Mechanical injury and inflammatory cytokines affect cartilage integrity and tissue homeostasis: a mass spectrometric analysis of proteins with relevance to arthritis

by

Anna L. Stevens
B.S. Chemistry, MIT, 2000

Submitted to the Department of Biological Engineering
in Partial Fulfillment of the Requirements for the Degree of

Doctor of Philosophy in Molecular and Systems Toxicology
at the
Massachusetts Institute of Technology
September, 2006

Signature of Author: _____
Department of Biological Engineering
July 24, 2006

Certified by: _____
Alan J. Grodzinsky
Professor of Electrical, Mechanical and Biological Engineering, Thesis Advisor

Certified by: _____
Steven R. Tannenbaum
Professor of Biological Engineering and Chemistry
Thesis Advisor

Accepted by: _____
Douglas A. Lauffenburger
For the Graduate Student Committee, Biological Engineering

Thesis Committee

Dr. Alan J. Grodzinsky ..... Professor of Electrical, Mechanical and Biological Engineering
Massachusetts Institute of Technology

Dr. Steven R. Tannenbaum ..... Professor of Chemistry and Biological Engineering
Massachusetts Institute of Technology

Dr. Forest White ..... Assistant Professor of Biological Engineering
Massachusetts Institute of Technology

Dr. Mary B. Goldring ..... Associate Professor of Medicine (Cell Biology)
Beth Israel Deaconess Medical Center, Harvard Medical School

Dr. Ram Sasisekharan ..... Professor of Biological Engineering
Massachusetts Institute of Technology

Mechanical injury and inflammatory cytokines affect cartilage integrity and tissue homeostatis: A mass spectrometric analysis of proteins with relevance to arthritis.

by

Anna L. Stevens

Submitted to the Division of Biologcal Engineering on August 3, 2006 in Partial Fulfillment of the requirements for the Degree of Doctor of Philosophy in Molecular and Systems Toxicology at the Massachusetts Institute of Technology

Osteoarthritis is characterized by synovial joint degeneration, and its cardinal pathological feature is degeneration and loss of the articular cartilage joint surface. While the aetiology of osteoarthritis is unknown, risk factors include gender, age, obesity, and prior joint injury. Joint injuries, including tears of the anterior cruciate ligament (ACL) and meniscus, increase the risk for the development of OA and involve both mechanical damage to cartilage, meniscus and synovial tissues, and tissue degradation associated with cytokine-induced inflammation. While the role of inflammatory cytokines in OA is still controversial, their role in rheumatoid arthritis is evidenced by the successful use of anti-TNF-α and anti-IL-1 therapies to abrogate disease symptoms and progression. In vitro, both IL-1β and TNF-α promote chondrocyte-mediated matrix degradation and inhibit cartilage matrix synthesis, while mechanical damage causes cell death, matrix damage, and decreased cell biosynthesis. Understanding the similarities and differences in cartilage responses to inflammatory cytokines and mechanical injury is important in understanding the catabolic-anabolic shifts that typify OA progression. Therefore, the objectives of this thesis were (1) to identify the role of TNF-α and IL-1β induced nitric oxide (NO) as a mediator of cartilage tissue damage; (2) to characterize and compare the regulation by IL-1β, TNF-α, and mechanical injury of secreted factors, matrix degradation, and mechanisms of chondrocyte cell death using an SDS-PAGE-LC/MS/MS protein profiling approach; and (3) to further quantify the effects of IL-1β, TNF-α and injury using an isobaric isotope labeling (iTRAQ) based 2D-LC/MS/MS approach. Together these studies were designed to provide better understanding of matrix degradation, cell death, immune response, and evidence of cell-mediated repair processes.

NO is produced by chondrocytes in response to inflammatory cytokines TNF-α, IL-1β and IL-17, and can mediate cellular and extracellular events through cGMP signaling, protein modifications (e.g., S-nitrosation or tyrosine nitration), altered transcript stability, and altered sugar and lipid chemistry. Cartilage was treated with IL-1β or TNF-α left untreated in the presence or absence of the NO synthase inhibitor, L-N-methylarginine (L-NMA), and changes in gene expression and matrix breakdown were measured. We found that L-NMA treatment partially inhibited TNF-α-induced, aggrecanase-mediated aggrecan degradation as indicated by a decrease in sGAG loss to the medium and by an increase in the generation of aggrecanase-specific aggrecan fragments. No change was observed upon addition of L-NMA to IL-1β treated explants, but addition of L-NMA to combined IL-1β and TNF-α treated explants increased sGAG loss, suggesting that the effects of NO may be contextual. We hypothesized that this might be due to differences in aggrecanase expression (ADAMTS4 vs. ADAMTS5) or post-translational modification, but no aggrecanase was consistently identified in the samples. No

difference in MMP expression or activation was noted following addition of L-NMA, and no change in NO chemistry between IL-1β and TNF-α treatment was evident by nitrate and nitrite production. Gene expression analysis was conducted on a battery of 32 genes, including matrix proteins, inflammatory mediators, proteases, cytokines and growth factors, and housekeeping proteins. While IL-1β and TNF-α both increased the expression of proteases and inflammatory mediators, addition of L-NMA did not significantly affect expression of the genes tested. We concluded that the effects of TNF-α and IL-1β–induced NO production may depend on differences in cellular responses to each of these cytokines and possibly to differences in signaling or aggrecanase expression.

In the second study, newborn bovine calf cartilage explants were treated with 10 ng/ml IL-1β, 100 ng/ml TNF-α, radially-unconfined injurious compression (strain: 50%; strain rate 100%/sec), or no treatment, and cultured for five days. Pooled medium was subjected to SDS-PAGE-LC/MS/MS, and data were analyzed by Spectrum Mill proteomics software, focusing on protein identification, differences between treatments and matrix protein proteolysis. Over 250 proteins were identified among the four protein groups including CD109, platelet derived growth factor like protein, and scrapie responsive protein, which have not been previously identified in cartilage. IL-1β and TNF-α caused an increase in YKL39, YKL40, complement factor B, MMP-3, ECM-1, haptoglobin, serum amyloid A3, and clusterin. Injurious compression caused the release of intracellular proteins including GRP58, GRP78, alpha 4 actinin, pyruvate kinase, and vimentin, suggesting a loss of membrane integrity in a population of chondrocytes. Data on actin release within the first 24 hours suggested that this loss of membrane integrity occurred by mechanical cell disruption. Injurious compression also caused proteolysis of collagen type VI subunits, collagen type II, and COMP. Thrombospondin 1 fragments were seen in all treatment groups, and aggrecan proteolysis was predominant with cytokine treatment. Cartilage explants subjected to injurious compression released intracellular proteins and showed enhanced degradation of matrix proteins, while explants subjected to IL-1β or TNF-α released proteins involved in innate immunity and stress response.

In the third study, cartilage explants were subjected to injurious compression, TNF-α (100 ng/ml) or IL-1β (10 ng/ml), or no treatment, cultured in equal volumes of medium, and the medium was collected, pooled and the proteins deglycosylated by treatment with chondroitinase ABC. The proteins were subjected to trypsinization, and the peptides were labeled with one of four iTRAQ labels each containing a unique signature ion. The labeled peptides were subjected to nano-2D-LC/MS/MS on a QStar, quadrupole time of flight instrument. The study was done in analytical replicate on a pooled sample of greater than 70 explants from a total of 6-12 different animals. Data were analyzed by ProQuant to obtain a ProGroup peptide report containing identified spectra, which were combined to achieve a peptide, and then a protein level output of mean ratios, standard deviations of those ratios, and significance based on either Wilcoxan sign rank or Student's t-test both corrected for multiple comparisons. Because of our interest in catabolic and anabolic shifts, a targeted data analysis approach was taken in addition to a systems level PCA and K-means clustering approach. By focusing on particular protein domains, we identified a decrease in the synthesis of most fibrillar collagen subunits ($p<0.05$), and an increase in the release of the aggrecan G2 and G3 domains with IL-1β and TNF-α treatment ($p<0.05$). We also noted a significant increase in MMP-1, MMP-3, MMP-9, and MMP-13 in at least one condition and, in most cases, all conditions compared to the untreated sample. Increases in

proteins involved in innate immunity and immune cell recruitment were noted with IL-1β and TNF-α treatment, while an increase in intracellular protein release was seen most dramatically with mechanical compression injury. Since anabolic effects are often driven by the insulin-like growth factor family and the TGF-β superfamily, we specifically identified members of these pathways to understand which factors may mediate early repair processes. At the systems level, 2 principal components were sufficient to describe 97% of the covariance in the data. IL-1β and TNF-α caused a similar response in proteins identified; in contrast, a 'Y'-shaped distribution was observed upon projection of proteins based on their response injury vs. cytokine treatment. K-means clustering revealed six main clusters to further characterize the biology of mechanical injury versus cytokine effects on cartilage.

Thesis Supervisors: Dr. Alan J. Grodzinsky and Dr. Steven R. Tannenbaum

Acknowledgements

I have had the great fortune to do my thesis work at one of the best research institutions in the world. I am tremendously grateful for that opportunity and learning experience which has shaped me both as a future physician and as a scientist. I will always be grateful to MIT for giving me an education and the analytical skills to apply that education. I also thank the American Society for Engineering Education and the Office for Naval Rearch for the National Defense Science and Engineering graduate fellowship that funded my first three years in graduate school. I thank NIH grants AR45779, CA26731, ES02109. I thank the Biological Engineering Division for providing a unique collaborative research environment which allowed me to work side-by-side with students and post-docs trained in both science and engineering – I am a better scientist because of this experience. I thank Health Sciences and Technology for providing a basic medical sciences education that allowed me to take advantage of my research opportunities and the perspective to understand the strengths and limitations of my work. I thank the Harvard Medical School MD-PhD program for their support.

I thank my advisors, Prof. Alan Grodzinsky and Prof. Steven Tannenbaum for giving me the honor and pleasure of doing my thesis research in their laboratories. I thank Prof. Grodzinsky for giving me a unique opportunity to work in a bioengineering lab as a student trained in basic science – the difference in focus enlarged my perspective and approach to biological questions. I also thank Prof. Grodzinsky for always making time to sit down with me and think through problems or ideas and for always being optimistic even in the face of setbacks. I thank Prof. Tannenbaum for his guidance and his willingness to disagree but to still let me do what I thought was best – I valued his opinions greatly as he always offered a different insight into the problems I was facing. I have tremendous respect for my advisors as researchers and as people – I taught me a great deal.

In thanking my advisors, I must also thank Dr. J. S. Wishnok (Pete) who almost served as my unofficial third advisor. Pete was patient with me and dealt well with my concerns and insecurities as a young, but at times, overly independent scientist. He taught me the basics of mass spectrometry and then stood back and let me learn. I spent a great deal of time learning the hard way, but I guess that is the only way to assimilate the knowledge and the experience. In addition to his scientific assistance, I respect him for being a genuinely good person who listened to my ideas, concerns, thoughts and feelings passing wisdom without overtly passing judgment.

I thank my thesis committee members, Dr. Forest White, Dr. Ram Sasisekharan and Dr. Mary Goldring for their time, energies and insights. Dr. White served as chair of my thesis committee offering me the support and assistance that I need to accomplish my thesis goals. I am grateful for the time he spent teaching me about the QStar and helping me think through my iTRAQ experiments. I thank Dr. Mary Goldring for always reminding me to bring the work back to the biology which was the motivation of my work in the first place. She was helpful in placing a big picture on the details of my work – what the system was saying rather than what individual proteins were doing. I have tremendous respect for Dr. White and Dr. Goldring, and I appreciate them helping me grow as a scientist.

There is nothing better and no greater colleague than one who can turn around and understand any question and engage any thought – that was Diana Chai. I could literally turn around and chat with Diana about anything. She had the scientific mastery, knowledge, and perspective that allowed her to engage the questions and ideas that I tossed her way regularly. She made the entire graduate experience a little bit easier because she was always happy (99.9% of the time) and that made for a fun and pleasant environment.

In the Tannenbaum lab, the person that I turned to first and most was Dr. Patty Sun – we helped each other through many difficult situations and celebrated some really good times. Patty was a great resource for HPLC and mass spectrometry, and I relied on her expertise and on her columns a number of times in method development. I have great respect for her intellect and her sense of humor; she is an extraordinary friend and colleague.

Despite incredible raw intelligence that MIT brings in as graduate students every year, experimental science/engineering requires not only a mastery of ideas but an assimilation of those ideas which is far more difficult and limits success in experimental work. I thank those who helped me assimilate my knowledge and my research in order to be a better scientist – Dr. Michael DiMicco, Dr. Jon Fitzgerald, Dr. Patty Sun, Dr. Jimmy Flarakos, Dr. Eliot Frank, Dr. Delphine Dean, Dr. Laurel Ng, Dr. Monica Kristianson, Dr. Hongbin Yu, Dr. James Sherley, and Dr. William Thilly and Dr. Doug Lauffenburger. I thank the White lab, particularly Yi Zhang, Ale Wolf-Yadlin, Paul Huang, and Katrin Moser for always offering friendly assistance with proteomics questions. Importantly, I thank the Han Lab including Prof. J. Han, Jianping Fu, Ying-Chih Wang, and Yong-Ak Song for the opportunity to collaborate with them – They challenged me to continue to think about the basic methods that I use rather than just using them. I had a great deal of fun talking with them about their microfluidics research and working with them. I look forward to the future when I will use the technologies they are developing today. I thank my UROPs, Danette Ko and Yael Marshall who are extraordinary young scientists and enjoyable people to work with.

In the end, it is the little things that can create the biggest headaches. For that reason, I thank Han-Hwa Hung, Amy Francis, and Linda Bragman for taking care of many of the little things. Han-Hwa has a big job overseeing the Grodzinsky lab and teaching the young students experimental techniques, and she does it with care. I am grateful to her for her time and commitment to the lab. I thank Linda Bragman for her time and care as well. I thank Amy Francis for overseeing the Tannenbaum lab – she is an invaluable member of the lab, and her commitment and care is evident in everything she does. I thank her for being there to help.

Research is a collaborative activity that should not be done alone. Otherwise, it often lacks the intellectual vigor and creativity that comes with camaraderie. Therefore I thank my collaborators. I thank Cameron Wheeler for his real time PCR expertise – I am fortunate to have worked with him. I thank Dr. Mustafa Unlu who taught me a great deal about 2D-PAGE and protein work in general. I thank Dr. Vadiraja Bhat who aided in my early SDS-PAGE-LC/MS/MS analysis by offering me protocols that served as starting points in my work. I thank Dr. White for his assistance in the iTRAQ-2D-LC/MS/MS experimental design. I thank Dr. Flarakos for his helpful discussion on setting up an appropriate offline 2D-LC protocol. I thank Ramesh Babu Indrakanti for continuing the iTRAQ work on the cytokine-injury combination samples. I thank Dr. Eliot Frank for his helpful scientific discourse and suggestions.

Support is important for perseverance and I therefore must thank my friends and family. I thank Megan McBee and Diana Chai. Many hours were spent at Starbucks talking over experiments, talking over life and relationships, and talking about plans for the future. Ajit Dash is both my roommate and my friend, and I admire his perspective, grounding, and ability to achieve balance. I thank Eugene Kuznetsov who is my best friend; this PhD is recognition of his love and support for me over the last four years. I thank the Grodzinsky lab, the Tannenbaum lab, the 7th floor of building 56, and those who I have grown to know well through undergraduate, medical school, and graduate school. And finally, I thank my family for constantly reminding me the importance of dreaming

Table of Contents

Title		Page
Chapter 1	Introduction	13
1.1	Arthritis Overview	13
1.2	Epidemiology	13
1.3	Diarthrodial Joint and the Knee	14
1.4	Cartilage Structure and Composition	14
1.5	Cartilage Proteases: Damage and Remodeling	19
1.6	Cartilage Changes in Osteoarthritis Disease Development	23
1.7	Joint Injury in Osteoarthritis Development	24
1.8	In vitro Joint Injury / Cartilage Injury Model	25
1.9	Cytokines and inflammation in Cartilage Damage	28
1.10	Biomarkers of Osteoarthritis	33
1.11	Thesis Objectives	35
1.12	References	37
Chapter 2	The role of nitric oxide in TNF-α-induced, chondrocyte-mediated extra-cellular matrix damage compared to IL-1β in bovine cartilage explant cultures	
2.1	Abstract	48
2.2	Introduction	50
2.3	Methods	55
2.4	Results	60
2.5	Discussion	65
2.6	Figures	75
2.7	References	83
Chapter 3	An SDS-PAGE-LC/MS/MS analysis of cartilage tissue response to mechanical compression injury and inflammatory cytokines TNF-α and IL-1β	
3.1	Abstract	89
3.2	Introduction	91
3.3	Methods	95
3.4	Results	100
3.5	Discussion	105
3.6	Figures	118
3.7	References	128

Table of Contents (cont.)

Title		Page
Chapter 4	An iTRAQ-2D-LC/MS/MS based quantitative comparison of cartilage response to mechanical compression injury and inflammatory cytokines, TNF-α and IL-1β – catabolism, immunity, cell death and possible repair	
4.1	Abstract	139
4.2	Introduction	141
4.3	Methods	145
4.4	Results	154
4.5	Discussion	163
4.6	Figures	184
4.7	References	197
Chapter 5	Summary and Conclusions	207
Appendix A	Protocols	
A.1	In-gel digestion protocol	209
A.2	Two-dimensional gel protocol	211
Appendix B	Additional Results	
B.1	Additional cytokine plus L-NMA results (Chapter 2 supplement)	217
B.2	Cytokine plus injury results	218
B.3	Two dimensional gel electrophoresis results	225
B.4	iTRAQ data analysis supplement (Chapter 4 supplement)	228
Appendix C	Protein lists from proteomics experiments	236
C.1	Protein list from SDS-PAGE-LC/MS/MS (Chapter 3 supplement)	236
C.2	Protein list from iTRAQ-2D-LC/MS/MS (Chapter 4 supplement)	246
C.3	Aggrecanase blots and protein list from detergent lyses TNF-α treated chondrocyte culture	253

List of Figures

Title	Page
Figure 2.1: Five day accumulated total nitrate and nitrite release to the medium in response to IL1β and TNF-α with and without L-NMA.	75
Figure 2.2: Twenty-four hour 5-^{3}H-proline and ^{35}S-sulfate incorporation day 6 post treatment IL-1β and TNF-α treatment with an without L-NMA	76
Figure 2.3: Accumulated sulfated glycosaminoglycan release to the medium with IL-1β and TNF-α with and without L-NMA.	77
Figure 2.4: Anti-G1-NITEGE-COOH immunoblot to probe mechanism IL-1β and TNF-α induced nitric oxide mediated sGAG loss.	78
Figure 2.5: Real-time PCR gene expression in response to IL-1β and TNF-α treatment with and without L-NMA projection plot of genes (A), centroid profiles (B), and table of gene expression relative to untreated control sample (C).	79
Figure 2.6: Gelatin and Casein zymograms for MMP release to the medium in response to treatment with TNF-α and IL-1β with and without L-NMA.	82
Figure 3.1: Flow chart of SDS-PAGE-LC/MS/MS approach used for protein identifications, comparisons, and degradation.	118
Figure 3.2: Global analysis of proteins identified in the medium in response to TNF-α, IL-1β, and injury: Venn diagram of proteins released with each treatment (A) proteins by location (B).	120
Figure 3.3: Immunoblot of actin (A) and fibronectin (B) release with injury compared to untreated (free swell).	124
Figure 3.4: Thromobospondin 1 breakdown with IL-1β, TNF-α and injury by graph of peptide ion intensity versus gel slice molecular weight.	125
Figure 3.5: Collagen type II breakdown with IL-1β, TNF-α and injury by graph of summed peptide ion intensity versus gel slice molecular weight.	126
Figure 3.6: Collagen type VI breakdown with injury compared to untreated (free swell) by graph of summed peptide ion intensities versus gel slice molecular weight (A) and confirmation by immunoblot analysis (B).	127
Figure 3.7: Cartilage oligomeric matrix protein (COMP) breakdown with IL-1β, TNF-α and injury by graph of summed peptide ion intensity versus gel slice molecular weight	128
Figure 3.8: Actin release 24 hours and 96 hours after mechanical compression injury compared to untreated (free swell).	129
Figure 4.1: Schematic of the iTRAQ-2D-LC/MS/MS process and data analysis	184
Figure 4.2: Analytical variation and reproducibility: Histogram of the log2(mean protein ratio1/mean protein ratio2).	185
Figure 4.3: Matrix protein release to the medium with IL-1β TNF-α and injury treatment compared to the untreated sample: most abundant matrix proteins (A), collagen C-terminal telopeptides (B), aggrecan release by globular region (C), and matrix metalloproteinases (D).	187

List of Figures

Title	Page
Figure 4.4: Proteins released with treatments from different biological relevant pathways: innate immune proteins (A), chemokines and cytokines (B), transforming growth factor superfamily related proteins (C), and IGF pathway related proteins (D).	190
Figure 4.5: Projection plot of all the proteins represented by their response to each treatment in log base 2 space.	193
Figure 4.6: Centroid profiles from K-means clustering (six clusters)	194
Figure 4.7: Intracellular protein release with IL-1β, TNF-α and injury	195
Fig. B.1.1: Immunoblot for collagen type II degradation IL-1β and TNF-α treatment with and without L-NMA	217
Fig. B.1.2: Anti-fibronectin immunoblot for fibronectin release and degradation with IL-1β and TNF-α treatment with and without L-NMA	217
Fig. B.2.1: Nitrite release over 5 days after treatment with IL-1β, TNF-α and/or injury	218
Fig. B.2.2: sGAG release with combined cytokine (IL-1β or TNF-α) and injury treatments (5-day)	219
Fig. B.2.3: Biosynthesis day 6 post cytokine (IL-1β and TNF-α) and injury treatment	220
Fig. B.2.4: Gelatin zymograms from day-5 medium cytokine and injury treatment	221
Fig. B.2.5: Casein zymogram from day-5 medium for IL-1 and injury treatment	222
Fig. B.2.6: Collagen type II degradation by immunoblot for cytokine (IL-1β and TNF-α) and injury treatment	222
Fig. B.2.7: Silver stain 4-15% SDS-PAGE gel of IL-1β and injury treatments	223
Fig. B.2.8: Actin immunoblot of medium from TNF-α and injury treatments	223
Fig. B.2.9: Aggrecan G-1 immunoblot for TNF-α and injury treatments	224
Fig. B.2.10: MMP-3 immunoblot of medium from IL-1β and injury treatments	224
Fig. B.2.11: MMP-9 immunblot of medium from TNF-α and injury treatments	225
Fig. B.3.1: Silver-stained 2D-PAGE from untreated 5-day culture medium	226
Fig. B.3.2: Silver-stained 2D-PAGE from NMA-only (A) and IL-1β plus TNF-α (B)	227
Fig. B.3.3: DIGE-2D-PAGE gels of 5-day medium from IL-1β and untreated with and without L-NMA	228
Fig. B.4.1: Histogram of peptide quantitation for Chondrotinase ABC in log2 space	230
Fig. B.4.2: Histograms of interinjection variation at a protein level for each signature ion ratio	231
Fig. B.4.3: Signature ion ratio reproducibility (log2(ratio1/ratio2)) values versus the mean ratio values (interinjection variability)	232
Fig. B.4.4: Histograms of analytical duplicate comparisons	233
Fig. B.4.5: Signature ion ratio reproducibility (log2(ratio1/ratio2)) values versus the mean ratio values (analytical duplicate reproducibility)	234
Fig. B.4.6: Comparison of quantitation by matlab scripts to ProGroup (ABI) Proteins summaries	235
Fig. B.4.7: Comparison of analytical duplicates using ProGroup (ABI) summaries	236
Fig. C.3.1: ADAMTS4/5 immunoblot of chondrocyte agarose cultures detergent lysis	253

List of Tables

Title		Page
Table 3.1:	SDS-PAGE-LC/MS/MS peptide and protein identification statistics.	119
Table 3.2:	Protein elevated with IL-1β, TNF-α, and/or injury over the untreated control sample	122
Table 4.1:	Chondroitinase ABC normalization statistics for iTRAQ ratios	185
Table 4.2:	p-values for collagen telopeptide and aggrecan (by globular domain) differences with IL-1β, TNF-α and injury compared to the untreated	189
Table 4.3:	p-values for matrix metalloproteinases with IL-1β, TNF-α and injury compared to the untreated control.	189
Table 4.4:	Additional potentially relevant biological regulators identified by iTRAQ-2D-LC/MS/MS analysis	196
Table B.4.1:	Table of Chondrotinase ABC normalization values	229
Table B.4.2:	Contributions of False ID/quantitation to iTRAQ error: the effect of peptide number on reproducibility	235
Table C.1:	SDS-PAGE-LC/MS/MS protein identification by Spectrum Mill of protein released into the medium from cartilage explants subjected to IL-1β, TNF-α or injury	237
Table C.2:	iTRAQ-2D-LC/MS/MS protein identification, quantitation and pvalues values	247
Table C.3:	SDS-PAGE-LC/MS/MS of detergent lyses of three week chondrocyte cultures in agarose after 36 hour TNF-α treatment	257

Chapter 1: Introduction

1.1 Arthritis Overview

Arthritis is characterized by degeneration of one or more synovial joints. Joint degeneration results from degradation and loss of the articular cartilage joint surface and leads to bone on bone contact and the accompanying clinical symptoms of pain, stiffness, swelling, and loss of joint motion [1]. The two major forms of arthritis include osteoarthritis and rheumatoid arthritis. Rheumatoid arthritis is a multi-system autoimmune disease which is characterized by a "persistent inflammatory synovitis" which ultimately leads to cartilage degeneration and bone erosion [2]. Osteoarthritis is a degenerative joint disease that has classically been considered a disease of mechanical wear-and-tear and is frequently localized to weight-bearing joints such as the knees and hips [2].

1.2 Epidemiology

A recent study by the Center for Disease Control suggests approximately 1 in 3 adult Americans suffer from symptoms of arthritic disease, which is significantly higher than the previous estimate of 16% from the Arthritis Foundation [1, 3]. The incidence of rheumatoid arthritis is approximately 1% of the population with women being approximately 3 times more likely to suffer from the disease than men [2]. The disease may be quite variable in presentation. While some cases may be of limited duration and cause only mild damage, many others will progress to cause complete joint destruction. Osteoarthritis is the most common joint disease [2]. While age is the most important risk factor for OA, joint trauma, repetitive joint use, obesity, and gender are also risk factors for the diseases [2]. Arthritis is the number one cause of disability in

the United States affecting a significant proportion of the population and making it an important focus for improving medical treatments and prevention.

1.3 Diarthrodial Joint and the Knee

Diarthrodial or synovial joints occur at the interface of two bones and allow for low friction mobility and force dissipation. Mobility and force dissipation are achieved by the articular cartilage covering the surface of the bones within a joint cavity, where synovial membrane cells secrete a lubricating substance known as synovial fluid [4]. The knee joint is a load bearing hinge joint that allows movement in one axis for flexion and extension [4]. The knee joint is formed by the articulation of the medial and lateral femoral condyles between the tibial plateau and the articulation between the patella and patellofemoral groove [4]. The joint is directly stabilized by the menisci that also serve to absorb shock and by ligaments including the anterior cruciate ligament, the posterior cruciate ligament, and the medial and collateral ligaments [4]. The leg muscles, particularly the quadriceps femoris provide additional stability and strength to the joint.

1.4 Cartilage Structure and Composition

Articular cartilage is an approximately 1 mm thick white, glistening material covering the surface of the bone in synovial joints [1]. The articular cartilage is responsible for weight distribution, dissipation, and low-friction joint motion [1]. Cartilage contains only a single cell type, called chondrocytes, which are responsible for production and maintenance of the dense extracellular matrix (ECM) [1]. Because cartilage is an avascular and aneural tissue, the chondrocytes must rely on diffusion from the synovial fluid or from the underlying bone for nutrients and oxygen. Making up approximately 90-99% of the cartilage volume, the ECM is composed primarily of collagen type II and aggrecan, which are responsible for the weight-

bearing properties of the tissue [5, 6]. Aggrecan is a large negatively charged proteoglycan responsible for the compressive stiffness of cartilage while the type II collagen network is thought to provide tensile strength to the tissue and thus prevents tissue swelling [5, 6]. In addition, the ECM contains a number of small proteoglycans, growth factors, structural proteins, proteins involved in cell-matrix interactions, and hyaluronic acid [1].

1.4.1 Aggrecan Structure

Aggrecan is a large aggregating proteoglycan of approximately 2-3 MDa in size, and it makes up approximately 35% of the dry weight protein of cartilage [7]. The aggrecan core protein is composed of four domains: the first globular domain, the second globular domain, the central sGAG rich domain, and the third globular domain. The first globular domain, often referred to as G1, is responsible for hyaluronan-binding and interacts with proteoglycan link protein [8]. The purpose of the second globular domain, G2, is unknown; however it may play an active role in inhibiting aggrecan secretion prior to addition of the sGAG chains [9, 10]. Between the G1 and G2 sits a 127 amino acid, rigid interglobular domain which is highly susceptible to protease cleavage [11, 12]. The sGAG binding region follows the G2 domain, and it is broken down into the keratin sulfate rich region and the chondroitin sulfate rich region. The keratin sulfate rich region of aggrecan contains a hexapeptide repeat in which between 4-23 keratin sulfate chains which are O-linked to serine residues [12-14]. There are two chondroitin sulfate rich regions which contain a total of 120 consensus sequences for chondroitin sulfate attachment [12, 15-17], from which chondroitin sulfate chains up to 50-100 disaccharide units long may be attached [7]. These chondroitin sulfate chains are responsible for the high fixed charge density of aggrecan which is critical to the function of the molecule [5]. The third globular domain, G3, makes up the C-terminal region of aggrecan. The G3 domain may be

important in aggrecan intracellular trafficking [18], it may protect the aggrecan molecule against degradation of the core protein [19], and it also may play a role in aggrecan aggregate formation and interaction with other matrix components [19].

In young cartilage, each aggrecan interacts with one molecule of proteoglycan link protein to form a strong non-covalent bond with hyaluronic acid [20]. However, as cartilage ages, aggrecan gets cleaved in various regions including the IGD domain and various locations within the chondroitin sulfate binding region (CS2), which leads to the accumulation of aggrecan fragments within the tissue that no longer resist compression, as well as the full length molecule due to loss of the sGAG binding regions.

1.4.2 Type II collagen

Collagen accounts for approximately 2/3 of the tissue dry weight with fibril forming collagen type II accounting for 90% of collagen composition [21]. The collagen fibril network of cartilage is a heteropolymeric structure of collagen type II, collagen type XI, and collagen type IX with collagen type II making up the majority by weight [21]. The type II collagen fibril is composed of triple helices which are homotrimers composed of three alpha 1 (II) subunits [22]. The alpha 1 (II) subunit contains N-terminal and C-terminal pro-peptides, important for fibril formation and post-translational processing, and an uninterrupted fibril forming region [1]. The fibril-forming region usually contains a triplet repeat Gly-X-Y peptide where X is often proline and Y hydroxyproline [23]. Collagens contain a number of modifications including glycosylation, proline hydroxylation, lysine hydroxylation, and various cross-links that are important for the overall stability of the collagen helix and the fibril [21]. The type II/XI/IX collagen heterofibril network is laid down early in development, and it possesses little capability for repair if damage in late life [21]. Collagen fibril direction varies with cartilage depth.

Superficial collagen fibrils run parallel to the surface in thin fibrils while those of the intermediate layer tend to be thicker and appear to run in a more random pattern when visualized by TEM [21]. Finally, collagen fibrils of the deep layer appear to be orthogonal to the joint surface and run in larger bundles. These differences in collagen fibril patterns contribute to the zonal architecture of the tissue. The contribution of collagens IX and XI are greater in thin fibrils of the superficial surface than in thicker fibrils of the deeper cartilage. Cartilage collagen structure also varies between the pericellular matrix region and the interterritorial matrix regions with the fibrils in the pericellular matrix more fine than those of the interterritorial matrix.

1.4.3 Other Matrix Molecules

In addition to aggrecan and type II collagen, cartilage contains a number of other important ECM structural proteins and protein complexes including other collagens, COMP, matrilins and other large proteoglycans. The cartilage collagen fibril network is composed primarily of type II collagen, type XI collagen and type IX collagen, accounting for approximately 2-3% of the collagen in adult cartilage[1, 21, 24]. Type XI collagen, more highly expressed in young tissue, may contribute to the collagen fibril formation and size while collagen IX plays an important role in fibril cross-linking which is essential for the stability of the collagen network [24]. Other collagens such as collagen VI, XII, and XIV may be expressed in the pericellular matrix of cartilage [1]. Though initially considered a sign of disease or contamination from vasculature in the underlying bone, small amounts of collagen III may co-localize with type II collagen fibrils, and likewise, collagen type V subunits may be associated with collagen XI fibrils [21].

In addition to collagens, matrilins and cartilage oligomeric matrix protein (COMP) may aid in maintaining the structural integrity of the extracellular matrix. COMP forms a disulfide-

bonded pentameric structure which binds calcium in the ECM [25]. In adult cartilage, COMP is primarily located in the interterritorial matrix, where it is thought to help stabilize the collagen framework [1]. COMP is susceptible to proteolytic cleavage, and its fragments may serve as useful biomarkers of active arthritic disease [26, 27]. Matrilin-1 and matrilin 3 are expressed by chondrocytes and are capable of forming collagen-dependent and collagen independent filaments (for review, [28]). In addition, Matrilin-1 also binds tightly to aggrecan and may become covalently attached, particularly as tissue ages. Although matrilin-3 is an integral ECM component in cartilage, increased expression may be associated with an increase in disease severity [29].

Large aggregating (aggrecan and versican) and non-aggregating proteoglycans (perlecan) may also be present in the matrix. Versican, like aggrecan is a large aggregating proteoglycan normally found in many connective tissues. Perlecan is a non-aggregating large proteoglycan thought to play a greater role in the pericellular environment interacting with cellular adhesion molecules and other matrix molecules and sequestering growth and differentiation factors in the pericellular matrix [1, 30, 31].

In addition to large structural ECM components, a number of matrix proteins may bridge the chondrocytes with the surrounding matrix. These cell-matrix interactions may be important in transmitting mechanical loads and maintaining cell phenotype. Proteins known to be involved in chondrocyte matrix interactions include fibronectin, thrombospondin-1, tenascin-c, collagen VI, collagen II, and perlecan. Fibronectin is present in cartilage in a number of different splice-variant isoforms; some of these isoforms are thought to be cartilage specific and critical for normal development and maintenance of the tissue (for review [32]). Fibronectin binds to cell surface proteins known as integrins, through specific alpha subunits (alpha v, alpha 3, and alpha

5) of the integrin α-β heterodimer. Fibronectin fragments have been shown to activate chondrocytes to release matrix proteases through their interactions with the alpha 5 integrin subunit [32, 33]. Thrombospondin-1 is also present in normal and arthritic cartilage and may be involved in cell-matrix interactions by binding to CD36 (GPIIIb, GPIV) and CD51 (α-v integrin via an RGD domain) present on the surface of chondrocytes in the superficial and middle/deep layers respectively [34, 35]. Tenascin-c is a large ECM protein found primarily in the pericellular matrix of deep cartilage, and like fibronectin and perlecan, it is thought to play a critical role in the development and maintenance of the articular cartilage phenotype through its interaction with cell surface receptors (for review [36]. Although tenascin is up-regulated in arthritic and in normal cartilage exposed to IL-1, this process is not associated with the loss of proteoglycans and may play a role in early repair processes [37].

In addition to the large structural proteins and proteoglycans in the extracellular matrix, small leucine-rich repeat proteoglycans (SLRPs) are also present in the matrix and are thought to play a role in regulating collagen fibril formation, cell adhesion, and growth factor regulation [38, 39]. While SLRPs such as decorin and biglycan have a well-characterized role in regulating collagen type II fibril size, a number of the other SLRP such as PRELP, epiphycan, and mimecan are less understood. The role of SLRPs in the ECM may extend beyond collagen fibril formation, for example, chondroadherin, a SLRP known to play a role in cell-matrix interactions through binding to type II collagen and α_1-β_2 integrin on the chondrocyte cell surface [40, 41].

1.5 Cartilage proteases: Damage and remodeling

Finally, the extracellular matrix contains proteases and protease inhibitors important for remodeling and for maintaining the extracellular matrix. Chondrocytes mediate matrix degradation primarily through the production of proteases, in particular, two classes of

metalloproteinases, matrix metalloproteinases (MMPs) and a disintegrin and metalloproteinase with thrombospondin motifs (ADAM-TSs) (for review [42, 43]). The MMP family currently contains 24 enzymes while the ADAM-TS contains 19 enzymes [42, 44]. All metalloproteinases are neutral proteases that possess zinc at the active site, which is responsible for coordinating a water molecule to attack the amide bond of particular substrates and sites. In addition to metalloproteases, the chondrocytes may release serine and cysteine proteases including cathepsins, calpains, and HTRA1, and plasmin [45, 46].

1.5.1 Matrix Metalloproteinases in Cartilage

The MMP family is composed of neutral proteases that can cleave a wide variety of substrates, and many of the MMPs are found in cartilage. The MMP family possesses three collagenases (MMP-1, MMP-8, MMP-13) that are capable of cleaving collagen fibrils with MMP-13 having the greatest affinity for type II collagen fibrils [47]. Gene expression of both, MMP-1 and MMP-13, is present in normal and OA cartilage; however MMP-13 gene expression is up regulated in OA cartilage [48, 49]. Immuno-histochemical analysis shows increased expression of all three collagenases (MMP-1, MMP-8, and MMP-13) in OA cartilage compared to an almost undetectable expression in normal cartilage [50]. The gelatinases, MMP-2 and MMP-9, are responsible for degrading partially denatured collagen fibrils, and they are present in normal cartilage with MMP-9 up regulated in osteoarthritic cartilage [49]. The stromelysins (MMP-3, MMP-10 and MMP-11) are a third group of MMPs with only MMP-3 present in cartilage. MMP-3 cleaves a wide range of substrates, including aggrecan [51], COMP[52], and fibronectin[53], and is up regulated following joint injury and in early OA at the protein level [50, 54]. A number of other MMPs such as MMP-12, MMP-19, and MMP-27 are present at the

mRNA level in cartilage [49]; however their role in matrix damage and remodeling has not been well studied and their functions are less well understood.

1.5.2 Cartilage ADAMTS's – the Aggrecanases

"Aggrecanase" was the named given to the proteolytic activity that cleaved Glu373-Ala374 bond (G1-NITEGE-COO- neo-eptiope) bond in aggrecan [55]. It was the identification of this unique cleavage site that led to the discovery that MMP-3 was not the enzyme responsible for acute aggrecan degradation in response to IL-1 and retinoic acid, and it began the search for the aggrecanases [51, 56, 57]. Reports over the next 7-8 years suggested a soluble and a membrane bound aggrecanase activity as determined by immunoreactivity with neo-epitope antibodies [58, 59]. In 1999, Tortorella et al. published the identification of the first aggrecanase purified from bovine nasal cartilage; aggrecanase 1 was identified as ADAMTS4 [60]. Shortly after, aggrecanase 2 was purified, cloned and identified as ADAMTS5 [61, 62]. Since then, there is evidence that ADAMTS1, 4, 5, 8, 9 may all have some aggrecanase ability meaning that they are all capable of cleaving aggrecan [63-66]. However, only ADAMTS4 and ADAMTS5 have been shown to have potent activity to the E373-A374 bond that originally characterized aggrecanase activity [64]. Real time PCR results indicate that ADAMTS1, ADAMTS4 and ADAMTS5 are expressed in normal and osteoarthritic cartilage, and ADAM-TS4 has been shown to be up-regulated at a transcription level in late stage osteoarthritic cartilage[48]. Aggrecanases (ADAMTS4 and ADAMTS5) are thought to be synthesized as a pre-protein and enter the secretory pathway where they are activated by an intracellular pro-protein convertase, furin, prior to secretion [67, 68]. The actual localization of the aggrecanases after secretion is still somewhat in question. Tortorella et al. extracted ADAMTS4 and ADAMTS5 from osteoarthritic cartilage using the chaotropic agent, guanidine, suggesting that

the enzyme may be associated with the proteoglycans [69]. To further support this possibility, Flannery et al. showed that both ADAMTS4 and ADAMTS5 have high sGAG binding affinity which is localized predominantly to the thrombospondin motif region [70]. At the same time, work by Pratta et al. using immunofluorescence in monolayer chondrocyte culture showed that ADAMTS4 remains associated with the cell surface rather than being released into the medium [71]. The work by Gao et al. and Patwari et al. have shown optimal ADAMTS4 isolation using a detergent lyses rather than guanidine extraction suggesting the molecule may be associated with the membrane or membrane proteins [67]. At the same time, they were also able to detect enzyme in the medium suggesting that it may simply be freely secreted [67]. Most in vitro work has focused on ADAMTS4; however recent in vivo work using ADAMTS4 and ADAMTS5 knockout mice indicate that only the ADAMTS5 knockout mice are protected against cartilage destruction in both joint trauma and inflammatory arthritis [72-74]. While often difficult to find in cartilage, aggrecanases are hypothesized to play a significant role in cytokine and retinoic acid induced aggrecan degradation in cartilage explants generating a G1-NITEGE^{373} neoepitope [67].

1.5.3 Cartilage Protease Inhibitors – Tissue inhibitor of metalloproteinases (TIMPs)

Matrix metalloproteinases and aggrecanases may be inhibited by one or more of the four tissue inhibitors of matrix metalloproteinases (TIMPs) [43]. TIMP-1 and TIMP-2 are broad spectrum inhibitors of the MMP family including collagenases, gelatinases, matrilysins, and stromelysins. In addition, TIMP-1 and TIMP-2 may have additional roles in regulating activation and proteolytic activity among the latent MMPs [75, 76]. TIMP-3 is a potent inhibitor of the aggrecanases, ADAMTS4 and ADAMTS5, as well as inhibiting many members of the MMP family [43]. TIMP-4 is also a broad spectrum MMP inhibitor that was originally

identified in the heart and is found in lesser abundance in other tissues [77]. TIMP-1 and TIMP-3 gene expression has been shown to be up regulated in OA cartilage, and they are generally thought to play a protective role [49].

1.5.4 Other classes of proteases and inhibitors in cartilage

In addition to the MMPs and their inhibitors, the TIMPs, cartilage contains the serine proteases, urokinase, tissue plasminogen activator (tPA) and serine protease (HTRA1), and at least two serine protease inhibitors, plasminogen activator inhibitor-1 (PAI-1) and alpha-1-antitrypsin[46, 78-81]. Urokinase, tPA, and HTRA1 are increased in OA cartilage while PAI is decreased [78].

Cysteine proteases known as cathepsins are also thought to play an important role in cartilage damage in arthritis. Cathepsin G and neutrophil elastase secreted from PMNs are immunolocalized to the cartilage surface in some cases of rheumatoid arthritis where the enzymes may play a role in cartilage breakdown[82]. The intracellular protease, cathepsin B is up regulated in synovial cells from RA patients compared to normal [83]. HTRA1 is a newly identified serine protease found in cartilage which degrades extracellular matrix proteins, such as decorin, fibromodulin, fibronectin, aggrecan and gelatins, and it inhibits TGF-β signaling[45, 46]. In addition, HTRA1 is elevated synovial fluid from OA and RA patients as well as in mouse models of experimental arthritis [45, 46, 82, 83]. Under normal conditions, the proteases and their inhibitors are at an equilibrium that allows for constant matrix remodeling; however, under inflammatory conditions, these proteases may enhance matrix degradation creating an imbalance between degradation and synthesis associated with arthritis [84].

1.6 Cartilage changes with Osteoarthritis disease development

Arthritis results from a progressive wearing away of the articular cartilage of the joint surface caused by mechanical injury, by joint instability, or by an inappropriate response to normal mechanical stimuli [84]. The molecular pathogenesis of the disease seems to require loss of aggrecan, damage to the collagen framework, and ultimately loss of normal chondrocyte phenotype and (some limited) chondrocyte cell death [84]. In response to joint injury or cytokine stimulation, latent matrix proteases or newly secreted proteases may rapidly degrade aggrecan [42, 60, 61, 85]. Although loss of aggrecan may significantly alter the mechanical properties of the tissue [86], chondrocytes may synthesize and replace lost aggrecan with a concomitant return of the tissue moduli and function without long term damage [87, 88]. Unlike aggrecan degradation, collagen damage and/or degradation are thought to constitute an irreversible step in the pathogenesis of arthritis [84]. Protease induced collagen degradation occurs after aggrecan depletion suggesting that aggrecan may protect collagen fibrils from proteolytic degradation [71]. Chondrocyte dedifferentiation, marked by the decrease in type II collagen and aggrecan and an increase in collagen type I and type X, occurs as the disease progresses and marks the beginning of the inevitable end as dedifferentiated cells can no longer synthesize useful matrix material [84]. Although the mechanism of matrix loss and the driving force for the disease progression are not completely understood, acute mechanical injury and prolonged inflammatory insult increase the risk of developing arthritis [54].

1.7 Joint Injury in osteoarthritis development

Research in vivo and in vitro suggests that mechanical injury leads to damage of the extracellular matrix and, at times, death to the chondrocytes. This damage, resulting in a change in matrix composition and mechanical properties, may be partly responsible for increasing the risk of arthritis, given that the chondrocytes are rarely able to repair the damage [89]. Knee

injury, particularly anterior cruciate ligament (ACL) tears and meniscal tears, may dramatically increase the risk for developing osteoarthritis. Joint injury including ACL or meniscal tear may significantly increase the relative risk of developing OA with the mean relative risk values ranging from 3 to 20 with the risk increasing with age of injury and time following injury [90-92]. While joint instability may contribute to secondary disease development, ACL correction has not been shown to decrease risk of OA development, implying that the acute traumatic event may have been sufficient to trigger a cascade of events initiating arthritic progression [93-96]. Acute knee injury is accompanied by an increase in pro-inflammatory cytokines, TNF-α and IL-1β [97–99], as well as by increases in MMP-3, COMP fragments, collagen II cross-links and aggrecan fragments [100-104].

1.8 In vitro joint injury/ cartilage injury models

In vitro models of injury have attempted to better characterize the effects of high stress and high strain mechanical compression on both the chondrocytes and the matrix. Most compression injury models suggest that chondrocytes may undergo apoptosis in response to injury [67, 105-107]; however high stress repetitive loading induces necrosis [108]. Loening et al. showed that apoptosis correlated with a decreased unconfined equilibrium and dynamic stiffness in response to unconfined compression injury [105]. These changes in physical properties were accompanied by an increase in swelling in hypotonic solution suggesting damage to the collagen framework [105]. Apoptosis by TUNEL was observed at peak stresses as low as 4.5 MPa, which was well below the ~12 MPa loads required to induce significant changes in mechanical properties compared to the free swelling control [105]. To validate the TUNEL findings, Patwari et al. subjected explants to a single 50% strain at 100 %/sec strain rate single compression, and showed that the TUNEL staining was consistent with the EM morphology

findings of apoptosis [67]. D'Lima et al. showed a similar apoptotic response from loading [106, 107]. A single mechanical compression injury, yielding a peak stress of 14 MPa, resulted in 34% of the chondrocytes undergoing apoptosis by DNA fragmentation assay 96 hours after injury [106]. Only 4% of the chondrocytes were apoptotic in the uninjured control group [106]. Lucchinetti et al. used a stress-controlled confined compression with many repetitions [108]. In this model, chondrocyte death occurred soon after the injury, and chondrocytes were determined to be necrotic by morphology by TEM [108]. In vitro injury models usually involve the application of high-strain/ high strain rate or high stress/ high stress rate controlled mechanical compression which may be either confined (more characteristic of the physiologic situation) or unconfined. The high rate of compression causes tissue pressurization in the center of the explants while the periphery may experience more strain [19] suggesting a spatial gradient of how the tissue experiences and responds to the compression. While this spatial gradient may exist, most studies have focused on the pressurized central region of the cartilage to avoid cutting artifacts [105] which is where abundant apoptosis can be seen by DNA fragmentation or by EM morphology. Patwari et al. suggests that compression injury may alter cell-matrix interactions sufficiently to initiate apoptosis [67]. Mechanical injury-induced cell death and accompanying damage to the extracellular matrix may explain why acute injury so frequently leads to arthritis; however the contribution of cell death to arthritis is still somewhat controversial [19, 109, 110].

In addition to studies on apoptosis, research has focused on characterizing biosynthetic responses to cartilage following injury. Kurz et al. showed that increasing strain rate of mechanical injury significantly decreased tissue recovery from injury (as measured by biosynthetic rates) [19]. Kurz et al. observed that higher strain rates (O.1 and 1Hz but not 0.01 Hz) led to a small increase in cell death with a more dramatic decrease in ^{35}S-sulfate

incorporation and ^{3}H-proline incorporation three days after the injury even in the presence of stimulatory dynamic compression[19]. Quinn et al. similarly showed a decrease in biosynthesis and increased cell death at the higher strain rates when testing osteochondral explants at strain rates between 0.003 Hz and 0.7 Hz and peak stresses between 3.5 and 14 MPa [111]. The study also showed that matrix damage occurred primarily in the superficial zone with higher strain rates[111]. While these studies included observations only early time points following injury, they suggest that mechanical injury may cause a change in chondrocyte behavior leading to decreased extracellular matrix production, which may potentiate further degeneration.

Mechanical injury may also cause loss of matrix molecules. Studies by Chen et al. and Thibault et al. tested the effects of mechanical injury on the production the collagenase-generated neoepitope of type II collagen [112, 113]. In both confined and unconfined compression injury models, injury caused an increase in collagenase-generated collagen fragments, which Thibault et al. postulated may be the result of mechanical denaturation of the collagen fibril making it susceptible to cleavage by latent metalloproteinases [113]. A study focusing on repair secondary to mechanical compression injury suggested that both fibronectin and proteoglycan synthesis were increased relative to controls over the ten days following injury which is similar to that seen in early OA [112]. DiMicco et al. characterized sulfated glycosaminoglycan release to the medium over the seven days following injury [19]. In this study, they noted a small but statistically significant increase in sGAG release, which they attributed to mechanical disruption of the matrix as well as a longer period of sGAG release that, while not elevated over the untreated, controls, is responsive to an MMP inhibitor [19].

Recent work, using real time RT-PCR and gene array technology, has focused on characterizing the initial changes in chondrocyte gene expression that may suggest a cause for

the changes in behavior observed with injury. Lee et al. performed real-time PCR time course profiles on 24 cartilage genes involved in normal cartilage maintenance to look for changes in gene expression following unconfined compression injury [67]. In this study, Lee et al identified MMP-3, ADAMTS5, and TGF-β which were elevated more than over 5 fold within four hours of injury and remained elevated at 24 hours after injury [67]. Transcription of MMP-1, MMP-9, and MMP-13 were also increased at the 24 hour time point, but matrix proteins aggrecan, type II collagen and fibronectin were not significantly altered. Additionally, increased transcription of c-Fos and c-Jun within the first hour of injury suggested that the AP-1 pathway may be an important response pathway in injury [67]. A similar study by Chan et al. used a combination of gene arrays and real time PCR to look for changes in transcription three hours after unconfined compression injury [114]. This study identified a decrease in transcription of adhesion molecules and growth factors ICAM-3, NCAM, N-cadherin, VCAM-1, and IGF-1 while the chemokine receptor CCR10, HMGB2, neurogranin, and ezrin were among the proteins that were up regulated [114].

1.9 Cytokines and Inflammation in cartilage damage

In vivo mechanical injury occurs with concomitant inflammation. Osteoarthritis has an inflammatory component, which involves the production of cytokines and local low-level inflammation without inflammatory cell migration and accompanying systemic immune response. Pro-inflammatory cytokines IL-1 and, to a lesser extent, TNF-alpha are known to cause cartilage extracellular matrix breakdown and may contribute to osteoarthritis.

1.9.1 Tumor Necrosis Factor alpha (TNF-α) and cartilage damage

Tumor necrosis factor alpha (TNF-α) is a 17 kDa protein produced primarily by inflammatory cells but it may be produced by synoviocytes and by chondrocytes [114-118].

TNF-alpha has been identified in the synovial joints of patients with inflammatory arthritis [119]. TNF-alpha is thought to play a role in joint disease because of its ability to initiate an inflammatory response and because it may play a role in cartilage and bone damage [114]. In vitro, TNF-alpha inhibits proteoglycan synthesis [120, 121], and increases proteoglycans degradation, though at a higher concentration than IL-1 [120]. TNF-alpha also stimulates the production of MMP-13 (collagenase-3) and MMP-9 (gelatinase-2) that may be responsible for collagen degradation [122, 123]. TNF-alpha also increases inflammatory mediators, such as PGE2 and nitric oxide [124, 125], and up-regulate adhesion molecules on endothelial cells leading to an inflammatory cell migration into the synovium [126, 127]. TNF-alpha up regulates the transcription of IL-1, TNF-alpha, and IL-6 genes in cartilage from osteoarthritic joints[128], and the production of IL-1 and GM-CSF by synovial cells [129, 130]. In vivo, transgenic mice over-expressing TNF-alpha spontaneously develop inflammatory arthritis[131]. In addition, anti-TNF-alpha antibody therapy has decreases inflammation and histological scores in mice [132-135], and is used successfully to treat humans with poorly controlled rheumatoid arthritis [134-137]. TNF-alpha and TNF-alpha receptors are not only present in rheumatoid arthritis but are increased in a canine model of osteoarthritis [138] as observed by immuno-histochemistry. TNF-alpha clearly plays an important role in rheumatoid arthritis through its ability to enhance inflammation and to promote breakdown of cartilage; however, less is known about the role of this cytokine in OA.

1.9.2 Interleukin 1beta in cartilage damage

Interleukin-1 or IL-1 is an 18 kDa protein present in two primary forms, IL-1alpha and IL-1beta [1]. IL-1 was first described as "mononuclear cell factor" for its ability to stimulate stellate synovial fibroblasts to produce collagenase in culture and then as "lymphocyte activating

factor" and "endogenous pyrogen" (for review [139]). Dingle et al. also identified IL-1 as secreted from synovium and described it as 'catabolin' for its ability to enhance chondrocyte mediated extracellular matrix degradation [140-142].

IL-1 plays a critical role in driving cartilage destruction in inflammatory arthritis, rheumatoid arthritis, and osteoarthritis [124]. IL-1, like TNF-alpha, can act on chondrocytes, synovial cells, and endothelial cells to enhance the production of collagenase, prostaglandins, cytokines, chemokines (IL-8 and leukotrienes), nitric oxide and cell adhesion molecules [42, 87, 120, 124, 143-145]. In inflammatory arthritis models, inhibition of TNF-alpha and IL-1 limits inflammation, and inhibition of IL-1 protects against cartilage (and bone) destruction [146]. IL-1 is frequently present in the synovial fluid of arthritic joints [147], and the inhibition of IL-1 may help to decrease cartilage and bone resorption in human disease[148]. While inhibition of IL-1 can be protective, IL-1beta gene deletion in mice may lead to an increased risk of osteoarthritis suggesting that IL-1 plays a critical but complex role in normal matrix remodeling [149].

In vitro studies suggest that IL-1 enhances cartilage degradation by activating chondrocytes to increase protease expression. IL-1 increases the loss of aggrecan, and thus sGAG, through the production of ADAM-TS4 (aggrecanse-1), possibly ADAM-TS5, and to a lesser extent MMP-3 [55, 56]. Using specific neoepitope antibodies, proteoglycan fragments released from IL-1-treated cartilage explants and cell cultures were shown to be primarily the result of aggrecanase cleavage (G1-NITEGE^{373}) along the core protein rather than MMP-3 cleavage (G1-VDIPEN^{341}) [55]. Recent work by Gao et al. suggests that activation of ADAM-TS4 by C-terminal cleavage appears to be associated with GPI-linked MT4-MMP (MMP17)[67, 150]. Following cleavage, the active form of ADAM-TS4 remains near the cell through its

association with syndecan-1[67]. This mechanistic model may begin to explain Dingle's observation that aggrecan cleavage occurs near the cells[67, 141].

Type II collagen molecules are cleaved by collagenases (MMP-1, 8, 13) into a 1/4 and 3/4 fragment, which can be further degraded by gelatinases, MMP-2 and MMP-9[42, 143]. Chondrocytes express MMP-1, MMP-3, MMP-8, MMP-9, and MMP-13 in response to IL-1 while MMP-2 is constitutively expressed by chondrocytes in explant culture[48, 79, 143, 150-157]. IL-1 induced up-regulation of collagenases, especially in the presence of the gelatinases, may lead to substantial damage to the collagen fibrillar network with concomitant decrease in tissue tensile strength visible as tissue swelling in hypotonic solution [6, 71, 158]. While MMP-3 is substantially upregulated in response to IL-1, its actions are unclear, as it does not play an active role in aggrecan or collagen breakdown early in the response to IL-1 [55]. In addition to collagen and aggrecan, IL-1 may also play a role in the degradation of COMP and fibromodulin while sparing most of the small leucine rich repeat proteoglycans[26, 159].

At a broad level, IL-1 inhibits the synthesis of proteins including aggrecan and collagen. At a gene expression level, IL-1 inhibits the synthesis of aggrecan, collagen type II and collagen IX as well as cartilage derived retinoic acid sensitive protein (CD-RAP) [160-162]. IL-1 significantly decreases extracellular matrix protein synthesis including collagens as measured by ^{3}H-proline incorporation and hydroxyproline, decorin, biglycan, and tenascin-c [37, 142, 163]. IL-1-induced chondrocyte mediated extracellular matrix degradation results from up-regulation of proteases and inflammatory mediators that may damage the matrix.

1.9.3 Mechanical changes associated with IL-1beta treatment

To study the effects inflammatory cytokines on tissue mechanical properties, Bonassar et al. studied the change in mechanical properties of cartilage explants treated with 100ng/ml of IL-

1β [158, 164]. IL-1β treatment led to a substantial and significant reduction in the compressive equilibrium modulus, dynamic stiffness and streaming potential as a result of sulfated glycosaminoglycan loss [158, 164]. By the eighth day of IL-1 treatment, ninety percent of the sulfated glycosaminoglycan had been released, large amounts of hyaluronic acid had also been released, the equilibrium modulus was only 20% of the starting value, and the tissue showed signs of swelling in hypotonic solution suggesting damage to the collagen network [158, 164]. Aggrecan loss in this study was shown to be mediated by aggrecanase cleavage and not by MMP-3, though the overall changes in mechanical properties were similar to those seen by Bonassar et al. upon treatment with APMA, a mercurial compound known to activate matrix metalloproteinases [164, 165]. Clearly, aggrecan was associated with much of the compressive stiffness of the tissue; however, there may be other structural proteins that may also contribute to the tissue mechanical properties or the response of the chondrocyte to the mechanical loads.

1.9.4 Combining cytokine treatment with cartilage mechanical compression injury

Because joint injury involves both injury to the joint and inflammation secondary to that injury, in vitro modeling of both components may be helpful in understanding the outcome caused by injury. Patwari et al. combined high strain, high strain rate compressive injury with exogenous IL-1 (1-10ng/ml) and TNF-a (100ng/ml) which resulted in synergy with respect to sulfated glycosaminoglycan loss compared to either cytokine or by mechanical injury alone [67, 166]. This study was critical in that it suggested that mechanical injury and cytokine-induced, chondrocyte-mediated degradation caused changes in tissue behavior and properties in complementary and synergistic ways.

1.9.5 The role of nitric oxide in cytokine-induced, chondrocyte-mediated cartilage damage

In addition to cytokines and other inflammatory mediators, Farrell et al. observed that synovial fluid from rheumatoid arthritic joints and osteoarthritic joints also contained large amounts of nitrite suggesting the up-regulation of nitric oxide production in inflamed synovial joints [167]. In vitro studies have shown that inflammatory cytokines, in particular IL-1, induce abundant production of nitric oxide by chondrocyte cultures and cartilage explants [144]. In vitro studies on chondrocyte or cartilage explant cultures have tested the role of nitric oxide in IL-1 induced catabolic effects using inhibitors such as L-NMA, L-NAME, and L-NIO [168-176]. Inhibition of IL-1 and TNF-alpha induced nitric oxide production was associated with increased proteoglycan synthesis as measured by a decrease in ^{35}S-sulfate incorporation in all species tested (human, rabbit, equine, bovine) [125, 169, 171-173, 175, 176]. In addition to inhibition of synthesis, studies suggest that the inhibition of IL-1-induced nitric oxide may inhibit matrix breakdown [168], have no significant effect on matrix breakdown [20], or enhance matrix breakdown [172, 173]. At a mechanistic level, nitric oxide activates matrix metalloproteinases [133, 168, 177], which may degrade collagen and aggrecan. Activation of MMPs would likely result in increased matrix degradation and not protection. Further research will have to be done to determine how nitric oxide affects collagen breakdown and further evaluate the findings suggesting that it protects against aggrecan degradation.

1.10 Biomarkers of osteoarthritis

Biomarkers in arthritis typically target indicators of inflammation or indicators of matrix degradation. To date, joint space narrowing as determined by radiographic imaging is the only tried-and-true indicator of arthritis and disease progression. Joint space narrowing occurs only after much cartilage degeneration making it reasonably specific; however this metric is likely not sufficiently sensitive to diagnose the disease for early intervention. Thus, better biomarkers are

needed to diagnose, to assess disease activity, to predict disease outcome, and to evaluate new therapeutics [178]. While there are many candidate biomarkers for OA, a method to test the sensitivity and specificity of the marker for OA and disease progression is not yet available. A method to test biomarkers requires the ability to show a dose response relationship – a marker must increase with disease progression and decrease with treatment. Unfortunately, no disease modifying therapy exists for OA, and therefore no control for disease progression exists. With no sensitive biomarker indicating disease progression/regression, candidate disease modifying agents will remain difficult and costly to test. Thus, identification of good biomarkers will benefit from disease modifying therapies, and the development and testing of good disease modifying therapies will require decent biomarkers. The lack of efficacious therapies and decent biomarkers for disease are evidence of how little we understand the disease.

Despite these challenges, new, more sensitive biomarkers for OA are needed and biochemical and imaging biomarkers are being tested. Biochemical biomarker candidates mainly focus on evidence of cartilage turnover and include hyaluronic acid, type II collagen N-propeptide, type II collagen C-propeptide (CTX-II), cross-linked collagen II peptides from the C-telopeptide, collagen III N-terminal propeptide (PIIINP), COMP, osteocalcin, pyridinoline, AgKS (keratan sulfate containing aggrecan fragment), ykl-40 [178]. In a cross sectional study evaluating several biomarkers in patient knee OA, Glc-Gal-PYD and CTX-II correlated well with WOMAC index scores and joint damage respectively [179].

Osteoarthritis is very much defined by its cardinal pathological feature -- cartilage degeneration. Thus, osteoarthritis is then the clinical endpoint of a pathologic process, but it is not the pathological process itself. Therefore defining biomarkers of disease around an endpoint sets the system to fail because the effects of the pathologic process (disease) are visible, but the

cause, which may be the cartilage or aspects of the joint itself, may be no longer present for evaluation. To treat the disease requires understanding of the pathologic process or the ability to ablate the clinical symptoms associated with the outcome. While we have certainly achieved the latter with joint replacement surgeries, we still struggle with the former.

1.11 Thesis Objectives

Cartilage degeneration is driven by the entire synovial joint, but the chondrocyte, by virtue of its position within the tissue, must play a primary role in this degeneration by producing matrix degrading proteases, by altering synthesis of matrix molecules, and by producing inflammatory cytokines and inappropriate levels of morphogenetic or growth factors [180]. To further characterize the mechanisms by which chondrocytes may sense and respond to its surrounding physical and chemical environment, we have chosen to use an in vitro explant model system. While we recognize the limitations of the system, we also believe that an in vitro model is necessary to begin to dissect the potential role of the chondrocyte in cartilage degeneration. In this work, we focused on the role of injurious mechanical compression and inflammatory cytokines, TNF-α and IL-1β, to characterize the cartilage and chondrocyte response at a tissue level. We recognize that such a model cannot recapture the component effects of traumatic joint injury or even RA, where TNF-α and IL-1β are known to play a very key role in the disease process. At the same time, this model may help elucidate the contribution of the chondrocyte to the disease process as well as provide hints of particular cartilage specific biomarkers that may be useful in monitoring cartilage damage in arthritic diseases.

The goal of this thesis is to better understand the contributions of inflammatory cytokine and nitric oxide induced (IL-1β and TNF-α), chondrocyte-mediated matrix degradation and injurious mechanical compression to cartilage damage which may be important in the

pathogenesis of arthritis. To this end, **Chapter 2** will focus on the contribution of IL-1β and TNF-α induced nitric oxide to cartilage matrix degradation and changes in gene expression. **Chapter 3** begins description of the systems-level analysis of proteins released from cartilage treated with IL-1β or TNF-α, mechanical injured, or untreated using an SDS-PAGE-LC/MS/MS approach with the purpose of understanding chondrocyte and matrix response to each of these treatments. **Chapter 4** continues with the goals of Chapter 3, but the purpose is to quantify and to identify real similarities and real differences between the treatments using an iTRAQ-2D-LC/MS/MS approach in order to understand the anabolic and catabolic shifts that are known to occur with treatments. Finally **Chapter 5** concludes with the basic points taken from each of the studies.

1.12 References

1. Klippel, J.H., Crofford, L. J., Stone, J. H., Weyand, C. M. , ed. *Primer on the Rheumatic Diseases*. 12 ed. Vol. 1. 2001, Arthritis Foundation: Altlanta, GA. 700.
2. Kasper, D.L., Braunwald, E., Fauci, A. S., Hauser, S. L., Hauser, D. L., Longo, J. L. J., Issebacher, K. J., ed. *Harrison's Principles of Internal Medicine*. 16 ed. Vol. 1. 2005, McGraw-Hill Companies.
3. Series, E.M., *Prevalence of self-reported arthritis or chronic joint symptoms among adults, 2001*, in *Morbidity and Mortality Weekly reports*. 2002.
4. Moore, K.L., Dalley, A. F. , *Clinically Oriented Anatomy*. 4th ed. 1999, Baltimore, MD: Lippincott Williams & Wilkens.
5. Grodzinsky, A.J., *Electromechanical and physicochemical properties of connective tissue.* Crit Rev Biomed Eng, 1983. **9**(2): p. 133-99.
6. Maroudas, A.I., *Balance between swelling pressure and collagen tension in normal and degenerate cartilage.* Nature, 1976. **260**(5554): p. 808-9.
7. Dudhia, J., *Aggrecan, aging and assembly in articular cartilage.* Cell Mol Life Sci, 2005. **62**(19-20): p. 2241-56.
8. Morgelin, M., et al., *Cartilage proteoglycans. Assembly with hyaluronate and link protein as studied by electron microscopy.* Biochem J, 1988. **253**(1): p. 175-85.
9. Luo, W., et al., *Divergent secretory behavior of the opposite ends of aggrecan.* J Biol Chem, 1996. **271**(28): p. 16447-50.
10. Kiani, C., et al., *Roles of aggrecan domains in biosynthesis, modification by glycosaminoglycans and product secretion.* Biochem J, 2001. **354**(Pt 1): p. 199-207.
11. Paulsson, M., et al., *Extended and globular protein domains in cartilage proteoglycans.* Biochem J, 1987. **245**(3): p. 763-72.
12. Doege, K.J., et al., *Complete coding sequence and deduced primary structure of the human cartilage large aggregating proteoglycan, aggrecan. Human-specific repeats, and additional alternatively spliced forms.* J Biol Chem, 1991. **266**(2): p. 894-902.
13. Antonsson, P., D. Heinegard, and A. Oldberg, *The keratan sulfate-enriched region of bovine cartilage proteoglycan consists of a consecutively repeated hexapeptide motif.* J Biol Chem, 1989. **264**(27): p. 16170-3.
14. Barry, F.P., et al., *Length variation in the keratan sulfate domain of mammalian aggrecan.* Matrix Biol, 1994. **14**(4): p. 323-8.
15. Doege, K., M. Sasaki, and Y. Yamada, *Rat and human cartilage proteoglycan (aggrecan) gene structure.* Biochem Soc Trans, 1990. **18**(2): p. 200-2.
16. Bourdon, M.A., et al., *Identification and synthesis of a recognition signal for the attachment of glycosaminoglycans to proteins.* Proc Natl Acad Sci U S A, 1987. **84**(10): p. 3194-8.
17. Krueger, R.C., Jr., et al., *Chick cartilage chondroitin sulfate proteoglycan core protein. I. Generation and characterization of peptides and specificity for glycosaminoglycan attachment.* J Biol Chem, 1990. **265**(20): p. 12075-87.
18. Domowicz, M.S., et al., *Role of the C-terminal G3 domain in sorting and secretion of aggrecan core protein and ubiquitin-mediated degradation of accumulated mutant precursors.* J Biol Chem, 2000. **275**(45): p. 35098-105.

19. Kisiday, J.D., et al., *Evaluation of medium supplemented with insulin-transferrin-selenium for culture of primary bovine calf chondrocytes in three-dimensional hydrogel scaffolds.* Tissue Eng, 2005. **11**(1-2): p. 141-51.
20. Bird, J.L., et al., *IL-1 beta induces the degradation of equine articular cartilage by a mechanism that is not mediated by nitric oxide.* Biochem Biophys Res Commun, 1997. **238**(1): p. 81-5.
21. Eyre, D., *Collagen of articular cartilage.* Arthritis Res, 2002. **4**(1): p. 30-5.
22. Eyre, D.R., *Collagen: molecular diversity in the body's protein scaffold.* Science, 1980. **207**(4437): p. 1315-22.
23. Voet, D., and Voet, J. G., *Biochemistry*. 2 ed. Vol. 1. 1995, USA: John Wiley and Sons. 1392.
24. Eyre, D.R., et al., *Recent developments in cartilage research: matrix biology of the collagen II/IX/XI heterofibril network.* Biochem Soc Trans, 2002. **30**(Pt 6): p. 893-9.
25. Adams, J.C., *Thrombospondins: multifunctional regulators of cell interactions.* Annu Rev Cell Dev Biol, 2001. **17**: p. 25-51.
26. Dickinson, S.C., et al., *Cleavage of cartilage oligomeric matrix protein (thrombospondin-5) by matrix metalloproteinases and a disintegrin and metalloproteinase with thrombospondin motifs.* Matrix Biol, 2003. **22**(3): p. 267-78.
27. Di Cesare, P.E., et al., *Increased degradation and altered tissue distribution of cartilage oligomeric matrix protein in human rheumatoid and osteoarthritic cartilage.* J Orthop Res, 1996. **14**(6): p. 946-55.
28. Deak, F., et al., *The matrilins: a novel family of oligomeric extracellular matrix proteins.* Matrix Biol, 1999. **18**(1): p. 55-64.
29. Pullig, O., et al., *Matrilin-3 in human articular cartilage: increased expression in osteoarthritis.* Osteoarthritis Cartilage, 2002. **10**(4): p. 253-63.
30. Costell, M., et al., *Perlecan maintains the integrity of cartilage and some basement membranes.* J Cell Biol, 1999. **147**(5): p. 1109-22.
31. Gomes, R.R., Jr., M.C. Farach-Carson, and D.D. Carson, *Perlecan functions in chondrogenesis: insights from in vitro and in vivo models.* Cells Tissues Organs, 2004. **176**(1-3): p. 79-86.
32. Clements, K.M., N. Burton-Wurster, and G. Lust, *The spread of cell death from impact damaged cartilage: lack of evidence for the role of nitric oxide and caspases.* Osteoarthritis Cartilage, 2004. **12**(7): p. 577-85.
33. Forsyth, C.B., J. Pulai, and R.F. Loeser, *Fibronectin fragments and blocking antibodies to alpha2beta1 and alpha5beta1 integrins stimulate mitogen-activated protein kinase signaling and increase collagenase 3 (matrix metalloproteinase 13) production by human articular chondrocytes.* Arthritis Rheum, 2002. **46**(9): p. 2368-76.
34. Pfander, D., et al., *Expression of thrombospondin-1 and its receptor CD36 in human osteoarthritic cartilage.* Ann Rheum Dis, 2000. **59**(6): p. 448-54.
35. Miller, R.R. and C.A. McDevitt, *Thrombospondin 1 binds to the surface of bovine articular chondrocytes by a linear RGD-dependent mechanism.* FEBS Lett, 1995. **363**(3): p. 214-6.
36. Pacifici, M., *Tenascin-C and the development of articular cartilage.* Matrix Biol, 1995. **14**(9): p. 689-98.

37. Chevalier, X., et al., *Influence of interleukin 1 beta on tenascin distribution in human normal and osteoarthritic cartilage: a quantitative immunohistochemical study.* Ann Rheum Dis, 1996. **55**(10): p. 772-5.
38. Hocking, A.M., T. Shinomura, and D.J. McQuillan, *Leucine-rich repeat glycoproteins of the extracellular matrix.* Matrix Biol, 1998. **17**(1): p. 1-19.
39. Comalada, M., et al., *Decorin reverses the repressive effect of autocrine-produced TGF-beta on mouse macrophage activation.* J Immunol, 2003. **170**(9): p. 4450-6.
40. Mansson, B., et al., *Association of chondroadherin with collagen type II.* J Biol Chem, 2001. **276**(35): p. 32883-8.
41. Camper, L., D. Heinegard, and E. Lundgren-Akerlund, *Integrin alpha2beta1 is a receptor for the cartilage matrix protein chondroadherin.* J Cell Biol, 1997. **138**(5): p. 1159-67.
42. Murphy, G., et al., *Matrix metalloproteinases in arthritic disease.* Arthritis Res, 2002. **4 Suppl 3**: p. S39-49.
43. Nagase, H. and M. Kashiwagi, *Aggrecanases and cartilage matrix degradation.* Arthritis Res Ther, 2003. **5**(2): p. 94-103.
44. Cal, S., et al., *Cloning, expression analysis, and structural characterization of seven novel human ADAMTSs, a family of metalloproteinases with disintegrin and thrombospondin-1 domains.* Gene, 2002. **283**(1-2): p. 49-62.
45. Grau, S., et al., *The role of human HtrA1 in arthritic disease.* J Biol Chem, 2006. **281**(10): p. 6124-9.
46. Tsuchiya, A., et al., *Expression of mouse HtrA1 serine protease in normal bone and cartilage and its upregulation in joint cartilage damaged by experimental arthritis.* Bone, 2005. **37**(3): p. 323-36.
47. Knauper, V., et al., *Biochemical characterization of human collagenase-3.* J Biol Chem, 1996. **271**(3): p. 1544-50.
48. Bau, B., et al., *Relative messenger RNA expression profiling of collagenases and aggrecanases in human articular chondrocytes in vivo and in vitro.* Arthritis Rheum, 2002. **46**(10): p. 2648-57.
49. Kevorkian, L., et al., *Expression profiling of metalloproteinases and their inhibitors in cartilage.* Arthritis Rheum, 2004. **50**(1): p. 131-41.
50. Tetlow, L.C., D.J. Adlam, and D.E. Woolley, *Matrix metalloproteinase and proinflammatory cytokine production by chondrocytes of human osteoarthritic cartilage: associations with degenerative changes.* Arthritis Rheum, 2001. **44**(3): p. 585-94.
51. Flannery, C.R., M.W. Lark, and J.D. Sandy, *Identification of a stromelysin cleavage site within the interglobular domain of human aggrecan. Evidence for proteolysis at this site in vivo in human articular cartilage.* J Biol Chem, 1992. **267**(2): p. 1008-14.
52. Ganu, V., et al., *Inhibition of interleukin-1alpha-induced cartilage oligomeric matrix protein degradation in bovine articular cartilage by matrix metalloproteinase inhibitors: potential role for matrix metalloproteinases in the generation of cartilage oligomeric matrix protein fragments in arthritic synovial fluid.* Arthritis Rheum, 1998. **41**(12): p. 2143-51.
53. Chin, J.R., G. Murphy, and Z. Werb, *Stromelysin, a connective tissue-degrading metalloendopeptidase secreted by stimulated rabbit synovial fibroblasts in parallel with collagenase. Biosynthesis, isolation, characterization, and substrates.* J Biol Chem, 1985. **260**(22): p. 12367-76.

54. Lohmander, L.S., et al., *Stromelysin, tissue inhibitor of metalloproteinases and proteoglycan fragments in human knee joint fluid after injury.* J Rheumatol, 1993. **20**(8): p. 1362-8.
55. Sandy, J.D., et al., *Catabolism of aggrecan in cartilage explants. Identification of a major cleavage site within the interglobular domain.* J Biol Chem, 1991. **266**(14): p. 8683-5.
56. Sandy, J.D., A.H. Plaas, and T.J. Koob, *Pathways of aggrecan processing in joint tissues. Implications for disease mechanism and monitoring.* Acta Orthop Scand Suppl, 1995. **266**: p. 26-32.
57. Lark, M.W., et al., *Cell-mediated catabolism of aggrecan. Evidence that cleavage at the "aggrecanase" site (Glu373-Ala374) is a primary event in proteolysis of the interglobular domain.* J Biol Chem, 1995. **270**(6): p. 2550-6.
58. Billington, C.J., I.M. Clark, and T.E. Cawston, *An aggrecan-degrading activity associated with chondrocyte membranes.* Biochem J, 1998. **336 (Pt 1)**: p. 207-12.
59. Arner, E.C., et al., *Cytokine-induced cartilage proteoglycan degradation is mediated by aggrecanase.* Osteoarthritis Cartilage, 1998. **6**(3): p. 214-28.
60. Tortorella, M.D., et al., *Purification and cloning of aggrecanase-1: a member of the ADAMTS family of proteins.* Science, 1999. **284**(5420): p. 1664-6.
61. Abbaszade, I., et al., *Cloning and characterization of ADAMTS11, an aggrecanase from the ADAMTS family.* J Biol Chem, 1999. **274**(33): p. 23443-50.
62. Hurskainen, T.L., et al., *ADAM-TS5, ADAM-TS6, and ADAM-TS7, novel members of a new family of zinc metalloproteases. General features and genomic distribution of the ADAM-TS family.* J Biol Chem, 1999. **274**(36): p. 25555-63.
63. Kuno, K., et al., *ADAMTS-1 cleaves a cartilage proteoglycan, aggrecan.* FEBS Lett, 2000. **478**(3): p. 241-5.
64. Tortorella, M.D., et al., *Characterization of human aggrecanase 2 (ADAM-TS5): substrate specificity studies and comparison with aggrecanase 1 (ADAM-TS4).* Matrix Biol, 2002. **21**(6): p. 499-511.
65. Collins-Racie, L.A., et al., *ADAMTS-8 exhibits aggrecanase activity and is expressed in human articular cartilage.* Matrix Biol, 2004. **23**(4): p. 219-30.
66. Somerville, R.P., et al., *Characterization of ADAMTS-9 and ADAMTS-20 as a distinct ADAMTS subfamily related to Caenorhabditis elegans GON-1.* J Biol Chem, 2003. **278**(11): p. 9503-13.
67. Patwari, P., et al., *Analysis of ADAMTS4 and MT4-MMP indicates that both are involved in aggrecanolysis in interleukin-1-treated bovine cartilage.* Osteoarthritis Cartilage, 2005. **13**(4): p. 269-77.
68. Wang, P., et al., *Proprotein convertase furin interacts with and cleaves pro-ADAMTS4 (Aggrecanase-1) in the trans-Golgi network.* J Biol Chem, 2004. **279**(15): p. 15434-40.
69. Malfait, A.M., et al., *Inhibition of ADAM-TS4 and ADAM-TS5 prevents aggrecan degradation in osteoarthritic cartilage.* J Biol Chem, 2002. **277**(25): p. 22201-8.
70. Flannery, C.R., et al., *Autocatalytic cleavage of ADAMTS-4 (Aggrecanase-1) reveals multiple glycosaminoglycan-binding sites.* J Biol Chem, 2002. **277**(45): p. 42775-80.
71. Pratta, M.A., et al., *Aggrecan protects cartilage collagen from proteolytic cleavage.* J Biol Chem, 2003. **278**(46): p. 45539-45.
72. Stanton, H., et al., *ADAMTS5 is the major aggrecanase in mouse cartilage in vivo and in vitro.* Nature, 2005. **434**(7033): p. 648-52.

73. Glasson, S.S., et al., *Deletion of active ADAMTS5 prevents cartilage degradation in a murine model of osteoarthritis.* Nature, 2005. **434**(7033): p. 644-8.
74. Glasson, S.S., et al., *Characterization of and osteoarthritis susceptibility in ADAMTS-4-knockout mice.* Arthritis Rheum, 2004. **50**(8): p. 2547-58.
75. Ogata, Y., Y. Itoh, and H. Nagase, *Steps involved in activation of the pro-matrix metalloproteinase 9 (progelatinase B)-tissue inhibitor of metalloproteinases-1 complex by 4-aminophenylmercuric acetate and proteinases.* J Biol Chem, 1995. **270**(31): p. 18506-11.
76. Kazes, I., et al., *Platelet release of trimolecular complex components MT1-MMP/TIMP2/MMP2: involvement in MMP2 activation and platelet aggregation.* Blood, 2000. **96**(9): p. 3064-9.
77. Greene, J., et al., *Molecular cloning and characterization of human tissue inhibitor of metalloproteinase 4.* J Biol Chem, 1996. **271**(48): p. 30375-80.
78. Martel-Pelletier, J., et al., *Plasmin, plasminogen activators and inhibitor in human osteoarthritic cartilage.* J Rheumatol, 1991. **18**(12): p. 1863-71.
79. Sadowski, T. and J. Steinmeyer, *Differential effects of nonsteroidal antiinflammatory drugs on the IL-1 altered expression of plasminogen activators and plasminogen activator inhibitor-1 by articular chondrocytes.* Inflamm Res, 2002. **51**(8): p. 427-33.
80. Fischer, D.C., et al., *Induction of alpha1-antitrypsin synthesis in human articular chondrocytes by interleukin-6-type cytokines: evidence for a local acute-phase response in the joint.* Arthritis Rheum, 1999. **42**(9): p. 1936-45.
81. Gray, C.W., et al., *Characterization of human HtrA2, a novel serine protease involved in the mammalian cellular stress response.* Eur J Biochem, 2000. **267**(18): p. 5699-710.
82. Velvart, M. and K. Fehr, *Degradation in vivo of articular cartilage in rheumatoid arthritis and juvenile chronic arthritis by cathepsin G and elastase from polymorphonuclear leukocytes.* Rheumatol Int, 1987. **7**(5): p. 195-202.
83. Trabandt, A., et al., *Cathepsin B in synovial cells at the site of joint destruction in rheumatoid arthritis.* Arthritis Rheum, 1991. **34**(11): p. 1444-51.
84. Aigner, T. and L. McKenna, *Molecular pathology and pathobiology of osteoarthritic cartilage.* Cell Mol Life Sci, 2002. **59**(1): p. 5-18.
85. Tortorella, M.D., et al., *The role of ADAM-TS4 (aggrecanase-1) and ADAM-TS5 (aggrecanase-2) in a model of cartilage degradation.* Osteoarthritis Cartilage, 2001. **9**(6): p. 539-52.
86. Tyler, J.A., *Articular cartilage cultured with catabolin (pig interleukin 1) synthesizes a decreased number of normal proteoglycan molecules.* Biochem J, 1985. **227**(3): p. 869-78.
87. Pettipher, E.R., G.A. Higgs, and B. Henderson, *Interleukin 1 induces leukocyte infiltration and cartilage proteoglycan degradation in the synovial joint.* Proc Natl Acad Sci U S A, 1986. **83**(22): p. 8749-53.
88. Arner, E.C., et al., *In vivo studies on the effects of human recombinant interleukin-1 beta on articular cartilage.* Agents Actions, 1989. **27**(3-4): p. 254-7.
89. Buckwalter, J.A., *Articular cartilage injuries.* Clin Orthop Relat Res, 2002(402): p. 21-37.
90. Gelber, A.C., et al., *Joint injury in young adults and risk for subsequent knee and hip osteoarthritis.* Ann Intern Med, 2000. **133**(5): p. 321-8.

91. Roos, H., et al., *Osteoarthritis of the knee after injury to the anterior cruciate ligament or meniscus: the influence of time and age.* Osteoarthritis Cartilage, 1995. **3**(4): p. 261-7.
92. von Porat, A., E.M. Roos, and H. Roos, *High prevalence of osteoarthritis 14 years after an anterior cruciate ligament tear in male soccer players: a study of radiographic and patient relevant outcomes.* Ann Rheum Dis, 2004. **63**(3): p. 269-73.
93. Roos, E.M., et al., *Knee Injury and Osteoarthritis Outcome Score (KOOS)--development of a self-administered outcome measure.* J Orthop Sports Phys Ther, 1998. **28**(2): p. 88-96.
94. Lohmander, L.S. and H. Roos, *Knee ligament injury, surgery and osteoarthrosis. Truth or consequences?* Acta Orthop Scand, 1994. **65**(6): p. 605-9.
95. Fithian, D.C., et al., *Prospective trial of a treatment algorithm for the management of the anterior cruciate ligament-injured knee.* Am J Sports Med, 2005. **33**(3): p. 335-46.
96. Buckwalter, J.A. and T.D. Brown, *Joint injury, repair, and remodeling: roles in post-traumatic osteoarthritis.* Clin Orthop Relat Res, 2004(423): p. 7-16.
97. Irie, K., E. Uchiyama, and H. Iwaso, *Intraarticular inflammatory cytokines in acute anterior cruciate ligament injured knee.* Knee, 2003. **10**(1): p. 93-6.
98. Cameron, M.L., et al., *Synovial fluid cytokine concentrations as possible prognostic indicators in the ACL-deficient knee.* Knee Surg Sports Traumatol Arthrosc, 1994. **2**(1): p. 38-44.
99. Cameron, M., et al., *The natural history of the anterior cruciate ligament-deficient knee. Changes in synovial fluid cytokine and keratan sulfate concentrations.* Am J Sports Med, 1997. **25**(6): p. 751-4.
100. Lohmander, L.S., et al., *Procollagen II C-propeptide in joint fluid: changes in concentration with age, time after knee injury, and osteoarthritis.* J Rheumatol, 1996. **23**(10): p. 1765-9.
101. Lohmander, L.S., T. Saxne, and D.K. Heinegard, *Release of cartilage oligomeric matrix protein (COMP) into joint fluid after knee injury and in osteoarthritis.* Ann Rheum Dis, 1994. **53**(1): p. 8-13.
102. Tchetverikov, I., et al., *MMP protein and activity levels in synovial fluid from patients with joint injury, inflammatory arthritis, and osteoarthritis.* Ann Rheum Dis, 2005. **64**(5): p. 694-8.
103. Lohmander, L.S., et al., *Changes in joint cartilage aggrecan after knee injury and in osteoarthritis.* Arthritis Rheum, 1999. **42**(3): p. 534-44.
104. Lohmander, L.S., et al., *The release of crosslinked peptides from type II collagen into human synovial fluid is increased soon after joint injury and in osteoarthritis.* Arthritis Rheum, 2003. **48**(11): p. 3130-9.
105. Loening, A.M., et al., *Injurious mechanical compression of bovine articular cartilage induces chondrocyte apoptosis.* Arch Biochem Biophys, 2000. **381**(2): p. 205-12.
106. D'Lima, D.D., et al., *Cartilage injury induces chondrocyte apoptosis.* J Bone Joint Surg Am, 2001. **83-A Suppl 2**(Pt 1): p. 19-21.
107. D'Lima, D.D., et al., *Human chondrocyte apoptosis in response to mechanical injury.* Osteoarthritis Cartilage, 2001. **9**(8): p. 712-9.
108. Lucchinetti, E., et al., *Cartilage viability after repetitive loading: a preliminary report.* Osteoarthritis Cartilage, 2002. **10**(1): p. 71-81.
109. Aigner, T., et al., *Apoptotic cell death is not a widespread phenomenon in normal aging and osteoarthritis human articular knee cartilage: a study of proliferation, programmed*

cell death (apoptosis), and viability of chondrocytes in normal and osteoarthritic human knee cartilage. Arthritis Rheum, 2001. **44**(6): p. 1304-12.
110. Roach, H.I., T. Aigner, and J.B. Kouri, *Chondroptosis: a variant of apoptotic cell death in chondrocytes?* Apoptosis, 2004. **9**(3): p. 265-77.
111. Quinn, T.M., et al., *Matrix and cell injury due to sub-impact loading of adult bovine articular cartilage explants: effects of strain rate and peak stress.* J Orthop Res, 2001. **19**(2): p. 242-9.
112. Schlaak, J.F., et al., *Different cytokine profiles in the synovial fluid of patients with osteoarthritis, rheumatoid arthritis and seronegative spondylarthropathies.* Clin Exp Rheumatol, 1996. **14**(2): p. 155-62.
113. Thibault, M., A.R. Poole, and M.D. Buschmann, *Cyclic compression of cartilage/bone explants in vitro leads to physical weakening, mechanical breakdown of collagen and release of matrix fragments.* J Orthop Res, 2002. **20**(6): p. 1265-73.
114. Brennan, F.M., et al., *Inhibitory effect of TNF alpha antibodies on synovial cell interleukin-1 production in rheumatoid arthritis.* Lancet, 1989. **2**(8657): p. 244-7.
115. Pennica, D., et al., *Human tumour necrosis factor: precursor structure, expression and homology to lymphotoxin.* Nature, 1984. **312**(5996): p. 724-9.
116. Wang, A.M., et al., *Molecular cloning of the complementary DNA for human tumor necrosis factor.* Science, 1985. **228**(4696): p. 149-54.
117. Brennan, F.M., et al., *Cytokine production in culture by cells isolated from the synovial membrane.* J Autoimmun, 1989. **2 Suppl**: p. 177-86.
118. Shinmei, M., et al., *The role of cytokines in chondrocyte mediated cartilage degradation.* J Rheumatol Suppl, 1989. **18**: p. 32-4.
119. Charles, I.G., et al., *Cloning, characterization, and expression of a cDNA encoding an inducible nitric oxide synthase from the human chondrocyte.* Proc Natl Acad Sci U S A, 1993. **90**(23): p. 11419-23.
120. Saklatvala, J., *Tumour necrosis factor alpha stimulates resorption and inhibits synthesis of proteoglycan in cartilage.* Nature, 1986. **322**(6079): p. 547-9.
121. Wilbrink, B., et al., *Role of TNF alpha, in relation to IL-1 and IL-6 in the proteoglycan turnover of human articular cartilage.* Br J Rheumatol, 1991. **30**(4): p. 265-71.
122. Lefebvre, V., C. Peeters-Joris, and G. Vaes, *Production of gelatin-degrading matrix metalloproteinases ('type IV collagenases') and inhibitors by articular chondrocytes during their dedifferentiation by serial subcultures and under stimulation by interleukin-1 and tumor necrosis factor alpha.* Biochim Biophys Acta, 1991. **1094**(1): p. 8-18.
123. Liacini, A., et al., *Induction of matrix metalloproteinase-13 gene expression by TNF-alpha is mediated by MAP kinases, AP-1, and NF-kappaB transcription factors in articular chondrocytes.* Exp Cell Res, 2003. **288**(1): p. 208-17.
124. Dayer, J.M., et al., *Human recombinant interleukin 1 stimulates collagenase and prostaglandin E2 production by human synovial cells.* J Clin Invest, 1986. **77**(2): p. 645-8.
125. Goodstone, N.J. and T.E. Hardingham, *Tumour necrosis factor alpha stimulates nitric oxide production more potently than interleukin-1beta in porcine articular chondrocytes.* Rheumatology (Oxford), 2002. **41**(8): p. 883-91.
126. Gamble, J.R., et al., *Stimulation of the adherence of neutrophils to umbilical vein endothelium by human recombinant tumor necrosis factor.* Proc Natl Acad Sci U S A, 1985. **82**(24): p. 8667-71.

127. Cavender, D., Y. Saegusa, and M. Ziff, *Stimulation of endothelial cell binding of lymphocytes by tumor necrosis factor.* J Immunol, 1987. **139**(6): p. 1855-60.
128. Shlopov, B.V., M.L. Gumanovskaya, and K.A. Hasty, *Autocrine regulation of collagenase 3 (matrix metalloproteinase 13) during osteoarthritis.* Arthritis Rheum, 2000. **43**(1): p. 195-205.
129. Alvaro-Gracia, J.M., et al., *Cytokines in chronic inflammatory arthritis. VI. Analysis of the synovial cells involved in granulocyte-macrophage colony-stimulating factor production and gene expression in rheumatoid arthritis and its regulation by IL-1 and tumor necrosis factor-alpha.* J Immunol, 1991. **146**(10): p. 3365-71.
130. Husby, G. and R.C. Williams, Jr., *Synovial localization of tumor necrosis factor in patients with rheumatoid arthritis.* J Autoimmun, 1988. **1**(4): p. 363-71.
131. Keffer, J., et al., *Transgenic mice expressing human tumour necrosis factor: a predictive genetic model of arthritis.* Embo J, 1991. **10**(13): p. 4025-31.
132. Piguet, P.F., et al., *Evolution of collagen arthritis in mice is arrested by treatment with anti-tumour necrosis factor (TNF) antibody or a recombinant soluble TNF receptor.* Immunology, 1992. **77**(4): p. 510-4.
133. Murrell, G.A., D. Jang, and R.J. Williams, *Nitric oxide activates metalloprotease enzymes in articular cartilage.* Biochem Biophys Res Commun, 1995. **206**(1): p. 15-21.
134. Elliott, M.J., et al., *Randomised double-blind comparison of chimeric monoclonal antibody to tumour necrosis factor alpha (cA2) versus placebo in rheumatoid arthritis.* Lancet, 1994. **344**(8930): p. 1105-10.
135. Elliott, M.J., et al., *Treatment of rheumatoid arthritis with chimeric monoclonal antibodies to tumor necrosis factor alpha.* Arthritis Rheum, 1993. **36**(12): p. 1681-90.
136. den Broeder, A.A., et al., *Long term anti-tumour necrosis factor alpha monotherapy in rheumatoid arthritis: effect on radiological course and prognostic value of markers of cartilage turnover and endothelial activation.* Ann Rheum Dis, 2002. **61**(4): p. 311-8.
137. Rankin, E.C., et al., *The therapeutic effects of an engineered human anti-tumour necrosis factor alpha antibody (CDP571) in rheumatoid arthritis.* Br J Rheumatol, 1995. **34**(4): p. 334-42.
138. Kammermann, J.R., et al., *Tumor necrosis factor-alpha (TNF-alpha) in canine osteoarthritis: Immunolocalization of TNF-alpha, stromelysin and TNF receptors in canine osteoarthritic cartilage.* Osteoarthritis Cartilage, 1996. **4**(1): p. 23-34.
139. Dayer, J.M., *The process of identifying and understanding cytokines: from basic studies to treating rheumatic diseases.* Best Pract Res Clin Rheumatol, 2004. **18**(1): p. 31-45.
140. Dingle, J.T., *Heberden oration 1978. Recent studies on the control of joint damage: the contribution of the Strangeways Research Laboratory.* Ann Rheum Dis, 1979. **38**(3): p. 201-14.
141. Dingle, J.T. and T.T. Dingle, *The site of cartilage matrix degradation.* Biochem J, 1980. **190**(2): p. 431-8.
142. Dingle, J.T., et al., *A cartilage catabolic factor from synovium.* Biochem J, 1979. **184**(1): p. 177-80.
143. Shingu, M., et al., *The effects of cytokines on metalloproteinase inhibitors (TIMP) and collagenase production by human chondrocytes and TIMP production by synovial cells and endothelial cells.* Clin Exp Immunol, 1993. **94**(1): p. 145-9.
144. Stadler, J., et al., *Articular chondrocytes synthesize nitric oxide in response to cytokines and lipopolysaccharide.* J Immunol, 1991. **147**(11): p. 3915-20.

145. Arner, E.C. and M.A. Pratta, *Independent effects of interleukin-1 on proteoglycan breakdown, proteoglycan synthesis, and prostaglandin E2 release from cartilage in organ culture.* Arthritis Rheum, 1989. **32**(3): p. 288-97.
146. van den Berg, W.B., et al., *Animal models of arthritis in NOS2-deficient mice.* Osteoarthritis Cartilage, 1999. **7**(4): p. 413-5.
147. Westacott, C.I., et al., *Tumor necrosis factor alpha can contribute to focal loss of cartilage in osteoarthritis.* Osteoarthritis Cartilage, 2000. **8**(3): p. 213-21.
148. Cohen, S.B. and A. Rubbert, *Bringing the clinical experience with anakinra to the patient.* Rheumatology (Oxford), 2003. **42 Suppl 2**: p. ii36-40.
149. Clements, K.M., et al., *Gene deletion of either interleukin-1beta, interleukin-1beta-converting enzyme, inducible nitric oxide synthase, or stromelysin 1 accelerates the development of knee osteoarthritis in mice after surgical transection of the medial collateral ligament and partial medial meniscectomy.* Arthritis Rheum, 2003. **48**(12): p. 3452-63.
150. Kandel, R.A., et al., *Fetal bovine serum inhibits chondrocyte collagenase production: interleukin 1 reverses this effect.* Biochim Biophys Acta, 1990. **1053**(2-3): p. 130-4.
151. Hutchinson, N.I., et al., *In vivo expression of stromelysin in synovium and cartilage of rabbits injected intraarticularly with interleukin-1 beta.* Arthritis Rheum, 1992. **35**(10): p. 1227-33.
152. Hembry, R.M., et al., *Immunolocalisation studies on six matrix metalloproteinases and their inhibitors, TIMP-1 and TIMP-2, in synovia from patients with osteo- and rheumatoid arthritis.* Ann Rheum Dis, 1995. **54**(1): p. 25-32.
153. Chubinskaya, S., et al., *Chondrocyte matrix metalloproteinase-8: up-regulation of neutrophil collagenase by interleukin-1 beta in human cartilage from knee and ankle joints.* Lab Invest, 1996. **74**(1): p. 232-40.
154. Koshy, P.J., et al., *The modulation of matrix metalloproteinase and ADAM gene expression in human chondrocytes by interleukin-1 and oncostatin M: a time-course study using real-time quantitative reverse transcription-polymerase chain reaction.* Arthritis Rheum, 2002. **46**(4): p. 961-7.
155. Ogata, Y., et al., *Matrix metalloproteinase 9 (92-kDa gelatinase/type IV collagenase) is induced in rabbit articular chondrocytes by cotreatment with interleukin 1 beta and a protein kinase C activator.* Exp Cell Res, 1992. **201**(2): p. 245-9.
156. Saito, S., et al., *Involvement of MMP-1 and MMP-3 in collagen degradation induced by IL-1 in rabbit cartilage explant culture.* Life Sci, 1998. **62**(22): p. PL 359-65.
157. Dozin, B., et al., *Response of young, aged and osteoarthritic human articular chondrocytes to inflammatory cytokines: molecular and cellular aspects.* Matrix Biol, 2002. **21**(5): p. 449-59.
158. Bonassar, L.J., et al., *Inhibition of cartilage degradation and changes in physical properties induced by IL-1beta and retinoic acid using matrix metalloproteinase inhibitors.* Arch Biochem Biophys, 1997. **344**(2): p. 404-12.
159. Sztrolovics, R., et al., *Resistance of small leucine-rich repeat proteoglycans to proteolytic degradation during interleukin-1-stimulated cartilage catabolism.* Biochem J, 1999. **339 (Pt 3)**: p. 571-7.
160. Goldring, M.B., et al., *Interleukin 1 suppresses expression of cartilage-specific types II and IX collagens and increases types I and III collagens in human chondrocytes.* J Clin Invest, 1988. **82**(6): p. 2026-37.

161. Kondo, S., et al., *Cytokine regulation of cartilage-derived retinoic acid-sensitive protein (CD-RAP) in primary articular chondrocytes: suppression by IL-1, bfGF, TGFbeta and stimulation by IGF-1.* J Orthop Res, 2001. **19**(4): p. 712-9.
162. Benton, H.P. and J.A. Tyler, *Inhibition of cartilage proteoglycan synthesis by interleukin I.* Biochem Biophys Res Commun, 1988. **154**(1): p. 421-8.
163. von den Hoff, H., et al., *Interleukin-1 reversibly inhibits the synthesis of biglycan and decorin in intact articular cartilage in culture.* J Rheumatol, 1995. **22**(8): p. 1520-6.
164. Bonassar, L.J., et al., *Activation and inhibition of endogenous matrix metalloproteinases in articular cartilage: effects on composition and biophysical properties.* Arch Biochem Biophys, 1996. **333**(2): p. 359-67.
165. Bonassar, L.J., et al., *Changes in cartilage composition and physical properties due to stromelysin degradation.* Arthritis Rheum, 1995. **38**(2): p. 173-83.
166. Patwari, P., et al., *Proteoglycan degradation after injurious compression of bovine and human articular cartilage in vitro: interaction with exogenous cytokines.* Arthritis Rheum, 2003. **48**(5): p. 1292-301.
167. Farrell, A.J., et al., *Increased concentrations of nitrite in synovial fluid and serum samples suggest increased nitric oxide synthesis in rheumatic diseases.* Ann Rheum Dis, 1992. **51**(11): p. 1219-22.
168. Tamura, T., et al., *Nitric oxide mediates interleukin-1-induced matrix degradation and basic fibroblast growth factor release in cultured rabbit articular chondrocytes: a possible mechanism of pathological neovascularization in arthritis.* Endocrinology, 1996. **137**(9): p. 3729-37.
169. Hauselmann, H.J., et al., *Nitric oxide and proteoglycan biosynthesis by human articular chondrocytes in alginate culture.* FEBS Lett, 1994. **352**(3): p. 361-4.
170. Hauselmann, H.J., et al., *Differences in nitric oxide production by superficial and deep human articular chondrocytes: implications for proteoglycan turnover in inflammatory joint diseases.* J Immunol, 1998. **160**(3): p. 1444-8.
171. Jouzeau, J.Y., et al., *Nitric oxide (NO) and cartilage metabolism: NO effects are modulated by superoxide in response to IL-1.* Biorheology, 2002. **39**(1-2): p. 201-14.
172. Stefanovic-Racic, M., et al., *Nitric oxide and proteoglycan turnover in rabbit articular cartilage.* J Orthop Res, 1997. **15**(3): p. 442-9.
173. Stefanovic-Racic, M., et al., *The role of nitric oxide in proteoglycan turnover by bovine articular cartilage organ cultures.* J Immunol, 1996. **156**(3): p. 1213-20.
174. Stefanovic-Racic, M., et al., *Modulation of chondrocyte proteoglycan synthesis by endogeneously produced nitric oxide.* Inflamm Res, 1995. **44 Suppl 2**: p. S216-7.
175. Hickery, M.S. and M.T. Bayliss, *Interleukin-1 induced nitric oxide inhibits sulphation of glycosaminoglycan chains in human articular chondrocytes.* Biochim Biophys Acta, 1998. **1425**(2): p. 282-90.
176. Taskiran, D., et al., *Nitric oxide mediates suppression of cartilage proteoglycan synthesis by interleukin-1.* Biochem Biophys Res Commun, 1994. **200**(1): p. 142-8.
177. Gu, Z., et al., *S-nitrosylation of matrix metalloproteinases: signaling pathway to neuronal cell death.* Science, 2002. **297**(5584): p. 1186-90.
178. Punzi, L., F. Oliviero, and M. Plebani, *New biochemical insights into the pathogenesis of osteoarthritis and the role of laboratory investigations in clinical assessment.* Crit Rev Clin Lab Sci, 2005. **42**(4): p. 279-309.

179. Garnero, P., et al., *Cross sectional evaluation of biochemical markers of bone, cartilage, and synovial tissue metabolism in patients with knee osteoarthritis: relations with disease activity and joint damage.* Ann Rheum Dis, 2001. **60**(6): p. 619-26.
180. Goldring, M.B., *Cytokines, Growth Factors and Bone-derived factors in cartilage.* 2006.

Chapter 2:

The role of nitric oxide in TNF-α-induced, chondrocyte-mediated extracellular matrix damage compared to IL-1β in bovine cartilage explant cultures

Anna L. Stevens(1), Cameron A. Wheeler(1), Alan J. Grodzinsky(1,2,3), Steven R. Tannenbaum (1,4)

Biological Engineering Division, Massachusetts Institute of Technology, Cambridge, MA, USA (1); Department of Electrical Engineering and Computer Science, Massachusetts Institute of Technology, Cambridge, MA, USA (2); Department of Mechanical Engineering, Massachusetts Institute of Technology, Cambridge, MA, USA (3); Department of Chemistry, Massachusetts Institute of Technology, Cambridge, MA, USA (4).

2.1 Abstract

Objective: Chondrocytes produce large amounts of nitric oxide (NO) when stimulated with pro-inflammatory cytokines, and thus NO may mediate some of the deleterious effects of cytokine treatment. The objective of this study was to determine the role of NO in TNF-α induced chondrocyte mediated extracellular matrix damage compared to IL-1β in bovine cartilage explant cultures

Methods: Cartilage explants were subjected to treatment with TNF-α (100 ng/ml) and with IL-1β (10 ng/ml) and with or without nitric oxide synthase inhibitor, N-methylarginine (L-NMA; 1.25 mM) for 24 hours (RNA) or five days with 10% medium collection and supplementation every 24 hours to monitor NO and sulfated glycosaminoglycan (sGAG) release. After 24 hours, explants were for RNA and real time PCR. The final collected medium was analyzed for sGAG, nitrate and nitrite, MMP activity by zymography, collagen degradation and aggrecan degradation by

immunoblotting of collagen type II and aggrecan G1 and aggrecan-G1-NITEGE respectively.

Results: TNF-α and IL-1β treatment caused a 3- to 5-fold increase sGAG release with an increase in aggrecanase specific aggrecan breakdown, an increase in nitrate and nitrite production, an increase in transcription of protases(MMP3, MMP13, ADAMTS4 and ADAMTS5) and pro-inflammatory enzymes iNOS and COX2, a decrease in ^{35}S-sulfate incorporation as a measure of new sGAG synthesis, and an increase MMP3 and MMP9 secretion. N-methylarginine treatment partially inhibited sGAG release induced by TNF-α treatment with concomitant decrease in the aggrecanase-specific neo-epitope of aggrecan released into the medium. However, the addition of L-NMA with IL-1β or TNF-α treatment had no detectable effect on sGAG biosynthesis, gene expression among the 31 genes tested, MMP secretion or activation, or collagen breakdown.

Conclusion: Inhibiting NO production in response to TNF-α partially suppressed aggrecan proteolysis by the aggrecanases and the concomitant release of sGAG-containing aggrecan fragments to the culture medium. L-NMA had a global effect on protein synthesis as measured by ^{3}H-5-proline where it partially reversed the cytokine induced inhibition. IL-1β-induced matrix degradation was unaffected by the inhibition of NO production by L-NMA; however nitric oxide was protective against sGAG release due to IL-1β and TNF-α in combination.

2.2 Introduction

Nitric oxide (NO) is a neutral free radical with potent biological effects through its actions as a signaling molecule activating cGMP production as well as through various oxidative and nitrosative chemistries that have been shown to modulate gene expression and to alter protein structure and function [1]. While the role of NO in many diseases is well characterized, its role in the pathogenesis of arthritis remains unclear.

In 1991, Stadler et al. first showed that lapine chondrocytes in monolayer produced substantial amounts of NO in response to IL-1β, LPS, or in combination with TNF-α [2]. Shortly after, inducible nitric oxide synthase (iNOS) was cloned from human chondrocytes treated with IL-1, and studies demonstrated that iNOS mRNA expression increased in response to IL-1β, TNF-α, and endotoxin treatment [3-5]. Since these first reports, numerous studies have shown that chondrocyte or explant cultures may produce NO in response to IL-1β, IL-1α, and TNF-α in most species tested [6-11]. Other pro-inflammatory factors such as IL-17, IL-18, ICE, and fibronectin fragments may increase NO production in chondrocytes [12-15].

With the identification of NO production by iNOS, a number of in vitro studies have used NOS inhibitors, L-NMA (L-N-methyl-arginine), L-NAME, aminoguanidine, and L-NIO (N-iminoethyl-L-ornithine) to evaluate the role of nitric oxide in IL-1β-induced changes in chondrocyte metabolism and matrix degradation in explant, hydrogel, and monolayer culture. With the exception of the bovine explant studies [7], inhibition of NOS partially reversed IL-1-induced inhibition of proteoglycan synthesis in rabbit, human, and rat cartilage explants or chondrocyte cultures [16-20]. TNF-α has been shown to decrease proteoglycan synthesis in a NO-dependent manner as well [10]. The

exogenous NO donor, SNAP (100 uM), also decreased proteoglycan synthesis [16, 17]. IL-1-stimulated NO production as well as exogenous NO donors decreased collagen synthesis in an mRNA independent fashion indicating that NO may post-transcriptionally regulate collagen production possibly through its actions on prolyl-hydroxylase, which is consistent with findings that protein disulfide isomerases may be susceptible to regulation via S-nitrosation [21, 22] .

Studies on matrix degradation have focused on the role of NO on IL-1β–mediated degradation and have suggested that NO may alter matrix degradation. Inhibition of NO production induced by IL-1β treatment enhances [7, 8, 23] or has no effect [24] on aggrecan degradation as measured by sGAG release. While studies have not yet explored the role of NO in collagen or other matrix damage, they suggest that NO produced in response to IL-1 does not induce proteoglycan degradation.

Studies focusing on mechanisms of matrix degradation indicate that IL-1 induced NO may enhance matrix metalloproteinase activity or expression in cartilage. Despite differences in methods, most findings supporta role for NO (exogenous or endogenous by IL-1 activation) in altering gelatinase (MMP-2 and MMP-9) [2, 25, 26] and stromelysin (MMP-3) [7, 25] expression or activity. Inhibition of NOS decreased IL-1β induced gelatinase activity and expression [2, 25]. Stadler et al. further showed that treating chondrocytes with a combination of either IL-1β and LPS or IL-1β and TNF-α and inhibiting NOS by L-NMA actually increased gelatinase activity [2]. Studies of stromelysin activity are less clear. Murrell et al. showed that inhibiting NOS decreased LPS induced MMP-3 activity with an insignificant decrease seen with IL-1β treatment. Similarly, treatment with SNAP was also able to stimulate MMP-3 activity, and the

effects were shown to be dependent on new protein synthesis [25]. Stefanovic-Racic, et al. showed that inhibiting NO production in response to IL-1 caused an increase in stromelysin activity [7]. These findings indicate that nitric oxide alone or in response to IL-1β treatment may enhance gelatinase activity while having a less straight-forward effect on MMP-3 activity.

Following the discovery of NO production by chondrocytes in response to inflammatory stimuli, Farrell et al. showed that the NO end-product, nitrite, was elevated in the synovial fluid of rheumatoid and to a lesser extent in osteoarthritic joints [27]. Since this discovery, animal models of inflammatory arthritis and osteoarthritis have been employed to test the role of NO in disease development and progression. Studies using rodent arthritis models have generally shown that prophylactic inhibition of NOS with a non-specific NOS inhibitor may lead to partial or full protection against the disease development with less promising results reported with more selective inhibitors [28-34]. At the same time, studies using NOS2-/- mice in inflammatory arthritis models generally show a decrease in tissue damage compared to the wild-type controls [35-37]. Further, Kato et al. also saw a decrease in nitrotyrosine, a decrease in apoptosis via TUNEL, a decrease in MMP-3 and MMP-9, and a decrease in serum IL-1β and NO derivatives in iNOS deficient animals.

In a canine osteoarthritis model (ACL resection/joint instability), the effects of nitric oxide inhibition by selective iNOS inhibitor, L-NIL, has shown promising effects, reducing cartilage damage, reducing MMP-1 and MMP-3 expression, reducing IL-18 and ICE production, and reducing apoptosis [14, 38-40]. NOS2-/- mouse models have shown both an increase and decrease in OA development with joint instability [37, 41]; however

NOS2-/- models are physiologically distinct from those treated with iNOS inhibitors, in which nitric oxide production decreases to baseline while NOS2-/- animals have no baseline iNOS activity. Additional complexity may exist as few NOS inhibitors are completely specific to one form or the other of the enzyme. Despite these caveats, these results suggest that nitric oxide may play a deleterious role in the development of osteoarthritis.

In addition to nitric oxide and IL-1, TNF-α also plays an important role in rheumatoid arthritis and likely in osteoarthritis as well. TNF-α was identified in synovial exudates of rheumatoid and osteoarthritic joints [42, 43]. In RA patients, TNF-α may contribute to IL-1 production as determined by anti-TNF therapy [44]. Hukkanen et al. found a correlation between nitric oxide production and the development and progression of polyarthritis in a transgenic TNF-α mouse model [45]. While TNF-α may play a greater role in inflammation than in tissue damage, *in vitro* evidence suggests that TNF-α alone or in combination with IL-1 may cause cartilage breakdown and a decrease in new matrix synthesis by chondrocytes [46].

TNF-α may play a role in the pathogenesis of osteoarthritis. Brennan et al. showed that spontaneous IL-1 production in OA synovial cells was low even though TNF-α was high suggesting a role for TNF-α in driving disease progression [44]. Shinmei et al. showed that OA chondrocytes had a larger population of IL-1, TNF-α, IL-6 and MMP3 positive chondrocytes compared to chondrocytes from healthy joints [47, 48]. At the same time, OA cartilage explants are more susceptible to IL-1 and TNF-α treatment [49-51]. Increased susceptibility to TNF-α may in part be the result of increased TNF-α receptor expression, as Webb et al. showed that there is a strong

correlation between TNF-R p55 (but not p75) expression and sGAG loss in cartilage [52]. In addition, synovial fluid from OA joints increased TNF-R p55 (and p75) receptor expression, which was partially blocked with IL-1 and IL-6 neutralizing antibodies [53]. TNF-α may be present in synovial fluid and serum from OA patients as well as being expressed in chondrocytes in OA tissue [54, 55]. Finally, using a high-through-put screening method, TNF-R1A was identified as a gene whose up regulation contributed to induction of a set of OA markers [56]. These data together suggests that TNF-α may play a role in cartilage breakdown in osteoarthritis and this breakdown may be modulated by the expression of iNOS via its production of nitric oxide.

IL-1 and TNF-α are known to induce chondrocyte mediated sulfated glycosaminoglycan release via cleavage of aggrecan. While a number of enzymes are known to cleave aggrecan, two classes of proteases, the matrix metalloproteases (MMPs) and the ADAMTSs (a disintegrin and metalloproteinase with a thrombospondin motif) have been well studied for their ability to cleave aggrecan. Using antibodies to the neoepitopes generated with protease-specific proteolysis of aggrecan, studies suggest that IL-1 and TNF-α induce "aggrecanase," not MMPs mediated cleavage of aggrecan [57, 58]. After much research the "aggrecanases", ADAMTS4 and ADAMTS5, were cloned from cartilage and shown to have a high affinity and activity against aggrecan with the ability to cleave at the "aggrecanase" site in aggrecan interglobular domain and be present in human arthritic joints [59-64].

The purpose of this study was to determine whether and by what mechanism nitric oxide plays a role in matrix loss in response to TNF-α and to compare this degradation to that found with IL-1β using NOS inhibitor, N-methylarginine (L-NMA).

Matrix degradation was measured by sGAG release, by collagen fragment release, and ^{35}S-sulfate incorporation on day 6 was used to monitor the effects on new sGAG synthesis. Mechanisms of proteoglycan degradation and matrix breakdown were probed by blotting for aggrecan fragments and by zymography for MMP activity. To test more globally the effects of nitric oxide in modulating cytokine-induced up-regulation of pro-catabolic genes, real time PCR on a battery of 32 genes were performed to look at the effects of L-NMA on cytokine induced changes in gene expression. These results suggest that NOS inhibitor, L-NMA, plays a role in decreasing TNF-α but not IL-1β induced aggrecanase-mediated aggrecan degradation. No differences were seen in metalloproteinase activity, gene expression by real time PCR, sGAG biosynthesis, or collagen fragments with L-NMA treatment. This suggests that the role of NO may be limited to modulation of aggrecan degradation at early time points in this model.

2.3 METHODS

Reagents. Insulin, transferrin and selenium medium supplement (ITS) and NOS inhibitor, N-methyl-arginine, were purchased from Sigma (St Louis, MI). Recombinant human IL-1β and TNF–α were purchased from R&D systems (Minneapolis, MN), Polyacrylamide gels and loading buffers were purchased from BioRad (Hercules, CA). Protease-free chondroitinase and keratanase II were purchased from Seikagaku (Japan). Common chemicals were purchased from ICN, Mallenkrodt, or Sigma.

Cartilage explant harvest and pre-experiment culture and weighing: Articular cartilage disks were obtained from the patello-femoral groove of 1-2 week old calves as described previously [65]. Cartilage cylinders (9 mm diameter) were cored from the patello-femoral groove, perpendicular to the joint surface. The cylinders were then cut

into two 1 mm thick disks using a microtome to insure similar geometry. A 6 mm diameter dermal punch was used to core out the center of each of the 9mm slice generating a 6 mm diameter by 1 mm thick cartilage disk. Each disk was placed into 1 well of a 12 well plate containing 2.5 ml of high glucose DMEM containing 1% ITS as described previously [66]. The medium was changed every two days during the seven-day resting period prior to experimentation with explant weights were taken on day 5.

TNF–α, IL-1β, and L-NMA treatments. Cytokines were resuspended in 0.1% BSA at a concentration of 10 ug/ml for TNF–α or 2.5 ug/ml for IL-1β. On day seven of culture, explants were treated with 10 ng/ml of IL-1β or 100 ng/ml of TNF–α or untreated in 2 ml of medium without 1% ITS for five days. Two hours after cytokine treatment, samples were treated with 1.25 mM L-NMA. Explants for real time PCR analysis were cultured for 24 hours after the addition of L-NMA and snap frozen in liquid nitrogen. For all other experiments, cartilage explant cultures were subjected to a 10% medium change every 24 hours-- 200 ul of medium was removed and 200 ul of fresh medium with one-half ascorbate was supplemented-- for an overall 40% medium change over the five day culture period (0.6 ml medium/explant/day). On day 5, medium and explants were collected, pooled to each treatment group, and stored at -80C.

Radiolabel incorporation as a measure of biosynthesis. For a subset of explant experiments, five-day conditioned culture medium was removed and replaced with fresh ITS containing medium supplemented with 10 microCi 5-^{3}H-Proline and 5 microCi disodium ^{35}S-sulfate for 24 hours to measure biosynthesis. Following 24 hour radiolabel treatment, explants were washed four times for 20 minutes in PBS containing 1mM proline and 1 mM disodium sulfate to remove unincorporated radiolabel. The explants

were then digested overnight in 0.2 mg/ml proteinase K at 60C. A portion of the digest was subjected to liquid scintillation counting to measure radioactive decay.

Sulfated Glycosaminoglycan (sGAG) Assay. Sulfated glycosaminoglycans were measured as an indicator of aggrecan release. sGAG in the medium was measured by dimethylmethylene blue (DMMB) assay using shark chondroitin C as a standard as described previously [67].

Nitrate/Nitrite Analysis. Medium samples were diluted 1:2 in water prior to nitrate nitrite analysis by Greiss assay [68]. Total nitrogen oxides were determined by cadmium column reduction of nitrate to nitrite followed by direct nitrite detection by Greiss reaction. Nitrite was assayed directly, and nitrate was calculated as the difference between the total nitrogen oxides and the nitrite.

Gelatin and Casein Zymography for MMPs. Zymograms were performed as described[69]. Briefly, conditioned medium from day 5 was mixed with 4X non-reducing SDS-sample buffer and electrophoresed in a 10%/12% gelatin or casein zymogram gels. Gels were renatured in 2.5% triton X-100 solution, and placed in solution of 50 mM Tris and 5mM $CaCl_2$ for 18 hours at 37C. Gels were then fixed and stained with Coomassie brilliant blue and destained until bands became visible and distinct. Gels were immediately scanned. EDTA was added to the incubation buffer to verify MMP activity. MMP-3 and MMP-9 were verified by western blotting.

Ethanol Precipitation and deglycosylation for aggrecan western blot analysis. The medium equivalent of 10 or 20 ug sGAG was precipitated by the addition of 3 volumes of ice-cold ethanol. The samples were resuspended (50 mM Tris-Acetate, 10mM EDTA) and sequentially deglycosylated beginning with 5 mU of protease-free chondroitinase

ABC for three hours followed by 0.1 mU of keratanase II and 0.1 mU of endo-β-galactosidase for an additional four hours.

Dialysis and Deglycosylation for western blot analysis. Chondroitinase ABC (80 mU) was added to 2.0 ml of pooled sample medium from each explant experiment was dialyzed and deglycosylated in a 7.5 kDa cutoff dialysis cassette (Pierce, city) overnight at 37C against 10 mM Tris-acetate, 10 mM NaCl, 10 mM sodium acetate, and 5 mM EDTA followed by dialysis against pure water at 4C for 12 hours. The sample was frozen and concentrated to 10X. For aggrecan westerns, the appropriate amount of sample was taken to achieve 10 or 20 ug sGAG for each sample and further deglycosylated as described above. For the MMP and collagen western blots, equal volumes of sample were loaded.

Western blot analysis Concentrated samples (10-15 ul) were run out on denaturing SDS-PAGE on a 4-15% gradient gel run at 15 mA for 2 hours. Proteins were then transferred to Immobilon (PVDF) membrane, and proteins were detected using monoclonal antibody to type II collagen (NeoMarkers, Lab vision), monoclonal antibody to the Aggrecan-G1-NITEGE-COOH fragment of aggrecan (C. Flannery, Wyeth Pharmaceuticals), and a polyclonal antibody to the G1 domain of aggrecan (J. Sandy).

RNA extraction and real time PCR. Two to three cartilage explants per condition (untreated, L-NMA, TNF-α, TNF-α and L-NMA, IL-1β, and IL-1β and L-NMA) per joint from a total of 8 joints (from 8 different animals) were pulverized under liquid nitrogen and homogenized in Trizol (Invitrogen, San Diego,CA). Homogenates were transferred to Phase Gel tubes according to the manufacturer's instructions (Eppendorf, Hamburg, Germany) and spun at 10,000rpm for 10 minutes at 4° C. The clear RNA

containing supernatant was removed from Phase Gel tubes and subjected to RNAeasy mini-kit clean-up (Qiagen, Chatsworth, CA) according to manufacturer's instructions. RNA quantification was determined by nano-drop method measuring absorbance at 280 nm and 260 nm. Equal amounts of RNA were subjected to reverse transcription using AmpliTaq-Gold reverse transcription kit (ABI, Foster City, CA) to generate cDNA for real time PCR analysis. Real time PCR analysis was performed using Applied Biosystems SYBR-Green master mix in combination with cDNA and primers. An ABI prism 7900HT real time PCR machine, equipped with 384 well loading plate, was used for analysis. Both forward and reverse primers were designed using Primer3 software based on the bovine genomic sequence. Primers from 32 cartilage relevant genes were measured: 18S-RNA, aggrecan, collagen II, fibromodulin, fibronectin, proteoglycan link protein, MMP1, MMP3, MMP9, MMP13, ADAMTS4, ADAMTS5, TIMP1, TIMP2, TIMP3, COX2, iNOS, G3PDH, β-actin, IGF-1, IGF2, TGF-β, TNF-α, IL-1β, IL-4, IL-6, TXNIP, HSP90, CD44, HAS2, bFGF, and OP-1. Standard curves analysis was performed on each of the primers to determine the efficiency of amplification and proper primer concentration. The measured cycle threashold (CT) was determined and converted to relative copy number using information from standard curves for comparisons.

Data analysis and statistics: Real time PCR data from each sample were normalized to the 18S-RNA and then the data were secondarily normalized to the untreated (control) sample within each sample set (animal). The normalized data was compared as the mean +/- SEM of each condition. Principle component analysis and k-means clustering analysis was performed on the real time PCR data using components of the Matlab

Statistics toolbox. The Kruskal-Wallis test and Wilcoxon sign-rank test with Bonferroni correction for multiple comparisons were used to determine statistical significance of the L-NMA effect and pairwise comparisons between treatments respectively. For the remaining quantitative assays-- sGAG, biosynthesis by radiolabel incorporation, and nitrate/nitrite assays -- multi-way ANOVA followed by a post-hoc Student's t-test with Bonferroni correction for multiple comparisons were used to determine statistical significance defined as $p<0.05$. All statistical analyses were performed using Systat 11, Richmond CA.

2.4 RESULTS

Explant Cultures: Cartilage explants were allowed to rest one week before beginning cytokine treatment and then treated with 100 ng/ml TNF–α, 10 ng/ml IL-1β, a combination of TNF-α (50 ng/ml) and IL-1β (10 ng/ml), or left untreated in 2 ml of DMEM. After 2 hours, one-half of each treatment group was further treated with 100X L-NMA for a final concentration of 1.25 mM L-NMA. Every 24 hours, the cultures underwent a 10% (200 ul) medium removal and supplementation, and the collected medium was frozen for sGAG and nitrate/nitrite determination. Over the course of the five-day experiment, there was no observable difference between the cytokine-treated and control samples. TNF–α +/- L-NMA and IL-1β +/- L-NMA treatments were performed as separate experiments. The results represent data collected from between 3 and 8 different animals with at least two explants per joint per condition. Because no statistical difference was noted between the untreated or L-NMA only groups in each experiment, the data were combined to simplify presentation.

Nitrate/Nitrite: Nitrate and nitrite are NO end products produced from NO interacting with superoxide or oxygen respectively. Nitrite and total nitrate and nitrite were determined by Greiss assay with nitrate reduction to nitrite performed by flowing samples through a cadmium column prior to Greiss reaction [68]. Nitrate was calculated as the difference between the total NO end products and the nitrite. The graph in **Figure 1** shows the accumulated total nitric oxide end products generated during the five-day treatment period, which includes both nitrate and nitrite. IL-1β and TNF–α similarly increased total nitric oxide end product production compared to the untreated control ($p < 0.001$), and the amounts were similar between the two cytokine treatments by day five. Treatment of samples with L-NMA inhibited NO production to at or near control levels.

^{35}S-sulfate and ^{3}H proline incorporation. Radiolabeled sulfate and proline incorporation were performed to measure protein and sulfate sGAG synthesis. To test the effects of L-NMA on new sGAG biosynthesis we subjected explants to ^{35}S-sulfate incorporation while ^{3}H-proline was used to measure protein synthesis. **Figure 2** shows the biosynthesis data based on the 24-hour radiolabel incorporation following the five-day treatment. sGAG biosynthesis was significantly decreased by TNF-α, IL-1β, and IL-1β and TNF-α treatment; however no significant effect was seen with L-NMA. Proline incorporation, as a measure of protein synthesis, was decreased only by the IL-1β and TNF-α combination treatment. L-NMA partially reversed the decrease in proline incorporation seen with cytokine treatment ($p = 0.05$).

Sulfated glycosaminoglycan release: sGAG release to the medium measured by DMMB assay was used as a sensitive indicator of sGAG loss which is predominantly the result of aggrecan degradation in cartilage explant studies. Both cytokines, TNF–α, IL-

1β, and the TNF-α and IL-1β combination caused a substantial (3-7 fold) and significant increase in sGAG release to the medium (**Figure 3**; $p<0.001$ for all three cytokine treatments compared to control at all time points). Treatment with L-NMA partially inhibited TNF–α induced sGAG release ($p<0.003$; all time points), but L-NMA significantly increased the rate of sGAG release with IL-1β and TNF-α in combination compared to the cytokine combination without L-NMA ($p<0.05$ for days 1-4; not significant on day 5). However with the exception of the 24-hour time point in which L-NMA partially inhibited sGAG release, L-NMA had no effect on IL-1β-induced sGAG release ($p = 0.015$ first 24 hours; $p>0.745$ for all other points). No L-NMA effect was seen in the untreated group. These results suggest that NO is partially responsible for sGAG release in response to TNF–α treatment, partially protective in response to TNF-α and IL-1β in combination, and has little or no effect on IL-1β treatment alone.

Western blotting analysis for Aggrecan G1 domain and aggrecanase generated neo-epitope. We then investigated whether L-NMA was able to decrease sGAG release by decreasing aggrecanase cleavage of aggrecan. Western blotting was performed on medium containing equal amounts of sGAG to probe for both the aggrecan first globular domain (aggrecan G-1) and the aggrecan-G1 neoepitope (G1-NITEGE-COOH) generated from aggrecanase hydrolysis of the 373E-374G bond. The aggrecan-G1 was detected at 200-300kDa suggestive of full length aggrecan and within the region of ~50-80 kDa which may correspond to aggrecan-G1 fragments generated from aggrecanase cleavage (ADAMTS-4 and ADAMTS-5) (not shown). To probe specifically for aggrecanase cleavage, an immunoblot to the aggrecan-G1-NITEGE-COOH was performed and shown in **Figure 4**. The aggrecan-G1-NITEGE-COOH immunoblot shows that IL-1β and

TNF–α, at the concentrations used in this study, caused the appearance of 60-80 kDa doublet bands. While the addition of L-NMA to IL-1β treatment had no effect on anti-aggrecan-G1-NITEGE-COOH stained doublet, the sample treated with TNF–α and L-NMA showed marked decrease in both bands compared to the sample treated with TNF-α alone. This decrease in anti-aggrecan-G1-NITEGE-COOH neoepitope bands strongly indicates that the decrease in sGAG release seen with the addition of L-NMA to TNF–α treatment is the result of decreased aggrecanase proteolysis of aggrecan. NO is partially responsible for TNF–α-induced sGAG release by increasing aggrecanase cleavage of aggrecan. However, it remains unclear whether this is a result of decreased ADAM-TS4 or ADAM-TS5 expression or activity.

Real time PCR analysis. To determined whether L-NMA may be altering transcription of aggrecanases and/or other proteases or matrix molecules, real time PCR analysis of a 32-gene set was performed on explants from 8 different animals subjected to 26 hours of IL-1β or TNF-α treatment with or without L-NMA. The relative copy numbers were normalized to 18S-RNA and expressed in terms of the fold increase or decrease over the untreated, control sample within each set. **Figure 5A** is a representation of the 31 genes plotted in principal component space. The data represented in the first three principle components account for approximately 95% of the variance in the data. K-means clustering analysis indicated that the genes segregate well into two spacially distinct populations indicated by the red triangles and blue squares. The centroid profiles for each group are represented in **Figure 5B** as the mean+/-SEM of each centroid. The first population of genes comprises those that have little response or are slightly down regulated by IL-1β and TNF-α treatment (Group 1). The second population of genes

contains those that are strongly up regulated by IL-1β and TNF-α treatment (Group 2). **Figure 5C** is a list of proteins from Group 1 and Group 2 described as average-fold-change relative the untreated sample (control) +/- SEM with asterisks representing statistical significance compared to the untreated sample at $p<0.05$. While addition of L-NMA often slightly decreased gene transcription compared to IL-1β or TNF-α alone, this decrease was not statistically significant. However, a trend toward significance ($p\sim0.1$) was seen in the effects of L-NMA on IL-1β induced increase of MMP-3 and TIMP-2 synthesis and on TNF-α induced increase of HSP90 expression.

Zymography for Metalloproteinase Measurements: To determine whether inhibition of NO production changed protease release to the medium in response to cytokine treatment, zymography was performed to look at the expression and activation of MMPs on day- five collected medium. Specifically, gelatin zymography was used to identify changes in gelatinases, MMP-2 and MMP-9 (**Figure 6a**), while casein zymography was used to monitor MMP-3 activity in medium samples (**Figure 6b**). To verify that the bands were from MMP activity, negative controls containing EDTA were performed and shown to be devoid of all bands (not shown).

Gelatin zymography, (**Figure 6a**) demonstrates two bands running between 75kDa and 50kDa (closed arrows), which represent the pro- and the active forms of MMP-2. No qualitative differences were observed in the MMP-2 bands between treatment groups. In addition to the MMP-2 bands, the upper band, ~90kDa (open arrow), is indicative of pro-MMP-9 activity and is present only in the cytokine treated samples. Results of the gelatin zymography indicate that L-NMA has no observable

effect on either MMP-2 or MMP-9 activation or release to the medium. MMP-9 expression was verified by western blotting and mass spectrometry (data not shown).

To evaluate MMP-3 secretion and activation in response to NOS inhibition and cytokine treatment, a casein zymogram was performed on medium samples. **Figure 6b** is a representative casein zymogram on medium samples from each of the treatment groups. Samples subjected to IL-1β treatment show a prominent, but diffuse clearing (containing a doublet—with the lower band most prominent) between 50 kDa and 75 kDa, representing secreted pro-MMP-3 activity while TNF-α treatment showed only a slight doublet band and the control medium contained no observable band. No activated MMP-3 band (at 45kDa) was visible in any of the samples at the medium amounts used. L-NMA had no observable effect on pro-MMP-3 release into the medium. The results of the zymogram were verified by Western blot analysis to show no difference in MMP-3 release to the medium in the IL-1β treated sample compared to the IL-1β and L-NMA sample (not shown).

2.5 DISCUSSION

Inflammatory cytokines, IL-1β and to a lesser extent, TNF–α, are capable of inducing chondrocyte-mediated extracellular matrix degradation. In vivo observations indicate that aggrecan degradation occurs first while collagen degradation occurs later [70]. While the role of NO in IL-1β-induced matrix damage has been explored, less is known about the role of NO in TNF–α induced matrix degradation. The purpose of this study was to use an explant *in vitro* model to explore how NO modulates cartilage matrix loss in response to both TNF–α and IL-1β. In this study, we found that treatment with

the NOS inhibitor, L-NMA, was able to partially inhibit TNF–α induced sGAG release, and this inhibition resulted from a decrease in cleavage of aggrecan by aggrecanase. Beyond its effect on TNF–α induced sGAG release to medium, iNOS inhibition by L-NMA was not shown to modulate biosynthesis, mRNA transcription of select genes (including matrix proteins, cytokines and growth factors, and proteases), MMP secretion, or collagen fragment release with cytokine treatment.

Differences in NO chemistry may dictate how NO modulates responses to IL-1β and TNF-α treatment. NO may combine with oxygen to form nitrous anhydride, a nitrosating agent, which may react with amine- or thiol-containing biomolecules or may react with water to form nitrite. Alternatively, NO may combine with superoxide radical to form peroxynitrite, a strong nitrosating agent that, when combined with carbon dioxide will form nitrosoperoxicarbonate, may release nitrogen dioxide and carbonate radical, oxidizing agents that cause lipid and protein oxidation, or may recombine to form nitrate and bicarbonate. **Figure 1** indicates that there is little difference in accumulated NO end products between TNF–α and IL-1β treatments, nitrate and nitrite each correspond to half of the nitric oxide production (not shown), suggesting similarity in the chemistry among these samples; however NO production occurred earlier in response to TNF-α treatment than to IL-1β (data not shown). It is possible that differences in rates of NO production at an earlier time point rather than the total amount produced may have played a role in the deleterious effects of NO.

Previous studies have explored the role of NO in IL-1β induced aggrecan degradation and sGAG release; however this is the first study to test the effect of NO on TNF-α induced sGAG release and its mechanism. Studies by Stefanovic-Racic et al., in

bovine, human, and rabbit explants, showed that treatment with L-NMA in the presence of IL-1β caused a significant increase in sGAG release compared to IL-1β alone[7, 8]. Using an equine explant model, Bird et al., showed that IL-1β in combination with L-NIO, had no effect on sGAG release compared to IL-1 alone [24], but in a more recent study, Bird et al. showed that both endogenous and exogenous NO had a protective effect against sGAG release via inhibiting aggrecanase cleavage of aggrecan [23]. Similar to the first study [23], we also found that IL-1β in combination with L-NMA was not different than treatment with IL-1β alone in mediating sGAG release. We did, however, observe some inter and intra-experiment variation in response to IL-1β alone and IL-1β with L-NMA by the explants. Results of experiments with the IL-1β and TNF–α combination and L-NMA suggest that the cytokine combination in the presence of L-NMA caused a significant increase in sGAG release compared to the cytokine combination alone **Figure 3**. The protective effect of NO seen with the combination of IL-1β and TNF-α was similar to that shown previously [7, 8, 24]. These results may point to an additional factor or concentration required for the protective effects of NO. Inhibiting NO production with L-NMA did inhibit TNF-α-induced sGAG loss to the medium by nearly half. The effects of NOS inhibition on sGAG release appear to be situational: In all cases, NO has either no effect or a protective effect in the presence of IL-1β; however NO enhances matrix degradation in response to TNF-α treatment.

Inhibition of TNF-α-inducedsGAG loss to the medium by L-NMA may be the result of a decrease in new proteoglycan synthesis, or it may be due to a decrease in expression or activity of an aggrecan cleaving protease. To test whether L-NMA altered cartilage biosynthesis in response to IL-1β or TNF-α treatment, explants were subjected

to 24 hour radiolabeling with ^{35}S-sulfate to measure new sGAG synthesis following the end of the five day cytokine treatment. **Figure 2** shows both sulfate incorporation as a measure of sGAG synthesis and proline incorporation as a measure of new protein synthesis for each condition. Explants, subjected to cytokine treatment alone or in combination, showed a decrease in new sGAG synthesis, however L-NMA alone or in combination with the cytokine treatment had no statistically significant effect on sGAG synthesis. Our findings are consistent with a study by Stefanovic-Racic et al. using bovine explants, but differ from studies using other animal models [7, 8, 10, 16-18]. L-NMA did cause a statistically significant effect on protein synthesis measured by ^{3}H-proline ($p = 0.05$), partially reversing cytokine-induced inhibition, which is consistent with previous findings [21]. The effects of the L-NMA on day 6 after cytokine treatment may vary from those seen early in response to cytokine treatment. However, because L-NMA has little effect on biosynthesis, we can conclude that decrease in sGAG loss was not due to a decrease in synthesis.

Because aggrecanases are known to mediate aggrecan degradation in response to cytokines, we further hypothesized that the mechanism of L-NMA inhibition of TNF–α-induced sGAG release was likely through a decrease in aggrecanase cleavage of aggrecan. The ADAMTS family is a metalloproteinase family of which ADAMTS1, 4, 5, 8, 9, 15 have all been shown to cleave aggrecan with ADAMTS4 and ADAMTS5 able to cleave the interglobular domain (IGD) of aggrecan at the 341-E-A-342 bond, known as the aggrecanase cleavage site [59, 63, 71]. While other proteases including the MMP family have been shown to cleave aggrecan in the IGD, only ADAMTS4 and ADAMTS5 are known to cleave after the glutamine-341 of aggrecan making it a specific epitope

associated with "aggrecanase" activity [57, 72]. Since the discovery of the aggrecanase cleavage site by Sandy et al., aggrecan degradation in response to inflammatory cytokine treatment has been attributed to aggrecanase and not to MMP activity [57, 58].

Thus, to test whether aggrecanase activity is responsible for differences in sGAG release seen with TNF-α and NOS inhibitor treatment, we used an antibody, which recognizes the aggrecanase-specific neo-epitope generated on the first globular domain of aggrecan, aggrecan-G1-NITEGE-COOH. The immunoblot to the aggrecanase generated neo-epitope resulted in the appearance of a doublet band at 60-80 kDa with a lighter band evident with TNF-α and L-NMA treatment compared to TNF-α alone or to IL-1beta and IL-1beta with L-NMA (**Figure 4**). Thus, the addition of L-NMA to TNF-α treatment decreases the generation and/or release of the aggrecanase generated G1 fragments. These results are consistent with the sGAG results in this study. However the effects of IL-1β in this study differ from the Bird et al. study where they found that L-NMA and IL-1β increased the aggrecanase cleavage fragments compared to IL-1β alone [23]. These results indicate that NO is partially responsible for TNF-α induced aggrecanase activity, and this inhibition may result from a decrease in aggrecanase expression or a change post-translational activation state.

To test the relative contributions of each of the ADAMTS4 and ADAMTS5 enzymes in aggrecanase degradation, we attempted to perform an immunoblot analysis of both the medium and the detergent lysis of the explants at day 5. While we were able to detect the recombinant protein, no reproducible signal was identified in any of the samples (data not shown). This may be due to the low abundance of the enzymes, or it may be that the antibodies used cannot detect bovine ADAMTS4 and ADAMTS5 since

the antibodies were made against the human enzymes. Finally, one cannot rule out the possibility that the aggrecanase activity is the result of another protease whose aggrecan cleaving ability has yet to be characterized and/or species-specific differences among those ADAMs and ADAMTS activities.

Because we were unable to find reproducibly either ADAMTS4 or ADAMTS5 at a protein level in explant or agarose samples, real time PCR analysis was conducted on explants subjected to IL-1β or TNF-α treatment in the presence or absence of L-NMA. While we evaluated ADAMTS4 and ADAMTS5, we took the opportunity to more broadly characterize the effects of NOS inhibition by L-NMA on IL-1β and TNF-α induced changes in gene transcription. In this study we focused exclusively on the 26-hour time point, which showed a small but significant increase in sGAG loss suggesting that the chondrocytes had begun to respond to the cytokine treatment. The panel of 32 genes is shown in figure 5C as the mean +/- SEM fold increase over control with the bold and asterisk indicating whether they were significantly decreased (Group 1) or significantly elevated compared to the control (Group2). While IL-1β and TNF-α treatment caused a number of large and statistically significant changes in gene expression, L-NMA caused no statistically significant change in gene expression among the 31 genes evaluated in this study.

Previous work with this model and by others has shown that ADAMTS4 and ADAMTS5 are up-regulated by IL-1β and TNF-α treatment respectively [73, 74]. Patwari et al. noted a significant increase in ADAMTS4 transcription after 24 hours of IL-1α treatment in this model system [73]. Caterson et al. reported that TNF-α caused a strong increase in ADAMTS5 transcription while IL-1β increased ADAMTS4

transcription in young bovine explants [74]. In this study, we see a stronger increase in ADAMTS5 with TNF-α than with IL-1β; however the effects of ADAMTS4 are similar at 26 hours after cytokine treatment. This may point to a role for ADAMTS5 in the NO dependent increase in aggrecan degradation with TNF-α; however the effect of L-NMA on ADAMTS5 gene expression was minimal and not statistically significant.

Previous work by Sasaki et al. noted a NO dependent increase in bFGF and MMP-9 in response to IL-1β in rabbit chondrocytes grown in monolayer [75]. While we did note an increase in the mean transcription level of bFGF and MMP-9 with TNF-α and IL-1β, the variance was sufficiently large such that no significant effect could be found, and no L-NMA effect was observed. In addition, the time point chosen for analysis may have been too early to probe these effects, as they noted that MMP and bFGF transcription occurred following an increase in iNOS, which was seen in this study [75].

NO has been implicated in activating MMPs; this may occur through disruption of the zymogen's cysteine switch via nitrosation or oxidation [76]. To evaluate whether NO may play a role in expression or activation of MMPs in our system, we used zymography to test whether the activation state or expression of MMPs in the explant medium were altered in response to treatment with L-NMA. **Figure 6A and 6B** show the results from the zymography. IL-1β and TNF–α caused a consistent increase in MMP-9, and IL-1β (and to a lesser extent, TNF-α) caused a consistent increase in MMP-3 secretion to medium. There was no band indicating the active form of either MMP-9 or MMP-3, and L-NMA caused no change in these profiles. MMP-2 was expressed under all conditions, and its expression and activation was unchanged by the presence of L-NMA. The results of the zymograms match well to those of the real-time PCR data in

that MMP-3 dramatically increases with IL-1β and less with TNF-α, and in that MMP-9 transcription shows a general increase with cytokine treatment compared to control (although these results are not statistically significant).

The zymography results were similar to those of Dozin et al. in that they failed to see an effect of NOS inhibition on MMPs by zymography when treating chondrocyte monolayers with a combination of IL-1α + TNF-α [77], but different from those of Tamura et al. who noted an increase in MMP-2 and MMP-9 expression by IL-1β that was blocked by L-NMA in rabbit chondrocyte monolayers [26]. Work by Stadler et al. and Murrell et al., using a gelatinase in solution activity assay, showed that inhibition of NO decreased gelatinase activity with IL-1β treatment [2, 25]. The reason for the difference between this study and the solution assay studies may be that zymography is not sufficiently quantitative, and that low levels of gelatinase activity or changes in gelatinase expression may not be readily identified. However, it is also possible that the differences may be the result of changes in the TIMP expression rather than changes in MMP activity. The increase in MMP-3 expression was similar to Murrell et al. who saw no NO-dependent caseinolytic activity with IL-1β treatment [25]. However, Stefanovic-Racic et al. saw an increase in latent caseinolytic activity using an in-solution activity assay [7]. These differences may again be attributed to differences in sensitivity, specificity, or model systems. The lack of qualitative differences in MMP-2, MMP-3, and MMP-9 expression or activation state in this study suggests that NO is not likely playing a significant role in MMP activation or expression.

No change in collagen fragment release was detected (not shown), suggesting that no significant increase in collagen breakdown resulted from treatment with cytokines (not

shown). In addition, L-NMA had no effect on the baseline degradation. This is not surprising in that the culture period was short and existing aggrecan likely protected the collagen framework against damage from collagenases [70]. Because so little collagen degradation was seen, any conclusion about the role of NO on collagen degradation would be premature. A longer study will be necessary to determine whether NO plays a role in collagen breakdown.

In this work, we have attempted to better characterize the role of NO in the catabolic responses to inflammatory cytokines, IL-1β and TNF-α. Inhibiting NOS partially inhibits aggrecanase mediated aggrecan degradation and concomitant sGAG release to the medium in response to TNF-alpha treatment. However, no effect was seen with IL-1β and the inverse effect was noted with the combination of IL-1β and TNF-α. This situational behavior of nitric oxide suggests possible differences in nitric oxide production or chemistry between TNF-α and IL-1β, but none was noted with the exception of a slightly slower increase in nitric oxide production with IL-1β treatment, which we attribute to a slower diffusion into the tissue due to the lower concentration gradient compared to TNF-α. Another possible reason for the difference may be differences in cell death due to the cytokine treatment; however no qualitative difference was noted by live/dead assay after the five-day cytokine treatments among any groups (data not shown).

Differences in cell signaling between the cytokines may define a different context for the cell response to NO chemistry and signaling. Previous studies probing chondrocyte signaling in response to TNF-α and IL-1β have implicated ERK1/2, p38, JNK as well as transcription factors, AP-1, NFkB, ESE-1 in pro-catabolic and anti-

anabolic cellular responses[78-82]. IL-1β activates C/EBPδ and C/EBPβ in chondrocytes, and TNF-α activates C/EBPβ in MC3T3-E1 cells [83, 84]. While the two cytokines share much of the same signaling machinery, differences in signaling are necessary to explain the effects of NOS inhibition aggrecan degradation. The activation of C/EBPβ or C/EBPδ may represent a possible difference in TNF-α and IL-1β signaling, and these factors are known to activate gene expression of proinflammatory molecules such as COX-2 [84].

While inhibiting NOS has no detectable effect on IL-1β or TNF-α induced MMPs expression or activation, collagen type II fragments, or gene expression after 24 hours of cytokine treatment, this study indicates that NO plays a complicated and situational role in matrix degradation. Inhibiting NOS is partially protective against TNF-α induced sGAG release, which is mediated through aggrecanase cleavage of aggrecan in the interglobular domain (aggrecan-G1-NITEGE-COOH). However, NOS inhibition with IL-1β and TNF-α treatment in combination has a deleterious impact on sGAG release, and IL-1β has no detectable effect on sGAG release in this study. These results imply that the role of NO in modulating matrix breakdown may depend on the inflammatory stimuli driving this catabolic response in chondrocytes. These findings may help shed light on the variability of in vivo studies that test the role of NO on arthritis development. These findings indicate that effects of NO may depend on the characteristics of the disease, in particular, the cytokines driving the catabolic response.

Acknowledgements. I would like to thank J. Glogowski for his technical assistance with the nitrate/nitrite anlaysis. I would like to thank the NDSEG and Centocor for funding (ALS).

2.6 FIGURES

Figure 1.1

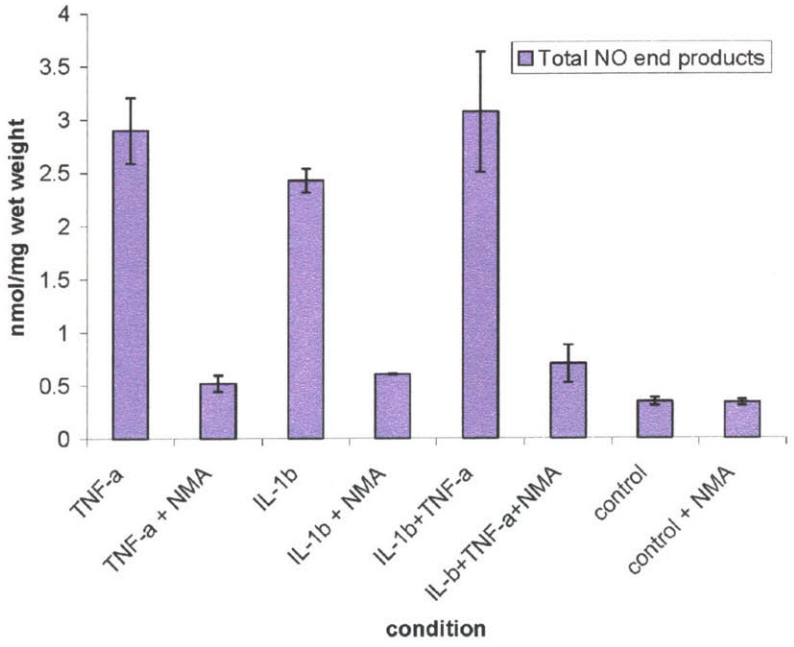

Figure 1: Five day accumulated total nitrate and nitrite release to the medium (nmol/mg wet weight) as a measure of NO production. Medium from day 5 was dilute 1:2 in water and analyzed by Greiss assay. IL-1β, TNF-α and TNF-α and IL-1β in combination caused 7-9 fold increase total nitrate and nitrite ($p<0.001$). Treatment with L-NMA (IL-1β + L-NMA, TNF-α + L-NMA, and IL-1β + TNF-α +NMA) prevented the production of nitrate and nitrite to at or near control levels. Data plotted as mean +/- SEM from greater than 3 explants per joint from five animals.

Figure 2.2

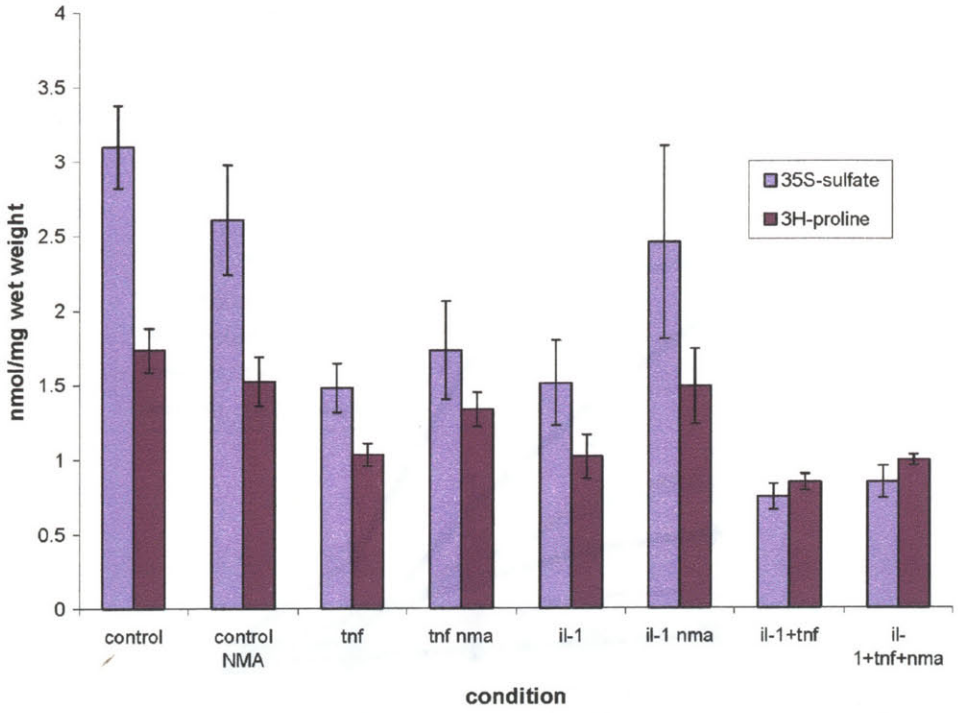

Figure 2: Twenty-four hour 5-^{3}H-proline and ^{35}S-sulfate incorporation following the 5 day cytokine treatment with L-NMA. The biosynthesis data are plotted as mean+/- SEM from at least 4 explants from at least 3 joints. The results indicate the combination of IL-1β and TNF-α caused a decrease in sulfate and proline incorporation (sGAG and protein biosynthesis) while TNF-α and IL-1β alone cause a statistically significant decrease in sulfate incorporation. No statistically significant effect on sGAG synthesis was seen with L-NMA treatment; however, NMA partially blocked the inhibition of protein synthesis by cytokine treatment $p = 0.05$.

Figure 2.3

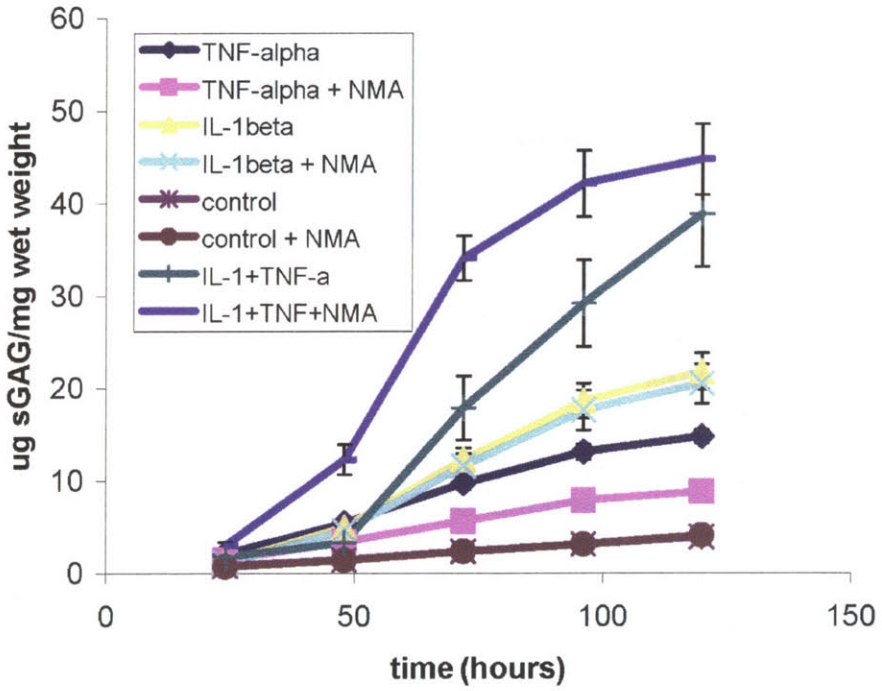

Figure 3: Accumulated sulfated glycosaminoglycan (sGAG) release to medium over five day cytokine treatment in the presence or absence of L-NMA. IL-1β and TNF-α alone and in combination caused multifold increase in sGAG release to the medium ($p<0.001$ for all points). L-NMA inhibited roughly half the sGAG released caused by treatment with TNF-α ($p<0.01$ for all time points), but L-NMA had no effect on sGAG release after the first 24 hours in response to IL-1β treatment. L-NMA caused a significant increase in sGAG release to the medium over the first four days in combination with IL-1β and TNF-α compared to IL-1β and TNF-α alone suggesting an increase in the rate of release ($p<0.03$ for days 1-4). No difference was seen in the untreated control when treated with L-NMA. The data is plotted as mean +/- SEM from greater than 3 explants from at least five different animals.

Figure 2.4

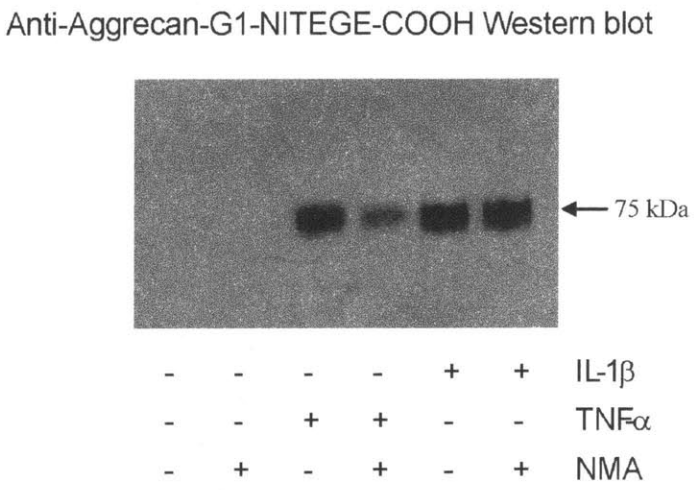

Figure 4: Anti-Aggrecan-G1-NITEGE-COOH immunoblot to probe mechanism of sGAG loss in response to IL-1β and TNF-α treatment with and without NOS inhibitor, L-NMA. A doublet is visualized in all cytokine treated conditions; however the TNF-α and L-NMA band is significantly lighter than that of the TNF-α alone or the IL-1β with and without L-NMA. Immunoblot is representative blot from five experiments.

Figure 2.5

Figure 2.5a

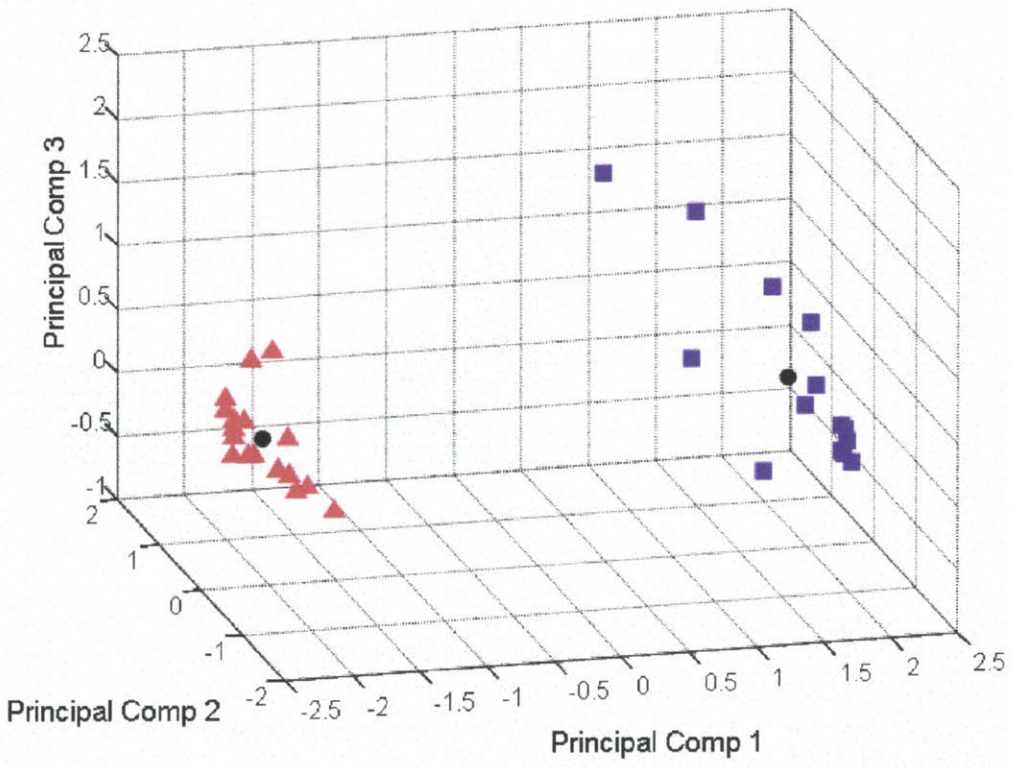

Figure 5A: Figure 5A is a projection plot of gene behavior represented by the first three principal components. As can be clearly seen in the figure, the genes can readily separated into 2 clusters which correspond to genes that respond positively to the IL-1β and TNF-α treatment and those genes that either don't respond or respond negatively to the cytokine treatment.

Figure 2.5b

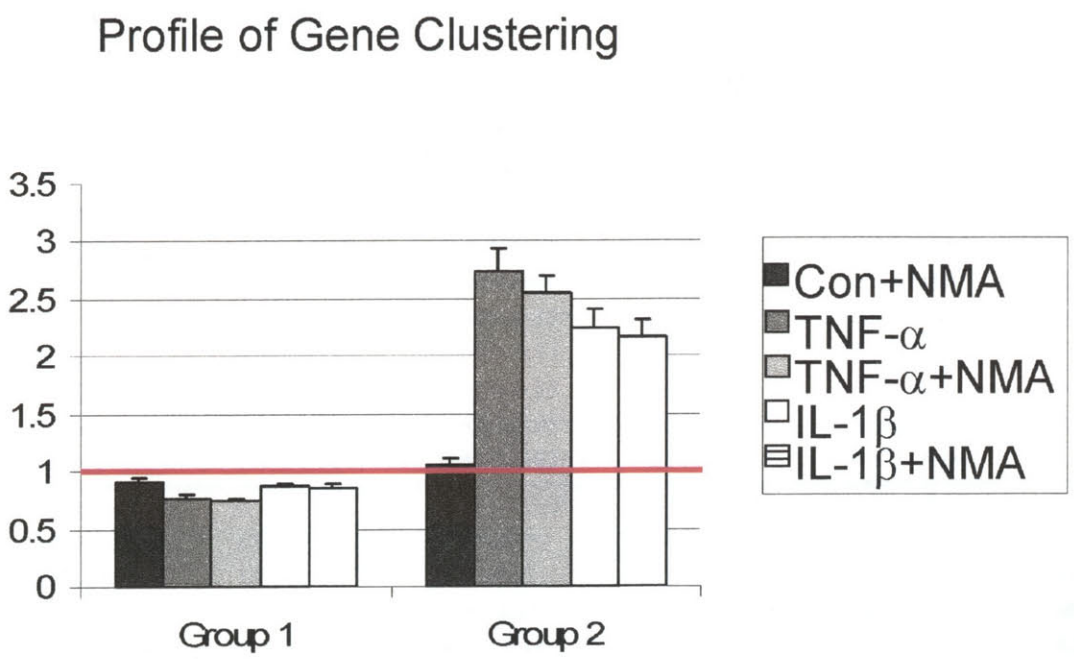

Figure 5B: Figure 5B represents the centroid profiles of the gene clusters indicated in Figure 5A. Group 2 contains genes that are up regulated in response to cytokine treatment while group 1 contains genes that are unresponsive or respond negatively. While there does seem to be an overall slight decrease in Group 2 gene expression with NMA, no genes were found to be significantly increased or decreased with the NMA treatment.

Figure 2.5c

Gene	*NMA only*	*TNF-alpha*	*TNF-α +NMA*	*IL-1β*	*IL-1β +NMA*
Aggrecan	0.98+/-0.06	**0.74+/-0.07***	0.69+/-0.09	0.91+/-0.05	**0.83+/-0.05***
Collagen II	0.98+/-0.13	0.73+/-0.11	0.77+/-0.12	0.81+/-0.10	0.67+/-0.11
Fibromodulin	1.18+/-0.12	**0.59+/-0.06***	**0.60+/-0.04***	0.86+/-0.06	0.96+/-0.10
Link protein	1.0+/-0.10	**0.46+/-0.06***	**0.48+/-0.05***	0.81+/-0.08	0.82+/-0.13
TIMP-2	0.99+/-0.12	**0.53+/-0.03***	**0.52+/-0.06***	**0.50+/-0.08***	0.71+/-0.16
TIMP-3	0.61+/-0.11	1.1+/-0.37	0.77+/-0.21	0.97+/-0.27	0.98+/-0.34
MMP-1	0.88+/-0.09	0.92+/-0.08	0.94+/-0.11	0.98+/-0.09	0.88+/-0.10
G3DPH	0.90+/-0.12	0.72+/-0.15	0.80+/-0.09	0.89+/-0.19	1.2+/-0.16
b-actin	0.95+/-0.08	0.81+/-0.06	0.88+/-0.06	0.86+/-0.07	0.84+/-0.07
IGF-1	1.0+/-0.13	**0.50+/-0.12***	**0.53+/-0.13***	0.64+/-0.10	0.61+/-0.12
IL-4	0.82+/-0.11	0.78+/-0.11	0.83+/-0.13	0.91+/-0.13	0.81+/-0.12
IL-6	0.77+/-0.13	0.82+/-0.15	0.70+/-0.14	1.1+/-0.16	0.95+/-0.18
TXNIP	0.92+/-0.09	**0.55+/-0.05***	**0.63+/-0.04***	**0.66+/-0.05***	**0.73+/-0.05***
HAS2	1.0+/-0.12	**0.49+/-0.03***	**0.54+/-0.05***	**0.47+/-0.04***	**0.47+/-0.03***
Fibronectin	0.96+/-0.08	**1.60+/-0.15***	1.48+/-0.23	**1.41+/-0.15***	1.25+/-0.13
MMP-3	1.0+/-0.18	**11+/-2.7***	**8.7+/-2.8***	**34+/-9.1***	**24.5+/-7.7***
MMP-9	1.1+/-0.24	115+/-60	99+/-44	74+/-54	**81+/-58***
MMP-13	0.83+/-0.17	**12+/-4.4***	**7.7+/-1.7***	**76+/-23***	**69+/-25***
ADAMTS4	0.98+/-0.09	**8.0+/-1.1***	**6.7+/-0.61***	**5.9+/-1.4***	**5.3+/-1.8***
ADAMTS5	1.26+/-0.23	**68+/-9.1***	**59+/-8.8***	**17.4+/-6.9***	**13.9+/-3.3***
TIMP-1	1.01+/-0.16	**4.6+/-1.3***	**3.3+/-0.45***	**3.4+/-0.64***	3.3+/-0.89
COX2	1.2+/-0.11	**11.4+/-2.7***	**13.4+/-5.1***	**17.6+/-5.0***	**17.5+/-5.7***
NOS2	1.5+/-0.57	**4513+/-1495***	**4694+/-1300***	**894/-183***	**873+/-304***
IGF-2	0.99+/-0.10	0.92+/-0.08	1.3+/-0.37	1.1+/-0.11	1.3+/-0.18
TGF-beta	0.92+/-0.07	2.3+/-0.20	**2.4+/-0.17***	**1.7+/-0.18***	**1.6/-0.19***
TNF-alpha	2.0+/-0.98	2.5+/-1.6	2.6+/-1.4	3.7+/-2.6	2.8+/-1.7
IL-1beta	0.95+/-0.12	4.4+/-2.8	3.2+/-2.0	4.3+/-2.4	4.3+/-2.6
HSP90	0.85+/-0.07	**2.2+/-0.27***	**1.9+/-0.23***	1.3+/-0.14	1.3+/-0.20
CD44	1.0+/-0.17	**20+/-3.0***	**20+/-3.0***	**11+/-2.1***	**11+/-3.0***
bFGF	9.0+/-7.0	1722+/-1109	1854+/-1783	61+/-48	9.1+/-3.8
OP-1	1.6+/-0.41	**80+/-16***	**69+/-20***	**26+/-10***	**20+/-6.0***

Figure 5C: The list of genes probed by real time PCR in group 1 and group 2 represented as the mean fold change over control +/-SEM. The * indicates statistical significance compared to the untreated control sample by pair-wise comparison (Wilcoxan Sign Rank test with Bonferroni correction for multiple comparison; $p<0.05$). Data represent experiments from eight animals with 2 or 3 explants pooled per animal for RNA extraction.

Figure 2.6

Figure 6A

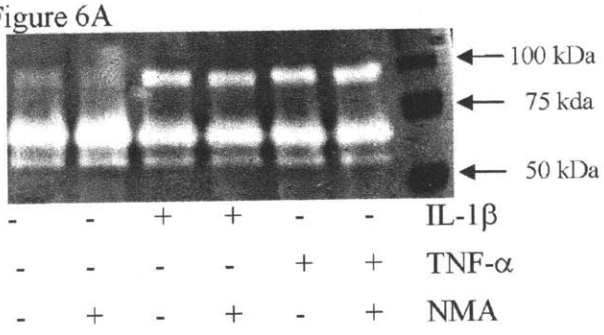

Figure 6B

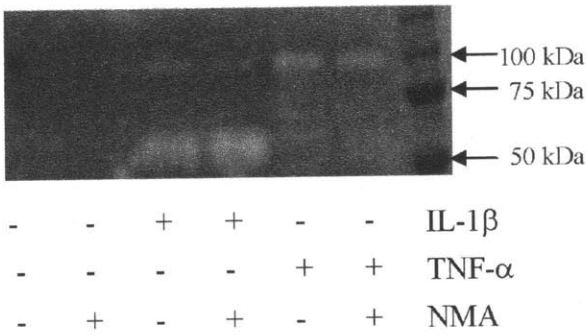

Figure 6. Gelatin (6A) and Casein zymograms (6B). Gelatin zymogram of five day culture medium (figure 6A). All samples contained a 72 kDa band (arrow) and a lower 65 kDa band corresponding to the pro- and active from of MMP-2 respectively. Only cytokine treated samples have a 92 kDa band corresponding to MMP-9. L-NMA had no affect on MMP-9 or MMP-2 expression or activation in medium. Casein zymogram of day 5 medium (figure 6B). The casein zymogram contains a 54 kDa band corresponding to pro-MMP-3. On closer observation the 54 kDa band actually appears as a doublet, a lighter upper band and a "brighter" lower band for both IL-1β and IL-1β-L-NMA. Only a very faint doublet can be detected for TNF-α treatment. In addition, a 90 kDa band can be seen with cytokine treatment in the casein gel as well. This may also correspond to MMP-9, or it may correspond to another calcium dependent protease. The data are representative zymograms from five experiments.

2.7 REFERENCES

1. Miersch, S. and B. Mutus, *Protein S-nitrosation: biochemistry and characterization of protein thiol-NO interactions as cellular signals.* Clin Biochem, 2005. **38**(9): p. 777-91.
2. Stadler, J., et al., *Articular chondrocytes synthesize nitric oxide in response to cytokines and lipopolysaccharide.* J Immunol, 1991. **147**(11): p. 3915-20.
3. Palmer, R.M., et al., *Induction of nitric oxide synthase in human chondrocytes.* Biochem Biophys Res Commun, 1993. **193**(1): p. 398-405.
4. Charles, I.G., et al., *Cloning, characterization, and expression of a cDNA encoding an inducible nitric oxide synthase from the human chondrocyte.* Proc Natl Acad Sci U S A, 1993. **90**(23): p. 11419-23.
5. Maier, R., et al., *Inducible nitric oxide synthase from human articular chondrocytes: cDNA cloning and analysis of mRNA expression.* Biochim Biophys Acta, 1994. **1208**(1): p. 145-50.
6. Stefanovic-Racic, M., et al., *Modulation of chondrocyte proteoglycan synthesis by endogeneously produced nitric oxide.* Inflamm Res, 1995. **44 Suppl 2**: p. S216-7.
7. Stefanovic-Racic, M., et al., *The role of nitric oxide in proteoglycan turnover by bovine articular cartilage organ cultures.* J Immunol, 1996. **156**(3): p. 1213-20.
8. Stefanovic-Racic, M., et al., *Nitric oxide and proteoglycan turnover in rabbit articular cartilage.* J Orthop Res, 1997. **15**(3): p. 442-9.
9. Rediske, J.J., et al., *The inducible production of nitric oxide by articular cell types.* Osteoarthritis Cartilage, 1994. **2**(3): p. 199-206.
10. Goodstone, N.J. and T.E. Hardingham, *Tumour necrosis factor alpha stimulates nitric oxide production more potently than interleukin-1beta in porcine articular chondrocytes.* Rheumatology (Oxford), 2002. **41**(8): p. 883-91.
11. Vuolteenaho, K., et al., *Effects of TNFalpha-antagonists on nitric oxide production in human cartilage.* Osteoarthritis Cartilage, 2002. **10**(4): p. 327-32.
12. Cai, L., et al., *Interleukin 17 induced nitric oxide suppresses matrix synthesis and protects cartilage from matrix breakdown.* J Rheumatol, 2002. **29**(8): p. 1725-36.
13. Olee, T., et al., *IL-18 is produced by articular chondrocytes and induces proinflammatory and catabolic responses.* J Immunol, 1999. **162**(2): p. 1096-100.
14. Boileau, C., et al., *The in situ up-regulation of chondrocyte interleukin-1-converting enzyme and interleukin-18 levels in experimental osteoarthritis is mediated by nitric oxide.* Arthritis Rheum, 2002. **46**(10): p. 2637-47.
15. Pichika, R. and G.A. Homandberg, *Fibronectin fragments elevate nitric oxide (NO) and inducible NO synthetase (iNOS) levels in bovine cartilage and iNOS inhibitors block fibronectin fragment mediated damage and promote repair.* Inflamm Res, 2004. **53**(8): p. 405-12.
16. Taskiran, D., et al., *Nitric oxide mediates suppression of cartilage proteoglycan synthesis by interleukin-1.* Biochem Biophys Res Commun, 1994. **200**(1): p. 142-8.
17. Hauselmann, H.J., et al., *Nitric oxide and proteoglycan biosynthesis by human articular chondrocytes in alginate culture.* FEBS Lett, 1994. **352**(3): p. 361-4.

18. Hickery, M.S. and M.T. Bayliss, *Interleukin-1 induced nitric oxide inhibits sulphation of glycosaminoglycan chains in human articular chondrocytes.* Biochim Biophys Acta, 1998. **1425**(2): p. 282-90.
19. Hickery, M.S., Palmer, R. M. J., Charles, I. G., Moncada, S., Bayliss, M. T. *The role of Nitric Oxide in the IL-1- and TNF-alpha induced inhibition of proteoglycan synthesisi in human articular cartilage.* in *Transactions of the Orthopaedic Research Society.* 1994.
20. Jarvinen, T.A.H., Moilanen, T., Jarvinen, T. L. N., Moilanen, E., *Endogenous nitric oxide and prostaglandin E2 do not regulate the synthesis of each other in interleukin-1beta - stimulated rat articular cartilage.* Inflammation, 1996. **20**(6): p. 683-392.
21. Cao, M., et al., *Nitric oxide inhibits the synthesis of type-II collagen without altering Col2A1 mRNA abundance: prolyl hydroxylase as a possible target.* Biochem J, 1997. **324 (Pt 1)**: p. 305-10.
22. Sliskovic, I., A. Raturi, and B. Mutus, *Characterization of the S-denitrosation activity of protein disulfide isomerase.* J Biol Chem, 2005. **280**(10): p. 8733-41.
23. Bird, J.L., S. May, and M.T. Bayliss, *Nitric oxide inhibits aggrecan degradation in explant cultures of equine articular cartilage.* Equine Vet J, 2000. **32**(2): p. 133-9.
24. Bird, J.L., et al., *IL-1 beta induces the degradation of equine articular cartilage by a mechanism that is not mediated by nitric oxide.* Biochem Biophys Res Commun, 1997. **238**(1): p. 81-5.
25. Murrell, G.A., D. Jang, and R.J. Williams, *Nitric oxide activates metalloprotease enzymes in articular cartilage.* Biochem Biophys Res Commun, 1995. **206**(1): p. 15-21.
26. Tamura, T., et al., *Nitric oxide mediates interleukin-1-induced matrix degradation and basic fibroblast growth factor release in cultured rabbit articular chondrocytes: a possible mechanism of pathological neovascularization in arthritis.* Endocrinology, 1996. **137**(9): p. 3729-37.
27. Farrell, A.J., et al., *Increased concentrations of nitrite in synovial fluid and serum samples suggest increased nitric oxide synthesis in rheumatic diseases.* Ann Rheum Dis, 1992. **51**(11): p. 1219-22.
28. Ialenti, A., et al., *Modulation of acute inflammation by endogenous nitric oxide.* Eur J Pharmacol, 1992. **211**(2): p. 177-82.
29. Ialenti, A., S. Moncada, and M. Di Rosa, *Modulation of adjuvant arthritis by endogenous nitric oxide.* Br J Pharmacol, 1993. **110**(2): p. 701-6.
30. McCartney-Francis, N., et al., *Suppression of arthritis by an inhibitor of nitric oxide synthase.* J Exp Med, 1993. **178**(2): p. 749-54.
31. McCartney-Francis, N.L., et al., *Selective inhibition of inducible nitric oxide synthase exacerbates erosive joint disease.* J Immunol, 2001. **166**(4): p. 2734-40.
32. Stefanovic-Racic, M., et al., *N-monomethyl arginine, an inhibitor of nitric oxide synthase, suppresses the development of adjuvant arthritis in rats.* Arthritis Rheum, 1994. **37**(7): p. 1062-9.
33. Stefanovic-Racic, M., et al., *Comparison of the nitric oxide synthase inhibitors methylarginine and aminoguanidine as prophylactic and therapeutic agents in rat adjuvant arthritis.* J Rheumatol, 1995. **22**(10): p. 1922-8.

34. Presle, N., et al., *Cartilage protection by nitric oxide synthase inhibitors after intraarticular injection of interleukin-1beta in rats.* Arthritis Rheum, 1999. **42**(10): p. 2094-102.
35. Sakaguchi, Y., et al., *Effects of selective iNOS inhibition on type II collagen-induced arthritis in mice.* Life Sci, 2004. **75**(19): p. 2257-67.
36. Kato, H., et al., *Effect of NOS2 gene deficiency on the development of autoantibody mediated arthritis and subsequent articular cartilage degeneration.* J Rheumatol, 2003. **30**(2): p. 247-55.
37. van den Berg, W.B., et al., *Animal models of arthritis in NOS2-deficient mice.* Osteoarthritis Cartilage, 1999. **7**(4): p. 413-5.
38. Pelletier, J.P., et al., *Reduced progression of experimental osteoarthritis in vivo by selective inhibition of inducible nitric oxide synthase.* Arthritis Rheum, 1998. **41**(7): p. 1275-86.
39. Pelletier, J., et al., *Reduction in the structural changes of experimental osteoarthritis by a nitric oxide inhibitor.* Osteoarthritis Cartilage, 1999. **7**(4): p. 416-8.
40. Pelletier, J.P., et al., *Selective inhibition of inducible nitric oxide synthase in experimental osteoarthritis is associated with reduction in tissue levels of catabolic factors.* J Rheumatol, 1999. **26**(9): p. 2002-14.
41. Clements, K.M., et al., *Gene deletion of either interleukin-1beta, interleukin-1beta-converting enzyme, inducible nitric oxide synthase, or stromelysin 1 accelerates the development of knee osteoarthritis in mice after surgical transection of the medial collateral ligament and partial medial meniscectomy.* Arthritis Rheum, 2003. **48**(12): p. 3452-63.
42. Yocum, D.E., et al., *Characteristics of tumor necrosis factor production in rheumatoid arthritis.* Cell Immunol, 1989. **122**(1): p. 131-45.
43. Di Giovine, F.S., Nuki, G., Duff, G. W., *Tumor necrosis factor in synovial exudates.* Annals of the Rheum, 1988. **47**: p. 768-772.
44. Brennan, F.M., et al., *Inhibitory effect of TNF alpha antibodies on synovial cell interleukin-1 production in rheumatoid arthritis.* Lancet, 1989. **2**(8657): p. 244-7.
45. Hukkanen, M., et al., *Induction of inducible nitric oxide synthase, argininosuccinate synthase, and GTP cyclohydrolase I in arthritic joints of human tumor necrosis factor-alpha transgenic mice.* J Rheumatol, 2003. **30**(4): p. 652-9.
46. Saklatvala, J., *Tumour necrosis factor alpha stimulates resorption and inhibits synthesis of proteoglycan in cartilage.* Nature, 1986. **322**(6079): p. 547-9.
47. Shinmei, M., et al., *Production of cytokines by chondrocytes and its role in proteoglycan degradation.* J Rheumatol Suppl, 1991. **27**: p. 89-91.
48. Harigai, M., et al., *Interleukin 1 and tumor necrosis factor-alpha synergistically increase the production of interleukin 6 in human synovial fibroblast.* J Clin Lab Immunol, 1991. **34**(3): p. 107-13.
49. Pelletier, J.P., et al., *Cytokines and inflammation in cartilage degradation.* Rheum Dis Clin North Am, 1993. **19**(3): p. 545-68.
50. Ismaiel, S., et al., *Susceptibility of normal and arthritic human articular cartilage to degradative stimuli.* Br J Rheumatol, 1992. **31**(6): p. 369-73.

51. Westacott, C.I., Ismaiel, S., Langkamer, V. G., Atkins, R. M., Elson, C. J. . *Human Articular Cartilage Degradation and Chondrocyte Expression of TNF-alpha Receptors.* in *Transactions of the Orthopaedic REsearch Society.* 1993. San Francisco, CA.
52. Webb, G.R., C.I. Westacott, and C.J. Elson, *Chondrocyte tumor necrosis factor receptors and focal loss of cartilage in osteoarthritis.* Osteoarthritis Cartilage, 1997. **5**(6): p. 427-37.
53. Webb, G.R., C.I. Westacott, and C.J. Elson, *Osteoarthritic synovial fluid and synovium supernatants up-regulate tumor necrosis factor receptors on human articular chondrocytes.* Osteoarthritis Cartilage, 1998. **6**(3): p. 167-76.
54. Hrycaj, P., et al., *Microheterogeneity of acute phase proteins in patients with clinically active and clinically nonactive osteoarthritis.* Clin Rheumatol, 1995. **14**(4): p. 434-40.
55. Schlaak, J.F., et al., *Different cytokine profiles in the synovial fluid of patients with osteoarthritis, rheumatoid arthritis and seronegative spondylarthropathies.* Clin Exp Rheumatol, 1996. **14**(2): p. 155-62.
56. Daouti, S., et al., *Development of comprehensive functional genomic screens to identify novel mediators of osteoarthritis.* Osteoarthritis Cartilage, 2005. **13**(6): p. 508-18.
57. Sandy, J.D., et al., *The structure of aggrecan fragments in human synovial fluid. Evidence for the involvement in osteoarthritis of a novel proteinase which cleaves the Glu 373-Ala 374 bond of the interglobular domain.* J Clin Invest, 1992. **89**(5): p. 1512-6.
58. Arner, E.C., et al., *Cytokine-induced cartilage proteoglycan degradation is mediated by aggrecanase.* Osteoarthritis Cartilage, 1998. **6**(3): p. 214-28.
59. Tortorella, M.D., et al., *Characterization of human aggrecanase 2 (ADAM-TS5): substrate specificity studies and comparison with aggrecanase 1 (ADAM-TS4).* Matrix Biol, 2002. **21**(6): p. 499-511.
60. Tortorella, M.D., et al., *Sites of aggrecan cleavage by recombinant human aggrecanase-1 (ADAMTS-4).* J Biol Chem, 2000. **275**(24): p. 18566-73.
61. Tortorella, M.D., et al., *The role of ADAM-TS4 (aggrecanase-1) and ADAM-TS5 (aggrecanase-2) in a model of cartilage degradation.* Osteoarthritis Cartilage, 2001. **9**(6): p. 539-52.
62. Abbaszade, I., et al., *Cloning and characterization of ADAMTS11, an aggrecanase from the ADAMTS family.* J Biol Chem, 1999. **274**(33): p. 23443-50.
63. Tortorella, M.D., et al., *Purification and cloning of aggrecanase-1: a member of the ADAMTS family of proteins.* Science, 1999. **284**(5420): p. 1664-6.
64. Malfait, A.M., et al., *Inhibition of ADAM-TS4 and ADAM-TS5 prevents aggrecan degradation in osteoarthritic cartilage.* J Biol Chem, 2002. **277**(25): p. 22201-8.
65. Sah, R.L., et al., *Biosynthetic response of cartilage explants to dynamic compression.* J Orthop Res, 1989. **7**(5): p. 619-36.
66. Kisiday, J.D., et al., *Evaluation of medium supplemented with insulin-transferrin-selenium for culture of primary bovine calf chondrocytes in three-dimensional hydrogel scaffolds.* Tissue Eng, 2005. **11**(1-2): p. 141-51.

67. Farndale, R.W., D.J. Buttle, and A.J. Barrett, *Improved quantitation and discrimination of sulphated glycosaminoglycans by use of dimethylmethylene blue.* Biochim Biophys Acta, 1986. **883**(2): p. 173-7.
68. Green, L.C., et al., *Analysis of nitrate, nitrite, and [15N]nitrate in biological fluids.* Anal Biochem, 1982. **126**(1): p. 131-8.
69. Clark, I.M., *Matrix Metalloproteinase Protocols.* Methods in molecular Biology, ed. I.M. Clark. Vol. 151. 2001, Clifton, NJ: Humana Press.
70. Pratta, M.A., et al., *Aggrecan protects cartilage collagen from proteolytic cleavage.* J Biol Chem, 2003. **278**(46): p. 45539-45.
71. Stewart, M.C., et al., *ADAMTS5-mediated aggrecanolysis in murine epiphyseal chondrocyte cultures.* Osteoarthritis Cartilage, 2006.
72. Flannery, C.R., M.W. Lark, and J.D. Sandy, *Identification of a stromelysin cleavage site within the interglobular domain of human aggrecan. Evidence for proteolysis at this site in vivo in human articular cartilage.* J Biol Chem, 1992. **267**(2): p. 1008-14.
73. Patwari, P., et al., *Analysis of ADAMTS4 and MT4-MMP indicates that both are involved in aggrecanolysis in interleukin-1-treated bovine cartilage.* Osteoarthritis Cartilage, 2005. **13**(4): p. 269-77.
74. Caterson, B., et al., *Mechanisms involved in cartilage proteoglycan catabolism.* Matrix Biol, 2000. **19**(4): p. 333-44.
75. Sasaki, K., et al., *Nitric oxide mediates interleukin-1-induced gene expression of matrix metalloproteinases and basic fibroblast growth factor in cultured rabbit articular chondrocytes.* J Biochem (Tokyo), 1998. **123**(3): p. 431-9.
76. Gu, Z., et al., *S-nitrosylation of matrix metalloproteinases: signaling pathway to neuronal cell death.* Science, 2002. **297**(5584): p. 1186-90.
77. Dozin, B., et al., *Response of young, aged and osteoarthritic human articular chondrocytes to inflammatory cytokines: molecular and cellular aspects.* Matrix Biol, 2002. **21**(5): p. 449-59.
78. Mendes, A.F., et al., *Role of nitric oxide in the activation of NF-kappaB, AP-1 and NOS II expression in articular chondrocytes.* Inflamm Res, 2002. **51**(7): p. 369-75.
79. Mendes, A.F., et al., *Role of mitogen-activated protein kinases and tyrosine kinases on IL-1-Induced NF-kappaB activation and iNOS expression in bovine articular chondrocytes.* Nitric Oxide, 2002. **6**(1): p. 35-44.
80. Grall, F., et al., *Responses to the proinflammatory cytokines interleukin-1 and tumor necrosis factor alpha in cells derived from rheumatoid synovium and other joint tissues involve nuclear factor kappaB-mediated induction of the Ets transcription factor ESE-1.* Arthritis Rheum, 2003. **48**(5): p. 1249-60.
81. Liacini, A., et al., *Induction of matrix metalloproteinase-13 gene expression by TNF-alpha is mediated by MAP kinases, AP-1, and NF-kappaB transcription factors in articular chondrocytes.* Exp Cell Res, 2003. **288**(1): p. 208-17.
82. Relic, B., et al., *TNF-alpha protects human primary articular chondrocytes from nitric oxide-induced apoptosis via nuclear factor-kappaB.* Lab Invest, 2002. **82**(12): p. 1661-72.

83. Yamamoto, K., et al., *Transcriptional roles of nuclear factor kappa B and nuclear factor-interleukin-6 in the tumor necrosis factor alpha-dependent induction of cyclooxygenase-2 in MC3T3-E1 cells.* J Biol Chem, 1995. **270**(52): p. 31315-20.
84. Thomas, B., et al., *Critical role of C/EBPdelta and C/EBPbeta factors in the stimulation of the cyclooxygenase-2 gene transcription by interleukin-1beta in articular chondrocytes.* Eur J Biochem, 2000. **267**(23): p. 6798-809.

Chapter 3:

An SDS-PAGE-LC/MS/MS analysis of cartilage tissue response to mechanical compression injury and inflammatory cytokines TNF-alpha and IL-1beta

Anna L. Stevens(1), John S. Wishnok(1), Alan J. Grodzinsky(1,2,3), Steven R. Tannenbaum (1,4)

Biological Engineering Division, Massachusetts Institute of Technology, Cambridge, MA, USA (1); Department of Electrical Engineering and Computer Science, Massachusetts Institute of Technology, Cambridge, MA, USA (2); Department of Mechanical Engineering, Massachusetts Institute of Technology, Cambridge, MA, USA (3); Department of Chemistry, Massachusetts Institute of Technology, Cambridge, MA, USA (4).

3.1 ABSTRACT

Objective: The objective of this study is to compare cartilage ECM and chondrocyte response to injurious mechanical compression, IL-1β treatment, TNF-α treatment and no treatment by focusing on proteins lost to the medium from in vitro cartilage explant culture.

Methods: Cartilage explants taken from young bovine stifle joint were treated with 10 ng/ml IL-1β, 100 ng/ml TNF-α, or subjected to radially-unconfined injurious mechanical compression (strain: 50%; strain rate 100%/sec), and cultured for five days. Pooled medium was subjected to SDS-PAGE-LC/MS/MS, and the data was analyzed by Spectrum Mill proteomics software focusing on protein identification, comparisons, and matrix protein proteolysis.

Results: Just over 250 proteins were identified among the four protein groups including CD109, platelet derived growth factor like protein, and scrapie responsive protein 1 which have not been previously identified in cartilage. IL-1β and TNF-α caused an increase in YKL39, YKL40, complement factor B, MMP-3, ECM-1, haptoglobin, serum amyloid A3, and clusterin. Injurious compression caused the release of intracellular proteins, including GRP58, GRP78, alpha 4

actinin, pyruvate kinase, and vimentin suggesting a loss of membrane integrity in a population of chondrocytes. Injurious compression also caused proteolysis of collagen type VI subunits, collagen type II, and COMP. Thrombospondin 1 fragments were seen in all treatment groups, and aggrecan proteolysis was predominant with cytokine treatment.

Conclusion: Mechanical compression causes loss of cartilage integrity including degradation of matrix molecules and damage to cell membrane integrity likely through strain-induced mechanical disruption of cells at the periphery of the explant. IL-1β and TNF-α cause the release of proteins invoke an innate immune and stress response by the chondrocytes, which may play a role in host defense against pathogens or may protect cells against stress induced damage.

3.2 INTRODUCTION

Articular cartilage is composed of chondrocytes and large amounts of extracellular matrix (ECM) rich in collagen type II and aggrecan which are responsible for the tensile strength and compressive stiffness of the tissue, respectively [1, 2]. A number of other ECM molecules are also present and responsible for normal tissue homeostasis, including other structural proteins, proteins involved in cell matrix interactions, and various extracellular signaling regulators.

Osteoarthritis is characterized by cartilage degeneration, which results from an imbalance between matrix synthesis and matrix degradation. While OA is a disease of the entire synovial joint, the chondrocyte likely plays a primary role in cartilage breakdown and local inflammation. Chondrocytes are capable of causing cartilage degeneration both through production of matrix degrading enzymes and small molecules and through modulation of the amount and type of matrix molecules that are synthesized and incorporated into the matrix.

Tumor necrosis factor alpha (TNF-α) is a secreted homotrimer composed of 17 kDa protein subunits produced primarily by inflammatory cells but also by synoviocytes and by chondrocytes, and detected in synovial fluid of OA and RA joints [3-9]. Importantly, anti-TNF-α therapy is used successfully to treat humans with poorly controlled rheumatoid arthritis [10-13]. In cartilage explant and chondrocyte cultures *in vitro*, TNF-α inhibits proteoglycan synthesis [14, 15] and increases proteoglycan degradation, albeit at a higher concentration than IL-1. TNF-α may also stimulate the production of aggrecanases, ADAMTS4 and 5, and matrix metalloproteinases, MMP-3, MMP-13 (collagenase-3) and MMP-9 (gelatinase-2) [16-20]. In addition, TNF-α may increase inflammatory mediators, such as PGE2 [20] and nitric oxide [21], and it increases transcription of IL-1, TNF-α, and IL-6 genes in cartilage from osteoarthritic joints [22].

Interleukin-1 or IL-1 is an 18 kDa protein present in two primary forms, IL-1α and IL-1β. IL-1 is frequently present in the synovial fluid of arthritic joints [23-25], and the inhibition of IL-1 may help to decrease cartilage and bone resorption in human disease [26]. IL-1 acts on chondrocytes, synovial cells, and endothelial cells to enhance the production of inflammatory mediators such as prostaglandins, cytokines, chemokines (IL-8 and leukotrienes), nitric oxide, and cell adhesion molecules [27-35]. *In vitro* treatment of cartilage explant cultures causes a substantial increase in aggrecan degradation that is likely mediated by ADAMTS4 and/or ADAMTS5, followed in time by degradation and loss of type II collagen by the up-regulated MMPs [36-39]. Chondrocytes are known to increase expression of ADAMTS4, ADAMTS5, MMP-1, MMP-3, MMP-8, MMP-9, and MMP-13 in response to IL-1 [31, 37, 40-46], many of which have been implicated in the degradation of a number of matrix molecules including fibronectin, matrilins, collagens, and COMP [47-51]. In addition to promoting matrix degradation, IL-1 also potently decreases new aggrecan and collagen synthesis [52, 53]. At a gene expression level, IL-1 inhibits the synthesis of aggrecan, collagen type II and collagen IX as well as cartilage derived retinoic acid sensitive protein (CD-RAP) [54-56]. Thus, both IL-1 and TNF-α are able to promote matrix destruction, increase inflammatory mediators, and decrease new matrix synthesis.

Joint injury is a significant risk factor for developing osteoarthritis. Development of osteoarthritis secondary to joint injury varies from roughly 15% to 75% over follow-up periods of 14 to 22 years which translates to an average relative risk of between 3 and 20 of developing osteoarthritis given traumatic joint injury [57-60]. Further, corrective surgery has little or no impact on the risk of developing OA post traumatic joint injury [58, 61, 62]. *In vitro* injury models have been developed to better understand the contribution of acute, mechanical

compression injury to the development of osteoarthritis. Studies have shown that high stress or high strain injury may lead to chondrocyte apoptosis[63-66], tissue fissuring and swelling, changes in the dynamic tissue modulus consistent with damage to the collagen network, increase in type II collagen degradation particularly at the boundaries of the tissue where the strain is highest, and increased proteoglycan loss [63, 67-74]. In addition, cytokines and injury together may enhance matrix damage compared to either stimuli alone[72]. Finally, co-culture with joint capsule tissue may also enhance cartilage degeneration by decreasing proteoglycan composition and decreasing stiffness of the tissue (Lee, J et al. in press).

To better understand changes in chondrocyte behavior following injury, studies have focused on changes in transcription within the first 24 hours following injury. Lee et al. performed real-time PCR time course profile on 24 cartilage genes involved in normal cartilage maintenance to detect changes in gene expression following unconfined compression injury [75]. In this study, Lee et al. identified MMP-3, ADAMTS5, and TGF-β which were elevated more than over 5 fold within four hours of injury and remained elevated at 24 hours after injury. Transcription of the matrix proteins, aggrecan, type II collagen, and fibronectin, and of matrix proteases, MMP-1, MMP-9, and MMP-13, were also increased at the 24 hour time point [75]. Additionally, increased transcription of c-fos and c-jun within the first hour of injury suggests that AP-1 pathway may be an important response pathway in injury. A similar study by Chan et al. used a combination of gene arrays and real time PCR to detect changes in transcription three hours after unconfined compression injury [76]. This study identified a decrease in transcription of adhesion molecules and growth factors, ICAM-3, NCAM, N-cadherin, VCAM-1, and IGF-1, while the chemokine receptor, CCR10, HMGB2, neurogranin, and ezrin were among the proteins that were upregulated [76].

Mass spectrometry has recently been used for protein identification and protein profiling to identify arthritis biomarkers and study changes in disease phenotype. Recent studies searching for protein biomarkers for OA and RA in synovial fluid have led to the identification of serum amyloid A, calgranulin A, B, and C, which are proteins correlated with increased RA disease severity [77, 78]. A study by Hermannson, et al., using a 2D gel approach to identify differences in newly synthesized protein released into the medium between osteoarthritic and normal cartilage, identified inhibin beta A and the C-terminal telopeptide of collagen in OA cartilage but not in cartilage from healthy joints. In addition, they were able to identify the production of connective tissue growth factor (CTGF) and cytokine like protein C17 in both normal and OA cartilage samples. Finally, studies on the effects of bFGF and IL-1 used ^{35}S-methionine labeling for new synthesis to show increased expression of TIMP-1, MMP-1, MMP-3, gp38 (ykl40), and serum amyloid A in response to these stimuli [79-81].

Mechanical injury and cytokines, TNF-α and IL-1β, cause changes in tissue properties and chondrocyte behavior, and both injury and long term cytokine exposure may lead to long term cartilage degeneration. The objective of the study was to identify and compare changes in protein release from cartilage explants into the medium in response to acute mechanical compression injury and to treatment with cytokines IL-1β or TNF-α. In this study, we use a systems-level mass spectrometry based proteomics method to identify and compare proteins released, including matrix protein proteolytic fragments. Protein level differences in the medium may reflect both differences in matrix degradation and differences in new protein synthesis. The goal of this study was to better understand the contribution of mechanical injury and cytokines to cartilage degeneration.

3.3 METHODS

Cartilage explantation and culture. Joints from 2-3 week old calves were obtained from the local abattoir (Research '87, Hopkinton, MA) and explanted as described previously [82]. Briefly, articular cartilage was removed from the femoropatellar groove as 9 mm cylinders cored out perpendicular to the joint surface, and the cores were sliced by microtome into 2 – 1mm thick slices which were punched by with 6 mm diameter dermal punch or by 3 mm dermal punch. Explanation yielded either 1 – 6mm diameter by 1 mm thick disk per slice (for untreated and cytokine treated studies) or 4 -3 mm diameter by 1mm thick explants per slice (for injury studies). Each 6 mm diameter disk or a set of 4- 3 mm diameter disks was placed into 1 well of a 24 well plate containing approximate 2.0 ml of culture medium with 1% ITS (high glucose (25mM glucose) DMEM supplemented with 10mM HEPES, 0.1 mM non-essential amino acids, 115 uM ascorbic acid, 400 uM L-proline, 100 U/ml penicillin, 100 ug/ml streptomycin, and 0.25 ug/ml amphotericin B powder (PSA for tissue culture), and 1mM sodium pyruvate). All treatments were performed on day 7 post explantation.

Mechanical Injury: Injurious compression was performed using an incubator-housed custom designed loading apparatus as described previously [72, 73, 75, 83]. Briefly, 3mm diameter x 1 mm thick cartilage disks were individually loaded into a polysulfone chamber and placed in the compression apparatus that performs unconfined compression by placing the cartilage between two impermeable platens. Explants were subjected to a single compression to 50% strain at a strain rate of 100%/second and a velocity of 1 mm/second which resulted in a load cell measured peak stress of 18.3+/-0.7 MPa (mean+/- SEM). The injured explants were placed in sets of four explants per culture well in 2.0 ml of medium, yielding the same cartilage volume per ml of medium as a single 6 mm diameter explant used for the cytokine and untreated explants.

TNF-α and IL-1β and post-treatment culture: Cytokines were resuspended in 0.1% BSA at a concentration of 10 ug/ml (TNF-α) or 2.5 ug/ml (IL-1β). On day seven of culture, 6 mm diameter explants were treated with 10 ng/ml of IL-1β or 100ng/ml of TNF-α or untreated in 2.0 ml of medium without 1% ITS for five days. All explant cultures were subjected to a 10% medium removal and 10% medium supplementation every 24 hours until the cultures were ended on day 5 (0.6 ml medium/explant/day) by placing the medium and explants at -80C.

Deglycosylation and SDS-PAGE. Medium from explants taken from at least 5 different joints were pooled, and a 2 ml aliquot of the pooled medium was treated with 3 mM EDTA and subjected to deglycosylation prior to SDS-PAGE. Samples were dialyzed in a 7.5 kDa cutoff membrane for 2 hours against buffer containing 10 mM Tris acetate, 10 mM NaCl, 10 mM sodium acetate, and 3 mM EDTA. After 2 hours, 50 mU of chondroitinase ABC was added to the dialyzing samples with buffer change, and the samples were dialyzed at 37C overnight. The samples were dialyzed against pure water at 4C overnight before freezing and concentrating samples by speedvac. Concentrated samples (10-15 ul) were combined with equal volume of 2X SDS-sample buffer containing 10 mM DTT. Samples were boiled for eight minutes, and loaded on a 4-15% gradient gel and run at 15 mA. Gels were washed with water, stained with Coomassie Blue Safestain (Invitrogen, Carlsbad, CA) for 30 minutes, and destained overnight with a change of water to enhance resolution. Gels were scanned using an Epson scanner, and saved as jpeg images.

Western blotting of fibronectin, type VI collagen, and actin. Equal amounts of concentrated medium (150ul/200ul) from injured or untreated explants from 4 randomly chosen experiments were run out on a 4-15% gel and transferred to PVDF for immunoblotting. Fibronectin blots were done using a monoclonal antibody to fibronectin (1:2000; BD Biosciences) while the type

VI collagen and actin antibodies were goat polyclonal antibodies (1:250; Chemicon –AB782; 1:500; Santa Cruz—C11). Appropriate secondary antibodies conjugated to HRP (anti-mouse- Amersham and anti-goat- Santa Cruz) were used for chemiluminescence detection.

Reduction, alkylation, trypsinization, and extraction from gel slices. Each sample, contained within a lane of the PAGE gel, was divided into approximately 30+/-2 equal slices (figure 1). The gel slices were destained, reduced, alkylated and in-gel digested as described by Shevchenko et al. with minor modifications [84]. Briefly, each gel slice was reduced with 1 mg/ml TCEP for 10 minutes, alkylated with 10 mg/ml iodoacetamide in the dark for 45 minutes, and treated with 10 ng/ml of trypsin gold (Promega, Madison, WI) in 50 mM ammonium bicarbonate for one hour on ice followed by overnight incubation at 37C. The extracted peptides were desalted using Millipore C18 Ziptip according to the manufacturer's instructions. Peptides from adjacent gel slices were combined to yield approximately 16 peptide samples for injection per treatment condition.

RP-LC. Capillary columns were prepared in-house using pulled and fritted capillaries purchased from New Objective. Capillaries were packed with 5um, 300A Vydac protein/peptide C18 material (Vydac, Hesperia, CA) to yield final column dimensions of 75 um ID X 160 mm with a 10 um tip. Samples were injected by manual injection with a Rheodyne injector possessing a 0.5ul internal sample loop. Chromatography was carried out on an Agilent micro-flow HPLC attached to a passive splitter which allowed about a 250 nl/min flow rate through the column. Peptides were eluted on a linear gradient from 0% B to 60% B (1.2% v/v/v in 93.8% acetonitrile, 5% water) over 120 minutes before equilibrating at starting conditions (Buffer A: 1.2% Acetic Acid (v/v) in water) over the following 80 minutes.

Tandem Mass Spectrometry. The LC was connected to an Applied Biosystems QStar XL, quadrupole-time-of-flight, equipped with a nanospray source and running Analyst version 1.0 [85]. Data was acquired during the entire chromatographic run (200 minutes) using an information dependent acquisition method with a16 second cycle time. Each cycle consisted of one MS scan (*m/z* 400-1800) followed by 3 MS/MS scans (*m/z* 100-2000) of the three most abundant ions exceeding 10 counts with a charge of 2 to 4 and *m/z* of 400 to 1800 and excluding previous ions and isotopes for 60 seconds.

Spectrum Mill data extraction, peptide validation, and protein identification and comparison. Data was analyzed using Spectrum Mill proteomics software Rev A.03.02.060. Raw data was extracted under default conditions. The data extractor extracted only spectra that have good signal to noise ratio (S/N>25), and all spectra that may represent peptide fragmentation (sequence tag > 1). The extracted data was searched against bovine sequences in the NCBInr database compiled in February of 2006 using trypsin as the protease, allowing 2 missed cleavages, and including variable modifications of oxidized methionine and N-terminal glutamine conversion to pyroglutamic acid in the search. Protein identification scores are calculated as the sum of the unique peptide scores, and a protein score of greater than 20 is considered sufficient for identity. Peptide identification scores are determined using a "shared peak count" scoring system where the 25 most abundant ions are matched with points given for b and y ions and unmatched ions result in penalties [86]. Peptides with a forward-reverse score of greater than 2 and a rank 1- rank 2 score of greater than 2 were considered valid with the following charge, score threshold, and % scored peak intensity (SPI): $z = 2$; score: 7.67, 60% SPI; $z = 1$, score: 7.67, 70% SPI; $z = 3$; score: 8.0, 70% SPI; $z = 4$; score: 8.0; 70% SPI. Doubly charged peptides were considered valid with a score greater than 7.67 and an SPI of 90% if the

differences in forward - reverse scoring and rank 1-2 score was greater than 1.0. These criteria should yield a false positive rate of less than 1% according to Kapp et al. [86]. Because the bovine database is not completely annotated and protein sequences not yet released, all unidentified spectra were subjected to a second search against the NCBInr mammalian databases in identity mode to increase chances of protein identification. Only proteins, with 2 or more validated peptides and a total score greater than 25, were considered valid for reporting. To compare proteins identified between each of the treatment groups, the number of spectra and summed ion intensity of peptides for each protein (total ion intensity) were used as indicators of protein amounts. Because these are semi-quantitative metrics, only qualitative information can be gained from this approach. Thus, we only consider those proteins with at least 5 additional spectra and at least a 10-fold increase in total ion intensity sufficiently different for reporting.

Spectrum Mill approach for Matrix degradation. To evaluate extracellular matrix degradation, we composed a database containing ECM proteins that were identified by the searches described above. To focus on matrix breakdown, we chose to eliminate all pro-peptides sequences from the matrix molecule protein sequences contained in our database. In order to achieve a complete database, we used as many bovine specific sequences as were available. The remainder of the protein sequences consisted of mammalian homologs that matched in the original Spectrum Mill identification search and of sequences that were spliced together between the bovine and the human protein sequences currently available. To allow better identification of collagens and other matrix molecules known to be rich in post-translational modifications, we added a number of "custom" amino acid modifications including hydroxyl-prolines, hydroxyl-lysine, sulfotyrosine, glucosamine N-linked to asparagines, and hexose O-linked to threonine or serine. These alterations to the search resulted in an efficient and focused search of the

maximum number of peptides (and their modifications) from the abundant ECM proteins. We set validation criteria slightly higher (peptides with a score >13; with all other criteria the same as described for standard identification procedures) and manually validated peptides with modifications. Using this method, we were able to identify modified peptides, particularly collagen type II peptides containing hydroxyproline and hydroxylysine modifications suggesting that both the database and the custom amino acid modifications were in fact picking out the appropriate spectra and proteins. Using our database consisting of only the structural regions of the ECM proteins of interest in conjunction with molecular weight obtained from the gel slice, we were able to identify signs of matrix degradation.

3.4 RESULTS

Explant treatment and culture. At least 3 explants per joint were taken from at least five different animals. Explants were allowed to rest one week before being subjected to mechanical compression, or treatment with 100 ng/ml TNF-α or 10 ng/ml IL-1β, or no treatment in 2 ml of serum-free DMEM without ITS. No difference was observed between the treatment groups. The medium was collected and pooled for analysis by SDS-PAGE-LC/MS/MS. The deglycosylated samples were subjected to SDS-PAGE followed by in-gel digestion of the gel slices to extract peptides [84]. The samples were then injected onto a reversed phase column connected to a QStar XL (quadrupole-time-of-flight) mass spectrometer with a nanospray source for peptide separation and data dependent MS/MS analysis for peptide identification.

Spectrum Mill Identification of proteins. Using an SDS-PAGE-LC/MS/MS technique and the Spectrum Mill criteria outline above, we identified 252 proteins with a score of 25 or greater which corresponds to MS/MS sequences that match 2 or more unique peptides from each protein. A complete list of identified proteins can be found in the supplementary table. Core

protein pIs ranged from <4.16 (aggrecan) to 11.06 (histone H2a) with the mean core protein pI of 6.86. The molecular weight (MW) similarly ranged from a core protein MW of ~482 kDa of perlecan to ~11 kDa of S100beta suggesting that the technique is compatible with proteins of varying pIs and MWs. The identification statistics for Spectrum Mill are shown in **Table 1** including the number of spectra collected and identified, the number of peptides identified, and the number of proteins identified. Using the identity conditions outline above and setting the threshold at 25, Spectrum Mill was able to identify approximately 15-20% of the spectra obtained for each sample set. Over 100 proteins per sample were identified with over 900 peptides positively identified from each sample. **Figure 2A** describes the overlap in identification between samples. For simplicity, TNF-α and IL-1β were grouped together as "cytokine" given that of the 153 and 138 proteins identified in each, 115 proteins were identified in common. The highest scoring and highest total intensity proteins were predominantly proteins that comprise the extracellular matrix. Among the 12 highest scoring cartilage proteins were aggrecan and collagen α 1 (II), perlecan, fibronectin, COMP, collagen α 1 (VI) and α 3 (VI), thrombospondin 1, and chitinase 3 like 1, link protein, and complement factor B. In addition to these proteins, we identified proteins such as AEBP1(likely ACLP)[87], CD109, scrapie-responsive protein 1, nucleobindin, and platelet derived growth factor receptor like protein, and peptidoglycan recognition protein all of which to our knowledge have not been identified previously in cartilage. We also identified a number of proteins recently described in cartilage including cytokine-like protein C17, CTGF, IL-17B, HTRA1, mimecan, retinoic acid binding protein, and follistatin like protein [88-98].

Differences between treatment groups. We wanted to focus on global differences and well as differences seen between individual proteins. **Figure 2B** is a set a pie graphs that show the

protein composition of the medium samples broken down by the protein location. While, both cytokine-treated samples look very similar to the control, the injury sample possesses a large number of intracellular proteins compared to the other treatments. To look more specifically at these differences, we have chosen to use spectra number and total ion intensity as an indicator to compare protein amounts between samples. Only differences of greater than 5 spectra and greater than 10 fold elevation in total ion intensity are reported. Based on these criteria, **Table 2** provides a list of elevated proteins, function, and location with the total ion intensity fold elevation over control or magnitude of total ion intensity (indicated by + signs) in the case when no spectra were identified in the control. Proteins increased in the medium in response to both IL-1β and TNF-α treatment include complement factor B, chitinase 3 like 1 and 2 (ykl39 and ykl40), MMP-3, clusterin, serum amyloid A3, ECM-1, haptoglobin, and acid-1-glycoprotein. In addition at the cutoff level specified, CD14, complement C1q α, lactoferrin, and C1r are also increased in the medium with IL-1β treatment, and VCAM-1, annexin A8, annexin A2, N-acetylmuramoyl-L-alanine amidase (PGRP-long), C1 inhibitor, and angiopoeitin-like 7 are increased only with TNF-α. While these proteins are somewhat of a mix, most appear to have something to do with innate immunity and stress response.

The largest increases in protein release to the medium in response to injury were due to prolyl-4-hydroxylase (beta subunit), GRP58, vimentin, alpha-4-actinin, pyruvate kinase, and UDP-glucose pyrophosphorylase, which are all intracellular proteins. GRP58 and prolyl-4-hydroxylase beta subunit are both protein disulfide isomerases, which reside in the endoplasmic reticulum and are important for the proper folding of proteins in the secretory pathway. Vimentin and alpha-actinin are proteins involved in actin cytoskeletal organization while pyruvate kinase M1/M2 is a key enzyme in the glycolysis pathway. Because the increase in

intracellular proteins suggests a loss of membrane integrity, we performed an anti-actin Western blot **(Figure 3a)** on medium from four sets of 3 mm diameter explants to verify the increases in intracellular protein release. **Figure 3a** shows that, in medium from four different experiments, mechanical injury increases release of actin to the medium with little variability, no band was visible with the untreated sample. This is consistent with the SDS-PAGE-LC/MS/MS findings and suggests that there is some loss of membrane integrity in a population of the chondrocytes present in the tissue.

In addition to the release of intracellular proteins, SDS-PAGE-LC/MS/MS results indicated that fibronectin, MMP-3, chitinase 3 like protein 1, and epiphycan, were also elevated in the medium compared to the control. Because fibronectin fragments are known to promote catabolic behavior of chondrocytes, an anti-fibronectin Western blot was performed on medium from 3 mm diameter explants to verify the increase in fibronectin release and to determine whether there were signs of fibronectin breakdown. Fibronectin release was increased with mechanical compression injury compared to the untreated controls in all four of the experiments **(Figure 3b)**. MMP-3 and chitinase 3 like protein 1 were also elevated in the cytokine-treated samples suggesting that there may be an overlap in response to these treatments, which is consistent with the findings of Gruber et al [81]. The increase in MMP-3 was verified by zymography (not shown).

Matrix protein degradation. One major focus of this work was to evaluate ECM degradation. The SDS-PAGE LC/MS/MS method provides molecular weight information that may be used to interpret whether the protein is full-length or cleaved to fragments of lower molecular weight. Using a custom database of matrix proteins that excludes sequences from signal peptides and telopeptides and searching for custom amino acid modifications that are known to exist in matrix

proteins, we searched for peptides from matrix protein in molecular weight regions that are smaller than that of the full length protein.

Using the methods outlined, proteins degraded irrespective of treatment and proteins that were degraded specifically with either cytokine or injury treatment were identified (Figure 4-7). The degradation data was graphed as total ion intensity versus approximate molecular weight which was based on the gel slice position and the proteins present within the slice. Each sample is represented by a different curve on the graph. Among those degraded regardless of treatment was thrombospondin 1 **(Figure 4)**. The increased total ion intensity (sum of all the peptide extracted ion intensities) at 30-50 kDa suggests that thrombospondin 1 is actively degraded and released into the medium irrespective of treatment conditions. A closer look at the peptides present in the gel slices from the 30-50 kDa region indicated that they are from the N-terminal region of the protein (first 500 or so amino acids).

Collagen type II, collagen type VI and COMP were among proteins that showed signs of proteolysis in the medium from the injuriously compressed explants. **Figure 5** is a graph of the fibril-forming region of collagen type II. The peak around 100-150 kDa represents the full-length collagen type II which appears to be most abundant in the untreated sample. The increase total ion intensity around 35 kDa and near 75 kDa in the injury sample is likely indicative of type II collagen proteolysis at or near the collagenase cleavage site. The finding of increased collagen degradation with injury is supported by Western blotting using an antibody that binds to a region within the C-terminal quarter fragment (not shown). This result is consistent with the findings from other injury models [68, 69].

Type VI collagen showed signs of degradation in response to injury compared to untreated explants as well. **Figure 6a** is a plot of all three type VI collagen subunits in the

control and injured samples. Collagen alpha 1 (VI) gave the highest intensity of all of the collagen VI subunits with a peak intensity at 100-150 kDa in the untreated and injured explant medium. An additional increase in intensity was also present at 50-75 kDa in the injury sample. Similarly, collagen alpha 3 (VI) and collagen alpha 2 (VI) had an elevated total ion intensity in the 50-75 kDa region consistent with proteolysis. To verify this finding, we performed a Western blot of type VI collagen to compare medium from untreated and injured explants from four different experiments **(Figure 6b)** using a polyclonal antibody against type VI collagen which may identify one or more of the collagen type VI subunits. A doublet at roughly 50-75 kDa may represent one or all of the collagen VI subunit fragments based on mass spectrometry data. Further, the band at 150 kDa fragment may correspond to the increase in either an alpha 3(VI) fragment or full-length alpha 1 (VI) based on the mass spectrometry findings. Together these data indicate a possible increase in collagen type VI subunit proteolysis in response to injury.

In addition to degradation of collagens, signs of COMP degradation were also evident with mechanical injury. **Figure 7** is a plot of COMP total ion intensity versus molecular weight. A peak at roughly 100 kDa is indicative of the full length protein. The shoulder in the band from IL-1 treated explants toward lower molecular weight is consistent with COMP cleavage from 120 kDa to the 110 kDa form which is frequently present with IL-1 treatment. The peaks at 60 kDa and 40 kDa in the injury sample may represent cleavage near the middle of the protein.

3.5 DISCUSSION

The purpose of the study was to characterize and compare, at the protein level, the cartilage tissue response to injurious mechanical compression and to treatment with pro-inflammatory cytokines, TNF-α and IL-1β, all of which are stimuli known to cause cartilage

damage and increase the risk of developing arthritis. Equal volumes of media from explants subjected to no treatment, to injurious mechanical compression, or to treatment with IL-1β or TNF-α were probed for differences in protein composition as well as protein degradation compared to the untreated (control) sample. Because of the small sGAG-associated variations in sample electrophoresis, because of the stochastic nature of the mass spectrometry analysis, and because of the small surface area differences between the 6 mm diameter and 4- 3mm diameter explants, a strict quantitative analysis of these data is not possible. However, a comparative study focusing on large differences is both useful and warranted. Total ion intensity is the sum of the extracted ion chromatograms for each of the peptide peaks identified for a protein, and it provides a means of performing a semi-quantitative comparison of the data to identify protein level differences [78]. Protein difference criteria were set high at a 10-fold elevation in total ion intensity and an increase in 5 spectra or more over the untreated sample to insure only good quality findings. Changes with mechanical injury compared to untreated controls were validated by immunoblotting using explants of the same geometry. Matrix protein degradation was determined using molecular weight information for each of the gel slice fractions, and a custom database was generated to exclude telopeptides and signal peptides from complicating analyses.

Proteins accumulated in the medium over the five days of culture represent a combination of new protein synthesis and secretion as well as passive diffusion of pre-existing proteins previously sequestered in the matrix. To help eliminate the contributions of sequestered plasma proteins, the cartilage explants were rested for seven days with four medium changes prior to treatment. Cartilage explants were incubated in treatment medium for five days because the sGAG accumulation in the medium plateaued between day 4 and day 5 of cytokine treatment suggesting the approaching of an equilibrium state following the treatment (data not shown) –

The early response of the cartilage to each treatment was represented in the accumulated protein in the medium. Although this experiment was not designed to distinguish between newly synthesized protein secretion and passive release of molecules from the matrix, the relative amount of some proteins in response to IL-1β and TNF-α treatment was many fold increased over the untreated control compared to the elevation of aggrecan suggesting that these proteins are newly synthesized rather than sequestered and then released from the matrix. Further support for new synthesis and secretion comes from the identity and biological activity of many of these proteins. Thus, the time scale and design of the experiment seemed suitable to identify differences among the various treatment groups.

As expected, many of the proteins present in the medium were present irrespective of treatment (**figure 2**). The matrix proteins were among the proteins present in all samples including collagen type II, XI, IX, VI, XII, XIV, XVI, and III. Proteoglycans and small leucine-rich repeat proteoglycans were also identified, including aggrecan, perlecan, NG2, lumican, fibromodulin, mimecan, biglycan, decorin, chondroadherin, and epiphycan. Other cartilage ECM proteins were also found including COMP, matrilin 1, matrilin 3, fibronectin, thrombospondin 1, nucleobindin, and osteonidogen.

In addition to the well-characterized cartilage proteins, other proteins such as CD109, scrapie responsive protein 1, platelet derived growth factor receptor like, angiopoeitin like 7, and peptidoglycan recognition proteins were also observed. CD109 is a 170 kDa GPI-linked protein recently identified as a member of the α-2-macroglobulin and the complement C3, C4, and C5 gene family, which are proteins which contain activated thioesters [99, 100]. The similarity of CD109 to α-2-macroglobulin suggests that it may serve as a protease inhibitor in cartilage. Alternatively, CD109 may play a role in complement activity as there is evidence of other

complement factors present in the tissue. Scrapie responsive protein 1 is a small secreted protein whose transcription is increased with that of glial fibrillary acidic protein following neuron infection with Creutzfeldt-Jakob disease [101, 102]. Glial fibrillary acidic protein has been previously identified in articular cartilage and cartilage tissue within gliomas [103-105]. No biological function has been attributed to scrapie like protein 1. Similarly, no biolgocal role for platelet derived growth factor receptor like protein has been reported beyond its similarity to the PDGF receptor; however we may speculate that release of this protein may represent a way of regulating the PDGF pathway in cartilage. Angiopoeitin-like-7 has been identified as a product of the cornea stromal cells, and it may serve to inhibit angiogenesis and promote cornea stromal cell phenotype [106, 107]. Finally, peptidoglycan recognition protein L (PGRP-L), or N-acetylmuramoyl-L-alanine amidase, was also released from the cartilage [108, 109]. PGRP-L, a transmembrane and secreted protein, is capable of binding and cleaving the lactylamide bond between the peptide chain and muramic acid of the peptidoglycans which form the cell wall of bacteria [109-111]. While the family of PGRPs are generally bacteriolytic, PGRP-L may play a role in decreasing the biologic response to peptidoglycans [110, 112]. The release of PGRP-L may aid in quelling the inflammatory response to peptidoglycan. The presence of these proteins suggests that the cartilage and likely chondrocytes play a role in regulating pathways as diverse as angiogenesis and innate immunity.

Proteins listed in **Table 2** are elevated with each treatment compared to the untreated control. Overall, the proteins identified with IL-1β treatment and TNF-α treatment were similar suggesting that the cytokines may have similar global effects, which include the secretion of proteins including chitinase 3 like protein 1 and 2, MMP-3, complement factor B, haptoglobin, and serum amyloid A3. Chitinase 3 like 2 but not chitinase like 1 may be elevated with OA

[113]. Chitinase 3 like 1 is elevated by IL-1 treatment in rat cartilage explants but not in human explants [113-115]. This may represent a species-specific difference or could possibly result from differences in experimental methods. Addition of chitinase 3 like 1 counters the effects of IL-1, suggesting that it may be tissue protective [116]. Complement factor B expression is elevated in OA cartilage compared to normal cartilage, and it is also expressed in developing cartilage [88, 117]. Lactoferrin is not known to be expressed by chondrocytes, but it has been identified in articular joints together with lysozyme, RNase7, and β-defensin 2 and 3 [118] and does play a role in innate immunity.

Serum amyloid A, haptoglobin and alpha-1-acid glycoprotein are acute phase proteins that were increased with IL-1β and TNF-α treatment. Gruber et al. noted an increase in protein synthesis of porcine serum amyloid A3 when the tissue was treated with IL-1β [81]. Furthermore bovine serum amyloid A3 is similar to human serum amyloid A, which is elevated in synovial fluid of patients with rheumatoid arthritis [77, 78, 119, 120]. Similarly, elevation of haptoglobin is associated with increased RA severity, and alpha-1-acid glycoprotein glycation varies in synovial fluid of RA patients compared to normal suggesting that there may be local expression in the joint [77, 121, 122]. While elevated serum amyloid A, complement factor B, alpha-1-acid glycoprotein, and haptoglobin in synovial fluid has been attributed the systemic response to inflammation, the cartilage itself may be contributing to the production of these proteins and may increase the local concentration of these proteins, which may play a role in the disease process. For example, serum amyloid A3 induces an increase in catabolic behavior by chondrocytes which suggests that it may play an active role in degradation [119].

In addition to secreted proteins, membrane proteins CD14 and VCAM-1 were elevated by IL-1β and TNF-α treatment respectively. VCAM-1 is increased in TNF-α treated medium,

and previous work indicates that chondrocytes increase expression of VCAM-1 when treated with IL-1 and TNF-α [33]. Additionally, VCAM-1 is shed from endothelial cells in response to IL-1 and TNF-α treatment possibly through the action of a metalloproteinase [123, 124]. VCAM-1 is known to be expressed in synovial tissue and soluble VCAM-1 in synovial fluid and serum correlates with RA severity[125-127]. CD14 is expressed on the surface of chondrocytes by FACs analysis, although the antigen is susceptible to degradation during enzymatic cell isolation[128]. Our results suggest that CD14 may be released in response to IL-1β treatment. Soluble CD14 may be important to enhance the LPS response in tissue expressing no or low copy number of CD14 [129] consistent with its role in LPS signaling.

While TNF-α induced some changes similar to mechanical compression injury, the latter produced proteins that were globally different from the other three treatments in that there were a higher proportion of intracellular proteins present. As indicated in **Table 2**, most proteins elevated in the medium of explants subjected to radially-unconfined compression injury are of intracellular origin suggesting that membrane integrity in at least a subpopulation of cells must have been compromised. To verify the release of intracellular proteins, we performed an anti-actin immunoblot on medium from four different experiments comparing untreated (free swell explants) medium from explants subjected to mechanical injury. The Western blot analysis confirmed the SDS-PAGE finding that explants subjected to mechanical injury release actin and thus likely the other intracellular proteins identified in **Table 2**.

Loss of membrane integrity may occur with both apoptosis and necrosis; however the release of ER and heat shock proteins is more common during necrosis than apoptosis [130]. Some of the heat shock proteins, namely hsp70, gp96, and calreticulin, may serve as adjuvants when complexed with antigenic peptides and presented to antigen-presenting cells (APCs) [131-

134]. This ability to stimulate antigen-specific immunity may be dictated through binding to CD91, lipoprotein receptor like protein, on APCs [134, 135]. At the same time, previous work on this injury model implicates apoptosis as the primary mechanism of cell death—both TUNEL and EM imaging support this finding [63, 136]. These microscopic evaluations characterizing apoptosis and necrosis avoided the explant periphery, as it is common to have cell death due to cutting which could complicate the interpretation of the effects of loading [63, 137].

Work done with confined and unconfined compression injury models suggests that cell death, as determined by live-dead assay, is most abundant at the explant surface or around the periphery of the explant where the strain is highest [68, 69, 73, 138, 139]. Lucchinetti et al. also reported that chondrocytes nearest to the loading surface in confined loading were not only dead by live-dead cell assay but stained negative by TUNEL suggesting necrotic cell death. This cell death occurred over 6-12 hours of stress-controlled loading in which creep may play a role in cell death. Because the peripheral regions are typically excluded from apoptosis/necrosis characterization, it is possible that these cells may be undergoing mechanical lysis or necrosis and have not been well-characterized beyond live-dead cell assays.

Loss of membrane integrity with apoptosis is likely to occur over time during the five-day culture period, while mechanical cell lysis is likely to occur at the time of injury and intracellular proteins are released relatively rapidly in culture. Using medium collected over the five days in culture, we compared actin release at day 1 and day 4 to determine whether release of actin occurred at early time points or whether it accumulated over time. **Figure 8** shows a representative actin immunoblot, which suggests that release of actin occurred primarily in the first 24 hours in culture, consistent with loss of membrane integrity as a result of acute mechanical cell lyses. While some leaking of intracellular proteins may occur with time, this

early release of intracellular proteins indicates that mechanical disruption is likely a primary mechanism of actin release in this unconfined compression model. While cells in the internal portion of the cartilage explants are susceptible to apoptosis, a population of cells at the surface, on the periphery, and around the occasional blood vessel found in these immature cartilage explants may experience mechanical disruption in response to the high strain. However, we cannot rule out the possibility that there is population of cells that may leak some intracellular proteins, yet they still appear to undergo apoptosis by TUNEL or EM. These results extend the previous work using this unconfined compression injury model by demonstrating that there may be spacial, or at least population, differences in the chondrocyte response to the unconfined compression.

The final major goal of this work was to identify protein degradation fragments released into the medium. The SDS-PAGE-LC/MS/MS method provides a means to probe for matrix protein degradation by proteolysis. Inflammatory cytokines are known to increase the release of a number of proteases that can degrade matrix structural proteins -- such as aggrecan, collagens, COMP, and matrilins; however, much less is known about whether matrix damage by mechanical compression injury leads to matrix remodeling. Thrombospondin 1, a protein that links the chondrocytes to their surrounding matrix, showed signs of degradation in all samples analyzed (**Figure 4**). Thrombospondin 1 is present on platelets and is readily cleaved by thrombin to release a 30 kDa heparin binding fragment and a 150 kDa fragment, and both fragments are capable of binding to fibronectin [140, 141]. In addition, thrombospondin 1 is known to bind to pro-MMP-2 and active MMP-2 as well as LRP1 (LDL receptor like protein 1) suggesting that it may play a role in the clearance of MMP-2 by LRP1 in the pericellular matrix of chondrocytes [142]. Thrombospondin 1 has also been implicated in the activation of latent

TGF-beta [143]. Because all samples show signs of thrombospondin 1 proteolysis, this breakdown cannot be attributed to any of the treatment in this study. However, such a means of MMP-2 regulation may be plausible in this tissue, and degradation of thrombospondin-1 may reflect normal remodeling regulation of the chondrocyte pericellular matrix. More work will need to be done to test whether thrombospondin 1 is playing a role in gelatinase regulation in cartilage.

Signs of protein degradation with injury include fibronectin, collagen type II, collagen type VI, COMP and aggrecan. As indicated in **Figure 3b**, injury causes an increase in fibronectin release. Injury also causes a small increase in fibronectin proteolysis as indicated by the laddering of bands seen on immunoblot which are more pronounced in the injured explant medium compared to the untreated explant medium (not shown). The increase in fibronectin release with injury is consistent with previous work by Burton-Wurster et al. who showed that compressive loading increases synthesis of fibronectin [144-146]. Fibronectin accumulation is increased in OA cartilage compared to cartilage from healthy joints [147, 148]. In addition, some fibronectin fragments may provoke a catabolic response by chondrocytes [149], so more specific evaluation of the role of fibronectin fragments with injury may be warranted.

Searching with custom amino acid modifications, we were able to identify a small increase in collagen type II staining around the 25 kDa region suggesting an increase in type II collagen fibril degradation which we were able to show by western blotting and is consistent with previous injury models [68, 69]. These data are consistent with the hypothesis that mechanical injury causes collagen proteolysis secondary to collagen fibril denaturation [68]; however because this is young tissue, proteolysis of newly synthesized collagen cannot be excluded as a possible explanation.

Collagen type VI also showed signs of possible degradation with a particularly large increase the roughly 75 kDa band from collagen alpha 1 (VI) and a less dramatic fragment of collagen alpha 3 (VI) around 150 kDa **(Figure 6A)**. Using an antibody to type VI collagen, we were able to detect bands in the molecular weight region consistent with the collagen alpha 1 (VI) and collagen alpha 3 (VI) fragments. These data may represent an increase in collagen type VI subunit proteolysis; however it is unclear whether this is indicative of damage to the matrix or to newly synthesized collagen VI subunits. Previous work indicates that mature cartilage pericellular matrix (PCM) may stain more intensely for collagen VI than immature cartilage[150, 151]. Work on the mechanical properties of the chondron suggests that while the PCM is much more compliant than the surrounding ECM, and the variations in the PCM stiffness may still be important in transmitting forces to the chondrocyte [152] . Work on correlating load induced cell death to the collagen VI staining intensity in the PCM indicates that 1 MPa loading for 1 hr caused a generalized flattening of the superficial zone chondrocyte PCM in immature compared to mature tissue [150]. It is possible that this flattening of the PCM may be associated with damage to the collagen VI network which could explain the apparent collagen VI fragment release in this study.

Mass spectrometry analysis indicated signs of COMP degradation **(Figure 7)** with injury and possibly with IL-1β treatment. COMP release from cartilage is known to be elevated in response to exercise and to injury [153-157], and COMP levels in serum and synovial fluid correlates with arthritic disease progression [157]. COMP fragments between 50 and 90 kDa have also been identified in synovial fluid from RA, OA, and reactive arthritis patients; and these fragments may be produced by synovial fibroblasts *in vitro* [158, 159]. Small COMP fragments (50-90 kDa) have also been demonstrated in synovial fluid within the first 2 months after

anterior cruciate ligament tear but not in synovial fluid from the healthy contralateral knee joint [160]. The results of this study indicate the injurious mechanical compression may cause the release of 50-70 kDa COMP fragments from cartilage, which may be the source of some of the COMP fragments identified in synovial fluid *in vivo*. COMP fragmentation with injury could be the result of mechanical denaturation and proteolysis of the pentameric COMP molecule or it may be the result of increase protease activity. In addition, COMP fragmentation in response to IL-1β treatment leads to the release of a 110kDa and a 10 kDa fragment respectively, and this activity may be mediated by ADAMTS4 [48].

The SDS-PAGE-LC/MS/MS was chosen because it provided a means to do systems level profiling as well as identify signs of protein degradation both of which were important in characterizing the effects of mechanical injury and inflammatory cytokine treatment. The power of this study is the ability to look at protein differences and protein degradation at a systems-level without being limited to proteins already known to be present in the system. The weakness is that the study does not provide quantitative data, that the study is limited to high abundance proteins, and that the findings are only correlations in which further work will be necessary to ascertain mechanisms and causation. The profiling aided in the identification of small secreted factors in response to IL-1β and TNF-α and the molecular weight information from the gel allowed protein degradation to be carefully evaluated for a number of matrix proteins in response to mechanical injury. In response to IL-1β and TNF-α cartilage explants release complement proteins, acute phase proteins, and stress response proteins as well as aggrecan fragments. We were surprised by the predominantly "generic" response. Acute phase proteins are predominantly produced by the liver in response to IL-6 even though IL-1β and TNF-α are sufficient to release some of these proteins [161]. While the presence of these proteins may be

the result of sequestered plasma proteins in the explant, the seven day rest period and large differences between treatments suggests that acute phase and complement proteins are likely the result of new protein synthesis in response to the cytokine treatment. The results of this study indicate chondrocytes are also capable of producing several of the acute phase and complement proteins in response to TNF-α and IL-1β, many of which play a role in innate immunity.

Explants subjected to this unconfined compression injury model have been shown to display changes in gene expression, small but significant loss of sGAG, apoptosis, changes in biosynthesis, and dynamic tissue stiffness [63, 71, 73, 75, 136]. This study demonstrates that injury is causing loss of cell membrane integrity early after injury which may be indicative of mechanical cell disruption and may be in part responsible for the decrease in biosynthesis. In addition the release of intracellular proteins may cause a change in gene expression or trigger apoptosis in surrounding cells. Release of matrix proteins and protein fragments with mechanical compression injury suggests damage to the matrix which is supported by the change in dynamic modulus. Damage to the matrix may lead to changes in cell-matrix interactions which could be responsible for apoptosis, for changes in gene expression, or for the decrease in dynamic compression induced stimulation of biosynthesis.

This work describes differences in cartilage and chondrocyte protein level response to mechanical injury and treatment with inflammatory cytokines TNF-α and IL-1β compared to control. In this work we identified proteins that were increased in response to treatment including intracellular proteins involved protein folding, glycolysis, and cytoskeletal structure with injury and proteins involved in innate immune or stress response such as MMP3, ykl39, ykl40, haptoglobin, lactoferrin complement factor B, serum amyloid A3, and clusterin. In addition we used the molecular weight information from the SDS-PAGE, to identify proteolysis

of thrombospondin 1, collagen type II and VI, fibronectin, aggrecan and COMP. Overall, this method provided information about cartilage damage and chondrocyte response to known damaging stimuli.

Acknowledgements. I would like to thank Dr. Vadiraja Bhat for his technical assistance with this work.

3.6 FIGURES
Figure 3.1

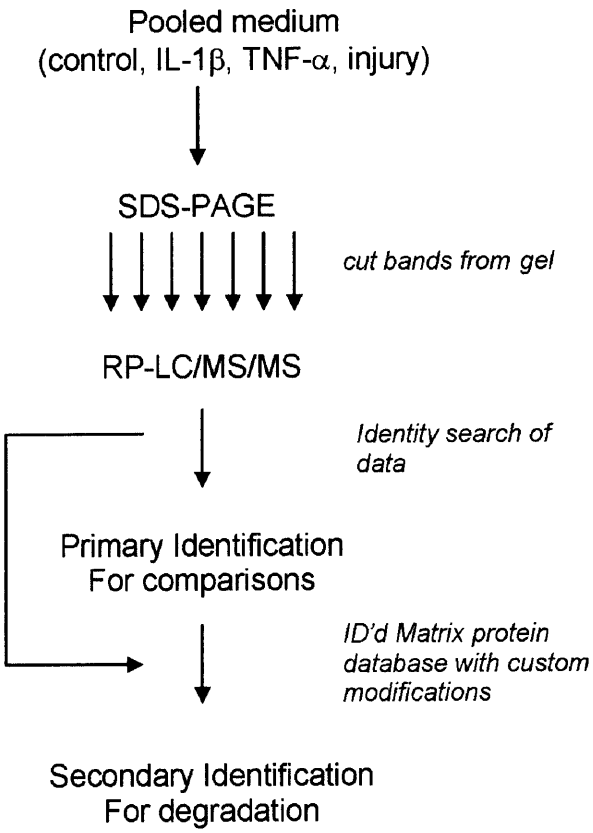

Figure 1: Flow chart of SDS-PAGE-LC/MS/MS approach used for protein identification and comparisons as well as degradation. Like samples are pooled together and separated out by SDS-PAGE. Gels are divided into 17 +/- 1 fraction for nano-RP-LC/MS/MS analysis. Data collected is searched in identity mode (modifications limited to pyroglutamic acid and oxidized methionine). Based on these results, the sequences (excluding signal sequences and telopeptides) from the highest scoring matrix proteins were entered into a custom database, and the data was subjected to a second global search which include modifications that were known to be present in matrix proteins including hydroxyl-proline, hydroxylysine, N-linked hexosamine, sulfotyrosine,

Table 3.1

ID statistics	Control	IL-1β	TNF-α	Injury
# extracted spectra	15238	16974	21525	21689
# identified spectra	3407	6466	6001	4252
# peptides	994	931	1136	1200
# proteins identified (SCORE >25)	114	139	153	167
# protein ID'd by bovine database	106	125	136	153

Table 1: Spectrum Mill identification statistics. Identification statistics for each sample is shown above including the number of extracted spectra, number of identified spectra, number of peptides, number of proteins identified by 2 peptides and a score of greater than 25, and number of proteins that were identified with the bovine database (which included at least a partial sequence of each of the identified proteins)

Figure 3.2
Figure 3.2a

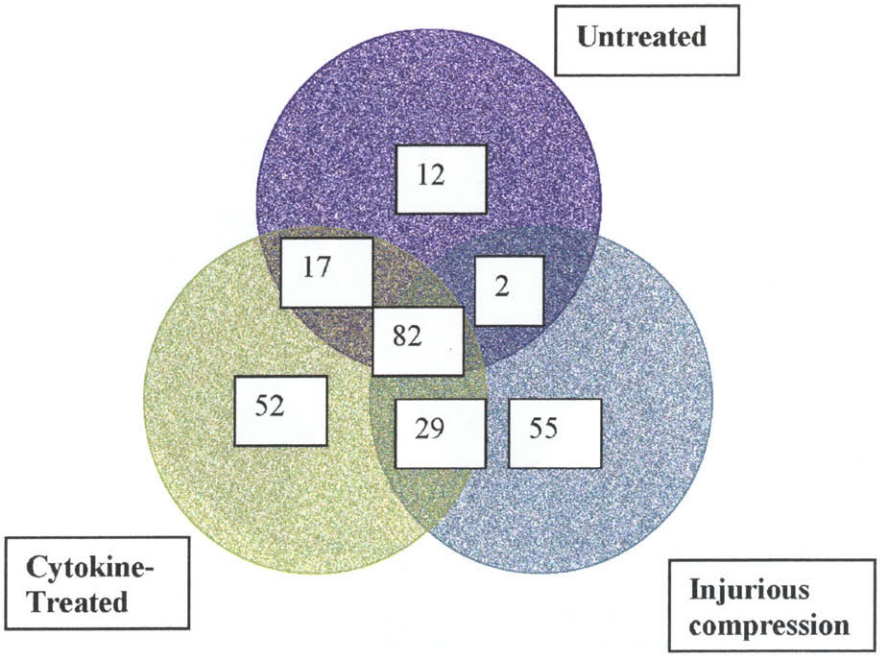

Figure 2: Global analysis of proteins identified with each experimental condition. Figure 2A is a Venn diagram of the proteins identified in the untreated, injuriously compressed, and the cytokine-treated (which includes both TNF-α and IL-1β). Eighty-two proteins were identified among all four samples while 119 proteins were identified in only a single treatment class. Significant overlap was noted between the TNF-α and IL-1β such that 115 of the 153 and 138 proteins were identified by both respectively. **Figure 2B** are a pie charts describing the composition of the medium protein samples based on the protein location. This figure shows a larger component of intracellular proteins in the injury samples compared to the other treatments.

Figure 3.2b

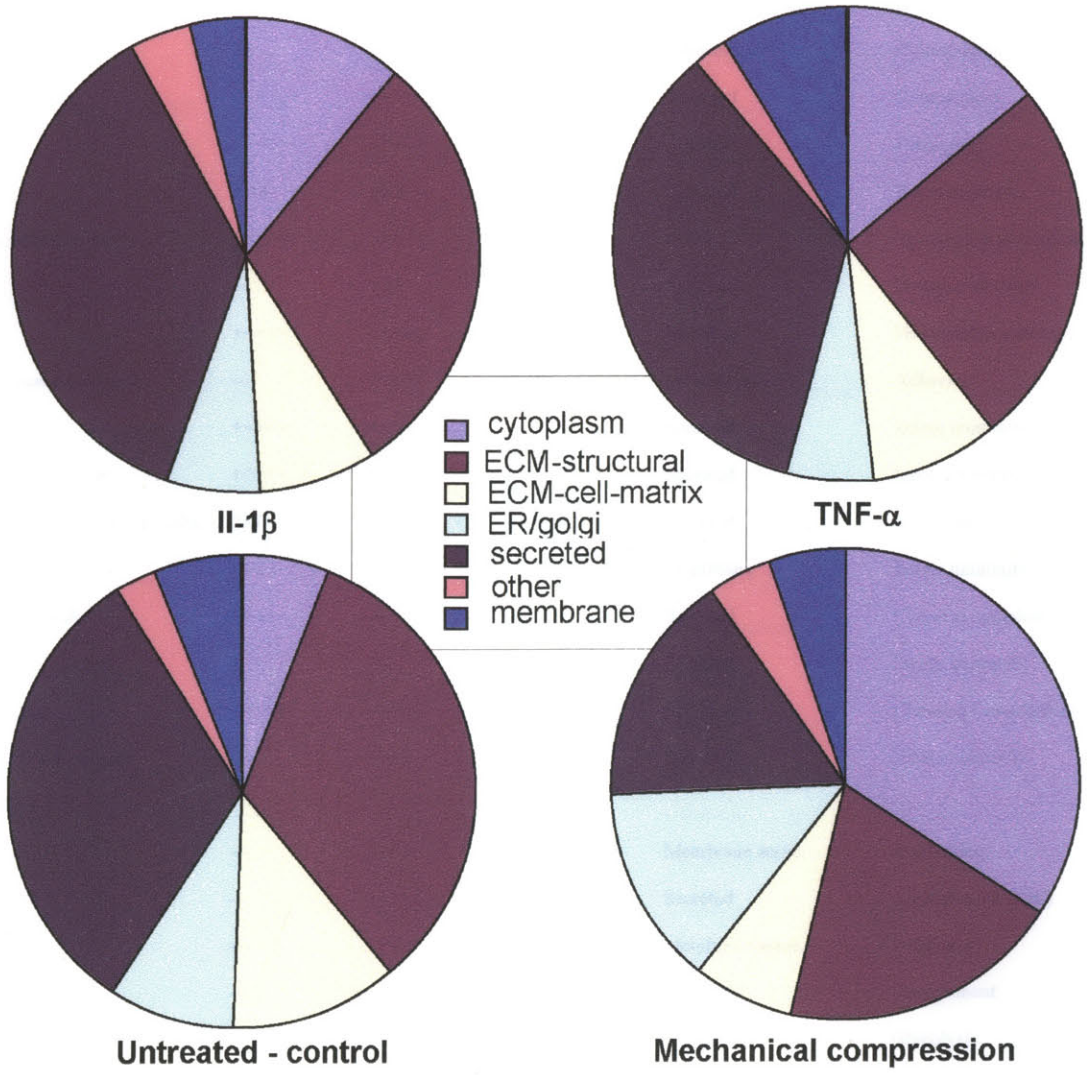
cytoplasm
ECM-structural
ECM-cell-matrix
ER/golgi
secreted
other
membrane
Il-1β
TNF-α
Untreated - control
Mechanical compression

Table 3.2

Protein Name	IL-1β Fold elevation	TNF-α Fold elevation	Injury Fold elevation	Protein Location	Protein Function
Chitinase 3 like 1 isof. 2	200	99	14.2	Secreted	Stress response
Stromelysin 1 (MMP-3)	++++++	+++++	+++++	Secreted	Metalloproteinase
Peroxiredoxin 1	++++	++++	+++++	Cytoplasm	Redox
Vimentin	38	35	283	Intracellular	Cytoskeleton
Complement factor B	++++++	++++++	---	Secreted	Complement
Chitinase 3 like 2	++++++	+++++	---	Secreted	Unknown
Clusterin	11.8	17.8	---	Secreted	Stress response
Extracellular matrix protein 1	++++++	+++++	---	ECM	Structural organization
C1 inhibitor	---	12.1	---	Secreted	Protease inhibitor
Haptoglobin	+++++	++++	---	Secreted	Hemoglobin scavenger
Vascular adhesion molecule 1	---	+++++	---	Membrane	Adhesion
Serum amyloid A3	+++++	+++++	---	Secreted	Innate immunity/stress
Alpha-1-acid glycoprotein	+++++	+++++	---	Secreted	Innate immunity
Neutrophil gelatinase assoc. lipocalin	23.0	---	---	Secreted	Lipocalin
CD14	+++++	---	---	Membrane	Innate immunity
Complement C1q alpha	+++++	---	---	Secreted	Classical complement
Lactoferrin	+++++	---	---	Secreted	Innate immunity
Complement C1r	+++++	---	---	Secreted	Classical Complement
N-acetylmuramoyl-L-alanine amidase (PGRP-L)	---	++++	---	Secreted	Innate immunity
Annexin 1	---	++++	---	Membrane assoc.	Trafficking
Angiopoeitin like 7	--	+++++	---	Secreted	Angiogenesis (anti)
Annexin A8	---	++++	---	Membrane assoc.	Unknown
Complement C3	---	++++	---	Secreted	Complement
Triosephosphate isomerase	---	+++++	+++++	Cytoplasm	Glycolysis
Lactate dehydrogenase A	---	++++	+++++	Cytoplasm	Metabolism
Beta actin	---	+++++	++++++	Intracellular	Cytoskeleton
Collagen alpha 2 (VI)	12.1	---	10.2	ECM	Structural
14-3-3 theta	---	++++	+++++	Cytoplasm	Regulatory
Annexin A2	---	++++	++++	Membrane assoc.	Trafficking
Proline hydroxylase alpha	---	---	15.6	Endoplasmic reticulum	Post-translation mod.
Actinin alpha 4	---	---	307	Intracellular	Cytoskeleton

Glucose regulated 58 kDa (GRP-58)	---	---	+++++	Endoplasmic reticulum	Protein folding (PDI)
Fibronectin	---	---	13	ECM	Cell_matrix interactions
Pyruvate kinase M1/M2	---	---	+++++	Cytoplasm	Glycolysis
UDP-glucose pyrophosphorylase 2	---	---	+++++	Cytoplasm	Metabolism
Cytoskeletal associated protein 4	---	---	+++++	Intracellular	Cytoskeleton
Protein disulfide isom. A6 (PDI-A6)	---	---	+++++	Endoplasmic reticulum	Protein folding (PDI)
Hsp90 alpha	---	---	+++++	Cytoplasm	Protein folding
78 kDa glucose regulated (GRP-78)	---	---	+++++	Endoplasmic reticulum	Protein folding/assembly
Phosphoglycerate kinase 1	---	---	+++++	Cytoplasm	Glycolysis
Tumor rejection antigen 1 (gp96)	---	---	+++++	Endoplasmic reticulum	Protein assembly/transport
Dermatan sulfate proteoglycan 3 (epiphycan)	---	---	+++++	ECM	SLRP
Protein disulfide isomerase A4 (ERp72)	---	---	+++++	Endoplasmic reticulum	Protein folding (PDI)
Lysine hydroxylase	---	---	+++++	Endoplasmic reticulum	PTM
ERp46	---	---	+++++	Endoplasmic reticulum	Protein folding
Glucose-6-phosphate isomerase	---	---	+++++	Cytoplasm	Metabolism
Calreticulin	---	---	+++++	Endoplasmic reticulum	Protein folding
Nucleotide diphosphate kianse	---	---	+++++	Cytoplasm	Metabolism
FK506 binding protein 9	---	---	+++++	Endoplasmic reticulum	Protein folding
Rab GDI beta	---	---	++++	Cytoplasm	Signaling
Parkisons disease 7	---	---	+++++	Cytoplasm	Unknown
Enolase 1	---	---	+++++	Cytoplasm	Glycolysis
PRDX2	---	---	++++	Cytoplasm	Redox
Collagen alpha 1 (IX)	---	---	0.02	ECM	Structural
Collagen alpha 1 (XVI)	---	---	0.08	ECM	Structural
MMP-2	---	---	0.09	Secreted	Metalloproteinase
Fibulin 4	---	0	---	Secreted	
PDGF receptor-like protein	---	---	0	Membrane	Receptor?

Table 2: Proteins identified by SDS-PAGE-LC/MS/MS from medium samples collected from cartilage treated with IL-1β, TNF-α, or unconfined compression injury. The proteins listed represent those proteins identified to be elevated with treatment compared to the untreated control. The table contains fold increase in total ion intensity over control, or if no spectra are identified in the untreated sample, the + signs represent the order of magnitude of the total ion intensity of each of the proteins.

Figure 3.3

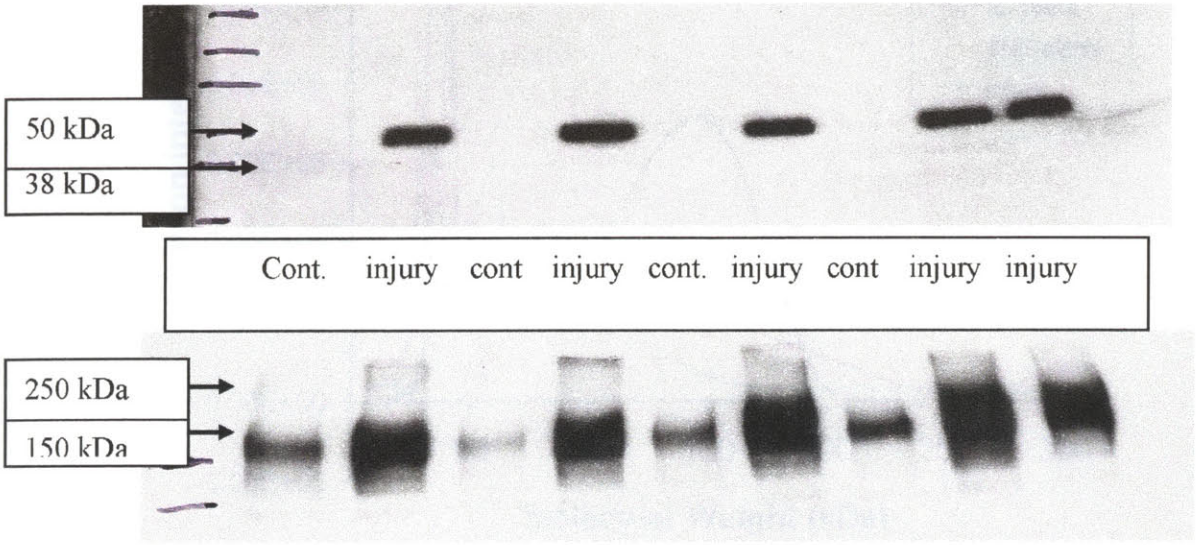

Figure 3A: Anti-Actin western blot of medium from explants subjected to injurious mechanical compression or untreated from four different experiments. The blot represents medium from four different explant experiments with each control and injury samples in adjacent lanes. These results indicate that mechanical compression injury causes release of actin and suggest possible loss of membrane integrity in at least a fraction of chondrocytes.
Figure 3B: Anti-fibronectin western blot of medium from explants subjected to injurious mechanical compression or untreated from four different experiments which ordered according to experiment with the untreated and injured samples adjacent for comparison. These results suggest that injury causes an increase in fibronectin release and breakdown (laddering more pronounced with longer exposure).

Figure 3.4

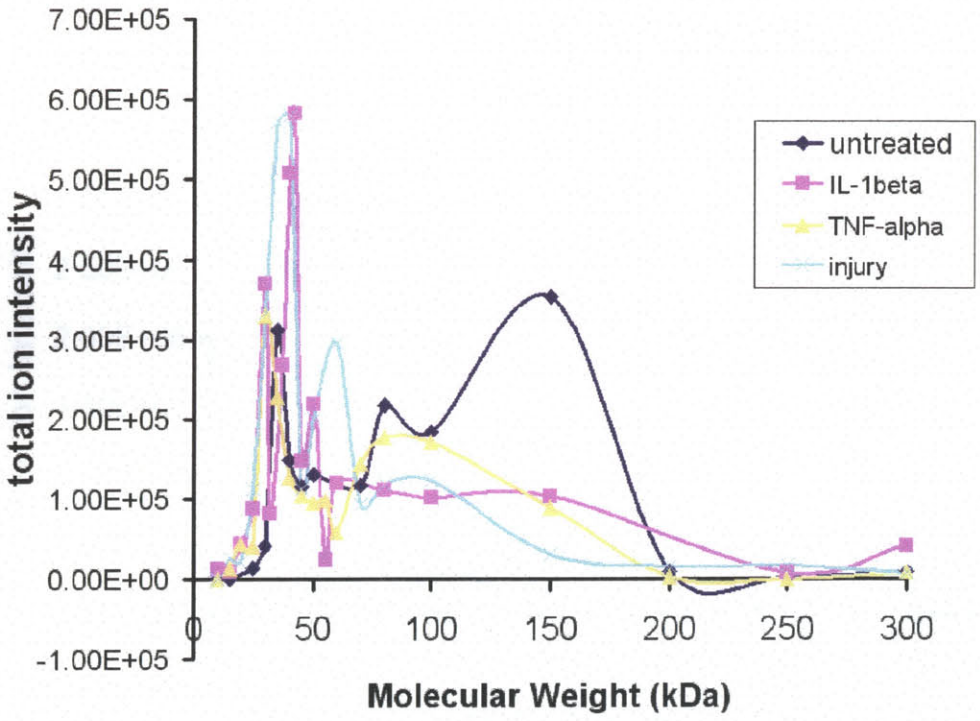

Figure 4: Graph of Thrombospondin 1 total ion intensity vs. molecular weight (MW) (as determined by proteins present in each slice). To determine whether matrix proteins were being broken down, we graphed the total ion intensity (summed ion intensity for all the peptides for thrombospondin in each gel slice and for each sample) versus the approximate molecular weight of each gel slice. Full length thrombopondin 1 has a molecular weight of approximately 130-180 kDa. Increased ion intensity in the 30-50 kDa regions indicates thrombospondin fragments which appear in all four treatment groups..

Figure 3.5

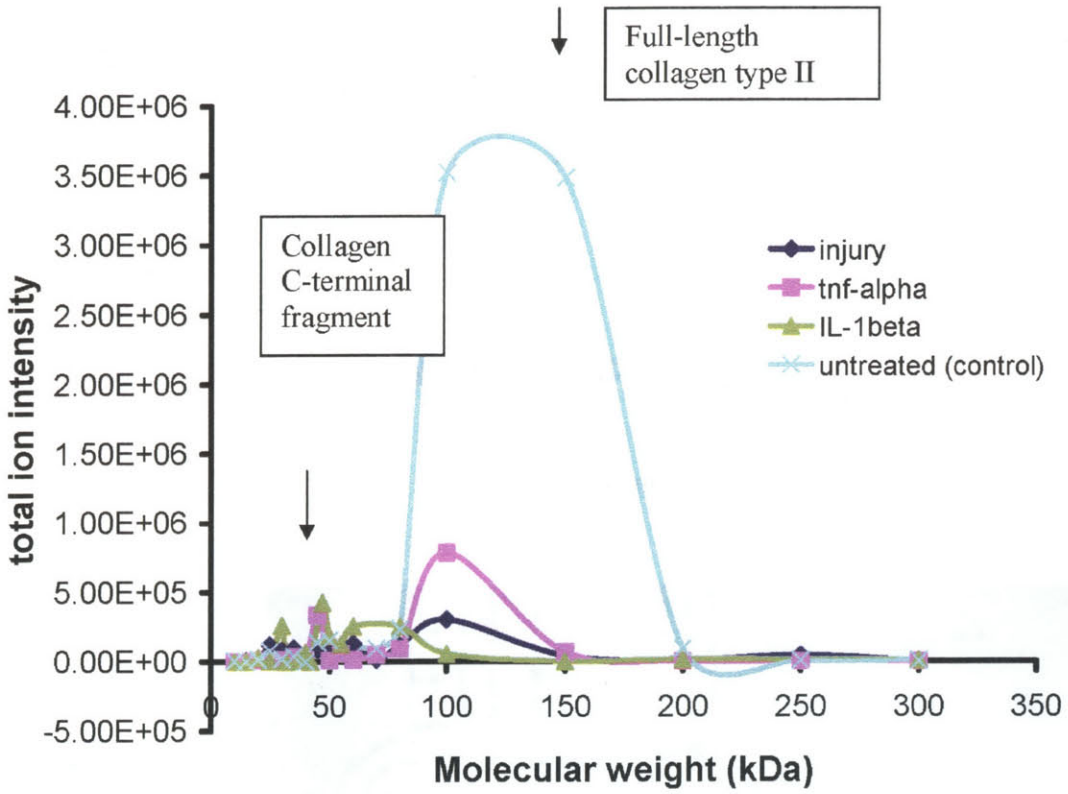

Figure 5: **Total ion intensity of peptides from the fibril portion of type II collagen release** as a function of molecular weight. The high intensity peak in the control sample at 100-150 kDa is indicative of full-length type II collagen release probably as a result of passive release of newly synthesized type II collagen. The sample subjected to injurious mechanical compression shows a slight increase in total ion intensity in the 20-35 kDa regions with peptides corresponding to the C-terminus suggesting collagen degradation possibly at the collagenase cleavage site.

Figure 3.6

Figure 3.6a

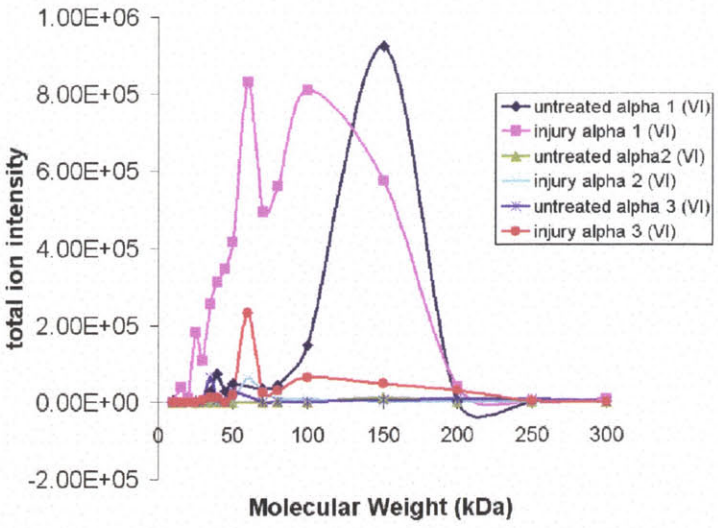

Figure 3.6b

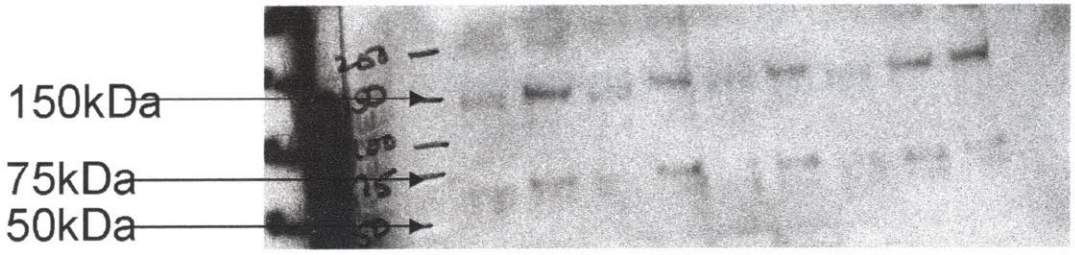

Figure 6A and 6B: **Collagen type VI degradation.** Figure 6A indicates the total ion intensity for each of the three collagen VI subunits vs approximate molecular weight (as determined by molecular weight marker and protein constituents) of untreated and injured medium from cartilage explants. Both collagen alpha 1 (VI) and collagen alpha 3 (VI) possess an increased intensity in the 50-75 kDa regions that is likely indicative of collagen VI breakdown. Figure 6B is a immunoblot of collagen type VI which indicates a stronger band at 150 kDa with injury as well as a doublet between 50 and 75 kDa in which the upper band appears to be more intense in the injury samples.

Figure 3.7

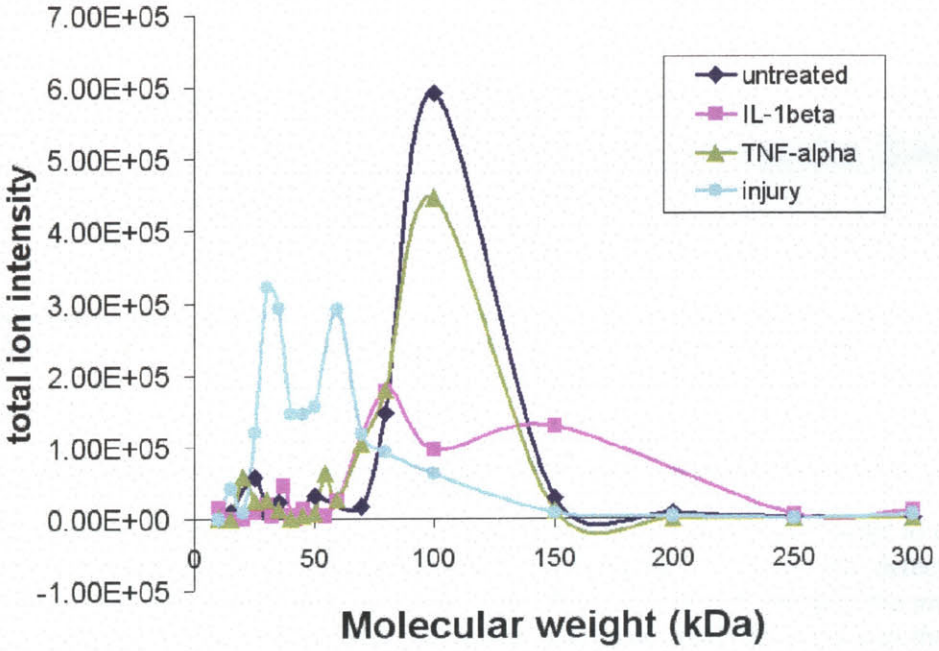

Figure 7A: COMP degradation in response to mechanical injury and treatment with cytokines, TNF-α and IL-1β, compared to control. The shift in COMP total ion intensity to lower molecular weight with mechanical injury suggests that COMP may be degraded in response to injury.

Figure 3.8

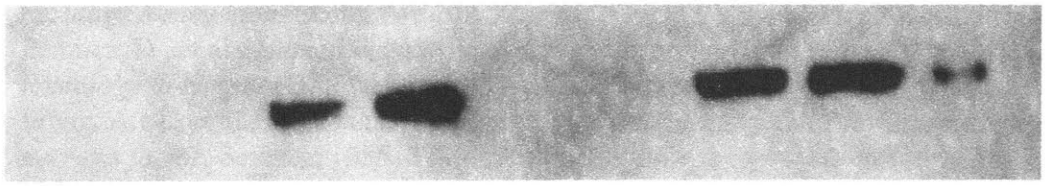

Cont. 24 hrs	Cont 96 hrs	Injury 24 hrs	Injury 96 hrs	Cont 24 hrs	Cont 96 hrs	Injury 24hrs	Injury 96 hrs	Cell lysis Pos. cont

Figure 8 is a representative anti-actin immunoblot from two different experiments to compare actin release to the medium at 24 hour and the 96 hour time point. Actin is only detected with injury and in the cell lysis (as a positive control), and there is little difference in the intensity of the bands at 24 hours and at 96 hours indicating that actin is primarily released into the medium within the first 24 hours of injury. This early release is suggestive of mechanical cell lysis.

3.7 REFERENCES

1. Maroudas, A.I., *Balance between swelling pressure and collagen tension in normal and degenerate cartilage.* Nature, 1976. **260**(5554): p. 808-9.
2. Grodzinsky, A.J., *Electromechanical and physicochemical properties of connective tissue.* Crit Rev Biomed Eng, 1983. **9**(2): p. 133-99.
3. Shinmei, M., et al., *Interleukin 1, tumor necrosis factor, and interleukin 6 as mediators of cartilage destruction.* Semin Arthritis Rheum, 1989. **18**(3 Suppl 1): p. 27-32.
4. Pennica, D., et al., *Human tumour necrosis factor: precursor structure, expression and homology to lymphotoxin.* Nature, 1984. **312**(5996): p. 724-9.
5. Wang, A.M., et al., *Molecular cloning of the complementary DNA for human tumor necrosis factor.* Science, 1985. **228**(4696): p. 149-54.
6. Hopkins, S.J. and A. Meager, *Cytokines in synovial fluid: II. The presence of tumour necrosis factor and interferon.* Clin Exp Immunol, 1988. **73**(1): p. 88-92.
7. Saxne, T., et al., *Detection of tumor necrosis factor alpha but not tumor necrosis factor beta in rheumatoid arthritis synovial fluid and serum.* Arthritis Rheum, 1988. **31**(8): p. 1041-5.
8. Di Giovine, F.S., G. Nuki, and G.W. Duff, *Tumour necrosis factor in synovial exudates.* Ann Rheum Dis, 1988. **47**(9): p. 768-72.
9. Westacott, C.I., et al., *Synovial fluid concentration of five different cytokines in rheumatic diseases.* Ann Rheum Dis, 1990. **49**(9): p. 676-81.
10. Elliott, M.J., et al., *Treatment of rheumatoid arthritis with chimeric monoclonal antibodies to tumor necrosis factor alpha.* Arthritis Rheum, 1993. **36**(12): p. 1681-90.
11. Ohshima, S., et al., *Long-term follow-up of the changes in circulating cytokines, soluble cytokine receptors, and white blood cell subset counts in patients with rheumatoid arthritis (RA) after monoclonal anti-TNF alpha antibody therapy.* J Clin Immunol, 1999. **19**(5): p. 305-13.
12. Rankin, E.C., et al., *The therapeutic effects of an engineered human anti-tumour necrosis factor alpha antibody (CDP571) in rheumatoid arthritis.* Br J Rheumatol, 1995. **34**(4): p. 334-42.
13. Elliott, M.J., et al., *Randomised double-blind comparison of chimeric monoclonal antibody to tumour necrosis factor alpha (cA2) versus placebo in rheumatoid arthritis.* Lancet, 1994. **344**(8930): p. 1105-10.
14. Saklatvala, J., *Tumour necrosis factor alpha stimulates resorption and inhibits synthesis of proteoglycan in cartilage.* Nature, 1986. **322**(6079): p. 547-9.
15. Wilbrink, B., et al., *Role of TNF alpha, in relation to IL-1 and IL-6 in the proteoglycan turnover of human articular cartilage.* Br J Rheumatol, 1991. **30**(4): p. 265-71.
16. Tortorella, M.D., et al., *The role of ADAM-TS4 (aggrecanase-1) and ADAM-TS5 (aggrecanase-2) in a model of cartilage degradation.* Osteoarthritis Cartilage, 2001. **9**(6): p. 539-52.
17. Arner, E.C., et al., *Cytokine-induced cartilage proteoglycan degradation is mediated by aggrecanase.* Osteoarthritis Cartilage, 1998. **6**(3): p. 214-28.
18. Lefebvre, V., C. Peeters-Joris, and G. Vaes, *Production of gelatin-degrading matrix metalloproteinases ('type IV collagenases') and inhibitors by articular chondrocytes during their dedifferentiation by serial subcultures and under stimulation by interleukin-1 and tumor necrosis factor alpha.* Biochim Biophys Acta, 1991. **1094**(1): p. 8-18.

19. Liacini, A., et al., *Induction of matrix metalloproteinase-13 gene expression by TNF-alpha is mediated by MAP kinases, AP-1, and NF-kappaB transcription factors in articular chondrocytes.* Exp Cell Res, 2003. **288**(1): p. 208-17.
20. Bunning, R.A. and R.G. Russell, *The effect of tumor necrosis factor alpha and gamma-interferon on the resorption of human articular cartilage and on the production of prostaglandin E and of caseinase activity by human articular chondrocytes.* Arthritis Rheum, 1989. **32**(6): p. 780-4.
21. Goodstone, N.J. and T.E. Hardingham, *Tumour necrosis factor alpha stimulates nitric oxide production more potently than interleukin-1beta in porcine articular chondrocytes.* Rheumatology (Oxford), 2002. **41**(8): p. 883-91.
22. Shlopov, B.V., M.L. Gumanovskaya, and K.A. Hasty, *Autocrine regulation of collagenase 3 (matrix metalloproteinase 13) during osteoarthritis.* Arthritis Rheum, 2000. **43**(1): p. 195-205.
23. Wood, D.D., et al., *Isolation of an interleukin-1-like factor from human joint effusions.* Arthritis Rheum, 1983. **26**(8): p. 975-83.
24. Fontana, A., et al., *Interleukin 1 activity in the synovial fluid of patients with rheumatoid arthritis.* Rheumatol Int, 1982. **2**(2): p. 49-53.
25. Smith, J.B., et al., *Occurrence of interleukin-1 in human synovial fluid: detection by RIA, bioassay and presence of bioassay-inhibiting factors.* Rheumatol Int, 1989. **9**(2): p. 53-8.
26. Cohen, S.B. and A. Rubbert, *Bringing the clinical experience with anakinra to the patient.* Rheumatology (Oxford), 2003. **42 Suppl 2**: p. ii36-40.
27. Saklatvala, J. and S.J. Sarsfield, *Lymphocytes induce resorption of cartilage by producing catabolin.* Biochem J, 1982. **202**(1): p. 275-8.
28. Saklatvala, J., et al., *Pig catabolin is a form of interleukin 1. Cartilage and bone resorb, fibroblasts make prostaglandin and collagenase, and thymocyte proliferation is augmented in response to one protein.* Biochem J, 1984. **224**(2): p. 461-6.
29. Saklatvala, J., V.A. Curry, and S.J. Sarsfield, *Purification to homogeneity of pig leucocyte catabolin, a protein that causes cartilage resorption in vitro.* Biochem J, 1983. **215**(2): p. 385-92.
30. Pettipher, E.R., G.A. Higgs, and B. Henderson, *Interleukin 1 induces leukocyte infiltration and cartilage proteoglycan degradation in the synovial joint.* Proc Natl Acad Sci U S A, 1986. **83**(22): p. 8749-53.
31. Shingu, M., et al., *The effects of cytokines on metalloproteinase inhibitors (TIMP) and collagenase production by human chondrocytes and TIMP production by synovial cells and endothelial cells.* Clin Exp Immunol, 1993. **94**(1): p. 145-9.
32. Dayer, J.M., et al., *Human recombinant interleukin 1 stimulates collagenase and prostaglandin E2 production by human synovial cells.* J Clin Invest, 1986. **77**(2): p. 645-8.
33. Kienzle, G. and J. von Kempis, *Vascular cell adhesion molecule 1 (CD106) on primary human articular chondrocytes: functional regulation of expression by cytokines and comparison with intercellular adhesion molecule 1 (CD54) and very late activation antigen 2.* Arthritis Rheum, 1998. **41**(7): p. 1296-305.
34. Stadler, J., et al., *Articular chondrocytes synthesize nitric oxide in response to cytokines and lipopolysaccharide.* J Immunol, 1991. **147**(11): p. 3915-20.

35. Arner, E.C. and M.A. Pratta, *Independent effects of interleukin-1 on proteoglycan breakdown, proteoglycan synthesis, and prostaglandin E2 release from cartilage in organ culture.* Arthritis Rheum, 1989. **32**(3): p. 288-97.
36. Patwari, P., et al., *Analysis of ADAMTS4 and MT4-MMP indicates that both are involved in aggrecanolysis in interleukin-1-treated bovine cartilage.* Osteoarthritis Cartilage, 2005. **13**(4): p. 269-77.
37. Koshy, P.J., et al., *The modulation of matrix metalloproteinase and ADAM gene expression in human chondrocytes by interleukin-1 and oncostatin M: a time-course study using real-time quantitative reverse transcription-polymerase chain reaction.* Arthritis Rheum, 2002. **46**(4): p. 961-7.
38. Pratta, M.A., et al., *Aggrecan protects cartilage collagen from proteolytic cleavage.* J Biol Chem, 2003. **278**(46): p. 45539-45.
39. Kozaci, L.D., D.J. Buttle, and A.P. Hollander, *Degradation of type II collagen, but not proteoglycan, correlates with matrix metalloproteinase activity in cartilage explant cultures.* Arthritis Rheum, 1997. **40**(1): p. 164-74.
40. Bau, B., et al., *Relative messenger RNA expression profiling of collagenases and aggrecanases in human articular chondrocytes in vivo and in vitro.* Arthritis Rheum, 2002. **46**(10): p. 2648-57.
41. Sadowski, T. and J. Steinmeyer, *Differential effects of nonsteroidal antiinflammatory drugs on the IL-1 altered expression of plasminogen activators and plasminogen activator inhibitor-1 by articular chondrocytes.* Inflamm Res, 2002. **51**(8): p. 427-33.
42. Kandel, R.A., et al., *Fetal bovine serum inhibits chondrocyte collagenase production: interleukin 1 reverses this effect.* Biochim Biophys Acta, 1990. **1053**(2-3): p. 130-4.
43. Hembry, R.M., et al., *Metalloproteinase production by rabbit articular cartilage: comparison of the effects of interleukin-1 alpha in vitro and in vivo.* Virchows Arch, 1994. **425**(4): p. 413-24.
44. Chubinskaya, S., et al., *Chondrocyte matrix metalloproteinase-8: up-regulation of neutrophil collagenase by interleukin-1 beta in human cartilage from knee and ankle joints.* Lab Invest, 1996. **74**(1): p. 232-40.
45. Saito, S., et al., *Involvement of MMP-1 and MMP-3 in collagen degradation induced by IL-1 in rabbit cartilage explant culture.* Life Sci, 1998. **62**(22): p. PL 359-65.
46. Dozin, B., et al., *Response of young, aged and osteoarthritic human articular chondrocytes to inflammatory cytokines: molecular and cellular aspects.* Matrix Biol, 2002. **21**(5): p. 449-59.
47. Ganu, V., et al., *Inhibition of interleukin-1alpha-induced cartilage oligomeric matrix protein degradation in bovine articular cartilage by matrix metalloproteinase inhibitors: potential role for matrix metalloproteinases in the generation of cartilage oligomeric matrix protein fragments in arthritic synovial fluid.* Arthritis Rheum, 1998. **41**(12): p. 2143-51.
48. Dickinson, S.C., et al., *Cleavage of cartilage oligomeric matrix protein (thrombospondin-5) by matrix metalloproteinases and a disintegrin and metalloproteinase with thrombospondin motifs.* Matrix Biol, 2003. **22**(3): p. 267-78.
49. von Bredow, D.C., et al., *Degradation of fibronectin fibrils by matrilysin and characterization of the degradation products.* Exp Cell Res, 1995. **221**(1): p. 83-91.
50. Muir, D. and M. Manthorpe, *Stromelysin generates a fibronectin fragment that inhibits Schwann cell proliferation.* J Cell Biol, 1992. **116**(1): p. 177-85.

51. Wagener, R., et al., *The matrilins--adaptor proteins in the extracellular matrix.* FEBS Lett, 2005. **579**(15): p. 3323-9.
52. Tyler, J.A., *Articular cartilage cultured with catabolin (pig interleukin 1) synthesizes a decreased number of normal proteoglycan molecules.* Biochem J, 1985. **227**(3): p. 869-78.
53. Herman, J.H., et al., *Cytokine modulation of chondrocyte metabolism--in vivo and in vitro effects of piroxicam.* Inflammation, 1984. **8 Suppl**: p. S125-37.
54. Goldring, M.B., et al., *Interleukin 1 suppresses expression of cartilage-specific types II and IX collagens and increases types I and III collagens in human chondrocytes.* J Clin Invest, 1988. **82**(6): p. 2026-37.
55. Kondo, S., et al., *Cytokine regulation of cartilage-derived retinoic acid-sensitive protein (CD-RAP) in primary articular chondrocytes: suppression by IL-1, bfGF, TGFbeta and stimulation by IGF-1.* J Orthop Res, 2001. **19**(4): p. 712-9.
56. Benton, H.P. and J.A. Tyler, *Inhibition of cartilage proteoglycan synthesis by interleukin I.* Biochem Biophys Res Commun, 1988. **154**(1): p. 421-8.
57. Gelber, A.C., et al., *Joint injury in young adults and risk for subsequent knee and hip osteoarthritis.* Ann Intern Med, 2000. **133**(5): p. 321-8.
58. Roos, H., et al., *Knee osteoarthritis after meniscectomy: prevalence of radiographic changes after twenty-one years, compared with matched controls.* Arthritis Rheum, 1998. **41**(4): p. 687-93.
59. von Porat, A., E.M. Roos, and H. Roos, *High prevalence of osteoarthritis 14 years after an anterior cruciate ligament tear in male soccer players: a study of radiographic and patient relevant outcomes.* Ann Rheum Dis, 2004. **63**(3): p. 269-73.
60. Felson, D.T., et al., *Risk factors for incident radiographic knee osteoarthritis in the elderly: the Framingham Study.* Arthritis Rheum, 1997. **40**(4): p. 728-33.
61. Roos, H., et al., *Osteoarthritis of the knee after injury to the anterior cruciate ligament or meniscus: the influence of time and age.* Osteoarthritis Cartilage, 1995. **3**(4): p. 261-7.
62. Daniel, D.M., et al., *Fate of the ACL-injured patient. A prospective outcome study.* Am J Sports Med, 1994. **22**(5): p. 632-44.
63. Loening, A.M., et al., *Injurious mechanical compression of bovine articular cartilage induces chondrocyte apoptosis.* Arch Biochem Biophys, 2000. **381**(2): p. 205-12.
64. D'Lima, D.D., et al., *Cartilage injury induces chondrocyte apoptosis.* J Bone Joint Surg Am, 2001. **83-A Suppl 2**(Pt 1): p. 19-21.
65. Borrelli, J., Jr. and W.M. Ricci, *Acute effects of cartilage impact.* Clin Orthop Relat Res, 2004(423): p. 33-9.
66. D'Lima, D.D., et al., *Human chondrocyte apoptosis in response to mechanical injury.* Osteoarthritis Cartilage, 2001. **9**(8): p. 712-9.
67. Kisiday, J., et al., *Self-assembling peptide hydrogel fosters chondrocyte extracellular matrix production and cell division: implications for cartilage tissue repair.* Proc Natl Acad Sci U S A, 2002. **99**(15): p. 9996-10001.
68. Thibault, M., A.R. Poole, and M.D. Buschmann, *Cyclic compression of cartilage/bone explants in vitro leads to physical weakening, mechanical breakdown of collagen and release of matrix fragments.* J Orthop Res, 2002. **20**(6): p. 1265-73.
69. Chen, C.T., et al., *Time, stress, and location dependent chondrocyte death and collagen damage in cyclically loaded articular cartilage.* J Orthop Res, 2003. **21**(5): p. 888-98.

70. Lin, P.M., C.T. Chen, and P.A. Torzilli, *Increased stromelysin-1 (MMP-3), proteoglycan degradation (3B3- and 7D4) and collagen damage in cyclically load-injured articular cartilage.* Osteoarthritis Cartilage, 2004. **12**(6): p. 485-96.
71. Kurz, B., et al., *Biosynthetic response and mechanical properties of articular cartilage after injurious compression.* J Orthop Res, 2001. **19**(6): p. 1140-6.
72. Patwari, P., et al., *Proteoglycan degradation after injurious compression of bovine and human articular cartilage in vitro: interaction with exogenous cytokines.* Arthritis Rheum, 2003. **48**(5): p. 1292-301.
73. DiMicco, M.A., et al., *Mechanisms and kinetics of glycosaminoglycan release following in vitro cartilage injury.* Arthritis Rheum, 2004. **50**(3): p. 840-8.
74. Quinn, T.M., et al., *Effects of injurious compression on matrix turnover around individual cells in calf articular cartilage explants.* J Orthop Res, 1998. **16**(4): p. 490-9.
75. Lee, J.H., et al., *Mechanical injury of cartilage explants causes specific time-dependent changes in chondrocyte gene expression.* Arthritis Rheum, 2005. **52**(8): p. 2386-95.
76. Chan, P.S., et al., *Gene expression profile of mechanically impacted bovine articular cartilage explants.* J Orthop Res, 2005. **23**(5): p. 1146-51.
77. Sinz, A., et al., *Mass spectrometric proteome analyses of synovial fluids and plasmas from patients suffering from rheumatoid arthritis and comparison to reactive arthritis or osteoarthritis.* Electrophoresis, 2002. **23**(19): p. 3445-56.
78. Liao, H., et al., *Use of mass spectrometry to identify protein biomarkers of disease severity in the synovial fluid and serum of patients with rheumatoid arthritis.* Arthritis Rheum, 2004. **50**(12): p. 3792-803.
79. Vincent, T., et al., *Basic FGF mediates an immediate response of articular cartilage to mechanical injury.* Proc Natl Acad Sci U S A, 2002. **99**(12): p. 8259-64.
80. Vincent, T.L., et al., *Basic fibroblast growth factor mediates transduction of mechanical signals when articular cartilage is loaded.* Arthritis Rheum, 2004. **50**(2): p. 526-33.
81. Gruber, J., et al., *Induction of interleukin-1 in articular cartilage by explantation and cutting.* Arthritis Rheum, 2004. **50**(8): p. 2539-46.
82. Sah, R.L., et al., *Biosynthetic response of cartilage explants to dynamic compression.* J Orthop Res, 1989. **7**(5): p. 619-36.
83. Frank, E.H., et al., *A versatile shear and compression apparatus for mechanical stimulation of tissue culture explants.* J Biomech, 2000. **33**(11): p. 1523-7.
84. Shevchenko, A., et al., *Mass spectrometric sequencing of proteins silver-stained polyacrylamide gels.* Anal Chem, 1996. **68**(5): p. 850-8.
85. Bhat, V.B., et al., *Comparative plasma proteome analysis of lymphoma-bearing SJL mice.* J Proteome Res, 2005. **4**(5): p. 1814-25.
86. Kapp, E.A., et al., *An evaluation, comparison, and accurate benchmarking of several publicly available MS/MS search algorithms: sensitivity and specificity analysis.* Proteomics, 2005. **5**(13): p. 3475-90.
87. Ith, B., et al., *Aortic carboxypeptidase-like protein is expressed in collagen-rich tissues during mouse embryonic development.* Gene Expr Patterns, 2005. **5**(4): p. 533-7.
88. Hermansson, M., et al., *Proteomic analysis of articular cartilage shows increased type II collagen synthesis in osteoarthritis and expression of inhibin betaA (activin A), a regulatory molecule for chondrocytes.* J Biol Chem, 2004. **279**(42): p. 43514-21.
89. Moseley, T.A., et al., *Interleukin-17 family and IL-17 receptors.* Cytokine Growth Factor Rev, 2003. **14**(2): p. 155-74.

90. Tardif, G., et al., *Differential gene expression and regulation of the bone morphogenetic protein antagonists follistatin and gremlin in normal and osteoarthritic human chondrocytes and synovial fibroblasts.* Arthritis Rheum, 2004. **50**(8): p. 2521-30.
91. Funaba, M., et al., *Follistatin and activin in bone: expression and localization during endochondral bone development.* Endocrinology, 1996. **137**(10): p. 4250-9.
92. Tsuchiya, A., et al., *Expression of mouse HtrA1 serine protease in normal bone and cartilage and its upregulation in joint cartilage damaged by experimental arthritis.* Bone, 2005. **37**(3): p. 323-36.
93. De Ceuninck, F., et al., *Assessment of some tools for the characterization of the human osteoarthritic cartilage proteome.* J Biomol Tech, 2005. **16**(3): p. 256-65.
94. Khan, I.M., et al., *Expression of clusterin in the superficial zone of bovine articular cartilage.* Arthritis Rheum, 2001. **44**(8): p. 1795-9.
95. Hu, B., et al., *Isolation and sequence of a novel human chondrocyte protein related to mammalian members of the chitinase protein family.* J Biol Chem, 1996. **271**(32): p. 19415-20.
96. Johansen, J.S., et al., *Serum YKL-40 levels in healthy children and adults. Comparison with serum and synovial fluid levels of YKL-40 in patients with osteoarthritis or trauma of the knee joint.* Br J Rheumatol, 1996. **35**(6): p. 553-9.
97. Johansen, J.S., H.S. Jensen, and P.A. Price, *A new biochemical marker for joint injury. Analysis of YKL-40 in serum and synovial fluid.* Br J Rheumatol, 1993. **32**(11): p. 949-55.
98. Kawashima-Ohya, Y., et al., *Retinol-binding protein is produced by rabbit chondrocytes and responds to parathyroid hormone (PTH)/PTH-related peptide-cyclic adenosine monophosphate pathway.* Endocrinology, 1999. **140**(3): p. 1075-81.
99. Lin, M., et al., *Cell surface antigen CD109 is a novel member of the alpha(2) macroglobulin/C3, C4, C5 family of thioester-containing proteins.* Blood, 2002. **99**(5): p. 1683-91.
100. Solomon, K.R., et al., *CD109 represents a novel branch of the alpha2-macroglobulin/complement gene family.* Gene, 2004. **327**(2): p. 171-83.
101. Dandoy-Dron, F., et al., *Gene expression in scrapie. Cloning of a new scrapie-responsive gene and the identification of increased levels of seven other mRNA transcripts.* J Biol Chem, 1998. **273**(13): p. 7691-7.
102. Dron, M., et al., *Characterization of the human analogue of a Scrapie-responsive gene.* J Biol Chem, 1998. **273**(29): p. 18015-8.
103. Kepes, J.J., L.J. Rubinstein, and H. Chiang, *The role of astrocytes in the formation of cartilage in gliomas. An immunohistochemical study of four cases.* Am J Pathol, 1984. **117**(3): p. 471-83.
104. Kepes, J.J. and E. Perentes, *Glial fibrillary acidic protein in chondrocytes of elastic cartilage in the human epiglottis: an immunohistochemical study with polyvalent and monoclonal antibodies.* Anat Rec, 1988. **220**(3): p. 296-9.
105. Kasantikul, V. and S. Shuangshoti, *Positivity to glial fibrillary acidic protein in bone, cartilage, and chordoma.* J Surg Oncol, 1989. **41**(1): p. 22-6.
106. Zhang, C.C., et al., *Angiopoietin-like proteins stimulate ex vivo expansion of hematopoietic stem cells.* Nat Med, 2006. **12**(2): p. 240-5.
107. Peek, R., et al., *The angiopoietin-like factor cornea-derived transcript 6 is a putative morphogen for human cornea.* J Biol Chem, 2002. **277**(1): p. 686-93.

108. Liu, C., et al., *Peptidoglycan recognition proteins: a novel family of four human innate immunity pattern recognition molecules.* J Biol Chem, 2001. **276**(37): p. 34686-94.
109. Gelius, E., et al., *A mammalian peptidoglycan recognition protein with N-acetylmuramoyl-L-alanine amidase activity.* Biochem Biophys Res Commun, 2003. **306**(4): p. 988-94.
110. Wang, Z.M., et al., *Human peptidoglycan recognition protein-L is an N-acetylmuramoyl-L-alanine amidase.* J Biol Chem, 2003. **278**(49): p. 49044-52.
111. Zhang, Y., et al., *Identification of serum N-acetylmuramoyl-l-alanine amidase as liver peptidoglycan recognition protein 2.* Biochim Biophys Acta, 2005. **1752**(1): p. 34-46.
112. Wang, H., et al., *Peptidoglycan recognition protein 2 (N-acetylmuramoyl-L-Ala amidase) is induced in keratinocytes by bacteria through the p38 kinase pathway.* Infect Immun, 2005. **73**(11): p. 7216-25.
113. Knorr, T., et al., *YKL-39 (chitinase 3-like protein 2), but not YKL-40 (chitinase 3-like protein 1), is up regulated in osteoarthritic chondrocytes.* Ann Rheum Dis, 2003. **62**(10): p. 995-8.
114. Johansen, J.S., et al., *Regulation of YKL-40 production by human articular chondrocytes.* Arthritis Rheum, 2001. **44**(4): p. 826-37.
115. Recklies, A.D., et al., *Inflammatory cytokines induce production of CHI3L1 by articular chondrocytes.* J Biol Chem, 2005. **280**(50): p. 41213-21.
116. Ling, H. and A.D. Recklies, *The chitinase 3-like protein human cartilage glycoprotein 39 inhibits cellular responses to the inflammatory cytokines interleukin-1 and tumour necrosis factor-alpha.* Biochem J, 2004. **380**(Pt 3): p. 651-9.
117. Andrades, J.A., et al., *Complement proteins are present in developing endochondral bone and may mediate cartilage cell death and vascularization.* Exp Cell Res, 1996. **227**(2): p. 208-13.
118. Varoga, D., et al., *Expression and regulation of antimicrobial peptides in articular joints.* Ann Anat, 2005. **187**(5-6): p. 499-508.
119. Vallon, R., et al., *Serum amyloid A (apoSAA) expression is up-regulated in rheumatoid arthritis and induces transcription of matrix metalloproteinases.* J Immunol, 2001. **166**(4): p. 2801-7.
120. Sukenik, S., et al., *Serum and synovial fluid levels of serum amyloid A protein and C-reactive protein in inflammatory and noninflammatory arthritis.* J Rheumatol, 1988. **15**(6): p. 942-5.
121. Charles, P., et al., *Regulation of cytokines, cytokine inhibitors, and acute-phase proteins following anti-TNF-alpha therapy in rheumatoid arthritis.* J Immunol, 1999. **163**(3): p. 1521-8.
122. Smith, K.D., et al., *The heterogeneity of the glycosylation of alpha-1-acid glycoprotein between the sera and synovial fluid in rheumatoid arthritis.* Biomed Chromatogr, 2002. **16**(4): p. 261-6.
123. Garton, K.J., et al., *Stimulated shedding of vascular cell adhesion molecule 1 (VCAM-1) is mediated by tumor necrosis factor-alpha-converting enzyme (ADAM 17).* J Biol Chem, 2003. **278**(39): p. 37459-64.
124. Singh, R.J., et al., *Cytokine stimulated vascular cell adhesion molecule-1 (VCAM-1) ectodomain release is regulated by TIMP-3.* Cardiovasc Res, 2005. **67**(1): p. 39-49.
125. Mason, J.C., P. Kapahi, and D.O. Haskard, *Detection of increased levels of circulating intercellular adhesion molecule 1 in some patients with rheumatoid arthritis but not in*

patients with systemic lupus erythematosus. Lack of correlation with levels of circulating vascular cell adhesion molecule 1. Arthritis Rheum, 1993. **36**(4): p. 519-27.
126. Wellicome, S.M., et al., *Detection of a circulating form of vascular cell adhesion molecule-1: raised levels in rheumatoid arthritis and systemic lupus erythematosus.* Clin Exp Immunol, 1993. **92**(3): p. 412-8.
127. Koch, A.E., et al., *Immunolocalization of endothelial and leukocyte adhesion molecules in human rheumatoid and osteoarthritic synovial tissues.* Lab Invest, 1991. **64**(3): p. 313-20.
128. Diaz-Romero, J., et al., *Immunophenotypic analysis of human articular chondrocytes: changes in surface markers associated with cell expansion in monolayer culture.* J Cell Physiol, 2005. **202**(3): p. 731-42.
129. Jersmann, H.P., *Time to abandon dogma: CD14 is expressed by non-myeloid lineage cells.* Immunol Cell Biol, 2005. **83**(5): p. 462-7.
130. Basu, S., et al., *Necrotic but not apoptotic cell death releases heat shock proteins, which deliver a partial maturation signal to dendritic cells and activate the NF-kappa B pathway.* Int Immunol, 2000. **12**(11): p. 1539-46.
131. Blachere, N.E., et al., *Heat shock protein-peptide complexes, reconstituted in vitro, elicit peptide-specific cytotoxic T lymphocyte response and tumor immunity.* J Exp Med, 1997. **186**(8): p. 1315-22.
132. Binder, R.J., N.E. Blachere, and P.K. Srivastava, *Heat shock protein-chaperoned peptides but not free peptides introduced into the cytosol are presented efficiently by major histocompatibility complex I molecules.* J Biol Chem, 2001. **276**(20): p. 17163-71.
133. Basu, S. and P.K. Srivastava, *Calreticulin, a peptide-binding chaperone of the endoplasmic reticulum, elicits tumor- and peptide-specific immunity.* J Exp Med, 1999. **189**(5): p. 797-802.
134. Basu, S., et al., *CD91 is a common receptor for heat shock proteins gp96, hsp90, hsp70, and calreticulin.* Immunity, 2001. **14**(3): p. 303-13.
135. Srivastava, P., *Roles of heat-shock proteins in innate and adaptive immunity.* Nat Rev Immunol, 2002. **2**(3): p. 185-94.
136. Patwari, P., et al., *Ultrastructural quantification of cell death after injurious compression of bovine calf articular cartilage.* Osteoarthritis Cartilage, 2004. **12**(3): p. 245-52.
137. Tew, S.R., et al., *The reactions of articular cartilage to experimental wounding: role of apoptosis.* Arthritis Rheum, 2000. **43**(1): p. 215-25.
138. Morel, V. and T.M. Quinn, *Cartilage injury by ramp compression near the gel diffusion rate.* J Orthop Res, 2004. **22**(1): p. 145-51.
139. Lucchinetti, E., et al., *Cartilage viability after repetitive loading: a preliminary report.* Osteoarthritis Cartilage, 2002. **10**(1): p. 71-81.
140. Zafar, R.S., Z. Zeng, and D.A. Walz, *Localization of two binding domains for thrombospondin within fibronectin.* Arch Biochem Biophys, 1992. **297**(2): p. 271-6.
141. Takahashi, K., et al., *Thrombospondin fragmentation by alpha-thrombin and resistance to gamma-thrombin.* Biochem J, 1984. **224**(2): p. 673-6.
142. Yang, Z., D.K. Strickland, and P. Bornstein, *Extracellular matrix metalloproteinase 2 levels are regulated by the low density lipoprotein-related scavenger receptor and thrombospondin 2.* J Biol Chem, 2001. **276**(11): p. 8403-8.
143. Leask, A. and D.J. Abraham, *TGF-beta signaling and the fibrotic response.* Faseb J, 2004. **18**(7): p. 816-27.

144. Burton-Wurster, N., et al., *Effect of compressive loading and unloading on the synthesis of total protein, proteoglycan, and fibronectin by canine cartilage explants.* J Orthop Res, 1993. **11**(5): p. 717-29.
145. Farquhar, T., et al., *Swelling and fibronectin accumulation in articular cartilage explants after cyclical impact.* J Orthop Res, 1996. **14**(3): p. 417-23.
146. Chen, C.T., et al., *Compositional and metabolic changes in damaged cartilage are peak-stress, stress-rate, and loading-duration dependent.* J Orthop Res, 1999. **17**(6): p. 870-9.
147. Burton-Wurster, N. and G. Lust, *Deposition of fibronectin in articular cartilage of canine osteoarthritic joints.* Am J Vet Res, 1985. **46**(12): p. 2542-5.
148. Burton-Wurster, N. and G. Lust, *Fibronectin and water content of articular cartilage explants after partial depletion of proteoglycans.* J Orthop Res, 1986. **4**(4): p. 437-45.
149. Homandberg, G.A., R. Meyers, and D.L. Xie, *Fibronectin fragments cause chondrolysis of bovine articular cartilage slices in culture.* J Biol Chem, 1992. **267**(6): p. 3597-604.
150. Levin, A.S., C.T. Chen, and P.A. Torzilli, *Effect of tissue maturity on cell viability in load-injured articular cartilage explants.* Osteoarthritis Cartilage, 2005. **13**(6): p. 488-96.
151. Poole, C.A., *Articular cartilage chondrons: form, function and failure.* J Anat, 1997. **191 (Pt 1)**: p. 1-13.
152. Guilak, F., et al., *The deformation behavior and mechanical properties of chondrocytes in articular cartilage.* Osteoarthritis Cartilage, 1999. **7**(1): p. 59-70.
153. Lohmander, L.S., T. Saxne, and D.K. Heinegard, *Release of cartilage oligomeric matrix protein (COMP) into joint fluid after knee injury and in osteoarthritis.* Ann Rheum Dis, 1994. **53**(1): p. 8-13.
154. Kuhne, S.A., et al., *Persistent high serum levels of cartilage oligomeric matrix protein in a subgroup of patients with traumatic knee injury.* Rheumatol Int, 1998. **18**(1): p. 21-5.
155. Mundermann, A., et al., *Serum concentration of cartilage oligomeric matrix protein (COMP) is sensitive to physiological cyclic loading in healthy adults.* Osteoarthritis Cartilage, 2005. **13**(1): p. 34-8.
156. Kersting, U.G., et al., *Changes in knee cartilage volume and serum COMP concentration after running exercise.* Osteoarthritis Cartilage, 2005. **13**(10): p. 925-34.
157. Sharif, M., et al., *Relationship between serum cartilage oligomeric matrix protein levels and disease progression in osteoarthritis of the knee joint.* Br J Rheumatol, 1995. **34**(4): p. 306-10.
158. Neidhart, M., et al., *Small fragments of cartilage oligomeric matrix protein in synovial fluid and serum as markers for cartilage degradation.* Br J Rheumatol, 1997. **36**(11): p. 1151-60.
159. Hummel, K.M., et al., *Analysis of cartilage oligomeric matrix protein (COMP) in synovial fibroblasts and synovial fluids.* Br J Rheumatol, 1998. **37**(7): p. 721-8.
160. Fang, C., et al., *Tissue distribution and measurement of cartilage oligomeric matrix protein in patients with magnetic resonance imaging-detected bone bruises after acute anterior cruciate ligament tears.* J Orthop Res, 2001. **19**(4): p. 634-41.
161. Castell, J.V., et al., *Interleukin-6 is the major regulator of acute phase protein synthesis in adult human hepatocytes.* FEBS Lett, 1989. **242**(2): p. 237-9.

Chapter 4:

An iTRAQ-2D-LC/MS/MS based quantitative comparison of cartilage response to mechanical compression injury and inflammatory cytokines, TNF-α and IL-1β — catabolism, immunity, cell death, and possible repair

4.1 ABSTRACT

The objective was to perform a quantitative comparison of proteins released from cartilage explants in response to IL-1β, TNF-α, and mechanical compression injury and to interpret their release in the context of the anabolic-catabolic shifts known to occur in cartilage in response to injury and cytokine treatment. Cartilage explants were subjected to injurious compression, TNF-α (100 ng/ml) or IL-1β (10 ng/ml), or no treatment, cultured in equal volumes of medium, and the medium was collected, pooled and the proteins deglycosylated by treatment with chondroitinase ABC. The proteins were subjected to trypsinization, and the peptides were labeled with one of four iTRAQ labels each containing a unique signature ion. The labeled peptides were subjected to nano-2D-LC/MS/MS on a QStar, quadrupole time of flight instrument. The study was done in analytical replicate on a pooled sample of greater than 70 explants from a total of 6-12 different animals. Data were analyzed by ProQuant to obtain a ProGroup peptide report containing identified spectra which were combined to achieve a peptide and then a protein level output of mean ratios, standard deviations of those ratios, and significance based on either Wilcoxan sign rank or Student's t-test both corrected for multiple comparisons. Because of our interest in catabolic and anabolic shifts, a targeted data analysis approach was taken in addition to a systems level PCA and K-means clustering

approach. By focusing on particular protein domains, we identified a decrease in the synthesis of most fibrillar collagen subunits ($p<0.05$), and an increase in the release of the aggrecan G2 and G3 domains with IL-1β and TNF-α treatment ($p<0.05$). We also noted a significant increase in MMP-1, MMP-3, MMP-9, and MMP-13 in at least one condition and, in most cases, all conditions compared to the untreated sample. An increase in proteins involved in innate immunity and immune cell recruitment were noted with IL-1β and TNF-α treatment, while an increase in intracellular protein release were seen most dramatically with mechanical compression injury. Anabolic effects are often driven by the insulin-like growth factor family and the TGF-β superfamily, so we specifically identified members of these pathways to understand which factors may mediate early repair processes. At the systems level, 2 principal components were sufficient to describe 97% of the covariance in the data. IL-1β and TNF-α caused a similar response in proteins identified; in contrast, a 'Y'-shaped distribution was observed upon projection of proteins based on their response injury vs. cytokine treatment. K-means clustering revealed six main clusters to further characterize the biology of mechanical injury versus cytokine effects on cartilage.

4.2 INTRODUCTION

Cartilage is the thin, glistening white tissue that covers the surface of the bone in diarthrodial joints where it is responsible for low friction movement and force dissipation with motion. Cartilage contains a single cell type, the chondrocyte, which composes approximately 2-5% of the tissue volume and is responsible for maintaining the encapsulating proteoglycan and collagen type II rich extracellular matrix that constitutes the remaining tissue volume.

Degeneration of cartilage is the cardinal feature of osteoarthritis, and this degeneration is characterized by changes in composition, changes in mechanical properties, and changes in chondrocyte phenotype [1-5]. While osteoarthritis is a disease of the entire joint, the chondrocytes are thought to play a primary role in cartilage destruction with changes in the biochemical, physical, and mechanical environment of the chondrocytes driving changes in normal chondrocyte phenotype which may further potentate disease progression [6]. Targeting the chondrocyte for arthritis therapy requires an understanding of the tissue as a whole and how the chondrocyte senses and responds to the various catabolic, anabolic, and morphogenetic stimuli in its matrix environment.

Pro-inflammatory stimuli, particularly inflammatory cytokines, TNF-α and IL-1β, are commonly present in both rheumatoid arthritic and osteoarthritic joints and synovial fluid [7-14], and these cytokines can promote cartilage degeneration and stimulate local and systemic inflammation [15-19]. IL-1β and, to a lesser extent, TNF-α are very potent pro-catabolic cytokines that cause a rapid loss of aggrecan, a transcriptional and post-transcriptional decrease in matrix molecule synthesis, and an increase in protease production – particularly neutral metalloproteinases, MMPs and ADAMTSs [20-25]. In

addition, both cytokines are capable of causing an increase in pro-inflammatory mediators such as nitric oxide, PGE_2, IL-8, IL-6 as well as adhesion molecules necessary for immune cell recruitment [26-28]. IL-1β and TNF-α are produced by synovial fibroblasts, by immune cells (macrophages) and by the chondrocytes themselves, and all of these cells respond to the cytokines in a pro-catabolic manner [29, 30]. The importance of these cytokines to rheumatoid arthritis has been illustrated by the effectiveness of anti-TNF-α and anti-IL-1 therapies which have abrogated disease progression in many with the disease [31-34]. Intraarticular injection of IL-1 leads to cartilage breakdown also induces proteoglycan release from cartilage and polymorphonuclear and mononuclear inflammatory infiltrates [16]. However, cartilage is capable of returning to normal following an injection with IL-1 [18]. Cartilage is capable of repairing itself following brief cytokine induced matrix breakdown and inflammation, but long term exposure may prove damaging to the tissue. While arthritis is a total joint disease, the contribution of pro-inflammatory cytokines to the degeneration of cartilage is likely significant, so understanding how chondrocytes respond to cytokine treatment may aid in identifying new disease treatments for OA and RA.

Joint injury may dramatically increase the risk for developing osteoarthritis. Knee injury, such as ACL or meniscal tear, may significantly increase the relative risk of developing OA with mean relative risk values ranging from 3 to 20 and increasing with age and time after injury [35-37]. Although joint instability may contribute to secondary disease development; ACL correction has not been shown to decrease the risk of secondary OA implying that the acute traumatic event may have been sufficient to trigger a cascade of events to initiate arthritic progression [38-40]. Acute knee injury is

normally accompanied by an increase in pro-inflammatory cytokines, TNF-α and IL-1β [41], as well as by an increase in MMP-3, COMP fragments, collagen II cross-links, and aggrecan fragments [42-46]. In vitro cartilage compression injury models have shown that compression injury may promote cell death, predominantly by apoptosis [47, 48], decrease matrix synthesis and abrogate synthesis stimulation with dynamic loading [49], increase collage type II degradation [50, 51], increase protease production [52], and alter gene transcription and subsequent protein release from the tissue [53, 54]. Following injury, cartilage makes initial, but often unfruitful attempts at repair (for review [55, 56].

Mass spectrometry has opened up the opportunity to perform systems level analyses in understanding the tissue level response of cartilage to both cytokines and mechanical injury, both of which can promote cartilage degeneration. Studies on the effects of "injury" and cytokines have led to the identification bFGF release with cutting injury to cartilage[57]. MMP-3, MMP-1, ykl40, serum amyloid A, and TIMP-1 synthesis have been shown to increase with IL-1β treatment compared to control [58]. A more recent study suggests that peroxiredoxin 1 may be released from chondrocytes and that MMP-1, MMP-3, ykl40, and cyclophilin fragments have also been identified with cytokine treatment [59]. A study comparing OA and normal cartilage identified new collagen synthesis and inhibin β secretion as the major protein differences [60]. In addition to *in vitro* cartilage studies, synovial fluid analysis for arthritis biomarkers have identified calgranulin A, B, and C as well as C reactive protein which were correlated with erosive RA [61]. While focusing specifically on proteins that are increased in response to various treatment or disease processes provides some information about

disease, it is difficult to appreciate the impact of its release without understanding the context in which the protein is expressed.

The emerging proteomics technologies provide a variety of means to identify and compare samples. While SDS-PAGE-LC/MS/MS is ideal for protein profiling and molecular weight determination, sample complexity prohibits quantifying protein on the gel, so the mass spectrometer must provide quantitative information. The 2D-PAGE approach allows appropriate level of separation for spot comparison and secondary protein identification; however, the complexity of the post-translational modification in many cartilage matrix proteins makes it difficult to visualize and compare individual spots without extensive sample clean up [59, 60]. In addition, it is not possible to look at all the spots in a 2D gel, and so most analyses are done only on spots that are differentially regulated. While peptide based separation techniques offer good separation and good protein coverage, sample comparison/quantitation must again occur by the mass spectrometer via isotope labeling. Protein samples can also be compared at the peptide level by mass spectrometry using chemical isotope labels such as ICAT or iTRAQ [62, 63]. iTRAQ is an amine-reactive NHS ester coupled to an isobaric reporter tag that contains 4 differentially isotope-labeled signature ions and balance groups which release signature ions (*m/z* 114.1, 115.1, 116.1, 117.1) with CID providing relative quantitation at the MS/MS level [63].

Our work using an SDS-PAGE-LC/MS/MS profiling approach indicated that pro-inflammatory cytokines may cause a release of proteins involved in innate immunity and stress response, and that mechanical injury may compromise the integrity of both cells and the surrounding matrix causing the release of fibronectin, collagen type II, collagen

type VI, and COMP fragments. The objective of this work is to take a quantitative mass spectrometry approach to understand how cartilage responds to inflammatory cytokines, TNF-α and IL-1β, and injurious mechanical compression probing the mechanisms and contributions of the cartilage tissue to damage, to inflammation, and to repair as well as to the potential development of arthritic disease. In particular, we hoped to begin to pull out biological pathways and consequences of treatments that may represent a shift in the anabolic-catabolic axes of the cartilage tissue. Proteins released from a controlled volume of cartilage into a controlled volume of medium are compared using an internal standard for normalization. IL-1β, TNF-α, and injury cause a decrease in collagen synthesis and an increase in a number of matrix metalloproteinases implicated in matrix degradation. IL-1β and TNF-α caused an increase in aggrecan degradation. Proteins involved innate immunity and inflammation are primarily elevated with TNF-α and IL-1β treatment. Anabolic pathways including TGF-β superfamily members and IGF-1 are altered with all treatments indicating a potential for tissue repair. This work also verifies the increase in release of intracellular proteins in response to injury which were found previously as well as increases in CTGF, semaphorin 3C, proenkephalin, and semaphorin 3C which may also contribute to repair processes.

4.3 METHODS

Overview. A diagram of the experimental process is outlined in **Figure 1** and described in detail in the methods section above. Equal volumes of cartilage from six or 12 animals were treated with one of the following treatments in equal volumes of medium: (1.) unconfined mechanical compression (injury) to 50% strain at 100%/s, (2) 10 ng/ml IL-1β, (3) 100 ng/ml TNF-α, or (4) subjected to no additional treatment. After five days,

the medium samples were collected, and the entire set was pooled and analyzed in analytical duplicate. Chondroitinase ABC was used both as a deglycosylase and as an internal standard to correct for any sample loss during work-up and labeling. Each sample (treatment condition) possessed a unique iTRAQ signature ion for quantitation – untreated: *m/z* /114.1; IL-1β treated: *m/z* 115.1; TNF-α treated: *m/z* 116.1; mechanically injured: *m/z* 117.1. The samples were combined and fractionated into approximately 45 injectable fractions by SCX chromatography. The fractions were subjected to RP-LC/MS/MS and the data was combined and analyzed using ProQuant and ProGroup report (ABI). The quantitative comparisons represent an average response of the cartilage to cytokine treatment and injury treatment compared to untreated controls, and the analytical variance and not biological variance is measured in this study to determine robustness and reproducibility for future studies.

Cartilage explantation and culture. Cartilage explants were obtained from the stifle joints of 2-3 week old calves as described previously [64]. Briefly, articular cartilage was obtained from the femoropatellar groove by coring 9 mm diameter cartilage-bone cylindrical cores perpendicular to the cartilage surface. Each core was then sliced into 2 – 9mm diameter by 1 mm thick slices using a microtome. Finally, 4 -3 mm diameter punches were taken from each 9 mm diameter by 1 mm thick slice and placed into individual wells of a 48 well culture plate. Between 8 and 12 explants, 3 mm diameter by 1 mm thick, per condition per animal were obtained from greater than six animals. Approximately, 75% of the cartilage was taken from the first 1-mm layer while the remaining 25% were taken from the second millimeter of cartilage. The cartilage explants were rested for 5 days prior to start of treatment and cultured in medium

containing 1% ITS (high glucose (25mM glucose) DMEM supplemented with 10mM HEPES, 0.1 mM Non-essential amino acids, 115 uM ascorbic acid, 400 uM L-proline, 100 U/ml penicillin, 100 ug/ml streptomycin, and 0.25 ug/ml amphotericin B powder (PSA for tissue culture), and 1mM sodium pyruvate. On the day of treatment, explants from each location-matched-slice were placed in different groups and cultured in sets of four in 2.0 ml of medium without ITS supplementation.

Mechanical Injury. Strain and strain rate-controlled unconfined compression was performed in an incubator housed loading apparatus as described previously [53, 65-67]. Each 3mm diameter explant was individually loaded into a polysulfone chamber which was placed into the loading apparatus for compression. The thickness (zero point) of the explant was found by slowly (-20 um/second) decreasing the displacement until a small load (25 g) was measured. The explant was then subjected to a single unconfined compression at a strain of 50% and a strain rate of 100%/second against a non-porous platen. The injured explants were then cultured in sets of four with medium not supplemented with ITS.

TNF-α and IL-1β and post-treatment culture. IL-1β and TNF-α were resuspended in 0.1% BSA at concentrations of 10 ug/ml and 2.5 ug/ml respectively (R&D systems). To begin treatment, explants were placed in sets of four with medium without ITS containing 10 ng/ml of IL-1β or 100 ng/ml of TNF-α or no additional treatment (untreated). Following treatments, explants were cultured for 120 hours with a 10% medium removal and 10% supplementation every 24 hours. Medium and explants were collected and stored at -80C.

Desalting and sGAG removal. Medium from between six and twelve animals were pooled for each condition – injuriously compressed, untreated, IL-1β treated, and TNF-α treated. Two sets of 3.0 ml of the pooled medium from each condition (sample set 1 and sample set 2) were supplemented with 5 mM EDTA, 100 ug/ml PMSF, and 5 mg/ml iodoacetamide. Samples were dialyzed in a 7.5 kDa cutoff membrane for 3 hours at room temperature against buffer containing 10 mM Tris acetate, 40 mM NaCl, and 5 mM EDTA. Seventy milli-units of chondroitinase ABC were added to the dialyzing samples to serves as both a deglycosylating enzyme and as an internal standard. The samples underwent deglycosylation by chondroitinase ABC and dialysis at 37C overnight. The samples were then dialyzed against 2 mm triethylammonium bicarbonate (TEAB) and 0.5 mM EDTA for 8 hours at room temperature followed by dialysis against 500 um TEAB. The samples were removed, frozen, and concentrated by speedvac to 10 times. The samples were subjected to protein estimation by microBCA assay kit (Pierce) according to the manufacturer's instructions.

Trypsinization. Samples were further concentrated to 150 ul and reduced and alklyated by addition of 2mM TCEP in 100 mM TEAB at 37C for 2 hours followed by addition of 5mM iodoacetamide in 100 mM TEAB at 37C for 2 hours. The samples were then subjected to acetone precipitation by addition of 6 volumes of ice cold acetone and placed at -20C overnight followed by centrifugation at 15,000 x g for 30 minutes at 4C. The pelleted samples were resuspended in 25 ul of 50 mM TEAB containing 0.1% SDS. Resuspended samples were subjected to protein estimation by microBCA assay. The sequencing grade modified trypsin was resuspended in 50 mM TEAB at a concentration of 0.1ug/ul just prior to use (Promega). Trypsin was added to each sample at a ratio of

1:37.5, trypsin to protein based on the first protein estimation by addition of 2/3 of the trypsin amount followed two hours later by the last 1/3 of trypsin. To verify complete trypsinization, sample set 2 was subjected to a second trypsinization at 1:75. Sample volume is taken to 40 ul by addition of water and acetonitrile (to 10%). The samples were incubated at 37C overnight and then speedvac'd to dryness. Samples were resuspended in 500 mM TEAB, and 500 fmol of angiotensin I, 500 fmol of bradykinin, and 500 fmol of angiotensin II antipeptide were added to each sample as peptide internal standards.

iTRAQ labeling. iTRAQ labeling was done according to manufacturer's instructions. Briefly, 100 ug (sample set 1) and 75 ug (sample set 2) of peptides in 26 ul of 500 mM TEAB from each of the 2 sets of four samples were taken (3.0 ml equiv. of control and injury sample; 2.0 ml TNF-α sample; 1.5 ml of IL-1β) following the addition of peptide standards for labeling. A set of iTRAQ labels was equilibrated at room temperature and then diluted with 70 ul of ethanol. The label was vortexed for 1 minute and centrifuged at 16,000 x g for 1 minute. iTRAQ reagent was added to each 100 ug sample of peptides from sample set 1 (75 ug peptides for sample set 2; 114.1: untreated, 115.1: IL-1β, 116.1 TNF-α, 117.1: injury), and the sample was vortexed for 1 minute, sonicated for 5 minutes, centrifuged at 16,000 x g for 1 minute, and then allowed to incubate at room temperature for 55 minutes. Following the reaction, samples were diluted to 200 ul total with water and combined based on the volume equivalent of proteins – 1.5 ml for the first sample set (200 ul IL-1β, 150 ul TNF-α, 100 ul of untreated and injury) and 1.0 ml equivalent in the second sample set. Combined samples were dried down to approximately 50 ul and combined with 1.0 ml of strong cation exchange buffer A (SCX

buffer A: 10 mM Potassium Phosphate pH 2.8, 25% acetonitrile) and 1% phosphoric acid to pH 3.5. Sample was further diluted with 3.0 ml of SCX buffer.

Strong cation exchange chromatography. An off-line 2D LC approach was taken similar to that described by Peng et al.[68]. The combined sample was injected by 4.0 ml sample loop onto a 2.1 mm X 100 mm strong cation exchange column (PolyLC) on an Agilent 1100 HPLC equipped with a UV cell and microfraction collector. Sample was injected on to the column at a flow rate of 250 ul/min for 20 minutes with 100% Bufer A followed by a gradient from 0 to 40% buffer B (10 mM Phosphate buffer pH 2.8, 400 mM KCl, 25% acetonitrile) over the following 40 minutes and then from 40% B to 95% B over 10 minutes holding at 95%B for five minutes before returning to the starting conditions (total run time – 80 minutes). The run was monitored by UV absorption at λ = 214 nm to determine when the peptides eluted during the gradient. Fractions were collected every 0.5 min (125 ul each) using an automated fraction collector. All fractions from the void volume were diluted and rerun to verify that no peptide was lost due to high salt and then discarded (plate 1). Approximately 90 fractions (plate 2) were collected during the gradient elution of the peptides (as determined by UV absorption). Fractions were transferred to 0.5 ml tubes and stored at -80C until use. Fractions were then concentrated by speedvac and desalted by ziptip combining adjacent ziptip'd fractions to obtain approximately 50 fractions for LC/MS/MS analysis.

LC/MS/MS. Desalted SCX fractions were injected by manual injection (Rheodyne, manual injector with 0.5 ul internal loop) onto a 75 um ID x 160 mm column with 10 um tip (New Objective) packed in house with Vydac protein/peptide C18 packing material (5um particle size, 300 angstrom) as described previously [69]. Peptides were loaded at

2% Buffer B (1.2% acetic acid in 90% acetonitrile; flow rate: 250 nl/min) for 12.5 minutes before elution on a 147.5 minute gradient from 2% to 40% B followed by a wash out for 20 minutes from 40% to 60% B and held at 60% B for five minutes before returning to 2% B over 15 minutes and equilibrating at 2% B for 60 minutes (Buffer A: 1.2% acetic acid in water). The LC is connected to a QStar, quadrupole time of flight mass spectrometer (ABI) equipped with a nanospray source [70]. Data was acquired through information dependent acquisition using Analyst 1.1 selecting for precursor ions between *m/z* 400 and *m/z* 1600 with a charge state between two and four and which exceeds 15 counts. The cycle time was 10 seconds and each cycle consisted of an MS scan (m/z 400-1600) followed by 3 data dependent MS/MS scan (m/z 100-1600) with ions excluded for 100 seconds after obtaining a single spectra. Data was collected for over the entire 240 minute chromatographic run with peptides typically eluting between 60 and 180 minutes. Many of the fractions containing large number of peptides were run twice and lumped together into the data set to improve analyses. All fractions from sample set one were run prior to running sample set two.

Data analysis. Data was analyzed using both ProQuant 1.0 with ProGroup Report (ABI) searching against the NCBInr (Genbank) bovine database assembled in December 2005 and the Genbank database release 153 with MS error set to +/- 0.25 Da and the MS/MS error was set at +/- 0.20 Da. Allowed modifications were limited to iTRAQ labeled tyrosine, oxidized methionine, and 1 missed trypsin cleavage. The spectra level output was assembled by ProGroup report, and the report was imported into Excel and sorted to remove all low confidence peptides (confidence < 90). Most of the peptides above this criteria were deemed high quality matches by manual inspection (>97%; only

~17/500 of the first viewed spectra did not have compelling matches). All peptides with no signature ratios for quantitation or those with ratios of 0 or 9999 were discarded. The resulting data were sorted according to protein and then by peptide sequence and were imported into Matlab (Mathworks). Matlab scripts combined redundant spectra for each peptide (including variable iTRAQ labeling and methionine oxidation) and excluded all peptides with a ratio below 7 and an error of greater than 33%, which aided in improving quantitation by eliminating some of the spectra with high error due to low signal intensity. Ratios above 7 were left unmodified as high ratios are subject to higher errors because of the mass spectrometer dynamic range limitations. The peptide list was then combined into a protein list again calculating the means and the standard deviations of all values. The data were normalized based on the geometric mean of the chondroitinase ABC ratios as it was added to the sample in equal amounts for deglycosylation at the beginning of the sample work-up to serve as an internal standard. All mathematical manipulations were done in log space, so data are represented as geometric means and the standard deviations are multiplicative and not additive (error factors). Histograms of much of the data were constructed to view the underlying distributions. Overall, the data displayed a normal distribution in log space as determined by Lilliefors test, a modification of Komolgorov-Smirnov test for normality which does not require a fixed mean or variance (Matlab). Exceptions to normality include distributions of proteins whose fragments were differentially lost leading to multi-modal distributions (typically bimodal). Thus, we conclude that the method gives rise to normally distributed data, and testing for normality is both useful and important given its biological relevance to the system. Based on the outcome of Lilliefor's test, either Student's t-test or Wilcoxan sign

rank test both with Bonferroni correction for multiple comparisons was performed to determine whether the protein amount was different with treatment compared to without treatment (untreated control). Protein identifications were verified by Spectrum Mill (Agilent). Proteins were subjected to manual validation (of both identification and quantitation) of at least one peptide per protein For proteins identified by 4 or fewer peptides, all peptides were evaluated for proper identity and adequate quantitation. Protein identification is defined as identification of least 2 peptides from the protein with a confidence of greater than 90%.

Clustering analysis. A final protein list was compiled from all proteins identified by 2 or more peptides from the first iTRAQ experiment (sample set 1) searched against the bovine database and supplemented with proteins identified only in the second experiment (sample set 2) as well as non-bovine proteins identified by Genbank search that represent proteins not yet annotated in the bovine genome. This complete list was clustered using a k-means clustering algorithm (Matlab statistics toolbox) of the log transformed mean signature ion ratios for each protein. The K-means clustering algorithm partitions the proteins into k clusters (defined by user) by iteratively minimizing the summed squared Euclidean distances of each protein within the cluster to the cluster centroid over the entire k clusters. The program was allowed to iterate as many as 1,000,000 times to achieve a minimum given a set of starting values, and we allowed 500,000 replicates beginning with k randomly chosen proteins to achieve the actual minimum for the dataset. The proteins were clustered into between 4 and 25 clusters to determine both the best fit (Silhouette plots) and a biologically useful number of clusters to interpret the system. A student's t-test was performed to determine whether the clusters were

significantly different from one another, and thus likely to describe unique biological phenomena.

4.4 RESULTS

Normalization of data using an internal standard – Chondroitinase ABC correction.

Because protein amounts were expected and known to be different between the samples, internal standard was used for ratio normalization. The chondroitin sulfate lyase, Chondroitinase ABC, was used to deglycosylate the samples prior to labeling and analysis, and it served as the internal standard as it was unlikely to be present or show strong similarity to other proteins present in the sample. **Table 1** provides data on the chondroitinase ABC standard and the mean ratio values which were used for correction. The second analytical duplicate appeared to suffer from some untreated (control) sample loss in work-up which caused the average signature ion ratios to be around 2-2.5 rather than the first duplicate sample set where all ratios were close to 1. Sample loss likely occurred with acetone precipitation based on protein estimates taken after sample concentration and after acetone precipitation.

The data was normalized by dividing the geometric mean of Chondroitinase ABC signature ion ratios by the corresponding signature ion ratios for each peptide and protein. This is equivalent to subtracting the Chondroitinase ABC signature ion ratios from the corresponding signature ion ratios for each protein on the log transformed data. While a more sophisticated normalization approach may have been used, this normalization was sufficient to correct the data such that the ratios for the first analytical experiment and the second analytical experiment were within 20%, which is sufficient to interpret biological effects in these samples.

Analytical duplicates – analytical variance and reproducibility. By performing analytical replicates on average samples (samples combined from multiple explants from multiple animals), we evaluate the average behavior of the cartilage explants to the treatment, and we can test whether our method is sufficiently robust and reproducible for further analysis of biological replicates where the variance is compose of both biological variation and analytical variation. The protein data from the analytical duplicates were compared by dividing the geometric mean of each signature ion ratio of each protein of the first duplicate (ratio1) by the geometric mean of the corresponding signature ion ratio of each protein from the second analytical duplicate (ratio2). To simplify the comparisons, only those proteins from the bovine-specific database with 2 peptides or greater were compared using the accession number for protein identification. **Figure 2** represents overlaid histograms comparing the all protein signature ion ratios represented as log2 (ratio1/ratio2). In this histogram, the log transform of the ratio of signature ion ratios should fall with a mean of zero, and the variance should be small suggesting good repeatability/reproducibility in the values obtained. In this case, we noted that the log2(ratio1/ratio2) values were shifted slightly off from zero with overall ratio mean+/- standard deviation for 115:114 of 0.0536 of +/-0.4597; for 116:114 of 0.2471 +/- 0.5087, and for 117:114 of 0.1368 +/- 0.4730. These values are similar to those obtained by comparing the ProGroup protein Summary for each dataset **(supplemental material)**. The slight shift from a mean of zero represents a 4-19% error in quantitative agreement between the two experiments and may be attributed to pipeting variation of the internal standard. The variance around zero, represented as the standard deviation of the log transformed data, is larger than reported by Keshamouni et al. [71], and analysis indicates

that both the large ratio values and poor identification/outliers appear to contribute to the variance **(supplemental data)**. Thus, with manual validation of identification and quantitation expect that this standard deviation may be closer to 0.35 for most proteins with ratios less than 4.

To gain a better idea of how this error may potentially affect interpretations of the results, we attempted to determine the consistency between the two data sets which we define as both duplicate ratios showing the same change – both ratios greater than one or both ratios less than one. Using this method, we obtained 1388 ratio values in agreement, 126 values that disagree (370 ratios that were not identified in both sets) representing consistency of 90% between datasets. Manual inspection indicates that most of the inconsistencies were the result of ratios of one or of close to one. The dataset from the first analytical duplicate was used as the primary list, and data from second analytical duplicate was added in the case where the protein was not found in the first sample or where the protein had a better identification and quantitation score (more peptides identified and signature ions were of sufficient intensity for good quantitation). In addition, proteins identified by Genbank from non-bovine species were used to supplement the protein list if the protein was not yet annotated in the bovine genome. All inconsistent values were labeled so they could be tracked during further analysis. The final protein list was subjected to manual validation of at least one peptide per protein and secondary validation by Spectrum Mill. All proteins identified by less than 4 peptides were manually inspected for accurate quantitation. While statistical significance has not been achieved for many of the proteins identified and quantified by only few peptides, the data comparisons in figure 2 suggest that any ratio that is greater than two

standard deviations of the log2(ratio1/ratio2) for the corresponding signature ion ratio likely represents a reproducible finding.

Matrix degradation and synthesis in response to mechanical compression and treatment with cytokines, IL-1β, TNF-α. Previous experiments have suggested that loss of matrix proteins to the medium may represent new matrix synthesis, matrix degradation or passive loss of components from the tissue. To explore the behavior of matrix proteins, **figure 3a** is a graph of the 14 highest scoring matrix proteins being released into the medium plotted as the log transformed mean ratio +/- SEM of over 40 peptides for each protein. Proteins such as collagen VI and fibronectin show an increase in release to the medium while proteins like COMP, nucleobindin 1 and NG-2 show a slight decrease compared to the control. While most of the proteins are showing a statistically significant change the variance represented in this findings are within a single experiment, and we suggest caution in interpreting findings suggesting less than a 40-50% increase. To better characterize the anabolic state of the tissue, **figure 3b** is a graph of collagen telopeptide relative quantitation for each of the fibrillar collagens. Collagen telopeptides are cleaved following collagen triple helix formation, and thus the release of the telopeptides to the medium should approximate new collagen synthesis. Based on **Figure 3b**, a decrease in all fibrillar collagen synthesis is seen in response to cytokine treatment (IL-1β and TNF-α) and to a lesser extent mechanical compression injury ($p<0.01$ for all collagen telopeptide in response to cytokine treatment; $p<0.05$ for collagen type II and the 2 collagen XI subunits in response to mechanical compression; **table 2**). A sharper decrease in collagen type I synthesis was seen with TNF-α compared to IL-1β or mechanical injury ($p<0.05$; student's t-test with Bonferroni correction). A

decrease in collagen synthesis is consistent with previous reports using other methods to determine collagen production [72, 73].

As mentioned previously, proteins possessing multimodal distributions with respect to its peptides are expected in this sample because of proteolytic degradation of existing matrix proteins. **Figure 3c** is a graph describing the quantitation of each globular domain of aggrecan based on the quantitation of each domain's peptide constituents. While the second and third globular domain of aggrecan (G2 and G3) are abundantly released to the medium in response to cytokine treatment ($p < 0.001$ for G2 and G3 for both cytokine treatments; **table 2**), the aggrecan G1 domain was not increased and was actually significantly decreased with TNF-α treatment compared to untreated ($p<0.05$ for G1 with TNF-α treatment; table 2). These results indicate that aggrecan's G2 and G3 domains are separated from the G1 domain, and the G1 domain is retained in the tissue longer than the G2 and G3 containing fragments. The decrease in G1 release with TNF-a treatment may also reflect a decrease in new proteoglycan synthesis which is seen in response to cytokine treatment and mechanical injury (data not shown).

Matrix degradation occurs in response to cytokine treatment and mechanical compression injury and is correlated with an increase in matrix metalloproteinase (MMP) production. **Figure 3d** is a graph of the identified members of the matrix metalloproteinase family and their response to IL-1β, TNF-α and injury treatment. MMP-3 and MMP-13 are most dramatically elevated with all treatments ($p<0.05$ for both proteases with all treatment except for MMP-13 with injury ($p=0.057$)). The only protease to decrease, MMP-2 decreased significantly with mechanical injury; however a concomitant increase in MMP-9 is seen suggesting a shift in gelatinase activity with

mechanical injury ($p<0.05$ for both MMP-2 and MMP-9 with injury). P-values indicating significant changes in MMP quantities with each treatment compared to control are given in **Table 3**. Cytokine treatment and mechanical compression generally caused an increase in MMP release to the medium which is likely the result of new protease synthesis. A shift in the anabolic-catabolic axes can be seen with the decrease in collagen c-terminal telopeptide production indicating a decrease in collagen synthesis with treatments; the increase catabolic behavior as seen with aggrecan G2 and G3 domain release to the medium; and the increase in MMP expression.

A targeted look at anabolic-catabolic shift. Before subjecting the data to systems-level analyses, the data was reviewed to explore relevant anabolic and catabolic pathways in an attempt to better understand the proteins released as systems rather than focusing only on the primary effectors. Among the most striking class of proteins, elevated in response to IL-1β, TNF-α and to a lesser extent mechanical injury, were proteins involved in innate immunity. **Figure 4a** is a graph describing the response profile of proteins involved in innate immunity including complement proteins and LPS binding proteins. Again, a number of the proteins are elevated both with cytokine treatment and with injurious compression (asterisks indicate $p<0.05$ change over the untreated sample. Complement factor B, C3, and C1r are significantly increased with all treatments (IL-1β, TNF-α, injury) compared to untreated ($p<0.05$). C1q is significantly increased with TNF-α and IL-1β and C1 inhibitor is increase with TNF-α and injury ($p<0.05$). Proteins involved in LPS binding, LBP is elevated with IL-1b, and CD14 is elevated with TNF-α and IL-1β treatment compared to untreated ($p<0.05$). Lactoferrin, serum amyloid A3 and chitinase 3 like 1 and 2 were also elevated with treatments

($p<0.05$ for all treatments and proteins except lactoferrin with injury). Cytokines and chemokines are involved in modulating inflammation and recruiting immune cells were also identified, and their profiles are shown in **Figure 4b**. While most of the cytokines and chemokines are not statistically significant due to the low number of peptides identified, the extent of their elevation compared to the error between analytical duplicates suggest that these are real increases in protein release. The presence particularly in response to IL-1β and TNF-α treatment, suggests that cytokine and chemokines may play a role in modulating the tissue inflammatory response as well as the recruitment of inflammatory cells into the joint area in vivo. IL-6, CCL-2, CCL-20, M-CSF and CXCL6 are all increased over five-fold with both IL-1β and TNF- treatments. IL-17B was the highest scoring of the cytokines, and it was significantly elevated with IL-1β treatment ($p<0.05$). The TGF-β superfamily is involved in modulating chondrocyte phenotype and enhancing cartilage matrix production. **Figure 4c** is a graph describing the response to of the TGF-β superfamily and its inhibitors. While connective tissue growth factor, CTGF, is not a member of the TGF-β family, it is known to be elevated in response to TGF-β and may be responsible for some of the well-characterized TGF-β effect so it was included. TGF-β superfamily members inhibin beta and CDMP-2 appear to be elevated with injury alone and injury and IL-1β respectively with a trend toward significance with inhibin beta with injury ($p\sim0.1$). TGF-β2 is largely unchanged with treatments. The BMP inhibitors, chordin like 1 and chordin like 2 are both decreased with all treatments ($p<0.05$) while gremlin is elevated with IL-1β and TNF-α treatment. BMP-1, a C-collagen endopeptidase known to degrade chordin [74], was elevated with all treatments as was LTBP-1S ($p<0.05$), and LTBP-2 was elevated

only with IL-1β and TNF-α treatment. Finally, CTGF is elevated with all treatments ($p<0.05$) while HTRA1, IGF-BP7 and inhibin beta inhibitor, follistatin like protein 1, are all unchanged with treatment.

As with the TGF-β superfamily of proteins, insulin-like growth factors (IGFs) and their binding proteins enhance matrix production and are considered highly anabolic factors for cartilage. **Figure 4d** describes the profile of IGF-II and the four IGF binding proteins (IGF-BP) found in the tissue. IGF-II appears to be elevated roughly 2 fold with injury; however it is not significant because of the limited number of peptides identified. IGF-BP3 and IGF-BP5 are both elevated with all treatments ($p<0.05$ for both treatments and all proteins except IGF-BP3 with injury where $p<0.1$). IGF-BP6 is also elevated with IL-1β treatment ($p<0.05$), and IGF-BP4 is largely unchanged. Changes in IGF-BP expression may suggest different amounts of free IGF-I or IGF-II are available for signaling. Shifts in the catabolic-anabolic balance and shift in inflammation and immunity responses are suggested by the changes in cytokine and chemokine production, changes in IGF-BP and changes in the TGF-β biological pathway.

Projection Plots and principal component analysis (PCA). In addition to focusing on specific classes of proteins, a systems-level analysis was also undertaken to better understand the global protein response to the treatments. The validated final protein list was subjected to principal component analysis. **Figures 5a-d** are projection plots of the proteins represented by their responses to the three treatment conditions. Principal component analysis of the data suggests that 75% of the covariance is described by one principal component, and 97% is described by two principal components. The existence of two major principal components suggests that at least two of the treatments

cause similar protein behavior. This can be observed visually in **Figure 5b** where a linear relationship is evident between the global protein response to IL-1β and TNF-α with a Pearson product-moment correlation coefficient, R of 0.87 ($R^2 = 0.7575$; $p<0.0001$). In fact, the plot of cytokine: untreated vs. injury: untreated are also well ordered, appearing almost Y-shaped (**figures 5c-d**). The Y-shape can be attributed to four major subsets of proteins -- a subset of proteins that is decreased regardless of treatment (stem of the Y), proteins whose amounts remain unchanged (junction) with treatment, proteins that are elevated slightly with cytokines and largely with injury (branch 1) and the other arm represents proteins which go up slightly with injury and largely with cytokine treatment (branch 2). Thus, while two dimensions may be sufficient to describe the protein data, we maintained the treated: untreated axes for k-means clustering as it offers a greater visual understanding of the data.

K-means Clustering

K-means clustering was used to divide the proteins into six groups based on their general proximity in space by minimizing the sum of the protein to centroid distances within clusters over all the clusters. Six groups (clusters) are indicated by the different colored and shaped icons for proteins (points) in the graphs in **Figure 5**. The clusters were shown to be statistically different from one another at $p<0.001$, and the six clusters represent a good biological fit for the data. **Figure 6** is shows a graph of the cluster centroid profiles represented as mean+/-SD, and the profiles are color-coded to match the clusters shown in Figure 5. Six clusters divide each branch of the 'Y' into two clusters in an attempt to understand biological differences between those proteins that respond very strongly and those that respond more moderately to treatments.

4.5 DISCUSSION

To compare and contrast the extracellular effects of cartilage mechanical injury and treatment with inflammatory cytokines, TNF-α and IL-1β, to untreated cartilage, cartilage medium from a 5 day culture was collected pooled and compared between sample groups using iTRAQ labeling and 2D-LC/MS/MS analysis (**Figure 1**). The goal of the experiment was to compare proteins lost from equal volumes of cartilage into equal volumes of medium as a result of each treatment. Different amounts of proteins were expected to be lost, so correction for sample loss during work-up was performed based on an internal standard protein, chondroitinase ABC.

The LC/MS/MS analysis was done on duplicate samples to provide information about the analytical variance and reproducibility of the method using an internal standard protein for correction. **Figure 2** and the **supplemental data** provide a detailed analysis of the analytical duplicates and the source of variance (error) identified in this experiment. Based on this analysis, we determine that the log2 (ratio1/ratio2) standard deviation is roughly 0.5 suggesting 95% of the log2 (ratio1/ratio2) values were within a factor of 2. We anticipate this to be a measure of the maximum error for the experiment as the error is in part the result of poor identification/ poor quantification as well as large mean ratio values due to the limited dynamic range of the instrument. To decrease error caused by poor identification or quantitation, all proteins with 4 or fewer peptides were manually validated considering both identification and quantitation. Proteins displaying large ratios in at least one signature isotope ratio possess slightly larger errors in the ratios. Mathematical outliers, defined as values 3 standard deviations away from the mean, were not removed. Outliers appear to be the result of signature ions outside of the

dynamic range of the detector, poor identifications, variable trypsinization, and/ or variable labeling, so removal of outliers may improve quantitation and reproducibility. The finalized protein list is organized by clusters and contains all ratios, SDs, peptide numbers, Spectrum Mill identification information, manual validation notes, consistency between the first and second analytical duplicate, and p values (**supplemental data**). Overall, good reproducibility and consistency was observed using this method with additional error resulting from proteins with very few peptides and proteins one or more large ratios which we attempt to remedy by manual verification of protein identification and quantitation.

As mentioned above, the samples exhibit some unusual properties that make data interpretation more complex. First, as mentioned above, some proteins may exhibit multimodal distributions due to loss of different domains of a protein at different rates due to proteolytic processing and release from the tissue. Protein release may result from new protein synthesis from proteolysis or from passive loss from the tissue due to an increase in transport in part due to loss of aggrecan (proteoglycan effects on transport [75]). The passive loss of proteins, due to an increase in transport from the tissue, should possess ratio values similar to aggrecan especially if the proteins are not anchored to other matrix constituents. This increase in transport does not mean that all proteins lost at a rate less than or equal to aggrecan represent passive loss; it simply means that there is additional complexity in interpreting the data. Mechanical compression injury may also change transport due to damage to the collagen network; however, this change is likely to be more subtle. At the same time, we chose a five day treatment because the aggrecan curves begin to flatten out suggesting that we achieved a new equilibrium. Finally, the

cartilage was harvested from 2-3 week old calves, and the cartilage may represent both chondroblastic and chondrocytic phenotypes rather than the chondrocytic phenotype expected from older tissue. In other words, young cartilage is more biologically active and still forming large amounts of matrix, particularly the collagen network. Thus, this model may not completely recapture the behavior of normal adult cartilage. At the same time, osteoarthritic cartilage is also known to exhibit some chondrobastic behavior, so this model may possess some similarities and differences compared to behaviors seen in OA cartilage. Ultimately, this is an observational experiment in which proteins lost to the matrix may represent some aspect of the biology going on in the tissue, and this biology may represent appropriate or inappropriate repair processes in response to the matrix damaging stimuli.

Mechanical injury and inflammatory cytokines, TNF-α and IL-1β, shift the anabolic-catabolic balance in cartilage. This shift has been described in the literature in response to cytokine treatment and in response to mechanical compression injury. For example, IL-1 and TNF-α are known to decrease collagen type II and type XI synthesis while not dramatically affecting its breakdown early in response to treatment [72, 73, 76]. Over time, IL-1 may also enhance the production of collagen type I and type III subunits although PGE2 is normally inhibits type I and type III collagen production in chondrocyte with IL-1 treatment [72, 77]. While no direct study on the effects of mechanical injury on collagen synthesis has been conducted, Lee et al., by real time RT-PCR, showed very little change in type II collagen transcription which may imply that mechanical injury does not alter collagen synthesis beyond its effects on cell death or that the inhibition of collagen synthesis may be a post-transcriptional effect [53]. Kurz et al.

showed an decrease in ^{3}H-proline incorporation compared to free swell controls following mechanical compression injury even when corrected for cell death [49]. Previous work by Sah et al. showed that approximately 80% of the proline incorporation represents new collagen synthesis in this young bovine model [78], which taken together with Kurz et al. suggests that there is likely a decrease in collagen synthesis with mechanical compression injury [49]. **Figure 3b** is a graph of the C-terminal telopeptides of the fibrillar collagens identified in the samples. The C-terminal telopeptides are important for collagen fiber formation, and their release is indicative of new collagen synthesis. **Figure 3b** suggests that there is a general decrease in collagen synthesis with treatments (**table 2** for p values). This decrease in collagen syntheses as described by collagen c-terminal telopeptide release to the medium is consistent with previous reports on collagen synthesis and represents an anti-anabolic shift in response to cytokine treatment and mechanical injury.

In response to IL-1β and TNF-α, aggrecan is rapidly degraded via the actions of aggrecanases, ADAMTS4 and ADAMTS5. Aggrecan is bound via its G1 domain and proteoglycan link protein to hyaluronic acid which is in turn bound to the chondrocyte cell surface through its interactions with CD44 (for review [79]). The proteolysis of aggrecan by aggrecanases occurs at multiple positions along the core protein with the most commonly characterized sites within the CS-rich region releasing aggrecan G3 or within the interglobular domain between G2 causing the release of all but the G1 aggrecan fragment. The aggrecan G1 and proteoglycan link protein are known to accumulate in cartilage with age [80]. Maroudas et al. measured the half life of aggrecan G1 and proteoglycan link protein to be approximately 25 years by aspartic acid

racemization method [81]. More recently confocal microscopy work by Fosang et al. showed that aggrecan G1-NITEGE fragments may be internalized [82], and Embry et al. provided further evidence that this may be a hyaluronic acid-dependent event mediated by CD44 [83]. The aggrecan G1 and link protein, with their high binding affinity to hyaluronic acid, may remain in the tissue and released more slowly with time or may be turned over via cellular internalization. **Figure 3c** is this study describes aggrecan release into the medium separated by globular domains. Aggrecan G2 and G3 domains are increased 3-5 fold with IL-1β and TNF-α respectively. However, aggrecan G1 is released at roughly the rate of the untreated explants suggesting that aggrecan G1 is retained in the tissue where it may be released more slowly or possibly internalized by the chondrocytes. Aggrecan proteolysis with accompanying release of the aggrecan G2 and G3 domains and with evidence of aggrecan G1 tissue retention is characteristic of the catabolic behavior seen with IL-1β and TNF-α treatment.

In response to IL-1β, TNF-α, and mechanical compression, chondrocytes produce proteases which may mediate extracellular matrix degradation. In particular, the MMPs have been implicated in the degradation of aggrecan, collagens, fibronectin, and COMP [84-87]. MMP expression is important for matrix remodeling and turnover to insure ECM integrity; however in response to pro-catabolic stimuli, the over expression of MMPs can lead to matrix degradation that is not balanced by new matrix synthesis yielding a negative equilibrium [88]. **Figure 3d** is a graphical representation of the identified MMP expression profiles with each treatment. Using the mechanical injury model described in this study, Lee et al. reported an increase in MMP-1, MMP-9, MMP-13 and MMP-3 gene expression 24 hours after compression injury compared to free swell

controls [53]. In this study, a statistically significant increase in MMP-3 and MMP-9 protein release is observed with mechanical injury compared to untreated (free swell controls) ($p<0.05$), and a trend towards and increase is seen for both MMP-1 and MMP-13 compared to untreated (free swell controls; $p\sim0.1$) [53]. Other explant and chondrocyte model systems have shown an increase in MMP-9 and MMP-13 expression with TNF-α treatment [73, 89], and an increase in MMP-1, MMP-3, MMP-8, MMP-9, and MMP-13 with IL-1β [87, 90–95]. In this study, MMP-1, MMP-3, MMP-9, and MMP-13 are elevated with IL-1β compared to untreated controls while TNF-α treatment results in an elevation of MMP-3, MMP-9 and MMP-13 relative to untreated controls ($p<0.05$, **table 3**). The identification and response of the MMPs found in this study are consistent with previous findings in this and other models for both cytokine treatment and mechanical injury. An increase in matrix metalloproteinases in response to both cytokine treatments and mechanical injury suggests a shift toward more pro-catabolic behavior of the chondrocytes.

TNF-α and IL-1β, both, play a role in the immune response and tissue damage which has motivated the successful use of anti-TNF-α and anti-IL-1 therapies in the treatment of rheumatoid arthritis [31, 32]. By focusing on the effects of these cytokines in an in vitro model, we hoped to better understand the contributions of the cytokines and chondrocytes to immune response inflammation and tissue destruction. In trying to understand the effects of both mechanical injury and inflammatory cytokine treatment, we assumed that the tissue behavior should be appropriate to illicit both an immune response and to initiate a repair process. Immune response and tissue repair is typified by dermal wound healing where there exists a well-characterized balance of pro and anti-

inflammatory factors and pro and anti-fibrotic factors which dictate both tissue protection against infection and scarring or repair processes. Dermal wound healing is an orchestrated systemic event; however cartilage, being avascular tissue, must mount an attempt at repair on its own.

Thus, proteins involved in the innate immune response were evaluated including complement factors and antimicrobials. **Figure 4a** is a graph showing the profiles of some of the protein that may play a role in innate immunity. Complement factor B, C3, and C1r are significantly increased with all treatments, C1q is significantly increased with TNF-α and IL-1β, and C1 inhibitor is elevated with TNF-α and injury. While not possible to determine the amount of protein present using this method, the coverage on both factor B and C3 suggest that these proteins may be present in reasonably large quantities. Factor B is involved in the activation of the complement alternative pathway through its interactions with C3, while C1 is involved in the lectin binding and classical complement pathways (for review of complement [96]). C3 is thought to initiate the alternative complement cascade through interactions with and deposition onto particulates such as LPS, yeast and plant polysaccharides, and virus particles [96]. Cartilage has been shown to produce factor B, and synovial cells produce complement factors including factor B and C2 and C3 suggesting that complement is synthesized within the joint particularly in inflammatory conditions [60, 97]. Skin fibroblasts have been shown to increase production of complement C3 and factor B in response to IL-1 and TNF-α [98]. Production of factor B rather than IGF-1 in TNF-α stimulated macrophages may be determined by the co-stimulation with IFN-β (IL-6) or IFN-γ representing a means by which TNF-α may contribute to both the immune response and

early repair [99]. Mice deficient in factor B and complement C3 ($B^{-/-}$, $C3^{-/-}$) both show an increased resistance to arthritis in collagen induced arthritis mouse models [100, 101]. CD14 and LBP are both involved in the transfer of LPS to the MD2-TLR4 complex required for cell signaling. However, elevation of these LPS handling proteins may also inhibit LPS response (for review [102, 103]). Peptidoglycan recognition proteins, PGRPs, are a class of peptidoglycan interacting proteins that may serve either as bacteriostatic or antibacterial agents that may play important roles in phagocytosis, cytokine response to microbes, and peptidoglycan degradation (for review [104]). In this study, PGRP-L, but not PGRP, was elevated with TNF-α treatment which may suggest that the tissue may be generating factors to break down pro-inflammatory peptidoglycans rather than generating bactericidal factors. Hanayama et al. recently showed that milk fat globule EGF factor 8 (MFG-E8) plays a critical role in the phagocytosis of apoptotic cells by binding to phosphatidylserine on the surface of dead cells and forming a bridge between the cell remains and the phagocyte [105]. This clearance of apoptotic cells may be important in preventing autoimmune disease as a lupus like syndrome when phosphatidylserine is masked by a dominant negative form of MGF-E8 [105, 106]. The effect of mechanical injury on apoptosis has been well characterized in this model, and we anticipate that approximately 30-40% of the cells may undergo apoptosis in response to the injury protocol used [47, 107]. Coincidently, the decrease in MFG-E8 is approximately 35% compared to the untreated control (**figure 4a**); this decrease may represent a decrease in synthesis or possibly retention of MFG-E8 in the tissue through its binding to apoptotic cells. Elevation of complement and LPS binding proteins

particularly with cytokine treatment suggests that cartilage serves as an active participant in the innate immune response against foreign pathogens.

In addition to elevation of the innate immune proteins, elevation of cytokines and chemokines were also noted particularly in response to IL-1β and TNF-α treatment. Three main families of chemokines exist based on structure and function, the CCL family, the CXCL family, the CX3CL family and the XCL family (for review [108]). The CCL family of chemokines, typified by macrophage chemotactic protein 1 (MCP-1), serve as chemotactic factors for monocytes and macrophages. Chemokine receptors often bind multiple chemokines, and they have been found on a diversity of cell types. Cartilage has been shown to produced MCP-1 in response to IL-1, TNF-α, TGF-β, LPS and LIF [109]. Pulsatelli et al. showed that human OA, RA, and normal chondrocytes produce IL-8, GRO-α, MCP-1 (CCL-2), MIP-1α (CCL-3) and RANTES (CCL-5) in response to IL-1 and TNF-a treatment [110]. Human chondrocytes also express chemokine receptors including CCR1, CCR2, CCR3, CCR5, CXCR1, and CXCR2 [111]. Chemokines CCL-2, CCL-20, CCL-5, and CXCL6 were all identified with mean ratios above 5 suggesting an increase in chemokine production with IL-1β and TNF-α treatment (Figure 4c). IL-17B was also elevated slightly with IL-1β treatment and has been previously identified in cartilage [112]. Cytokine like protein C17 has been previously identified in cartilage [60], and CCL16 (small inducible cytokine A16) has recently been identified in synovial tissue [113]. IL-6 and M-CSF are both known to be elevated in cartilage with IL-1 and TNF-α treatment [10, 114], and M-CSF has been shown to increase CTGF expression suggesting that it may play a role in repair processes [115]. To our knowledge, no prior work has been done exploring the effects of

mechanical injury on the production of cytokines and chemokines that may play a role immune cells recruitment and inflammation following injury. Unfortunately because of the large differences seen with cytokine treatment, the elevation of cytokines and chemokines are difficult to determine. In response to IL-1β and TNF-α treatment, cartilage releases chemokines and cytokines which may modulate the inflammatory processes and immune recruitment as well as begin to promote tissue repair.

The TGF-β gene superfamily and related biological pathways play a role in cartilage phenotype determination, anabolic response, and more generally in wound repair. The TGF-β gene superfamily is composed of TGF-β 1, 2, and 3 as well as the activins/inhibins and the bone morphogenetic protein (BMP) family (for review [116]). TGF-β1-3 are complexed with latent TGF-β binding proteins (LTBPs) for secretion. TGF-β is released from these latent complexes through proteolytic cleavage MMP-2 or MMP-9 or through interactions with thrombospondin 1 or $\alpha_v\beta_6$ integrin (for review [117]). Early work on the effects of TGF-β on cartilage matrix synthesis and chondrocyte dedifferentitation by Galera et al. indicate TGF-β has little effect on chondrocyte dedifferentiation when cultured in monolayer with serum, and TGF-β may decrease collagen synthesis in primary chondrocytes [118]. Luyten et al. compared the effects of bone morphogenetic protein 4 (BMP-4), activin and TGF-β1on cell proliferation and sulfate incorporation (as a measure of sGAG synthesis) [119]. This study showed that BMP-4 and TGF-β1, and to a lesser extent activin, promoted sulfate incorporation indicating an increase in matrix production [119]. Since then, TGF-β as well as the BMPs have become widely used in stimulating mesenchymal stem cell differentiation towards a chondrocyte phenotype (for review[120]). TGF-β also plays a

primary role in wound healing and fibrosis which is mediated in part through its elevation of connective tissue growth factor (CTGF) expression, a member of the CCN family (for review [121]). To support its role in cartilage repair, Nishida et al. showed injection of CTGF into an implantable hydrogel enhanced new tissue growth following experimental defect formation in a rat OA model [122]. In addition, *ctgf*$^{-/-}$ mice suffer from impaired chondrocyte proliferation and inappropriate aggrecan and link protein deposition within the cartilage matrix[123]. Work by Omoto et al. indicates that CTGF is expressed more highly in OA cartilage than normal cartilage, and this expression is associated with chondrocyte proliferation and possible changes in chondrocyte phenotype [122]. Transfection of mouse synovial membrane cells with CTGF resulted in fibrosis (as determined by collagen type I expression and matrix deposition), an increase TGF-β, an increase in matrix degrading enzymes, and cartilage damage [124].

Bone morphogenetic proteins were first identified as factors involved in osteochondral differentiation, development, and phenotype maintenance (for review [125]). BMP-2 and BMP-4 are found in developing and OA cartilage; however very little is present in normal adult cartilage [126]. Bobacz et al. reports BMP-6 expression in normal cartilage, and shows treatment of cartilage with BMP-6 enhances proteoglycan synthesis [127]. IL-1β has been shown to increase BMP-2 expression in a chondrosarcoma cell line and in human cartilage [128, 129]; however IL-1β also suppresses the anabolic effects of BMP stimulation with the exception of BMP-7 [130-132]. BMP activity is regulated by the BMP antagonists, DAN, gremlin, chordin, and noggin. Studies focusing on the differential expression of BMP antagonists in human normal versus OA cartilage and with cytokine treatment indicate that gremlin is

decreased with both IL-1β and TNF-α treatment, that follistatin is increased with TNF-α treatment, and that chordin is unaffected by IL-1β and TNF-α treatment [133, 134].

Activins are inhibin homodimers while inhibins are heterodimers, so in the absence of other inhibins, it is likely that activin A is the biologically relevant signaling molecule in response to injury. The presence of follistatin suggests a role for the activin/inhibin family in cartilage, and Hermannson et al. reported an increase inhibin beta A protein synthesis in OA cartilage compared to normal cartilage [60]. More recently, this same group also reported inhibin beta expression by fine chopping of cartilage as well as treatment with IL-1 and TGF-β [135]. While activin A may play a role in tissue repair as a member of the TGF-β superfamily of proteins, there is also evidence that it may also serve as a pro-inflammatory molecule as it is released within minutes following LPS or yeast stimulation and its production may be stimulated by TNF-α and IL-1α (for review of activin A in systemic inflammation [136]).

Because of the important role the TGF-β superfamily of proteins and their regulators play in cartilage maintenance, we chose to take a targeted look at the response of these proteins to treatments. **Figure 4c** is a graph showing the behavior of TGF-β family proteins, their inhibitors and their binding proteins. Only three TGF-β superfamily members were identified, TGF-β2, inhibin beta, and CDMP-2. Inhibin beta was shown to be elevated in response to injury with a trend towards significance ($p \sim 0.1$) while follistatin like protein 1 was unchanged. TGF-β2 was not changed with treatment; however, a large increase in LTBP-1S and LTBP-2 were noted which may suggest an increase in TGF-β synthesis or activity. CDMP-2 shows signs of elevation with IL-1β and injury though is not statistically significant. BMP antagonist gremlin was slightly

elevated with IL-1β and TNF-α treatment while the chordin like 1 and chordin like 2 were decreased with all treatments. These profiles are markedly different than those described by Tardif et al. in human chondrocytes stimulated with TNF-α and IL-1β [133, 134]. This difference may be species based difference, or it may represent differences in cartilage/chondrocyte behavior with age and tissue maturation. No change was seen with HTRA1, a serine protease, thought to play a role in modulating TGF-β signaling and was reported to be elevated as much as 7 fold in OA cartilage explants [137]. CTGF is elevated roughly 4-fold over the untreated sample with all treatments in this study ($p<0.05$), and peptides from other CCN family members, WISP-3 and NOV were also identified. CTGF may be elevated in cartilage by BMP-2, TGF-β, or M-CSF [115, 138]. The elevation of CTGF in this system may be mediated by M-CSF which is elevated with cytokine treatment and possibly by inhibin which was elevated with injury. We hypothesize that elevation of inhibin beta and CTGF may suggest signs of early tissue repair processes. The TGF-β related biological pathways are responsive to treatment with IL-1β, TNF-α and injurious mechanical compression, and these changes may be important in mediating tissue repair.

In addition to the TGF-β related pathways, insulin-like growth factors (IGF-I and IGF-II) are important in promoting anabolic activity in cartilage, and may play a role in limiting tissue damage and promoting tissue repair. IGF-1 is produced in the liver under the regulation of growth hormone, and it is typically bound to serum IGF binding proteins (IGF-BPs; IGF-BP3 is the primary binding protein in serum) which increases it half-life in the blood (for review [139]). IGF-1 has been shown to promote anabolic behavior and inhibit catabolism in cartilage (for review [140]), and IGF binding proteins

are found within the cartilage matrix and may regulate IGF-1 stores and activity. IGF-BP6 and IGF-BP2 are the primary IGF-BPs isolated from adult steer cartilage [141]. IGF-BP3, IGF-BP4 and IGF-BP5 are increased in human OA cartilage tissue, and IGF-BP3 synthesis is increased in OA suggesting a role for IGF pathway in OA [142, 143]. At the same time, IGF-BP5 and IGF-BP3 may undergo proteolysis which eliminates its bioactivity [144]. C1r and C1s have been implicated in the break down IGF-BP5 [145]; however, Zumbrunn et al. identified HTRA1 which possesses an IGF binding domain and can act as an IGF-BP protease [146, 147]. More recently, IGF-BP3 and IGF-BP5 has been shown to have IGF-independent activities, and IGF-BP3 may enhance apoptosis in mesenchymal chondroprogenitor cells independent of IGF binding [148, 149]. Thus, both IGF-1 and IGF-2 may play an important role in maintaining cartilage catabolic activity, and IGF-BPs play a primary role in transport, storage and modulating IGF activity with IGF-BP3 possessing some IGF independent functions. Thus, **figure 4d** is a graph showing the profiles of IGF-II and IGF-BPs identified in this study and their relative quantitation with treatments. IGF-II is elevated slightly with mechanical injury, and is likely produced locally within the tissue. IGF-BP3 and IGF-BP5 are elevated with both cytokines and with injury compared to untreated controls while IGF-BP6 is only elevated with IL-1β treatment ($p<0.05$) and IGF-BP4 is largely unchanged. The elevation of IGF-BP6 may be the result of increased transport or proteolysis if it represents the most abundant IGF-BP6 normally found in bovine cartilage [150]. IGF-BP3 and IGF-BP5 are elevated sufficiently and in all conditions to suggest that they may be newly synthesized. Because both IGF-BP3 and IGF-BP5 may have both IGF-

dependent and IGF-independent activities, the elevation of these binding proteins is difficult to interpret although it likely represents a shift in tissue response to IGF.

By looking specifically at biological pathways, we were able to see evidence of increased catabolism, a decrease in anabolism, shifts in pathways regulating innate immunity and inflammation and anabolic and phenotypic response. These observations possess some similarities with normal wound healing with inflammation and innate immunity important to protect the host against infection and with repair orchestrated through TGF-β and IGF biological pathways. This analogy likely represents an oversimplification of the events occurring; however it is helpful in organizing a more targeted discussion of events before subjecting the data to a systems-level analysis.

To better understand the effects of IL-1β, TNF-α and injurious mechanical compression at a more global level, we plotted each protein as points in three dimensional space which represent each protein's response to each treatment (**Figure 5a**), and they distributed in space almost as a plane which can be seen more readily in the 2D projection plots (**figures 5b-d**). We were somewhat surprised by the linear response observed in the cytokine: untreated conditional space. Looking at individual proteins, differences between IL-1β and TNF-α can be seen; however from a systems-level view, the response of proteins to the cytokine is quite similar, and these similarities represented well by a Pearson-product-moment correlation coefficient, R of 0.87 ($R^2 = 0.7575$). The behavior of proteins in cytokine: untreated vs. injury: untreated also possesses a great deal of order, appearing almost 'Y'-shaped. The principal component analysis indicating 75% of the covariance is within a single principal component and 97% within 2 principal components exemplifies this ordering. This 'Y' shaped behavior in protein response to

cytokine treatment and to injury is consistent with known effects of each treatment. In particular, both cytokine treatment and mechanical injury are known to decrease proteoglycan and collagen synthesis as described above. In addition, mechanical injury has been shown to cause cell death primarily by apoptosis, some matrix degradation while cytokine treatment promotes an inflammatory response, cartilage matrix degradation, and possibly some apoptosis. The projection of the proteins represented as points based on the protein's response to treatment displays the overall similarities and differences between treatments in this study.

To group the proteins according to their responses to treatment, we performed K-means clustering. While four clusters may be sufficient to pull out proteins which are largely represented as decreased with treatment, unchanged with treatments, increased primarily with injury, and increased primarily with cytokine treatment, we chose six clusters in hopes of teasing out more biological details of the system. Six clusters separates those proteins that are moderately elevated (2-5 fold) from those that are more dramatically elevated (7-10 fold) in response to cytokine treatment and injury treatment. **Figure 6** is a graph of the centroid profiles represented as mean +/- SD of proteins present in the cluster in response to each treatment.

In dividing the data into six clusters, we hoped to gain further insight into cell death in this model. In our SDS-PAGE-LC/MS/MS profiling, we identified intracellular proteins released into the medium in response to the injurious mechanical compression. In this study, we identified and quantified the release of a large number of intracellular proteins that were elevated between 5 and 20 fold with mechanical injury compared to untreated and elevated 2-4 fold with cytokine treatment compared to untreated samples.

The release of intracellular proteins in response to injurious mechanical compression may result from mechanical disruption of the cells or from loss of membrane integrity in cells undergoing apoptosis. While unlikely to cause necrosis, cytokines, and TNF-α in particular, may induce apoptosis in chondrocytes, so the increase in intracellular protein release with TNF-α may be the result of apoptosis. Previous unpublished work suggests that treatment with 100 ng/ml of TNF-α promotes apoptosis in as many as 10% of the cells. IL-1β, however, is not known to cause apoptosis in chondrocytes. TNF-α causes only a moderate increase in intracellular proteins compared to IL-1β, and both cause elevated intracellular proteins over the untreated samples. Another explanation for the increase of intracellular proteins with cytokine treatment is that TNF-α and IL-1β cause an increase in transport through aggrecan degradation. This increase in transport may cause the release of intracellular proteins from cells that were damaged during explant harvesting. This alternative hypothesis is weak given the rapid release of actin post injury compared to the length of the entire study and how few intracellular protein were found in the medium of untreated explants in the gel based profiling study. In an attempt to understand the leaking of intracellular contents suggesting loss of membrane integrity and cell death, we looked more specifically at the protein differences between cluster 4 and cluster 6. In particular, we assumed that ER proteins are more likely to be released with necrosis than apoptosis. Proteins from clusters 4 and 6 were sorted according to different intracellular location and plotted based on the relative elevation with each treatment (**figure 7**). While we noted a small but statistically significant increase (~40%) in cytoplasmic and metabolic proteins compared to cytoskeletal proteins and ER proteins, this trend was consistent across all treatments relative to the untreated sample, so no

conclusions about the contributions of necrotic compared to apoptotic proteins can be made. Mechanical injury and cytokines to a lesser extent cause an elevation in intracellular proteins which may be due to mechanical cell lysis and apoptosis.

Among non-intracellular proteins identified as elevated with mechanical injury (clusters 4 and 6) were CTGF, inhibin beta, semaphorin 3C, and proenkephalin. Semaphorin 3C is known to play a role in axon guidance, repelling sympathetic nerve fibers (for review[151]). Semaphorins are thought to signal, with the help of cell surface neuropilins which signal through plexins and alter signaling through Rho-GTPases. Neuropilin-2, identified in this study, also serve as co-receptors for VEGF165 and VEGF145 [152]. Mangasser-Stephan, et al. described the expression of Semaphorin 3C (semaphorin E) expression in rheumatoid synovial cells and suggested that it may serve an immunosuppressive role[153]. Miller et al. reported expression more recently again in synovial cells and suggested that semaphorin 3C may be playing a role in inhibiting axon growth of sympathetic nerves which may serve a pro-inflammatory role by decreasing norepinephrine which may in turn lead to greater TNF-a production[154]. The presence of both semaphorin 3C and its receptor neuropilin-2 suggest a role for semaphorin 3C within the cartilage. The quantitation of both semaphorin 3C and neuropilin 2 is found in Table 4. The expression is elevated between 3 and 5 fold with all treatments giving it an expression pattern similar to CTGF. Thus, we hypothesize that semaphorin 3C may play a role in either immuosuppression or early repair processes in the tissue; however more work must be done to characterize the effects of semaphorin 3C in this model. In addition to semaphorin 3C, we also noted the elevation of proenkephalin, which was elevated only with mechanical compression injury. Proenkephalin is the precursor for

enkephalins which are opioid-like peptides that serves as neurotransmitters in the brain. Proenkephalin is abundantly expressed in bone and cartilage during organogenesis [155], and Rosen et al hypothesize that the production of opioid peptides may play a role both in tissue regeneration with injury and in pain control [156]. Consistent with its role in organogenesis and repair, Villiger et al. showed chondrocyte proliferation correlated well with proenkephalin gene expression [157]. TGF-β and PDGF stimulated cell proliferation and proenkephalin release while retinoic acid and IL-1β inhibited production [157]. Taken together, proenkephalin may play a role in cartilage repair after injury.

While many of the proteins elevated in response to cytokine treatment have already been reviewed in the targeted analysis above, some additional proteins identified with cytokine treatment included pleiotrophin and oncostatin M receptor. Pleiotrophin is a very basic cytokine (pI 10.1) and protooncogene that has been implicated in tumor transformation, apoptosis, angiogeneisis, and mitogenesis (for review[158]). Pleiotrophin leads to such diverse responses by signaling through transmembrane receptor tyrosine phosphatase (RPTP) β/γ which modulates β-catenin signaling by disrupting beta-catenin and E-cadherin association. β-catenin is an important member in the wnt signaling pathway which signals by binding frizzled and inactivating GSK-3β which targets β-catenin for degradation through phosphorylation (for review[159]). Pleiotrophin is found in abundance in the resting zone of fetal epiphyseal but not in adult normal cartilage [160]. Pleiotrophin and the wnt signaling pathway, more generally, are important in osteoblast differentiation [160, 161]. Overexpression of pleiotrophin in transgenic mice led to the expression of pleiotrophin in cartilage with poor bone-cartilage delineation and

type I collagen production within the cartilage [162]. Pufe et al. recently described pleiotrophin expression in the synovial tissue from rheumatoid arthritis patients, and showed pleiotrophin expression was elevated with TNF-α treatment. This suggests that pleiotrophin expression is increased with both IL-1β and TNF-α treatment. In addition to pleiotrophin, we note that a number of secreted frizzled proteins, inhibitors of the wnt signaling pathway were also present. Pleiotrophin represents a possible means of altering β-catenin behavior which may impact wnt signaling. We thus suggest that pleiotrophin may be involved in repair or possibly in dedifferentiation of cells with inflammatory cytokine treatment.

In conclusion, we have used iTRAQ labeling and 2D-LC/MS/MS analysis of proteins released from cartilage that was untreated, injuriously compressed, and treated with cytokine IL-1β and TNF-α, and proteins involved with injury, immunity, and repair processes were observed. Among the proteins involved in injury were intracellular proteins which we believe were primarily released in response to mechanical cell disruption; however the increase with cytokine treatment suggests that loss of membrane integrity with apoptosis may also be occurring. Protein associated with immunity were most pronounced with cytokine treatment with a increase in complement proteins factor B, C3, C1r and C1q noted as well as proteins associated with LPS binding and LPS response. Elevation of these proteins was accompanied by elevation of cytokines and chemokines which include IL-6, CCL-20, CCL-2 and M-CSF which may play a role in modulating inflammation and immune cell recruitment in vivo. Evidence of altered anabolic pathways may suggest signs of repair. TGF-β superfamily members, TGF-β2, inhibin beta, and CDMP-2 were identified. Inhibin beta was elevated with mechanical

compression injury, LTBPs were elevated with cytokine treatment as well as a decrease in BMP antagonist, chordin like 1 and chordin like 2. A release of different IGF binding proteins may suggest a shift in IGF pathway with the potential to increase the extracellular stores of the enzyme. Of note, both IGF-BP3 and IGF-BP5 may serve IGF-independent functions and were shown to be elevated with all treatments. Finally, we note an increase in CTGF, semaphorin 3C, proenkephalin, and possibly pleiotrophin as proteins that may also play a role in tissue repair processes. In response to cytokine treatment and mechanical injury, cartilage possesses some ability to repair damage as long as the injury is not too severe and inflammation not too prolonged. The observations of protein response in this study reflect tissue damage, immunity, and potentially signs of repair. Understanding of these pathways and their effects on cartilage may aid in identifying new therapeutic strategies to treat disease processes.

Acknowledgments. I thank to Dr. Forest White for his invaluable assistance with the experimental design and mass spectrometry assistance. I thank Dr. Jimmy Flarakos for his technical assistance with the offline 2D-LC/MS/MS experimental approach.

4.7 FIGURES

Figure 4.1

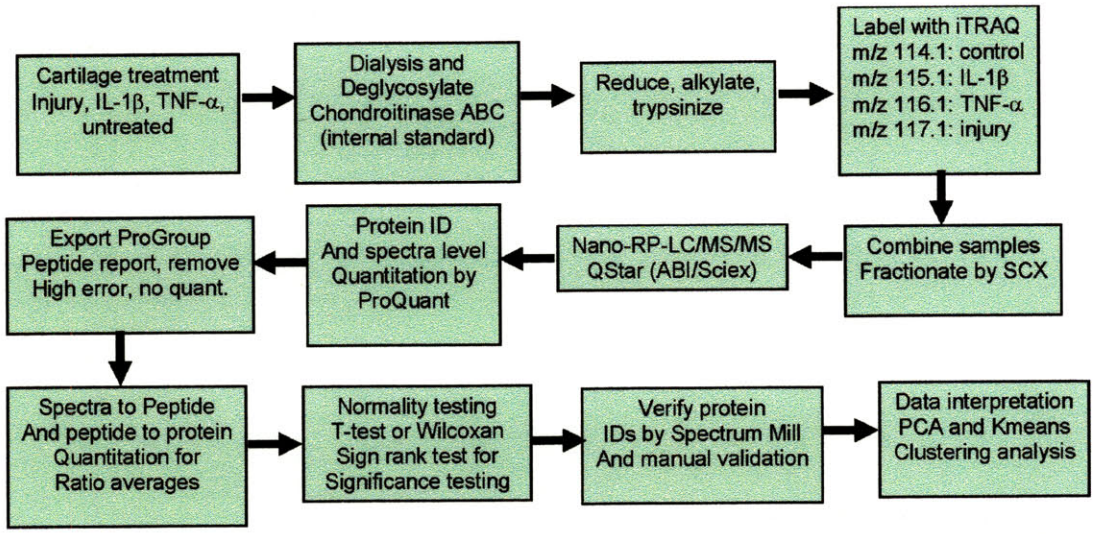

Figure 1: Figure 1 is a schematic of 2D-LC/MS/MS data analysis process. Samples are first deglycosylated with Chondroitinase ABC. The proteins are then subjected to reduction, alkylation and trypsinization before labeling with the iTRAQ reagent. Each sample is labeled with a reporter tag with a unique signature ion, and the samples are combined and subjected to SCX chromatography and the fractions are analyzed by LC/MS/MS (QStar). Data is collected and analyzed by ProQuant, and the assembled peptide list from ProGroup report is imported to excel where low confidence peptides are removed as are peptides with incomplete quantitation. The data is imported into matlab where the spectra are combined to peptide averages and then the peptide averages are combined to get a protein level average with statistical analyses being done using both t-tests and Wilcoxan tests with Bonferroni correction for multiple comparisons. Finally, protein identifications are verified by a combination of Spectrum Mill and manual validation prior to further analyses.

Table 4.1

Table 1

Expt	Peptides	115:114	115 SD	116:114	116 SD	117:114	117 SD	Normal
Itraq1	65	1.29	1.30	0.995	1.22	1.23	1.19	Yes (3)
Itraq2	55	2.43	1.76	2.81	2.14	2.26	1.68	Yes(1)

Table 1: Chondroitinase ABC normalization statistics. Table 1 provides the Chondroitinase ABC geometric mean signature ion ratios which were used to normalize data. Normalization was performed by dividing all protein signature ion ratios by the corresponding Chondroitinase ABC ratio. Some sample loss occurred with untreated (*m/z* 114.1 labeled sample) which led to high correction values for the second set of samples.

Figure 4.2: Comparison of the first and second analytical duplicates

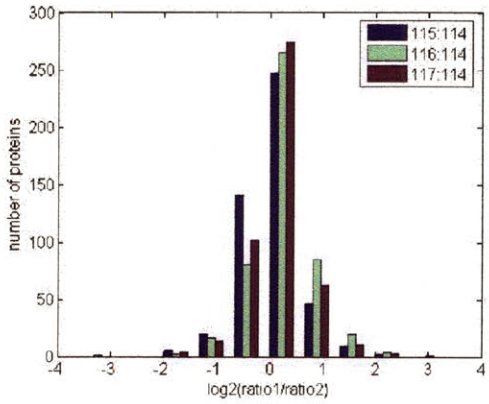

Figure 2 Analytical variation and reproducibility. Figure 2a are overlaid histograms comparing the mean protein ratios between the first analytical duplicate and the second analytical duplicate after internal standard correction. The data are plotted as log2(mean protein ratio experiment 1 / mean protein ratio experiment 2). The mean log2(protein ratio1/protein ratio2) +/- SD for 115:114 is 0.0311 +/-0.5602 for 116:114 is -0.2371+/-0.5736 and for 117:114 is 0.1596 +/- 0.5435. As for the inter-injection graphs, a mean of 0 is expected, and we see here an offset as high as 17% for the 116:114 ratio. The error described by the variance of the log2(ratio1/ratio2) is in part dependent on error caused by large ratios and poor identification/quantitation (supplemental data).

Figure 4.3: Matrix proteins Released

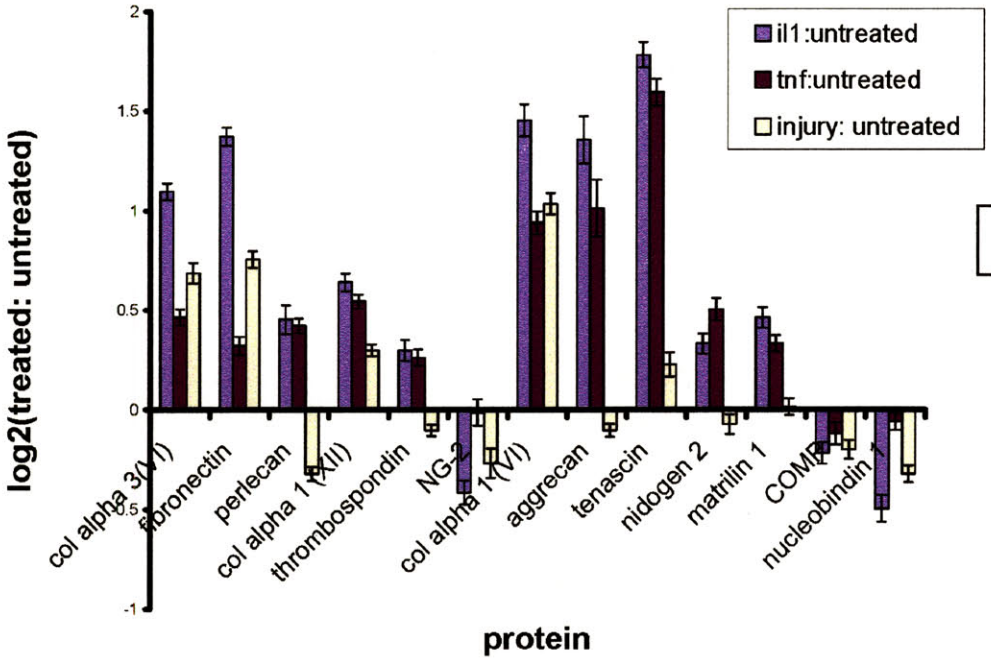

Figure 3a

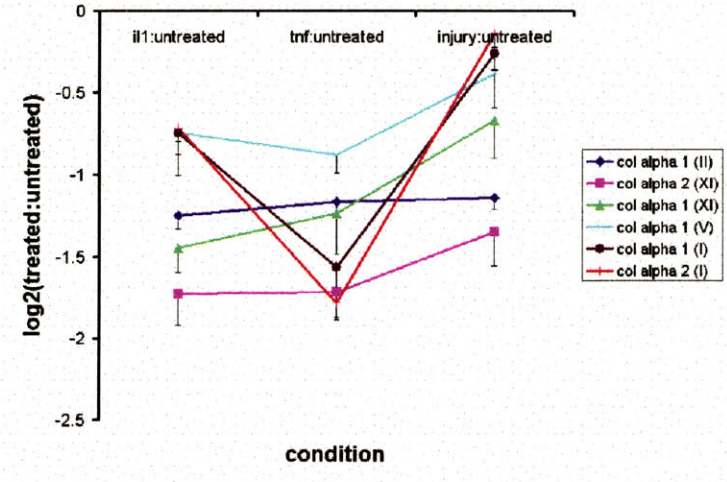

Figure 3b

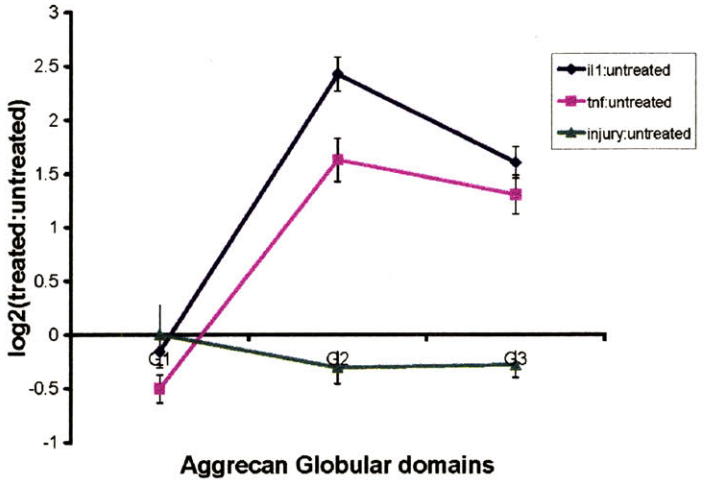

Figure 3c

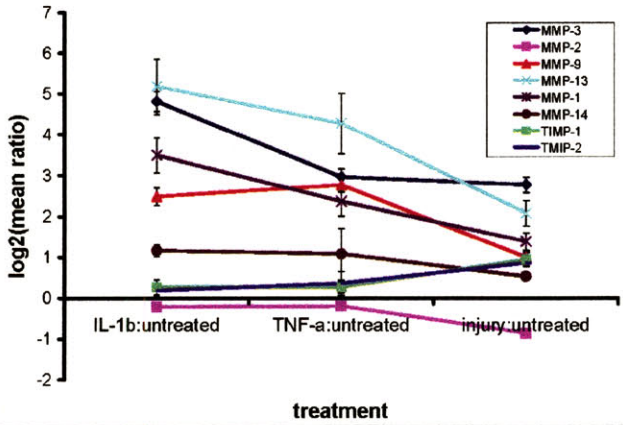

Figure 3d

Figure 3: Matrix Proteins and MMPs released to the medium. Figure 3a is a graph displaying the behavior of the top 14 scoring matrix proteins. With the exception of nidogen and matrilin 1 with injury and nucleobindin 1 and COMP with TNF-alpha treatment, all changes are statistically significant at $p < 0.05$. Caution should be used in interpreting statistical significance of finding that represents less than a 50% increase. To better characterize the anabolic state of the system, Figure 3b is a graph of the C-terminal telopeptides of fibrillar collagens, col2A1, col11A1, col11A2, col5A1, col1A1, col1A2. The release of these telopeptides may approximate the production of new fibrillar collagens, and this data suggest that collagen synthesis is generally decreased with all treatments. Figure 3c is a graph of aggrecan quantitation based on peptides from each globular domain. Aggrecan is a proteoglycan that is rapidly proteolyzed in response to IL-1beta and TNF-alpha treatment. The graph suggests that G2 and G3 are lost more readily than G1 which is consistent with known behavior of the proteoglycan. Figure 3d displays the response of MMP identified in the medium with each treatment. All data is represented as mean +/- SEM of between 3 and 100 peptides.

Table 4.2

Table 2: p values for collagen C-terminal telopeptides and aggrecan globular domain release

Condition	Col2A1	Col11A1	Col11A2	Col5A1	Col1A1	Col1A2	G1	G2	G3
IL-1β:cont	<0.005	<0.005	<0.005	<0.05	<0.005	<0.005	ns	<0.005	<0.005
TNF-α:cont	<0.005	<0.01	<0.005	<0.005	<0.005	<0.005	<0.05	<0.005	<0.005
Injury:cont	<0.005	<0.05	<0.005	~0.6	~0.9	~0.3	ns	~0.3	~0.3

Table 2 lists the p values of collagen C-terminal telopeptides and aggrecan globular domains for statistical comparisons treatment and control using Student's t-test with Bonferroni correction for multiple comparisons

Table 4.3

Table 3: p values for statistical significance in comparing treatment to untreated by Student's t-test with correction for multiple comparisons

Protein	p value IL-1β:untreated	p value TNF-α:untreated	p value Injury:untreated
MMP-3	<0.001	<0.001	<0.001
MMP-2	0.004	0.02	<0.001
MMP-9	<0.001	<0.001	<0.001
MMP-13	0.009	0.027	0.057
TIMP-1	1.23	0.54	0.023
MMP-1	0.001	0.09	0.10
MMP-14	0.09	1.3	0.008
TIMP-2	0.36	5.4	<0.001

Table 3 lists the p values for statistical significance in comparison each treatment to the untreated control by Student's t-test with Bonferroni correction for multiple comparisons. All p values smaller than 0.001 are indicated as <0.001.

Figure 4.4

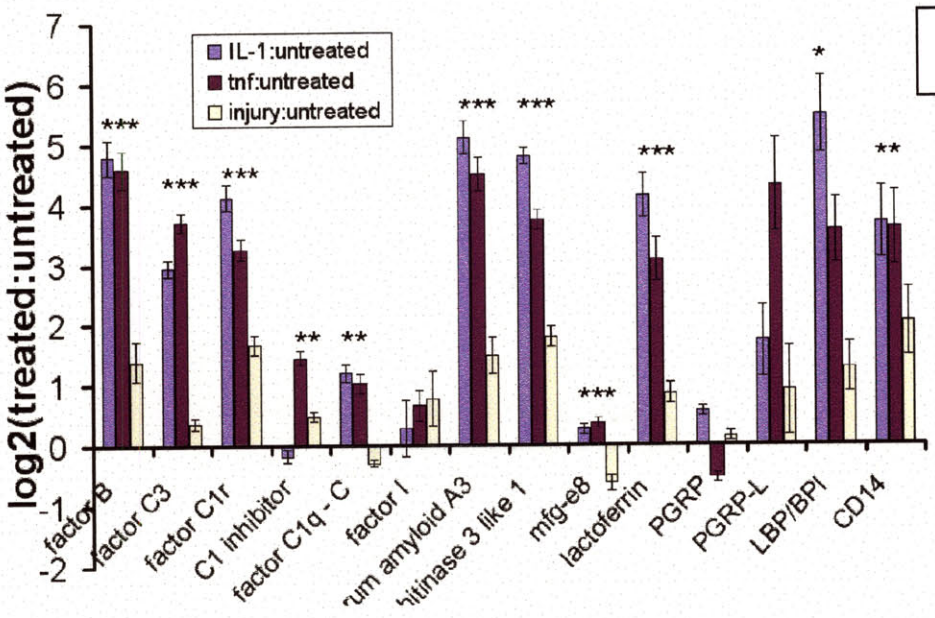

Figure 4a

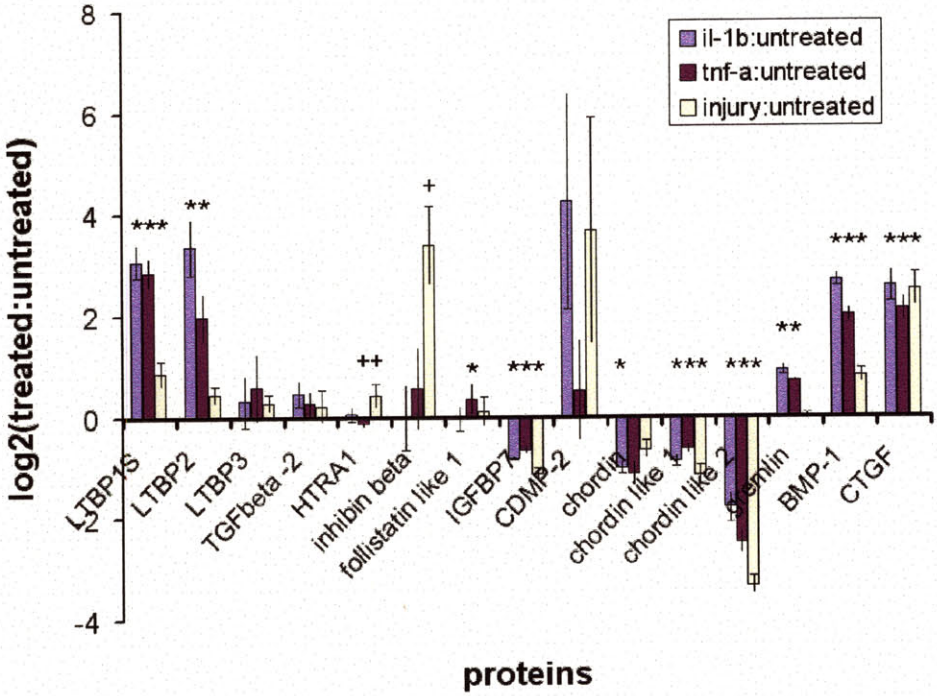

Figure 4c

Figure 4B

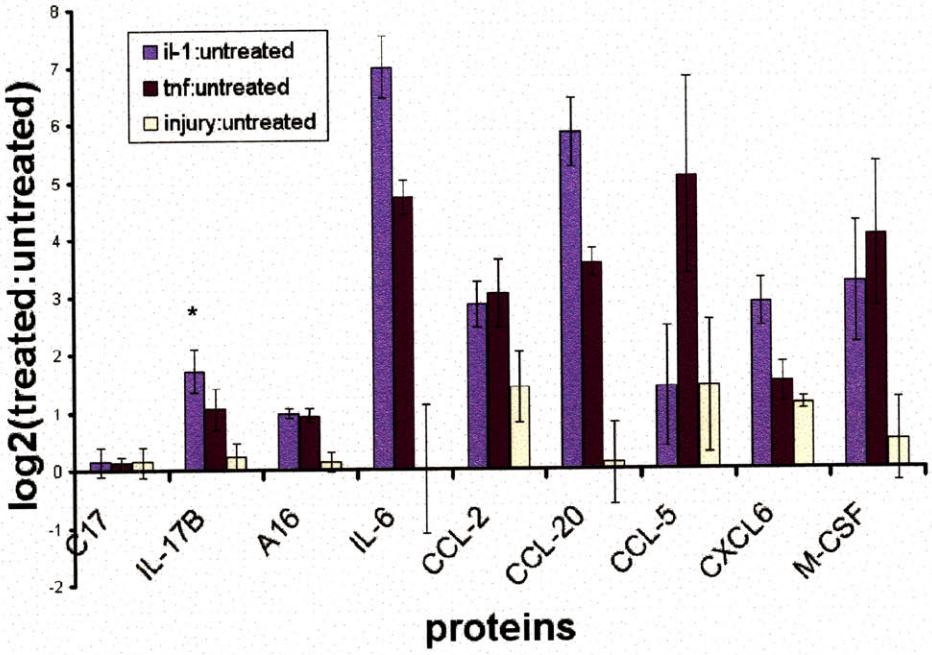

Figure 4D

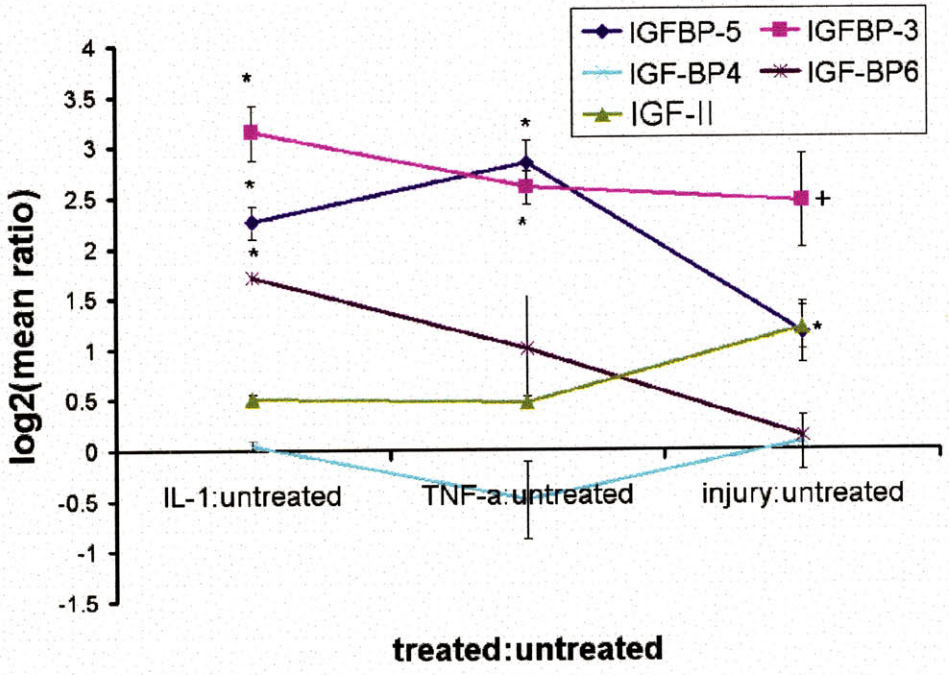

Figure 4. Figure 4 are a set of graphs focusing on biological pathways to better understand the effects of treatments. Figure 4a is a graph of proteins involved in innate immunity including complements and antimicrobials. Figure 4b is showing the behavior of proteins involved in the signaling of TGF-beta superfamily members and their inhibitors. Figure 4c is a set of cytokines and chemokines and their production with each treatment. Figure 4d are the IGF binding proteins. All data are plotted as the mean ratio value for each treatment +/- SEM with the number of peptides ranging from 2 to 35. The asterisks indicate $p<0.05$ for significance of treatment compared to control and the '+' indicates $p<0.1$ indicating a trend towards significance. All statistical analyses were done by either Wilcoxan Sign rank or Student's t-test with Bonferroni correction for multiple comparisons.

Figure 4.5

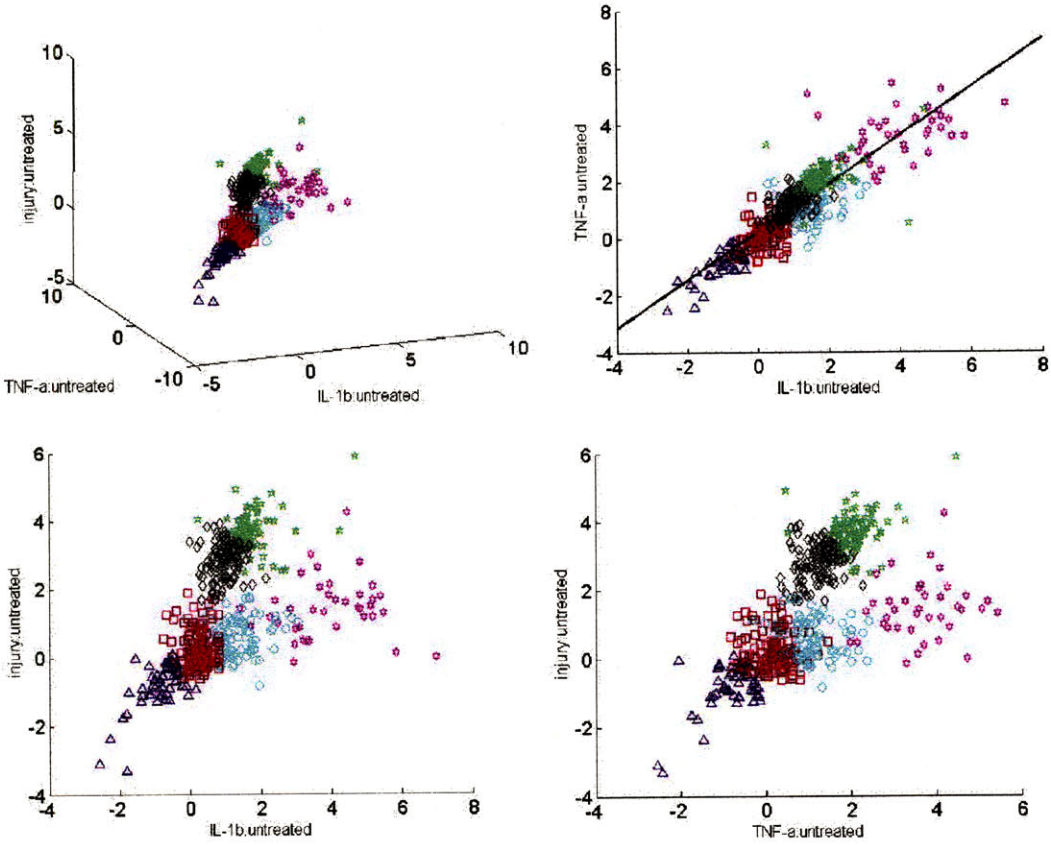

Figure 5: Projection plot of proteins represented by the three treated:untreated ratio conditions with colors representing the protein clusters defined by K-means clustering. Figure 5a includes all three dimensions and appears almost planar in the threedimensional condition space. Figures 5b-d represent the three 2D projections of the data. Figure 5b has been fitted to a line with a slope of 0.8465, an intercept of 0.2152 and Pearson product moment correlation coefficient, R, of 0.87, indicating a robust and statistically significant relationship between the response of proteins to TNF-alpha and to IL-1beta ($p<0.0001$). Figure 5c-d proteins are arranged in a 'Y' shaped pattern suggesting similarities and differences exist between the response to cytokine treatment and injurious mechanical compression.

Figure 4.6

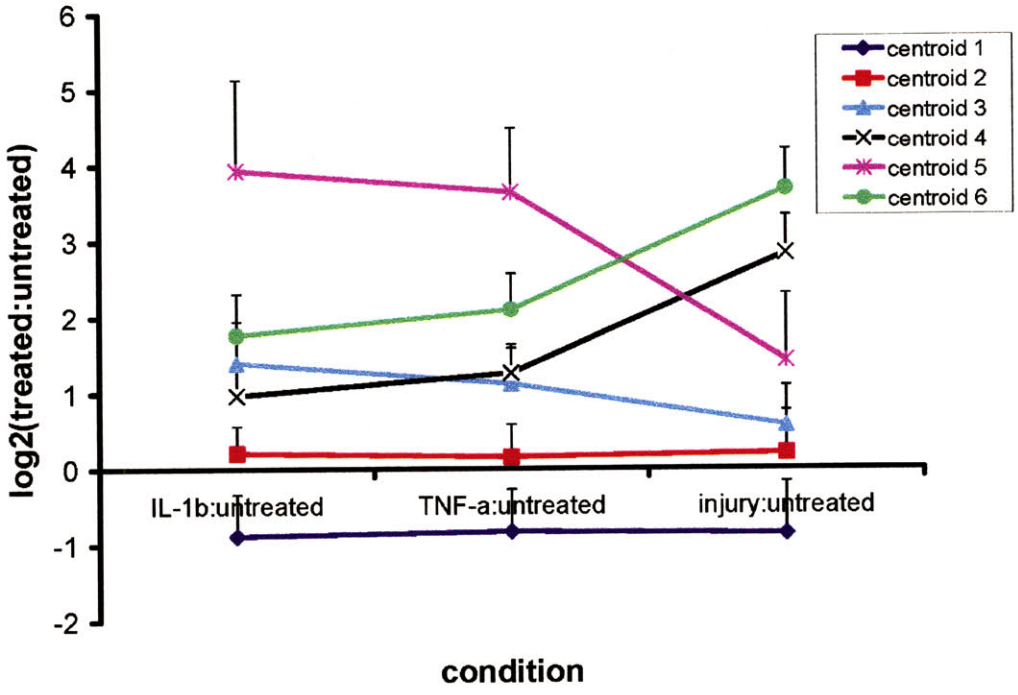

Figure 6: Centroid profiles for the six clusters identified by K-means clustering. Data is displayed as centroid mean +/- SD, and all clusters are significantly different from one another ($p<0.001$). Each cluster contains between 42 and 156 proteins, and they represent the proteins response to the treatments.

Figure 4.7

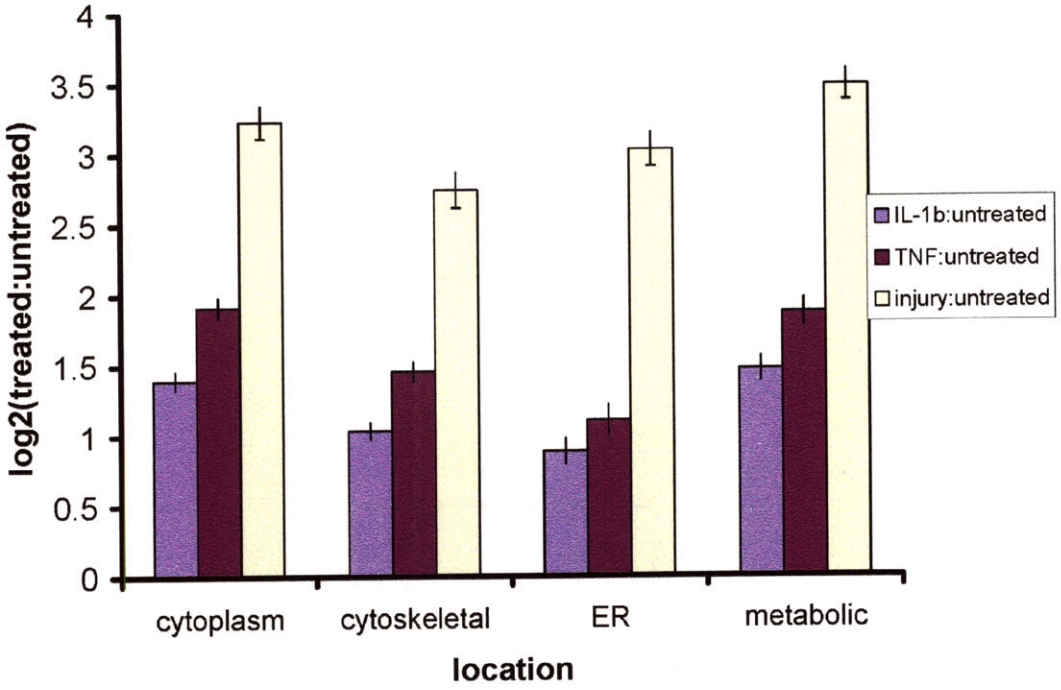

Figure 7. Intracellular proteins released in response to treatment separated by intracellular function or location. Mechanical injury, TNF-α and IL-1β causes a significant increase in the release of intracellular proteins compared to the untreated control. A slight increase in the release of cytoplasmic and metabolic proteins was seen compared to cytoskeletal and ER proteins. This difference was consistent with all treatments. This difference in loss may reflect different modes of cell death or normal differences in release rates for different intracellular components.

Table 4.4: Other Potentially Relevant Regulators

Protein Name	IL-1β: untreated	TNF-α: untreated	Injury: untreated
Semaphorin 3C	**4.48**	**2.73**	**4.88**
Neuropilin 2	**1.83**	**2.34**	1.03
Proenkephalin	2.5	1.39	29.9
Pleiotrophin	**9.82**	**4.43**	1.37
Frizzled related protein	1.81	1.77	0.83
Secreted frizzled 1	**2.3**	**1.9**	1.13
sFRP4	3.6	2.5	**1.4**
PDGF-like receptor	1.07	0.98	**0.79**
Angiopoeitin like 7	**1.54**	**2.23**	**2.45**
GAS6	0.74	*0.64*	*0.61*
Fibroleukin	**2.13**	**2.34**	1.03
APP	**0.52**	**0.62**	**0.41**

Table 4: Potentially relevant regulators. Table 4 is a list of some of the other potential regulatory proteins identified in the samples and their relative quantitation.

4.7 REFERENCES

1. Pfander, D., R. Rahmanzadeh, and E.E. Scheller, *Presence and distribution of collagen II, collagen I, fibronectin, and tenascin in rabbit normal and osteoarthritic cartilage.* J Rheumatol, 1999. **26**(2): p. 386-94.
2. Maroudas, A.I., *Balance between swelling pressure and collagen tension in normal and degenerate cartilage.* Nature, 1976. **260**(5554): p. 808-9.
3. Kleemann, R.U., et al., *Altered cartilage mechanics and histology in knee osteoarthritis: relation to clinical assessment (ICRS Grade).* Osteoarthritis Cartilage, 2005. **13**(11): p. 958-63.
4. Wilson, T.C., et al., *Pulmonary and systemic induction of SAA3 after ventilation and endotoxin in preterm lambs.* Pediatr Res, 2005. **58**(6): p. 1204-9.
5. Chevalier, X., *Fibronectin, cartilage, and osteoarthritis.* Semin Arthritis Rheum, 1993. **22**(5): p. 307-18.
6. Goldring, M.B., *Update on the Chondrocyte Lineage and Implications for Cell Therapy in Arthritis*, in *Osteoarthritis*, L. Sharma, Berenbaum, F., Editor. in press, Elsevier.
7. Westacott, C.I., et al., *Synovial fluid concentration of five different cytokines in rheumatic diseases.* Ann Rheum Dis, 1990. **49**(9): p. 676-81.
8. Wood, D.D., et al., *Isolation of an interleukin-1-like factor from human joint effusions.* Arthritis Rheum, 1983. **26**(8): p. 975-83.
9. Smith, J.B., et al., *Occurrence of interleukin-1 in human synovial fluid: detection by RIA, bioassay and presence of bioassay-inhibiting factors.* Rheumatol Int, 1989. **9**(2): p. 53-8.
10. Shinmei, M., et al., *The role of cytokines in chondrocyte mediated cartilage degradation.* J Rheumatol Suppl, 1989. **18**: p. 32-4.
11. Saxne, T., et al., *Detection of tumor necrosis factor alpha but not tumor necrosis factor beta in rheumatoid arthritis synovial fluid and serum.* Arthritis Rheum, 1988. **31**(8): p. 1041-5.
12. Hopkins, S.J. and A. Meager, *Cytokines in synovial fluid: II. The presence of tumour necrosis factor and interferon.* Clin Exp Immunol, 1988. **73**(1): p. 88-92.
13. Fontana, A., et al., *Interleukin 1 activity in the synovial fluid of patients with rheumatoid arthritis.* Rheumatol Int, 1982. **2**(2): p. 49-53.
14. Di Giovine, F.S., G. Nuki, and G.W. Duff, *Tumour necrosis factor in synovial exudates.* Ann Rheum Dis, 1988. **47**(9): p. 768-72.
15. Cooper, W.O., et al., *Acceleration of onset of collagen-induced arthritis by intra-articular injection of tumour necrosis factor or transforming growth factor-beta.* Clin Exp Immunol, 1992. **89**(2): p. 244-50.
16. Pettipher, E.R., G.A. Higgs, and B. Henderson, *Interleukin 1 induces leukocyte infiltration and cartilage proteoglycan degradation in the synovial joint.* Proc Natl Acad Sci U S A, 1986. **83**(22): p. 8749-53.
17. Pettipher, E.R., et al., *Leucocyte infiltration and cartilage proteoglycan loss in immune arthritis in the rabbit.* Br J Pharmacol, 1988. **95**(1): p. 169-76.
18. Arner, E.C., et al., *In vivo studies on the effects of human recombinant interleukin-1 beta on articular cartilage.* Agents Actions, 1989. **27**(3-4): p. 254-7.

19. Hawkins, D.L., et al., *Effect of tumor necrosis factor antibody on synovial fluid cytokine activities in equine antebrachiocarpal joints injected with endotoxin.* Am J Vet Res, 1995. **56**(10): p. 1292-9.
20. Goldring, M.B., *The role of the chondrocyte in osteoarthritis.* Arthritis Rheum, 2000. **43**(9): p. 1916-26.
21. Goldring, S.R. and M.B. Goldring, *The role of cytokines in cartilage matrix degeneration in osteoarthritis.* Clin Orthop Relat Res, 2004(427 Suppl): p. S27-36.
22. Saklatvala, J., *Tumour necrosis factor alpha stimulates resorption and inhibits synthesis of proteoglycan in cartilage.* Nature, 1986. **322**(6079): p. 547-9.
23. Saklatvala, J., et al., *Pig catabolin is a form of interleukin 1. Cartilage and bone resorb, fibroblasts make prostaglandin and collagenase, and thymocyte proliferation is augmented in response to one protein.* Biochem J, 1984. **224**(2): p. 461-6.
24. Arner, E.C., et al., *Cytokine-induced cartilage proteoglycan degradation is mediated by aggrecanase.* Osteoarthritis Cartilage, 1998. **6**(3): p. 214-28.
25. Burrage, P.S., K.S. Mix, and C.E. Brinckerhoff, *Matrix metalloproteinases: role in arthritis.* Front Biosci, 2006. **11**: p. 529-43.
26. Henrotin, Y.E., et al., *Effects of exogenous IL-1 beta, TNF alpha, IL-6, IL-8 and LIF on cytokine production by human articular chondrocytes.* Osteoarthritis Cartilage, 1996. **4**(3): p. 163-73.
27. Henrotin, Y.E., et al., *Nitric oxide downregulates interleukin 1beta (IL-1beta) stimulated IL-6, IL-8, and prostaglandin E2 production by human chondrocytes.* J Rheumatol, 1998. **25**(8): p. 1595-601.
28. Kienzle, G. and J. von Kempis, *Vascular cell adhesion molecule 1 (CD106) on primary human articular chondrocytes: functional regulation of expression by cytokines and comparison with intercellular adhesion molecule 1 (CD54) and very late activation antigen 2.* Arthritis Rheum, 1998. **41**(7): p. 1296-305.
29. Pettipher, E.R., *Pathogenesis and treatment of chronic arthritis.* Sci Prog, 1989. **73**(292 Pt 4): p. 521-34.
30. Grall, F., et al., *Responses to the proinflammatory cytokines interleukin-1 and tumor necrosis factor alpha in cells derived from rheumatoid synovium and other joint tissues involve nuclear factor kappaB-mediated induction of the Ets transcription factor ESE-1.* Arthritis Rheum, 2003. **48**(5): p. 1249-60.
31. Furst, D.E., *Anakinra: review of recombinant human interleukin-I receptor antagonist in the treatment of rheumatoid arthritis.* Clin Ther, 2004. **26**(12): p. 1960-75.
32. Furst, D.E., et al., *Updated consensus statement on biological agents, specifically tumour necrosis factor alpha (TNFalpha) blocking agents and interleukin-1 receptor antagonist (IL-1ra), for the treatment of rheumatic diseases, 2004.* Ann Rheum Dis, 2004. **63 Suppl 2**: p. ii2-ii12.
33. Dayer, J.M., *The saga of the discovery of IL-1 and TNF and their specific inhibitors in the pathogenesis and treatment of rheumatoid arthritis.* Joint Bone Spine, 2002. **69**(2): p. 123-32.
34. Dayer, J.M., *Interleukin 1 or tumor necrosis factor-alpha: which is the real target in rheumatoid arthritis?* J Rheumatol Suppl, 2002. **65**: p. 10-5.

35. Gelber, A.C., et al., *Joint injury in young adults and risk for subsequent knee and hip osteoarthritis.* Ann Intern Med, 2000. **133**(5): p. 321-8.
36. Roos, H., et al., *Osteoarthritis of the knee after injury to the anterior cruciate ligament or meniscus: the influence of time and age.* Osteoarthritis Cartilage, 1995. **3**(4): p. 261-7.
37. von Porat, A., E.M. Roos, and H. Roos, *High prevalence of osteoarthritis 14 years after an anterior cruciate ligament tear in male soccer players: a study of radiographic and patient relevant outcomes.* Ann Rheum Dis, 2004. **63**(3): p. 269-73.
38. Daniel, D.M., et al., *Fate of the ACL-injured patient. A prospective outcome study.* Am J Sports Med, 1994. **22**(5): p. 632-44.
39. Roos, H., et al., *Knee osteoarthritis after meniscectomy: prevalence of radiographic changes after twenty-one years, compared with matched controls.* Arthritis Rheum, 1998. **41**(4): p. 687-93.
40. Buckwalter, J.A. and T.D. Brown, *Joint injury, repair, and remodeling: roles in post-traumatic osteoarthritis.* Clin Orthop Relat Res, 2004(423): p. 7-16.
41. Irie, K., E. Uchiyama, and H. Iwaso, *Intraarticular inflammatory cytokines in acute anterior cruciate ligament injured knee.* Knee, 2003. **10**(1): p. 93-6.
42. Lohmander, L.S., T. Saxne, and D.K. Heinegard, *Release of cartilage oligomeric matrix protein (COMP) into joint fluid after knee injury and in osteoarthritis.* Ann Rheum Dis, 1994. **53**(1): p. 8-13.
43. Cameron, M., et al., *The natural history of the anterior cruciate ligament-deficient knee. Changes in synovial fluid cytokine and keratan sulfate concentrations.* Am J Sports Med, 1997. **25**(6): p. 751-4.
44. Tchetverikov, I., et al., *MMP protein and activity levels in synovial fluid from patients with joint injury, inflammatory arthritis, and osteoarthritis.* Ann Rheum Dis, 2005. **64**(5): p. 694-8.
45. Lohmander, L.S., et al., *The release of crosslinked peptides from type II collagen into human synovial fluid is increased soon after joint injury and in osteoarthritis.* Arthritis Rheum, 2003. **48**(11): p. 3130-9.
46. Lohmander, L.S., et al., *Changes in joint cartilage aggrecan after knee injury and in osteoarthritis.* Arthritis Rheum, 1999. **42**(3): p. 534-44.
47. Loening, A.M., et al., *Injurious mechanical compression of bovine articular cartilage induces chondrocyte apoptosis.* Arch Biochem Biophys, 2000. **381**(2): p. 205-12.
48. D'Lima, D.D., et al., *Human chondrocyte apoptosis in response to mechanical injury.* Osteoarthritis Cartilage, 2001. **9**(8): p. 712-9.
49. Kurz, B., et al., *Biosynthetic response and mechanical properties of articular cartilage after injurious compression.* J Orthop Res, 2001. **19**(6): p. 1140-6.
50. Thibault, M., A.R. Poole, and M.D. Buschmann, *Cyclic compression of cartilage/bone explants in vitro leads to physical weakening, mechanical breakdown of collagen and release of matrix fragments.* J Orthop Res, 2002. **20**(6): p. 1265-73.
51. Chen, C.T., et al., *Compositional and metabolic changes in damaged cartilage are peak-stress, stress-rate, and loading-duration dependent.* J Orthop Res, 1999. **17**(6): p. 870-9.

52. Lin, P.M., C.T. Chen, and P.A. Torzilli, *Increased stromelysin-1 (MMP-3), proteoglycan degradation (3B3- and 7D4) and collagen damage in cyclically load-injured articular cartilage.* Osteoarthritis Cartilage, 2004. **12**(6): p. 485-96.
53. Lee, J.H., et al., *Mechanical injury of cartilage explants causes specific time-dependent changes in chondrocyte gene expression.* Arthritis Rheum, 2005. **52**(8): p. 2386-95.
54. Vincent, T.L., et al., *Basic fibroblast growth factor mediates transduction of mechanical signals when articular cartilage is loaded.* Arthritis Rheum, 2004. **50**(2): p. 526-33.
55. Hunziker, E.B., *Articular cartilage repair: basic science and clinical progress. A review of the current status and prospects.* Osteoarthritis Cartilage, 2002. **10**(6): p. 432-63.
56. Hunziker, E.B., *Articular cartilage repair: are the intrinsic biological constraints undermining this process insuperable?* Osteoarthritis Cartilage, 1999. **7**(1): p. 15-28.
57. Vincent, T., et al., *Basic FGF mediates an immediate response of articular cartilage to mechanical injury.* Proc Natl Acad Sci U S A, 2002. **99**(12): p. 8259-64.
58. Gruber, J., et al., *Induction of interleukin-1 in articular cartilage by explantation and cutting.* Arthritis Rheum, 2004. **50**(8): p. 2539-46.
59. Catterall, J.B., et al., *Development of a novel 2D proteomics approach for the identification of proteins secreted by primary chondrocytes after stimulation by IL-1 and oncostatin M.* Rheumatology (Oxford), 2006.
60. Hermansson, M., et al., *Proteomic analysis of articular cartilage shows increased type II collagen synthesis in osteoarthritis and expression of inhibin betaA (activin A), a regulatory molecule for chondrocytes.* J Biol Chem, 2004. **279**(42): p. 43514-21.
61. Liao, H., et al., *Use of mass spectrometry to identify protein biomarkers of disease severity in the synovial fluid and serum of patients with rheumatoid arthritis.* Arthritis Rheum, 2004. **50**(12): p. 3792-803.
62. Gygi, S.P., et al., *Quantitative analysis of complex protein mixtures using isotope-coded affinity tags.* Nat Biotechnol, 1999. **17**(10): p. 994-9.
63. Ross, P.L., et al., *Multiplexed protein quantitation in Saccharomyces cerevisiae using amine-reactive isobaric tagging reagents.* Mol Cell Proteomics, 2004. **3**(12): p. 1154-69.
64. Sah, R.L., et al., *Biosynthetic response of cartilage explants to dynamic compression.* J Orthop Res, 1989. **7**(5): p. 619-36.
65. Frank, E.H., et al., *A versatile shear and compression apparatus for mechanical stimulation of tissue culture explants.* J Biomech, 2000. **33**(11): p. 1523-7.
66. DiMicco, M.A., et al., *Mechanisms and kinetics of glycosaminoglycan release following in vitro cartilage injury.* Arthritis Rheum, 2004. **50**(3): p. 840-8.
67. Patwari, P., et al., *Proteoglycan degradation after injurious compression of bovine and human articular cartilage in vitro: interaction with exogenous cytokines.* Arthritis Rheum, 2003. **48**(5): p. 1292-301.

68. Peng, J., et al., *Evaluation of multidimensional chromatography coupled with tandem mass spectrometry (LC/LC-MS/MS) for large-scale protein analysis: the yeast proteome.* J Proteome Res, 2003. **2**(1): p. 43-50.
69. Hsieh, Y.L., et al., *Automated analytical system for the examination of protein primary structure.* Anal Chem, 1996. **68**(3): p. 455-62.
70. Bhat, V.B., et al., *Comparative plasma proteome analysis of lymphoma-bearing SJL mice.* J Proteome Res, 2005. **4**(5): p. 1814-25.
71. Keshamouni, V.G., et al., *Differential protein expression profiling by iTRAQ-2DLC-MS/MS of lung cancer cells undergoing epithelial-mesenchymal transition reveals a migratory/invasive phenotype.* J Proteome Res, 2006. **5**(5): p. 1143-54.
72. Goldring, M.B., et al., *Interleukin 1 suppresses expression of cartilage-specific types II and IX collagens and increases types I and III collagens in human chondrocytes.* J Clin Invest, 1988. **82**(6): p. 2026-37.
73. Lefebvre, V., C. Peeters-Joris, and G. Vaes, *Modulation by interleukin 1 and tumor necrosis factor alpha of production of collagenase, tissue inhibitor of metalloproteinases and collagen types in differentiated and dedifferentiated articular chondrocytes.* Biochim Biophys Acta, 1990. **1052**(3): p. 366-78.
74. Petropoulou, V., L. Garrigue-Antar, and K.E. Kadler, *Identification of the minimal domain structure of bone morphogenetic protein-1 (BMP-1) for chordinase activity: chordinase activity is not enhanced by procollagen C-proteinase enhancer-1 (PCPE-1).* J Biol Chem, 2005. **280**(24): p. 22616-23.
75. Torzilli, P.A., et al., *Effect of proteoglycan removal on solute mobility in articular cartilage.* J Biomech, 1997. **30**(9): p. 895-902.
76. Reginato, A.M., et al., *Transcriptional modulation of cartilage-specific collagen gene expression by interferon gamma and tumour necrosis factor alpha in cultured human chondrocytes.* Biochem J, 1993. **294 (Pt 3)**: p. 761-9.
77. Goldring, M.B., *Control of collagen synthesis in human chondrocyte cultures by immune interferon and interleukin-1.* J Rheumatol, 1987. **14 Spec No**: p. 64-6.
78. Sah, R.L., et al., *Effects of compression on the loss of newly synthesized proteoglycans and proteins from cartilage explants.* Arch Biochem Biophys, 1991. **286**(1): p. 20-9.
79. Dudhia, J., *Aggrecan, aging and assembly in articular cartilage.* Cell Mol Life Sci, 2005. **62**(19-20): p. 2241-56.
80. Roughley, P.J., R.J. White, and A.R. Poole, *Identification of a hyaluronic acid-binding protein that interferes with the preparation of high-buoyant-density proteoglycan aggregates from adult human articular cartilage.* Biochem J, 1985. **231**(1): p. 129-38.
81. Maroudas, A., et al., *Aggrecan turnover in human articular cartilage: use of aspartic acid racemization as a marker of molecular age.* Arch Biochem Biophys, 1998. **350**(1): p. 61-71.
82. Fosang, A.J., et al., *Generation and novel distribution of matrix metalloproteinase-derived aggrecan fragments in porcine cartilage explants.* J Biol Chem, 2000. **275**(42): p. 33027-37.
83. Embry, J.J. and W. Knudson, *G1 domain of aggrecan cointernalizes with hyaluronan via a CD44-mediated mechanism in bovine articular chondrocytes.* Arthritis Rheum, 2003. **48**(12): p. 3431-41.

84. Flannery, C.R., M.W. Lark, and J.D. Sandy, *Identification of a stromelysin cleavage site within the interglobular domain of human aggrecan. Evidence for proteolysis at this site in vivo in human articular cartilage.* J Biol Chem, 1992. **267**(2): p. 1008-14.
85. Ganu, V., et al., *Inhibition of interleukin-1alpha-induced cartilage oligomeric matrix protein degradation in bovine articular cartilage by matrix metalloproteinase inhibitors: potential role for matrix metalloproteinases in the generation of cartilage oligomeric matrix protein fragments in arthritic synovial fluid.* Arthritis Rheum, 1998. **41**(12): p. 2143-51.
86. Chin, J.R., G. Murphy, and Z. Werb, *Stromelysin, a connective tissue-degrading metalloendopeptidase secreted by stimulated rabbit synovial fibroblasts in parallel with collagenase. Biosynthesis, isolation, characterization, and substrates.* J Biol Chem, 1985. **260**(22): p. 12367-76.
87. Knauper, V., et al., *Biochemical characterization of human collagenase-3.* J Biol Chem, 1996. **271**(3): p. 1544-50.
88. Aigner, T. and L. McKenna, *Molecular pathology and pathobiology of osteoarthritic cartilage.* Cell Mol Life Sci, 2002. **59**(1): p. 5-18.
89. Liacini, A., et al., *Induction of matrix metalloproteinase-13 gene expression by TNF-alpha is mediated by MAP kinases, AP-1, and NF-kappaB transcription factors in articular chondrocytes.* Exp Cell Res, 2003. **288**(1): p. 208-17.
90. Sadowski, T. and J. Steinmeyer, *Differential effects of nonsteroidal antiinflammatory drugs on the IL-1 altered expression of plasminogen activators and plasminogen activator inhibitor-1 by articular chondrocytes.* Inflamm Res, 2002. **51**(8): p. 427-33.
91. Kandel, R.A., et al., *Fetal bovine serum inhibits chondrocyte collagenase production: interleukin 1 reverses this effect.* Biochim Biophys Acta, 1990. **1053**(2-3): p. 130-4.
92. Hembry, R.M., et al., *Metalloproteinase production by rabbit articular cartilage: comparison of the effects of interleukin-1 alpha in vitro and in vivo.* Virchows Arch, 1994. **425**(4): p. 413-24.
93. Koshy, P.J., et al., *The modulation of matrix metalloproteinase and ADAM gene expression in human chondrocytes by interleukin-1 and oncostatin M: a time-course study using real-time quantitative reverse transcription-polymerase chain reaction.* Arthritis Rheum, 2002. **46**(4): p. 961-7.
94. Dozin, B., et al., *Response of young, aged and osteoarthritic human articular chondrocytes to inflammatory cytokines: molecular and cellular aspects.* Matrix Biol, 2002. **21**(5): p. 449-59.
95. Chubinskaya, S., et al., *Chondrocyte matrix metalloproteinase-8: up-regulation of neutrophil collagenase by interleukin-1 beta in human cartilage from knee and ankle joints.* Lab Invest, 1996. **74**(1): p. 232-40.
96. Lachmann, P., *Complement before molecular biology.* Mol Immunol, 2006. **43**(6): p. 496-508.
97. de Ceulaer, C., S. Papazoglou, and K. Whaley, *Increased biosynthesis of complement components by cultured monocytes, synovial fluid macrophages and skynovial membrane cells from patients with rheumatoid arthritis.* Immunology, 1980. **41**(1): p. 37-43.

98. Katz, Y., et al., *IL-17 regulates gene expression and protein synthesis of the complement system, C3 and factor B, in skin fibroblasts.* Clin Exp Immunol, 2000. **120**(1): p. 22-9.
99. Lake, F.R., et al., *Functional switching of macrophage responses to tumor necrosis factor-alpha (TNF alpha) by interferons. Implications for the pleiotropic activities of TNF alpha.* J Clin Invest, 1994. **93**(4): p. 1661-9.
100. Hietala, M.A., et al., *Complement deficiency ameliorates collagen-induced arthritis in mice.* J Immunol, 2002. **169**(1): p. 454-9.
101. Hietala, M.A., et al., *Complement activation by both classical and alternative pathways is critical for the effector phase of arthritis.* Eur J Immunol, 2004. **34**(4): p. 1208-16.
102. Triantafilou, M. and K. Triantafilou, *Lipopolysaccharide recognition: CD14, TLRs and the LPS-activation cluster.* Trends Immunol, 2002. **23**(6): p. 301-4.
103. Kitchens, R.L. and P.A. Thompson, *Modulatory effects of sCD14 and LBP on LPS-host cell interactions.* J Endotoxin Res, 2005. **11**(4): p. 225-9.
104. Steiner, H., *Peptidoglycan recognition proteins: on and off switches for innate immunity.* Immunol Rev, 2004. **198**: p. 83-96.
105. Hanayama, R., et al., *Autoimmune disease and impaired uptake of apoptotic cells in MFG-E8-deficient mice.* Science, 2004. **304**(5674): p. 1147-50.
106. Asano, K., et al., *Masking of phosphatidylserine inhibits apoptotic cell engulfment and induces autoantibody production in mice.* J Exp Med, 2004. **200**(4): p. 459-67.
107. Patwari, P., et al., *Ultrastructural quantification of cell death after injurious compression of bovine calf articular cartilage.* Osteoarthritis Cartilage, 2004. **12**(3): p. 245-52.
108. Charo, I.F. and R.M. Ransohoff, *The many roles of chemokines and chemokine receptors in inflammation.* N Engl J Med, 2006. **354**(6): p. 610-21.
109. Villiger, P.M., R. Terkeltaub, and M. Lotz, *Monocyte chemoattractant protein-1 (MCP-1) expression in human articular cartilage. Induction by peptide regulatory factors and differential effects of dexamethasone and retinoic acid.* J Clin Invest, 1992. **90**(2): p. 488-96.
110. Pulsatelli, L., et al., *Chemokine production by human chondrocytes.* J Rheumatol, 1999. **26**(9): p. 1992-2001.
111. Borzi, R.M., et al., *Human chondrocytes express functional chemokine receptors and release matrix-degrading enzymes in response to C-X-C and C-C chemokines.* Arthritis Rheum, 2000. **43**(8): p. 1734-41.
112. Moseley, T.A., et al., *Interleukin-17 family and IL-17 receptors.* Cytokine Growth Factor Rev, 2003. **14**(2): p. 155-74.
113. Haringman, J.J., et al., *Chemokine and chemokine receptor expression in paired peripheral blood mononuclear cells and synovial tissue of patients with rheumatoid arthritis, osteoarthritis, and reactive arthritis.* Ann Rheum Dis, 2006. **65**(3): p. 294-300.
114. Campbell, I.K., G. Ianches, and J.A. Hamilton, *Production of macrophage colony-stimulating factor (M-CSF) by human articular cartilage and chondrocytes. Modulation by interleukin-1 and tumor necrosis factor alpha.* Biochim Biophys Acta, 1993. **1182**(1): p. 57-63.

115. Nakao, K., et al., *Collaborative action of M-CSF and CTGF/CCN2 in articular chondrocytes: possible regenerative roles in articular cartilage metabolism.* Bone, 2005. **36**(5): p. 884-92.
116. de Caestecker, M., *The transforming growth factor-beta superfamily of receptors.* Cytokine Growth Factor Rev, 2004. **15**(1): p. 1-11.
117. Annes, J.P., J.S. Munger, and D.B. Rifkin, *Making sense of latent TGFbeta activation.* J Cell Sci, 2003. **116**(Pt 2): p. 217-24.
118. Galera, P., et al., *Effect of transforming growth factor-beta 1 (TGF-beta 1) on matrix synthesis by monolayer cultures of rabbit articular chondrocytes during the dedifferentiation process.* Exp Cell Res, 1992. **200**(2): p. 379-92.
119. Luyten, F.P., et al., *Recombinant bone morphogenetic protein-4, transforming growth factor-beta 1, and activin A enhance the cartilage phenotype of articular chondrocytes in vitro.* Exp Cell Res, 1994. **210**(2): p. 224-9.
120. Roelen, B.A. and P. Dijke, *Controlling mesenchymal stem cell differentiation by TGFBeta family members.* J Orthop Sci, 2003. **8**(5): p. 740-8.
121. Leask, A. and D.J. Abraham, *TGF-beta signaling and the fibrotic response.* Faseb J, 2004. **18**(7): p. 816-27.
122. Nishida, T., et al., *Regeneration of defects in articular cartilage in rat knee joints by CCN2 (connective tissue growth factor).* J Bone Miner Res, 2004. **19**(8): p. 1308-19.
123. Ivkovic, S., et al., *Connective tissue growth factor coordinates chondrogenesis and angiogenesis during skeletal development.* Development, 2003. **130**(12): p. 2779-91.
124. Blaney Davidson, E.N., et al., *Connective tissue growth factor/CCN2 overexpression in mouse synovial lining results in transient fibrosis and cartilage damage.* Arthritis Rheum, 2006. **54**(5): p. 1653-61.
125. Chen, D., M. Zhao, and G.R. Mundy, *Bone morphogenetic proteins.* Growth Factors, 2004. **22**(4): p. 233-41.
126. Nakase, T., et al., *Localization of bone morphogenetic protein-2 in human osteoarthritic cartilage and osteophyte.* Osteoarthritis Cartilage, 2003. **11**(4): p. 278-84.
127. Bobacz, K., et al., *Expression of bone morphogenetic protein 6 in healthy and osteoarthritic human articular chondrocytes and stimulation of matrix synthesis in vitro.* Arthritis Rheum, 2003. **48**(9): p. 2501-8.
128. Aida, Y., et al., *Effect of IL-1alpha on the expression of cartilage matrix proteins in human chondrosarcoma cell line OUMS-27.* Life Sci, 2004. **75**(26): p. 3173-84.
129. Fukui, N., et al., *Stimulation of BMP-2 expression by pro-inflammatory cytokines IL-1 and TNF-alpha in normal and osteoarthritic chondrocytes.* J Bone Joint Surg Am, 2003. **85-A Suppl 3**: p. 59-66.
130. Glansbeek, H.L., et al., *Bone morphogenetic protein 2 stimulates articular cartilage proteoglycan synthesis in vivo but does not counteract interleukin-1alpha effects on proteoglycan synthesis and content.* Arthritis Rheum, 1997. **40**(6): p. 1020-8.

131. van der Kraan, P.M., et al., *Role of nitric oxide in the inhibition of BMP-2-mediated stimulation of proteoglycan synthesis in articular cartilage.* Osteoarthritis Cartilage, 2000. **8**(2): p. 82-6.
132. Huch, K., et al., *Effects of recombinant human osteogenic protein 1 on the production of proteoglycan, prostaglandin E2, and interleukin-1 receptor antagonist by human articular chondrocytes cultured in the presence of interleukin-1beta.* Arthritis Rheum, 1997. **40**(12): p. 2157-61.
133. Tardif, G., et al., *Differential regulation of the bone morphogenic protein antagonist chordin in human normal and osteoarthritic chondrocytes.* Ann Rheum Dis, 2006. **65**(2): p. 261-4.
134. Tardif, G., et al., *Differential gene expression and regulation of the bone morphogenetic protein antagonists follistatin and gremlin in normal and osteoarthritic human chondrocytes and synovial fibroblasts.* Arthritis Rheum, 2004. **50**(8): p. 2521-30.
135. Alexander, S., Hermannson, M. A., Wait, R., Wallace, A. L., Saklatvala. *Activin A is a novel regulatory protein produced by human articular cartilage in response to mechanical injury and osteoarthritis*. in *52nd Annual Meeting of the Orthopaedic Research Society* 2006. Chicago, Ill: Orthopaedic Research Society.
136. Jones, K.L., et al., *Activin A and follistatin in systemic inflammation.* Mol Cell Endocrinol, 2004. **225**(1-2): p. 119-25.
137. Hu, B., et al., *Isolation and sequence of a novel human chondrocyte protein related to mammalian members of the chitinase protein family.* J Biol Chem, 1996. **271**(32): p. 19415-20.
138. Nakanishi, T., et al., *Cloning of a mRNA preferentially expressed in chondrocytes by differential display-PCR from a human chondrocytic cell line that is identical with connective tissue growth factor (CTGF) mRNA.* Biochem Biophys Res Commun, 1997. **234**(1): p. 206-10.
139. Pollak, M.N., E.S. Schernhammer, and S.E. Hankinson, *Insulin-like growth factors and neoplasia.* Nat Rev Cancer, 2004. **4**(7): p. 505-18.
140. Trippel, S.B., *Growth factor actions on articular cartilage.* J Rheumatol Suppl, 1995. **43**: p. 129-32.
141. Bhakta, N.R., et al., *The insulin-like growth factors (IGFs) I and II bind to articular cartilage via the IGF-binding proteins.* J Biol Chem, 2000. **275**(8): p. 5860-6.
142. Iwanaga, H., et al., *Enhanced expression of insulin-like growth factor-binding proteins in human osteoarthritic cartilage detected by immunohistochemistry and in situ hybridization.* Osteoarthritis Cartilage, 2005. **13**(5): p. 439-48.
143. Eviatar, T., H. Kauffman, and A. Maroudas, *Synthesis of insulin-like growth factor binding protein 3 in vitro in human articular cartilage cultures.* Arthritis Rheum, 2003. **48**(2): p. 410-7.
144. Clemmons, D.R., et al., *Inhibition of insulin-like growth factor binding protein 5 proteolysis in articular cartilage and joint fluid results in enhanced concentrations of insulin-like growth factor 1 and is associated with improved osteoarthritis.* Arthritis Rheum, 2002. **46**(3): p. 694-703.

145. Moralez, A., W.H. Busby, Jr., and D. Clemmons, *Control of insulin-like growth factor binding protein-5 protease synthesis and secretion by human fibroblasts and porcine aortic smooth muscle cells.* Endocrinology, 2003. **144**(6): p. 2489-95.
146. Zumbrunn, J. and B. Trueb, *Primary structure of a putative serine protease specific for IGF-binding proteins.* FEBS Lett, 1996. **398**(2-3): p. 187-92.
147. Oka, C., et al., *HtrA1 serine protease inhibits signaling mediated by Tgfbeta family proteins.* Development, 2004. **131**(5): p. 1041-53.
148. Longobardi, L., et al., *A novel insulin-like growth factor (IGF)-independent role for IGF binding protein-3 in mesenchymal chondroprogenitor cell apoptosis.* Endocrinology, 2003. **144**(5): p. 1695-702.
149. Beattie, J., et al., *Insulin-like growth factor-binding protein-5 (IGFBP-5): a critical member of the IGF axis.* Biochem J, 2006. **395**(1): p. 1-19.
150. Garcia, A.M., et al., *Transport and binding of insulin-like growth factor I through articular cartilage.* Arch Biochem Biophys, 2003. **415**(1): p. 69-79.
151. Kruger, R.P., J. Aurandt, and K.L. Guan, *Semaphorins command cells to move.* Nat Rev Mol Cell Biol, 2005. **6**(10): p. 789-800.
152. Gluzman-Poltorak, Z., et al., *Neuropilin-2 is a receptor for the vascular endothelial growth factor (VEGF) forms VEGF-145 and VEGF-165 [corrected].* J Biol Chem, 2000. **275**(24): p. 18040-5.
153. Mangasser-Stephan, K., et al., *Identification of human semaphorin E gene expression in rheumatoid synovial cells by mRNA differential display.* Biochem Biophys Res Commun, 1997. **234**(1): p. 153-6.
154. Miller, L.E., et al., *Increased prevalence of semaphorin 3C, a repellent of sympathetic nerve fibers, in the synovial tissue of patients with rheumatoid arthritis.* Arthritis Rheum, 2004. **50**(4): p. 1156-63.
155. Rosen, H., et al., *Proenkephalin A in bone-derived cells.* Proc Natl Acad Sci U S A, 1991. **88**(9): p. 3705-9.
156. Rosen, H. and Z. Bar-Shavit, *Dual role of osteoblastic proenkephalin derived peptides in skeletal tissues.* J Cell Biochem, 1994. **55**(3): p. 334-9.
157. Villiger, P.M. and M. Lotz, *Expression of prepro-enkephalin in human articular chondrocytes is linked to cell proliferation.* Embo J, 1992. **11**(1): p. 135-43.
158. Deuel, T.F., et al., *Pleiotrophin: a cytokine with diverse functions and a novel signaling pathway.* Arch Biochem Biophys, 2002. **397**(2): p. 162-71.
159. Krishnan, V., H.U. Bryant, and O.A. Macdougald, *Regulation of bone mass by Wnt signaling.* J Clin Invest, 2006. **116**(5): p. 1202-9.
160. Neame, P.J., et al., *Pleiotrophin is an abundant protein in dissociative extracts of bovine fetal epiphyseal cartilage and nasal cartilage from newborns.* J Orthop Res, 1993. **11**(4): p. 479-91.
161. Tare, R.S., et al., *Pleiotrophin/Osteoblast-stimulating factor 1: dissecting its diverse functions in bone formation.* J Bone Miner Res, 2002. **17**(11): p. 2009-20.
162. Tare, R.S., et al., *Effects of targeted overexpression of pleiotrophin on postnatal bone development.* Biochem Biophys Res Commun, 2002. **298**(3): p. 324-32.

Chapter 5: *Summary and Conclusions*

The first objective of this thesis was to identify the effects of TNF-α and IL-1β–induced nitric oxide as a mediator of cartilage tissue damage. A detailed analysis of the data presented in Chapter 2 leads to the following conclusions:

- Nitric oxide may be partially responsible for TNF-α induced aggrecanase mediated aggrecan degradation. In contrast, nitric oxide may protect against aggrecan degradation in response to combined IL-1β and TNF-α–induced matrix degradation.
- Inhibiting nitric oxide production in response to TNF-α and Il-1β treatment had no effect on gene expression after 26 hours on a survey of 32 genes including matrix proteins, proteases (including aggrecanases ADAMTS4 and ADAMTS5).
- The effect of nitric oxide on aggrecan degradation appears to be contextual – that is, it may depend on the other signaling mechanisms in play and/or yet uncharacterized shifts in protein expression.
- Nitric oxide may partially mediate inhibition of protein synthesis as determined by ^{3}H-proline incorporation. A partial reverse in cytokine-induced protein synthesis inhibition is seen following the addition of L-NMA.

The second objective was to determine the effects of IL-1β, TNF-α, and mechanical injury on secreted factors, matrix degradation, and mechanisms of chondrocyte cell death using an SDS-PAGE-LC/MS/MS protein profiling approach. Our main conclusions are:

- Mechanical injury may promote degradation of matrix proteins (this may result from mechanical damage to the matrix or increased breakdown of newly synthesized matrix components) – especially collagen VI, collagen II, COMP, and fibronectin.
- Mechanical injury causes an increase in the release of intracellular proteins. The release of actin occurred primarily in the first 24 hours after injury, suggesting mechanical compression injury may cause mechanical disruption of the chondrocyte cell membrane. We hypothesize that this mechanical disruption occurs in the periphery of the 3mm-diameter explants where the radial strain is highest. Previous work has implicated cell death by apoptosis in the central region of the tissue that experiences pressurization with high strain, high strain rate compression (strain 50%, strain rate 100%/sec).
- IL-1β and TNF-α cause an increase in some acute phase proteins including acid-1-alpha glycoprotein, haptoglobin, and serum amyloid A3.

The third objective of this study was to further quantify the effects of IL-1β, TNF-α and injury treatments using an isobaric labeling (iTRAQ) based 2D-LC/MS/MS approach to better understand matrix degradation, cell death, immune response, and evidence of cell-mediated repair processes. The main conclusions from these experiments were:

- Mechanical injury may release proteins that are important in promoting tissue repair by serving as pro-anabolic stimuli -- Inhibin beta, proenkephalin, CTGF, CDMP-2, IGF-II, and semaphorin 3C were all elevated to different degrees in response to mechanical injury. BMP inihitors, chordin like and chordin like 2 were decreased, while inhibin inhibitor, follistatin 1 was unchanged.

- Mechanical injury and cytokine treatment may promote matrix degradation or matrix remodeling through the production of MMPs (ADAMTS proteases were not identified) – MMP-1, MMP-13, MMP-9, and MMP3 were elevated with treatments and in most cases the elevation was significant.
- Mechanical injury again showed evidence of intracellular protein release with proteins elevated roughly 10 fold compared to untreated controls. Slight differences were seen between the release of cytosolic and ER proteins; however this difference was not sufficiently different to directly attribute release to a particular mechanism of cell death.
- Inflammatory cytokines, TNF-α and IL-1β may also cause the release of intracellular proteins compared to no treatment. The increase of intracellular protein release may occur with apoptosis and cell leaking or the increase in intracellular protein release may be the result of increased tissue transport that may enhance the loss of intracellular proteins of cells dead prior to the start of the experiment.
- Inflammatory cytokine (IL-1β and TNF-α) and mechanical injury may decrease collagen synthesis (as evidenced by decrease in C-terminal telopeptide release)
- Inflammatory cytokines may promote aggrecan degradation as measured by sGAG release, increases in NITEGE fragment release, by separation of G1 from G2 and G3 domain regions by gel and 2D-LC/MS/MS analysis.
- IL-1β and TNF-α may enhance the production of alternative pathway complement and LPS surveillance proteins relative to untreated – complement factor B, C3, and C1r were elevated
- Mechanical injury causes a slight increase in complement proteins and proteins involved in innate immunity.
- IL-1β and TNF-α also increased the release of immune modulatory and immune recruitment proteins including CCL2, CCL20, CXCL6, IL-6 and M-CSF. IL-17B release was increased with IL-1β treatment and CCL-5 appeared elevated with TNF-α treatment.
- Potential catabolic proteins such as CTGF, pleiotrophin, and semaphorin 3C were also elevated possibly suggesting tissue repair.

Future Work

Current experiments suggest some similarities and some differences between mechanical compression injury and treatment with inflammatory cytokines, TNF-α and IL-1β. In addition, previous work in the lab has indicated that combination of cytokines, IL-1β and TNF-α, and injury may have additive effects on decreases in synthesis and nitric oxide production and synergistic effects with respect to sGAG release. These effects of the combination of treatments will be further characterized by conducting a second systems level analysis using the iTRAQ-LC/MS/MS approach of chapter three and comparing cytokine and injury in combination to each cytokine alone. While these *in vitro* models cannot directly recapture *in vivo* effects of joint injury, they provide information on the anabolic and catabolic changes that may occur *in vivo* and may lead to greater understanding the disease.

Appendix A.1 In-gel Digestion Protocol

1. Excision of protein bands from polyacrylamide gels
    a. Wash gel 2 with ddH_20 ten minutes each
    b. Excise the band of interest. Cut as close to the protein band as possible to reduce the amount of "background" gel. Cut into 1mm x 1mm cubesand place in 0.65 ml tube (do not crush or clog pipet tips)

2. Washing gel pieces
    a. Wash the gel pieces with ~400 ul of water, 15 min.
    b. Wash with water/MeCN 1:1, 15 min (vortex) (200 ul + 200 ul is a good volume for all subsequent wash steps)
    c. Remove liquid, add MeCN to cover gel pieces (vortex)
    d. After pieces shrink and turn sticky white, remove MeCN
    e. Rehydrate in 100 mM NH_4HCO_3 (AMBIC) (vortex) AMBIC = ammonium bicarbonate
    f. After 5 min, add equal volume of MeCN (to get 1:1 ratio) (vortex)
    g. Incubate 15 minutes then remove solvent
    h. Dry down in speed vac

3. Reduction and alkylation (200 ul is sufficient for TCEP and iodoacetamide steps)
    a. Rehydrate in 1 mg/ml TCEP in 100 mM AMBIC
    b. Incubate at RT for 10 min (vortex)
    c. Remove solvent, replace with same volume of 55 mM (10 mg/ml) iodoacetamide in 100 mM AMBIC
    d. Incubate 45 minutes at room temp in the dark
    e. Remove solvent
    f. Wash with Ambic and MeCN as in step 2e.
    g. All the Coomassie blue stain should be removed at this time. If residual Coomassie still remains, repeat wash with AMBIC/MeCN (1:1) until removed
    h. Gel pieces should be dried completely in speed vac

4. In-gel Digestion
    a. Dilute 20 ug of Promega sequencing grade modified trypsin in 200 ul of 50 mM AMBIC (0.1 ug/ul) (trypsin solution)
    b. Dilute trypsin solution 1:10 in 50 mM AMBIC (10 ng/ul trypsin solution)
    c. Add 60 ul of 10 ng/ul trypsin solution to gel pieces and leave on ice for 1 hour.
    d. Incubate at 37°C overnight

5. Extraction of Peptides (never let the supernatant go dry, just concentrate (~10 ul))
    a. Add 20 ul of formic acid to gel pieces (this stops trypsin reaction)
    b. Vortex 10 mins (sonicating 30 min is a very good idea instead of vortexing).
    c. Remove supernatant and concentrate it in the speed vac

d. The following steps are optional but may enhance peptide recovery
    i. Add 200 ul 100 mM AMBIC, sonicate 30 min, and add supernatant to the supernatant you are currently drying in the speed vac
    ii. Add 0.1% trifluroacetic acid (TFA) in water, sonicate, speed vac supernatant (as in step i)
    iii. Add 0.1% TFA in water/MeCN (1:1), sonicate, speedvac supernatant (2 times)

6. Sample desalting
    a. Use Millipore Reverse-Phase ZipTip
        i. Follow instructions included with ZipTips, briefly
            1. Wet tip with 0.1% TFA in 50% MeCN
            2. Equilibrate with 0.1% TFA in water (5 x 10 ul)
            3. Load sample onto tip (20 x 10 ul)
            4. Wash with 0.1% TFA, 5% MeOH in water (5 x 10 ul)
            5. Elute with 0.1% TFA in 50-60% MeCN (10 ul)
            6. You may speed vac the desalted sample to concentrate but don't dry
7. RP-LC/MS/MS
    a. New Objective 75 um ID with 10 um tip capillary packed with Vydac C18 300A, 5 um particle size using a pressure bomb to ~16cm.
    b. Manual injector equipped with 0.5 ul loop
    c. LC architecture
        i. Tubing is 50 um with the exception of the split line after connectors and should be ~32 cm of 20 um tubing
        ii. Flow rate is typically between 4-7 ul/min depending on column (for a ~250 nl/min flow through the column)
    d. Buffer system:
        i. Buffer A -- 1.2% Acetic Acid (v/v) in water
        ii. Buffer B – 1.2% Acetic Acid in 90% ACN, 8.8% water (v/v/v)
    e. LC Gradients for nano-LC/MS/MS (optimal approach)
        i. 2% B to 40% B in 2-2.5 hours
        ii. 40% to 60% in 10 minutes
        iii. Hold at 60% for 10 minutes
        iv. Re-equilibrate to 2% over ~2 hours

Appendix A.2 – Two-dimensional Gel Electrophoresis of cartilage medium samples.

Following the initial SDS-PAGE-LC/MS/MS profiling experiments and work, we considered both iTRAQ and DIGE-2D-PAGE. Although we decided to pursue the iTRAQ route in part because of the significant number of differences between the samples, I did develop a reasonably reliable method to get two-dimensional gels for comparison. In order to get clean 2D gels (spots and not smears), we performed deglycosylation with three enzymes – Chondroitinase ABC, Keratanase II, and PNGase F. This supplement will begin with a detailed working protocol for experiments followed by some silver stained gels and some DIGE-2D-PAGE experiments done using an imager being developed by Millenium Pharmaceuticals through Dr. Mustafa Unlu, a former research scientist for CSBi. Dr. Unlu contributed to this work by teaching me how to run 2D-PAGE, and Debby Pheasant assisted with putting together the 2D gel protocol when we were learning together.

Medium samples were the result of a five-day treatment of 40-50 ml of cartilage in 2.0 ml of medium with a 10% medium removal and 10% supplementation every 24 hours.

Deglycosylases: Chondroitinase ABC and Keratanase II were purchase from Seikagaku; PNGase F was purchased from New England Biolabs

Protease free Chondroitinase ABC: 2U + 200 ul water – 5 ul aliquots at –80C
Keratanase II : 0.1 U + 200 ul water – 5 ul aliquots at –80C
PNGase in glycerol: use 2.5 ul / 2.0 mls store in –20C

Sample dialysis and deglycosylation. Samples were deglycosylated in 7.5 kDa cutoff dialysis cassette (Pierce) in a similar fashion to the SDS-PAGE protocol

Dialysis Buffer: 10 mM Tris Acetate pH 7.8, 80 mM Sodium Chloride, 3 mM EDTA

To a 2.0 ml aliquot of medium, 5 ul of Chondroitinase ABC and 5 ul Keratanase II was added and the sample dialyzed for 12 hours. 2.5 ul PNGase F added followed by further dialysis for another 12-24 hours. The dialysis was done at 37C in buffer in 100-1000 fold excess during deglycosylation. The buffer was then changed to water for another 2 x 12 hours in water at room temperature – it can be difficult to keep proteins in solution as deglycosylation generally decreases protein solubility – transferring the proteins to 4C may enhance chance of precipitates forming.

The pH of deglycosylation/dialysis buffer is near optimal for Chondroitinase ABC (pH 8.0), but a bit far from the optimal pH for Keratanase II. However based on previous experiments, this protocol was sufficient for deglycosylation (Chondrotin sulfate is likely the largest sugar component in the sample).

Following dialysis in water, protein solutions were collected and dried by speedvac. The dried samples were reconstituted in 75ul of lysis buffer (see below for 2D gel details).

Before Getting Started: 2D gel BUFFER STOCKS

Stock Solutions Needed

1 M DTT
1 M Na HEPES, pH 8.5
x M Tris HCl, pH 6.8
10 % SDS (in ddH2O)
87% glycerol stock

Lysis Buffer (Sample Buffer)

Recipe for 50 ml to be aliquotted and stored at -80C

6 M Urea **18.0 g**

Make up to 40 ml with ddH20 and dissolve urea

2 M Thiourea **7.6 g**

Dissolve mixture

10 mM DTT **500 ul of 1 M DTT stock**

2% CHAPS **1.0 g**

Dissolve

10 mM NaHEPES, pH 8.5 **500 ul of 1 M HEPES stock**

Add water to 50 ml. At this point keep it cold to prevent urea breakdown.
Aliquot into 1.0-1.5 ml aliquots and store at -80C

Rehydration Buffer

Recipe for 20 ml of Rehydration Buffer

6 M Urea **7.2 g**

Make up to about 15 ml and dissolve urea

2 M Thiourea **3.0 g**

Dissolve

2 mM Acetic Acid **2.7 ul Glacial Acetic Acid (17 M)**

Add

1% ASB-14 or 2% Chaps (depending on protein mix)
(ASB-14 is better for membrane proteins)

Add water to 20 ml
Reducing agent

2-4 mM Tributylphosphine **1:50 or 1:100 from 200 mM TBP (Biorad)**

or

10 mM DTT **200 ul of 1M DTT stock**

trace bromophenol blue

Store at 4C.

Add
1:200 IPG buffer (containing ampholytes) at are added just prior to use.

Equilibration Buffer

Recipe for 100 ml Equilibration Buffer.

125 mM Tris HCl	**25 ml Tris HCl stock, pH 6.8**
1% SDS (2% if DIGE)	**10 or 20 ml of 10% SDS stock**
8.7% glycerol	**10 ml 87% glycerol stock**

Store at 4C or room temp

2-4 mM TBP is added to Equilibration Buffer to make Equilibration buffer 1, 2% Iodoacetamide and trace of bromophenol blue is added to make equilibration buffer 2. Add just prior to use.

ISOELECTRIC FOCUSING

Rehydrating strips

1. The Amersham strips are stored at -20°. Bring them to room temperature before opening the package to prevent condensation from forming on them.

2. Immobiline DryStrips can be purchased from Amersham Biosciences (GE). Either 11cm or 13cm Immobiline DryStrips can be used in conjunction with the Criterion gel boxes. If you are using 13 cm strips, you will need to cut off the plastic tabs on the edge. Most of protocol is based on 11/13 cm Immobiline DryStrip 3-11 NL. If using other strips, it may be useful to check recommended IPG buffer/ rehydration amounts.

3. Prepare Rehydration Buffer. For 11 cm strips, Combine 200 ul rehydration buffer + 1 ul of IPG buffer / strip; for 13 cm – 250 ul + 1.25 ul IPG buffer. For other strip lengths, follow the manufacturer directions. Generally speaking, for the 3-11 NL (non-linear) add 0.5% IPG buffer (ampholytes) to rehydration buffer. Store remaining opened IPG buffer at 4C; return unused rehydration buffer to 4C as well. Add the Rehydration buffer to the rehydration tray spreading out the buffer over most of the length of the IPG strip.

4. Level the preswelling tray, then add the appropriate volume of buffer to each lane (200 ul for 11 cm strip), loading it all at one end. Remove the strip from its package, noting that the gel is on the side whose writing you can't read. Flex the strip slightly to release the thin protective plastic from the gel and remove that. There is a 5 mm space at each end of the strip, which has no gel on it so it's safe to grab the strip there. Lay the strip on the buffer **gel-side down** being careful that no bubbles are trapped under the gel. Once the gel strip is placed on the buffer, slide the strip back and forth to be sure that everything is evened out.

5. Close the lid on the preswelling tray and place it into a Ziploc bag containing two wet paper towels. This will retard evaporation of the buffer. Seal the bag and leave it on the bench overnight. Gels will swell to 0.5 mm thickness.

Sample preparation

If you are using cup loading, you are limited to approximately 100 ul and 100 ug of protein. If you need to go higher (with regards to protein amount or volume, consider loading during the rehydration step).

1. Dry down 10-100 ug protein in a Speed-Vac overnight to remove volatile buffer components.
2. Add IPG buffer (ampholytes) to LB at 2ul per 100 ul of LB just prior to resuspending the samples. If you are DIGE dyes, do NOT add IPG buffer until AFTER labeling sample.
3. Resuspend sample in 20-100 ul Lysis Buffer (LB).

Running the focusing

1. Level the Multiphor II. Clean the white tray and align it correctly on the electrode plate. Add 108 ml light mineral oil over all 12 lanes even if only running a few.

2. Place the gel strips into the center lanes, gel side up. Put the + end at the top with the end of the plastic just below the center hole in the tray. Be sure strip is centered within the lane and **completely covered with oil**. Center strips between indentation within the well.

3. Pre-wet the wicks on a plastic surface using 150 ul high-quality water/wick. Use two wicks per gel strip. (The wicks prevent salts and excess proteins from reaching the electrodes as well as providing enough water to prevent electroendosmosis.)

4. At the top of the strip, place the wick so that it touches the feet of the cup, and at the bottom, place it so that it is over some of the gel. Place the wicks at both ends of the gel such that the wick contacts the end of the gel. Submerge the wick the wicks in the mineral oil. The wicks should cover the + signs at the anode.

5. Place the sample cups over the gel (on the + side of the gel) just in contact with the wicks.

6. Load sample (>20ul and <100ul) in each cup, placing the pipette tip under the surface of the oil as you deliver sample.

7. Place the top electrode with diagonal lines toward you so that it contacts both the wicks and the gold cathode plate at the outside edges. Snap it into place with the knobs at the sides. Place the bottom electrode similarly, having it contact the anode plate.

8. Close the lid and enter your protocol. A sample protocol (for 11 cm 3-11 NL strips) is shown below:

a. No rehydration time (since that was already done)
b. Temp. to 20°C and current to 50 uA per strip
c. Step, 500 V, 2 hour (goes to 500 V immediately)
d. Grad, 1000 V, 2 hour (ramps up to 1000 V over 1 hour)
e. Grad, 6000 V, 2 hours
f. Step, 6000 V, 30 min

13 cm can be taken to 8000 V and held for 30 min. See accompanying Immobiline Drystrip booklet (comes with the gels) for more protocol information.

9. Press Edit and give the file a name.

10. To begin the focusing run, hit Start twice. At 500 V, you should see some number of uA which means that current is moving through the gel. Seeing 0 uA would indicate trouble – you are not making a connection – go back and make sure that salt bridges/ wicks are contacting gels and electrode for example. Note that while you are running in voltage controlled setting, the machine limits the current to 50 uA, so you may be current limited at least initially in runs. As focusing progresses, the uA should go down allowing voltage to go up. If current only allows a very small voltage, that would indicate that your samples have too much salt in them. Next time desalt sample. If you desperately need this data, consider changing salt bridges possibly repeatedly to pull salt out of system. Ideally, everything should be fine and you should be able to approach if not reach the upper voltage limit.

11. Toward the end of the run, prepare two Equilibration Buffers, 7 ml each for each strip. Make one batch with DTT and one with iodoacetamide.

12. When the run is over, record the total Vh before turning off the machine.

13. Pull each strip out of the oil and blot excess oil off the back of it onto a paper towel. Curl the strip around the inside edge of a small Petri dish, gel side in. Add 7 ml of the DTT containing equilibration buffer and shake gently at RT for 15 min.

14. Pour out the DTT –equilibration buffer and rinse the gel strip briefly with water to remove the DTT. Add 7 ml of the equilibration buffer containing 2% iodoacetamide and shake gently at RT for 15 min. At this point, the gel strip could be frozen at -80° for running later.

15. Meanwhile, set up the 2nd dimension SDS gel and rinse its top surface off with water. All experiments were performed on Criterion pre-cast Tris-HCl gel second dimensions which allowed the use of 11 or 13 cm strips (BioRad). Add the gel strip into the slot with the + end at the left. Orient the strip so that its plastic is against the back wall of the slot and the gel is facing forward into the air. Be sure the strip is in contact with the top of the SDS gel down its entire length – it is

important to avoid air bubbles! Add molten agarose (with bromphenol blue and 0.1% SDS) to just cover the gel on the strip and remove any bubbles, which might occur. Label the face plate of the SDS gel with the sample name.

16. Run the 2nd dimension gel at 20 mA/gel for approximately 3 hours and stain with Coomassie blue or Silver Stain.

Appendix B.1 Additional Cytokine + L-NMA experiments

The purpose of **Figure B.1.1** is to determine whether addition of L-NMA altered collagen degradation. Medium from five day experiment was partially deglycosylated as described in the methods of chapter 2, and it was then subjected to Western blotting for collagen using a monoclonal antibody specific for collagen type II (Neomarkers).

Figure B.1.1

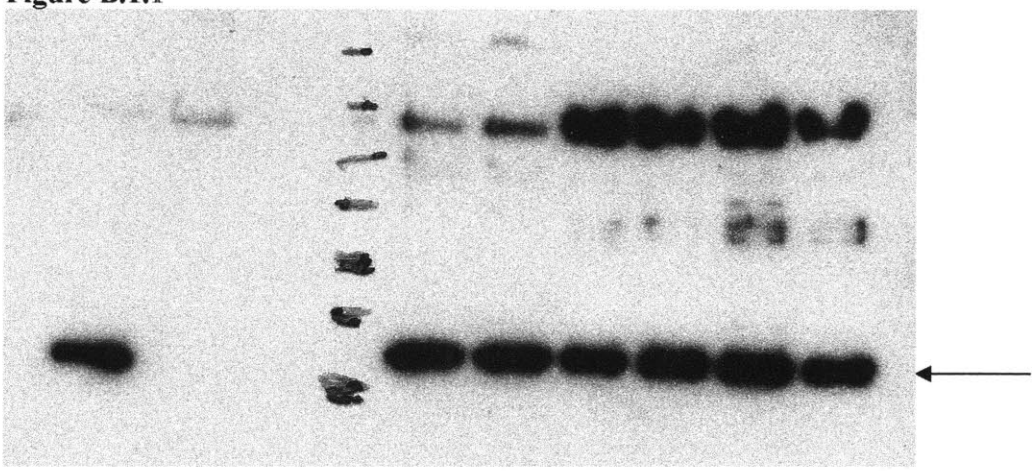

Figure B.1.1: Western Blot of collagen type II (arrow indicates C-terminal fibril fragment while upper band is indicative of full-length collagen

Based on this blot, there is little or no additional collagen degradation with cytokine treatment and no effect with L-NMA. This is consistent with the literature in that collagen degradation occurs after aggrecan release.

Because differences in fibronectin release were seen with injury, we also decided to look at the effects of cytokine treatment on fibronectin. **Figure B.1.2** is a Western blot probing for fibronectin and fibronectin breakdown and indicates the cytokine treatment causes and increase in fibronectin release and in fibronectin breakdown

Figure B.1.2

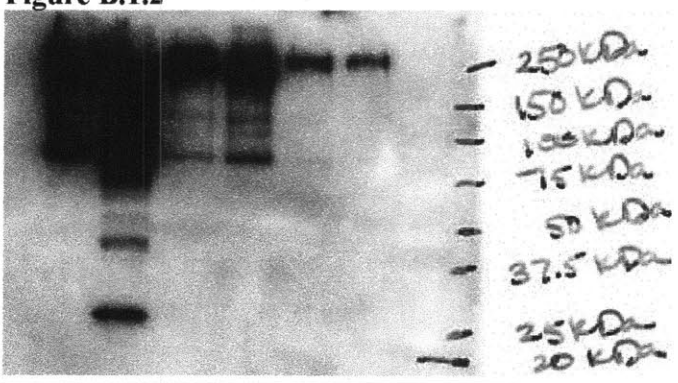

IL-1 NMA	IL-1	TNF NMA	TNF	CON NMA	CON	MW

Appendix B.2: Additional Cytokine + injury experiments and Data

To determine the overall nitric oxide (NO) production for the experiment, NO end product, nitrite, was measured on the five-day medium. Based on previous cytokine data, nitrite should represent about 50% of the total nitric oxide end products. **Figure B.2.1** is a graph of the nitric oxide production with cytokine, TNF-α and IL-1β, treatment and mechanical injury plotted as mean +/- SEM for 2-3 sets of explants per animal from five animals respectively.

Figure B.2.1

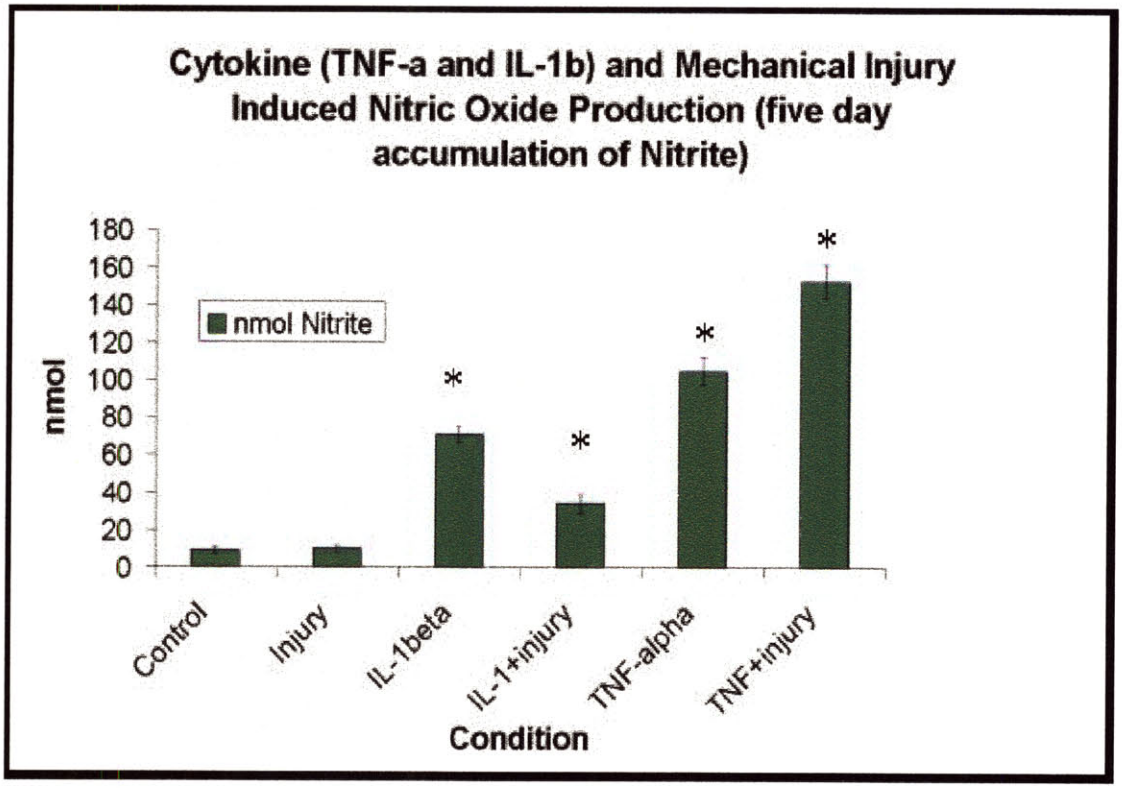

Cytokine treatment alone but not injury alone is sufficient to elevate nitric oxide production 3-5 fold over control ($p<0.01$; Student's t-test with Bonferroni correction for multiple comparisons). The combination of injury with TNF-α led to an elevation of nitric oxide production above that of the TNF-α treated alone while IL-1β in combination with injury decreased nitric oxide compared to IL-1β alone.

To monitor the effects of the cytokine and injury treatments in these studies, sGAG loss was also monitored using the medium collected every 24 hours for each set of explants over the five day time course. **Figure B.2.2** describes the effects of IL-1β and TNF-α in combination with injury on sGAG release over the five-day time course. Data is represented as mean +/- SEM for five (TNF-α), six (IL-1β), or 11 (injury and control) animals with 2-3 sets of 4 explants per animal. The double asterisks indicate a significant difference between TNF-α and TNF-α plus injury at all times points except 24 hours ($p<0.01$; Student's t-Test with Bonferroni correction for multiple comparisons) while the single asterisk indicates differences compared to control ($p<0.01$; Student's t-test with Bonferroni correction for multiple comparisons). Mechanical compression injury showed a small, but significant increase in sGAG loss to the medium at the 24 hour time point ($p<0.05$). No difference was seen between IL-1β and IL-1β plus injury ($p>0.5$ at all points).

Figure B.2.2

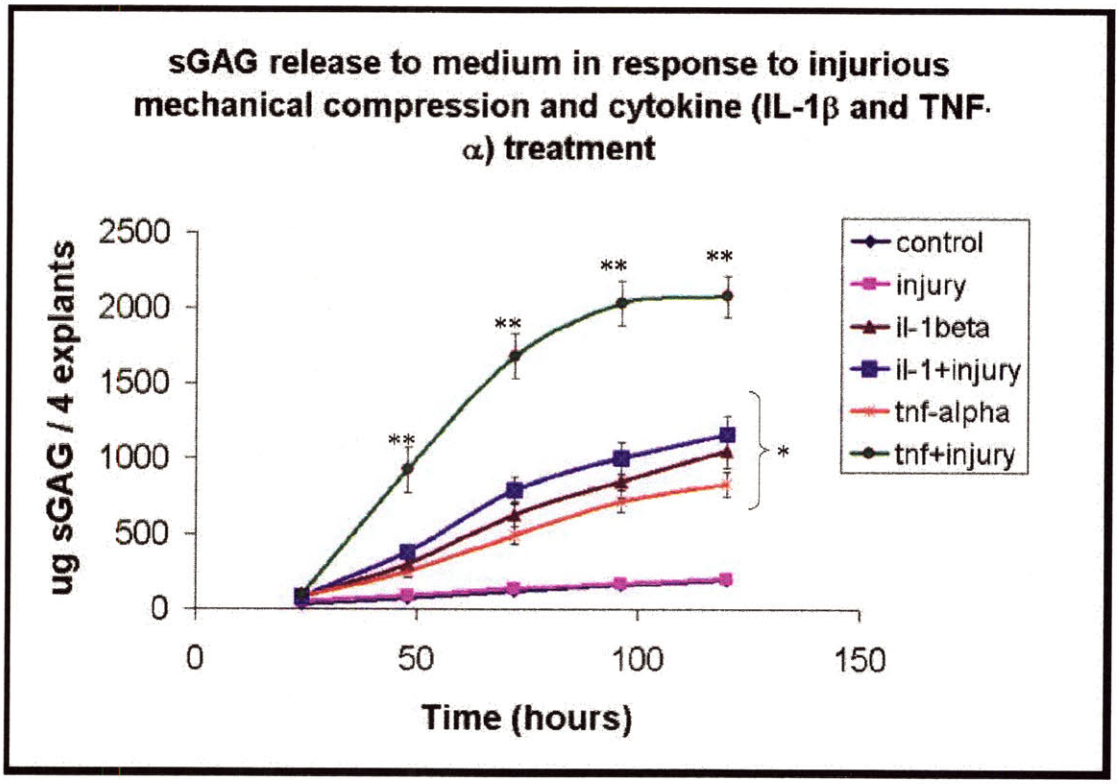

In addition, a dramatic increase in sGAG release with TNF-α in combination with injury compared to TNF-α alone; however, the synergy was not seen with IL-1β in combination with injury. While no signaling differences have been delineated between IL-1β and IL-1α, this is one possible explanation for the differences. While the effects of IL-1 in combination with injury were not significant, the effects of TNF-α in combination with injury caused a large and significant increase in sGAG release to the medium compared to TNF-α alone.

The differences nitric oxide and sGAG release in IL-1β and TNF-α response in combination with injury represent additional differences between the effects of these cytokines. Nitric oxide product differences mirror the sGAG release for TNF-α and TNF-α with injury in which sGAG release is elevated with nitric oxide production. In the cytokine-NMA study described in **Chapter 2**, nitric oxide seems to stimulate sGAG loss with TNF-α treatment as indicated by a decrease in sGAG loss with L-NMA. The data above in combination with the cytokine-NMA study of **chapter 2** beg the question of whether the increase in sGAG production seen with injury is driving the increase in sGAG release. In addition, the TNF-α-induced increase in sGAG release with nitric oxide is the exact opposite effect as that seen with IL-1β and TNF-α in combination. In the above data, a decrease in nitric oxide was seen with IL-1β in combination with injury relative to IL-1β alone. This is accompanied by very little change in sGAG release with IL-1β and injury in combination. At the very least, this data further supports the different mechanism by which IL-1β and TNF-α alter cell behavior and the use nitric oxide as a signaling molecule.

Further characterizations of the cytokine-injury experiments were performed by measuring ^{3}H-proline and ^{35}S-sulfate incorporation on the day six following the five-day treatment. While this incorporation rate may be artificially decreased with cytokine treatment due to an increase in transport, radiolabel incorporation provides an estimate of biosynthesis rates for the tissue. **Figure B.2.3** is the radiolabel incorporation data for day six following the five-day treatment. The data is represented as mean +/- SEM for five or six different animals and 2-3 explant sets per animal.

Figure B.2.3

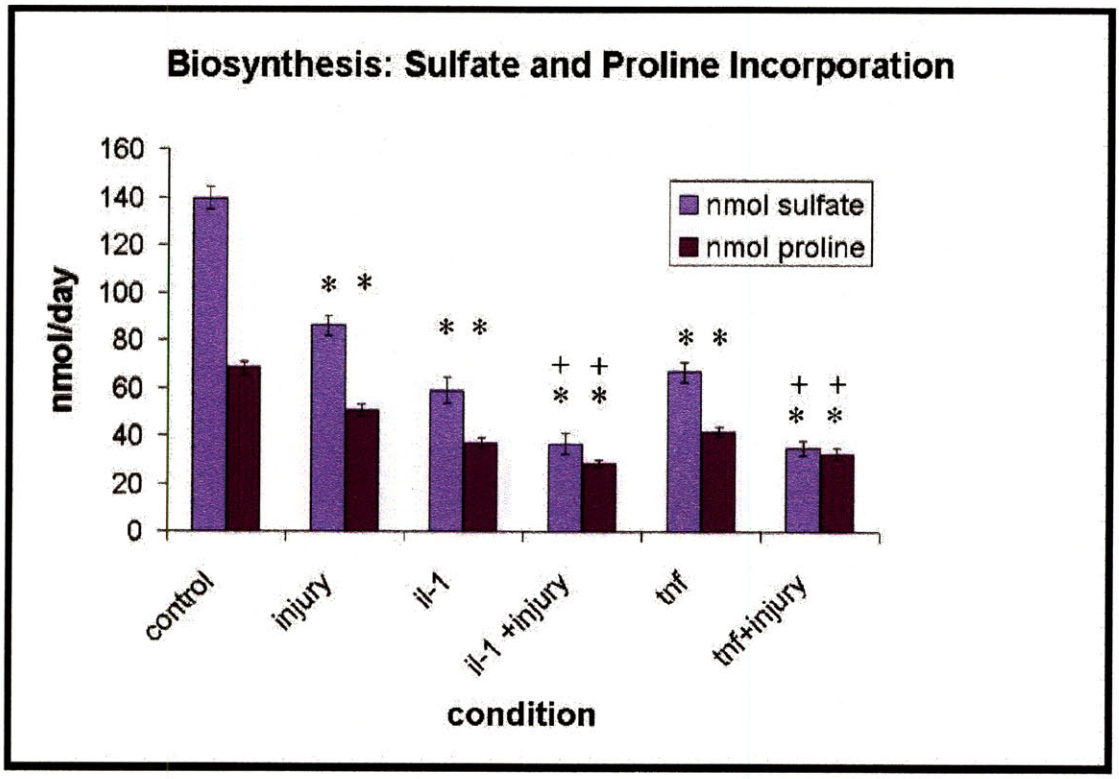

The asterisks represent a significant decrease in incorporation rate relative to the control ($p<0.01$ for all treatments by Student's t-Test with Bonferroni correction for multiple comparisons). The '+' indicates a significant decrease in incorporation rates in the combination treatment relative to cytokine treatment alone or injury alone ($p<0.01$; Student's t-Test with correction for multiple comparisons).

To determine changes in MMP activity in the medium, zymograms were performed of the medium. **Figures B.2.4** are representative zymograms from five-day accumulated medium. **Figure B.2.4a** is a gelatin zymogram with treatment conditions labeled below. The lower doublet represents MMP-2 and is found in all conditions while the upper band is likely indicative of MMP-9 activity, which is more pronounced with TNF-α and TNF-α and injury combination treatment though increased with injury as well. **Figure B.2.4b** is a casein zymogram showing MMP-3 activity, which is weak in all samples although small amounts of activity may be seen with TNF-α, injury, and TNF-α and injury combination treatment.

Figure B.2.4

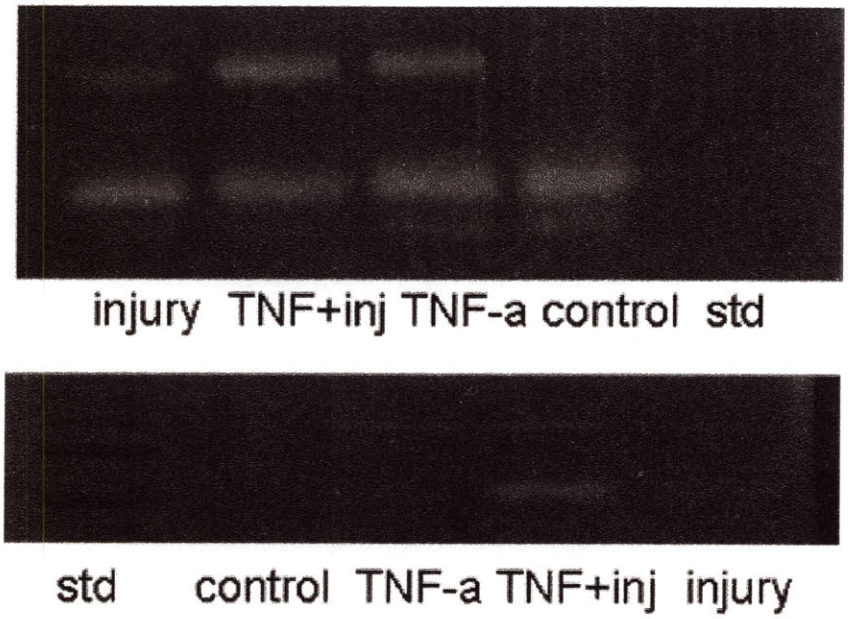

Figure B.2.5 is a casein zymogram of the five day accumulated medium from an il-1-injury experiment. MMP-3 activity is increased most dramatically with IL-1β treatment, no additional increase is seen with IL-1β and injury in combination, and very little activity is seen with injury in comparison.

Figure B.2.5

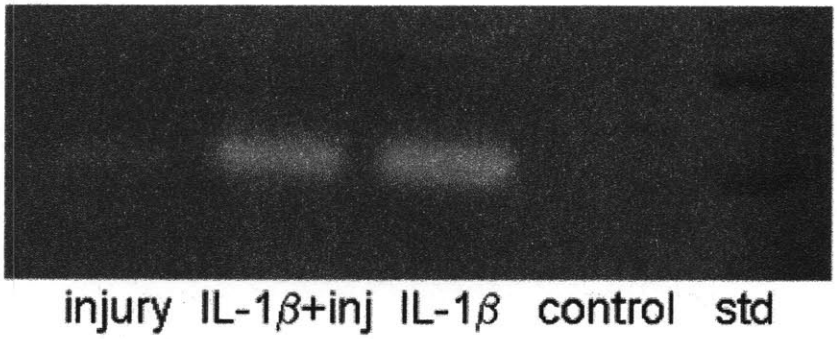

Because changes in mechanical properties with injury suggest damage to the collagen framework, we probed collagen type II fragments in the medium by Western blot to determine whether the damage is accompanied by collagen degradation. **Figures B.2.6** are collagen western blots of medium from cytokine-injury experiments. In both blots, a ~30 kDa band can be seen with all treatments; however it is more pronounced with injury with not additional increase in intensity with injury and cytokine in combination. Based on the size of the fragment, this band may correspond to the ¼ collagenase cleavage fragment, which is shown in the blot on the right. These findings are similar to those of Thibault et al. [JOR, 2002] and Chen et al., [JOR, 2003] and the increase in potential collagenase cleavage fragment likely results from mechanical denaturation of the collagen fibril with secondary collagenase (MMP) cleavage.

Figures B.2.6

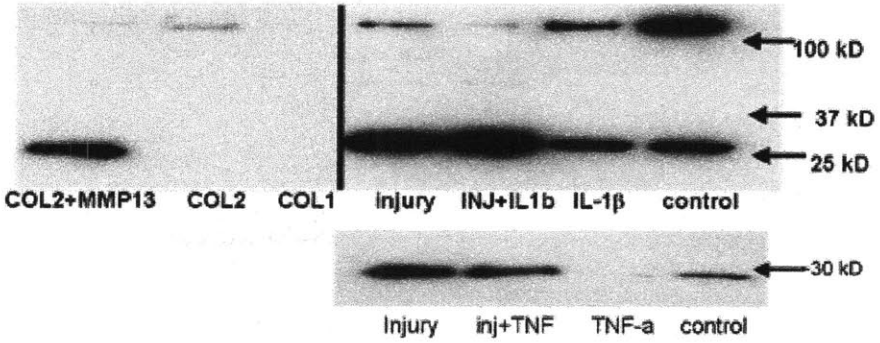

To look at global differences in the proteins released into the medium, we performed SDS-PAGE with silver staining. **Figure B.2.7** is a silver-stained gel of IL-1b-injury treatment in duplicate with one set at 100 ul and the other at 250 ul.

Figure B.2.7

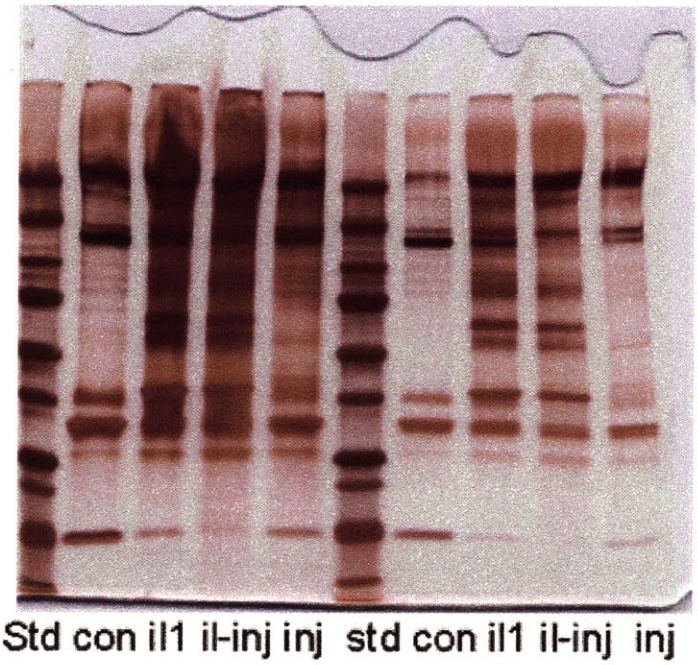

A number of differences can be readily seen between conditions by SDS-PAGE. iTRAQ based analysis of medium from IL-1-injury and TNF-injury experiments are currently underway and may begin to explain some of these differences. The conditions across the bottom of the gel are as follows: std- MW standard; Con – control; il1 – IL-1β; il-inj – IL-1β and injury; inj – injury.

Additional survey experiments and results include an anti-actin blot of medium from a TNF-α-injury experiment. Approximately 100 ul of medium from each condition (untreated, tnf-α, tnf-α+injury, and injury) was probed for by anti-actin antibody (**Figure B.2.8**). This blot was only done with medium from one experiment, so conclusions would be premature. However, this result is worth at least verifying as it may imply that TNF-α treatment may alter amount of actin release or at least the proteolytic degradation of actin that has been released. This result may make more sense when the iTRAQ experiment is complete. It may also be worthwhile to repeat this experiment to verify its reproducibility. This blot is being included because it may provide insight into experiments currently being performed.

Figure B.2.8

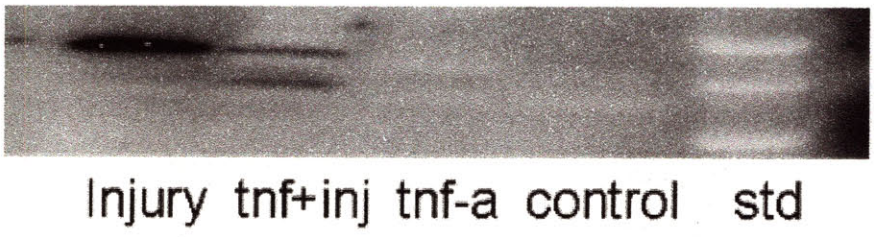

The aggrecan G1 blot from a TNF-injury experiment also only performed once however it is worth at least noting the effects of the combination treatment on G1 fragments in the medium (**Figure B.2.9**).

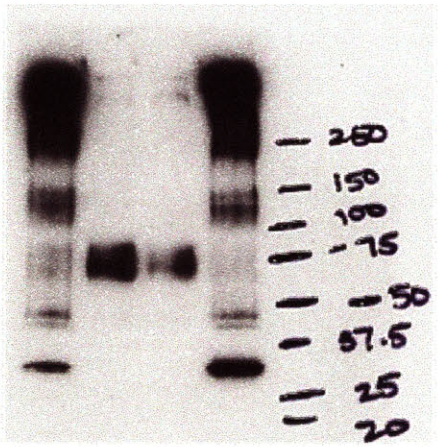

Aggrecan G1- Blot: Inj—injury, t-inj—TNF-α + injury, tnf—TNF-α, cont- control, std--standard

The aggrecan G1-immunoblot above was performed as an sGAG controlled experiment – equal volumes of sGAG are loaded per condition. TNF-α and TNF-α with injury both have a sharp band around 75 kDa, which may represent the aggrecanase cleavage fragments of G1. A small increase is seen with injury compared to untreated samples. This suggests that TNF-α and injury in combination cause a greater increase in aggrecan G1 fragments then TNF-α, which is greater than injury, which is greater than the untreated. If all G1 fragments are identified with equal intensity, then it seems that there is more G1 released per sGAG with injury and control than there is with TNF-α treatment or with TNF-α and injury together. This is consistent with the iTRAQ results for aggrecan release by globular domain with cytokine treatment.

Because we recognized the possibility that a number of other MMPs in addition to MMP-3 could contribute to the clearing by casein gel zymography, we wished to verify the MMP-3 activity. Thus, below is an MMP-3 immunoblot for the IL-1-injury experiment (**Figure B.2.10**). We chose the IL-1β experiment because IL-1β causes a significant increase in MMP-3. I believe this was 100-150 ul of medium. This result confirms MMP-3 protein expression with injury. The effects of injury in combination with IL-1β appear limited.

Figure B.2.10

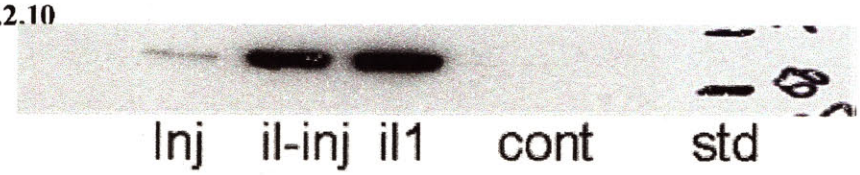

Finally, a blot for MMP-9 was done to confirm its presence with TNF-α and with injury. The MMP-9 antibody did cross-react with MMP-2; however it did give a band at around 90 kDa that corresponds in appropriate intensity with the gelatin zymograms suggesting that is able to detect MMP-9 (Figure B.2.11).

Figure B.2.11

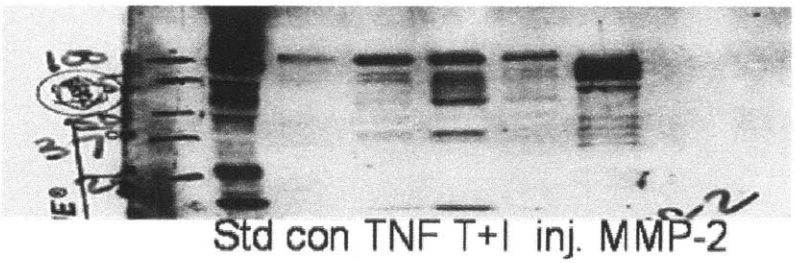

Ant-MMP-9 Blot – Std: standard, con: control (untreated), TNF: TNF-α, T+I: TNF-α and injury, inj: injury, MMP-2: matrix metalloproteinase 2

Appendix B.3: 2D-PAGE results.

Below are some representative 2D PAGE results from various medium types.

Figure B.3.1 is a 2D-PAGE gel of untreated medium in 4-15% second dimension gradient gel stained with Silver Snap 2 silver stain (Pierce); The streaking is likely due to insufficient deglycosylation and desalting as this represents one of the first gels with only chondroitinase ABC and Keratanase II used at low concentration. All subsequent gels will be 8-16% second dimension gels. Note that the anode is on the left and the cathode is on the right – gel dimensions are approximately 14 cm x 7-8 cms.

Figure B.3.1

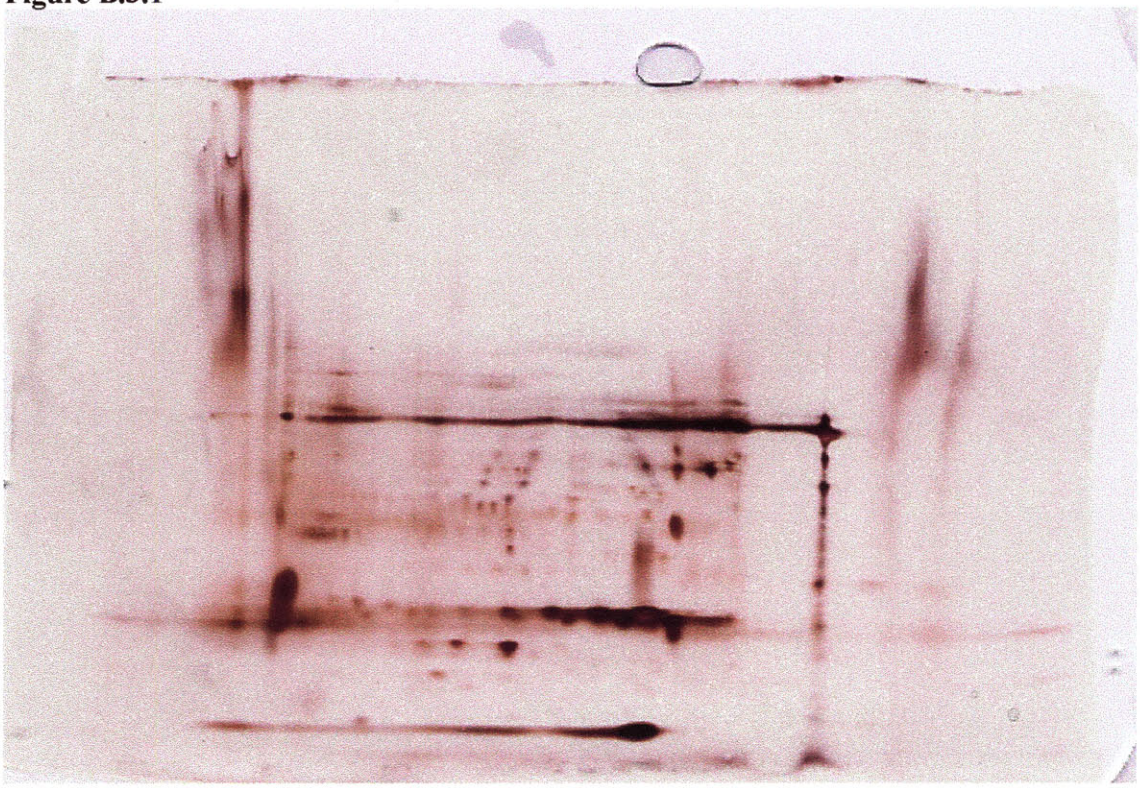

Similar to the **Figure B.3.1** above, **Figure B.3.2a-b** is a picture of a 2D-PAGE gel of NMA only treated sample deglycosylated as described above, run out on an 8-16% gel and silver-stained. (Control-NMA sample should be similar to the control only; however the control-NMA was used because more medium samples were available).

Figure B.3.2a

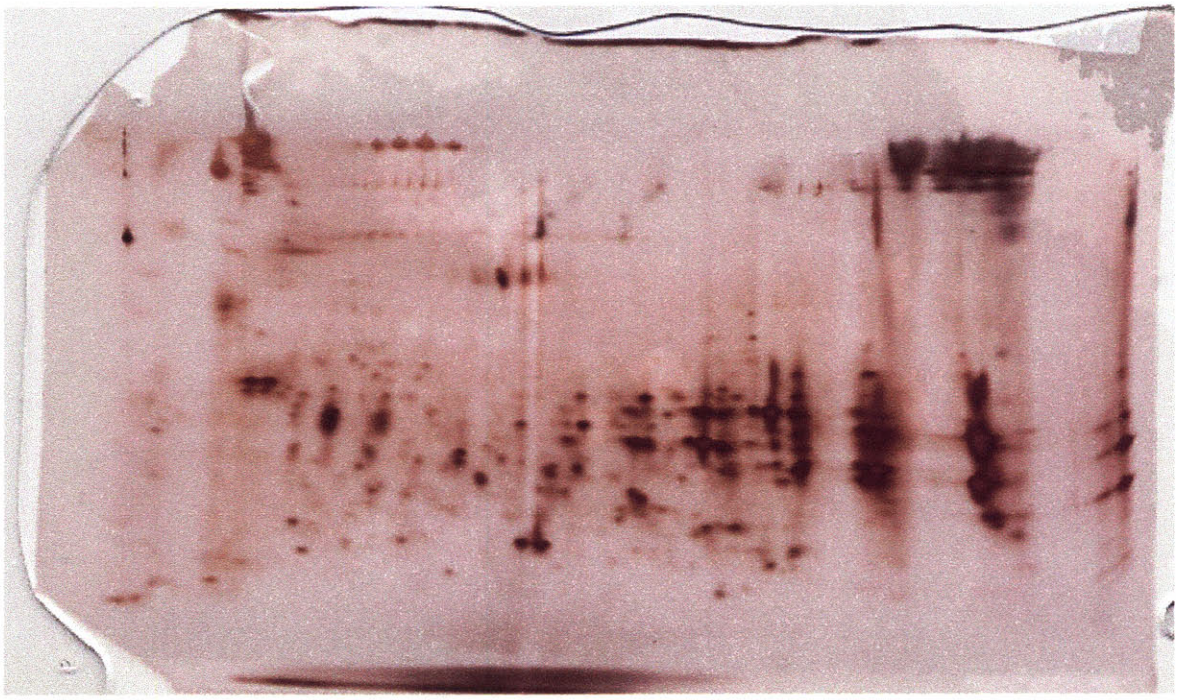

Figure B.3.2 is a silver-stained gel with an 8-16% second dimension of medium from IL1β and TNF-α combination treatment. This represents the most complicated of the samples that were run with respect to the number of spots observed on the gel.

Figure B.3.2b

Once the method was sufficiently developed and verified, some DIGE labeling was used to compare IL-1 medium samples to IL-1 and NMA medium samples as well as untreated samples with NMA only samples. **Figure B.3.3** is a set of gels comparisons of IL-1 and untreated with or without NMA. Some spots were picked, but this project was not followed up on.

Figure B.3.3

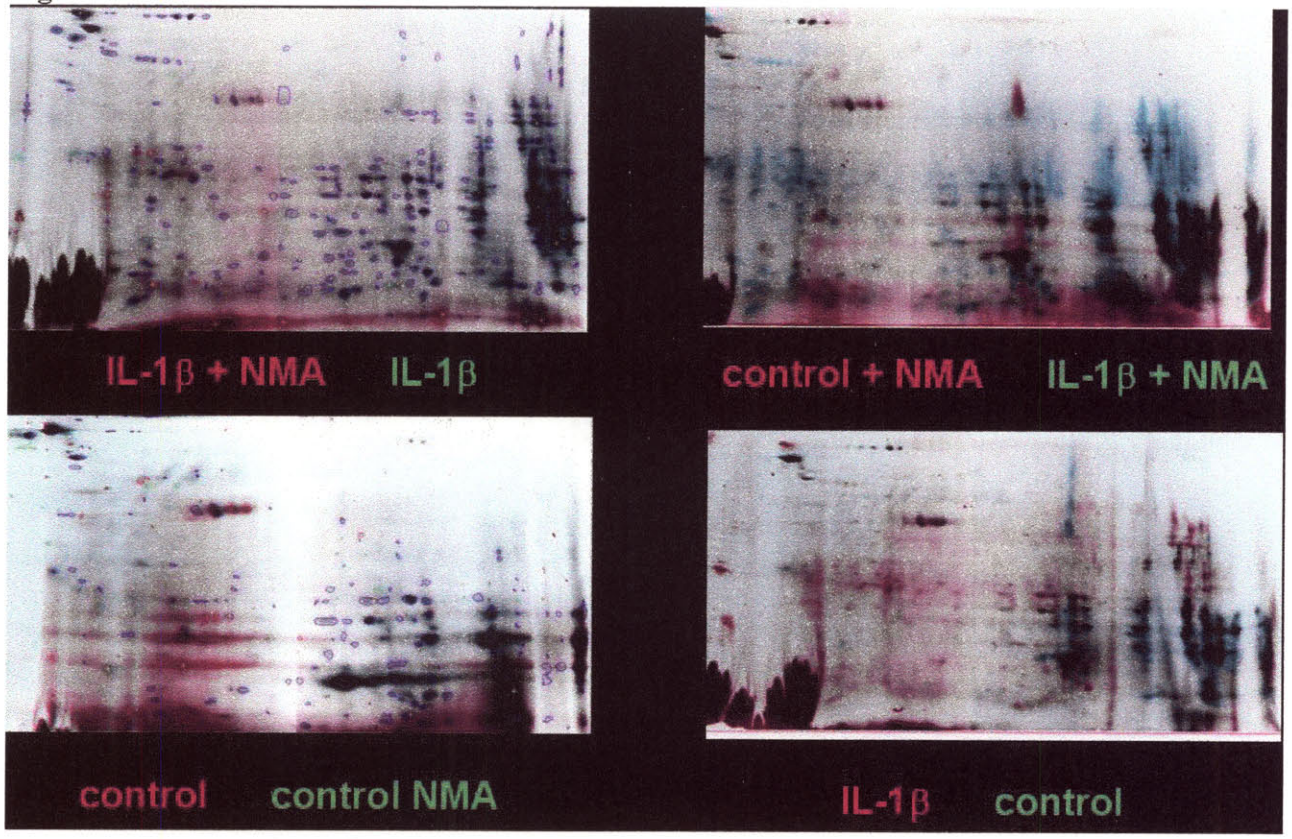

While the DIGE method with the described work-up is capable of providing reproducible results, the sample complexity makes this method very labor intensive because identification takes place at the mass spectrometry level and in-gel digestion of each spot is necessary for peptide-based protein identification. In addition, most software attempts to normalize based on the assumption that you are always comparing equal amounts of protein – this represents an equal volume experiment, and it may be somewhat difficult to normalize based an internal standard. The DIGE method is ideal for a set of experiments in which the differences expected are small and the samples are protein controlled. The lab doing the experiments should have access to appropriate imaging and spot-picking technologies, and automated in-gel digestion machinery as well as a MALDI interface may provide further benefit.

Appendix B.4: iTRAQ Supplemental Information and Data analysis

Because the samples represent proteins released into an equal volume of medium from an equal volume of cartilage, protein amounts were expected to be and known to be different. In addition, the sample work-up was somewhat lengthier and more complicated than many, and thus, it may represent a source of error prior to sample labeling and analysis. Therefore, it was not prudent to accept ProQuant sample normalization or to assume no normalization at all. Thus, we chose to use the deglycosylase, chondrotinase ABC, as the internal standard which was added in equal amounts at the beginning of sample work-up. **Table B.4.1** provides data on the chondrotinase ABC standard and the mean ratio values which were used for correction. Correction was performed simply by dividing each protein's iTRAQ signature ion ratios by the mean chondroitinase ABC signature ion ratios. **Figures B.4.1a-f** are the histograms for the chondroitinase ABC peptides for each of the signature ion ratios and for the analytical duplicates. While a more sophisticated normalization approach may have been use, this normalization was sufficient to correct the data such that the ratios for the first analytical experiment and the second analytical experiment were within 20%, which is small compared to most differences seen in this experiment.

Table B.4.1

Expt	Peptides	115:114	115 SD	116:114	116 SD	117:114	117 SD	Normal
Itraq1	65	1.29	1.30	0.995	1.22	1.23	1.19	Yes (3)
Itraq2	55	2.43	1.76	2.81	2.14	2.26	1.68	Yes(1)

Itraq2 median 115 – 2.21; Median 116 – 2.55; Median 117 – 2.15
Itraq1 median 115 – 1.28; Median 116 – 0.9716; Median 117 – 1.2349

Figure B.4.1a-f

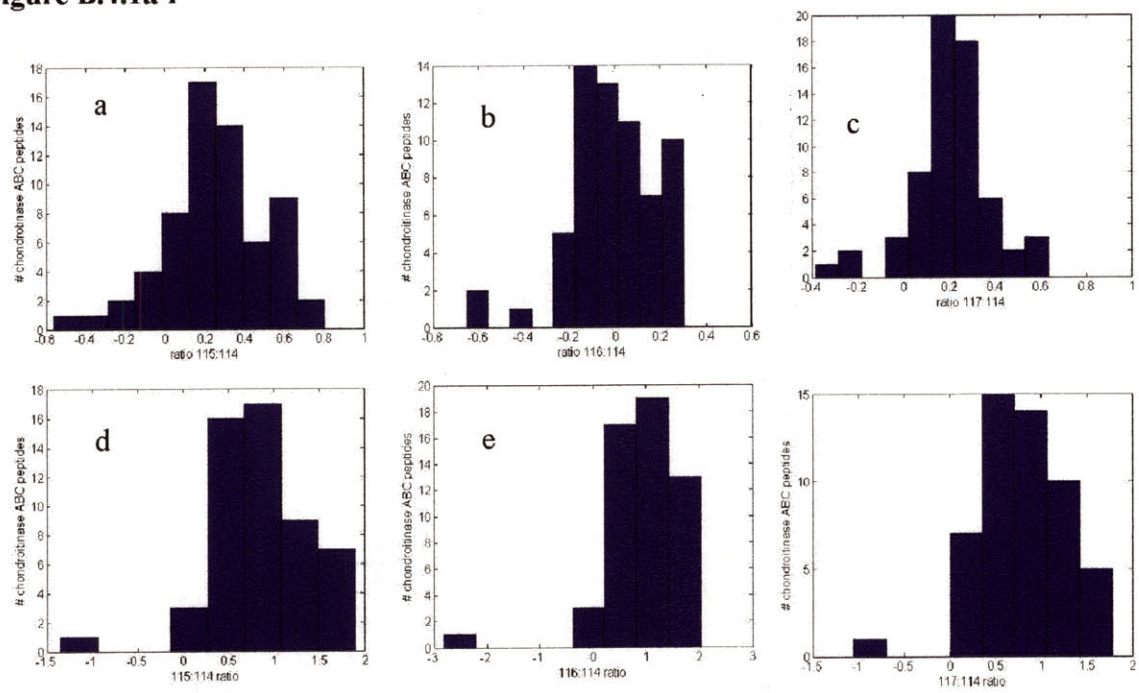

Histograms of Chondroitinase ABC peptides in log_2 space. Figure B.4.1 is a set of histograms representing the ratio values for the Chondroitinase ABC peptides in log_2 space. The top panel represents data from the first experiment and the bottom panel the data from the second experiment. The peptide distributions for the first duplicate experiment due pass Lilliefor's test for normality while only the 117: 114 ratio experiment 2 qualifies. The mean values were used as correction factors in this experiment, and this may account for up to a 10% error based on the mean to median difference. The statistics for the ratio corrections are given in Table 1 above.

Because the samples being compared in this experiment represent samples which vary in amount of protein (by a factor of 2), in post-translational modifications (particularly glycosylation and proteolysis), and in proteins present (ratios from 0.1 to 100), understanding the limits of quantitation and reproducibility is key to interpreting the data. Thus, we chose to take a systematic look at the protein level quantitation reproducibility in a number of placing starting with reproducibility between injections. A number of the SCX fractions were sufficiently complex that we chose to inject them in duplicate to increase coverage of proteins present in the sample. This data on duplicate injections provided sufficient data to look at interinjection variance as a source of error in the data. Approximately 20 fractions were subjected to duplicate injection, so the data was divided into first injection files and second injection files, and the data was subjected to the treatment described in the data analysis section. Briefly, all spectra with no quantitation or with uninterpretable quantitation (0 or 9999) and with an identification confidence less than 90 were removed. Redundant spectra were averaged to generate a

non-redundant peptide list which was then averaged to generate a final protein list. Using protein accession number, the protein list from the first injection and the second injection were compared as the ratio of the first injection mean isotope ratio to the second injection mean isotope ratio.

To generate symmetry for values greater than one and values less than one, the data were log transformed. Thus, if the data matched perfectly, log transformed ratios would all equal 0, and since the data are prone to a number of small error sources, we can expect a normal distribution with a mean of 0 and the variance would provide a numerical estimate of the reproducibility between injections. Duplicate analysis of the same set of SCX samples led to the identification of an addition 72 proteins with a score greater than 3. **Figures B.4.2** are the histograms for the first and second injection datasets for the first analytical duplicate. The data represent 316 proteins with an original ProQuant score of 3 or higher in both datasets. The data generally appear to be normally distributed with the 116:114 and 117:114 ratios looking slightly offset from zero with a mean of -0.1416 and -0.1936 respectively which represent as much as a 15% error. The variance was larger than expected with a standard deviation of approximately 0.4 for all ratios indicating that 95% of the data fall between ratio of 0.6 and 1.7. In this experiment, the geometric mean of each treated to untreated ratio is 2 or greater, so while this error must be dealt with appropriately, the error is unlikely to impact the results from this experiment.

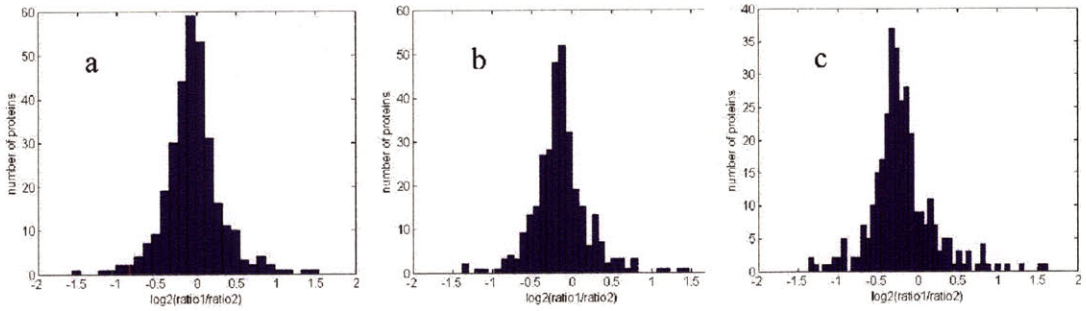

Figure B.4.2 Interinjection variation in quantitation at a protein level. Figure 2 are the histograms for the three signature ion ratios (*m/z* 115:114 (a), *m/z* 116:114 (b), *m/z* 117:114(c)). The distributions generally appear normal with mean +/- SD for each isotope ratio are -0.0504 +/-0.4208, -0.1416+/-0.3874, -0.1973 +/- 0.3997 for the 115:114, 116:114, and 117:114 ratios respectively. The slight shift in mean and slightly large standard deviation may be in part due to proteins with one or more large ratios. This data represents 316 proteins with original ProQuant scores of greater than 3 in both datasets

At the same time, understanding the source of the error might aid in the experimental interpretations. Thus, one possible explanation for the interinjection variance is that many of the ratios were much larger than one, so quantitation may be limited by the dynamic range of the detector. To get a better feel for the impact of large ratios on the variance of the data, we decided to look only at those proteins in which all ratios were less than 10 and then all ratios that had means up to 50 which is likely outside the dynamic range of the mass spectrometer detector. **Figure B.4.3** is a plot of the mean

ratio of dataset 1 versus the $\log_2$ (ratio1/ratio2) with **Figure B.4.3a** representing only proteins with all ratios less than 10 and **Figure B.4.3b** representing all proteins with ratios less than 50. If the large ratio values were a cause of error, the data spread for the $\log_2$ (ratio1/ratio2) would appear to widen out as mean ratio values became increasingly large. This is seen to some extent in both **figure B.4.3A** and **B.4.3B**. To provide further support for the additional error associated with large ratios, we computed the average and variance based on the ratio size. When only proteins with all ratios between 0.25 and 4 were included, the standard deviation dropped to between 0.2 and 0.25 which is consistent with previous reports. When proteins with ratios between 0.1 and 10 were included, then the variance increased to between 0.30 and 0.35, and then to around 0.40 when all proteins were included. While large ratios (meaning one or more than one signature ion peak is greater than the other ones) are unlikely the cause of all interinjection error, it appears that large ratio values may contribute some to the variation seen between injections. This effect of large ratios likely results from the limited dynamic range of the detector compared to the range of the proteins within the sample. All interinjection variation analyses were done prior to normalization of chondroitinase ABC internal standard.

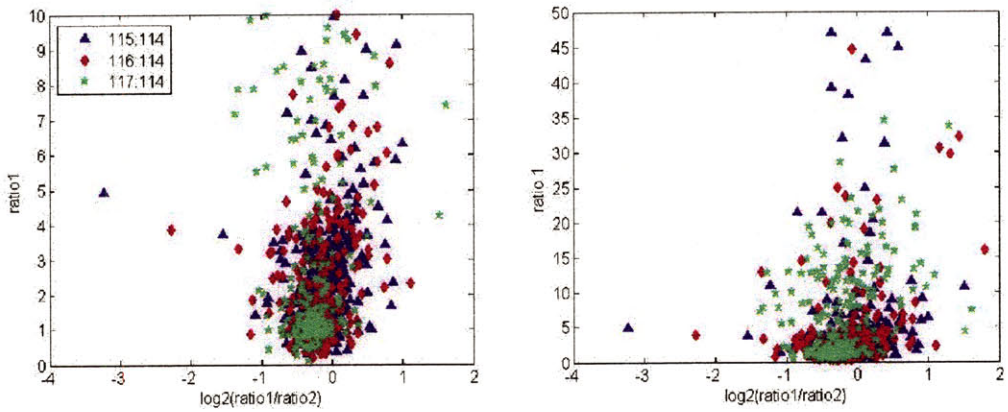

Figure B.4.3 the effects of the ratio mean on the reproducibility between experiments. Figure 3 is a plot log2(ratio1/ratio2) values obtained in figure 2 versus the sample 1 ratio for each protein and signature ion ratio. There is some additional spreading of the data with larger ratios, so the effects of large ratios on quantitation is one source contributing to interinjection variation.

Analytical Variation

The analytical duplicates are susceptible to variation, which includes inter-injection variation as well as errors from sample collection and work-up not corrected by the chondroitinase ABC, and errors associated with the use of an internal standard (pipeting error of standard, inappropriate normalization method). Thus, a similar approach is taken to the chondrotinase ABC normalized data. Quantitaton data for all proteins with an original ProQuant score greater than 2 were used for comparison. **Figure B.4.4a-c** are the histograms displaying the distributions of the log2(ratio1/ratio2) values this time comparing the first analytical duplicate (ratio1) and the second analytical duplicate (ratio2) for each of the signature ion ratios. Again, the data is expected to be

normally distributed centered at zero with a variance being small compared to the average ratio value. As seen with the inter-injection variation, a slight shift from zero is noted with the mean +/- SD for the 115:114, 116:114and 117:114 of 0.0346+/-0.4861, 0.2364 +/- 0.5505, 0.1327 +/- 0.5139. The shift in the mean suggests as much as a 20% error and is similar to that seen with the interinjection variation. This shift may be properly attributed to an error in internal standard normalization; however this shift is similar to that seen with the intrasample variation which cannot be explained by this. Because this shift is small compared to the differences seen in this data, we will consider this error when making conclusion about the data. Finally, the standard deviations are slightly larger (as much as ~0.15) than those seen with the interinjection variation which should be expected unless unless the mass spectrometer is the greatest source of error in the measurement. Thus, this additional error may be the result improper normalization, variation in extent of deglycosylation, trypsinization, or labeling which are not completely accounted for with normalization used. In addition, false identifications may account for some of the error in quantitations as we are expecting a false identification rate of approximately 3% at a peptide level. One additional source of error for the 116:114 ratios may be error in the signature ion quantitation due to interference of an ion intensity occasionally seen around m/z 116.06; this error is usually not seen with the other isotope ratios, and it is likely to be a error that should be consistent throughout the experiment.

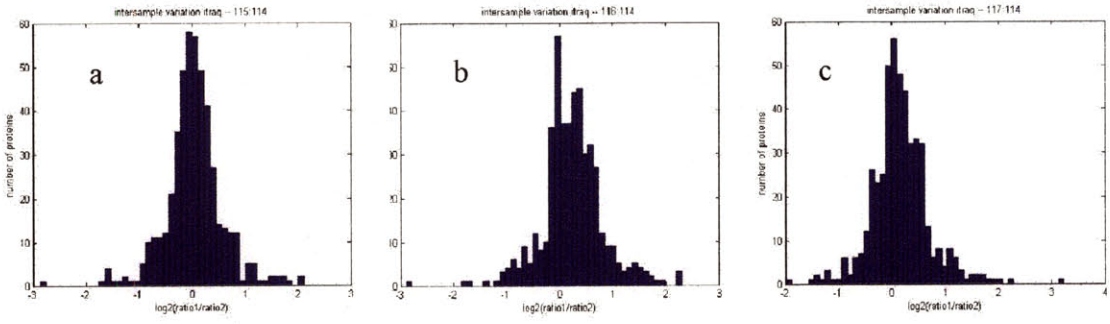

Figure B.4.4: Comparison of analytical duplicates. Figure 4a-c are frequency plots of log2(ratio1/ratio2) for each signature ion ratio (115:114 (a), 116:114 (b), 117:114 (c)). The mean +/- SD for each ratio are as follows – 115:114 0.0346 +/- 0.4861, 116:114 0.2361 +/- 0.5506, 0.1327 +/- 0.5130.

However, a closer look again at large ratios as well as identification certainty was made. First, as before **Figure B.4.5** is a plot of the $\log_2$ (ratio1/ratio2) versus the mean ratio 1 values to determine whether the variance again showed some dependence on ratio. While it is likely that most of this type of variance is accounted for in the interinjection variation, the large correction values for the second duplicate may contribute to some additional variance. Again, there does appear to be some contribution of ratio size to the variance; however, it does not appear to be the only cause of variance in the data.

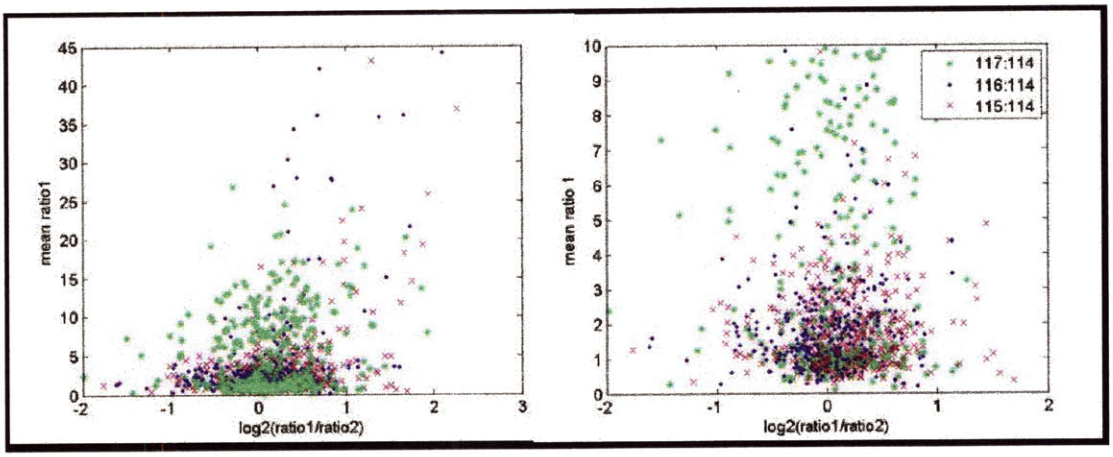

Figure B.4.5: The effects of large ratios on analytical variation. Figure 5 is a set of plots of the log2(ratio1/ratio2) versus the mean ratio 1 for all proteins with ratios less than 10 (a) and less than 50 (b). 'x' represents 115: 114 ratios; '.' represents 116: 114 ratios; and '*' represents 117: 114 ratios.

Another important source of variance is false protein identifications or quantitation outliers which will be most pronounced in proteins with very little peptide data. In the case of false identifications, the variance should decrease if the criteria for protein identification were increased. Thus, we chose to compare the distributions generated from data with 2 or more peptides, 3 or more peptides, or 4 or more peptides. If poor identification is the problem, we would expect the variance to decrease as more peptides were required for identification (and thus more peptides used for quantitation which would decrease the effect of a single outlier). Table 2 displays the mean and standard deviation data from comparing $\log_2$ (ratio1/ratio2) the two analytical duplicates including proteins identified by 2 peptides or more, 3 peptides or more, or 4 peptides or more. The change in variance ranged from 0.06 to 0.09 when increasing identification criteria from 2 peptides to 3 peptides. This suggests that false identifications or outliers in quantitation may account for roughly ½ the increase in variance seen between the interinjection variance and the analytical duplicate variances. The effects of false identification/false quantitation also appear to mask the initial effects of the large ratios in analytical variation. The impact of large ratios becomes more clear once the data from less than 2 or 3 peptides has been removed (contributes again between 0.06 and 0.09 or so to the variation). It appears that poor protein identification and large ratios may both contribute to the variance in comparing both analytical duplicates.

Identification cutoff	Mean 115:114	SD 115:114	Mean 116:114	SD 116:114	Mean 117:114	SD 117:114
2 peptides	0.0346	0.4861	0.2364	0.5506	0.1327	0.5130
3 peptides	0.0538	0.4266	0.2435	0.4833	0.1237	0.4207
4 peptides	0.0647	0.4233	0.2609	0.4642	0.1268	0.3958

Table B.4.2: Contributions of false identifications or outliers in quantitation. Table 2 provides the mean and standard deviation (of log2 transformed data) for the $\log_2$ (ratio1/ratio2) comparison between the first and second analytical duplicates. The variance appears to decrease substantially when increasing the identification criteria from 2 peptides to three peptides suggesting that false identifications may be contributing to the analytical variance comparing the analytical duplicates.

The analysis above suggests that secondary verification of protein identification and possibly peptide identification as well as manual validation may be important for data in which the quantitation is based on only 2 or 3 peptides. Thus, all data will be verified by Spectrum Mill, and at least one peptide per protein will be manually validated to improve accuracy of the data. In addition, for proteins identified and quantified by four or fewer peptides, all spectra will be verified manually. Errors caused by large ratios (one or a couple signature ions much larger than the others) may alter interpretation of all the ratios for that protein. Thus, we anticipate we can decrease the overall error in the experiment through manual validation and secondary validation of the data; however large ratios will have larger intrinsic errors.

Comparison of Matlab Scripts to ProQuant and ProGroup Protein Summary

As a means of verifying our chosen quantitation method, we compared our results to those of ProQuant and ProGroup protein report. **Figure B.4.6** is the histograms for each of the signature ion ratios. The mean +/- SD for each ratio are as follows – 115:114: 0.0752 +/- 0.4505, 116:114: 0.1440 +/- 0.4450, 117:114: 0.1791 +/- 0.6012. While some differences in the data were noted, the consistency (both data sets in agreement about whether the value is above or below 1) was approximately 92%. These values seem reasonable given the slightly different approaches to the data. (Also ProQuant protein summary is based on a 20% confidence limit, so there may be more intrinsic error due to false identification of peptides.

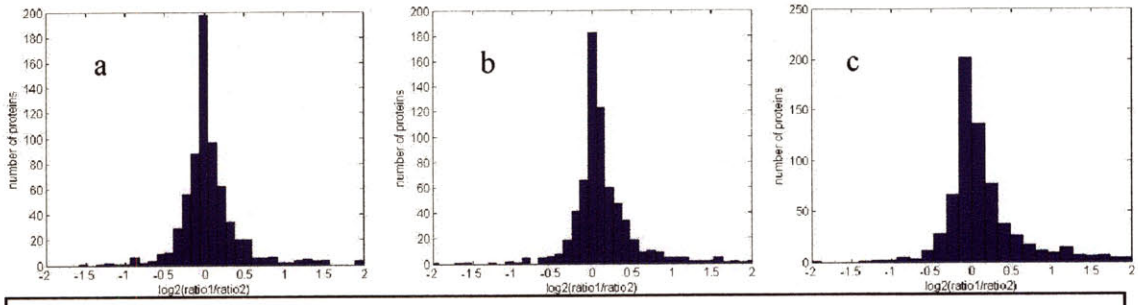

Figure B.4.6: Comparison of Matlab scripts to ProGroup Protein Summary. Figure 6a-c are histograms of the $\log_2$ (ratio1/ratio2) as a measure of error for each of the signature ion ratios.

The ProGroup protein summary from the first and second analytical duplicate was also compared as described above. **Figure B.4.7** is a set of histograms representing the signature ion ratios. The mean +/- SD for each of the curves were 115:114, 0.0362 +/- 0.5787; 116:114, 0.1926 +/- 0.6705; 117:114, 0.1383+/-0.5552. Overall, there is not a dramatic difference between the output of the Matlab scripts and the ProGroup protein summary with the exception of a slight decrease in the variance seen with the Matlab scripts. Similar to that found with the Matlab scripts, the data was approximately 90% consistent in the outcomes.

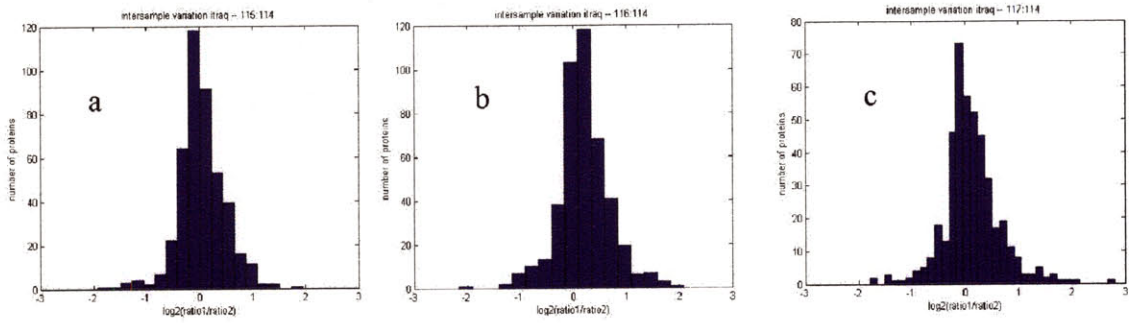

Figure B.4.7: ProGroup protein summary comparison for the analytical duplicates. Figure 7a-c are the histograms for the three signature ion ratios used for quantitation, 115: 114 (a), 116: 114 (b), 117: 114 (c).

Appendix C.1: Protein List from SDS-PAGE-LC/MS/MS with Spectrum Mill (Agilent) identification

Table C.1 on the following page provide information on proteins identified from the SDS-LC-MS/MS analysis by Spectrum Mill Proteomics Software (Agilent). Table 1 provides information that was used for the samples comparisons made in Chapter 3.

Column 1: **untreated** (control):
- Row 1: Number of spectra
- Row 2: Summed peptide ion intensity for each protein

Column 2: **IL-1β**
- Row 1: Number of spectra
- Row 2: Summed peptide ion intensity for each protein

Column 3: **TNF-α**
- Row 1: Number of spectra
- Row 2: Summed peptide ion intensity for each protein

Column 4: **Injury**
- Row 1: Number of spectra
- Row 2: Summed peptide ion intensity

Column 5: **Protein MW**: Protein molecular weight (kDa)
Column 6: **Protein pI**: Protein isoelectric point
Column 7: **Species:** Animal species of matched protein sequences
Column 8: **Accession**: Database accession number
Column 9: **% coverage**: The percent coverage of protein
Column 10: **Peptides**: Number of peptide identified
Column 11: **Score**: Summed score based on peak ions matched and uniqueness
Column 12: **Protein name**: Name of protein identified
Column 13: **Function**: Categorical function of protein identified
Column 14: **Location**: Normal location of protein identified

untreated (Control)	IL-1β	TNF-α	Injury	Protein MW	Protein pI	species	accession	% coverage	peptides	score	group #	Protein NAME	Function	Locations
87 4.57E+05	96 7.12E+06	138 7.04E+06	97 6.32E+05	482534	6.06	Bos taurus	76663616	23	76	1240.93	1	perlecan	cell matrix interactions	ECM
98 6.44E+05	274 2.34E+06	189 1.69E+06	449 8.37E+06	262428.1	5.5	Bos taurus	76610128	40	63	1211.36	2	fibronectin	cell matrix interactions	ECM
49 1.45E+05	415 6.26E+06	882 2.87E+07	36 3.31E+05	69323.9	5.82	Bos taurus	30794280	75	53	1003.91	3	albumin	contaminant--plasma transport	secreted
27 1.30E+05	38 4.93E+05	21 1.11E+05	70 4.72E+05	320152.9	6.34	Bos taurus	76614732	21	49	789.89	4	collagen alpha 3 (VI)	ECM structure	ECM
240 3.37E+06	1081 1.61E+07	665 1.46E+07	310 7.23E+06	246478.3	4.16	Bos taurus	37953324	14	37	690.35	5	aggrecan	ECM structure	ECM
137 1.70E+06	160 2.96E+06	149 1.74E+06	147 2.66E+06	129534.7	4.74	BOVIN	12644428	34	37	618.19	6	Thrombospondin-1 precursor	cell matrix interactions	ECM
89 1.42E+06	295 3.26E+06	134 1.94E+06	233 5.05E+06	108697.3	5.24	Bos taurus	76667061	32	28	534.26	7	collagen alpha 1 (VI)	ECM structure	ECM
46 4.81E+05	13 2.70E+05	18 1.84E+05	0 0.00E+00	77080.4	6.68	Homo sapiens	62897069	42	26	473	8	transferrin variant	contaminant--plasma transport	secreted
98 1.87E+06	127 2.36E+06	202 4.11E+06	66 1.69E+06	40287.8	7.93	Bos taurus	27805853	79	25	449.38	9	cartilage linking protein 1	ECM structure	ECM
9 8.41E+04	906 1.69E+07	352 8.30E+06	48 1.20E+06	43765.9	8.87	Bos taurus	76636770	67	25	474.77	10	chitinase 3 like 1 isoform 2	innate immunity/stress respon	secreted
77 1.22E+06	242 4.36E+06	126 2.88E+06	34 1.06E+06	176804.7	6.53	Bos taurus	76649917	14	23	424.29	11	collagen alpha2 (XI)	ECM structure	ECM
0 0.00E+00	33 6.93E+05	40 9.68E+05	0 0.00E+00	83190.4	8.32	Bos taurus	76650936	42	23	422.2	12	complement factor B	innate immunity - complement	secreted
463 1.70E+07	924 2.09E+07	691 1.54E+07	262 7.84E+06	141875.1	6.82	Canis familiaris	55742776	17	26	468.84	13	collagen alpha 1 (II)	ECM structure	ECM
34 3.82E+05	9 1.26E+05	12 1.46E+05	6 3.11E+04	73777.4	5.42	Bos taurus	27807447	43	22	400.01	14	matrix metalloproteinase 2 (72 KDa type IV collagenase)	protease	ECM
24 3.37E+04	7 4.06E+04	12 2.85E+04	16 6.74E+04	339186.8	5.38	Bos taurus	76625440	11	28	399.78	15	collagen alpha1 (XII) long isoform	ECM structure	ECM
97 1.84E+06	60 6.87E+06	67 9.72E+05	99 1.80E+06	82707	4.57	Bos taurus	76620782	36	20	377.56	16	Cartilage oligomeric matrix protein precursor (COMP) isofor	ECM structure	ECM
50 1.32E+06	12 7.34E+04	52 1.80E+06	109 7.66E+05	62064.6	5.14	Homo sapiens	55956899	45	21	349.58	17	keratin 9	contaminant - cytoskeletal	cytoplasm
38 5.14E+05	18 1.43E+06	33 4.86E+05	27 3.55E+05	54982.7	5.11	Bos taurus	76641931	50	20	348.49	18	nucleobindin 1	ECM structure	ECM
156 4.73E+06	167 3.86E+06	163 7.05E+06	70 3.13E+06	34613.4	4.71	Bos taurus	77567785	55	19	338.8	19	Secreted protein, acidic, cysteine-rich [osteonectin]	cell matrix interactions	ECM
67 4.61E+05	4 6.74E+04	17 6.46E+04	53 4.45E+05	164983	5.27	Bos taurus	76673087	25?	27	449.03	20	CD109	protease inhibitor?	membrane
66 3.11E+05	44 3.05E+06	76 7.31E+05	131 1.32E+06	66067	8.15	Homo sapiens	17318569	25	19	315.5	21	keratin 1	contaminant - cytoskeletal	cytoplasm
33 1.14E+05	0 0.00E+00	1 1.28E+04	9 7.86E+04	254778.7	5.33	Bos taurus	76662186	11	21	311.81	22	melanoma associated chondroitin sulfate proteoglycan 4 (N	cell matrix interactions	membrane
0 0.00E+00	28 6.23E+05	28 2.49E+05	0 0.00E+00	43244.7	8.57	Bos taurus	76613223	60	16	302.62	23	chitinase 3 like 2	unknown - sugar binding	secreted
7 4.55E+04	6 3.89E+04	4 5.33E+04	37 7.11E+05	57265.9	4.8	Bos taurus	27806501	44	23	343.76	24	procollagen-proline, 2-oxoglutarate 4-dioxygenase	PTM	ER
42 6.87E+05	61 1.07E+06	46 7.97E+05	84 1.74E+06	41590.3	6.83	Bos taurus	60650302	53	16	290.98	25	biglycan preproprotein	ECM structure	ECM
23 1.25E+05	43 1.48E+06	125 2.22E+06	9 1.16E+05	51114.2	5.73	Bos taurus	27806907	38	16	286.35	26	clusterin	innate immunity/complement c	secreted
27 1.15E+05	48 4.31E+05	42 1.98E+05	12 6.71E+04	211706.5	4.88	Bos taurus	76625285	11	17	301.18	27	tenascin precursor	cell matrix interactions	ECM
18 9.57E+04	21 1.37E+05	11 9.44E+04	9 1.01E+05	166628.5	5.65	Bos taurus	76627657	13	15	269.7	28	nidogen precursor (osteonidogen)	cell matrix interactions	ECM
260 4.98E+06	139 2.69E+06	261 4.31E+06	92 2.11E+06	91492.4	6.01	Bos taurus	76669942	40	30	528.61	29	collagen alpha 1 (XI)	ECM structure	ECM
43 3.09E+05	61 7.82E+05	40 2.89E+05	31 3.59E+05	54065.4	8.43	Bos taurus	76611076	38	16	267.47	30	Cartilage matrix protein precursor (Matrilin-1)	ECM structure	ECM
19 8.99E+04	7 1.49E+05	12 1.48E+05	13 9.70E+04	83564.7	6.13	Bos taurus	27806477	24	16	260.23	31	procollagen-lysine, 2-oxoglutarate 5-dioxygenase precursor	PTM	ER
0 0.00E+00	78 1.72E+06	13 2.85E+05	14 1.78E+05	54414.8	5.36	Bos taurus	61863538	42	15	258.26	32	Stromelysin-1 precursor (Matrix metalloproteinase-3) (MMP-	protease	secreted
18 2.06E+05	5 7.24E+04	5 5.15E+04	24 2.73E+05	80731.1	5.54	Bos taurus	74356373	29	16	258.09	33	Hypothetical protein LOC535077	other	secreted
15 1.92E+05	64 1.18E+06	76 6.25E+05	15 2.93E+05	40887.5	9.49	Bos taurus	27806687	49	14	277.81	34	chondroadherin	cell matrix interactions	ECM
17 7.84E+04	4 2.69E+04	10 8.73E+04	2 1.16E+04	77610.1	8.75	Bos taurus	76652955	28	14	249.98	35	xylosyltransferase I	PTM	golgi
23 5.05E+04	10 2.29E+04	50 1.54E+05	100 3.66E+05	59527.9	5.17	Homo sapiens	28317	29	13	244.87	36	unnamed protein product	contaminant - cytoskeletal	cytoplasm
11	12	17	17			Canis						collagen, type XIV, alpha 1	ECM structure	ECM

untreated (Control)	IL-1β	TNF-α	Injury	Protein MW	Protein pI	species	accession	% coverage	peptides	score	group #	Protein NAME	Function	Locations
5.46E+04	3.24E+04	5.46E+04	8.24E+04	193349.2	5.22	familiaris	73974565	9	15	243.45	37			
0 0.00E+00	23 6.52E+05	6 6.06E+04	0 0.00E+00	63427.9	6.5	Bos taurus	76612740	32	13	241.3	38	extracellular matrix protein 1 isoform 1 precursor isoform 14	ECM structure	ECM
11 4.79E+04	0 0.00E+00	10 4.26E+04	9 1.88E+04	81444.6	6.36	Bos taurus	76623057	32	15	239.5	39	Transforming growth factor-beta induced protein IG-H3 prec	cell matrix interactions	ECM
1 4.98E+02	0 0.00E+00	0 0.00E+00	24 1.63E+05	106355.6	5.29	Bos taurus	76641275	21	14	233.4	40	actinin, alpha 4 isoform 11	cytoskeleton	cytoplasm
0 0.00E+00	1 5.01E+03	0 0.00E+00	18 3.09E+05	56929.9	6.23	Bos taurus	27805905	32	14	224.8	41	glucose regulated protein 58kD	PDI	ER
18 7.40E+04	63 6.39E+05	44 6.96E+05	26 3.16E+05	51723.5	6.19	Bos taurus	27807349	30	12	215.73	42	serine (or cysteine) proteinase inhibitor, clade G (C1 inhibitc	protease inihibitor (complemer	secreted
2 1.75E+03	4 6.87E+04	12 6.16E+04	37 4.98E+05	53677.1	5.21	Bos taurus	27806785	27	14	214.69	43	vimentin	cytoskeleton	cytoplasm
0 0.00E+00	0 0.00E+00	42 6.77E+05	0 0.00E+00	51061.3	4.95	Homo sapiens	38114739	26	13	213.4	44	KRT13 protein	contaminant - cytoskeletal	cytoplasm
0 0.00E+00	4 3.37E+04	2 2.84E+03	33 2.55E+05	61428	8.62	Bos taurus	73567283	31	14	213	45	LOC512571 protein	metabolism	cytoplasm
28 1.22E+05	39 4.16E+05	68 5.72E+05	71 1.07E+06	110331.5	5.48	Bos taurus	76617906	12	13	211.89	46	keratin 4 isoform 9	contaminant - cytoskeletal	cytoplasm
58 1.01E+06	73 1.46E+06	40 1.31E+06	71 1.81E+06	43037.9	5.57	Bos taurus	74356334	36	10	211.53	47	Fibromodulin	ECM structure	ECM
50 5.75E+05	33 4.89E+05	20 2.55E+05	36 5.89E+05	38756.6	5.93	Bos taurus	74354899	42	12	211.3	48	Lumican	ECM structure	ECM
32 3.61E+05	24 6.41E+05	24 4.13E+05	23 4.99E+05	23743.6	9.33	Bos taurus	74268324	49	12	205.44	50	PPIB protein	PTM	ER
46 3.63E+05	12 5.36E+04	17 1.02E+05	6 6.22E+03	99493	8.75	Bos taurus	76625388	17	12	201.32	51	Collagen alpha 1(IX) chain precursor, partial	ECM structure	ECM
12 1.31E+05	19 1.91E+05	5 4.15E+04	5 5.00E+04	138939.2	5.61	Bos taurus	75775290	9	11	193.72	52	Collagen, type I, alpha 1	ECM structure	ECM
9 3.20E+04	1 7.70E+03	6 4.73E+04	6 2.28E+04	80694.8	5.53	Bos taurus	76607158	20	12	188.96	53	Melanotransferrin precursor (CD228 antigen)	transport	membrane
0 0.00E+00	2 4.34E+03	1 3.25E+03	19 3.71E+05	56903.5	7.69	Bos taurus	41366780	27	12	188.67	54	UDP-glucose pyrophosphorylase 2	metabolism	cytoplasm
14 1.01E+05	9 1.14E+05	7 6.89E+04	27 4.21E+05	46104.2	6.05	Bos taurus	27806941	30	12	187.67	55	serine (or cysteine) proteinase inhibitor, clade A (alpha-1ant	protease inhibitor	secreted
0 0.00E+00	1 4.60E+03	0 0.00E+00	12 2.67E+05	80352.5	6.36	Bos taurus	76619055	20	11	181.65	56	cytoskeleton-associated protein 4	cytoskeleton	cytoplasm
31 1.41E+05	27 3.21E+05	41 4.34E+05	69 6.60E+05	54848.5	5.05	Bos taurus	479	16	11	180.63	57	cytokeratin VIb	contaminant? - cytoskeleton	cytoplasm
12 9.24E+04	15 1.29E+05	26 1.57E+05	32 2.16E+05	34209.7	5.43	BOVIN	129077	37	10	176.65	58	Mimecan precursor (Osteoglycin) osteoinductive factor	ECM structure	ECM
2 1.80E+04	3 1.31E+04	6 9.72E+03	12 1.20E+05	36089	4.86	Bos taurus	59858367	39	10	173.02	59	annexin 5	cell matrix interactions	membrane
0 0.00E+00	1 2.91E+02	6 7.63E+04	11 2.20E+05	26689.6	6.45	Bos taurus	74267824	49	10	163.55	60	Triosephosphate isomerase	metabolism	cytoplasm
0 0.00E+00	2 3.01E+04	10 3.10E+04	11 2.71E+05	36597.8	8.12	Bos taurus	27806559	36	10	159.68	61	lactate dehydrogenase A	metabolism	cytoplasm
9 9.80E+04	18 1.51E+05	5 2.72E+04	6 1.73E+05	129064.2	9.23	Bos taurus	27806257	8	10	157.51	62	collagen, type I, alpha 2	ECM structure	ECM
0 0.00E+00	18 3.30E+05	9 3.33E+04	0 0.00E+00	44859.4	7.83	Bos taurus	76640813	27	11	153.07	63	Haptoglobin precursor isoform 4	transport	secreted
0 0.00E+00	0 0.00E+00	0 0.00E+00	16 1.05E+05	48514.9	4.91	Bos taurus	76630218	31	9	152.58	64	Protein disulfide-isomerase A6 precursor	PDI	ER
19 5.39E+04	4 2.27E+04	4 1.43E+04	10 5.30E+04	82366.3	4.74	Bos taurus	27807319	16	10	152.45	65	AE binding protein 1	cell matrix interactions - unkno	ECM
0 0.00E+00	6 5.76E+04	5 4.81E+04	12 2.60E+05	22209.7	8.59	Bos taurus	59858511	52	10	151.55	66	peroxiredoxin 1	redox	cytoplasm

untreated (Control)	IL-1β	TNF-α	Injury	Protein MW	Protein pI	species	accession	% coverage	peptides	score	group #	Protein NAME	Function	Locations
1 6.29E+03	6 6.19E+04	10 4.26E+04	0 0.00E+00	36039.1	5.67	Bos taurus	74355004	34	9	150.1	67	Apolipoprotein E	lipid regulation	secreted
0 0.00E+00	0 0.00E+00	0 0.00E+00	12 1.06E+05	84731.2	4.93	Bos taurus	34362343	14	10	147.09	68	90-kDa heat shock protein alpha	chaperone	cytoplasm
0 0.00E+00	2 1.90E+04	0 0.00E+00	21 1.92E+05	61243.3	4.72	Bos taurus	76630567	32	14	236.26	69	78 kDa glucose-regulated protein precursor (GRP 78) (BiP) (	chaperone	ER
0 0.00E+00	2 3.66E+04	2 2.03E+04	18 1.63E+05	44537.9	8.48	Bos taurus	74353972	21	9	146.16	70	Phosphoglycerate kinase 1	metabolism	cytoplasm
6 6.51E+04	37 3.41E+05	19 3.18E+05	11 1.09E+05	60882.3	7.88	Bos taurus	76630143	19	8	145.43	71	matrilin 3	ECM structure	ECM
0 0.00E+00	0 0.00E+00	23 2.66E+05	0 0.00E+00	57285.5	6.25	Homo sapiens	27769210	17	9	144.53	72	Keratin 4	contaminant -cytoskeleton	cytoplasm
12 1.82E+05	8 2.66E+05	13 1.71E+05	16 3.64E+05	34856.6	5.46	Bos taurus	62968316	32	10	141.54	73	follistatin-like 1	signal negative	secreted
28 1.96E+05	7 6.94E+04	22 1.26E+05	14 1.37E+05	100000	9.64	Bos taurus	76677607	38	7	231.12	74	Collagen alpha 1(V) chain precursor	ECM structure	ECM
9 4.18E+04	23 2.35E+05	13 1.88E+05	11 1.18E+05	22766.5	9.74	Bos taurus	74353857	37	7	138.64	75	Unknown (protein for IMAGE:7942574)	contaminant-ribonuclease	secreted
0 0.00E+00	0 0.00E+00	0 0.00E+00	13 9.54E+04	92427.2	4.76	Bos taurus	75775556	13	10	137.01	76	Tumor rejection antigen (gp96) 1	chaperone	ER
0 0.00E+00	3 1.09E+05	9 6.70E+04	23 5.60E+05	41676	5.36	Bos taurus	22655316	32	9	133.15	77	beta-actin	cytoskeleton	cytoplasm
4 2.31E+04	3 7.42E+03	2 6.92E+03	24 4.27E+05	36687.9	4.76	Bos taurus	27805823	28	8	131.7	78	dermatan sulfate proteoglycan 3	ECM structure	ECM
0 0.00E+00	0 0.00E+00	21 4.70E+05	0 0.00E+00	25644.5	6.44	Homo sapiens	4337115	54	11	156.05	79	tumor necrosis factor	contaminant-cytokine	secreted
0 0.00E+00	0 0.00E+00	0 0.00E+00	10 6.51E+04	72498.4	4.96	Bos taurus	76616203	16	9	129.71	80	Protein disulfide-isomerase A4 precursor (Protein ERp-72)	PDI	ER
5 4.70E+03	0 0.00E+00	2 6.26E+03	13 8.26E+04	68587.5	6.14	Bos taurus	76607976	14	8	124.39	81	procollagen-lysine, 2-oxoglutarate 5-dioxygenase 2 isoform	PTM	ER
7 7.57E+04	3 1.45E+05	3 4.70E+04	5 5.13E+04	39879.3	8.72	Bos taurus	54660107	25	8	121.96	83	decorin	ECM structure	ECM
0 0.00E+00	0 0.00E+00	2 4.67E+03	9 5.82E+04	53989.5	5.43	Bos taurus	76617955	16	9	120.65	84	PREDICTED: similar to keratin, hair, basic, 1	contaminant - cytoskeletal	cytoplasm
9 4.92E+04	39 2.28E+05	20 2.70E+05	4 5.77E+04	36234.2	8.75	Bos taurus	27806625	26	7	119.59	85	frizzled-related protein	signal-negative/positive	secreted/membrane
4 3.61E+04	9 6.22E+04	3 2.24E+04	2 6.63E+03	47862.6	6.8	Bos taurus	74354284	19	8	119.31	86	MFGE8 protein	cell matrix interactions	secreted
0 0.00E+00	4 4.14E+04	7 6.61E+04	0 0.00E+00	81398.7	5.3	Bos taurus	41386707	11	7	117.59	87	vascular cell adhesion molecule 1	cell matrix interactions	membrane
0 0.00E+00	0 0.00E+00	1 1.69E+03	10 8.59E+04	38672.8	6.28	Bos taurus	76676583	23	7	117.46	88	Thioredoxin domain containing protein 5 precursor (Endopl	PDI	ER
0 0.00E+00	1 6.23E+02	4 1.09E+04	7 7.69E+04	29174.1	4.63	Pan troglodyte	55644755	32	6	117.34	89	epsilon isoform of 14-3-3 protein	signal	cytoplasm
0 0.00E+00	22 3.93E+05	12 1.10E+05	0 0.00E+00	14769.7	9.35	Bos taurus	79158764	40	8	116.75	90	Serum amyloid A 3	innate immunity- lipid regulati	secreted
2 1.03E+04	13 1.25E+05	3 3.42E+04	10 1.06E+05	97178.2	5.53	Bos taurus	76607764	11	8	114.9	91	alpha 2 type VI collagen isoform 2C2a precursor isoform 1	ECM structure	ECM
6 1.63E+04	4 1.75E+04	3 1.79E+04	4 2.39E+04	106888.1	5.25	Bos taurus	61845535	10	8	114.74	92	EMILIN 1 precursor (Elastin microfibril interface-located pro	ECM structure	ECM
115 5.81E+06	188 3.31E+06	170 5.00E+06	238 8.14E+06	24409.6	7	PIG	136429	31	6	113.8	93	Trypsin precursor	contaminant protease	secreted
14 1.42E+05	5 1.19E+05	5 3.94E+04	6 5.12E+04	49753.1	8.48	Bos taurus	76661652	16	12	189.11	94	EGF-like repeats and discoidin I-like domains-containing pr	cell matrix interactions	ECM
0 0.00E+00	0 0.00E+00	10 2.05E+04	3 2.63E+04	36787.3	5.3	Bos taurus	27806317	25	7	107.8	95	annexin A8		membrane associate
17 2.21E+05	10 3.52E+05	20 1.79E+05	4 2.40E+04	138850.1	6.39	Bos taurus	76609270	5	7	107.52	96	Collagen alpha 1(III) chain precursor isoform 2	ECM structure	ECM
6 3.96E+04	2 1.89E+04	8 1.79E+04	3 2.39E+04	41081.8	10.45	Bos taurus	76674078	23	6	107.11	97	retinol-binding protein 4, plasma precursor	transport	secreted
2 2.70E+03	4 5.89E+04	1 1.55E+03	7 2.54E+04	46506.9	9.01	Bos taurus	76636117	21	6	107.04	98	Collagen-binding protein 2 precursor (Colligin 2)	chaperone	ER
0 0.00E+00	15 1.34E+05	7 8.16E+04	0 0.00E+00	23182.6	5.61	Bos taurus	74268094	30	6	105.41	99	Unknown (protein for MGC:128004) - lipocalin	transport	secreted
3 1.19E+04	10 2.74E+05	3 2.79E+04	2 2.72E+04	42342.7	9.64	Bos taurus	76630593	19	6	104.83	100	Neutrophil gelatinase-associated lipocalin precursor (NGAL	transport	secreted
3 3.19E+04	9 8.76E+04	6 1.03E+05	0 0.00E+00	26399.4	9.54	Bos taurus	76611613	29	6	104.24	101	complement component 1, q subcomponent, beta polypepti	innate immunity	secreted
0 0.00E+00	0 0.00E+00	4 6.38E+03	11 1.13E+05	63639.9	7.36	Bos taurus	76640991	14	6	101.54	102	Glucose-6-phosphate isomerase (GPI)	metabolism	cytoplasm

untreated (Control)	IL-1β	TNF-α	Injury	Protein MW	Protein pI	species	accession	% coverage	peptides	score	group #	Protein NAME	Function	Locations
16 1.27E+05	9 2.96E+05	10 1.24E+05	8 1.22E+05	32629.8	5.92	Bos taurus	76620265	23	7	101.02	103	Fibulin-5 precursor (FIBL-5)	signal	secreted
0 0.00E+00	0 0.00E+00	2 2.76E+04	10 3.51E+05	48038.7	4.31	Bos taurus	27806723	19	8	100.42	104	calreticulin	chaperone	ER
4 1.04E+04	6 3.23E+04	4 2.07E+04	0 0.00E+00	48211.2	8.13	Bos taurus	76853981	17	6	99.2	105	Procollagen C-proteinase enhancer protein precursor (PCP	PTM	ER
5 3.66E+04	1 5.49E+03	5 1.11E+05	2 2.77E+04	41503.9	8.69	Bos taurus	76808113	22	6	97.19	106	acid phosphatase-like 2	PTM	secreted
0 0.00E+00	3 3.22E+04	5 3.88E+04	8 1.23E+05	50743.9	8.28	Bos taurus	76630316	15	6	96.84	107	14-3-3 protein theta (14-3-3 protein tau)	signal	cytoplasm
6 1.69E+04	4 6.26E+04	4 5.51E+04	0 0.00E+00	41820	8.84	Bos taurus	78369684	24	6	95.13	108	platelet-derived growth factor receptor-like protein	signal	membrane/secreted
9 3.40E+04	17 2.92E+05	17 1.41E+05	17 2.57E+05	18354.5	10.62	Bos taurus	76651044	34	6	95.06	109	Histone H2B 291B	DNA architecture	nucleus
8 5.08E+04	5 1.70E+04	3 2.16E+04	2 3.79E+03	121440.4	7.84	Bos taurus	76611086	6	7	108.1	110	alpha 1 type XVI collagen precursor	ECM structure	ECM
0 0.00E+00	6 6.28E+04	2 1.50E+04	0 0.00E+00	25802.2	9.11	Bos taurus	62460582	32	5	91.22	111	complement component 1, q subcomponent, alpha polypept	innate immunity	secreted
3 2.66E+04	5 2.17E+05	6 1.90E+05	3 2.40E+04	14547.9	9.25	bovine	7513476	49	6	90.67	112	chondromodulin II	signal	secreted
1 3.31E+03	0 0.00E+00	3 1.18E+04	9 2.41E+05	17316.2	7.76	Bos taurus	74354800	44	6	89.88	114	Unknown (protein for MGC:127630)	metabolism	cytoplasm
0 0.00E+00	0 0.00E+00	8 5.93E+04	0 0.00E+00	56676	5.86	Pan troglodyte	55631825	13	5	88.85	115	PREDICTED: annexin I	transport - exocytosis	membrane associated
7 3.96E+04	12 2.26E+05	5 3.02E+04	5 1.47E+05	24371.4	7.44	Bos taurus	74354677	29	6	109.19	116	Tissue inhibitor of mettaloproteinase 2	protease inhibitor	secreted
6 3.18E+04	7 4.96E+04	3 3.21E+04	3 3.89E+04	55970.7	8.7	Bos taurus	61863334	9	5	86.6	117	Serine protease HTRA1 precursor (L56)	protease	secreted
0 0.00E+00	0 0.00E+00	7 1.31E+04	8 3.85E+04	38612.3	6.92	Bos taurus	27807289	20	5	86.36	118	annexin A2	transport - exocytosis	membrane associated
2 1.59E+04	23 2.59E+05	17 1.03E+05	2 1.82E+04	33343.2	9.32	Bos taurus	76690954	21	4	86.21	119	secreted modular calcium-binding protein 2	ECM structure	ECM
0 0.00E+00	0 0.00E+00	1 3.53E+03	4 6.54E+04	28852.1	6.68	Bos taurus	77404217	33	5	85.88	120	phosphoglycerate mutase	metabolism	cytoplasm
0 0.00E+00	0 0.00E+00	9 2.80E+04	0 0.00E+00	77245	6.3	Bos taurus	76621268	12	5	84.74	121	N-acetylmuramoyl-L-alanine amidase precursor (Peptidogly	innate immunity	secreted
0 0.00E+00	0 0.00E+00	6 4.56E+04	1 2.35E+03	38992	6.38	Bos taurus	61553085	17	6	84.59	122	annexin I	transport - exocytosis	membrane associated
5 1.10E+05	6 2.16E+05	10 2.00E+05	5 2.97E+05	26176.1	8.52	Bos taurus	76634746	19	5	84.24	124	collagen triple helix repeat containing 1	ECM structure	ECM
0 0.00E+00	0 0.00E+00	0 0.00E+00	8 6.24E+04	63535.4	4.92	Bos taurus	76615361	15	6	84.02	125	FK506 binding protein 9	rotamase	ER
8 3.62E+04	1 1.19E+04	0 0.00E+00	2 6.42E+03	49515	4.88	Bos taurus	76657493	15	5	82.69	126	EGF-containing fibulin-like extracellular matrix protein 2 pre	ECM structure	ECM
0 0.00E+00	5 1.02E+05	0 0.00E+00	0 0.00E+00	78168	8.78	Bos taurus	408926	7	5	82.46	127	lactoferrin	innate immunity - iron transpo	secreted
14 9.88E+03	4 3.90E+04	16 2.77E+04	28 1.28E+05	24529.1	4.98	Bos taurus	30794348	26	4	81.98	128	casein alpha-S1	transport	secreted
0 0.00E+00	0 0.00E+00	0 0.00E+00	8 2.85E+04	50512.4	6.02	BOVIN	13638228	13	5	80.33	129	Rab GDP dissociation inhibitor beta (Rab GDI beta)	signal	cytoplasm
0 0.00E+00	2 1.49E+04	1 4.36E+03	4 1.13E+04	15057.5	8.46	Bos taurus	73586531	47	5	80.07	130	Profilin 1	cytoskeleton	cytoplasm
9 2.16E+04	12 1.81E+05	16 1.22E+05	12 7.27E+04	35525.3	10.2	Bos taurus	76831272	13	4	79.7	131	germinal histone H4 gene	DNA architecture	nucleus
0 0.00E+00	0 0.00E+00	1 1.47E+03	5 4.25E+04	45371.5	5.96	Bos taurus	601	16	5	78.14	133	plasminogen activator inhibitor	protease inhibitor	secreted
4 2.18E+04	2 2.99E+03	2 5.70E+03	0 0.00E+00	62118.1	9.78	Bos taurus	76609723	13	5	78.14	134	Carbohydrate sulfotransferase 11 (Chondroitin 4-O-sulfotrar	PTM	golgi
6 1.54E+04	9 1.84E+05	7 6.12E+04	3 1.45E+04	17003.6	9.09	Bos taurus	84202584	42	5	77.88	135	Unknown (protein for MGC:137015)	contaminant- riboncuelease	secreted
0 0.00E+00	0 0.00E+00	1 8.99E+02	5 9.17E+04	20035.4	6.84	Bos taurus	62751848	43	5	77.74	136	Parkinson disease (autosomal recessive, early onset) 7 (glu	metabolism	cytoplasm
0 0.00E+00	4 5.02E+04	0 0.00E+00	6 5.53E+04	47326.4	6.38	Bos taurus	74354056	18	5	77.6	137	Unknown (protein for MGC:127526)	metabolism	cytoplasm
0 0.00E+00	2 4.61E+03	8 1.33E+05	4 5.73E+04	39456.8	7.55	Bos taurus	62460514	14	4	77.01	138	angiopoietin-like 7	signal	secreted
0 0.00E+00	8 5.44E+04	2 2.38E+04	0 0.00E+00	39681	5.37	Bos taurus	41386760	13	4	76.79	139	CD14 antigen	innate immunity - signal	membrane/secreted
0 0.00E+00	9 1.53E+05	0 0.00E+00	0 0.00E+00	44557.7	5.76	Bos taurus	74354137	13	4	76.3	140	Complement component 1, r subcomponent	innate immunity - complement	secreted
6 6.78E+04	6 4.77E+04	5 4.58E+04	4 1.04E+05	15632.5	7.6	Bos taurus	76620378	24	5	75.94	141	Cytokine-like protein C17 precursor	signal	secreted

untreated (Control)	IL-1β	TNF-α	Injury	Protein MW	Protein pI	species	accession	% coverage	peptides	score	group #	Protein NAME	Function	Locations
5 4.07E+04	2 1.51E+04	0 0.00E+00	2 1.70E+04	75133.1	5.29	Bos taurus	27806095	10	6	74.6	142	protein S (alpha)	signal	secreted
1 1.99E+03	2 2.51E+04	3 7.00E+03	0 0.00E+00	18357.3	8.96	Bos taurus	76616163	42	4	73.43	143	retinoic acid receptor responder (tazarotene induced) 2 isof	unknown	secreted
0 0.00E+00	0 0.00E+00	2 2.02E+03	5 4.30E+04	21946.1	5.36	Bos taurus	74353992	26	4	72.64	144	PRDX2 protein	redox	cytoplasm
13 6.21E+04	10 1.04E+05	9 1.35E+05	15 2.13E+05	37765	11.05	Bos taurus	76612880	14	5	71.64	145	H3 histone, family 2 isoform 2	DNA architecture	nucleus
0 0.00E+00	0 0.00E+00	6 3.15E+04	0 0.00E+00	187315.2	6.41	Bos taurus	76622036	4	5	70.11	146	PREDICTED: similar to Complement C3 precursor isoform 2	innate immunity - complement	secreted
4 1.22E+04	1 3.23E+03	0 0.00E+00	0 0.00E+00	16356	7.63	Bos taurus	61097917	46	4	68.73	147	cystatin E/M	protease inhibitor	cytoplasm?
0 0.00E+00	4 1.90E+04	2 1.39E+04	1 3.21E+03	43877.4	9.56	Bos taurus	27807207	15	4	68.3	148	plasminogen activator inhibitor type 1, member 2	protease inhibitor	secreted
3 3.16E+04	2 2.16E+04	2 1.12E+04	3 2.14E+04	21063.2	9.59	Bos taurus	19550242	23	4	67.85	149	oligosaccharide-binding protein	innate immunity	secreted
2 1.80E+04	4 7.23E+04	4 8.66E+04	4 4.65E+04	23031.7	8.46	Bos taurus	27806161	25	4	67.53	151	tissue inhibitor of metalloproteinase 1	protease inhibitor	secreted
1 9.76E+02	1 8.84E+02	2 4.51E+03	5 5.15E+04	29798.7	4.62	Bos taurus	76642117	18	4	66.88	152	reticulocalbin 3, EF-hand calcium binding domain	chaperone	ER
0 0.00E+00	0 0.00E+00	3 1.69E+04	2 1.15E+04	21004.9	7.73	Bos taurus	74354599	25	4	66.69	153	Phosphatidylethanolamine binding protein	metabolism	cytoplasm
0 0.00E+00	0 0.00E+00	5 1.95E+04	5 1.06E+04	51268.1	4.98	Homo sapiens	24430197	11	4	66.52	154	keratin 16	contaminant - cytoskeletal	cytoplasm
3 1.19E+04	3 1.02E+04	0 0.00E+00	0 0.00E+00	131227.5	8.77	Bos taurus	76621011	5	4	66.24	155	Cartilage intermediate layer protein 2 precursor (CILP-2)	ECM structure	ECM
0 0.00E+00	0 0.00E+00	0 0.00E+00	4 6.82E+03	53048.5	6.29	Bos taurus	76625476	20	4	65.26	156	NADP-dependent malic enzyme (NADP-ME) (Malic enzyme 1	metabolism	cytoplasm
0 0.00E+00	4 1.95E+04	3 1.32E+04	0 0.00E+00	17684.4	6.32	Bos taurus	74356489	28	4	64.28	157	Unknown (protein for IMAGE:7989842)	transport	secreted
1 3.70E+02	2 2.38E+04	0 0.00E+00	7 1.25E+04	58120.9	5.13	BOVIN	13878928	11	4	63.27	159	Proactivator polypeptide precursor [Contains: Saposin A (P	other	lysosome
0 0.00E+00	0 0.00E+00	0 0.00E+00	5 5.01E+04	34378.9	9.22	Bos taurus	2293575	22	4	62.33	160	elongation factor 1 alpha	translation	cytoplasm
0 0.00E+00	0 0.00E+00	0 0.00E+00	7 5.94E+04	79731.2	4.56	Bos taurus	76682896	6	5	62.19	161	nucleolin-related protein isoform 9	DNA architecture	nucleus
2 5.99E+03	2 7.89E+03	0 0.00E+00	3 2.49E+04	82977.8	6.45	Bos taurus	76628833	5	4	62.01	162	lysyl oxidase-like 3 precursor	PTM	ECM
0 0.00E+00	0 0.00E+00	0 0.00E+00	5 2.18E+04	37685.5	7.03	Bos taurus	83638723	16	4	61.82	163	Unknown (protein for MGC:133714)	metabolism	cytoplasm
0 0.00E+00	0 0.00E+00	1 5.99E+03	5 5.53E+04	25635	6.91	Bos taurus	73586890	24	4	61.69	164	Glutathione S-transferase M1	redox	cytoplasm
6 2.54E+04	0 0.00E+00	0 0.00E+00	2 3.79E+03	64589.1	5.8	Bos taurus	76632004	7	4	60.66	165	growth arrest-specific 6	signal	secreted
8 1.19E+05	24 4.19E+05	4 1.43E+05	1 5.40E+03	14353.6	7.65	Bos taurus	27806849	33	3	60.01	166	melanoma inhibitory activity	signal	secreted
0 0.00E+00	0 0.00E+00	0 0.00E+00	5 2.00E+04	95368.7	6.41	Bos taurus	74353984	7	5	59.38	167	Unknown (protein for MGC:127305)	translation	cytoplasm
0 0.00E+00	3 9.17E+03	1 3.28E+03	2 4.57E+04	25067.1	6	Bos taurus	27807167	19	4	58.96	168	anti-oxidant protein 2 (non-selenium glutathione peroxidase	redox	cytoplasm
4 5.49E+04	2 1.40E+04	7 4.82E+04	2 3.18E+04	14247.2	5.5	Bos taurus	76619933	32	3	58.85	169	Insulin-like growth factor binding protein 7 precursor (IGFBF	signal	secreted
4 9.96E+03	0 0.00E+00	0 0.00E+00	0 0.00E+00	30276.5	5.71	Bos taurus	74268269	17	4	58.81	170	Apolipoprotein A1	lipid transport	secreted
0 0.00E+00	0 0.00E+00	0 0.00E+00	6 3.80E+04	64355.4	5.98	Bos taurus	76659545	7	4	58.21	172	PREDICTED: similar to Moesin (Membrane-organizing exten	cytoskeleton	cytoplasm

untreated (Control)	IL-1β	TNF-α	Injury	Protein MW	Protein pI	species	accession	% coverage	peptides	score	group #	Protein NAME	Function	Locations
6 1.51E+04	6 7.12E+04	3 1.23E+04	0 0.00E+00	14340	8.83	Bos taurus	76691025	34	4	58.06	173	scrapie responsive protein 1	unknown	secreted
2 1.83E+04	2 8.33E+02	3 2.74E+04	1 9.56E+03	18450.6	9.53	Bos taurus	27806923	31	4	57.83	174	angiogenin	signal - ribonuclease	secreted
2 7.15E+03	4 7.94E+04	6 2.00E+04	7 2.89E+04	83173.9	9.18	Homo sapiens	62088140	5	5	95.37	175	quiescin Q6 isoform a variant	unknown	cytoplasm
0 0.00E+00	2 2.73E+04	1 3.17E+03	0 0.00E+00	111838.2	7.28	Bos taurus	76624630	3	3	57.04	176	Bone morphogenetic protein 1 precursor (BMP-1) (Procollag	PTM-protease	secreted
0 0.00E+00	0 0.00E+00	5 5.70E+04	0 0.00E+00	46285.2	5.67	Bos taurus	62946669	10	4	56.78	177	muscle endopin 1a	protease inhibitor	cytoplasm
1 4.82E+02	2 4.08E+03	4 1.99E+04	9 6.97E+04	10668	4.57	Bos taurus	73587373	40	3	56.71	178	Hypothetical protein LOC525716	S100/ICaBP	cytoplasm?
0 0.00E+00	1 7.34E+03	2 2.37E+03	4 3.86E+04	36719.5	5.57	Bos taurus	73586701	14	3	55.91	179	CTSB protein	protease	cytoplasm/secreted
1 1.73E+04	4 6.37E+04	3 1.46E+04	2 3.23E+04	27390.2	6.59	Bos taurus	76680741	14	3	55.34	180	PREDICTED: similar to Extracellular superoxide dismutase [	redox	secreted
0 0.00E+00	5 3.33E+04	0 0.00E+00	1 3.26E+03	37924.5	8.29	Bos taurus	11096307	8	3	54.79	181	connective tissue growth factor precursor	signal	secreted
3 1.94E+04	3 6.20E+04	1 2.84E+04	5 3.25E+04	83596.7	6.47	Homo sapiens	16741721	5	3	54.42	182	Lysyl hydroxylase, precursor	PTM	ER
6 1.01E+05	6 1.18E+05	0 0.00E+00	0 0.00E+00	64963	9.23	Bos taurus	76686297	5	3	54.13	183	Collagen alpha 2(IX) chain precursor	ECM structure	ECM
1 3.26E+03	11 1.16E+05	3 7.65E+04	0 0.00E+00	14997.2	8.53	Bos taurus	76669311	30	3	53.09	184	secreted modular calcium-binding protein 1	ECM structure	ECM
3 4.39E+04	8 1.53E+05	5 6.61E+04	0 0.00E+00	28997.4	9.16	Bos taurus	76611607	11	3	52.94	185	Complement C1q subcomponent, C chain precursor isoform	innate immunity - complement	secreted
0 0.00E+00	2 4.32E+04	5 1.79E+04	0 0.00E+00	34763.1	9.05	Bos taurus	27806139	14	3	52.59	186	secreted frizzled-related protein 1	signal	secreted
0 0.00E+00	0 0.00E+00	3 6.71E+03	2 1.50E+04	15682.6	5.85	Bos taurus	73586543	41	4	51.43	187	SOD1 protein	redox	cytoplasm
5 3.07E+04	8 4.67E+03	15 6.00E+04	1 5.65E+03	12217	9.27	Bos taurus	27807275	24	3	50.63	188	matrix Gla protein	cell matrix interactions	ECM
0 0.00E+00	1 1.06E+03	0 0.00E+00	4 2.31E+04	45385.6	7.58	Bos taurus	76658398	9	4	50.02	189	Cathepsin D precursor isoform 3	protease	lysosome
4 1.97E+03	1 6.62E+03	3 6.87E+03	2 3.16E+03	54027	9.93	Bos taurus	76658905	11	3	49.94	190	Extracellular matrix protein 2 precursor (Matrix glycoprotein	ECM	secreted
0 0.00E+00	1 2.80E+03	3 3.71E+04	6 2.84E+05	21401.7	4.8	Bos taurus	81674721	16	3	49.92	191	Unknown (protein for MGC:133726)	metabolism/transport	cytoplasm
0 0.00E+00	0 0.00E+00	0 0.00E+00	6 1.18E+04	111465	6.19	Bos taurus	76657686	5	3	49.57	192	alpha glucosidase II alpha subunit isoform 2	metabolism	cytoplasm
1 7.53E+03	6 6.54E+04	3 2.06E+04	0 0.00E+00	65538.7	8.94	Bos taurus	76680598	3	3	48.59	193	secreted modular calcium-binding protein 2	ECM structure	ECM
0 0.00E+00	3 1.22E+04	2 1.42E+04	0 0.00E+00	22215.7	9.04	Bos taurus	27807147	20	3	47.95	194	cartilage C-type lectin	signal	secreted
2 1.26E+05	0 0.00E+00	3 4.57E+04	5 4.35E+04	20493.9	7.58	Bos taurus	76628646	20	3	47.16	195	T07H6.5	innate immunity -complement	secreted
0 0.00E+00	1 7.92E+02	0 0.00E+00	4 5.47E+03	33602.1	4.65	Bos taurus	76672694	11	3	47.14	196	Reticulocalbin-1 precursor, partial	chaperone	ER
0 0.00E+00	0 0.00E+00	4 4.67E+04	0 0.00E+00	18163.1	8.86	Homo sapiens	21702983	18	4	45.86	197	esophagin	contaminant - keratinocyte diff	cytoplasm
2 1.04E+04	1 5.73E+02	1 3.89E+03	0 0.00E+00	56974.9	7.93	Rattus norvegicu	62648493	8	3	45.68	198	Cocoacrisp protein	protease inhibitor?	secreted
0 0.00E+00	0 0.00E+00	0 0.00E+00	4 1.53E+04	64512.8	5.68	Bos taurus	76649691	6	3	45.59	199	FK506 binding protein 10 precursor (Peptidyl-prolyl cis-tran	rotamase	ER
0 0.00E+00	0 0.00E+00	0 0.00E+00	4 1.52E+04	11702.1	4.53	Bos taurus	82571755	40	3	45.52	200	Ribosomal protein, large P2	translation	cytoplasm
4 1.74E+03	1 4.93E+03	3 3.44E+03	0 0.00E+00	192346.3	7	Bos taurus	76663447	6	6	84.93	201	laminin, alpha 4 precursor	cell matrix interactions	ECM
5 1.07E+04	0 0.00E+00	0 0.00E+00	0 0.00E+00	72898.2	4.6	Bos taurus	76679431	7	3	44.73	202	PREDICTED: hypothetical protein XP_602993; HA binding lir	ECM structure	ECM
0 0.00E+00	2 5.19E+03	0 0.00E+00	0 0.00E+00	162937	4.85	Bos taurus	76622653	2	2	44.18	203	fibrillin 2 precursor	ECM structure	ECM
0 0.00E+00	1 3.81E+03	2 5.32E+03	0 0.00E+00	16292.3	9.68	Bos taurus	76627333	27	3	43.74	204	Gremlin-1 precursor (Cysteine knot superfamily 1, BMP anta	singal	secreted
0 0.00E+00	0 0.00E+00	1 1.72E+03	2 7.30E+03	36438.4	6.16	Bos taurus	74354869	10	3	43.7	205	Hypothetical protein LOC535182; malate dehydrogenase	metabolic	cytoplasm
3 1.59E+03	0 0.00E+00	6 2.98E+04	0 0.00E+00	26018.8	8.54	Bos taurus	27806963	13	3	42.2	206	casein alpha-S2	transport - Calcium phosphate	secreted

untreated (Control)	IL-1β	TNF-α	Injury	Protein MW	Protein pI	species	accession	% coverage	peptides	score	group #	Protein NAME	Function	Locations
0	5	5	0									Ran GTPase-activating protein 1	signal	cytoplasm
0.00E+00	1.04E+05	6.01E+04	0.00E+00	142453.3	5.46	Canis familiaris	73969443	2	2	41.32	207			
0	0	1	3			Bos						transketolase	metabolism	cytoplasm
0.00E+00	0.00E+00	1.65E+03	9.79E+03	67906.2	7.56	taurus	50844503	8	3	41.22	208			
2	0	3	1			Bos						procollagen-lysine, 2-oxoglutarate 5-dioxygenase 3 precurse	PTM	ER
1.65E+04	0.00E+00	3.33E+04	1.05E+04	86469.6	5.82	taurus	76653827	4	2	39.11	210			
0	4	0	0			Bos						vanin 1 precursor	signal	membrane
0.00E+00	2.94E+04	0.00E+00	0.00E+00	56947	5.31	taurus	66792902	6	2	38.45	211			
0	0	0	3			Bos						Fructose-bisphosphate aldolase A (Muscle-type aldolase) is	metabolism	cytoplasm
0.00E+00	0.00E+00	0.00E+00	2.80E+04	39436.3	8.45	taurus	76653617	9	3	38.13	213			
4	17	11	6			Bos						prostaglandin H2 D-isomerase	transport	membrane
3.87E+04	7.22E+04	2.17E+05	8.95E+04	21229.3	6.43	taurus	27807521	11	2	36.13	214			
7	0	1	0			Bos						Collagen alpha 1(IX) chain precursor, partial	ECM structure	ECM
5.94E+04	0.00E+00	3.19E+04	0.00E+00	26967.6	8.76	taurus	76686475	11	3	36.02	215			
0	0	2	2			Bos						GSTP1 protein	redox	cytoplasm
0.00E+00	0.00E+00	4.37E+03	6.75E+03	23613.3	6.89	taurus	74268086	19	2	35.92	216			
0	0	1	2			Rattus						transaldolase	metabolism	cytoplasm
0.00E+00	0.00E+00	9.24E+02	2.92E+03	37476.3	6.57	norvegicu	12002054	9	2	35.77	217			
1	0	1	0			Bos						C1q and tumor necrosis factor related protein 3 isoform b is	signal	secreted
1.36E+03	0.00E+00	3.01E+03	0.00E+00	34953.3	6.67	taurus	76674304	7	2	35.3	218			
4	0	1	0			Bos						Amyloid beta A4 protein precursor (APP) (ABPP)	signal	membrane
1.17E+04	0.00E+00	8.28E+03	0.00E+00	63986.8	4.73	taurus	76607645	6	2	35.03	219			
0	0	0	2			Canis						Cofilin-1 (Cofilin, non-muscle isoform)	cytoskeleton	cytoplasm
0.00E+00	0.00E+00	0.00E+00	7.31E+03	23481.6	8.92	familiaris	73946791	12	2	34.71	220			
0	0	0	4			Bos						tubulin, alpha 1	cytoskeleton	cytoplasm
0.00E+00	0.00E+00	0.00E+00	1.77E+04	51290.3	4.96	taurus	76610661	6	2	34.51	221			
0	6	0	0			Bos						cystatin C (amyloid angiopathy and cerebral hemorrhage)	protease inhibitor	secreted
0.00E+00	8.81E+03	0.00E+00	0.00E+00	16265	9.23	taurus	27806675	30	2	34.42	222			
0	0	0	2			Bos						endoplasmic reticulum protein 29 precursor	chaperone	ER
0.00E+00	0.00E+00	0.00E+00	4.33E+04	28806.2	5.63	taurus	76639231	8	2	34	223			
0	0	1	3			Bos						serine (or cysteine) proteinase inhibitor, clade B (ovalbumin	protease inhibitor	secreted
0.00E+00	0.00E+00	3.16E+03	1.75E+04	42560.9	5.44	taurus	27807517	5	2	33.72	224			
0	1	2	3			Bos						PPIA protein	PTM	ER
0.00E+00	1.66E+04	9.07E+03	9.08E+03	17869.5	8.34	taurus	75948300	10	2	33.58	225			
2	1	0	0									Chordin-like protein 2 precursor (Chordin-related protein 2)	signal	secreted
1.22E+04	1.36E+04	0.00E+00	0.00E+00	60199.5	8.94	Bos taurus	76675768	5	2	33.44	226			
0	0	0	3			Canis						platelet-activating factor acetylhydrolase, isoform Ib, beta su	cytoskeleton	cytoplasm
0.00E+00	0.00E+00	0.00E+00	2.27E+04	63827.5	7.66	familiaris	73955102	4	2	33.35	227			
0	2	1	0			Bos						Interleukin-17B precursor (IL-17B) (Interleukin-20) (IL-20) iso	signal	secreted
0.00E+00	1.66E+04	5.94E+03	0.00E+00	24932.3	9.47	taurus	76623570	10	2	33.31	228			
0	3	0	0			Bos						hypothetical protein LOC512242	innate immunity - lipid binding	secreted
0.00E+00	3.52E+04	0.00E+00	0.00E+00	53698.3	6.61	taurus	84579853	4	2	33.29	229			
8	1	3	0									Microfibril-associated glycoprotein 4 precursor	cytoskeleton	cytoplasm
9.96E+04	9.99E+03	2.12E+04	0.00E+00	28558.3	5.09	BOVIN	62906887	9	2	32.85	230			
0	0	1	2			Bos						Hypoxanthine-guanine phosphoribosyltransferase (HGPRT)	metabolism	cytoplasm
0.00E+00	0.00E+00	1.65E+03	9.79E+03	24575.5	6.44	taurus	76614147	10	2	32.81	231			
0	2	0	0			Bos						matrix metalloproteinase 1	protease	secreted
0.00E+00	1.79E+04	0.00E+00	0.00E+00	53354.3	5.97	taurus	27806541	5	2	32.77	232			
4	1	2	0			Bos						alpha 1 type XV collagen precursor	ECM structure	ECM
1.09E+04	4.22E+03	1.69E+04	0.00E+00	21825.1	7.73	taurus	76624758	12	2	32.55	233			
0	0	0	2									Dihydropyrimidinase-related protein 2 (DRP-2) (Neural-spec	metabolism	cytoplasm
0.00E+00	0.00E+00	0.00E+00	1.48E+04	62277.9	5.95	BOVIN	3122018	4	2	32.31	234			
0	0	0	2			Bos						heat shock protein, alpha-crystallin-related, B6	chaperone	ER
0.00E+00	0.00E+00	0.00E+00	1.09E+04	21044.1	9.45	taurus	76640845	11	2	32.18	235			
0	0	0	2			Bos						TIP120 protein isoform 3	translation	cytoplasm
0.00E+00	0.00E+00	0.00E+00	1.73E+03	122998	5.66	taurus	76661740	2	2	31.99	236			
0	0	0	4			Bos						Ras GTPase-activating-like protein IQGAP1 (p195) isoform 1	signal	cytoplasm
0.00E+00	0.00E+00	0.00E+00	4.03E+03	157942.8	5.61	taurus	76646935	3	2	31.77	237			
0	0	0	3			Bos						liver glycogen phosphorylase isoform 6	metabolism	cytoplasm
0.00E+00	0.00E+00	0.00E+00	8.15E+03	98258.3	6.34	taurus	76627833	2	2	31.45	238			
0	1	2	0			Bos						beta-2-microglobulin	immunity - MHC class I beta ch	membrane
0.00E+00	3.36E+02	7.37E+03	0.00E+00	13676.7	7.79	taurus	41386683	33	2	31.38	239			
0	0	0	4									Protein CutA precursor (Brain acetylcholinesterase putative	other	membrane
0.00E+00	0.00E+00	0.00E+00	9.52E+03	18976.2	8.64	BOVIN	62286494	23	2	31.3	240			
0	1	1	0			Bos						von Willebrand factor A domain-related protein isoform 1; W	ECM structure	ECM
0.00E+00	2.66E+03	3.04E+03	0.00E+00	52047.5	8.93	taurus	76637679	6	2	31.06	241			
2	1	2	0									Angiogenin-2	signal	secreted
6.05E+03	3.29E+03	9.02E+03	0.00E+00	14522.4	9.97	BOVIN	2500561	24	2	30.25	242			
0	0	0	4			Bos						beta tubulin	cytoskeleton	cytoplasm
0.00E+00	0.00E+00	0.00E+00	8.16E+03	49937.3	4.78	taurus	50844501	6	2	30.14	243			
0	0	3	1			Bos						plakoglobin	signal	cytoplasm
0.00E+00	0.00E+00	5.68E+03	1.17E+03	81821.3	5.76	taurus	20336613	3	2	29.98	245			

untreated (Control)	IL-1β	TNF-α	Injury	Protein MW	Protein pI	species	accession	% coverage	peptides	score	group #	Protein NAME	Function	Locations
0 0.00E+00	3 1.09E+05	2 8.96E+04	0 0.00E+00	76101.8	4.78	Sus scrofa	38455786	2	2	29.9	246	complement C1s	innate immunity - complement	secreted
0 0.00E+00	2 1.26E+04	0 0.00E+00	0 0.00E+00	68723.4	7.13	Homo sapiens	1304126	23	2	29.56	247	polyubiquitin	catabolism	cytoplasm
1 3.72E+03	2 1.58E+04	0 0.00E+00	0 0.00E+00	16640.4	8.2	Bos taurus	27806881	16	2	29.28	248	Niemann-Pick disease, type C2	metabolism	lysosome
9 2.45E+04	2 1.99E+04	8 2.03E+04	6 1.17E+04	72972.2	8.74	Bos taurus	76661312	3	2	29.24	249	alpha 3 type IX collagen	ECM structure	ECM
0 0.00E+00	0 0.00E+00	0 0.00E+00	3 1.98E+04	34400.8	5.72	Bos taurus	74353873	6	2	29.12	250	Ribosomal protein, large, P0	translation	cytoplasm
0 0.00E+00	2 1.34E+04	0 0.00E+00	0 0.00E+00	26531.2	4.83	Mus musculus	51092303	15	2	28.77	251	Try10-like trypsinogen	protease	secreted
0 0.00E+00	0 0.00E+00	3 2.16E+04	0 0.00E+00	85142.8	5.98	Bos taurus	76635840	3	2	28.73	252	CEGP1 protein	cell matrix interactions	secreted
0 0.00E+00	2 4.72E+03	1 1.54E+03	1 2.00E+02	151091.9	9.53	Homo sapiens	1572721	2	2	28.6	253	megakaryocyte stimulating factor; MSF	ECM structure	ECM
0 0.00E+00	0 0.00E+00	0 0.00E+00	3 8.84E+03	14598.1	6.42	Homo sapiens	51468838	12	2	28.55	254	ribosomal protein S12	translation	cytoplasm
0 0.00E+00	0 0.00E+00	0 0.00E+00	2 1.07E+04	28727.2	5.6	Bos taurus	73587123	11	2	27.63	255	Unknown (protein for MGC:128498) ; glutathione S transfera	redox	cytoplasm
0 0.00E+00	2 1.97E+04	0 0.00E+00	0 0.00E+00	54372.1	6.07	Pan troglodyte	55600491	5	2	27	256	interleukin 1, beta proprotein; preinterleukin 1 beta; catabol	signal	secreted
0 0.00E+00	1 1.06E+04	0 0.00E+00	3 6.14E+04	27646.2	8.87	Bos taurus	76668658	9	2	26.95	257	Galectin-3	cell matrix interactions	ECM
0 0.00E+00	0 0.00E+00	1 1.05E+04	2 9.92E+03	22679.4	5.77	Bos taurus	71037405	12	2	26.94	258	heat shock 27kDa protein 1	cytoskeleton	cytoplasm
0 0.00E+00	0 0.00E+00	0 0.00E+00	2 1.12E+04	37747.6	4.44	Bos taurus	76615715	7	2	26.93	259	calumenin isoform 2 isoform 2	PTM	ER/secreted
0 0.00E+00	0 0.00E+00	1 1.13E+03	4 1.09E+04	16961.2	4.46	Bos taurus	74268208	15	2	26.83	260	MYL6 protein	lipid transport	lysosome
0 0.00E+00	0 0.00E+00	0 0.00E+00	2 4.10E+03	88976.3	6.82	Bos taurus	76847456	3	2	26.76	261	Protein transport protein Sec23A (SEC23-related protein A) (	vessicle trafficking	cytoplasm
3 1.29E+04	0 0.00E+00	0 0.00E+00	0 0.00E+00	77979.2	6.37	Rattus norvegicu	62655664	3	2	25.5	263	PREDICTED: similar to RIKEN cDNA 4933437K13; similar to	redox	cytoplasm
0 0.00E+00	0 0.00E+00	2 1.59E+04	0 0.00E+00	65122	6.53	Bos taurus	74354719	4	2	25.33	264	LMNA protein	contaminant? - cytoskeleton	cytoplasm
0 0.00E+00	0 0.00E+00	1 5.12E+03	7 2.11E+04	57417.2	4.86	Canis familiaris	73964749	4	1	22.5	268	prolyl 4-hydroxylase, beta subunit		
0 0.00E+00	0 0.00E+00	1 9.80E+03	0 0.00E+00	23840.2	5.1	Rattus norvegicu s	27716369	4	1	22.2	269	microfibril-associated glycoprotein 1		
1 5.43E+02	1 1.22E+04	1 2.32E+03	1 2.05E+03	21269.5	6.29	Bos taurus	27881412	5	1	21.22	270	casein kappa		
0 0.00E+00	1 3.56E+03	0 0.00E+00	0 0.00E+00	11588.9	9.4	Bos taurus	11464505	10	1	20.94	273	granulocyte chemotactic protein-2 precursor		
1 7.77E+03	2 1.32E+04	2 8.42E+04	0 0.00E+00	54958.7	8.95	Rattus norvegicu	56090421	1	1	20.91	274	similar to RIKEN cDNA C130099A20		
0 0.00E+00	0 0.00E+00	2 7.76E+03	0 0.00E+00	114886.4	8.26	Bos taurus	76625413	1	2	20.84	275	filamin A interacting protein 1		
0 0.00E+00	1 7.60E+03	0 0.00E+00	0 0.00E+00	70872.9	8.97	Bos taurus	17941422	2	1	20.82	276	vitrin		
0 0.00E+00	2 2.16E+04	0 0.00E+00	0 0.00E+00	68733	5.79	Mus musculus	74137565	4	1	20.29	278	unnamed protein product		
0 0.00E+00	0 0.00E+00	3 5.22E+03	2 6.00E+03	312253.4	4.82	Bos taurus	27806637	0	1	20.27	279	fibrillin 1		
0 0.00E+00	0 0.00E+00	2 1.40E+04	0 0.00E+00	16782.6	9.92	Bos taurus	51012437	8	1	20.25	280	milk lysozyme		
0 0.00E+00	0 0.00E+00	0 0.00E+00	1 1.82E+04	19561.4	4.84	Bos taurus	74356483	8	1	20.23	281	Tumor protein, translationally-controlled 1		
0 0.00E+00	0 0.00E+00	1 1.70E+03	1 4.55E+03	23421.5	5.12	Bos taurus	28603774	12	1	20.14	282	Rho GDP dissociation inhibitor (GDI) alpha		
0 0.00E+00	0 0.00E+00	0 0.00E+00	3 6.29E+03	11588.3	4.77	Pan troglodyte	55641109	14	1	20.13	283	PREDICTED: similar to 60S acidic ribosomal protein P1		

Appendix C.2: Protein list of iTRAQ-2D-LC/MS/MS with ProQuant (ABI): Protein identification relative Quantitation and p values sorted by K-means Clustering

Table C.2 is the protein list for experiments and data described in chapter 4 including the protein identification, quantitation for each treatment relative to the untreated sample, and significance values.

Column 1: **Order**: Final Protein number
Column 2: **Protein Name**: Name of protein
Column 3: **Protein #**: Protein number
Column 4: **Score**: $10^{(-\text{score})}$ is the p value for the protein ID (ProGroup score)
Column 5: **Score 2**: $10^{(-\text{score})}$ is the adjusted p value for protein ID (matlab scripts)
Column 6: **Mass Coverage**: Summed peptide molecular weight for each protein
Column 7: **outliers**: 0 indicate no outliers for all signature ion ratios; 1 indicates presence of outliers in one or more signature ion ratios
Column 8: **pvalue 115**: p value for 115:114 ratios based on Wilcoxan Rank-sum or Student's t-Test with Bonferroni correction for multiple comparisons
Column 9: **pvalue 116:** p value for 116:114 ratios based on Wilcoxan Rank-sum or Student's t-Test with Bonferroni correction for multiple comparisons
Column 10: **pvalue 117**: p value for 117:114 ratios based on Wilcoxan Rank-sum or Student's t-Test with Bonferroni correction for multiple comparisons
Column 11: **115: 114**: Geometric mean for 115:114 ratios
Column 12: **SD**: error factor for the 115:114 ratio (SD of log transformed ratio)
Column 13: **116: 114**: Geometric mean for 116:114 ratios
Column 14: **SD**: error factor for 116:114 ratios (SD of log transformed ratio)
Column 15: **117: 114**: Geometric mean for 117:114 ratios
Column 16: **SD**: error factor for 117:114 ratios (SD of log transformed ratio)
Column 17: **Accession**: database accession number
Column 18: **Sig 115**: Consistency – Analytical duplicate agreement for 115:114 ratio – greater than 1 or less than 1 (3 indicates agreement, 1 indicates found in 1 sample, 0 indicates disagreement
Column 19: **Sig 116**: Analytical duplicate agreement for 116:114 ratio -- greater than 1 or less than 1 (3 indicates agreement, 1 indicates found in 1 sample, 0 indicates disagreement
Column 20: **Sig 117**: Analytical duplicate agreement for 117:114 ratio -- greater than 1 or less than 1 (3 indicates agreement, 1 indicates found in 1 sample, 0 indicates disagreement
Column 21: **SM-ID**: Spectrum Mill verification of protein identification (yes/no)
Column 22: **coverage**: Spectrum Mill coverage of protein
Column 23: **manual**: Manual validation of identification and quantitation
Column 24: **Idexer**: Sorting indexer from K-means clustering (6 clusters)

order	Protein Name	protein #	score	peptides	score 2	mass cov	outliers	pval 116	pval 118	pval 117	116:114	SD	116:114	SD	117:114	SD	Accession	sig 116	sig118	sig117	SM-ID	coverage	manual	indexer k8
22	PREDICTED: similar to Gelsolin precursor (Actin-depolymerizing factor) (ADF) (Brevin) (AGE	22	50.29	31	59.987	47621	0	1.03E-05	1.27E-05	0.074632	0.70913	1.1726	0.58723	1.2915	1.0588	1.4278	76625353	3	3	3	yes	31	yes	1
27	collagen, type I, alpha 2	27	52.41	28	47.915	43412	1	0.000298	1.33E-09	0.12126	0.64052	1.5711	0.45372	1.4855	0.83364	1.4536	27806257	3	3	3	no		yes	1
28	matrix metalloproteinase 2 (72 KDa type IV collagenase)	28	52.05	30	56.092	48456	1	0.003627	0.021477	2.91E-14	0.85989	1.2397	0.87414	1.2616	0.55016	1.2477	27807447	3	3	3	yes	43	yes	1
35	PREDICTED: similar to procollagen, type I, alpha 1 isoform 1 ; PREDICTED: similar to proco	35	48.1	28	51.285	43609	0	0.005763	2.07E-12	0.44871	0.78417	1.5737	0.46119	1.3681	0.85656	1.5559	76644335	3	3	3	no		yes	1
53	PREDICTED: similar to xylosyltransferase I	53	37.05	19	36.046	31886	0	0.003214	0.000619	0.000931	0.66349	1.3185	0.80998	1.2039	0.41374	1.4306	76652955	3	3	3	yes	30	yes	1
58	PREDICTED: similar to CD109	58	36.2	23	41.137	39750	0	1.04E-06	1.56E-05	0.043117	0.65249	1.3	0.6744	1.3367	0.79136	1.4605	76673087	3	3	0	yes	14	yes	1
66	secreted protein, acidic, cysteine-rich (osteonectin) [Bos taurus]	66	32.62	24	44.461	48133	0	7.28E-12	2.8E-09	3.32E-12	0.46067	1.3156	0.58846	1.288	0.47164	1.2918	27806147	3	3	3	yes	48	yes	1
70	AE binding protein 1	70	32	17	33.046	29716	0	7.45E-05	0.003016	0.013527	0.64936	1.311	0.64616	1.3479	0.88757	1.1451	27807319	3	3	3	yes	25	yes	1
78	PREDICTED: similar to Transforming growth factor-beta induced protein IG-H3 precursor (Be	78	27.55	15	28.046	22794	0	0.013824	0.001541	0.000497	0.77275	1.3083	0.72692	1.2715	0.71789	1.2467	76623057	3	3	3	yes	16	yes	1
80	PREDICTED: similar to alpha 1 type XI collagen isoform A preproprotein, partial	80	27.12	26	52	48150	0	0.001314	0.000712	6.38E-07	0.50208	2.0142	0.51747	1.7778	0.54387	1.5258	76678255	3	3	3	yes	22	yes	1
91	protein S (alpha)	91	26.07	13	25.523	20242	0	3.87E-09	6.64E-08	8.28E-08	0.38242	1.2121	0.40085	1.2724	0.45835	1.2332	27806095	3	3	3	yes	21	yes	1
100	PREDICTED: similar to Chordin-like protein 1 precursor (Neuralin) (Ventroptin), partial	100	24.82	12	23.699	22197	0	0.00099	0.001574	0.001519	0.55393	1.3537	0.64715	1.2882	0.44767	1.5476	76699190	3	3	3	yes	25	yes	1
110	PREDICTED: similar to Carbohydrate sulfotransferase 11 (Chondroitin 4-O-sulfotransferase	110	23.4	11	21.523	15511	0	0.23438	1.3945	0.001072	0.62815	1.75	0.87481	1.3623	0.4746	1.4713	76609723	3	3	3	yes	14	yes	1
131	PREDICTED: similar to alpha 1 type XVI collagen precursor	131	20.51	13	23.666	21448	0	1.958	0.041343	2.92E-06	1.1226	1.5029	0.80962	1.2635	0.52211	1.2726	76611086	0	3	3	yes	8	yes	1
144	melanoma inhibitory activity	144	18.69	9	18	19750	0	0.0026	0.15279	0.00208	0.55289	1.3088	0.81441	1.2279	0.59786	1.2526	27806849	3	3	3	yes	63	yes	1
151	PREDICTED: similar to Collagen alpha 1(V) chain precursor	151	18	9	18	14173	0	0.001141	0.007011	0.61002	0.64025	1.2289	0.70219	1.2407	0.88474	1.2198	76677607	3	3	3	yes	33	yes	1
152	PREDICTED: similar to Calsyntenin-1 precursor	152	17.87	9	17.097	12109	0	0.000393	0.002558	0.001368	0.52285	1.2935	0.54433	1.373	0.69734	1.1868	76637438	3	3	3	yes	8	yes	1
155	PREDICTED: similar to EGF-like repeats and discoidin I-like domains-containing protein 3, p	155	17.4	9	15.614	14167	0	7.72E-06	0.023438	2.48E-06	0.38581	1.2495	0.40686	1.1792	0.40497	1.2001	76681652	3	3	3	yes	22	yes	1
172	PREDICTED: similar to growth arrest-specific 6	172	15.77	8	15	13120	0	0.30997	0.055288	0.065354	0.74255	1.4325	0.63515	1.3743	0.61089	1.5003	76632004	3	3	3	yes	15	yes	1
182	PREDICTED: similar to insulin-like growth factor binding protein 7 (predicted), partial	182	15.05	12	23.046	19477	0	4E-09	7.18E-05	5.11E-06	0.57019	1.1044	0.63985	1.229	0.46331	1.3104	76619957	3	3	3	yes	42	yes	1
185	PREDICTED: similar to carbohydrate (chondroitin 6) sulfotransferase 3	185	14.72	8	14.569	13419	0	0.20145	0.049794	0.4867	0.71973	1.423	0.72405	1.2473	0.77578	1.4228	76631783	3	3	3	yes	12	yes	1
191	PREDICTED: similar to Chordin-like protein 2 precursor (Chordin-related protein 2) (Breast ti	191	14.14	7	13.398	14337	0	0.006015	0.000317	8.12E-06	0.28639	1.7428	0.1829	1.5562	0.10055	1.3759	76675788	3	3	3	yes	20	yes	1
199	PREDICTED: similar to procollagen, type V, alpha 2	199	13.73	8	12.589	15008	0	0.040912	0.00484	0.62355	0.61384	1.4398	0.46328	1.4697	0.90628	1.1608	76609282	3	3	3	no		yes	1
203	PREDICTED: similar to Amyloid beta A4 protein precursor (APP) (ABPP) (Alzheimers diseas	203	13.23	9	16.921	16614	0	0.001734	0.006592	0.048875	0.51536	1.3254	0.61678	1.2929	0.40958	1.4254	76607645	3	3	3	yes	13	yes	1
209	PREDICTED: similar to retinol-binding protein 4, plasma precursor	209	12.89	6	12	9057.6	0	0.010115	0.1875	0.1875	0.75499	1.119	0.61305	1.2475	0.82693	1.0978	76674078	3	3	3	yes	14	yes	1
214	PREDICTED: similar to Collagen alpha 2(IX) chain precursor	214	12.4	9	16.396	14419	0	1.5	0.036201	0.807	0.76018	1.7666	0.57526	1.5655	0.74946	1.6815	76686297	3	3	3	yes	6	yes	1
222	PREDICTED: similar to procollagen, type V, alpha 1	222	12.03	9	18	17637	0	1.2188	1.1719	0.98438	0.69747	2.3314	0.70252	2.399	0.93888	2.1969	76631238	3	3	3	yes -r	5	yes - 1 bad peptide	1
224	PREDICTED: similar to scrapie responsive protein 1	224	12	6	12	10841	0	0.000409	0.002915	0.1875	0.44764	1.1767	0.41883	1.3043	0.46521	1.0905	76691025	3	3	3	yes	52	yes	1
266	PREDICTED: similar to glypican 1 precursor, partial	266	9.61	5	9.0458	9012.5	0	0.11103	0.096196	0.052257	0.5853	1.3663	0.50443	1.485	0.53815	1.3354	76614725	3	3	3	yes	6	yes	1
268	PREDICTED: hypothetical protein XP_602993	268	9.52	5	9.5229	9152.6	0	0.012267	0.054972	0.057297	0.28669	1.4796	0.29586	1.4981	0.31744	1.7332	76679431	3	3	3	no		yes	1
269	chondromodulin I precursor [leukocyte cell-derived chemotaxin 1] [Bos taurus]	269	9.38	7	13.046	14143	0	0.014637	0.036234	1.2188	0.44462	1.5349	0.55831	1.4506	0.84053	1.2847	27806265	3	3	3	yes	14	yes	1
281	PREDICTED: similar to Angiotensinogen precursor	281	8.8	5	8.7959	9131.5	0	0.18481	0.073461	1.5064	0.29535	1.4616	0.43964	1.3533	0.49287	2.1526	76656943	3	3	3	no		yes/poor quant	1
303	PREDICTED: similar to Chordin precursor	303	8	4	8	7186	0	0.025004	0.37997	0.19276	0.49771	1.1922	0.45735	1.4308	0.63933	1.2659	76607523	3	3	3	yes	5	yes/poor quant	1
304	PREDICTED: similar to immunoglobulin superfamily containing leucine-rich repeat isoform 4	304	8	4	8	6129.5	0	4.5291	1.3965	0.013805	0.95571	1.3033	0.87661	1.1932	0.45905	1.1734	76647324	3	3	3	yes	10	yes	1
325	microfibrillar-associated protein 2	325	7.05	4	7.0458	6398.3	0	0.44442	2.8686	0.078645	0.54718	1.5842	0.81813	1.58	0.63923	1.1839	27805997	1	1	1	yes	14	yes	1
328	PREDICTED: similar to Alpha-mannosidase II (Mannosyl-oligosaccharide 1,3-1,6-alpha-man	328	7.05	4	7.0458	6711.5	0	0.43823	2.8337	0.1474	0.58598	1.4831	0.8941	1.3139	0.67212	1.208	76693348	0	3	3	yes	3	yes	1
333	PREDICTED: similar to SPARC-related modular calcium binding protein 1	333	6.92	3	6	4280.2	0	2.2952	1.5052	0.95616	0.72385	1.6557	0.6829	1.5114	0.69525	1.3322	76679410	3	3	3	yes	13	yes	1
334	PREDICTED: similar to cococrisp, partial	334	6.92	4	6.9208	8101.8	0	0.12701	0.6131	0.059257	0.20598	1.4987	0.35697	1.8587	0.19434	1.3285	76689069	3	3	3	yes	15	yes	1
340	PREDICTED: similar to ectonucleotide pyrophosphatase/phosphodiesterase 2 (autotaxin)	340	6.57	3	4.5686	5097.6	0	0.45792	0.72618	0.047088	0.54165	1.3655	0.5358	1.5138	0.52035	1.1081	76635015	1	1	1	yes	2	yes/poor quant	1
348	PREDICTED: similar to UDP-GlcNAc:betaGal beta-1,3-N-acetylglucosaminyltransferase 7	348	6.33	3	6	5308.1	0	0.2739	1.9671	0.66928	0.46873	1.337	0.75687	1.4562	0.67002	1.2883	76610821	3	3	3	yes	7	yes/poor quant	1
352	PREDICTED: similar to microfibrillar-associated protein 4	352	6.16	3	5.5229	4376.2	0	0.045652	0.029083	0.16622	0.2658	1.223	0.32642	1.1451	0.29395	1.434	76644177	3	3	3	yes	14	yes	1
408	PREDICTED: similar to chondroitin beta1,4 N-acetylgalactosaminyltransferase	408	4.85	4	8	3513.9	0	0.11296	1.9873	0.19966	0.667761	1.03	0.783391	1.37	0.534964	1.12	76656022	1	1	1	yes	9	yes	1
441	PREDICTED: similar to fucosyltransferase 11 (alpha (1,3) fucosyltransferase)	441	4.13	3	6	6644.4	0	0.90723	0.92364	2.0227	0.58588	1.5036	0.59899	1.4851	0.69316	1.6603	76656663	3	3	3	yes	9	yes / very poor qua	1
476	PREDICTED: similar to plexin domain containing 2 precursor	476	4	2	4	2741.5	0	1.2368	2.7766	0.23689	0.61157	1.2829	0.9084	1.1284	0.42778	1.0774	76680089	3	0	3	yes	4	yes/ very poor quar	1
497	PREDICTED: similar to UDP-N-acetyl-alpha-D-galactosamine:polypeptide N-acetylgalactosa	497	3.76	2	3.5229	3107.7	0	0.1024	0.53537	6	0.63458	1.0174	0.75301	1.0582	0.89278	1	76609798	3	3	3	yes	2	yes	1
521	PREDICTED: similar to lethmin 1	521	3.4	2	3.3979	3425.9	0	4.9397	1.1934	0.28272	0.92066	1.5073	0.84787	1.0783	0.55137	1.0644	76632070	1	1	1	no		yes/ very poor quar	1
532	PREDICTED: similar to C1q and tumor necrosis factor related protein 3 isoform b isoform 2 ;	532	3.1	2	3.0998	2491.3	0	0.95491	0.99691	0.17857	0.38928	1.4059	0.54752	1.2555	0.53487	1.0423	76674304	3	3	3	yes	6	yes	1
551	PREDICTED: similar to plasma glutamate carboxypeptidase	551	3	2	3	3451.9	0	6	6	6	0.47984	1	0.50241	1	0.58814	1	76634864	1	1	1	yes	8	yes/ very poor quar	1
565	PREDICTED: similar to Fibroblast growth factor receptor 3 precursor (FGFR-3) (Heparin-bin	360	6	3	6	4061.6	0	0.32907	0.19542	0.26874	0.1681	2.127	0.17035	1.7633	0.11624	2.2827	76666960	3	3	3	yes	2	yes/ poor quant	1
601	PREDICTED: similar to C1q and tumor necrosis factor related protein 2, partial	501	3	2	3	3254.9	0	6	6	5.9084	0.34116	1	0.24175	1	0.97229	5.2473	76630529	1	1	1	yes		one good	1
2	PREDICTED: similar to Basement membrane-specific heparan sulfate proteoglycan core pro	2	165.83	90	173.19	156900	1	2.79E-09	1.56E-18	2.82E-13	1.3738	1.6184	1.3423	1.2668	0.80402	1.2556	76663616	3	3	3	yes	16	yes	2
3	PREDICTED: similar to alpha 1 type XII collagen long isoform precursor isoform 1 ; PREDIC	3	157.67	82	154.59	140470	1	3.88E-14	7.16E-14	2.83E-15	1.5625	1.3202	1.4564	1.2396	1.2284	1.1979	76625438	3	3	3	yes	28	yes	2
5	thrombospondin	5	115.04	71	138.01	114210	1	1.34E-06	5.18E-08	0.007771	1.2272	1.347	1.1968	1.2579	0.93387	1.1845	41386685	0	0	3	yes	41	yes	2
6	PREDICTED: similar to melanoma-associated chondroitin sulfate proteoglycan 4	6	103.22	53	101.98	88251	0	4.67E-08	2.5396	0.007091	0.74786	1.3492	0.98594	1.4013	0.82593	1.4525	76662196	3	3	3	yes	24	yes	2
12	PREDICTED: similar to Nidogen-2 precursor (NID-2) (Osteonidogen)	12	77.32	44	83.933	86319	0	3.46E-07	1.85E-10	0.87984	1.2599	1.2588	1.4162	1.2917	0.94963	1.2576	76627857	3	3	3	yes	24	yes	2
14	PREDICTED: similar to collagen, type XI, alpha 2 isoform 1 preproprotein	14	71.97	35	68.444	57100	1	0.029341	0.16097	2.9491	1.7601	2.683	1.3629	2.1791	1.0026	1.8163	76649817	3	0	0	yes	16	yes - bimod	2
15	PREDICTED: similar to Cartilage matrix protein precursor (Matrilin-1)	15	70.71	38	73.137	63169	0	4.38E-10	2.59E-09	3.8529	1.3822	1.248	1.2843	1.188	1.013	1.185	76611076	3	3	3	yes	59	yes	2
16	PREDICTED: similar to nucleobindin 1 isoform 1	16	67.31	37	73.523	66588	1	4.07E-08	0.87787	2.52E-08	0.71148	1.3089	0.95572	1.2007	0.79875	1.19	76641927	3	3	3	yes	61	yes	2
19	PREDICTED: similar to Cartilage oligomeric matrix protein precursor (COMP) isoform 1 ; PR	19	60.79	33	66	84263	1	0.00221	0.20534	0.000705	0.85948	1.2441	0.92407	1.2509	0.87146	1.1975	76620786	3	3	3	yes	44	yes	2
20	PREDICTED: similar to Cartilage intermediate layer protein 2 precursor (CILP-2)	20	57.2	28	53.569	43867	1	1.07E-06	1.24E-06	0.012392	1.3638	1.2883	1.325	1.241	0.90287	1.1719	76621011	3	3	3	yes	20	yes	2
30	cartilage linking protein 1	30	51.33	30	58.796	50333	0	0.000665	0.001252	0.022754	1.3011	1.3819	0.71473	1.3781	0.87905	1.2515	27805853	3	3	0	yes	63	yes	2
31	procollagen-lysine, 2-oxoglutarate 5-dioxygenase precursor	31	50.38	28	53.092	48065	0	4.5028	0.000175	0.14762	1.0135	1.2423	1.3417	1.213	1.0813	1.1855	27806477	3	3	3	yes	26	yes	2
39	PREDICTED: similar to Laminin alpha-4 chain precursor, partial	39	44.79	29	52.535	47213	0	3.74E-06	1.28E-09	2.44E-07	1.3	1.2469	1.5376	1.2715	0.70075	1.2832	76625667	3	3	3	yes	19	yes	2
40	biglycan	40	44.05	22	40.967	37963	0	4.69E-06	4.26E-07	0.001062	0.59684	1.4191	0.67385	1.2577	1.4519	1.2805	30315684	3	3	3	yes	57	yes	2
41	peptidylprolyl isomerase B	41	41.63	22	41.489	34624	1	6.53E-07	2.52E-06	1.2E-12	1.5374	1.278	1.4255	1.2473	2.1771	1.2499	27806469	3	3	3	yes	70	yes	2
48	vitrin	48	34.56	17	34	26109	0	0.23571	1.9208	0.020749	1.1851	1.366	1.0755	1.3397	0.87754	1.1702	27805781	3	3	0	yes	28	yes	2
52	PREDICTED: similar to Collagen alpha 1(III) chain precursor isoform 1 ; PREDICTED: simila	52	37.07	21	40.046	34532	0	0.23291	2.0175	0.030666	1.3247	1.7621	0.90738	1.5536	0.75316	1.5653	76609280	3	3	3	no		yes	2
54	PREDICTED: similar to thrombospondin 4 precursor isoform 3	54	37.02	23	43.62	42546	0	1.3249	0.022795	0.19727	1.1067	1.4442	1.1902	1.276	0.91805	1.1864	76626494	3	0	3	no		yes	2
55	serine (or cysteine) proteinase inhibitor, clade A (alpha-1antiproteinase, antitrypsin), member	55	36.54	19	35.614	30136	0	0.014018	0.53751	1.11E-06	1.3851	1.4934	0.84119	1.5032	1.6206	1.2759	27806841	3	0	3	yes	30	yes	2
56	follistatin-like 1	56	36.32	21	41.046	35992	0	4.4475	0.001474	0.22383	0.97551	1.3231	1.2831	1.2926	1.0791	1.1693	62988316	3	0	0	yes	55	yes	2
60	DCN protein	60	34.66	18	35	30696	0	0.029119	0.019961	4.44E-05	1.2486	1.4024	1.1752	1.2131	1.3343	1.2009	27806899	3	0	0	yes	43	yes	2
61	apolipoprotein E	61	34.59	18	33.188	28853	0	1.4629	0.011321	0.004185	1.1292	1.5326	1.2599	1.3059	0.80203	1.2427	27806739	3	3	3	yes	41	yes	2
72	PREDICTED: similar to Annexin A5 (Annexin V) (Lipocortin V) (Endonexin II) (Calphobindin I	72	31.19	17	32.398	28018	0	3.71E-08	3.93E-07	0.003595	0.62877	1.2748	0.63109	1.224	2.3799	1.6117	76619354	3	3	3	yes	33	yes	2
73	PREDICTED: similar to Collagen alpha 1(IX) chain precursor, partial	73	30.88	20	39	30201	1	1.3926	0.048075	0.21917	0.93806	1.7321	0.70248	1.6844	0.7716	1.5277	76625388	3	3	3	yes	12	yes	2
75	PREDICTED: similar to Procollagen C-proteinase enhancer protein precursor (PCPE) (Type	75	28.14	14	27.046	24758	0	0.004233	0.002232	1.7747	1.5612	1.4594	1.4517	1.3403	1.0909	1.4186	76653961	3	3	0	yes	25	yes	2
77	PREDICTED: similar to Extracellular matrix protein 2 precursor (Matrix glycoprotein SC1/EC	77	27.83	18	34.921	29359	0	1.3149	4.9826	2.5203	1.1096	1.3983	1.0165	1.3761	0.95445	1.2614	76658905	3	0	3	yes	19	yes	2
82	PREDICTED: similar to Collagen-binding protein 2 precursor (Collagin 2) (Rheumatoid arthriti	82	26.9	12	22.319	21988	0	0.032559	1.4376	4.78E-06	1.1911	1.1785	0.9308	1.2095	1.7355	1.1849	76636115	3	0	3	yes	48	yes	2
84	PREDICTED: similar to acid phosphatase-like 2	84	26.7	14	26.046	23734	0	0.63526	4.59E-06	5.89E-05	0.83759	1.4411	1.7538	1.2428	0.85268	1.2355	76608113	0	3	3	no		yes	2
85	PREDICTED: similar to Serine protease HTRA1 precursor (L56)	85	26.61	15	28.569	21571	1	4.0726	0.12158	0.090454	1.0519	1.4871	0.90872	1.1744	1.3361	1.909	61883334	0	3	3	yes	23	yes	2
92	PREDICTED: similar to Fibulin-5 precursor (FIBL-5) (Developmental arteries and neural cres	92	25.81	16	26.854	24299	0	3.8656	3.4871	4.74E-05	0.97379	1.2529	1.032	1.2508	0.69868	1.2412	76620265	3	0	3	yes	40	yes	2
93	serine (or cysteine) proteinase inhibitor, clade G (C1 inhibitor), member 1, (angioedema, here	93	25.8	14	25.489	20052	0	0.79695	7.89E-08	0.000952	0.88545	1.3126	2.7403	1.3096	1.3967	1.2496	27807349	0	3	3	yes	25	yes	2
94	lumican	94	25.77	14	27.523	24469	0	0.096376	0.01082	7.56E-06	1.3129	1.42	1.2882	1.2573	1.7784	1.2631	27806853	3	3	3	yes	37	yes	2
96	PREDICTED: similar to lysyl oxidase-like 3 precursor	96	25.6	14	24.535	24742	0	0.00299	0.001465	0.34913	1.3157	1.2333	1.3666	1.3205	1.1382	1.2497	76628833	3	3	3	yes	23	yes	2
97	PREDICTED: similar to Low-density lipoprotein receptor-related protein 1 precursor (LRP) (A	97	25.57	16	30.046	26500	0	0.44395	1.4582	1.8792	1.1349	1.3015	1.0701	1.2498	1.104	1.4423	76618581	3	0	0	yes	6	yes	2
101	PREDICTED: similar to procollagen-lysine, 2-oxoglutarate 5-dioxygenase 2 isoform a precurs	101	24.47	15	28.62	26052	0	1.27	0.005898	5.28E-11	1.076	1.2422	1.1777	1.1549	2.8142	1.2182	76607976	3	3	3	yes	35	yes	2
102	PREDICTED: similar to Lysyl oxidase homolog 2 precursor (Lysyl oxidase-like protein 2) (Lys	102	24.46	15	27.614	23821	0	0.024902	0.005048	0.88147	1.2389	1.2951	1.2964	1.2583	0.93077	1.2431	76624810	3	3	3	yes	24	yes	2
103	fibromodulin	103	24.44	15	28.921	25436	1	2.0824	0.8915	0.11214	1.1056	1.491	1.1428	1.4024	1.1939	1.2945	27806823	3	3	3	yes	34	yes	2
104	milk fat globule-EGF factor 8 protein	104	24.34	12	24	19808	0	0.021583	0.002513	0.003752	1.203	1.1898	1.2948	1.1971	0.65288	1.367	41386719	3	0	3	yes	23	yes	2
105	PREDICTED: similar to Melanotransferrin precursor (Melanoma-associated antigen p97) (CD	105	24.02	14	25.541	20511	0	0.001505	7.15E-08	1.04E-06	1.2664	1.1941	2.0319	1.2349	1.6918	1.2167	76607158	3	3	3	yes	13	yes	2
111	PREDICTED: similar to EGF-containing fibulin-like extracellular matrix protein 2 precursor (F	111	23.4	12	23.398	19509	0	0.68901	4.1046	0.000305	0.87787	1.3015	1.0352	1.3316	0.69121	1.2213	76657493	3	0	3	yes	19	yes	2
112	PREDICTED: similar to Nucleobindin 2 precursor (DNA-binding protein NEFA) (Gastric cance	112	23.14	12	22.444	23009	0	0.004302	0.2153	0.007907	1.2271	1.1375	1.1562	1.1887	1.6557	1.4158	76635537	3	3	3	yes	35	yes	2

order	Protein Name	protein #	score	peptides	score 2	mass cov	outliers	pval 116	pval 116	pval 117	116:114	SD	116:114	SD	117:114	SD	Accessior sig 116	sig116	sig117	SM-ID	coverage	manual	Indexer k6
114	osteoglycin (osteoinductive factor, mimecan)	114	22.71	10	20	14090	0	3.5739	0.96094	0.57083	0.94004	1.4268	0.90304	1.2963	1.122	1.2156	27806829	0	3	3 yes	31 yes		2
117	peptidylglycine alpha-amidating monooxygenase	117	22.15	11	20.444	18927	0	0.29883	0.018314	4.6075	1.0691	1.2858	0.82006	1.1847	1.0248	1.307	27806825	3	3	0 yes	17 yes		2
124	PREDICTED: similar to platelet-derived growth factor receptor-like protein	124	21.18	11	20.699	19263	0	0.24577	2.5255	0.006644	1.0705	1.0946	0.97808	1.0915	0.79418	1.1674	76655663	0	3	3 yes	34 yes		2
126	PREDICTED: similar to EMILIN 1 precursor (Elastin microfibril interface-located protein 1) (E	126	21.17	10	20	15730	0	0.33897	0.60915	2.7133	1.2613	1.3988	1.2548	1.4819	0.88525	1.5885	61845535	3	3	3 yes	11 yes		2
127	PREDICTED: similar to matrilin 4 isoform 2 precursor	127	21.02	13	23.614	17448	0	0.001465	5.89E-05	3.7077	1.656	1.3809	1.6054	1.2645	0.98177	1.1383	76833782	3	3	0 no	yes		2
128	PREDICTED: similar to CG12002-PA, isoform A / similar to NCAM	128	20.67	9	17.523	15630	0	0.003462	0.000467	0.15766	1.6373	1.3089	1.6207	1.2169	1.244	1.2723	76881898	3	3	3 yes	10 yes		2
133	tissue inhibitor of metalloproteinase 2	133	20.23	12	22.092	17705	0	0.36339	5.458	7.48E-07	1.1254	1.2161	1.2758	1.9881	1.8042	1.1871	27806163	0	0	3 yes	24 yes		2
137	PREDICTED: similar to Cathepsin D precursor isoform 2 ; PREDICTED: similar to Cathepsin	137	19.77	10	19	16748	0	4.5042	1.2237	9.39E-07	0.96762	1.3503	0.92696	1.1655	3.6959	1.3313	76858406	0	0	3 yes	23 yes		2
140	thrombospondin 2	140	18.98	11	20.523	17126	0	4.0167	1.7947	0.000187	0.98571	1.301	1.0813	1.2671	1.4211	1.1771	28875793	3	0	0 no	yes		2
147	dermatan sulfate proteoglycan 3	147	18.58	11	21	20375	0	2.6883	0.10098	0.023436	0.95471	1.1904	0.83429	1.2162	2.1942	1.386	27805823	0	3	3 yes	44 yes		2
148	annexin I	148	18.57	9	17.523	15492	0	0.007052	2.7371	0.025018	1.8945	1.328	1.1097	1.4133	1.3862	1.2477	28461193	3	3	3 yes	28 yes		2
159	peptidoglycan recognition protein	159	17.05	9	17.046	14550	0	0.001263	0.001495	0.58438	1.4782	1.2013	0.69059	1.1949	1.1073	1.186	27806640	3	3	0 yes	yes		2
160	cathepsin L	160	13.92	7	13.046	13072	0	3.4405	0.14725	7.5E-05	1.0533	1.2594	1.2833	1.2476	2.0075	1.1518	27806873	3	0	3 yes	31 yes		2
161	PREDICTED: similar to Olfactomedin-like protein 3 precursor (HNOEL-iso) (hOLF44)	161	16.91	9	16.268	14158	0	0.000968	4.0824	0.023436	1.5572	1.2213	1.034	1.2844	2.3859	1.4155	61811393	3	0	3 yes	18 yes		2
165	mannosidase, alpha, class 2B, member 1	165	16.47	8	15.046	11960	0	0.89063	0.20129	0.001557	1.2768	1.4001	1.2959	1.3205	2.4754	1.4601	31341666	3	3	3 yes	11 yes		2
175	PREDICTED: similar to Nidogen precursor (Entactin) isoform 2 ; PREDICTED: similar to Nid	175	15.84	8	15.523	14548	0	0.098042	0.003718	4.9207	1.4135	1.3656	1.6336	1.2669	0.975	1.3543	76856149	3	3	3 yes	6 yes		2
177	tissue inhibitor of metalloproteinase 1 (erythroid potentiating activity, collagenase inhibitor)	177	15.39	9	17.699	19843	0	1.2305	0.5377	0.023436	1.1961	1.4761	1.2043	1.3349	1.9095	1.3954	27808161	3	0	3 yes	30 yes		2
181	legumain	181	15.06	9	15.063	12874	0	0.2953	0.25262	0.000677	0.71707	1.5385	0.73251	1.4718	2.1491	1.3881	27806555	3	3	3 yes	16 yes		2
184	PREDICTED: similar to signal peptide, CUB domain, EGF-like 3	184	14.86	7	13	13733	0	0.007916	0.054857	0.5625	1.6594	1.2116	1.2974	1.1673	0.92131	1.1295	76850091	3	3	3 yes	11 yes		2
195	PREDICTED: similar to cell growth regulator with EF hand domain 1	195	14	7	14	16326	0	2.9362	3.1289	4.875	1.1207	1.5059	1.0854	1.3751	1.0033	1.1632	76829997	0	0	0 yes	32 yes		2
198	PREDICTED: similar to fibulin 1 isoform C precursor isoform 2 ; PREDICTED: similar to fibuli	198	14	14	27.046	24151	0	0.008855	0.000732	0.018085	1.2144	1.1979	1.3039	1.2578	0.79345	1.2687	76817190	3	3	3 yes	6 yes		2
200	PREDICTED: similar to alpha 1 type XI collagen isoform B preproprotein, partial	200	13.57	9	16.046	14006	0	0.29781	0.002246	0.25354	1.7531	2.0727	0.7126	1.1891	1.526	1.691	76874654	3	3	3 no	yes		2
204	PREDICTED: similar to Stem cell growth factor precursor (Lymphocyte secreted C-type lectir	204	13.23	7	12.046	10562	0	5.1909	2.4375	0.027232	0.9724	1.4673	0.80851	1.4449	0.85679	1.0806	76842160	3	3	3 yes	27 yes		2
208	PREDICTED: similar to secreted modular calcium-binding protein 2	208	12.97	7	12.569	10810	0	4.8279	5.825	0.017805	1.0821	2.2425	0.98727	1.675	0.69117	1.2252	76860599	3	0	3 yes	9 yes		2
210	PREDICTED: similar to Peptidyl-prolyl cis-trans isomerase C (PPIase) (Rotamase) (Cyclophi	210	12.85	9	16.444	12527	0	0.057286	0.17019	0.31639	1.3329	1.2899	1.2748	1.3136	1.3654	1.5087	76822582	3	3	3 yes	6 yes		2
212	fibrillin 1	212	12.8	6	11	10377	0	0.43154	0.16872	1.2968	1.529	1.4779	1.9471	1.554	0.89623	1.1817	27806637	3	3	3 yes	3 yes		2
215	keratin 10 (epidermolytic hyperkeratosis)	215	12.37	7	12.046	9523.2	0	0.006738	0.098356	3.8752	0.70716	1.1703	0.83838	1.1518	1.0228	1.1315	27805977	3	3	3 no	yes		2
216	PREDICTED: similar to Extracellular superoxide dismutase [Cu-Zn] precursor (EC-SOD) isof	216	12.36	6	12	9139.6	0	0.14999	0.44221	0.025418	1.1822	1.1384	1.104	1.1134	1.293	1.1352	76880741	3	3	3 yes	32 yes		2
218	PREDICTED: similar to retinoic acid receptor responder (tazarotene induced) 2 isoform 2	218	12.14	7	14	12084	0	0.09375	0.000612	0.020897	1.7333	1.275	1.5638	1.1398	0.78765	1.1453	76818163	3	3	3 yes	45 yes		2
225	PREDICTED: similar to von Willebrand factor A domain-related protein isoform 1	225	12	6	12	13361	0	1.6133	1.5441	0.32408	1.2091	1.4536	1.1822	1.3783	1.3106	1.3024	76837679	3	3	3 yes	13 yes		2
226	PREDICTED: similar to keratin 1 isoform 2 ; PREDICTED: similar to keratin 1 isoform 7 ; PRI	226	11.66	6	11	8963.4	0	5.6392	0.88943	5.4348	1.0231	2.022	1.5052	1.7973	0.98626	1.2368	76817878	3	0	3 yes	8 yes		2
227	angiogenin	227	11.54	5	10	7422.6	0	0.040463	1.5093	0.31404	1.7581	1.2779	1.1391	1.2429	1.3548	1.282	27806923	3	3	3 yes	82 yes		2
228	PREDICTED: similar to secreted modular calcium-binding protein 1	228	11.52	6	11.523	9972.6	0	1.7923	0.22075	0.029259	0.948	1.1194	0.7855	1.2327	0.75023	1.1579	76869311	3	3	3 yes	45 yes		2
234	prostaglandin H2 D-isomerase	234	11.05	6	10.444	9545.5	0	0.1875	0.3557	0.1875	0.7762	1.2147	1.74	1.7473	0.72266	1.4173	27807521	3	0	3 yes	18 yes		2
243	PREDICTED: similar to T07H8.5	243	10.59	5	10	8512.3	0	0.63614	0.39676	3.75	1.3616	1.3935	1.2645	1.2326	1.0294	1.5892	76828646	3	3	3 no	yes		2
245	PREDICTED: similar to mannosidase, alpha, class 2A, member 1	245	10.39	6	10	10307	0	0.32812	4.4594	2.3332	0.72833	1.3647	0.97301	1.2136	0.90527	1.2949	76824022	3	3	3 yes	13 yes		2
247	PREDICTED: similar to dermatan 4 sulfotransferase 1	247	10.27	5	10	7547.9	0	3.863	0.93634	0.16646	1.0348	1.1658	1.1149	1.1496	0.7415	1.2187	76827567	0	0	3 yes	6 yes		2
254	PREDICTED: similar to Cytokine-like protein C17 precursor	254	10	5	10	9374.6	0	3.4125	1.693	3.7283	1.1145	1.4782	1.0905	1.1688	1.1012	1.4967	76820378	3	3	3 yes	35 yes		2
255	PREDICTED: similar to collagen triple helix repeat containing 1	255	10	5	10	7351	0	0.375	0.014479	0.075993	1.2837	1.2924	1.4108	1.1194	1.4193	1.1998	76834746	3	3	3 yes	25 yes		2
259	PREDICTED: similar to Alpha-N-acetylgalactosaminidase precursor (Alpha-galactosidase B)	259	9.97	5	9.0458	7322.8	0	0.54167	0.22967	0.002449	1.2813	1.2831	1.3398	1.2397	1.9693	1.1498	76816903	3	3	3 yes	14 yes		2
264	PREDICTED: similar to fibulin 2 precursor, isoform a	264	9.67	5	9.5229	6925.2	0	0.51647	0.13067	3.0093	1.395	1.3028	1.3851	1.1597	1.1463	1.431	76849536	1	1	1 yes	2 yes		2
271	PREDICTED: similar to mannose receptor, C type 2	271	9.3	5	9.0458	7294.6	0	2.9367	5.483	2.0349	1.1166	1.3831	1.024	1.5861	0.67239	1.3251	76845205	3	3	3 yes	4 yes		2
288	5'-nucleotidase, ecto (CD73)	288	8.45	5	8.0915	8020.4	0	4.2417	0.58531	0.022791	1.0269	1.1371	1.1729	1.1433	1.9155	1.1718	27806507	0	0	3 yes	8 yes		2
300	cystatin E/M	300	8.13	4	8	8477.4	0	0.27281	0.035671	0.25402	0.69051	1.251	0.62707	1.1423	1.3765	1.2085	61097917	3	3	3 yes	21 yes		2
305	PREDICTED: similar to Collagen alpha 1(VII) chain precursor (Long-chain collagen) (LC coll	305	8	4	8	6499.8	0	0.12673	0.31714	2.9625	1.2398	1.1014	2.3189	1.7174	1.0796	1.2178	76848218	3	3	3 yes	2 yes/poor quant		2
310	PREDICTED: similar to integrin, beta-like 1 (with EGF-like repeat domains)	310	7.63	4	7.0458	6164.2	0	3.4885	5.0591	0.031875	0.89302	1.4438	1.0242	1.248	2.0173	1.2121	76861183	1	1	1 yes	11 yes/poor quant		2
311	PREDICTED: similar to prolyl 4-hydroxylase, alpha II subunit isoform 2 precursor isoform 2 ;	311	7.53	3	5.3979	3970.2	0	0.64658	0.17964	0.36825	1.4397	1.2535	1.2606	1.0736	2.9895	1.637	76822268	3	0	3 yes	4 yes/poor quant		2
314	PREDICTED: similar to transforming growth factor, beta 2 isoform 2 ; PREDICTED: similar to	314	7.51	3	5.0458	4174.1	0	1.7678	2.8985	3.8963	1.3844	1.4924	1.2143	1.4828	1.1628	1.6376	76870057	3	0	0 yes	8 yes		2
319	carboxypeptidase X	319	7.33	4	7	6177.4	0	5.0854	2.0188	3.9269	1.0385	1.4345	0.82469	1.4017	0.88054	1.6717	62751399	3	3	3 yes	13 yes		2
335	PREDICTED: similar to complement factor I	335	6.88	4	6.5686	7082.9	0	3.8375	0.92635	1.8542	1.2213	1.8843	1.5763	1.4217	1.708	1.8686	76819404	1	1	1 yes	6 yes/very poor quan		2
353	PREDICTED: similar to Cathepsin F precursor isoform 3 ; PREDICTED: similar to Cathepsin	353	6.15	3	6	3837.1	0	5.0567	0.10885	0.19414	0.99023	1.0784	1.2453	1.0089	1.8496	1.217	76858024	3	0	3 no	5 yes		2
355	PREDICTED: similar to secreted modular calcium-binding protein 1	355	6.14	3	6	4244.1	0	3.1156	2.3867	1.2734	0.8969	1.2752	0.80866	1.4117	0.78623	1.259	76869309	3	3	3 yes	13 yes		2
360	PREDICTED: similar to hyaluronan and proteoglycan link protein 3 (predicted)	360	6	4	8	6087.5	0	0.69416	5.4446	1.9878	1.434	1.3888	1.024	1.4555	0.84845	1.3288	76847007	3	0	3 yes	6 yes		2
361	matrix Gla protein	361	6	5	10	6241.1	0	3.75	0.375	3.2727	0.99149	1.5503	1.3271	1.3811	0.77558	2.3663	27807275	3	0	3 yes	24 yes		2
363	lysyl oxidase	363	6	3	6	4367.8	0	0.064634	0.084771	4.1033	1.6426	1.0941	0.62652	1.1022	0.90385	1.45	27808857	3	3	3 yes	9 yes		2
368	PREDICTED: similar to Annexin A6 (Annexin VI) (Lipocortin VI) (P68) (P70) (Protein III) (Chr	368	6	3	6	4516.8	0	5.3821	6	1.9977	0.97516	1.2436	0.5627	1	1.5865	1.4419	76823595	3	3	3 yes	5 yes/very poor quan		2
374	PREDICTED: similar to Tetranectin precursor (TN) (Plasminogen-kringle 4 binding protein)	374	6	3	6	5796.1	0	1.6775	0.64792	2.6109	1.6376	1.7868	1.1299	1.0788	0.89463	1.2205	61819259	0	0	3 yes	16 yes/poor quant		2
377	PREDICTED: similar to alpha 1 type XV collagen precursor	377	5.87	3	5.5229	4874.8	0	0.79108	5.2579	0.26309	1.257	1.1737	1.0164	1.1732	0.80582	1.0844	76824759	3	3	3 yes	25 yes		2
379	glutaminyl-peptide cyclotransferase (glutaminyl cyclase)	379	5.86	3	5.5229	5151.7	0	1.5156	1.9008	3.3943	1.2721	1.2995	1.1662	1.223	1.142	1.4011	29135303	3	3	3 yes	13 yes		2
384	PREDICTED: similar to Angiopoietin-related protein 2 precursor (Angiopoietin-like 2) isoform	384	5.68	3	5.0458	4525.1	0	3.3292	3.2889	1.7324	1.113	1.3018	1.0767	1.1958	1.1257	1.1541	76830450	3	3	3 yes	10 yes/very poor quan		2
401	PREDICTED: similar to Beta-hexosaminidase alpha chain precursor (N-acetyl-beta-glucosan	401	5.08	3	4.4437	4746.5	0	2.049	6	0.19681	1.6169	1.4978	1.0953	1	3.188	1.0882	76826683	3	3	3 yes	9 yes/very poor quan		2
404	paired basic amino acid cleaving enzyme [furin, membrane associated receptor protein] [Bos	404	5.05	2	3.0458	4728.3	0	1.631	6	0.55834	1.7265	1.421	0.8	1	2.379	1.1977	27806495	0	3	0 yes	22 yes/poor quant		2
406	insulin-like growth factor binding protein 4	406	5	3	5	5267.6	0	3.4894	2.8535	5.1751	1.0323	1.06	0.70674	1.5755	1.0516	1.3634	27807009	0	3	0 yes	9 yes		2
429	PREDICTED: similar to semaphorin 6D isoform 1 precursor	429	4.33	2	4	3823	0	2.0243	1.1284	1.5387	0.88787	1.1036	1.5008	1.1909	0.85917	1.2855	76827892	3	0	3 no	yes		2
433	PREDICTED: similar to Neogenin precursor, partial	433	4.28	2	4	3475.1	0	1.243	0.25289	3.5358	1.3289	1.1453	1.5518	1.0421	0.86965	1.3001	76872111	1	1	1 yes	4 yes		2
445	sialyltransferase ST3Gal-VI	445	4.11	2	3.5229	3343.9	0	0.38632	0.29525	4.8657	1.7169	1.0807	1.5263	1.0474	0.91159	1.5339	50872137	1	1	1 yes	9 yes		2
446	PREDICTED: similar to Collagen alpha 1(XVII) chain (Bullous pemphigoid antigen 2) (180 kD	446	4.04	2	3.3979	3127.5	0	1.015	1.3784	2.6171	1.7232	1.233	0.8207	1.1112	1.2321	1.2728	76854900	3	3	3 yes	4 yes/poor quant		2
450	PREDICTED: similar to esophageal cancer related gene 4 protein	450	4	2	4	2740.6	0	3.7548	3.6678	2.4262	0.76744	1.7537	0.71392	1.9759	2.5803	2.8644	76829589	3	3	3 yes	yes /very poor id		2
455	ATP6IP1 protein	455	4	2	4	4222.4	0	2.8427	6	0.35868	0.80411	1.3283	0.96483	1	0.75048	1.039	28461231	1	1	1 yes	7 yes		2
475	PREDICTED: similar to Beta-1,4-galactosyltransferase 4 (Beta-1,4-GalTase 4) (Beta4Gal-T4	475	4	2	4	4288.5	0	0.63965	0.75841	3.3763	1.5035	1.119	1.1981	1.1626	1.1086	1.1529	76829853	1	1	1 yes	0 yes/poor quant		2
483	PREDICTED: similar to Biotinidase precursor	483	4	2	4	3020.7	0	0.26006	2.1551	1.4599	0.83315	1.0178	0.76046	1.2777	1.1065	1.0592	76871919	3	3	3 yes	4 yes/poor quant		2
485	PREDICTED: similar to ectonucleotide pyrophosphatase/phosphodiesterase 1, partial	485	4	3.68	7.3979	6153.3	0	5.7652	5.9775	0.67755	1.0039	1.157	1.0007	1.3391	1.321	1.2849	76800000	0	3	0 yes	16 yes		2
500	PREDICTED: similar to Latent transforming growth factor beta binding protein 3 precursor (L	500	3.7	5	7.4949	8408.8	0	2.825	1.9704	0.52818	1.2499	1.8555	1.4974	2.2517	1.2201	1.219	61840215	0	3	3 yes	5 one		2
514	mannosidase, beta A, lysosomal	514	3.49	2	3	3286.8	0	3.3319	2.4917	3.4557	1.1896	1.3396	0.68453	1.506	0.84487	1.3544	27805995	1	1	1 yes	2 yes		2
523	PREDICTED: similar to Potential carboxypeptidase-like protein X2 precursor	523	3.31	2	3	2877.6	0	5.3813	3.8251	1.9322	0.97128	1.2869	1.0862	1.2004	0.77551	1.2204	76806193	0	0	3 yes	9 yes/poor quant		2
548	PREDICTED: similar to Thrombospondin-3 precursor isoform 1 ; PREDICTED: similar to Thr	548	3	5	9	8023.4	0	3.6344	1.8994	2.7529	1.0581	1.2533	1.153	1.3209	0.89722	1.3446	76812138	0	0	3 no	yes		2
617	type IIA procollagen	1	105.66	58	112.15	104530	0	4.7774	1.83E-07	0.36899	1.0049	2.7417	0.58162	1.5833	0.83995	2.191	gi|10947027				yes		2
627	Chondroitinase ABC	3	91.83	50	97.444	101060	0	3.1046	5.8757	4.1086	0.97565	1.2993	0.9992	1.2352	0.98883	1.2049	gi|5936742; gi|3991938; gi|3408155; gi|1607541				yes		2
629	PREDICTED: similar to C1q and tumor necrosis factor related protein 5 isoform 2 ; PREDICT	566	2.66	1	2	1917.1	0	6	6	6	1.7349	1	1.5985	1	1.1626	1	76835366	3	3	3 yes	6 yes-one		2
1	PREDICTED: similar to alpha 3 type VI collagen isoform 5 precursor isoform 1	1	207.94	107	207.68	170540	1	5.27E-18	1.35E-15	5.69E-17	2.1418	1.3516	1.3833	1.3368	1.6062	1.4487	76814736	3	3	3 yes	29 yes		3
4	PREDICTED: similar to Fibronectin precursor (FN) (Cold-insoluble globulin) (CIG) isoform 13	4	149.44	81	154.93	148410	1	6.89E-14	1.48E-09	9.73E-14	2.587	1.3201	1.2526	1.3212	1.6875	1.3007	76810128	3	3	3 yes	32 yes		3
8	PREDICTED: similar to Collagen alpha 1(VI) chain precursor isoform 1	8	93.86	59	111.85	101310	1	3.78E-10	8E-10	1.67E-09	2.7414	1.5273	1.9244	1.353	2.0468	1.3333	76867061	3	3	3 yes	40 yes		3
9	aggrecan 1	9	93.47	61	117.23	117440	0	1.21E-10	5.01E-07	0.006772	2.5815	1.8943	2.02	2.1569	0.92692	1.188	76826761	3	3	3 yes	15 yes		3
10	PREDICTED: similar to Tenascin precursor (TN) (Hexabrachion) (Cytotactin) (Neuronectin) (	10	86.63	47	92.523	85529	1	3.57E-26	4.36E-23	0.026206	3.4419	1.4115	3.0211	1.4443	1.1767	1.3998	76825295	3	3	3 yes	20 yes		3
38	PREDICTED: similar to matrilin 3 precursor	36	47.7	27	52	48784	0	2.6E-13	4.59E-10	3.8461	3.044	1.4833	2.1118	1.4054	1.0241	1.2867	76830143	3	3	3 yes	47 yes		3
44	PREDICTED: similar to Bone morphogenetic protein 1 precursor (BMP-1) (Procollagen C-pro	44	40.81	21	39.614	31714	1	1.42E-14	3.93E-11	7.35E-05	6.5221	1.4874	4.0243	1.567	1.7469	1.5599	76824630	3	3	3 yes	19 yes		3
49	PREDICTED: similar to alpha 2 type VI collagen isoform 2C2a precursor isoform 1	49	38.2	23	42.967	40490	0	2.7E-09	7.92E-07	1.81E-08	2.2131	1.4348	1.6686	1.344	2.0827	1.3982	76807764	3	3	3 yes	23 yes		3
57	chondroadherin	57	36.2	20	37.796	33238	0	3.62E-09	5.01E-06	0.6564	2.2459	1.3461	1.478	1.2616	1.1388	1.3999	27808697	3	0	0 yes	53 yes		3
71	clusterin	71	31.97	17	33.046	31086	0	2.72E-13	0.001758	0.45616	2.0374	1.1281	3.1776	1.1396	1.0772	1.1755	27806907	3	3	3 yes	33 yes		3
81	plasminogen activator inhibitor type 1, member 2	81	27.07	14	27.097	20805	1	2E-06	0.000732	2.58E-05	1.6726	1.2251	1.6042	1.4742	1.6027	1.2641	27807207	3	3	3 yes	28 yes		3
89	versican	89	26.42	17	30.313	25088	1	2.3E-05	4.87E-12	2.3403	1.6014	1.3271	2.2621	1.1812	1.0864	1.3498	30794358	3	3	0 yes	4 yes		3

order	Protein Name	protein #	score	peptides	score 2	mass cov	outliers	pval 115	pval 116	pval 117	116:114	SD	116:114	SD	117:114	SD	Accessior	sig 115	sig116	sig117	SM-ID	coverage	manual	Indexer k6
108	PREDICTED: similar to germinal histone H4 gene ; PREDICTED: similar to germinal histone	108	23.82	20	39.523	31972	0	1.26E-09	6.27E-10	0.000531	1.9211	1.2717	1.907	1.2561	1.9205	1.2104	61820747	3	3	3	yes	19	yes	3
118	PREDICTED: similar to Gremlin-1 precursor (Cysteine knot superfamily 1, BMP antagonist 1	118	22.05	10	20	21637	0	6.55E-05	3.96E-05	5.902	1.9048	1.2214	1.6428	1.1248	1.001	1.1534	61863230	3	3	3	yes	52	yes	3
120	PREDICTED: similar to Laminin gamma-1 chain precursor (Laminin B2 chain), partial	120	22	11	21.222	20122	0	0.011719	0.000232	0.74312	1.9279	1.3615	2.2236	1.463	1.2068	1.4494	76837875	3	3	0	yes	11	yes	3
123	PREDICTED: similar to Histone H2B 2918 ; PREDICTED: similar to Histone H2B 2918 ; PRI	123	21.35	12	21.063	14584	0	1.16E-09	2.17E-10	1.26E-08	2.1625	1.1292	2.0811	1.1039	2.2385	1.1717	76812878	3	3	3	yes	62	yes	3
129	PREDICTED: similar to H3 histone, family 2 isoform 2	129	20.64	11	19.541	15303	0	0.005859	0.000748	0.000131	2.5568	1.6482	2.1221	1.5112	2.2858	1.445	76812680	3	3	3	no	yes	yes	3
143	PREDICTED: similar to Fibroleukin precursor (Fibrinogen-like protein 2) (pT49) isoform 1	143	18.73	9	16.523	14544	0	0.00017	0.000143	5.4809	2.1304	1.3062	2.3364	1.3401	1.0279	1.3109	61880803	3	3	3	yes	23	yes	3
145	cyanogen bromide	145	18.68	9	17.398	14376	0	0.049006	1.4925	0.016549	2.6349	2.2984	0.79817	1.5952	2.1553	1.7172	47564048	3	3	3	yes	23	yes	3
156	domain) lectin, superfamily member 1(cartilage-derived)	156	17.36	9	17.046	13604	0	5.17E-05	0.000165	0.004954	2.955	1.3851	1.7482	1.2172	1.4849	1.2564	27807147	3	3	0	yes	53	yes	3
163	PREDICTED: similar to CEGP1 protein	163	16.66	8	16	13867	0	0.046875	6.35E-05	3.2061	1.3856	1.2028	2.781	1.2971	0.93191	1.357	76835840	3	3	3	yes	12	yes	3
169	cell-derived chemotaxin 2	169	16.27	9	17.046	13497	0	1.28E-05	0.000223	3.6232	2.1314	1.2081	1.7775	1.2349	1.036	1.2173	27805983	3	3	0	yes	70	yes	3
171	frizzled-related protein	171	16	8	16	12878	0	0.33215	0.23438	1.4107	1.8148	2.084	1.7689	1.6734	0.83489	1.4821	27806625	3	3	3	yes	24	yes	3
192	angiopoietin-like 7	192	14.06	8	15.046	14246	0	0.007967	0.000256	1.73E-06	1.5389	1.2673	2.2258	1.2859	2.45	1.1435	62460514	3	3	3	yes	27	yes	3
193	hemoglobin, gamma	193	14	7	14	11685	0	0.020797	3.65E-05	0.001786	1.3726	1.197	3.9346	1.2784	1.576	1.1749	62460494	3	3	3	no	alpha 1	yes	3
198	PREDICTED: similar to steroid-sensitive protein 1 isoform 1 ; PREDICTED: similar to steroid	198	13.78	7	13.046	11726	0	0.375	0.04666	0.1979	2.0468	1.8184	1.8653	1.4274	1.3513	1.2872	76860977	3	3	0	no	6	yes	3
201	PREDICTED: similar to Ceruloplasmin precursor (Ferroxidase) isoform 2 ; PREDICTED: sim	201	13.42	7	12.523	11672	0	0.014544	0.15964	0.067845	2.8555	1.5768	1.6544	1.487	1.958	1.5236	76807945	3	3	3	yes	2	yes/poor quant	3
205	RA87, member RAS oncogene family	205	13.2	6	12	11689	0	0.17044	0.006912	0.001376	1.5368	1.412	2.0449	1.301	1.6705	1.143	27806449	3	3	3	yes	9	yes	3
213	PREDICTED: similar to neuroplilin 2 isoform 3 precursor isoform 4 ; PREDICTED: similar to n	213	12.43	6	11.046	7934.6	0	0.00106	3.03E-05	0.87721	1.8262	1.1601	2.9102	1.1358	0.83486	1.2932	76810302	3	3	3	yes	8	yes	3
217	PREDICTED: similar to secreted modular calcium-binding protein 2	217	12.29	6	12	10758	0	7.05E-07	0.1875	0.13148	5.1799	1.0964	3.4587	1.2152	1.1654	1.121	76890954	3	3	3	yes	24	yes	3
237	secreted frizzled-related protein 1	237	10.81	5	10	8037.7	0	0.01045	0.006075	1.5117	2.2781	1.2807	1.9494	1.19	1.1359	1.2373	27806139	3	3	3	yes	13	yes	3
241	alpha-2-HS-glycoprotein	241	10.64	5	10	7328.6	0	0.000216	0.023836	0.096718	5.3197	1.204	1.8602	1.2621	2.0881	1.5002	27806751	3	3	3	yes	14	yes	3
251	PREDICTED: similar to proteoglycan 4	251	10.14	5	10	7968.3	0	0.000656	0.10295	0.010115	2.9952	1.0841	1.6446	1.2301	3.287	1.2459	76838019	3	3	3	yes	10	yes	3
257	PREDICTED: similar to Complement C1q subcomponent, C chain precursor isoform 1 ; PRE	257	10	5	10	7855.1	0	0.001881	0.007325	1.7248	2.3469	1.1784	1.956	1.2015	0.86913	1.2916	76811607	3	3	3	yes	21	yes	3
262	PREDICTED: similar to Histone H1.4 (H1 VAR.2) (H1e), partial	262	9.82	5	9.3979	6128.4	0	0.013293	0.038728	0.20584	3.0968	1.4364	1.8494	1.3017	1.6398	1.4196	76851042	3	3	3	yes	19	yes	3
263	PREDICTED: similar to collagen, type XXVII, alpha 1	263	9.71	4	8	5680.1	0	0.015729	0.03959	5.02	2.033	1.1646	1.8271	1.195	0.96662	1.3529	76825290	3	3	3	yes	4	yes	3
267	PREDICTED: similar to PDZ domain containing 6	267	9.52	6	11.523	12226	0	0.002099	0.006703	0.040765	2.1979	1.1687	1.6765	1.1481	1.1649	1.0686	76827221	3	3	0	yes	ribonuclea	yes	3
279	PREDICTED: similar to Procollagen C-endopeptidase enhancer 2 precursor (Procollagen CC	279	8.98	6	9.6144	8262.6	0	0.003805	0.010122	0.48175	2.5604	1.3503	2.1469	1.3576	1.483	1.5544	76886418	3	3	3	yes	21	yes	3
280	PREDICTED: hemoglobin alpha chain isoform 2 ; PREDICTED: similar to alpha 2 globin ; PF	280	8.88	4	7.5229	6646.7	0	3.4634	0.061226	2.3785	1.2073	1.83	3.73	1.5746	1.1318	1.2851	76852523	3	3	3	yes	5	yes	3
287	beta-2-microglobulin	287	8.45	4	8	7037.9	0	0.085642	0.014461	0.1152	3.2249	1.5772	4.8364	1.3897	1.6447	1.1288	41386683	3	3	3	yes	44	yes	3
290	PREDICTED: similar to ephrin A1 isoform a precursor isoform 1 ; PREDICTED: similar to epl	290	8.34	4	7.0458	5931.9	0	0.19545	0.16886	0.030655	2.7671	1.7167	2.5405	1.5953	2.7024	1.3092	76812106	3	3	3	yes	13	yes	3
294	PREDICTED: similar to olfactomedin-like 2B	294	8.16	4	7.5229	6882.3	0	0.00217	0.005483	0.2001	5.4148	1.2039	5.3627	1.2867	2.086	1.4817	76812910	1	1	1	no		yes/poor quant	3
299	PREDICTED: similar to interleukin-17B precursor (IL-17B) (Cytokine-like protein Zcyto7) (Ne	299	8.13	6	9.0458	9487.5	0	0.033331	0.19152	1.998	3.2761	1.8671	2.0732	1.8324	1.1778	1.4539	76823570	3	3	3	yes	16	yes	3
308	PREDICTED: similar to insulin-like growth factor binding protein 6 isoform 1	308	7.67	3	5.0458	4148.1	0	0.001239	1.2158	2.1877	3.2469	1.0297	1.9861	1.889	1.0989	1.1523	81883585	3	0	0	yes	25	yes	3
313	PREDICTED: similar to agrin	313	7.52	4	7.5229	6916.5	0	0.22779	0.1655	2.1757	1.8096	1.3962	2.091	1.4429	0.85804	1.2544	76837785	3	3	3	yes	1	yes	3
318	PREDICTED: similar to Laminin beta-1 chain precursor (Laminin B1 chain), partial	318	7.35	4	7.0458	5423.2	0	0.21927	0.23191	0.71611	1.7902	1.381	2.2869	1.59	1.28	1.2566	76815137	3	3	3	yes	1	yes	3
321	PREDICTED: similar to mannosidase, alpha, class 1A, member 1, partial	321	7.3	5	9.0458	7002.8	0	0.00159	0.29866	0.000995	2.028	1.1392	1.2069	1.1633	1.9832	1.1185	76874188	3	3	3	yes	5	yes	3
331	PREDICTED: similar to stromal cell derived factor 4	331	6.96	3	6	5630.1	0	0.2006	0.16551	0.21684	2.3381	1.3178	1.8272	1.1937	1.9972	1.2639	76837700	3	3	3	no		yes	3
332	PREDICTED: similar to complement component 1, q subcomponent, beta polypeptide precur	332	6.92	4	6.9208	6492.5	0	0.035275	0.058344	0.12758	2.3042	1.2674	2.0491	1.2753	0.8235	1.0915	76811613	3	3	0	yes	14	yes	3
341	PREDICTED: similar to thrombospondin repeat containing 1 isoform 1	341	6.46	3	5.0458	5148.6	0	0.067061	0.27336	2.0362	8.4456	1.4829	3.4737	1.6109	2.0173	2.6556	76812850	3	3	3	yes	1	yes	3
342	matrix metalloproteinase 14 (membrane-inserted)	342	6.45	3	6	4363.9	0	0.093255	1.3923	0.008975	2.2318	1.1917	2.1043	2.1382	1.4429	1.0249	27806001	3	3	3	yes	3	yes	3
345	PREDICTED: similar to polypeptide N-acetylgalactosaminyltransferase 2	345	6.35	4	6.3468	8623.1	0	2.3602	0.67332	3.7067	1.7267	2.4029	1.8085	1.4567	1.0838	1.3367	76858089	1	1	1	yes	3	yes/poor quant	3
350	PREDICTED: similar to alpha 3 type IX collagen	350	6.23	3	6	5790.2	0	2.099	5.5735	2.1982	2.8693	4.5205	0.9755	1.5317	2.029	2.6808	76861312	3	3	3	yes	7	yes/very poor quan	3
378	PREDICTED: similar to Apolipoprotein D precursor (Apo-D) (ApoD)	378	5.87	4	7.5229	6603.6	0	0.011808	0.46918	0.01436	3.9387	1.306	1.7225	1.5117	2.3809	1.1979	76807186	3	3	3	no		yes	3
386	transcobalamin II	386	5.67	2	3.5229	2911.7	0	0.76201	1.1606	3.3655	3.5337	1.4351	2.8451	1.5899	1.1779	1.3241	27806385	3	3	3	yes	5	yes	3
394	PREDICTED: similar to meteorin, glial cell differentiation regulator-like	394	5.52	2	4	3103.6	0	0.84338	0.60335	1.1323	6.8245	1.6397	3.9969	1.3663	2.441	1.4703	76845390	3	3	3	yes	2	yes	3
412	Niemann-Pick disease, type C2	412	4.7	2	3	3844.9	0	0.16132	0.82589	0.23929	3.2332	1.0726	1.3392	1.095	3.1921	1.1085	27806881	3	3	3	yes	26	yes	3
417	PREDICTED: similar to Cathepsin L precursor (Major excreted protein) (MEP)	417	4.62	2	4	3982.2	0	1.8776	2.0073	3.5479	4.9245	3.3438	3.6781	2.8098	1.7001	2.7289	61867538	3	3	3	yes	5	yes	3
418	H2A histone family, member Z ; PREDICTED: similar to H2A histone family, member V isofo	418	4.6	2	4	2745.6	0	1.0197	0.2817	0.35684	3.5854	1.6386	2.3516	1.0935	2.4367	1.1254	27807373	3	3	3	yes	24	yes	3
419	PREDICTED: similar to Periostin precursor (PN) (Osteoblast-specific factor 2) (OSF-2), parti	419	4.6	2	4	3603	0	0.56708	1.2927	0.4968	3.2168	1.2803	1.4924	1.2205	3.3349	1.2496	76883330	3	3	3	yes	6	yes	3
420	PREDICTED: similar to Vesicular integral-membrane protein VIP36 precursor (GP36b glycop	420	4.54	2	4	3217.9	0	0.50312	1.3271	0.2871	1.3673	1.0604	1.766	1.3381	2.1744	1.0862	61879717	3	3	3	yes	5	yes/poor quant	3
428	PREDICTED: similar to small inducible cytokine A16 precursor	428	4.33	2	4	3924.1	0	0.34773	0.45487	3.5976	1.952	1.0902	1.9129	1.116	1.0877	1.1776	76842911	3	3	0	yes	30	yes	3
431	PREDICTED: similar to Galectin-3 binding protein precursor (Lectin galactoside-binding solu	431	4.29	2	4	2633.4	0	0.63798	0.58341	0.10982	1.7531	1.1432	2.1676	1.1834	2.0038	1.0287	76845574	3	3	3	yes	3	yes	3
435	PREDICTED: similar to fibroblast growth factor receptor 1 isoform 5 precursor isoform 3 ; PR	435	4.24	2	4	3122.8	0	1.0661	0.9341	4.8271	2.6791	1.4909	4.4865	1.8985	1.1754	2.0557	76855919	3	3	3	yes	4	yes	3
447	PREDICTED: similar to ERGIC-53 protein precursor (ER-Golgi intermediate compartment 53	447	4.02	2	3.0458	3102.8	0	0.32841	0.23143	1.0232	1.7817	1.0732	2.3831	1.0773	1.5081	1.1729	76852230	3	3	0	yes	3	yes	3
458	PREDICTED: similar to Dipeptidyl-peptidase I precursor (DPP-I) (DPPI) (Cathepsin C) (Cathe	458	4	2	4	3739.9	0	2.0213	1.327	1.3936	2.0143	1.7848	2.0921	1.4594	2.9987	1.8097	76856982	3	3	3	yes	4	yes/poor quant	3
463	glycoprotein-4-beta-galactosyltransferase 2	463	4	2	4	2680.4	0	0.11605	0.29582	0.18874	3.2482	1.0519	2.2585	1.0935	2.1051	1.0534	29135321	3	3	3	no		yes	3
466	PREDICTED: similar to Syndecan-4 precursor (Amphiglycan) (SYND4) (Ryudocan core prot	466	4	2	4	5097	0	0.83529	0.74645	6	3.8677	1.5298	2.477	1.2891	0.5519	1	76833778	3	3	3	yes	20	yes	3
491	S100 calcium binding protein A12 (calgranulin C)	491	4	2	4	2824.5	0	0.021177	3.5171	1.051	3.0918	1.0089	1.1588	1.3155	1.6436	1.2194	27807183	3	3	3	yes	20	yes	3
507	PREDICTED: similar to Complement factor D precursor (C3 convertase activator) (Properdin	507	3.52	2	3.5229	3151.1	0	6	6	6	3.3821	1	1.6178	1	1.3	1	61882363	3	3	1	no		yes/poor quant	3
510	chemokine (C-X-C motif) ligand 6 (granulocyte chemotactic protein 2)	510	3.52	2	3.5229	2880.6	0	0.56539	0.64451	0.48187	7.2966	1.5206	2.7986	1.387	2.1787	1.1497	27805833	1	1	1	yes	20	yes	3
512	PREDICTED: similar to Secreted frizzled-related protein 4 precursor (sFRP-4) (Frizzled prote	512	3.52	2	3.5229	3401.9	0	0.070311	0.42691	0.032159	3.6055	1.034	2.4939	1.1561	1.4082	1.0041	76888934	1	1	1	yes	6	yes	3
520	PREDICTED: similar to Pentraxin-related protein PTX3 precursor (Pentaxin-related protein P	520	3.4	2	3.3979	3124.9	0	0.93377	0.46091	6	3.5898	1.5697	5.2072	1.327	0.93353	1	76807843	3	3	3	yes	6	yes/low quant/itraq;	3
525	PREDICTED: similar to ST4 oncofetal trophoblast glycoprotein	525	3.3	2	3.301	1934.8	0	1.7373	0.68317	2.7293	2.0832	1.6612	2.3157	1.2395	1.1919	1.2403	76825454	1	1	1	no		yes / poor quant	3
540	inter-alpha-trypsin inhibitor (protein HC), light	540	3.05	2	3.0458	3088.4	0	1.4021	1.0876	5.9503	2.3567	1.5939	3.0696	1.5908	1.0057	1.8567	27806743	3	3	0	yes	6	yes	3
566	PREDICTED: similar to Calgranulin B (Migration inhibitory factor-related protein 14) (MRP-14	378	5.1	3	5.0969	4042.5	0	0.1654	0.70991	0.012469	5.32	1.6338	2.3992	1.7747	2.2597	1.0666	61877405	1	1	1	yes	11	yes	3
570	PREDICTED: similar to chondroitin polymerizing factor	408	4.27	2	3.0458	2516.5	0	6	6	6	1.9812	1	2.2327	1	1.479	1	76810731	1	1	1	yes	2	check	3
575	PREDICTED: similar to KIAA1822 protein	424	4	2	4	2563.6	0	0.40503	1.0557	3.4743	2.4003	1.1409	1.2976	1.1102	1.0818	1.1152	76884173	1	1	1	yes	4	yes	3
580	endothelial protein C receptor	439	4	2	4	2710.7	0	1.7067	2.8985	5.9571	2.2248	1.7192	1.6869	2.0161	0.99736	1.3949	27806093	3	3	3	yes	9	yes	3
618	dystroglycan	199	8.92	4	8	7777.8	0	0.093677	0.004755	0.13318	1.8313	1.2754	2.356	1.1304	1.8303	1.2506	gi|2853448				no			3
621	fetuin ; Sequence 11 from patent US 5981483; Sequence 8 from patent US 5821227	244	6.28	3	5.3979	4812.3	0	0.044103	0.38838	1.2391	5.0464	1.2734	1.6801	1.2648	1.7561	1.6971	gi|344; gi|10058432; gi|6004706				no			3
607	PREDICTED: similar to WNT1 inducible signaling pathway protein 3 precursor (WISP-3)	595	6.66	3	6	4526.6	0	1.2454	0.31535	6	3.9111	1.9197	4.0296	1.1771	0.93676	1	76825668	3	3	3			yes - poor quant	3
11	procollagen-proline, 2-oxoglutarate 4-dioxygenase	11	75.44	42	78.678	64542	0	0.000001	2.2E-16	9.88E-08	1.5283	1.3102	1.7596	1.2735	6.8191	1.4874	27806501	3	3	3	yes	64	yes	4
17	PREDICTED: similar to cytoskeleton-associated protein 4	17	63.1	33	63.967	56982	0	1.71E-05	2.28E-13	3.21E-28	2.3667	1.5029	2.1782	1.3327	10.211	1.3927	76819055	3	3	3	yes	34	yes	4
18	vimentin	18	60.86	32	64	56049	0	1.69E-11	4.1E-15	5.65E-22	1.928	1.369	3.2209	1.4681	7.3978	1.5384	27806785	3	3	3	yes	53	yes	4
21	PREDICTED: similar to actinin, alpha 4 isoform 10 ; PREDICTED: similar to actinin, alpha 4 i	21	56.92	31	60.046	56807	1	2.45E-08	3.71E-12	2.27E-20	2.1135	1.6175	2.5895	1.4598	7.9337	1.6161	76841273	3	3	3	yes	27	yes	4
23	PREDICTED: similar to Lamin A/C (70 kDa lamin) isoform 2	23	52.99	26	49.666	40158	0	3.86E-14	3.28E-16	4.98E-05	2.3891	1.31	3.6026	1.3824	5.033	1.4233	76812306	3	3	3	yes	44	yes	4
24	glucose regulated protein 58kD	24	49.77	27	52.62	46919	0	3.16E-10	3.78E-09	3.36E-05	2.0702	1.4246	1.9936	1.4593	11.145	1.6678	27805905	3	3	3	yes	52	yes	4
33	PREDICTED: similar to Moesin (Membrane-organizing extension spike protein), partial	33	44.31	25	44.025	37278	0	5.53E-08	2.63E-11	1.03E-14	1.5359	1.2847	2.0805	1.3368	3.6403	1.429	76816391	3	3	3	no		yes	4
37	PREDICTED: similar to Filamin B (FLN-B) (Beta-filamin) (Actin-binding-like protein) (Thyroid	37	46.19	22	40.535	38423	0	4.61E-07	6.36E-07	3.78E-11	2.1906	1.5485	2.289	1.5667	4.4442	1.6164	76848770	3	3	3	yes	10	yes	4
38	PREDICTED: similar to 78 kDa glucose-regulated protein precursor (GRP 78) (Immunoglobu	38	45.78	36	69.313	62411	0	3.32E-10	6.62E-13	4.36E-24	1.5432	1.3139	1.9097	1.3789	6.2872	1.5114	76830567	3	3	3	yes	56	yes	4
46	heat shock 70 kDa protein 8	46	39.01	23	43.012	38106	0	1.12E-07	3.67E-08	0.000162	2.5489	1.5733	3.0182	1.7396	8.3729	2.0115	27805925	3	3	3	yes	30	yes	4
50	PREDICTED: similar to Ribosome-binding protein 1 (Ribosome receptor protein) (mRRp)	50	37.76	20	35.229	30009	0	1.38E-08	0.000297	6.27E-09	1.9506	1.2833	1.7425	1.5176	5.0704	1.9302	76832456	3	3	3	yes	21	yes	4
62	tumor rejection antigen (gp96) 1	62	32.7	16	30.569	23993	0	3.81E-07	1.78E-07	1.36E-12	1.8472	1.284	2.1447	1.3095	8.2182	1.4214	27807723	3	3	3	yes	24	yes	4
64	PREDICTED: similar to AHNAK nucleoprotein isoform 1	64	33.51	17	31.489	29634	0	0.003662	0.002197	3.06E-06	2.0551	2.0133	2.1582	2.0838	6.6047	2.6289	76857680	3	3	3	yes	8	yes	4
67	calreticulin	67	32.36	17	31.365	26831	0	0.00044	7.45E-06	1.28E-13	1.6397	1.4703	2.1585	1.5254	10.595	1.4638	27806723	3	3	3	yes	32	yes	4
68	actin, beta	68	32.31	18	35.046	31560	0	0.001179	2.56E-09	1.47E-14	1.8916	1.1925	2.2018	1.302	8.3205	1.3991	27806785	3	3	3	yes	42	yes	4
87	PREDICTED: similar to alpha glucosidase II alpha subunit isoform 2	87	25.51	12	20.915	18446	0	0.000261	4.31E-05	1.73E-08	1.6589	1.309	1.8384	1.3051	4.7907	1.3741	76857688	3	3	3	yes	17	yes	4
88	annexin A2	88	26.52	13	26	22733	0	0.011719	0.00019	5.82E-07	1.8239	1.4743	1.6129	1.249	3.474	1.4236	27807289	3	3	3	yes	37	yes	4
90	villin 2	90	28.15	23	39.581	34710	1	0.000185	4.88E-08	2.75E-12	1.6773	1.3331	1.9432	1.4243	3.5969	1.5036	27806351	3	3	3	yes	39	yes	4
95	PREDICTED: similar to Fructose-bisphosphate aldolase A (Muscle-type aldolase) isoform 2 ;	95	25.61	13	24.046	21404	0	0.000233	8.22E-05	3.29E-07	2.6231	1.5829	3.5932	1.7152	7.3126	1.8305	76853611	3	3	3	no	36	yes	4
98	PREDICTED: similar to glyceraldehyde-3-phosphate dehydrogenase isoform 2 ; PREDICTEI	98	25.4	13	25.398	21978	0	6.95E-07	7.82E-07	1.29E-08	1.9132	1.2348	2.4462	1.3417	9.534	1.673	76818518	3	3	3	yes	44	yes	4
107	heat shock 70 kD protein 1	107	24	17	32.092	25388	0	0.000823	0.001692	4.42E-07	1.8562	1.6283	2.0565	1.846	6.2754	2.2558	40254806	3	3	3	yes	16	yes	4

order	Protein Name	protein #	score	peptides	score 2	mass cov	outliers	pval 115	pval 116	pval 117	116:114	SD	116:114	SD	117:114	SD	Accession	sig 115	sig116	sig117	SM-ID	coverage	manual	Indexer k6	
116	PREDICTED: similar to Prolyl 4-hydroxylase alpha-1 subunit precursor (4-PH alpha-1) (Proc	116	22.24	11	21.523	18890	0	0.00301	0.000236	3.4E-07	1.5731	1.3112	1.6869	1.249	6.0755	1.5212	76656655	3	3	3 yes		18	yes	4	
119	PREDICTED: similar to FK506 binding protein 9	119	22	11	21.523	16426	0	0.000138	0.001357	0.011719	1.6732	1.2268	1.7244	1.2948	8.9699	1.8211	76615361	3	3	3 yes		21	yes	4	
121	PREDICTED: similar to tubulin, beta 5 isoform 4 ; PREDICTED: similar to tubulin, beta 5 isof	121	21.98	10	20	16069	0	0.058594	0.010907	1.65E-05	2.3814	1.7459	2.4178	1.7845	9.0842	1.968	76650558	3	3	3 yes		31	yes	4	
125	PREDICTED: similar to Thioredoxin domain containing protein 5 precursor (Thioredoxin-like	125	21.17	13	24.569	22070	0	8.5E-06	2.02E-06	1.42E-10	1.8862	1.231	2.5748	1.3039	10.271	1.4348	76676583	3	3	3 yes		39	yes	4	
132	eukaryotic translation elongation factor 1 alpha 1	132	20.24	9	16.092	14173	0	0.046875	0.046875	1.47E-05	2.6257	1.7755	2.5613	1.8311	10.06	1.7996	68299807	3	3	3 yes		18	yes	4	
135	PREDICTED: similar to semaphorin 3C	135	20.07	11	18.569	17820	0	2.13E-07	6.27E-05	3.58E-07	4.4829	1.3192	2.7332	1.3637	4.8794	1.2836	76615066	3	3	3 yes		14	yes	4	
136	PREDICTED: similar to liver glycogen phosphorylase isoform 7 ; PREDICTED: similar to live	136	19.9	10	17.137	15393	0	0.011719	0.023438	0.023438	2.0722	1.5308	2.6941	1.8119	8.0901	2.4748	76627635	3	3	3 yes		19	yes	4	
138	protein kinase C substrate 80K-H	138	19.44	11	19.012	18191	0	6.98E-05	6.81E-06	2.81E-07	2.1553	1.3235	2.7067	1.3148	10.692	1.7162	41386727	3	3	3 yes		18	yes	4	
139	Rho GDP dissociation inhibitor (GDI) alpha	139	19.27	9	17.523	13630	0	5.1E-05	3.97E-07	1.11E-06	2.2308	1.2722	3.2812	1.2088	8.437	1.2413	28603774	3	3	3 yes		30	yes	4	
141	PREDICTED: similar to Rab GDP dissociation inhibitor beta (Rab GDI beta) (GDI-2) isoform	141	18.92	10	17.137	15989	0	0.11994	0.074687	0.000172	2.1302	2.0408	2.746	2.3544	7.7034	2.3022	76632586	3	3	3 yes		35	yes - 1 bad peptide	4	
142	PREDICTED: similar to FK506 binding protein 10 precursor (Peptidyl-prolyl cis-trans isomera	142	18.76	9	18	14618	0	0.000651	0.030293	1.49E-07	1.6931	1.2517	1.6965	1.4503	12.626	1.4294	76649693	3	3	3 yes		21	yes	4	
153	peroxiredoxin 1	153	17.53	9	16.569	11963	0	0.023436	0.023436	6.42E-10	2.5563	1.1233	3.0856	1.136	7.7625	1.1563	27806081	3	3	3 no			yes	4	
164	PREDICTED: similar to actinin, alpha 1	164	16.62	18	34.092	29154	0	0.008076	1.02E-05	3.29E-09	1.8563	1.8893	2.5497	1.6403	5.6691	1.8035	76628185	3	3	3 no		4	yes	4	
167	PREDICTED: similar to Galectin-3 (Galactose-specific lectin 3) (Mac-2 antigen) (IgE-binding	167	16.3	8	16	12370	0	0.000562	0.001783	2.9E-06	2.3742	1.3594	2.6648	1.5195	8.3384	1.4079	76688658	3	3	3 yes		22	yes	4	
170	PREDICTED: similar to tropomyosin 3 isoform 2 isoform 3 ; PREDICTED: similar to tropomyc	170	16.16	8	14.62	12127	0	0.022373	0.046875	0.046875	1.661	1.4002	2.7045	1.4671	8.4013	1.6908	76692107	3	3	3 yes		43	yes	4	
176	PREDICTED: similar to calumenin precursor isoform 4 ; PREDICTED: similar to calumenin p	176	15.52	8	15.523	12374	0	0.017795	0.020098	2.32E-05	1.5591	1.326	1.3968	1.2425	3.7044	1.332	76615719	3	0	3 yes		24	yes	4	
179	PREDICTED: similar to Glucose-6-phosphate isomerase (GPI) (Phosphoglucose isomerase)	179	15.21	7	12.523	12411	0	0.12535	0.030034	9.09E-05	1.9531	1.4992	3.1334	1.7972	9.8053	1.6067	76640989	3	3	3 yes		15	yes	4	
183	cathepsin B	183	14.92	8	14.921	15061	0	0.013107	0.008018	0.002864	1.884	1.4629	1.8471	1.4015	3.8361	1.8598	27606971	3	3	3 yes		15	yes	4	
188	cofilin 1 (non-muscle)	188	14.47	7	14	8867.7	0	0.1875	0.09375	0.09375	2.2288	1.7388	3.5561	1.7288	7.7197	2.394	62751777	3	3	3 no	yes		yes	4	
189	PREDICTED: similar to nucleophosmin 1 isoform 1	189	14.26	7	13.523	8918.1	0	0.1875	0.000883	6.01E-06	2.1552	1.2309	2.8719	1.2628	6.9095	1.2906	76625542	3	3	3 yes?		29	yes	4	
197	PREDICTED: similar to archain isoform 2 ; PREDICTED: similar to archain isoform 1 ; PRED	197	13.87	6	12	9767	0	0.040655	0.1493	0.005633	2.023	1.4753	2.9577	1.9991	8.7098	2.1411	76635418	3	3	3 yes		19	yes	4	
206	scinderin	206	13.03	8	12.887	11997	0	0.09375	0.0024	0.000151	2.1497	1.5883	3.3483	1.5714	7.5129	1.7946	27808415	3	3	3 yes		8	yes	4	
230	PREDICTED: similar to calmodulin 1 ; PREDICTED: similar to calmodulin 1	230	11.37	7	12.444	13079	0	0.016257	0.000604	0.000645	1.8846	1.408	2.9479	1.3706	6.5365	1.7402	76687664	3	3	3 yes		34	yes	4	
231	tyrosine 3-monooxygenase/tryptophan 5-monooxygenase activation protein, epsilon polypep	231	11.26	9	17.046	13701	0	0.000341	7.78E-06	6.1E-06	2.0746	1.3284	2.878	1.2808	7.2043	1.5649	27806197	3	3	3 yes		40	yes	4	
239	PREDICTED: similar to reticulocalbin 3, EF-hand calcium binding domain	239	10.71	5	9.3979	9462.7	0	0.27448	0.040982	5.66E-06	1.2521	1.146	1.5763	1.1459	6.1022	1.0839	76642117	0	3	3 yes		24	yes	4	
240	peroxiredoxin 2	240	10.66	5	10	10284	0	0.22797	0.19271	0.000319	2.1569	1.0671	3.3397	1.0899	9.669	1.3207	27807469	3	3	3 yes		43	yes	4	
242	PREDICTED: similar to ubiquitin C isoform 11 ; PREDICTED: similar to ubiquitin C isoform 1	242	10.63	6	10.046	9077.1	0	0.000436	0.000524	0.1875	2.256	1.1617	3.0429	1.2676	4.5454	1.3353	76638714	3	3	3 yes		76	yes	4	
244	PREDICTED: similar to myosin, heavy polypeptide 9, non-muscle, partial	244	10.5	6	10.268	9575.3	0	0.1875	0.1875	0.000258	1.849	1.25	2.5953	1.339	3.2195	1.2404	76680332	3	3	3 yes		3	yes	4	
250	tyrosine 3-monooxygenase/tryptophan 5-monooxygenase activation protein, gamma polypep	250	10.14	8	15.046	11326	0	6.47E-05	1.68E-05	8.81E-06	2.1516	1.2158	3.0706	1.2639	8.799	1.5109	27807401	3	3	3 yes	gamma		yes	4	
252	GDP dissociation inhibitor 1	252	10.14	9	16.092	14227	0	0.18261	0.088619	0.000781	1.9755	2.0381	2.284	2.0684	6.617	2.2852	27806617	3	3	3 yes		30	yes	4	
253	PREDICTED: similar to Lamin B1	253	10.05	6	10.046	9205.1	0	0.1875	0.1875	0.000249	3.4268	2.7433	4.8478	2.6455	4.3337	1.1847	76660399	3	3	3 yes		7	yes - 1 bad peptide	4	
256	thioredoxin	256	10	7	13	11665	0	1.875	0.65625	0.091368	2.2511	4.035	3.3359	4.0626	7.5001	4.8869	27806783	3	3	3 yes		40	yes	4	
270	PREDICTED: similar to WD-repeat protein 1 (Actin interacting protein 1) (AIP1) (NORI-1)	270	9.3	5	9	8730.6	0	0.55224	0.05786	0.020084	1.5135	1.522	2.7414	1.6237	5.7243	1.8675	76620344	3	3	3 yes		7	yes	4	
272	PREDICTED: similar to Cystatin B (Liver thiol proteinase inhibitor) (CPI-B) (Stefin B)	272	9.27	5	9.0458	8171	0	0.14238	0.005687	0.000391	1.5393	1.3119	2.3943	1.2508	4.4906	1.214	76608395	3	3	3 no	E/M/C		yes	4	
273	peroxiredoxin 4	273	9.09	8	14.824	13903	0	0.09375	0.09375	0.000454	2.3337	1.6363	2.4799	1.6229	5.0508	1.7442	27806085	3	3	3 yes		46	yes	4	
274	PREDICTED: similar to endoplasmic reticulum protein 29 precursor	274	9.05	5	9.0458	7375.9	0	0.21565	0.10492	0.001511	1.9703	1.6289	2.6213	1.7367	12.816	1.5905	76639231	3	3	3 yes		14	yes	4	
282	PREDICTED: similar to Reticulocalbin-1 precursor, partial	282	8.64	4	8	6637.6	0	0.31649	0.17	0.002397	1.2692	1.1655	1.2795	1.1318	4.3057	1.1804	76672694	0	0	3 yes		21	yes	4	
283	hepatoma-derived growth factor (high-mobility group protein 1-like)	283	8.64	4	8	7691.8	0	0.049039	0.14586	0.037671	2.6498	1.3642	2.8955	1.6549	10.145	1.9603	28461287	3	3	3 yes		11	yes	4	
285	PREDICTED: similar to Reticulocalbin-2 precursor (Calcium-binding protein ERC-55) (Taipo>	285	8.62	4	8	8991.6	0	0.27874	0.14536	0.003827	1.8357	1.265	1.7525	1.1666	8.005	1.3186	76647200	3	3	3 yes		22	yes	4	
291	PREDICTED: similar to Puromycin-sensitive aminopeptidase (PSA) isoform 2 ; PREDICTED	291	8.3	4	7.5229	6430.5	0	0.78555	0.47481	0.22049	1.8361	1.8016	2.4148	1.9611	5.1362	2.4817	76644640	3	3	3 yes		4	yes/poor quant	4	
292	ribosomal protein L10e	292	8.26	4	8	6765.1	0	0.018375	0.017548	0.002274	2.0153	1.172	2.4804	1.2245	12.016	1.3198	62751847	3	3	3 yes		10	yes	4	
296	PREDICTED: similar to serine/threonine protein kinase MASK, partial	296	8.15	4	8	6693.4	0	0.039076	1.4025	0.033259	1.8124	1.1912	1.7448	1.7713	15.02	2.1246	76678376	3	3	3 yes		5	yes	4	
298	PREDICTED: similar to Filamin A (Alpha-filamin) (Filamin 1) (Endothelial actin-binding protei	298	8.14	5	9.5229	8435	0	0.085864	0.006172	0.002771	1.9427	1.4304	2.9176	1.3233	4.717	1.3906	76658941	3	3	3 yes		3	yes	4	
301	PREDICTED: similar to cytoplasmic beta-actin isoform 1 ; PREDICTED: similar to cytoplasm	301	8	12	24	24085	0	1.59E-06	1.87E-06	1.29E-09	2.0749	1.2209	2.3648	1.2707	9.4525	1.4296	76645442	3	3	3 yes		42	yes	4	
315	PREDICTED: similar to Phosphoacetylglucosamine mutase (PAGM) (Acetylglucosamine phc	315	7.5	4	7.0458	6445.9	0	0.27536	0.094967	0.02808	2.012	1.5285	2.2147	1.3789	5.2864	1.5306	76625467	3	3	3 yes		10	yes	4	
316	heat shock 27kDa protein 1	316	7.4	3	6	5496.2	0	0.18017	2.5651	0.047289	1.6044	1.1563	1.5029	2.0433	14.021	1.5044	71037405	3	3	3 yes		21	yes	4	
320	PREDICTED: similar to Proteasome subunit alpha type 6 (Proteasome iota chain) (Macropai	320	7.3	4	7.301	6103.7	0	0.053133	0.76143	0.009794	1.3775	1.054	1.9599	1.5844	6.2095	1.3961	76647405	3	3	3 yes		15	yes/poor quant	4	
324	superoxide dismutase 1, soluble ; PREDICTED: similar to Superoxide dismutase	324	7.13	3	6	5039.6	0	0.36942	0.48206	0.15292	3.0198	1.6459	3.006	1.7782	7.2872	1.7506	27807109	3	3	3 yes		16	yes	4	
327	ribosomal protein S12	327	7.05	4	7.0458	6262.4	0	0.81492	0.3663	0.024836	2.2231	1.7678	2.8801	1.6076	10.485	1.8051	62461611	3	3	3 yes		29	yes	4	
330	heat shock 10kDa protein 1 (chaperonin 10)	330	6.98	3	6	4060.3	0	1.6826	1.1892	0.85665	1.6105	1.7564	2.3916	2.2165	4.4957	3.0218	27805927	0	0	3 no			yes	4	
337	PREDICTED: similar to F-actin capping protein alpha-1 subunit (CapZ alpha-1) isoform 1 ; PI	337	6.76	3	6	5430.9	0	1.1883	6	0.70932	1.9887	1.367	3.3439	1	7.081	1.6821	61821561	1	1	1 no		13	yes	4	
343	PREDICTED: similar to Translational endoplasmic reticulum ATPase (TER ATPase) (15S Mg(	343	6.38	3	5.3979	5271.1	0	2.2566	6	0.27863	3.1228	2.9448	1.9795	1	8.3156	2.2692	76624455	3	3	3 no			yes / poor quant	4	
344	PREDICTED: similar to leucine proline-enriched proteoglycan (leprecan) 1 isoform 3 ; PRED	344	6.36	3	5.0458	5166.4	0	0.20288	0.091228	0.092119	1.6785	1.1844	1.6744	1.1178	4.7585	1.4031	76672344	0	3	3 yes		7	yes	4	
347	UDP-glucose dehydrogenase	347	6.33	3	6	6035.9	0	1.1045	0.20502	0.05181	2.5442	1.4812	2.524	1.0729	5.8242	1.3304	27806365	1	1	1 yes		11	yes	4	
354	heat shock 70 kD protein 3	354	6.14	12	23.523	20510	0	0.000139	3.47E-05	1.92E-07	2.5057	1.5095	2.7972	1.4821	7.5505	1.6738	41386899	1	1	1 no		4	yes	4	
358	PREDICTED: similar to MIR-interacting saposin-like protein precursor (Transmembrane prot	358	6.12	3	6	5172.9	0	0.57325	0.47248	0.061504	1.3996	1.2143	1.9572	1.4152	6.8967	1.4088	61813920	3	3	3 yes		27	yes	4	
369	PREDICTED: similar to Leukotriene A-4 hydrolase (LTA-4 hydrolase) (Leukotriene A(4) hydr	369	6	3	5	5323	0	6	6	0.20347	1.1717	1	1.5383	1	9.5211	2.0911	76618917	3	3	3 yes		4	yes/poor quant	4	
370	chloride intracellular channel 1	370	6	3	6	4328.3	0	1.6238	1.4661	0.086409	2.6224	1.8538	2.3352	1.6231	6.2524	1.4699	62751970	3	3	3 yes		11	yes	4	
373	gelsolin-like capping protein	373	6	3	6	5807.1	0	0.9385	0.2504	0.069861	1.2629	1.1996	1.723	1.2199	3.2278	1.2472	30468254	1	1	1 yes		13	yes	4	
380	PREDICTED: similar to Tumor necrosis factor receptor superfamily member 11B precursor (1	380	5.84	3	5.0458	4694.5	0	0.30287	0.15575	0.06267	2.8361	1.5247	1.7291	1.1687	4.2168	1.2927	76634663	3	0	3 yes		10	yes	4	
385	PREDICTED: similar to NG,NG-dimethylarginine dimethylaminohydrolase 1 (Dimethylarginin	385	5.68	3	5.3979	4636.6	0	0.31163	0.02152	0.016733	1.9391	1.3128	3.0909	1.1245	11.692	1.2528	76613543	3	3	3 yes		21	yes	4	
387	PREDICTED: similar to splicing factor, arginine/serine-rich 1 (ASF/SF2)	387	5.61	3	5.0458	4394.2	0	0.26775	0.32156	0.22339	2.3317	1.3779	2.944	1.5704	8.798	2.1122	76642711	3	3	3 yes		19	yes	4	
388	prosaposin	388	5.59	2	4	3007.6	0	0.96559	0.80702	0.18094	1.4822	1.1546	1.5784	1.109	3.298	1.0833	27806447	3	3	3 yes		14	yes	4	
390	PREDICTED: similar to Proteasome subunit alpha type 3 (Proteasome component C8) (Mac	390	5.54	3	5.3979	5293.3	0	6	1.5105	0.52992	1.8033	1	4.2121	2.337	8.5603	3.2714	76627984	3	0	3 yes		10	yes/poor quant	4	
397	ARP3 (actin-related protein 3, yeast) homolog	397	5.4	3	5.3979	5776	0	1.6467	0.18728	0.067529	2.3506	1.7436	2.5356	1.3385	8.5111	1.4871	27808335	1	1	1 no			yes	4	
399	PREDICTED: similar to Heterogeneous nuclear ribonucleoprotein G (hnRNP G) (RNA-bindin	399	5.33	3	4.0915	4078.2	0	0.16077	0.44384	0.25422	2.6446	1.0596	2.5816	1.1695	6.8066	1.1982	76658701	3	3	3 no			yes	4	
400	aminotransferase 1] [glutamic-oxaloacetic transaminase 1, soluble] [Bos taurus]	400	5.28	3	5	5463.1	0	0.682	0.71452	0.31761	1.9763	1.5463	2.523	1.8385	7.8441	2.3267	29135295	3	3	3 yes		9	yes	4	
409	myosin, light peptide 6, alkali, smooth muscle and non-muscle	409	4.82	2	4	2197.1	0	0.83517	0.41146	0.31312	2.1931	1.2799	2.8352	1.179	8.3223	1.2775	28461187	3	3	3 no			yes	4	
414	PREDICTED: similar to Thioredoxin domain containing protein 4 precursor (Endoplasmic reti	414	4.64	2	4	3157.6	0	6	6	6	1.704	1	1.8252	1	4.135	1	76655551	3	3	3 yes		15	yes/poor quant	4	
415	PREDICTED: similar to vesicle amine transport protein 1 homolog (T californica) isoform 3 ; I	415	4.64	2	4	3302.6	0	1.3687	0.079597	0.1319	1.2157	1.109	2.4363	1.0266	5.3316	1.0852	76671280	1	1	1 yes		5	yes/poor quant	4	
426	PREDICTED: similar to 1-phosphatidylinositol-4,5-biphosphate phosphodiesterase delta 1 (	426	4.34	2	4	3584.7	0	6	6	0.30482	2.6082	1	2.3412	1	6.9055	1.2443	76648298	3	3	3 no			yes/very poor quan	4	
430	PREDICTED: similar to FK506 binding protein 14 precursor (Peptidyl-prolyl cis-trans isomera	430	4.33	2	4	3516	0	6	1.4401	0.38829	1.2847	1	1.2704	1.1434	5.0878	1.2645	76615394	1	1	1 yes		11	check	4	
436	tyrosine 3-monooxygenase/tryptophan 5-monooxygenase activation protein, beta polypeptid	436	4.2	9	16.569	12285	0	2.08E-05	2.72E-06	0.023438	2.0629	1.2123	3.0727	1.2577	8.213	1.4412	27807403	3	3	3 no		3	yes	4	
449	PREDICTED: similar to Bifunctional 3-phosphoadenosine 5-phosphosulfate synthethase 2 (F	449	4	2	4	4180	0	6	6	0.19145	1.834467	1	2.103562	1	6.386901	1	76671596	1	1	1 yes		8	yes/very poor quan	4	
456	lectin, galactoside-binding, soluble, 1 (galectin 1)	456	4	2	4	3975	0	1.3374	0.38982	0.46768	1.9208	1.4009	2.8402	1.1632	7.1748	1.4091	28461189	3	3	3 yes		30	yes	4	
459	PREDICTED: similar to D-dopachrome tautomerase (Phenylpyruvate tautomerase II)	459	4	2	4	2402.4	0	0.25204	6	1.2668	1.906	1.0621	4.0193	1	7.5815	2.6818	76639463	3	3	3 yes		17	yes/poor quant	4	
462	S100 calcium-binding protein A10	462	4	2	4	3909.3	0	1.279	0.17852	0.62847	1.8077	1.3382	2.3001	1.0566	5.8581	1.5145	27807173	3	3	3 no			yes	4	
464	thymosin beta 4	464	4	2	4	2799.4	0	1.1865	0.81692	0.16622	1.4019	1.1657	1.6312	1.1622	14.122	1.1771	50872141	3	3	3 yes		12	yes/?	4	
467	PREDICTED: similar to Calgizzarin (S100 calcium-binding protein A11) (S100C protein) (MLI	467	4	2	4	3023.4	0	6	6	0.99397	1.5366	1	2.2812	1	7.8459	2.1721	76612513	3	3	3 yes		5	poor quant	4	
467	PREDICTED: similar to tissue specific transplantation antigen P35B	467	4	2	4	2970.4	0	1.3264	1.872	0.14098	3.0461	1.7685	2.5851	2.0474	8.7852	1.1217	76634698	1	1	1 yes		6	yes	4	
490	PREDICTED: similar to SWAP-70 protein, partial	490	4	2	4	3008.3	0	0.62087	0.67752	0.73847	3.1925	1.3089	2.5562	1.2686	9.5271	1.8686	76635779	1	1	1 no		1	yes	4	
503	protein O-fucosyltransferase 1	503	3.6	2	3	3507.8	0	6	6	0.79741	1.2391	1	2.8236	1	10.435	2.019	33695127	1	1	1 yes		5	yes/poor quant	4	
519	PREDICTED: similar to ubiquitin-conjugating enzyme E2N (homologous to yeast UBC13) iso	519	3.4	2	3.3979	4328.5	0	1.0442	0.63627	0.84479	1.7214	1.2403	2.9704	1.2955	7.7324	1.9163	76617540	3	3	3 yes		7	yes/poor id	4	
550	PREDICTED: similar to RAB1, member RAS oncogene family isoform 4 ; PREDICTED: simil	550	3	2	3	3468.1	0	1.2312	1.5792	0.17069	1.645	1.265	2.2274	1.6436	9.0551	1.1495	76629647	3	3	3 no			yes/poor quant	4	
555	PREDICTED: similar to high-mobility group box 2 isoform 23 ; PREDICTED: similar to high-m	555	7.65	4	7.0458	8196.3	0	1.948	1.4728	0.081262	1.5032	1.7249	1.6153	1.3169	6.493	2.0427	28461287	3	3	3 no		11	yes	4	
556	inhibin beta A	633	6.58	4	6.4437	6131.6	0	5.9854	3.3488	0.089372	1.005	2.1782	1.4823	2.661	10.466	2.5296	27805949	1	1	3 yes		6	yes	4	
562	PREDICTED: similar to Plasminogen activator inhibitor 1 RNA-binding protein (PAI1 RNA-bir	316	7.05	4	7.0458	5714.2	0	0.36498	0.67567	0.005656	2.42	1.4856	1.7741	1.4402	6.1185	1.3162	76625300	1	1	1 yes		4	yes	4	
564	PREDICTED: similar to heterogeneous nuclear ribonucleoprotein C isoform b isoform 6 ; PR	348	6	3	5.3979	4639.8	0	1.4229	1.3774	0.79472	2.5612	2.6545	2.6037	2.6374	6.3839	3.6752	76627027	1	1	1 no			yes -one bad peptic	4	
569	PREDICTED: similar to 14-3-3 protein theta (14-3-3 protein tau) (14-3-3 protein T-cell) (HS1	392	4.66	7	13.523	9824.4	0	0.02932	0.007911	0.002615	2.642	1.8086	3.1982	1.7235	8.8341	2.2883	76630316	1	1	1 no			yes/ poor quant	4	
573	PREDICTED: similar to actin related protein 2/3 complex, subunit 4	415	4.12	2	4	2564.5	0	6	0.32844	0.15279	1.5989	1	2.5725	1.1221	7.6375	1.122	76648493	1	1	1 yes		7	yes /poor quant	4	
579	PREDICTED: similar to CG11577-PA	436	4	2	4	3190.2	0	6	6	0.081278	1.8209	1	3.0006	1	10.113	1.0721	61866984	1	1	1 no			one low	4	

order	Protein Name	protein #	score	peptides	score 2	mass cov	outliers	pval 118	pval 116	pval 117	116:114	SD	116:114	SD	117:114	SD	Accessior	sig 116	sig116	sig117	SM-ID	coverage	manuel	Indexer k6
593	PREDICTED: similar to Testican-1 precursor (SPOCK protein), partial	471	3.52	2	3.5229	2823.7	0	0.68624	0.65664	0.18089	1.9204	1.1825	2.2116	1.2152	11.452	1.1775	27806687	1	1	1	yes	9	yes	4
605	PREDICTED: similar to SEC31-like 1 isoform 2	579	2.6	1	2	1447.7	0	6	6	6	1.7568	1	2.502	1	11.671	1	76860845	3	3	3	yes	2	one good	4
619	plectin 7 ; plectin 5 ; plectin 3 ; plectin 11 ; plectin 1 ; plectin 10 ; plectin 4 ; plectin 9 ; plectin :	206	8.27	3	5.3979	4739.8	0	0.57463	0.3089	0.48091	2.0239	1.1632	3.0224	1.1352	4.9873	2.3147	gi|40849920; gi|40849916; gi|40849890; gi|4	no						4
7	albumin	7	96.49	52	102.44	88672	0	3.36E-27	1.44E-32	1.78E-09	13.8	2.2347	43.125	2.481	2.4791	2.0395	30794280	3	3	3	yes	59	yes	5
13	PREDICTED: similar to Complement factor B precursor (C3/C5 convertase)	13	75.08	35	68.745	60808	1	5.31E-17	2.65E-15	0.000873	27.733	3.2967	24.001	3.514	2.6215	2.913	76650936	3	3	3	yes	47	yes	5
25	PREDICTED: similar to Complement C3 precursor isoform 1	25	55.54	29	53.405	47320	0	9.55E-18	7.64E-20	0.023691	7.7038	1.6898	12.993	1.7432	1.2815	1.447	76822034	3	3	3	yes	14	yes	5
26	PREDICTED: similar to Stromelysin-1 precursor (Matrix metalloproteinase-3) (MMP-3) (Tran	26	52.84	30	58.046	44259	0	3.52E-17	3.88E-13	5.63E-13	28.033	2.485	7.7705	2.1675	6.792	2.0838	61863538	3	3	3	yes	47	yes	5
29	PREDICTED: similar to chitinase 3-like 1 isoform 2	29	51.94	34	65.319	61405	0	1.11E-26	5.62E-21	3.38E-10	27.915	1.7561	13.279	1.8815	3.4717	2.0121	76836770	3	3	3	yes	67	yes	5
32	PREDICTED: similar to Complement C1r subcomponent precursor (Complement component	32	49.23	24	48	43922	0	4.39E-15	3.2E-14	2.72E-08	17.424	1.9464	9.5883	1.7649	3.1791	1.9684	76816391	3	3	3	yes	3	yes	5
34	PREDICTED: similar to extracellular matrix protein 1 isoform 1 precursor isoform 14 ; PREDI	34	48.62	26	49.489	50817	0	4.98E-05	1.56E-13	0.000163	26.937	2.2552	12.071	2.1767	2.6722	2.3007	76812740	3	3	3	yes	43	yes	5
59	PREDICTED: similar to Haptoglobin precursor isoform 4	59	36.03	18	34.589	27582	0	2.5E-08	4.3E-07	0.011921	42.035	4.2707	17.256	3.8335	3.4082	3.7186	76840813	3	3	3	yes	41	yes	5
69	serum amyloid A 3	69	32.19	20	37.569	28809	0	4.05E-13	9.37E-12	0.002989	34.317	2.2797	22.488	2.3733	2.7865	2.5288	38566896	3	3	3	yes	61	yes	5
83	matrix metalloproteinase 9 (gelatinase B, 92kDa matrix metalloproteinase 9 (gelatinase B, 92	83	26.75	14	26.092	23947	0	2.02E-07	4.31E-09	0.00014	5.5756	1.7464	6.8015	1.574	1.9893	1.4069	27807437	3	3	3	yes	12	yes	5
115	vascular cell adhesion molecule 1	115	22.36	12	21.589	19319	0	2.15E-05	2.33E-05	0.021812	15.135	2.6794	25.83	2.8245	3.5165	1.8201	41386707	3	3	3	yes	9	yes	5
122	PREDICTED: similar to insulin-like growth factor binding protein 5 isoform 1 ; PREDICTED: s	122	21.35	10	20	16040	0	8.13E-06	3.78E-06	0.040525	4.7706	1.4446	7.1549	1.6594	2.223	1.9377	76810359	3	3	3	yes	30	yes	5
134	lactoferrin [lactotransferrin] [Bos taurus]	134	20.11	10	20	16103	0	7.59E-06	8.09E-05	0.010457	17.533	2.2259	8.4221	2.2077	1.8144	1.4741	30794292	3	3	3	yes	12	yes	5
154	matrix metalloproteinase 13 (collagenase 3)	154	11.52	5	10	9438.5	0	0.009601	0.027022	0.057845	36.035	2.8668	19.221	3.1497	4.1771	1.6212	27805999	3	3	3	yes	12	yes	5
162	PREDICTED: similar to Chitinase 3-like protein 2 precursor (YKL-39) (Chondrocyte protein 3	162	16.66	8	16	13218	0	1.35E-08	7.62E-06	0.002529	36.035	1.6774	14.19	1.6369	2.218	1.4335	76813223	3	3	3	yes	16	yes	5
166	secreted phosphoprotein 1	166	16.33	8	16	15227	0	0.00119	0.046875	0.046875	21.672	3.4218	18.165	2.9584	18.777	3.059	27806401	3	3	3	yes	50	yes	5
173	PREDICTED: similar to latent transforming growth factor beta binding protein 1 isoform LTBF	173	15.76	17	29.967	29750	0	3.34E-07	2.42E-07	0.023186	8.4893	2.5296	7.2501	2.3157	1.8371	2.0401	76829029	3	3	3	yes	16	yes	5
178	pleiotrophin [heparin binding growth factor 8, neurite growth-promoting factor 1] [Bos taurus]	178	15.23	8	14.569	11570	0	1.14E-06	9.85E-06	0.036897	9.8194	1.3798	4.4331	1.3316	1.3697	1.2587	27806813	3	3	3	yes	38	yes	5
186	latent transforming growth factor beta binding protein 2 (NOTE:redefinition of symbol)	186	14.72	7	13.046	10673	0	0.005294	0.033508	0.29028	10.281	2.7485	3.9275	2.3595	1.3695	1.3451	27805991	3	3	3	yes	4	yes	5
219	vanin 1 precursor	219	12.14	6	11.523	9701.9	0	0.001091	0.004265	0.018554	21.035	2.1295	5.7239	1.7821	3.0505	1.6463	66792902	3	3	3	yes	12	yes	5
221	matrix metalloproteinase 1	221	12.13	7	10.717	11364	0	0.001136	0.090936	0.099695	11.257	2.2042	5.1186	1.9145	2.601	1.4817	27808541	3	3	3	yes	16	yes	5
232	insulin-like growth factor binding protein 3	232	11.25	5	10	7849	0	0.001723	0.004695	0.10359	8.8309	1.5066	6.0226	1.2915	5.4864	2.0343	27807007	3	3	3	yes	25	yes	5
235	PREDICTED: similar to lipopolysaccharide-binding protein precursor isoform 1 ; PREDICTEI	235	11.05	6	11.048	11006	0	0.002099	0.25837	6	44.095	2.9386	11.748	2.4977	2.4186	1	76833538	3	3	3	yes	44	yes	5
258	CD14 antigen	258	9.97	5	9.5229	7257	0	0.020509	0.025368	0.64504	12.808	2.5042	12.036	2.5832	4.0657	2.3826	41386760	3	3	3	yes	13	yes	5
307	PREDICTED: similar to Alpha-1-acid glycoprotein 1 precursor (AGP 1) (Orosomucoid 1) (OM	307	7.68	4	7.0458	5378.8	0	0.17749	0.19308	1.852	35.891	6.2221	36.859	6.7026	3.1865	4.4081	76625309	3	3	3	yes	21	yes - 1 bad peptide	5
346	PREDICTED: similar to N-acetylmuramoyl-L-alanine amidase precursor (Peptidoglycan reco	346	6.34	3	6	5996.5	0	0.60896	0.18647	2.0549	3.2954	2.0412	19.7	2.5396	1.8688	2.4049	76621288	3	3	3	yes	11	yes	5
349	PREDICTED: similar to Putative serum amyloid A-3 protein	349	6.28	11	21	15136	0	1.52E-07	5.22E-07	0.065925	30.296	2.0741	17.03	1.9928	2.2204	2.0667	76691395	3	3	3	no		yes	5
392	superoxide dismutase 2, mitochondrial	392	5.52	3	5.5229	4137	0	0.0679	0.058366	0.024124	12.342	1.5952	16.954	1.6277	6.1812	1.2222	41529822	3	3	3	yes	12	yes	5
451	PREDICTED: similar to ICOS ligand precursor (B7 homolog 2) (B7-H2) (B7-like protein Gl50)	451	4	2	4	2344.2	0	0.2047	0.25208	3.5176	7.5748	1.166	9.7855	1.2376	0.90017	1.2161	76808586	3	3	0	yes	5	yes	5
452	CD44 antigen [homing function and Indian blood group system] [Bos taurus]	452	4	3	6	4540.6	0	0.003789	0.024838	0.40004	7.9181	1.0029	10.579	1.0219	1.7514	1.0869	27806703	3	3	3	yes	5	yes	5
453	PREDICTED: similar to oncostatin M receptor, partial	453	4	2	4	3644	0	0.14057	0.28116	0.12327	10.656	1.1311	14.529	1.3219	7.9623	1.0994	76846489	3	3	3	yes	3	yes	5
454	chemokine (C-C motif) ligand 20	454	4	2	4	2401.3	0	0.38385	0.26072	6	57.082	1.7801	11.83	1.2698	1.0899	1	27806273	3	3	3	yes	16	yes	5
492	chemokine (C-C motif) ligand 5	492	4	2	4	3425.8	0	2.4277	1.2394	2.5787	2.6593	2.7743	33.736	5.3323	2.682	3.0557	28461277	0	3	0	no		yes	5
515	colony stimulating factor 1 (macrophage)	515	3.44	2	3.0458	2527.5	0	1.2052	1.1566	6	9.2933	2.7986	16.5	3.4504	1.396	1	27806879	3	3	0	yes	3	yes	5
522	chemokine (C-C motif) ligand 2	522	3.39	2	3.0458	3060.6	0	0.5464	0.73141	1.5622	7.163	1.4934	8.1491	1.7774	2.6496	1.8171	27806711	3	3	3	yes	14	yes	5
529	interleukin 6 (interferon, beta 2)	529	3.22	2	3.2218	3525.2	0	0.29186	0.24311	6	125.52	1.6874	26.379	1.3431	1	1	27806867	1	1	1	yes	12	yes	5
541	alpha-2-plasmin inhibitor	541	3.05	2	3.0458	2446.5	0	0.23683	0.42677	1.9454	15.428	1.2715	12.545	1.4938	4.3999	3.2224	27807209	1	1	1	yes	3	yes	5
633	PREDICTED: similar to chemokine (C-X3-C motif) ligand 1, partial	574	2.64	2	2	2054.8	0	6	6	6	5.2628	1	7.5261	1	3.1734	1	76682374	3	3	3	yes	20	yes - good id by 2	5
42	PREDICTED: similar to Pyruvate kinase, isozymes M1/M2 (Pyruvate kinase muscle isozyme	42	41.56	20	38.143	35709	0	0.001758	3.36E-07	3.15E-10	3.8482	1.8837	5.2343	1.9499	13.88	2.1582	76626899	3	3	3	yes	38	yes	6
43	PREDICTED: similar to phosphoglycerate kinase 1 isoform 3 ; PREDICTED: similar to phosp	43	41.45	22	40.86	34191	0	1.87E-08	8.27E-11	2.01E-15	3.1415	1.6888	4.311	1.5826	17.103	1.8049	76879981	3	3	3	yes	49	yes	6
45	PREDICTED: similar to Protein disulfide-isomerase A4 precursor (Protein ERp-72) (ERp72) (	45	39.83	20	37.489	34307	0	0.001179	1.14E-08	3.79E-13	2.1654	1.51	3.0406	1.5066	12.221	1.7883	76616203	3	3	3	yes	28	yes	6
47	heat shock 90kD protein 1, alpha	47	38.6	20	37.967	33941	0	1.1E-09	2E-11	2.64E-14	3.9242	1.5945	5.117	1.5493	12.448	1.6585	60592792	3	3	3	yes	29	yes	6
51	triosephosphate isomerase	51	37.61	19	37.097	30762	0	1.06E-10	2.36E-14	1.12E-14	2.9952	1.3839	4.5134	1.3144	9.9139	1.4896	61888856	3	3	3	yes	60	yes	6
63	UDP-glucose pyrophosphorylase 2	63	33.81	17	32	27938	0	0.001009	0.001465	0.001758	3.0746	2.3549	3.1054	1.7927	14.252	2.1232	41386780	3	3	3	yes	42	yes	6
65	PREDICTED: similar to nucleolin-related protein isoform 5 ; PREDICTED: similar to nucleolin	65	32.89	16	30.589	23811	0	2.27E-10	6.49E-11	4.66E-14	4.1137	1.3995	6.1708	1.4864	22.201	1.509	76682888	3	3	3	yes	21	yes	6
74	lactate dehydrogenase A	74	30.25	16	28.535	23252	0	9.12E-09	2.25E-09	0.002627	2.7646	1.3691	3.8254	1.4548	11.131	1.4917	27806559	3	3	3	yes	44	yes	6
76	PREDICTED: similar to transaldolase 1 isoform 1	76	27.86	14	26.62	19426	0	6.58E-06	3.87E-07	0.000732	3.0923	1.6404	4.4179	1.664	17.262	1.7348	76658465	3	3	3	yes	33	yes	6
79	transketolase	79	27.17	14	25.523	23238	0	1.9E-06	5.53E-07	1.75E-09	3.9754	1.5518	5.9628	1.6553	14.894	1.8121	51491841	3	3	3	yes	26	yes	6
86	PREDICTED: similar to phosphoglycerate mutase 1 like a isoform 6 ; PREDICTED: similar to	86	26.57	15	28.569	29874	0	9.21E-07	1.31E-08	1.24E-12	3.0427	1.5079	4.0101	1.4328	12.356	1.4399	76654685	3	3	3	yes	56	yes	6
106	tyrosine 3-monooxygenase/tryptophan 5-monooxygenase activation protein, zeta polypeptide	106	24.01	12	23.046	18300	0	3.71E-06	3.62E-08	5.53E-09	2.38	1.3432	3.5355	1.316	9.5453	1.5085	27807367	3	3	3	yes	40	yes	6
109	enolase 1	109	23.69	11	21.046	19284	0	7.6E-05	0.058594	3.35E-05	4.2717	1.8349	3.4549	2.4551	9.4742	2.3559	27806645	3	3	3	yes	54	yes	6
113	PREDICTED: similar to Protein disulfide-isomerase A6 precursor (Thioredoxin domain contai	113	23.09	10	20	18120	0	0.008166	0.004487	3.58E-05	4.9315	2.7127	5.6337	2.6714	15.588	2.5188	76630220	3	3	3	yes	30	yes/ poor quant	6
130	Parkinson disease (autosomal recessive, early onset) 7	130	20.52	11	20.523	17520	0	0.002799	0.000202	9.99E-07	2.9185	1.8849	4.8472	1.9303	14.892	2.0204	62751849	3	3	3	yes	41	yes	6
146	PREDICTED: similar to Tubulin alpha-2 chain (Alpha-tubulin 2) isoform 8 ; PREDICTED: sim	146	18.83	10	19.398	18981	0	0.007919	0.002061	0.025438	2.5775	1.6818	3.005	1.6189	12.588	1.7519	76618145	3	3	3	yes	25	yes	6
149	PREDICTED: similar to Heterogeneous nuclear ribonucleoproteins A2/B1 (hnRNP A2 / hnR	149	18.31	9	17.699	15650	0	0.023438	0.000268	0.001011	3.1215	2.1902	3.0399	1.4217	13.985	3.3139	76682749	3	3	3	yes	7	yes	6
157	anti-oxidant protein 2 (non-selenium glutathione peroxidase, acidic calcium-independent pho	157	17.33	8	15.222	11913	0	0.003934	2.34E-05	2.74E-05	2.9028	1.4146	4.2395	1.1776	11.588	1.5194	27807167	3	3	3	yes	33	yes	6
158	PREDICTED: similar to Cathepsin H precursor	158	17.17	8	15.046	12222	0	0.001851	0.000998	3.43E-06	2.9938	1.4785	3.2266	1.4533	14.536	1.5566	76847098	3	3	3	yes	22	yes	6
168	lactate dehydrogenase B	168	16.28	12	21.012	17690	0	2.66E-08	1.43E-06	7.1E-09	2.4717	1.2989	3.3206	1.3837	11.808	1.585	27806561	3	3	3	no		yes	6
174	PREDICTED: similar to heterogeneous nuclear ribonucleoprotein D isoform c isoform 13 ; PF	174	15.85	8	15.523	13640	0	0.003456	0.00076	2.28E-05	6.2452	2.0813	8.7929	1.9356	21.385	1.9515	76620256	3	3	3	yes	8	yes	6
180	PREDICTED: similar to Alcohol dehydrogenase [NADP+] (Aldehyde reductase) (Aldo-keto re	180	15.17	8	14.097	10520	0	0.000597	7.11E-05	3.95E-06	2.5434	1.3122	3.9897	1.4286	11.856	1.5179	76890510	3	3	3	no		yes	6
190	serine (or cysteine) proteinase inhibitor, clade B (ovalbumin), member 6	190	14.22	7	13.046	13705	0	0.00877	0.022379	0.008166	2.6905	1.4676	4.1319	1.9733	8.5335	2.266	27807517	3	3	3	yes	24	yes	6
194	annexin A8	194	14	7	14	10267	0	0.001238	0.000237	6.37E-05	2.9963	1.4389	5.537	1.5273	5.5473	1.4019	27806317	3	3	3	yes	26	yes	6
202	PREDICTED: similar to Phosphatidylethanolamine-binding protein (PEBP) (Prostatic binding	202	13.26	7	13.046	13058	0	5.54E-05	7.82E-05	5.86E-06	3.1745	1.2491	4.4369	1.3557	12.705	1.3968	76639068	3	3	3	yes	60	yes	6
207	connective tissue growth factor	207	13	7	13	10899	0	0.00098	0.09375	0.001782	5.9987	1.7675	4.3548	1.5696	5.7014	1.8524	27806677	3	3	3	yes	17	yes	6
211	PREDICTED: similar to Malate dehydrogenase, cytoplasmic isoform 1	211	12.81	5	9.3979	9274	0	0.051518	0.011623	0.000554	2.5966	1.3628	4.8755	1.5318	15.895	1.4789	61856478	3	3	3	no		yes	6
220	PREDICTED: similar to Fascin (Singed-like protein) (55 kDa actin bundling protein) (p55) (so	220	12.13	6	11.301	8563.8	0	0.006765	0.001296	0.000179	2.7107	1.4406	4.4201	1.4656	9.7656	1.4765	76654327	3	3	3	yes	11	yes	6
223	high-mobility group box 1	223	12	5	10	9245.6	0	0.015485	0.015447	0.000685	3.3754	1.2968	4.4589	1.3759	9.5795	1.3934	41386729	3	3	3	yes	33	yes	6
229	isocitrate dehydrogenase 1 (NADP+), soluble	229	11.38	6	11.046	9252	0	0.08799	0.049048	0.002358	3.0437	1.8308	4.3718	2.3482	11.187	2.0231	30794318	3	3	3	yes	15	yes	6
233	PREDICTED: similar to serine (or cysteine) proteinase inhibitor, clade B (ovalbumin), membe	233	11.16	5	9.0458	8717.2	0	0.00421	0.002966	0.00033	3.1448	1.3117	3.9541	1.1827	9.7674	1.3255	76851280	3	3	3	yes	16	yes	6
238	glutathione S-transferase M1	238	10.78	6	12	9563	0	0.16268	0.16933	0.01558	3.2492	1.7895	4.7354	2.181	12.066	2.2988	28461273	3	3	3	yes	32	yes	6
248	PREDICTED: similar to peptidylprolyl isomerase A isoform 1 isoform 1 ; PREDICTED: simila	248	10.22	6	12	8467.6	0	0.025396	0.040333	0.013582	3.2854	1.7984	3.8159	2.0911	7.3063	2.3395	76626930	3	3	3	yes		yes	6
249	PREDICTED: similar to glyoxalase 1	249	10.18	5	9.5229	7840.4	0	0.043425	0.01169	0.006937	2.9344	1.6109	3.4113	1.4621	12.242	1.9854	76650162	3	3	3	yes	30	yes	6
265	PREDICTED: similar to eukaryotic translation initiation factor 4A, isoform 1 isoform 20 ; PREI	265	9.66	5	9.5229	8533.8	0	0.09825	0.02549	0.001808	3.0692	1.5822	4.3522	1.1812	21.322	1.7911	76643173	3	3	3	yes	18	yes	6
275	profilin 1	275	9.05	5	9.0458	8707	0	0.002312	0.003113	0.003096	2.8729	1.1257	3.4875	1.1676	8.7527	1.3081	62751593	3	3	3	yes	26	yes	6
276	PREDICTED: similar to Elongation factor 1-gamma (EF-1-gamma) (eEF-1B gamma) isoform	276	9.05	5	9.0458	8354.7	0	0.053392	0.04406	0.375	3.1411	1.7118	4.9751	2.0412	12.177	1.5715	76657631	3	3	3	yes	14	yes	6
278	PREDICTED: similar to Stress-induced-phosphoprotein 1 (STI1) (Hsc70/Hsp90-organizing pr	278	9.04	4	7.5229	6454.8	0	0.10931	0.091345	0.26236	2.9163	1.2888	4.6945	1.8517	10.596	4.0752	76657889	3	3	3	yes		poor id/quant	6
284	PREDICTED: similar to ubiquitin-activating enzyme E1 isoform 2 ; PREDICTED: similar to ut	284	8.62	4	8	7811	0	2.4031	0.90238	0.045399	2.4553	2.5207	4.4043	3.087	13.093	2.2207	76655770	3	3	3	no		yes	6
286	ribosomal protein, large, P0	286	8.57	5	8.5686	7388.9	0	0.2395	0.17098	0.004531	3.7306	2.6674	5.3567	3.0629	20.735	2.0789	60592767	3	3	3	yes	8	yes	6
293	PREDICTED: similar to Alcohol dehydrogenase class III chi chain (Glutathione-dependent fo	293	8.25	4	7.0458	4798.5	0	0.58491	0.34822	0.13224	2.5106	2.1684	3.6876	2.3924	10.414	2.9157	76662148	3	3	3	no		yes	6
295	PREDICTED: similar to NADP-dependent malic enzyme (NADP-ME) (Malic enzyme 1)	295	8.15	4	8	7841.6	0	0.018298	0.008252	0.000785	3.7509	1.3486	5.838	1.3551	20.436	1.2659	76625476	3	3	3	yes	14	yes	6
297	PREDICTED: similar to SPUF protein precursor (Secreted protein of unknown function)	297	8.14	4	8	8243	0	0.081118	0.043642	0.10307	6.5042	2.0431	4.0768	1.5373	5.7758	2.0755	76636120	1	1	1	yes	36	yes	6
302	PREDICTED: similar to SH3 domain binding glutamic acid-rich protein like 3 isoform 2 ; PRE	302	8	5	10	8279.3	0	0.012948	0.00684	3.65E-05	2.8956	1.2382	5.0679	1.2968	17.044	1.2233	76611225	3	3	3	yes	28	yes	6
306	PREDICTED: similar to heat shock 70kD protein binding protein isoform 6 ; PREDICTED: sin	306	7.98	3	6	4216.4	0	0.45198	0.34472	0.11277	3.1269	1.7771	4.5437	1.9292	10.874	1.7768	76617020	3	3	3	no		yes	6
309	laminin receptor 1 (ribosomal protein SA, 67 kDA)	309	7.65	4	7.0458	5880.1	0	0.15562	0.084695	4.68E-05	3.7201	1.4532	3.7499	1.3164	23.866	1.103	27805981	3	3	3	yes	20	yes	6
312	glutathione S-transferase pi	312	7.52	4	7.5229	8402.8	0	0.021242	0.025482	0.021654	3.4071	1.339	4.488	1.4633	9.1752	1.7011	29135329	3	3	3	yes	36	yes	6
317	PREDICTED: similar to Splicing factor, proline-and glutamine-rich (Polypyrimidine tract-bindi	317	7.4	4	7.3979	6026.6	0	0.001584	0.004624	0.008789	5.2679	1.1785	7.3776	1.3274	15.578	1.6213	76614612	3	3	3	yes	4	yes	6
322	PREDICTED: similar to Stathmin (Phosphoprotein p19) (pp19) (Oncoprotein 18) (Op18) (Leu	322	7.28	3	6	3929.2	0	0.076918	0.051102	0.067625	5.1903	1.3855	6.6967	1.3579	6.135	1.3999	76611374	3	3	3	yes	17	yes	6
336	PREDICTED: similar to Phosphoglucomutase 1 (Glucose phosphomutase 1) (PGM 1), partia	336	6.84	3	5.5229	4741.7	0	0.11988	0.36937	0.18697	3.3568	1.3512	4.3019	1.9305	11.596	2.1541	76614007	3	3	3	yes	9	yes	6

order	Protein Name	protein #	score	peptides	score 2	mass cov	outliers	pval 116	pval 116	pval 117	116:114	SD	116:114	SD	117:114	SD	Accession	sig 115	sig116	sig117	SM-ID	coverage	manual	Indexer k8
339	eukaryotic translation elongation factor 1 beta 2	339	6.62	3	6	4651.5	0	0.29362	0.095879	0.011037	3.4306	1.6332	4.3987	1.3886	12.952	1.2099	62460568	3	3	3	yes	12	yes	6
357	PREDICTED: similar to Dihydropyrimidinase-related protein 2 (DRP-2) (Turned on after divis	357	6.12	6	12	10634	0	0.032186	0.002632	0.000405	2.2231	1.5172	3.6965	1.4777	9.8134	1.5864	76624847	3	3	3	yes	14	yes	6
359	PREDICTED: similar to Calpain-2 catalytic subunit (Calpain-2 large subunit) (Calcium-activat	359	6.06	3	5.3979	4667.6	0	0.36915	0.20305	0.34009	4.1324	1.8955	4.3802	1.6209	6.1498	2.1874	76636995	1	1	1	yes	4	bad quant	6
362	nucleoside-diphosphate kinase NBR-A ; nucleoside-diphosphate kinase NBR-B ; PREDICTE	362	6	3	6	4899.9	0	0.009368	0.007969	0.00095	2.7759	1.0725	4.0832	1.093	14.372	1.0598	61656159	3	3	3	yes	31	yes	6
367	peroxiredoxin 5 precursor	367	6	3	6	5875.6	0	0.83108	0.59984	0.21427	8.05	4.507	6.5984	3.0619	12.708	2.3518	27807445	3	3	3	yes	10	yes?	6
381	PREDICTED: similar to Protein transport protein Sec23A (SEC23-related protein A) isoform (	381	5.81	3	5.5229	5235.1	0	6	6	0.011284	3.1422	1	3.6375	1	19.15	1.2488	76647454	1	1	1	yes	7	yes/very poor quan	6
382	fusion, derived from t(12;16) malignant liposarcoma	382	5.72	3	5.3979	5729	0	0.007675	0.37365	0.077325	3.4937	1.0807	3.2736	1.1789	13.728	1.6822	27806887	3	3	3	yes	3	yes	6
383	endoplasmic reticulum thioredoxin superfamily member, 18 kDa	383	5.71	3	5.3979	5064	0	0.74821	0.60267	0.020978	2.9634	1.3584	3.6284	1.3362	16.587	1.3343	62751458	3	3	3	yes	13	yes	6
391	PREDICTED: similar to haloacid dehalogenase-like hydrolase domain containing 2 isoform 3	391	5.52	3	5.5229	3778.2	0	0.18241	0.38613	0.032072	3.3254	1.4496	3.7138	1.6016	13.306	1.3897	76652141	3	3	3	no	12	yes	6
393	PREDICTED: similar to Hypoxanthine-guanine phosphoribosyltransferase (HGPRT) (HGPRT	393	5.52	2	4	3157	0	6	6	0.074386	3.4363	1	6.5304	1	12.577	1.0722	76671371	3	3	3	no	15	yes / poor quant	6
395	PREDICTED: similar to CG1532-PA isoform 3 ; PREDICTED: similar to CG1532-PA isoform	395	5.5	2	4	3001.7	0	0.37138	0.091707	0.18533	2.7425	1.1493	3.5849	1.0443	13.745	1.1972	76643557	3	3	3	no		yes	6
396	ribosomal protein, large P2	396	5.4	3	5.3979	5760.1	0	0.38094	0.023492	0.000225	3.6236	1.209	5.6568	1.0152	19.187	1.0319	27807523	3	3	3	yes	40	yes	6
398	PREDICTED: similar to Ras GTPase-activating-like protein IQGAP1 (p195) isoform 1	398	5.39	3	5	5368.8	0	0.55743	0.28318	0.3281	4.3181	1.3554	3.4123	1.1376	7.5514	2.3497	76646935	3	3	3	yes	1	yes	6
405	C19orf10-like	405	5	3	5	3931.3	0	0.083237	0.04287	0.002855	2.1213	1.1677	3.1387	1.1834	16.796	1.1125	47564074	3	3	3	no		yes	6
407	PREDICTED: similar to 6-phosphogluconate dehydrogenase, decarboxylating	407	5	3	5	5179.8	0	0.22018	0.5004	0.10303	3.2559	1.4961	3.681	2.0061	9.819	1.6909	76637462	3	3	3	no		yes/ poor quant	6
411	epsilon subunit of coatomer protein complex	411	4.78	2	3.0458	4106.3	0	6	6	0.36883	3.5524	1	4.9035	1	13.619	1.4301	28603812	3	3	3	yes	20		6
416	PREDICTED: similar to Nucleosome assembly protein 1-like 1 (NAP-1 related protein) (hNRI	416	4.62	2	4	3862.1	0	6	6	0.11054	2.9707	1	4.1422	1	15.453	1.1186	76617371	1	1	1	yes	6	yes	6
423	polypyrimidine tract binding protein 1	423	4.4	2	4	2851.5	0	1.0569	0.87856	0.18448	3.5486	1.6631	6.19	1.8288	11.422	1.16	27806103	3	3	3	yes	9	yes	6
424	plasminogen activator inhibitor-1	424	4.35	2	4	2834.8	0	6	1.3985	0.98292	1.1919	1	9.7794	3.4433	16.29	2.8251	27806497	3	3	3	yes	4	yes	6
427	tumor protein, translationally-controlled 1	427	4.33	2	3.0458	3529	0	0.29666	0.49494	0.21849	2.919	1.1251	3.996	1.2908	12.108	1.2215	62177164	3	3	3	no	? Gp96?	yes	6
432	ribosomal protein L12	432	4.29	2	4	3105.9	0	6	6	0.085939	2.8481	1	3.3762	1	11.798	1.0817	45430019	1	1	1	yes	15	yes	6
438	platelet-activating factor acetylhydrolase, isoform Ib, beta subunit (30kD)	438	4.14	2	4	3324.9	0	6	6	6	3.0171	1	3.9509	1	14.504	1	27807193	3	3	3	no		yes	6
439	farnesyl diphosphate synthase	439	4.14	2	4	4106.2	0	1.1984	0.70248	0.57622	3.3093	1.7318	4.9358	1.5219	13.162	1.7403	29135283	3	3	3	yes		yes	6
448	glial fibrillary acidic protein	448	4	4	8	5917	0	0.25627	0.022707	0.011995	2.8927	1.8707	3.2047	1.1325	9.595	1.5569	28849921	3	3	3	yes	8	yes	6
472	PREDICTED: similar to Metallothionein-II (MT-II) (Metallothionein 2A)	472	4	2	4	2182	0	0.83766	0.77966	0.56389	25.812	2.7862	22.61	2.4915	58.193	2.3505	76640558	1	1	1	no		yes/poor quant	6
478	PREDICTED: similar to retinoblastoma binding protein 7 isoform 1 ; PREDICTED: similar to r	478	4	2	4	2679.7	0	1.0221	0.48019	0.45208	4.009	1.7132	4.7749	1.3224	11.947	1.5176	76659772	1	1	1	yes	2	yes/poor quant	6
488	PREDICTED: similar to Actin-related protein 2/3 complex subunit 3 (ARP2/3 complex 21 kDa	488	4	2	4	2366.3	0	0.23788	0.086819	0.19936	3.4799	1.1162	3.5154	1.0412	9.6674	1.1825	61883592	3	3	3	no	4	yes	6
493	PREDICTED: similar to glutathione-S-transferase, mu 5 isoform 2 ; PREDICTED: similar to g	493	3.99	3	3.0458	3739	0	0.45659	0.40046	0.2264	2.7841	1.681	3.5148	1.8086	10.953	2.291	76613059	3	3	3	yes	6	yes	6
502	fatty acid binding protein 5	502	3.67	2	3.0458	2142.1	0	0.7856	1.142	0.46688	2.7146	1.3428	3.7404	1.7772	9.7333	1.4849	27805805	3	3	3	yes	24	yes	6
508	PREDICTED: cartilage-derived morphogenetic protein 2	508	3.52	2	3.5229	3403	0	1.7659	6	2.0807	19.002	7.9664	1.4369	1	12.749	6.856	76634871	1	1	1	yes	6	yes	6
509	PREDICTED: similar to Proteasome subunit alpha type 4 (Proteasome component C9) (Mac	509	3.52	2	3.5229	3059.7	0	0.42695	0.25689	0.24844	2.3992	1.149	2.8117	1.1035	12.055	1.2577	61886385	1	1	1	no		yes	6
511	poly(rC) binding protein 1	511	3.52	2	3.5229	3406	0	0.11153	0.40344	0.28454	3.8396	1.0571	5.6908	1.2978	18.513	1.3315	62751650	1	1	1	no		yes	6
526	proenkephalin	526	5.52	3	5.5229	3433	0	6	6	0.15908	2.495	1	1.3936	1	29.855	2.6575	27806489	3	3	3	yes	13	yes	6
527	destrin (actin depolymerizing factor)	527	3.26	3	4.8198	3784.9	0	0.027064	0.01238	0.027489	2.566	1.1163	3.702	1.1086	11.141	1.3279	62751673	1	1	1	yes	3	yes	6
534	clathrin, light polypeptide B (light chain B)	534	3.05	2	3.0458	2813.3	0	1.0497	0.99862	0.28011	2.8197	1.5118	3.8061	1.6586	16.172	1.3079	27805873	3	3	3	yes	13	yes	6
545	thioredoxin reductase 1	545	3.05	2	3.0458	3091.9	0	6	6	0.35977	3.4982	1	4.9236	1	13.732	1.419	27807129	1	1	1	yes	6	yes	6
546	PREDICTED: similar to aldehyde dehydrogenase 9A1 isoform 1 ; PREDICTED: similar to ald	546	3.05	2	3.0458	2686.6	0	0.23702	0.018192	0.10033	3.1765	1.1069	3.4264	1.0083	14.658	1.1049	76611741	1	1	1	yes?	9	yes	6
547	PREDICTED: similar to eukaryotic translation initiation factor 4A2 isoform 2 ; PREDICTED: s	547	3	5	8.5229	8647.4	0	0.375	0.003006	0.001565	3.4078	1.9865	4.1234	1.1897	20.223	1.7368	76607308	3	3	3	yes	18	yes	6
563	PREDICTED: similar to Chloride intracellular channel protein 4 (mc3e5/mtCLIC)	329	6.44	3	5.5229	5493.9	0	0.63799	0.55424	0.21777	3.0017	1.9659	3.3991	1.9998	8.9071	2.1001	76658766	1	1	1	no		yes	6
567	PREDICTED: similar to TAF15 RNA polymerase II, TATA box binding protein (TBP)-associat	379	5.09	2	4	2278.1	0	0.66704	0.33473	0.092306	5.1079	1.5021	4.3176	1.1993	27.627	1.1201	76642871	1	1	1	no		yes/ poor quant	6
572	bucentaur	413	4.14	2	4	3139.8	0	0.1385	0.88717	0.23515	4.8231	1.0817	4.1716	1.6125	16.047	1.2737	27807389	1	1	1	yes	4	yes	6
592	PREDICTED: similar to dehydrogenase/reductase (SDR family) member 6 isoform 2 ; PRED	468	3.52	2	3.5229	2121.2	0	0.19725	0.21976	0.057973	3.7542	1.1015	4.4559	1.1294	15.487	1.0606	76640190	1	1	1	yes	8	yes	6
604	PREDICTED: similar to Heterogeneous nuclear ribonucleoprotein A1 (Helix-destabilizing prot	563	7.4	5	9.3979	7648.4	0	0.91064	0.36809	0.080439	2.8202	3.7111	4.251	3.5057	9.1461	3.2251	76617606	3	3	3	yes	34	yes - bad peptide	6
611	adenylate kinase 1, soluble	626	2.32	5	10	6781.9	0	0.17025	0.040117	0.015781	3.7275	2.4021	3.7025	1.7629	9.7007	2.143	61886850	3	3	3	yes	13	yes	6
634	PREDICTED: similar to SET protein (Phosphatase 2A inhibitor I2PP2A) (I-2PP2A) (Template	591	2.48	2	4	2846.6	0	1.2772	1.3987	0.35325	2.9056	1.6889	3.2524	1.8957	11.557	1.3785	76630803	3	3	3			yes	6

Appendix C.3: ADAMTS4 and ADAMTS5 blots and SDS-PAGE-LC/MS/MS of 3 week chondrocyte-agarose cultures treated with TNF-α

The following ADAMTS4 and ADAMTS5 blots are 3 agarose cultures that I did in Spring 2003 and they were primarily done so that I could learn 3D culture techniques and clearly not for the purpose of trying to find an aggrecanase. There are 3 sets of cultures on the gels: Set1 were cultured only about 1 week prior to treatment and then treated for 24 hours TNF-α +/-NMA (order: Control, Control-NMA, TNF-α, TNF-α-NMA); Set 2 were cultured 2-3 weeks initially in FBS for first ~2 medium changes and then with ITS. They were treated with TNF-α for 36 hours (order: control, TNF-α); Set 3 were cultured about 7 weeks in FBS and were overgrown routinely with fibroblastoid cells. They were treated with TNF-α for 48 hours (order: control, TNF-α). All these agarose sets were treated with approximately 100 ng/ml of TNF-α (in retrospect this concentration is way too high!). There is approximately 50 ug protein/well from a detergent lysis of agarose cultures (I don't believe that I still have the medium samples from these experiments).

Anti-ADAMTS4 blot – This blot was done under very mild washing conditions and antibody concentration at 1:1000, so there is a chance of non-specific binding

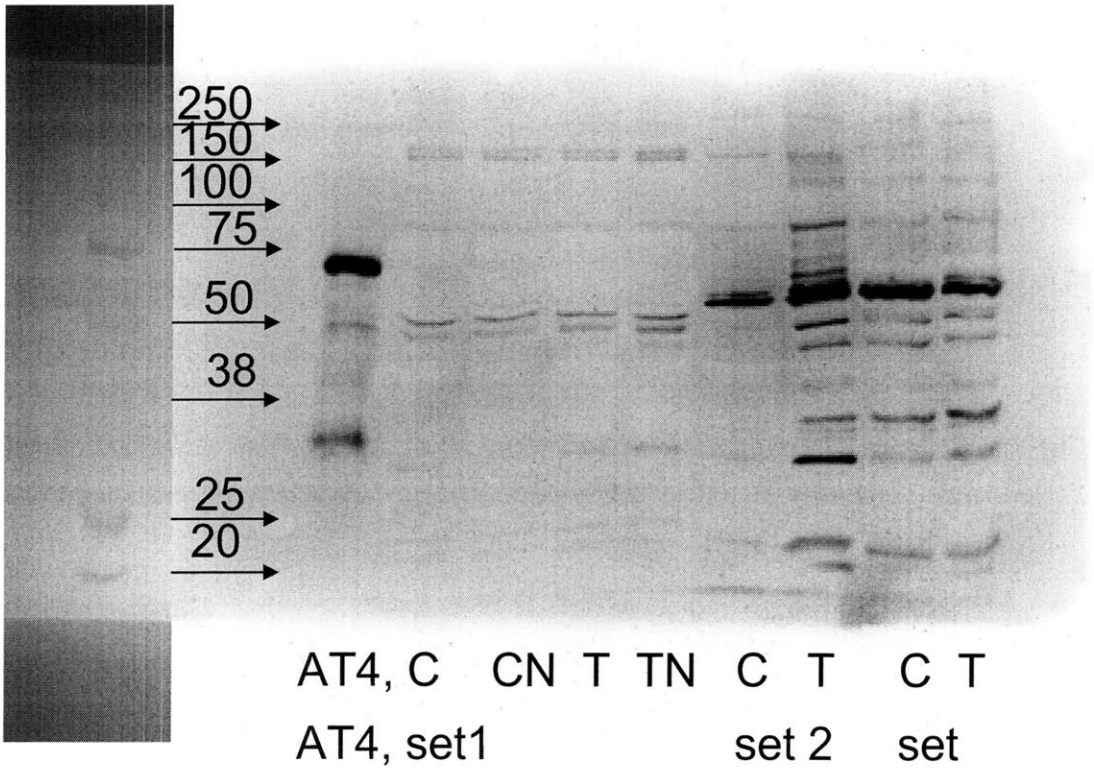

Anti-ADAMTS5. Information about the blot conditions and gel order are same as above. Only one band was seen, and I need to rule out secondary binding since there is a similar band in the ADAMTS4 blot.

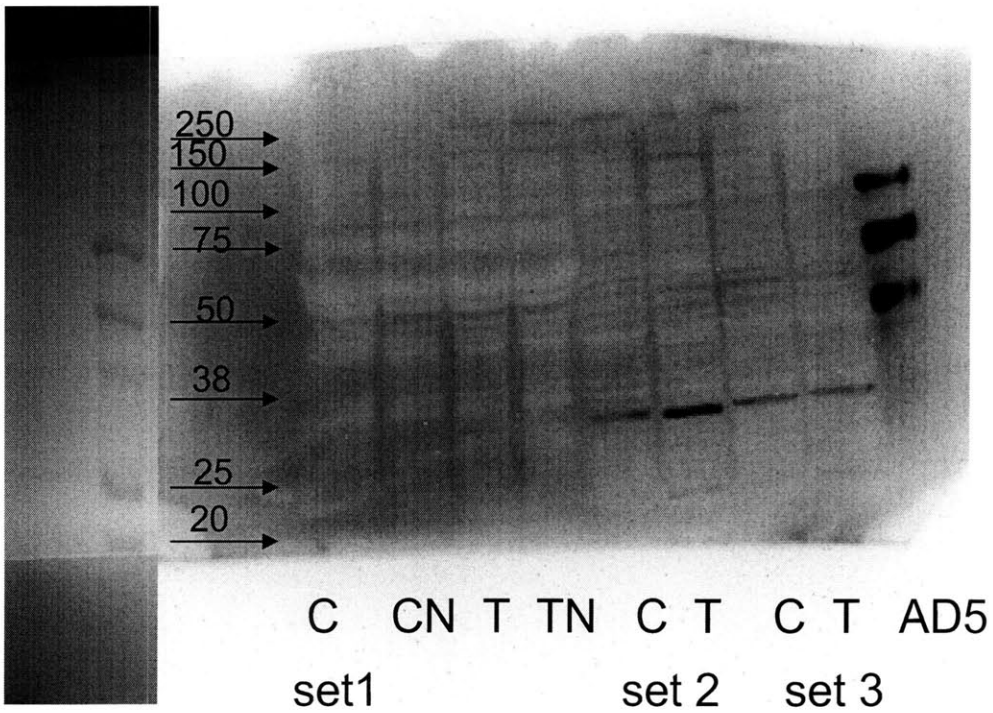

Additional work trying to identify ADAMTS4 and ADAMTS5 in the medium and from detergent extracts of explants samples from the cytokine + NMA experiment did not yield positive results. Below is a anti-ADAMTS5 blot of the medium. A faint band is visible at a molecular weight of roughly 200 kDa which was present in all conditions, but no additional bands were identified. The left lane bands indicate the recombinant ADAMTS5 protein.

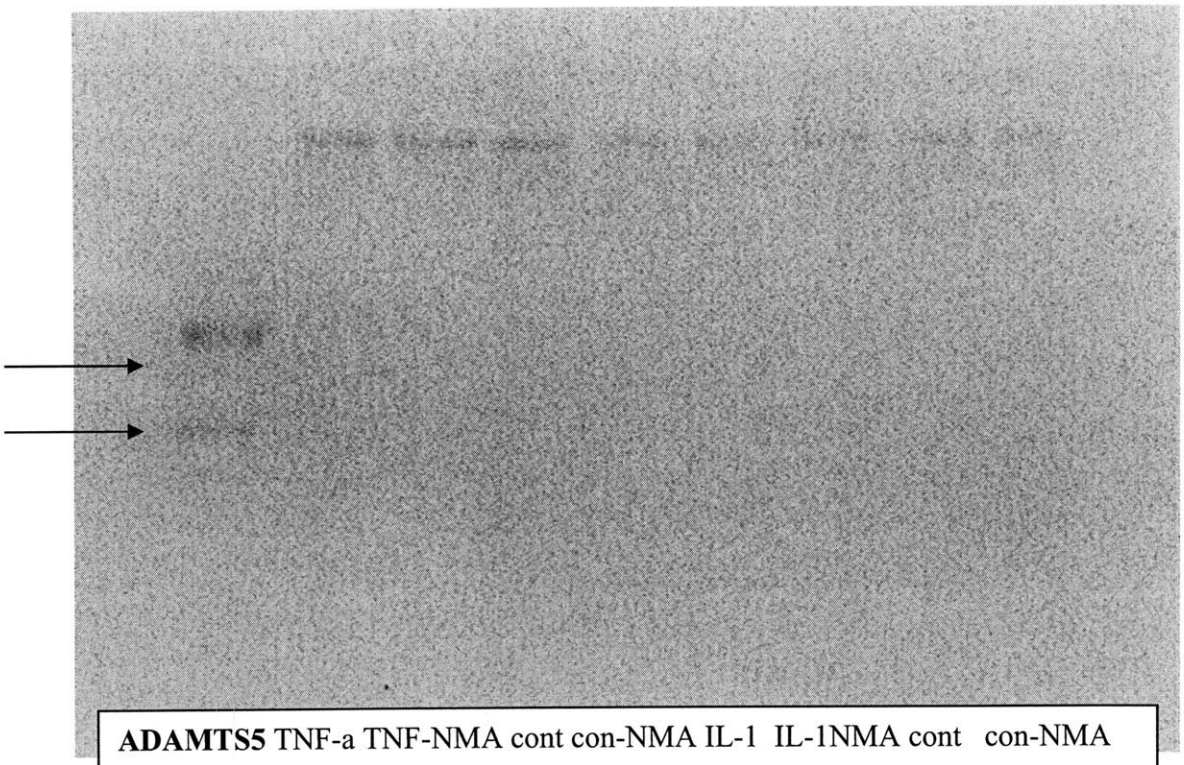

ADAMTS5 TNF-a TNF-NMA cont con-NMA IL-1 IL-1NMA cont con-NMA

The blot below is an anti-ADAMTS4 blot of the medium. Again there is a slight bad around 200 kDa or so but no bands are readily apparent in the ~80 kDa region which is the expected MW of ADAMTS4. The lane on the left is the recombinant ADAMTS4 protein.

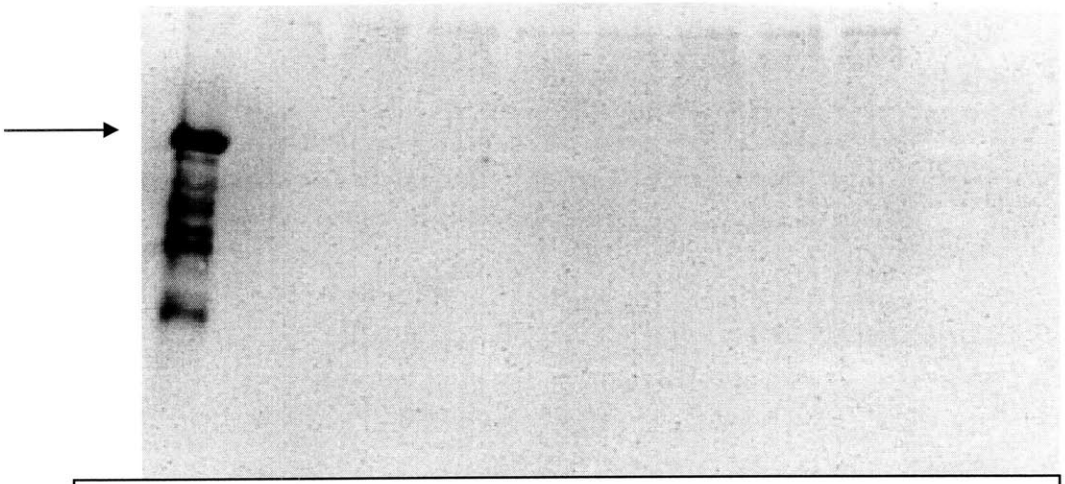

ADAMTS4 TNF T-NMA cont c-NMA IL-1 I-NMA cont con-NMA

No additional bands were found in the detergent lysis of the explants.

Table C.3 SDS-PAGE-LC/MS/MS analysis of detergent lyses of three week chondrocyte cultures in agarose after 36 hour TNF-a treatment

Table C.3 is the Spectrum Mill protein summary for the SDS-PAGE-LC/MS/MS analysis of 3 week chondrocyte cultures treated with TNF-α for 36 hours.

Column 1: **GroupNum**:	Protein number
Column 2: **Numspec.**:	Number of spectra
Column 3: **Uniquepep**:	Number of unique peptides
Column 4: **Uniquescore**:	Score based on unique peptide identifications
Column 5: **% Coverage**:	percentage of protein amino acid sequence found
Column 6: **TotalIInstensity**:	summed peptide ion intensity for each protein
Column 7: **MW**:	protein molecular weight
Column 8: **pI**:	protein isoelectric point
Column 9: **species**:	animal species
Column 10: **Database**:	Protein database
Column 11: **Accession**:	database accession number
Column 12: **Protein Name**:	name of the protein

The purpose for this experiment was to attempt to validate the ADAMTS4 bands that were identified by Western blotting. While there is ADAMTS4 present in the list, it is the result of carry-over from the positive control (ADAMTS4 recombinant protein). The intersesting findings in the list are iNOS, transcription factors such as STAT3, matrix proteins, innate immune proteins that were also identified in cartilage explants (supports new protein synthesis as the cause the release of innate immune proteins from explants), caspases (suggesting possible apoptosis with TNF-α treatment). In addition to the above findings that are primarily the result of TNF-α treatment, the increase in mitochondrial proteins was also noted which were not found with injury to explants in which a number of intracellular protein types were released. This may suggest a change in phenotype of the chondrocytes (and attempt to deal with the oxygen tension) or it may simply be that the mitochondrial proteins are not readily released with injury).

groupNun	numSpect	unique peptide	scoreUnique	% coverage	totalIntensity	mw	pI	species	database	accession	Protein name
1	151	46	776.81	71	2.03E+06	69323.9	5.82	Bos taurus	NCBInr	30794280	albumin
2	54	50	743.49	23	8.02E+04	341601.4	6.08	Bos taurus	NCBInr	76614728	PREDICTED: similar to alpha 3 type VI collagen isoform 1 precursor isoform 2
3	222	39	724.38	68	2.70E+06	61428	8.62	Bos taurus	NCBInr	73587283	LOC512571 protein
4	72	37	621.31	45	9.80E+05	84731.2	4.93	Bos taurus	NCBInr	34392343	90-kDa heat shock protein alpha
5	47	42	602.51	23	9.04E+04	229100.4	5.44	Bos taurus	NCBInr	27807325	myosin, heavy polypeptide 10, non-muscle
6	68	35	591.15	64	8.61E+05	56929.9	6.23	Bos taurus	NCBInr	27805905	glucose regulated protein 58kD
7	51	36	560.26	58	5.75E+05	64355.4	5.98	Bos taurus	NCBInr	76659545	Villin 2
8	34	33	539.2	50	4.96E+05	80352.5	6.36	Bos taurus	NCBInr	76619055	PREDICTED: similar to cytoskeleton-associated protein 4
9	37	30	498.43	48	6.74E+05	71239.9	5.49	BOVIN	NCBInr	123644	Heat shock cognate 71 kDa protein (Heat shock 70 kDa protein 8)
10	33	29	498.22	41	4.58E+05	84084.2	5.86	Bos taurus	NCBInr	76623595	annexin VI
11	34	34	492.62	19	3.88E+04	279440.9	5.53	Bos taurus	NCBInr	76648768	filamin A
12	43	28	465.74	43	3.94E+05	72498.4	4.96	Bos taurus	NCBInr	76616203	protein disulfide isomerase related protein
13	84	28	465.69	41	1.04E+06	80731.1	5.54	Bos taurus	NCBInr	74356373	Hypothetical protein LOC535077
14	166	26	464.26	61	2.09E+06	47326.4	6.38	Bos taurus	NCBInr	74354056	enolase 1
15	99	26	456.39	72	1.60E+06	44537.9	8.48	Bos taurus	NCBInr	74353972	Phosphoglycerate kinase 1
16	114	25	434.81	65	1.10E+06	38612.3	6.92	Bos taurus	NCBInr	27807289	annexin A2
17	68	28	432.04	51	1.06E+06	57265.9	4.8	Bos taurus	NCBInr	27806501	procollagen-proline, 2-oxoglutarate 4-dioxygenase
18	33	27	428.85	28	5.81E+04	157942.8	5.61	Bos taurus	NCBInr	76646935	PREDICTED: similar to Ras GTPase-activating-like protein IQGAP1 (p195) is
19	30	29	427.52	17	5.13E+04	269669.4	5.75	Homo sapie	NCBInr	16753233	talin 1
20	42	26	427.4	39	5.18E+05	80694.8	5.53	Bos taurus	NCBInr	76607158	PREDICTED: similar to Melanotransferrin precursor (Melanoma-associated a
21	56	27	424.55	40	2.97E+05	95368.7	6.41	Bos taurus	NCBInr	74353984	Unknown (protein for MGC:127305)
22	52	28	420.25	57	5.09E+05	53677.1	5.21	Bos taurus	NCBInr	27806785	vimentin
23	54	25	413.13	62	7.64E+05	39143.3	4.72	Bos taurus	NCBInr	76630567	heat shock 70kDa protein 5
24	94	23	400.88	68	1.12E+06	47830.1	4.8	Bos taurus	NCBInr	76650558	beta tubulin
25	50	21	391.15	51	5.54E+05	56283.8	5.15	Bos taurus	NCBInr	28461221	ATP synthase, H+ transporting, mitochondrial F1 complex, beta subunit
26	64	23	388.54	60	4.82E+05	38897.8	6.44	Bos taurus	NCBInr	74	annexin I
27	27	22	387.98	47	2.57E+05	75537	5.09	Bos taurus	NCBInr	76617127	PREDICTED: similar to CG1550-PA isoform 2
28	27	22	365.27	51	3.30E+05	60977.9	5.71	Bos taurus	NCBInr	76644268	LOC511913 protein
29	67	23	362.13	65	6.62E+05	39436.3	8.45	Bos taurus	NCBInr	76653617	ALDOC protein
30	72	19	359.34	53	7.56E+05	46506.9	9.01	Bos taurus	NCBInr	76636117	PREDICTED: similar to Collagen-binding protein 2 precursor (Colligin 2) (Rhe
31	48	22	358.37	58	5.65E+05	48038.7	4.31	Bos taurus	NCBInr	27806723	calreticulin
32	94	21	356.06	51	1.19E+06	48452	4.97	Bos taurus	NCBInr	76618161	Tubulin alpha-2 chain (Alpha-tubulin 2) (Alpha-tubulin isotype M-alpha-2)
33	57	22	349.18	60	5.73E+05	36787.3	5.3	Bos taurus	NCBInr	27806317	annexin A8
34	19	19	349.02	47	3.25E+05	62277.9	5.95	BOVIN	NCBInr	3122018	Dihydropyrimidinase-related protein 2 (DRP-2) (Neural-specific protein NSP6
35	47	21	348.26	48	6.09E+05	56903.5	7.69	Bos taurus	NCBInr	41386780	UDP-glucose pyrophosphorylase 2
36	27	20	346.81	40	3.14E+05	67906.2	7.56	Bos taurus	NCBInr	50844503	transketolase
37	30	21	344.2	31	9.19E+04	108355.6	5.29	Bos taurus	NCBInr	76641275	PREDICTED: similar to actinin, alpha 4 isoform 11
38	87	21	342.97	61	1.16E+06	43765.9	8.87	Bos taurus	NCBInr	76636770	chitinase 3-like 1
39	38	23	338.93	30	1.09E+05	102207.4	6.29	Bos taurus	NCBInr	33332343	hexokinase 1
40	22	21	333.1	48	2.69E+05	55136.6	7.51	Bos taurus	NCBInr	27806365	UDP-glucose dehydrogenase
41	82	21	332.68	60	7.01E+05	36088.1	4.94	Bos taurus	NCBInr	73586525	annexin 5
42	36	19	328.95	32	1.73E+05	89330.3	5.14	Bos taurus	NCBInr	73586667	Hypothetical protein LOC507345
43	27	21	327.94	37	2.94E+05	76758.3	8.41	Bos taurus	NCBInr	76629806	glutamine fructose aminotransferase
44	21	21	324.39	39	1.40E+05	65291	5.03	Bos taurus	NCBInr	79153525	Hypothetical protein LOC535321
45	55	18	311.5	51	5.92E+05	40287.8	7.93	Bos taurus	NCBInr	27805853	cartilage linking protein 1
46	66	19	297.92	27	3.95E+05	66067	8.15	Homo sapie	NCBInr	17318569	keratin 1
47	21	21	297.87	16	3.06E+04	211706.5	4.88	Bos taurus	NCBInr	76625295	PREDICTED: similar to Tenascin precursor (TN) (Hexabrachion) (Cytotactin)
48	23	19	296.21	30	1.79E+05	83492.5	6.34	Bos taurus	NCBInr	73586669	Hypothetical protein LOC510075
49	23	18	294.5	50	2.55E+05	35889	5.54	Bos taurus	NCBInr	48374083	annexin A4
50	69	18	291.74	54	5.98E+05	36597.8	8.12	Bos taurus	NCBInr	27806559	lactate dehydrogenase A
51	19	17	289.8	27	1.69E+05	86185.4	6.64	Bos taurus	NCBInr	76647458	PREDICTED: similar to Protein transport protein Sec23A (SEC23-related prot
52	34	16	284.95	45	3.86E+05	48075.6	6.1	Bos taurus	NCBInr	73586966	Hypothetical protein LOC505323

groupNun	numSpect	unique peptide	scoreUnique	% coverage	totalIntensity	mw	pI	species	database	accession	Protein name
53	40	17	284.01	34	4.33E+05	59719.9	9.21	Bos taurus	NCBInr	102	H(+)-transporting ATP synthase
54	19	18	282.85	26	1.90E+05	87124.2	5.8	Bos taurus	NCBInr	76661128	PREDICTED: similar to Signal transducer and activator of transcription 1-alph
55	25	17	279.9	34	2.01E+05	61631.6	8.03	Bos taurus	NCBInr	74354891	Glutamate dehydrogenase 1, mitochondrial precursor (GDH)
56	41	16	275.39	38	3.30E+05	50512.4	6.02	BOVIN	NCBInr	13638229	Rab GDP dissociation inhibitor beta (Rab GDI beta) (Guanosine diphosphate
57	18	17	273.69	33	1.77E+05	79321.8	8.8	Bos taurus	NCBInr	76659038	PREDICTED: similar to acyl-CoA synthetase long-chain family member 4 isof
58	20	15	272.33	33	2.71E+05	56709.1	7.54	BOVIN	NCBInr	118502	Aldehyde dehydrogenase, mitochondrial precursor (ALDH class 2) (ALDHI) (A
59	30	15	266.95	39	3.05E+05	51019.5	5.14	Bos taurus	NCBInr	74354615	Heterogeneous nuclear ribonucleoprotein K
60	21	17	266.6	25	1.42E+05	73742	5.97	Bos taurus	NCBInr	73586960	Heat shock 70kDa protein 9B (mortalin-2)
61	16	16	265.68	22	1.40E+05	85357.8	8.08	Bos taurus	NCBInr	27806769	aconitase 2, mitochondrial
62	133	15	265.51	45	1.96E+06	41676	5.36	Bos taurus	NCBInr	22655316	beta-actin
63	16	15	265.4	30	1.76E+05	79992.9	5	Bos taurus	NCBInr	76637003	Calpain-2 catalytic subunit (Calpain-2 large subunit) (Calcium-activated neutra
64	16	16	264.98	40	2.11E+05	54982.7	5.11	Bos taurus	NCBInr	76641931	PREDICTED: similar to nucleobindin 1 isoform 3
65	16	16	263.57	34	1.94E+05	64828.6	6.65	Bos taurus	NCBInr	76656655	PREDICTED: similar to Prolyl 4-hydroxylase alpha-1 subunit precursor (4-PH
66	20	17	262.87	27	5.17E+04	111465	6.19	Bos taurus	NCBInr	76657688	PREDICTED: similar to alpha glucosidase II alpha subunit isoform 2
67	23	18	262.76	21	5.75E+04	98258.3	6.34	Bos taurus	NCBInr	76627633	alpha-1,4-glucan orthophosphate glycosyl transferase
68	131	15	262.04	62	1.61E+06	24638.1	8.69	BOVIN	NCBInr	1174380	Superoxide dismutase [Mn], mitochondrial precursor
69	21	16	260.13	42	2.92E+05	62871	7.33	Bos taurus	NCBInr	73587307	Unknown (protein for MGC:127793)
70	17	17	258.93	28	1.54E+05	87797.3	6.86	Bos taurus	NCBInr	76654528	PREDICTED: similar to pyrroline-5-carboxylate synthetase isoform 1 isoform
71	49	18	258.53	8	4.81E+05	246478.3	4.16	Bos taurus	NCBInr	37953324	aggrecan
72	17	16	251.48	24	1.83E+05	83173.1	5.14	Bos taurus	NCBInr	76672350	PREDICTED: similar to leprecan 1 isoform 1
73	138	14	250.78	46	1.36E+06	35868.3	8.51	Bos taurus	NCBInr	73587299	Glyceraldehyde-3-phosphate dehydrogenase
74	18	15	244.98	26	1.68E+05	68782.9	6.15	Bos taurus	NCBInr	76633782	PREDICTED: similar to matrilin 4 isoform 2 precursor
75	17	15	242.87	20	1.18E+05	94091.4	5.55	Bos taurus	NCBInr	76640328	PREDICTED: similar to vacuolar protein sorting 35 isoform 2
76	14	14	241.35	34	1.14E+05	50824.4	8.96	Bos taurus	NCBInr	430	isocitrate dehydrogenase (NADP+)
77	20	13	241.15	25	2.01E+05	55761.4	7.13	Bos taurus	NCBInr	73586529	LOC514939 protein
78	21	15	236.36	40	1.35E+05	46759.6	6.13	Bos taurus	NCBInr	74354744	Isocitrate dehydrogenase 1 (NADP+), soluble
79	24	14	234.95	28	2.12E+05	50743.9	8.28	Bos taurus	NCBInr	76630316	tyrosine 3-monooxygenase/tryptophan 5-monooxygenase activation protein,
80	18	15	234.68	35	1.59E+05	55872	5.83	Bos taurus	NCBInr	76670156	glycyl-tran synthetase
81	20	14	233.7	44	1.67E+05	53048.5	6.29	Bos taurus	NCBInr	76625476	PREDICTED: similar to NADP-dependent malic enzyme (NADP-ME) (Malic e
82	48	14	232.1	37	5.06E+05	47502.2	6.81	Bos taurus	NCBInr	41386719	milk fat globule-EGF factor 8 protein
83	18	14	228.7	22	1.42E+05	83564.7	6.13	Bos taurus	NCBInr	27806477	procollagen-lysine, 2-oxoglutarate 5-dioxygenase precursor
84	26	14	227.7	40	1.61E+05	36617.3	6.8	Bos taurus	NCBInr	73586501	Unknown (protein for MGC:126928)
85	19	13	222.07	22	5.29E+04	83190.4	8.32	Bos taurus	NCBInr	76650936	PREDICTED: similar to Complement factor B precursor (C3/C5 convertase)
86	14	13	219.95	32	1.20E+05	58605.4	5.85	Bos taurus	NCBInr	27806419	seryl-tRNA synthetase
87	22	12	219.93	42	1.95E+05	48850.6	4.64	Bos taurus	NCBInr	74268096	Hypothetical protein LOC517087
88	18	14	218.54	44	2.51E+05	49414.8	9.14	Bos taurus	NCBInr	76674779	PREDICTED: similar to phosphoglucomutase 1
89	35	12	216.44	36	4.12E+05	48514.9	4.91	Bos taurus	NCBInr	76630218	PREDICTED: similar to Protein disulfide-isomerase A6 precursor (Thioredoxi
90	17	13	215.62	83	1.34E+05	22393.2	5.98	Bos taurus	NCBInr	74354863	heat shock 27kDa protein 1
91	15	15	214.22	23	4.48E+04	102892.1	5.48	Bos taurus	NCBInr	76644640	PREDICTED: similar to Puromycin-sensitive aminopeptidase (PSA) isoform 2
92	25	12	213.75	42	2.41E+05	37588.6	4.56	Bos taurus	NCBInr	76615717	PREDICTED: similar to calumenin precursor isoform 3
93	24	13	213.56	21	1.79E+05	81398.7	5.3	Bos taurus	NCBInr	41386707	vascular cell adhesion molecule 1
94	20	14	212.72	23	4.41E+04	97400.3	5.31	Bos taurus	NCBInr	83405754	Coatomer protein complex, subunit gamma 2
95	19	13	212.43	25	2.10E+05	54216	7.56	Bos taurus	NCBInr	78	annexin XI
96	31	12	211.18	70	3.55E+05	22209.7	8.59	Bos taurus	NCBInr	59858511	peroxiredoxin 1
97	24	12	209.08	44	1.89E+05	33602.1	4.65	Bos taurus	NCBInr	76672694	PREDICTED: similar to Reticulocalbin-1 precursor, partial
98	19	13	204.92	30	1.61E+05	62086.1	6.24	Bos taurus	NCBInr	24251217	l-caldesmon
99	17	13	203.79	39	8.01E+04	29032.8	4.75	Bos taurus	NCBInr	79153472	tropomyosin 1 alpha chain
100	15	13	203.3	33	1.85E+05	54414.8	5.36	Bos taurus	NCBInr	61863538	MMP-3
101	14	13	202.36	25	1.17E+05	63427.9	6.5	Bos taurus	NCBInr	76612740	PREDICTED: similar to extracellular matrix protein 1 isoform 1 precursor isof
102	13	13	201.67	28	2.04E+05	70954.7	6.37	Bos taurus	NCBInr	74268037	Hypothetical protein LOC504439
103	14	14	199.52	7	1.56E+04	274556	6.23	Bos taurus	NCBInr	38425281	fatty acid synthase
104	11	11	199.41	26	1.15E+05	55575.6	5.68	Bos taurus	NCBInr	410689	leucine aminopeptidase

groupNun	numSpect	unique peptide	scoreUnique	% coverage	totalIntensity	mw	pI	species	database	accession	Protein name
105	15	12	198.37	44	1.47E+05	38351.7	8.09	Bos taurus	NCBInr	74354951	GNB2L1 protein
106	19	12	197.37	32	1.99E+05	46104.2	6.05	Bos taurus	NCBInr	27806941	serine (or cysteine) proteinase inhibitor, clade A (alpha-1antiproteinase, antitr
107	17	12	196.89	54	1.31E+05	28727.2	5.6	Bos taurus	NCBInr	73587123	chloride channel protein p64H1
108	14	13	195.9	25	1.39E+05	58109.7	5.89	Bos taurus	NCBInr	76635420	PREDICTED: similar to archain isoform 3
109	16	12	195.76	29	2.10E+05	54785.7	6.55	Bos taurus	NCBInr	75773587	Fascin homolog 1, actin-bundling protein
110	14	13	195.58	23	1.35E+05	63535.4	4.92	Bos taurus	NCBInr	76615361	PREDICTED: similar to FK506 binding protein 9
111	12	12	195.42	18	9.37E+04	87643.7	6.44	Bos taurus	NCBInr	75948195	Hypothetical protein LOC514586
112	18	12	195.35	40	1.49E+05	44791.5	8.73	Bos taurus	NCBInr	76649531	PREDICTED: similar to transmembrane protein 43
113	13	13	193.64	8	1.65E+04	234747.7	5.79	Bos taurus	NCBInr	76661429	PREDICTED: similar to Myoferlin (Fer-1-like protein 3) isoform 3
114	13	12	192.5	18	2.96E+04	107736.6	5.81	Bos taurus	NCBInr	76635618	PREDICTED: similar to coatomer protein complex, subunit beta isoform 3
115	11	11	190.13	58	1.42E+05	24566.1	5.55	Bos taurus	NCBInr	76614007	PREDICTED: similar to Phosphoglucomutase 1 (Glucose phosphomutase 1)
116	12	12	187.41	18	3.59E+04	117945.6	5.46	Bos taurus	NCBInr	76655772	ubiquitin-activating emzyme E1
117	11	11	187.09	36	7.62E+04	42866.6	5.44	Bos taurus	NCBInr	74354268	26S proteasome p40.5 subunit
118	14	12	186.22	43	1.26E+05	29174.1	4.63	Pan troglody	NCBInr	55644755	14-3-3 protein epsilon isoform transcript variant 1
119	11	11	185.62	26	1.07E+05	60586.3	6.38	Bos taurus	NCBInr	74354953	T-complex protein 1, gamma subunit (TCP-1-gamma) (CCT-gamma)
120	13	12	184.47	18	8.71E+04	82032.1	5.09	Bos taurus	NCBInr	74268113	dipeptidyl peptidase III isoform 1
121	13	12	183.59	22	1.01E+05	82414.6	6.81	Bos taurus	NCBInr	76666079	PREDICTED: similar to DEAD (Asp-Glu-Ala-Asp) box polypeptide 1 isoform 2
122	16	12	183.13	31	1.62E+05	42236	5.71	Bos taurus	NCBInr	76651280	serine (or cysteine) proteinase inhibitor, clade B (ovalbumin), member 6
123	13	12	183.07	19	9.37E+04	89073.3	7.1	Bos taurus	NCBInr	76648296	1-phosphatidylinositol-4,5-bisphosphate phosphodiesterase delta 1 (Phospho
124	38	11	182.21	33	2.31E+05	39879.3	8.72	Bos taurus	NCBInr	54660107	decorin
125	27	11	181.27	22	1.97E+05	51114.2	5.73	Bos taurus	NCBInr	27806907	clusterin
126	32	12	181.12	30	1.61E+05	44859.4	7.83	Bos taurus	NCBInr	76640813	haptoglobin
127	29	11	180.96	21	1.56E+05	59527.9	5.17	Homo sapie	NCBInr	28317	Keratin, type I cytoskeletal 10 (Cytokeratin-10) (CK-10) (Keratin-10) (K10)
128	12	11	180.96	42	6.88E+04	33646.9	9.95	Bos taurus	NCBInr	76616406	PREDICTED: similar to B-cell receptor-associated protein 37 isoform 1
129	11	11	178.7	21	1.27E+05	60151.6	4.36	Bos taurus	NCBInr	74356454	Protein kinase C substrate 80K-H
130	15	11	178.5	62	1.65E+05	20035.4	6.84	Bos taurus	NCBInr	62751849	Parkinson disease (autosomal recessive, early onset) 7
131	12	10	178.15	54	1.72E+05	31375.1	5.29	Bos taurus	NCBInr	76688665	PREDICTED: similar to Bifunctional 3-phosphoadenosine 5-phosphosulfate s
132	14	10	177.26	43	2.53E+05	35143.1	5.75	Bos taurus	NCBInr	73586870	NP protein
133	13	11	176.62	17	8.81E+04	85058.1	6.91	Bos taurus	NCBInr	76684810	PREDICTED: similar to tumor necrosis factor, alpha-induced protein 2
134	42	11	176.59	25	1.72E+05	62064.6	5.14	Homo sapie	NCBInr	55956899	keratin 9
135	12	12	176.35	27	1.16E+05	59870.7	5.76	Bos taurus	NCBInr	76635779	PREDICTED: similar to SWAP-70 protein, partial
136	11	11	175.46	19	7.24E+04	78120.9	8.73	Bos taurus	NCBInr	506	lactotransferrin
137	14	12	174.9	19	8.40E+04	57162.5	5.45	Bos taurus	NCBInr	76658345	Hematopoietic cell-specific Lyn substrate 1
138	11	10	173.48	20	8.74E+04	63085.7	6.44	Bos taurus	NCBInr	285642	5'-nucleotidase precursor
139	19	11	173.38	21	2.19E+05	51091.8	4.44	Bos taurus	NCBInr	76690221	calnexin
140	11	10	173.33	29	1.13E+05	53812.3	5.49	Bos taurus	NCBInr	74354933	WARS protein
141	13	11	172.98	29	9.05E+04	57956.5	6.32	Bos taurus	NCBInr	75773567	Hypothetical protein LOC521540
142	17	12	167.98	15	2.78E+04	122998	5.66	Bos taurus	NCBInr	76661740	PREDICTED: similar to TIP120 protein isoform 3
143	14	10	166.85	18	1.32E+05	84354.8	5.67	Bos taurus	NCBInr	76630432	PREDICTED: similar to niban protein isoform 1
144	12	10	166.09	43	1.05E+05	28663.2	5.78	Bos taurus	NCBInr	66792738	hypothetical protein LOC510041
145	11	11	164.42	17	6.30E+04	83249	9.17	Bos taurus	NCBInr	74268185	FGF-2 binding protein
146	11	9	162.48	45	9.35E+04	25302.9	7.69	Bos taurus	NCBInr	76610134	5-aminoimidazole-4-carboxamide ribonucleotide formyltransferase/IMP cyclol
147	12	11	161.41	9	2.71E+04	191589.7	5.48	Bos taurus	NCBInr	27806689	clathrin, heavy polypeptide (Hc)
148	12	11	160.57	18	8.69E+04	62482.3	6.08	Bos taurus	NCBInr	78369310	hypothetical protein LOC617109
149	16	11	160.16	14	3.39E+04	288270.8	5.83	Bos taurus	NCBInr	76657613	AHNAK nucleoprotein isoform 1
150	20	9	160.1	37	1.61E+05	35668.7	8.82	Bos taurus	NCBInr	81674781	malate dehydrogenase 2, mitochondrial
151	11	10	159.62	33	4.78E+04	33253	5.66	Bos taurus	NCBInr	76643555	PREDICTED: similar to CG1532-PA isoform 1
152	10	9	159.13	40	1.11E+05	28852.1	6.68	Bos taurus	NCBInr	77404217	similar to phosphoglycerate mutase
153	11	11	158.58	15	2.92E+04	98924.3	5.45	Bos taurus	NCBInr	74267681	Major vault protein
154	19	10	158.08	27	1.08E+05	43514	8.67	Bos taurus	NCBInr	74353843	GALE protein
155	20	9	157.91	50	1.54E+05	21946.1	5.36	Bos taurus	NCBInr	74353992	PRDX2 protein
156	15	10	157.51	46	1.32E+05	30839.8	8.82	Bos taurus	NCBInr	73586892	Voltage-dependent anion channel 1

groupNun	numSpect	unique peptide	scoreUnique	% coverage	totalIntensity	mw	pI	species	database	accession	Protein name
157	14	9	155.57	36	1.28E+05	37328.7	5.41	Bos taurus	NCBInr	76649136	guanine nucleotide binding protein (G protein), alpha stimulating activity polyp
158	22	9	155.21	30	1.75E+05	40773.4	7.68	Bos taurus	NCBInr	76617076	NADH-cytochrome b5 reductase (B5R) (Diaphorase-1) (Cytochrome b5 reduc
159	20	9	154.83	27	1.71E+05	38672.8	6.28	Bos taurus	NCBInr	76676583	PREDICTED: similar to Thioredoxin domain containing protein 5 precursor (T
160	21	9	154.74	22	2.39E+05	49753.1	8.48	Bos taurus	NCBInr	76661652	PREDICTED: similar to EGF-like repeats and discoidin I-like domains-contain
161	14	9	154.29	29	1.41E+05	46836.4	5.13	Bos taurus	NCBInr	74354589	Thioredoxin domain containing 4 (endoplasmic reticulum)
162	16	9	150.93	28	1.39E+05	43683	9.59	Bos taurus	NCBInr	10834556	proline arginine-rich end leucine-rich repeat protein
163	9	9	150.84	11	8.16E+04	91506.5	6.36	Bos taurus	NCBInr	76672651	PREDICTED: similar to phosphofructokinase, platelet isoform 12
164	20	8	150.2	59	3.90E+05	23613.3	6.89	Bos taurus	NCBInr	74268086	GSTP1 protein
165	26	8	149.67	26	3.21E+05	43037.9	5.57	Bos taurus	NCBInr	74356334	Fibromodulin
166	9	9	148.46	29	7.28E+04	46285.8	5.35	Bos taurus	NCBInr	76608670	PREDICTED: similar to glucan (1,4-alpha-), branching enzyme 1 (glycogen bı
167	10	10	148.21	21	9.57E+04	58596.5	6.69	Bos taurus	NCBInr	76622660	PREDICTED: similar to antiquitin
168	17	10	147.41	22	1.67E+05	50419.4	6.31	Bos taurus	NCBInr	76657631	PREDICTED: similar to Elongation factor 1-gamma (EF-1-gamma) (eEF-1B g
169	66	9	146.91	32	7.07E+05	34378.9	9.22	Bos taurus	NCBInr	2293575	elongation factor 1 alpha
170	11	10	146.37	43	5.43E+04	29585.8	6.15	Bos taurus	NCBInr	74354782	Hypothetical protein LOC515503
171	16	9	145.96	22	1.17E+05	38484.7	6.49	Bos taurus	NCBInr	76620254	PREDICTED: similar to Heterogeneous nuclear ribonucleoprotein D0 (hnRNP
172	12	10	145.74	38	1.25E+05	31619.7	7.47	Bos taurus	NCBInr	62177148	voltage-dependent anion channel 2
173	12	10	145.69	38	7.53E+04	21623.8	5.99	Bos taurus	NCBInr	76649594	PREDICTED: similar to Dolichyl-diphosphooligosaccharide--protein glycosyltr
174	10	10	145.62	19	7.43E+04	70649.5	8.74	Bos taurus	NCBInr	74267810	ACADVL protein
175	14	9	145.11	28	1.93E+05	38419	5.26	Bos taurus	NCBInr	27806751	alpha-2-HS-glycoprotein
176	22	10	144.87	29	1.65E+05	34613.4	4.71	Bos taurus	NCBInr	77567785	Secreted protein, acidic, cysteine-rich [osteonectin]
177	10	9	144.47	23	5.72E+04	47150.7	7.46	Bos taurus	NCBInr	37962708	phosphoribosylaminoimidazole carboxylase
178	11	9	144.1	47	7.53E+04	21664.1	8.4	Bos taurus	NCBInr	61888850	adenylate kinase 1, soluble
179	9	9	143.31	17	7.82E+04	61471.3	6.08	Bos taurus	NCBInr	76620344	PREDICTED: similar to WD-repeat protein 1 (Actin interacting protein 1) (AIP
180	20	9	142.13	30	2.06E+05	27646.2	8.87	Bos taurus	NCBInr	76668658	PREDICTED: similar to Galectin-3 (Galactose-specific lectin 3) (Mac-2 antige
181	21	10	141.33	30	7.84E+04	37685.5	7.03	Bos taurus	NCBInr	83638723	transaldolase 1
182	13	10	138.46	55	4.19E+04	22426.6	8.4	Bos taurus	NCBInr	61888874	transgelin 2
183	9	9	137.5	10	1.58E+04	136063.2	8.62	Bos taurus	NCBInr	76643113	PREDICTED: similar to Nitric oxide synthase, inducible (NOS, type II) (Inducil
184	30	9	137.4	15	2.18E+05	54848.5	5.05	Bos taurus	NCBInr	479	cytokeratin VIb
185	13	9	137.09	35	9.02E+04	36438.4	6.16	Bos taurus	NCBInr	74354869	Hypothetical protein LOC535182
186	10	8	136.57	21	5.13E+04	56285	5.93	Bos taurus	NCBInr	76631190	PREDICTED: similar to UDP-N-acteylglucosamine pyrophosphorylase 1, like
187	11	8	136.36	16	1.10E+05	64427.6	5.56	Bos taurus	NCBInr	76649693	PREDICTED: similar to FK506 binding protein 10 precursor (Peptidyl-prolyl ci
188	13	8	136.23	31	1.30E+05	32884.3	4.8	Bos taurus	NCBInr	73587277	Laminin receptor 1 (ribosomal protein SA, 67 kDA)
189	9	8	135.31	18	5.45E+04	57210.7	8.81	Bos taurus	NCBInr	76644716	PREDICTED: similar to proteasome (prosome, macropain) 26S subunit, non-/
190	14	9	134.87	18	9.27E+04	59950.5	5.86	Bos taurus	NCBInr	76625467	PREDICTED: similar to Phosphoacetylglucosamine mutase (PAGM) (Acetylgl
191	8	8	134.31	38	1.01E+05	24152.9	8.05	Bos taurus	NCBInr	76671596	PREDICTED: similar to Bifunctional 3-phosphoadenosine 5-phosphosulfate s
192	9	9	133.36	17	8.69E+04	60206.8	5.8	Bos taurus	NCBInr	81673561	t-complex protein 4a
193	13	7	133.13	13	1.48E+05	69020.9	8.92	Pan troglody	NCBInr	55624160	EGF-like repeats and discoidin I-like domains-containing protein 3
194	17	7	132.18	29	1.84E+05	41170.6	6.46	Bos taurus	NCBInr	76626357	PREDICTED: similar to Acetyl-CoA acetyltransferase, cytosolic (Cytosolic ace
195	8	8	132.16	23	5.48E+04	46413.1	7.09	Bos taurus	NCBInr	184	aspartate aminotransferase
196	12	7	130.9	31	1.19E+05	29798.7	4.62	Bos taurus	NCBInr	76642117	PREDICTED: similar to reticulocalbin 3, EF-hand calcium binding domain
197	8	8	130.42	43	6.03E+04	26992	5.17	Bos taurus	NCBInr	74268283	Chloride intracellular channel 1
198	7	7	129.61	26	6.47E+04	41571.8	6.15	Bos taurus	NCBInr	84708845	Unknown (protein for MGC:133898)
199	8	8	129.43	23	8.81E+04	47513.8	9.19	Bos taurus	NCBInr	415324	aspartate aminotransferase
200	9	8	128.82	15	6.19E+04	83112.9	6.7	Bos taurus	NCBInr	81674209	STAT3 protein
201	8	8	126.29	18	5.84E+04	55605.8	7.62	Bos taurus	NCBInr	74268173	Serine hydroxymethyltransferase 2 (mitochondrial)
202	7	7	122.3	18	6.00E+04	57475.6	6.18	Bos taurus	NCBInr	73586876	Hypothetical protein LOC505313
203	11	7	122.07	35	9.47E+04	25101.7	6.6	Bos taurus	NCBInr	76649600	PREDICTED: similar to Dolichyl-diphosphooligosaccharide--protein glycosyltr
204	9	8	122.04	18	5.39E+04	59290.6	9.04	Bos taurus	NCBInr	76634481	PREDICTED: similar to Cytochrome P450 7B1 (Oxysterol 7-alpha-hydroxylas
205	10	8	120.68	12	6.70E+04	73257.3	6.71	Bos taurus	NCBInr	76622127	PREDICTED: similar to KH-type splicing regulatory protein (FUSE binding prc
206	10	9	120.32	20	6.56E+04	52240.7	6.01	Bos taurus	NCBInr	76643080	PREDICTED: similar to 26S proteasome non-ATPase regulatory subunit 11 (2
207	8	7	119.33	22	7.72E+04	50170.3	6.44	Bos taurus	NCBInr	76649598	PREDICTED: similar to Dolichyl-diphosphooligosaccharide--protein glycosyltr
208	8	8	118.72	18	4.71E+04	68917.3	5.69	Bos taurus	NCBInr	75773506	Eukaryotic translation initiation factor 4B

groupNun	numSpect	unique peptide	scoreUnique	% coverage	totalIntensity	mw	pI	species	database	accession	Protein name
209	7	7	117.62	20	6.53E+04	56451.9	6.47	Bos taurus	NCBInr	78042498	phosphoglycerate dehydrogenase
210	14	8	117.21	30	5.32E+04	26604.1	4.7	Bos taurus	NCBInr	28461287	hepatoma-derived growth factor (high-mobility group protein 1-like)
211	14	8	117.18	6	3.87E+04	138850.1	6.39	Bos taurus	NCBInr	76609270	PREDICTED: similar to Collagen alpha 1(III) chain precursor isoform 2
212	10	7	116.74	11	5.27E+04	97227.8	4.68	Bos taurus	NCBInr	76644624	PREDICTED: similar to karyopherin beta 1 isoform 2
213	9	8	116.24	15	8.85E+04	66153.3	6.05	Bos taurus	NCBInr	76619715	PREDICTED: similar to phosphoglucomutase 2
214	7	7	115.26	35	3.26E+04	22959.1	9.86	Bos taurus	NCBInr	28189605	similar to ribosomal protein S3
215	17	8	114.26	14	8.70E+04	71705	6.42	Homo sapie	NCBInr	25058739	ALB protein
216	8	8	114.23	29	3.03E+04	33072.2	9.34	Bos taurus	NCBInr	76632116	mitochondrial F1-ATPase gamma-subunit
217	8	8	113.24	13	5.96E+04	68475.7	5.42	Bos taurus	NCBInr	75775489	ATPase, H+ transporting, lysosomal (vacuolar proton pump), alpha polypeptic
218	7	7	113.17	35	3.37E+04	29820.3	5.57	Homo sapie	NCBInr	46360168	prohibitin
219	8	7	112.69	27	6.11E+04	31157.8	5.67	BOVIN	NCBInr	47117864	NG,NG-dimethylarginine dimethylaminohydrolase 1 (Dimethylargininase 1) (D
220	11	7	112.66	25	4.77E+04	28727.3	9.31	Bos taurus	NCBInr	74354583	Unknown (protein for MGC:127664)
221	10	8	112.57	28	1.24E+04	41590.3	6.83	Bos taurus	NCBInr	60650302	biglycan preproprotein
222	8	8	111.4	8	1.78E+04	125099.6	6.61	Bos taurus	NCBInr	76660845	PREDICTED: similar to SEC31-like 1 isoform 2
223	8	7	111.15	17	6.44E+04	51272.9	7.16	Bos taurus	NCBInr	74267948	CAP, adenylate cyclase-associated protein 1
224	17	6	110.53	24	9.89E+04	38624.7	5.64	Bos taurus	NCBInr	76608399	PREDICTED: similar to Pyridoxal kinase (Pyridoxine kinase)
225	14	7	110.51	39	7.75E+04	16702	4.65	Bos taurus	NCBInr	76676187	PREDICTED: similar to calnexin
226	7	7	110.2	16	4.12E+04	56135.4	5.01	Bos taurus	NCBInr	76617087	PREDICTED: similar to protein kinase C and casein kinase substrate in neurc
227	8	7	110.15	19	5.97E+04	39216.1	9.26	Bos taurus	NCBInr	61832036	PREDICTED: similar to IKK interacting protein isoform 2 isoform 1
228	10	7	109.61	24	5.44E+04	29772.7	5.65	Bos taurus	NCBInr	73587049	Unknown (protein for MGC:128392)
229	9	7	109.58	13	5.89E+04	58206.8	7.01	Bos taurus	NCBInr	83406133	Hypothetical protein LOC613336
230	16	6	108.2	20	1.30E+05	41445.1	5.22	Bos taurus	NCBInr	76617010	PREDICTED: similar to heat shock 70kD protein binding protein isoform 2
231	10	7	107.97	16	6.65E+04	60882.3	7.88	Bos taurus	NCBInr	76630143	PREDICTED: similar to matrilin 3 precursor
232	8	8	107.94	36	3.77E+04	34349.2	6.84	Bos taurus	NCBInr	75948237	Hypothetical protein LOC540838
233	9	8	107.78	9	5.30E+04	112885.4	5.14	Bos taurus	NCBInr	76607529	PREDICTED: similar to proteasome 26S non-ATPase subunit 2
234	8	6	106.58	10	6.26E+04	75217.1	7.12	Bos taurus	NCBInr	76620042	PREDICTED: similar to Lysosome membrane protein II (LIMP II) (Scavenger
235	7	7	106.51	29	3.83E+04	31235.5	10.25	Bos taurus	NCBInr	74267604	Ribosomal protein S2
236	13	6	106.51	19	1.39E+05	46182.2	5.32	Mus musculi	NCBInr	74139596	Eif4a1 protein
237	9	7	106.18	26	6.55E+04	38221.9	6.33	Bos taurus	NCBInr	76617802	PREDICTED: similar to Poly(rC)-binding protein 2 (Alpha-CP2) (Putative hete
238	6	6	105.97	18	4.20E+04	56240.2	6.23	Bos taurus	NCBInr	76634377	PREDICTED: similar to carbonic anhydrase VIII
239	7	7	105.5	34	5.15E+04	26879.6	3.88	Bos taurus	NCBInr	61857708	PREDICTED: similar to acidic (leucine-rich) nuclear phosphoprotein 32 family
240	9	7	103.88	19	6.12E+04	55311.6	8.36	Bos taurus	NCBInr	76622496	PREDICTED: similar to Vesicular integral-membrane protein VIP36 precursor
241	7	6	103.85	32	6.78E+04	21183.5	5.73	Bos taurus	NCBInr	76656657	PREDICTED: similar to Prolyl 4-hydroxylase alpha-1 subunit precursor (4-PH
242	7	7	102.6	3	6.87E+03	307583.1	7.99	Bos taurus	NCBInr	76639293	PREDICTED: similar to GCN1 general control of amino-acid synthesis 1-like '
243	9	6	101.89	22	4.62E+04	31308.3	4.9	Bos taurus	NCBInr	74267652	Hypothetical protein LOC540984
244	6	6	101.66	26	4.96E+04	29945.1	9.75	Bos taurus	NCBInr	74267633	Ribosomal protein S3A
245	7	7	101.65	33	5.18E+04	22612.1	6.73	BOVIN	NCBInr	121664	Glutathione peroxidase 1 (GSHPx-1) (GPx-1) (Cellular glutathione peroxidase
246	7	7	101.27	22	6.34E+04	39837.7	6.14	Bos taurus	NCBInr	82571797	Similar to GDP-mannose pyrophosphorylase B isoform 2
247	6	6	100.77	14	5.92E+04	49784.1	9.29	Bos taurus	NCBInr	76635122	PREDICTED: similar to Acetyl-CoA acetyltransferase, mitochondrial precurso
248	10	6	100.6	22	5.19E+04	38756.6	5.93	Bos taurus	NCBInr	74354899	Lumican
249	6	5	98.95	19	4.09E+04	50680.2	8.77	HUMAN	NCBInr	67472677	septin 7
250	8	7	97.93	37	6.41E+04	19581.4	4.84	Bos taurus	NCBInr	74356483	Tumor protein, translationally-controlled 1
251	7	6	97.76	16	5.27E+04	45797.3	7.64	Bos taurus	NCBInr	76626483	proteasome chain p42
252	9	8	97.03	26	3.94E+04	37429.9	8.97	Bos taurus	NCBInr	76662781	PREDICTED: similar to Heterogeneous nuclear ribonucleoproteins A2/B1 (hn
253	7	6	96.57	30	7.05E+04	24804.9	4.51	Bos taurus	NCBInr	62460568	eukaryotic translation elongation factor 1 beta 2
254	9	6	96.08	32	4.33E+04	22409	6.22	Bos taurus	NCBInr	74354052	Hypothetical protein LOC517171
255	5	5	95.99	45	5.82E+04	19987.8	5.88	Bos taurus	NCBInr	42564199	ferritin light polypeptide
256	6	6	95.86	13	4.96E+04	73413.6	7.03	Bos taurus	NCBInr	78042544	galactosidase, beta 1
257	8	6	95.14	30	5.19E+04	23544	6.39	Bos taurus	NCBInr	74354082	Hypothetical protein LOC509970
258	5	5	94.35	16	3.88E+04	47362.7	4.4	Bos taurus	NCBInr	76617377	PREDICTED: similar to Nucleosome assembly protein 1-like 1 (NAP-1 relatec
259	6	6	94.09	42	3.71E+04	18692.6	5.99	Bos taurus	NCBInr	74356487	ATP synthase, H+ transporting, mitochondrial F0 complex, subunit d
260	10	6	93.89	26	7.20E+04	34879.6	9.58	Bos taurus	NCBInr	77736103	hypothetical protein LOC532659

groupNun	numSpect	unique peptide	scoreUnique	% coverage	totalIntensity	mw	pI	species	database	accession	Protein name
261	11	6	93.71	12	1.00E+05	53451.4	5.49	Bos taurus	NCBInr	76656527	PREDICTED: similar to annexin VII isoform 2 isoform 4
262	6	6	93.36	24	6.69E+04	38876.4	6.17	Bos taurus	NCBInr	30466254	gelsolin-like capping protein
263	18	6	93.28	10	1.13E+05	60825.3	8.7	Bos taurus	NCBInr	76617862	keratin 5
264	7	6	92.98	12	3.34E+04	56309.9	8.72	Bos taurus	NCBInr	76644089	PREDICTED: similar to aldehyde dehydrogenase 3A2 isoform 1 isoform 2
265	11	7	92.08	11	4.94E+04	66921.2	6.76	Canis familia	NCBInr	73964981	MLL septin-like fusion protein MSF-A
266	6	5	92	15	3.69E+04	47638.3	5.88	Bos taurus	NCBInr	75773598	S-adenosylhomocysteine hydrolase
267	7	7	91.08	30	1.72E+04	26918.6	5.09	Bos taurus	NCBInr	76637711	PREDICTED: similar to EF hand domain containing 2 isoform 2
268	6	6	91.06	28	3.93E+04	24469.7	6.12	Bos taurus	NCBInr	83405346	RAB25, member RAS oncogene family
269	6	6	90.41	36	3.00E+04	23466.7	8.64	Bos taurus	NCBInr	77736431	hypothetical protein LOC613749
270	6	6	90.16	10	3.86E+04	75769	6.73	Bos taurus	NCBInr	76623789	PREDICTED: similar to arginyl-tRNA synthetase isoform 5
271	6	5	89.37	14	2.88E+04	44334.1	8.32	Bos taurus	NCBInr	73586687	Hypothetical protein LOC508324
272	8	6	89.27	27	1.87E+04	26689.6	6.45	Bos taurus	NCBInr	74267824	Triosephosphate isomerase
273	6	6	89.21	8	4.43E+04	80578.3	5.67	Bos taurus	NCBInr	473522	adseverin
274	5	5	87.82	14	2.16E+04	46535	8.09	Bos taurus	NCBInr	756	Sjogren syndrome antigen B (autoantigen La)
275	7	5	87.77	11	5.40E+04	51723.5	6.19	Bos taurus	NCBInr	27807349	serine (or cysteine) proteinase inhibitor, clade G (C1 inhibitor), member 1, (an
276	7	7	87.36	9	8.10E+03	119794.6	5.54	Bos taurus	NCBInr	76623926	PREDICTED: similar to leucyl/cystinyl aminopeptidase isoform 1
277	5	5	87.12	14	4.33E+04	46208.3	6.37	Bos taurus	NCBInr	76610535	PREDICTED: similar to GDP-mannose pyrophosphorylase A isoform 2
278	6	6	86.68	26	1.88E+04	28609.5	6.96	Bos taurus	NCBInr	81673887	Similar to proteasome (prosome, macropain) subunit, beta type 5
279	6	5	86.38	20	3.20E+04	21623.2	4.5	Bos taurus	NCBInr	76658622	membrane steroid binding protein
280	6	6	85.57	9	1.45E+04	131429	6.42	Bos taurus	NCBInr	76623638	PREDICTED: similar to Protein transport protein Sec24D (SEC24-related prot
281	29	5	85.15	3	2.03E+05	141875.1	6.82	Canis familia	NCBInr	55742776	alpha 1 type II collagen
282	6	5	84.96	10	4.00E+04	56704.8	6.89	Bos taurus	NCBInr	76611743	PREDICTED: similar to aldehyde dehydrogenase 9A1 isoform 2
283	6	5	84.44	31	3.02E+04	27379.8	5.31	Bos taurus	NCBInr	74267960	Proteasome activator subunit 2
284	9	6	84.33	10	3.81E+04	68587.5	6.14	Bos taurus	NCBInr	76607976	PREDICTED: similar to procollagen-lysine, 2-oxoglutarate 5-dioxygenase 2 is
285	7	5	83.36	26	2.55E+04	26496.9	8.27	Bos taurus	NCBInr	217606	adenylate kinase 2A
286	5	5	82.84	27	4.59E+04	32979.2	5.57	Bos taurus	NCBInr	74354976	Capping protein (actin filament) muscle Z-line, alpha 2
287	7	5	82.29	23	5.58E+04	22264.8	6.2	Bos taurus	NCBInr	76613178	PREDICTED: similar to Rho-related GTP-binding protein RhoC (Silica-induce
288	5	5	82	19	1.78E+04	33856	9.62	Bos taurus	NCBInr	76655832	PREDICTED: similar to cytidylate kinase
289	6	6	81.45	14	2.83E+04	40140	9.39	Bos taurus	NCBInr	27807185	solute carrier family 25 (mitochondrial carrier
290	5	5	81.33	17	4.39E+04	31581.2	4.98	Bos taurus	NCBInr	76670238	PREDICTED: similar to Thioredoxin domain containing protein 1 precursor (T
291	5	5	81.28	6	9.30E+03	107529.4	4.85	Bos taurus	NCBInr	79153667	Vesicle docking protein p115
292	6	5	80.79	28	2.45E+04	26246.2	8.26	Bos taurus	NCBInr	83638719	MGC133525 protein
293	5	5	80.16	22	4.14E+04	35569.7	8.32	Bos taurus	NCBInr	28603704	APEX nuclease (multifunctional DNA repair enzyme) 1
294	5	5	80.16	24	3.79E+04	30914.2	7.18	Bos taurus	NCBInr	76610491	PREDICTED: similar to Aflatoxin B1 aldehyde reductase member 2 (AFB1-AF
295	5	5	79.99	21	3.21E+04	34173.7	6.52	Bos taurus	NCBInr	74353940	sulfotransferase family, cytosolic, 1A, phenol-preferring, member 1
296	9	5	79.54	12	6.57E+04	44773.8	7.64	Bos taurus	NCBInr	61816796	PREDICTED: similar to Putative GTP-binding protein PTD004 isoform 1
297	5	5	79.37	21	2.40E+04	26661.9	6.82	Bos taurus	NCBInr	74355014	Dehydrogenase/reductase (SDR family) member 6
298	6	5	79.31	6	2.68E+04	86231.8	5.25	Bos taurus	NCBInr	76653005	PREDICTED: similar to CG1486-PA, isoform A
299	7	5	79.12	15	1.96E+04	40147.2	10.09	Bos taurus	NCBInr	76648962	PREDICTED: similar to Y55F3AM.10
300	6	5	78.54	17	3.59E+04	40976	8.69	Bos taurus	NCBInr	74355044	Actin related protein 2/3 complex, subunit 1B, 41kDa
301	8	5	78.47	11	3.84E+04	48927.4	5.14	Canis familia	NCBInr	73947624	Proteasome 26S ATPase subunit 4
302	5	5	78.41	1	3.23E+03	531958.1	6.01	Bos taurus	NCBInr	76647908	PREDICTED: similar to dynein, cytoplasmic, heavy polypeptide 1 isoform 3
303	7	5	78.35	11	3.38E+04	59070.7	5.12	Bos taurus	NCBInr	76627692	PREDICTED: similar to Sorting nexin-1 isoform 1
304	6	5	78.21	20	4.77E+04	34400.8	5.72	Bos taurus	NCBInr	74353873	Ribosomal protein, large, P0
305	5	4	77.96	19	3.05E+04	36754.3	6.28	Bos taurus	NCBInr	73586789	Proteasome (prosome, macropain) 26S subunit, non-ATPase, 7 (Mov34 hom
306	5	5	77.93	12	3.19E+04	46417.5	7.15	Bos taurus	NCBInr	74268328	Argininosuccinate synthetase
307	8	5	77.69	11	6.52E+04	48862.8	5.44	Sus scrofa	NCBInr	47523464	oligosaccharyltransferase OST48
308	5	5	77.69	15	3.63E+04	33194.6	5.39	Bos taurus	NCBInr	74353962	Chaperonin containing TCP1, subunit 5 (epsilon)
309	5	5	77.49	22	1.97E+04	24577.4	9.52	Bos taurus	NCBInr	76631901	PREDICTED: similar to prohibitin
310	7	4	77.27	10	5.20E+04	63572.1	6.87	Canis familia	NCBInr	73984196	Actr3 protein
311	5	5	77.16	15	4.66E+04	41375.9	6.5	Bos taurus	NCBInr	28461209	mitogen-activated protein kinase 1
312	7	5	75.62	14	4.58E+04	55559.3	5.64	Bos taurus	NCBInr	74353841	Hypothetical protein LOC507327

groupNun	numSpecI	unique peptide	scoreUnique	% coverage	totalIntensity	mw	pI	species	database	accession	Protein name
313	7	5	75.47	10	2.46E+04	74728.6	9.31	Bos taurus	NCBInr	76619804	PREDICTED: similar to Signal recognition particle 72 kDa protein (SRP72) isc
314	5	5	75.4	9	3.57E+04	72944.1	7.55	BOVIN	NCBInr	51338770	Succinate dehydrogenase [ubiquinone] flavoprotein subunit, mitochondrial pre
315	7	4	75.35	4	7.79E+04	95686.3	9.93	Pan troglody	NCBInr	55631158	YWHAZ protein
316	5	5	75.06	21	1.74E+04	33741.5	6.01	Bos taurus	NCBInr	1838956	capping protein, beta3 isoform
317	6	5	75.04	17	3.70E+04	32877.6	9.82	Bos taurus	NCBInr	32189336	solute carrier family 25 member 6
318	6	6	74.6	8	3.18E+04	71321.3	6.32	Bos taurus	NCBInr	74354788	Hypothetical protein LOC509624
319	5	5	74.45	6	3.46E+04	83990.8	8.48	Bos taurus	NCBInr	76638695	PREDICTED: similar to acetoacetyl-CoA synthetase, partial
320	6	5	74.31	18	3.68E+04	39668.1	6.76	Bos taurus	NCBInr	27807161	isocitrate dehydrogenase 3 (NAD+) alpha
321	6	6	74.16	8	1.05E+04	106548.7	5.25	Bos taurus	NCBInr	76610871	PREDICTED: similar to proteasome 26S non-ATPase subunit 1 isoform 8
322	5	5	73.66	12	4.23E+04	44911.5	6.1	Bos taurus	NCBInr	76648164	PREDICTED: similar to Cartilage-associated protein precursor, partial
323	118	4	73.51	25	1.79E+06	24409.6	7	PIG	NCBInr	136429	Trypsin precursor
324	6	5	73.33	12	3.53E+04	51036.9	6.13	Bos taurus	NCBInr	74354958	PSMC2 protein
325	5	5	73.14	19	1.73E+04	28821.8	9.42	Bos taurus	NCBInr	84490369	ATP synthase, H+ transporting, mitochondrial F0 complex, subunit b, isoform
326	8	4	72.96	13	9.67E+04	31721	4.41	Bos taurus	NCBInr	76668091	Myristoylated alanine-rich C-kinase substrate (MARCKS) (ACAMP-81)
327	5	5	72.81	17	3.20E+04	29595.9	10.16	Bos taurus	NCBInr	61835740	40S ribosomal protein S4
328	6	4	72.75	12	3.26E+04	56170.9	5.2	Bos taurus	NCBInr	76625333	PREDICTED: similar to 26S proteasome non-ATPase regulatory subunit 5 (2(
329	5	5	72.37	22	2.87E+04	31256.4	7.1	Bos taurus	NCBInr	75948233	PRDX3 protein
330	6	4	72.29	19	5.13E+04	26409.7	8.51	Pan troglody	NCBInr	55639371	RAN protein
331	6	5	71.64	12	4.52E+04	49212.8	5.87	Bos taurus	NCBInr	59858331	proteasome 26S ATPase subunit 1
332	5	5	71.34	23	2.19E+04	28718.6	8.91	Bos taurus	NCBInr	74356381	Shwachman-Bodian-Diamond syndrome
333	8	5	71.32	33	4.99E+04	17504.3	8.91	Bos taurus	NCBInr	76607963	PREDICTED: similar to procollagen-lysine, 2-oxoglutarate 5-dioxygenase 2 is
334	6	6	71.29	7	5.81E+04	71462.9	8.67	Bos taurus	NCBInr	76652230	PREDICTED: similar to ERGIC-53 protein precursor (ER-Golgi intermediate c
335	5	5	71.23	11	2.96E+04	60368	5.68	Bos taurus	NCBInr	76626675	PREDICTED: similar to Beta-hexosaminidase alpha chain precursor (N-acety
336	5	5	71.19	8	1.03E+04	101836.4	7.08	Bos taurus	NCBInr	76628078	PREDICTED: similar to C-1-tetrahydrofolate synthase, cytoplasmic (C1-THF s
337	5	4	70.78	12	3.84E+04	37391.2	5.6	Bos taurus	NCBInr	814	Guanine nucleotide-binding protein G(I)/G(S)/G(T) beta subunit 2 (Transducin
338	4	4	70.36	7	2.42E+04	80641.9	5.56	Bos taurus	NCBInr	27807495	prolyl oligopeptidase
339	6	4	70.21	11	5.20E+04	42840.7	6.03	Bos taurus	NCBInr	76671278	PREDICTED: similar to vesicle amine transport protein 1 isoform 1
340	5	4	69.27	8	2.52E+04	67818.2	6.39	Bos taurus	NCBInr	76613409	LOC512486 protein
341	4	4	69.09	12	2.43E+04	61657.5	5.47	Bos taurus	NCBInr	76657953	PREDICTED: similar to atlastin-like isoform 3
342	8	5	68.98	5	1.48E+04	108697.3	5.24	Bos taurus	NCBInr	76667061	PREDICTED: similar to Collagen alpha 1(VI) chain precursor isoform 1
343	5	4	68.95	15	3.22E+04	39677.4	7.46	Bos taurus	NCBInr	73586689	Hypothetical protein LOC505515
344	5	5	68.75	13	1.83E+04	44968.8	8.76	Bos taurus	NCBInr	76633465	PREDICTED: similar to Microtubule-associated protein RP/EB family member
345	7	5	68.72	26	4.83E+04	20161	5.09	Bos taurus	NCBInr	76629651	GTP binding protein Rab1a
346	4	4	68.24	7	2.35E+04	71006.3	6.41	Bos taurus	NCBInr	76607778	PREDICTED: similar to Lanosterol synthase (Oxidosqualene--lanosterol cycla
347	4	4	68.17	8	1.97E+04	85157.9	8.19	Bos taurus	NCBInr	76628858	PREDICTED: similar to Mannosyl-oligosaccharide glucosidase (Processing A
348	7	4	67.72	6	3.51E+04	73334.7	5.46	Bos taurus	NCBInr	76619718	PREDICTED: hypothetical protein XP_598213, partial
349	5	5	67.52	13	2.18E+04	42579.1	6.84	Bos taurus	NCBInr	76639219	PREDICTED: similar to Protein KIAA0152 precursor
350	4	4	67.15	9	3.35E+04	53959	5.22	Bos taurus	NCBInr	76651799	PREDICTED: similar to Ubiquitin carboxyl-terminal hydrolase 14 (Ubiquitin thi
351	5	5	67.12	9	2.85E+04	60107	7.1	Bos taurus	NCBInr	76628891	PREDICTED: similar to T-complex protein 1, eta subunit (TCP-1-eta) (CCT-et
352	5	5	67.11	8	2.33E+04	66993.8	8.24	Bos taurus	NCBInr	76611461	PREDICTED: similar to heterogeneous nuclear ribonucleoprotein R isoform 2
353	5	5	66.22	16	1.98E+04	38803.9	9.17	Bos taurus	NCBInr	76617606	Heterogeneous nuclear ribonucleoprotein A1 (Helix-destabilizing protein) (Sin
354	4	4	65.98	9	2.36E+04	55524.4	8.76	Bos taurus	NCBInr	76640954	PREDICTED: similar to Xaa-Pro dipeptidase (X-Pro dipeptidase) (Proline dipe
355	5	5	65.89	8	8.68E+03	104323.3	8.46	Bos taurus	NCBInr	76624106	PREDICTED: similar to Iron-responsive element binding protein 1 (IRE-BP 1)
356	5	4	65.88	9	2.85E+04	46691.2	7.51	Bos taurus	NCBInr	75773452	Hypothetical protein LOC537713
357	6	4	65.48	12	3.57E+04	45653.4	8.23	Homo sapie	NCBInr	976227	26S proteasome subunit p45
358	5	5	65.48	3	4.15E+03	193115.8	5	Mus musculi	NCBInr	30420885	collagen type XIV
359	9	4	65.24	5	6.67E+04	86925.2	8.91	Bos taurus	NCBInr	76622337	PREDICTED: similar to Septin-8
360	5	4	65.24	18	2.33E+04	28195.4	7.15	Bos taurus	NCBInr	27806083	peroxiredoxin 3
361	7	4	64.61	8	4.57E+04	48964.6	5.44	Bos taurus	NCBInr	74353855	HLA-B-associated transcript 1
362	4	4	64.42	15	2.16E+04	37187.1	5.84	Bos taurus	NCBInr	74356397	Hypothetical protein LOC538829
363	5	5	64.34	6	1.01E+04	119789.8	6.83	Bos taurus	NCBInr	79158721	ATP citrate lyase
364	4	4	64.3	14	1.68E+04	41919.7	10.33	Bos taurus	NCBInr	76666230	PREDICTED: similar to 40S ribosomal protein S7 (S8)

groupNun	numSpecI	unique peptide	scoreUnique	% coverage	totalIntensity	mw	pI	species	database	accession	Protein name
365	4	3	64.1	38	3.51E+04	15136.3	6.41	Bos taurus	NCBInr	76691672	PREDICTED: similar to 5-aminoimidazole-4-carboxamide ribonucleotide form
366	4	4	63.34	17	2.35E+04	33192.8	6.16	Bos taurus	NCBInr	75775302	Hypothetical protein LOC507313
367	5	5	63.26	22	2.15E+04	33454	7.73	Bos taurus	NCBInr	62460606	pyrroline-5-carboxylate reductase family, member 2
368	4	4	63.23	13	1.88E+04	34172.1	9.89	Bos taurus	NCBInr	32	2-oxoglutarate carrier
369	4	4	62.92	19	1.38E+04	25656	6.45	Bos taurus	NCBInr	76613071	Glutathione S-transferase M1
370	8	4	62.88	15	9.01E+04	36385.1	5.18	Bos taurus	NCBInr	76691116	eukaryotic translation initiation factor Eif4a2
371	4	4	62.65	6	1.86E+04	86558.4	6.45	Bos taurus	NCBInr	76645272	PREDICTED: similar to N-ethylmaleimide-sensitive factor isoform 4
372	7	4	62.63	6	6.92E+04	72341.8	8.68	Bos taurus	NCBInr	76661938	PREDICTED: similar to UV excision repair protein RAD23 homolog B (hHR23
373	4	4	62.56	14	4.14E+04	22474.7	9.26	Bos taurus	NCBInr	82571590	Similar to FK506 binding protein 11 precursor (Peptidyl-prolyl cis-trans isomer
374	4	4	62.27	14	2.02E+04	29511	7.58	Macaca fasc	NCBInr	67967814	Proteasome (prosome, macropain) subunit, alpha type 4
375	5	4	62.07	16	3.09E+04	34025.2	4.1	Bos taurus	NCBInr	76612860	PREDICTED: similar to acidic (leucine-rich) nuclear phosphoprotein 32 family
376	6	4	62	9	4.39E+04	51251.1	6.33	Bos taurus	NCBInr	76620649	PREDICTED: similar to Heterogeneous nuclear ribonucleoprotein H (hnRNP H
377	5	4	62	8	3.29E+04	53284.8	6.93	Bos taurus	NCBInr	76672944	PREDICTED: similar to solute carrier family 25 member 24 isoform 1 isoform
378	4	4	61.93	18	2.53E+04	35425.3	8.35	Bos taurus	NCBInr	74267964	PDZ and LIM domain 4
379	4	4	61.7	7	1.99E+04	89686.8	6.01	Bos taurus	NCBInr	76625842	PREDICTED: similar to Protein KIAA0776 isoform 1
380	4	4	61.38	20	1.91E+04	31548.1	6.5	Bos taurus	NCBInr	76631393	PREDICTED: similar to esterase D/formylglutathione hydrolase isoform 5
381	5	4	61.34	12	3.88E+04	40217.7	6.48	Bos taurus	NCBInr	61886357	PREDICTED: similar to N-acetylneuraminic acid phosphate synthase isoform
382	5	4	61.28	7	4.66E+04	70539.3	6.3	Bos taurus	NCBInr	76634024	PREDICTED: similar to eukaryotic translation elongation factor 1 delta isoforn
383	4	4	60.52	10	1.67E+04	40620.5	6.12	Bos taurus	NCBInr	27806463	peptidylprolyl isomerase D
384	4	4	60.5	34	2.48E+04	16384.9	9.25	Bos taurus	NCBInr	76613864	PREDICTED: similar to ER-Golgi intermediate compartment 32 kDa protein (E
385	3	3	60.05	11	2.11E+04	48148.8	8.8	Bos taurus	NCBInr	73586962	Ubiquinol-cytochrome c reductase core protein II
386	4	4	59.9	12	3.96E+04	41061.7	5.79	Bos taurus	NCBInr	76629739	PREDICTED: similar to actin-related protein 2, partial
387	4	4	59.88	6	2.09E+04	71710.8	7.49	Bos taurus	NCBInr	76619562	PREDICTED: similar to Phenylalanyl-tRNA synthetase beta chain (Phenylalar
388	5	4	59.84	8	3.05E+04	49718.7	5.26	Bos taurus	NCBInr	76635541	PREDICTED: similar to Nucleobindin 2 precursor (DNA-binding protein NEFA
389	4	4	59.12	15	2.63E+04	34335.9	8.4	Bos taurus	NCBInr	78042500	hypothetical protein LOC505126
390	4	4	58.93	9	1.50E+04	70798.4	5.41	Bos taurus	NCBInr	76659016	Lymphocyte cytosolic protein 1 (L-plastin)
391	11	4	58.57	10	7.16E+04	40001.9	6.42	Bos taurus	NCBInr	27806703	CD44 antigen [homing function and Indian blood group system]
392	3	3	58.2	10	1.83E+04	47897.6	5.01	Bos taurus	NCBInr	76620664	PREDICTED: sequestosome 1 isoform 1
393	6	4	58.14	11	3.18E+04	45894.6	5.03	Bos taurus	NCBInr	76662827	PREDICTED: similar to transmembrane emp24 protein transport domain cont
394	5	3	57.72	6	3.57E+04	67915.6	8.95	Bos taurus	NCBInr	76636495	LOC508448 protein
395	4	4	56.94	2	1.82E+03	237106.1	8.61	Bos taurus	NCBInr	76625277	PREDICTED: similar to Proteasome-associated protein ECM29 homolog (Ecr
396	7	5	56.91	6	6.46E+03	90280.5	8.6	Bos taurus	NCBInr	31982399	a disintegrin-like and metalloprotease (reprolysin type) with thrombospondin t
397	6	3	56.85	5	9.04E+04	81390.6	5.38	Pan troglody	NCBInr	55632315	PREDICTED: heat shock 70kDa protein 5 (glucose-regulated protein, 78kDa)
398	4	4	56.76	14	2.79E+04	37730.7	5.36	Bos taurus	NCBInr	76655900	PREDICTED: similar to SPFH domain protein 2 precursor
399	4	4	56.76	8	2.02E+04	76683.2	5.37	Bos taurus	NCBInr	76675970	PREDICTED: similar to nuclear receptor binding protein
400	3	3	56.67	9	2.26E+04	60682.2	6.35	Bos taurus	NCBInr	62751751	EH-domain containing 1
401	6	4	56.4	12	4.10E+04	37526.1	6.66	Homo sapier	NCBInr	460771	hnRNP-E1
402	3	3	56.32	21	2.02E+04	13737.7	8.25	Bos taurus	NCBInr	76662308	PREDICTED: similar to 3-oxoacid CoA transferase 1, partial
403	3	3	56.06	7	2.54E+04	61981.1	6.36	Bos taurus	NCBInr	76652215	PREDICTED: similar to Asparaginyl-tRNA synthetase, cytoplasmic (Asparagir
404	4	4	55.7	3	3.69E+03	198221.9	5.84	Bos taurus	NCBInr	76627770	PREDICTED: similar to talin 2
405	4	4	55.64	8	3.07E+04	68742.2	5.15	Bos taurus	NCBInr	76652904	PREDICTED: similar to G1 to S phase transition 1
406	5	4	55.3	13	2.03E+04	35403	8.34	Bos taurus	NCBInr	4097831	zeta-crystallin
407	5	4	55.12	3	2.04E+04	113018.4	9.2	Bos taurus	NCBInr	31341666	mannosidase, alpha, class 2B, member 1
408	4	4	55.03	7	1.77E+04	55488.8	8.59	Bos taurus	NCBInr	76619545	PREDICTED: similar to Enigma homolog (Enigma-like PDZ and LIM domains
409	4	4	54.93	5	7.93E+03	121587.6	5.64	Bos taurus	NCBInr	76672887	PREDICTED: similar to exportin 1, CRM1 homolog
410	3	3	54.61	20	2.16E+04	32035.3	6.82	Bos taurus	NCBInr	62460502	hypothetical protein LOC512526
411	4	4	54.21	2	3.07E+03	254778.7	5.33	Bos taurus	NCBInr	76662196	PREDICTED: similar to melanoma-associated chondroitin sulfate proteoglyca
412	7	4	53.86	10	4.26E+04	34856.6	5.46	Bos taurus	NCBInr	62988316	follistatin-like 1
413	4	3	53.8	7	2.05E+04	62135.1	4.9	Bos taurus	NCBInr	76617192	PREDICTED: similar to fibulin 1 isoform C precursor isoform 3
414	3	3	53.75	46	2.80E+04	9985.6	5.52	Bos taurus	NCBInr	76691670	PREDICTED: similar to 5-aminoimidazole-4-carboxamide ribonucleotide form
415	5	4	53.59	4	2.22E+04	100494.8	4.86	Bos taurus	NCBInr	76621399	PREDICTED: similar to transportin 2 (importin 3, karyopherin beta 2b) isoforn
416	4	3	53.54	11	2.71E+04	54723.9	6.07	BOVIN	NCBInr	3915188	Thioredoxin reductase 1, cytoplasmic (TR) (TR1)

groupNun	numSpect	unique peptide	scoreUnique	% coverage	totalIntensity	mw	pI	species	database	accession	Protein name
417	4	4	53.45	5	4.42E+03	111915.1	4.85	Bos taurus	NCBInr	27806553	microtubule-associated protein 4
418	3	3	53.3	6	4.50E+04	78539.6	6.39	Mus musculi	NCBInr	13183789	glutamine: fructose-6-phosphate amidotransferase 1 muscle isoform GFAT1M
419	4	4	53.17	12	1.05E+04	32541.8	10.89	Bos taurus	NCBInr	76631260	Histone H1.1
420	4	4	53.16	25	1.58E+04	21245.4	5.66	Bos taurus	NCBInr	76669166	PREDICTED: similar to Copine-3 (Copine III), partial
421	3	3	53.13	15	1.98E+04	27368.8	4.71	Bos taurus	NCBInr	74356321	Hypothetical protein LOC505637
422	3	3	52.85	5	1.27E+04	83352.3	6.64	Bos taurus	NCBInr	76619239	PREDICTED: similar to dynamin 1-like isoform 2
423	3	3	52.42	25	2.22E+04	18154.7	4.96	Bos taurus	NCBInr	81294317	Hypothetical protein LOC517857
424	4	4	52.36	21	1.60E+04	24306.1	8.26	Bos taurus	NCBInr	74267846	GrpE-like 1, mitochondrial
425	4	4	52.31	8	2.67E+04	49851.7	6.13	Bos taurus	NCBInr	76610199	LOC506562 protein
426	5	4	52.17	10	3.55E+04	37013.7	6.1	Bos taurus	NCBInr	76630782	PREDICTED: similar to protein phosphatase 2A, regulatory subunit B isoform
427	4	4	52.09	6	2.72E+04	79933.6	8.37	Bos taurus	NCBInr	76678705	PREDICTED: similar to protein kinase C, delta isoform 3
428	3	3	52.03	7	2.03E+04	66464.5	8.51	Mus musculi	NCBInr	50510663	PREDICTED: glutaminase isoform 5
429	3	3	51.53	15	1.82E+04	23712.6	4.95	Bos taurus	NCBInr	74354306	Hypothetical protein LOC533251
430	3	3	51.4	19	1.68E+04	23370	4.51	Bos taurus	NCBInr	74354935	Hypothetical protein LOC513312
431	5	4	51.29	16	1.34E+04	28405.3	5.19	Bos taurus	NCBInr	61553092	proteasome alpha 3 subunit isoform 1
432	4	3	51.27	19	2.68E+04	23349.7	9.91	Bos taurus	NCBInr	27806307	mitochondrial ATP synthase, O subunit
433	3	3	51	5	1.32E+04	76837.5	6.61	Bos taurus	NCBInr	27806089	protein kinase, C alpha
434	3	3	50.65	5	2.89E+04	81837	5.93	Homo sapie	NCBInr	28466983	leprecan-like 2
435	3	3	50.64	5	1.94E+04	64408.8	9.34	Bos taurus	NCBInr	76689356	PREDICTED: similar to septin 5
436	6	3	50.55	16	2.63E+04	29716.8	6.01	Bos taurus	NCBInr	76669942	type XI collagen alpha 1 chain
437	3	3	50.51	6	2.17E+04	48971.6	5.41	Bos taurus	NCBInr	76681614	LOC504752 protein
438	9	3	50.17	6	6.97E+04	47457.9	5.61	Bos taurus	NCBInr	76675550	PREDICTED: similar to actin-related protein 3-beta
439	3	3	50.15	15	5.58E+03	28666.8	10.85	Bos taurus	NCBInr	74267715	Ribosomal protein S6
440	4	3	50.04	8	3.49E+04	65626.6	6.87	Pan troglody	NCBInr	55615936	5-aminoimidazole-4-carboxamide ribonucleotide formyltransferase/IMP cyclol
441	4	3	49.96	8	2.39E+04	36730.9	7.05	Bos taurus	NCBInr	76655159	PREDICTED: similar to caspase 7 isoform delta
442	3	3	49.9	13	1.68E+04	31023.2	9.04	Bos taurus	NCBInr	73587441	NAD(P)H dehydrogenase, quinone 1
443	3	3	49.8	9	1.15E+04	61178.6	5.83	Bos taurus	NCBInr	76648277	PREDICTED: similar to EPM2A-interacting protein 1 (Laforin-interacting prote
444	3	3	49.25	23	1.55E+04	14894.1	5.3	Bos taurus	NCBInr	76650162	PREDICTED: similar to glyoxalase 1
445	3	3	49.2	8	2.51E+04	36167	9.41	Bos taurus	NCBInr	78045537	hypothetical protein LOC509983
446	3	3	49.02	5	6.17E+03	74787	9.49	Bos taurus	NCBInr	76637153	PREDICTED: similar to heterogeneous nuclear ribonucleoprotein U isoform b
447	4	3	49.01	7	2.64E+04	46560.9	5.34	Bos taurus	NCBInr	76616903	alpha-N-acetylgalactosaminidase precursor
448	4	3	48.99	15	2.18E+04	21424	7.52	Bos taurus	NCBInr	74353868	Ras-related C3 botulinum toxin substrate 2 (rho family, small GTP binding prc
449	4	3	48.76	12	2.38E+04	37171.2	6.75	Bos taurus	NCBInr	76673628	PREDICTED: similar to Ribose-phosphate pyrophosphokinase I (Phosphoribc
450	3	3	48.7	13	2.23E+04	34577.3	5.23	Bos taurus	NCBInr	73587111	Leucine zipper transcription factor-like 1
451	3	3	48.47	23	3.77E+03	22661.1	9.39	Bos taurus	NCBInr	76681980	PREDICTED: similar to Latent transforming growth factor beta binding protein
452	5	3	48.4	6	2.80E+04	70671.3	9.51	Bos taurus	NCBInr	74268035	Poly(A) binding protein, cytoplasmic 1
453	3	3	48.07	6	2.21E+04	53052.9	7.02	Bos taurus	NCBInr	76645357	PREDICTED: similar to 26S proteasome non-ATPase regulatory subunit 12 (2
454	4	3	48.07	14	2.93E+04	27842.6	4.58	Bos taurus	NCBInr	76685000	PREDICTED: hypothetical protein XP_588946, partial
455	6	3	47.96	5	6.95E+04	56822.3	8.82	Bos taurus	NCBInr	76631182	PREDICTED: similar to Ectonucleoside triphosphate diphosphohydrolase 2 (N
456	3	3	47.87	14	1.40E+04	33643.9	5.85	Bos taurus	NCBInr	76615466	PREDICTED: similar to Biliverdin reductase A precursor (Biliverdin-IX alpha-r
457	3	3	47.8	5	2.51E+04	84116.3	5.96	Bos taurus	NCBInr	76620459	PREDICTED: similar to Leucine zipper-EF-hand containing transmembrane p
458	3	3	47.67	21	3.64E+04	22201.6	9.36	Bos taurus	NCBInr	76633366	PREDICTED: similar to Copine-1 (Copine I) isoform 1
459	3	3	47.64	10	1.80E+04	36784.5	7.65	Bos taurus	NCBInr	30794344	aldo-keto reductase family 1, member C1 (dihydrodiol dehydrogenase 1
460	3	3	47.6	12	1.95E+04	37088.2	5.56	Bos taurus	NCBInr	76633362	PREDICTED: similar to Copine-1 (Copine I) isoform 9
461	3	3	47.45	6	1.99E+04	56576.1	5.66	Bos taurus	NCBInr	297129	H+-ATPase non-catalytic subunit B
462	3	3	47.37	23	2.85E+04	22132.5	6.58	Bos taurus	NCBInr	74354774	Biliverdin reductase B (flavin reductase (NADPH))
463	3	3	47.24	5	2.38E+04	61146.2	7.07	Bos taurus	NCBInr	76659718	PREDICTED: similar to ribosomal protein S6 kinase polypeptide 3, partial
464	3	3	47.23	12	4.13E+04	28806.2	5.63	Bos taurus	NCBInr	76639231	PREDICTED: similar to endoplasmic reticulum protein 29 precursor
465	3	3	46.97	1	1.48E+04	176804.7	6.53	Bos taurus	NCBInr	76649917	collagen type XI alpha 2
466	3	3	46.95	5	1.80E+04	71930.3	6.52	Pan troglody	NCBInr	55616117	PREDICTED: tubulin, alpha 1
467	5	4	46.92	15	1.32E+04	36719.5	5.57	Bos taurus	NCBInr	73586701	CTSB protein
468	4	3	46.79	15	1.01E+04	22964.6	9.76	Homo sapie	NCBInr	62897773	ribosomal protein S5 variant

groupNun	numSpecI	unique peptide	scoreUnique	% coverage	totalIntensity	mw	pI	species	database	accession	Protein name
469	5	4	46.67	24	6.04E+03	25015.6	7.94	Bos taurus	NCBInr	899229	thrombospondin-1
470	3	3	46.63	1	2.48E+03	292118.3	5.52	Bos taurus	NCBInr	76659571	PREDICTED: similar to ubiquitin specific protease 9, X-linked isoform 1 isofor
471	4	3	46.52	6	1.50E+04	74425.2	8.49	Bos taurus	NCBInr	76631992	PREDICTED: similar to Carnitine O-palmitoyltransferase II, mitochondrial prec
472	4	3	46.47	28	2.25E+04	20504.7	6.74	Bos taurus	NCBInr	83638644	Similar to ADP-ribosylation factor-like 3
473	3	3	46.36	6	1.31E+04	70068.6	5.63	Bos taurus	NCBInr	76655054	PREDICTED: similar to X-prolyl aminopeptidase (aminopeptidase P) 1, solubl
474	4	3	46.28	8	2.07E+04	43244.7	8.57	Bos taurus	NCBInr	76613223	PREDICTED: similar to Chitinase 3-like protein 2 precursor (YKL-39) (Chondr
475	3	3	46.22	8	1.49E+04	42497.4	8.85	Bos taurus	NCBInr	76632784	LOC613338 protein
476	3	3	46.2	17	1.77E+04	27298.5	7.76	Bos taurus	NCBInr	74267997	transmembrane emp24 protein transport domain containing 9
477	3	3	46	3	1.34E+04	77865	6.37	Bos taurus	NCBInr	83405734	LOC511200 protein
478	4	3	45.78	8	2.38E+04	52655.7	5.6	Bos taurus	NCBInr	73586898	Hypothetical protein LOC512626
479	3	3	45.6	5	3.53E+04	66727.3	5.93	Bos taurus	NCBInr	73586515	Eukaryotic translation initiation factor 3, subunit 6 interacting protein
480	3	3	45.29	9	1.58E+04	44976.7	6.58	Bos taurus	NCBInr	76654829	LOC514371 protein
481	4	3	44.91	9	2.10E+04	57105.5	9.22	Bos taurus	NCBInr	17298537	polypyrimidine-tract binding protein
482	3	3	44.68	14	1.09E+04	26155.4	7.7	Bos taurus	NCBInr	74355022	ATPase, H+ transporting, lysosomal 31kDa, V1 subunit E isoform 1
483	4	3	44.65	7	1.39E+04	36965.4	6.52	Bos taurus	NCBInr	76668080	PREDICTED: similar to N(4)-(beta-N-acetylglucosaminyl)-L-asparaginase pre
484	4	3	44.58	8	6.50E+03	56297.6	8.16	Bos taurus	NCBInr	76607166	PREDICTED: similar to ectonucleotide pyrophosphatase/phosphodiesterase
485	3	3	44.4	14	2.11E+04	23208	7.84	Bos taurus	NCBInr	76614885	PREDICTED: similar to high-mobility group box 2, partial
486	3	3	44.06	11	1.57E+04	32844.4	5.27	BOVIN	NCBInr	585322	Inorganic pyrophosphatase (Pyrophosphate phospho-hydrolase) (PPase)
487	6	3	43.63	8	1.89E+04	44294.3	5.05	Bos taurus	NCBInr	73586582	Hypothetical protein LOC527201
488	5	3	43.57	5	3.26E+04	59609.8	5.4	Bos taurus	NCBInr	73586947	Chaperonin containing TCP1, subunit 8 (theta)
489	3	3	43.56	13	9.54E+03	30025.8	10.61	Bos taurus	NCBInr	61886865	PREDICTED: similar to 60S ribosomal protein L7a
490	3	3	43.41	5	1.59E+04	51946.8	8.81	Bos taurus	NCBInr	76618666	citrate synthase
491	3	3	43.3	13	1.92E+04	25849.1	9.39	Bos taurus	NCBInr	76627860	PREDICTED: similar to Electron transfer flavoprotein alpha-subunit, mitochon
492	3	3	43.28	4	2.12E+03	92368.7	5.47	Bos taurus	NCBInr	76636780	PREDICTED: similar to Plasma membrane calcium-transporting ATPase 4 (P
493	3	3	43	9	1.78E+04	36746.8	9.02	Bos taurus	NCBInr	76654464	PREDICTED: similar to Short chain 3-hydroxyacyl-CoA dehydrogenase, mitoc
494	3	3	42.8	5	7.73E+03	101989.6	6.74	Bos taurus	NCBInr	30523262	100 kDa coactivator
495	4	3	42.78	9	2.29E+04	45533.6	5.54	Bos taurus	NCBInr	74354034	Proteasome (prosome, macropain) 26S subunit, non-ATPase, 6
496	4	4	42.7	3	6.72E+03	158004.5	9.35	Bos taurus	NCBInr	76632456	PREDICTED: similar to Ribosome-binding protein 1 (Ribosome receptor prote
497	3	3	42.65	10	3.20E+04	33328.3	5.34	Bos taurus	NCBInr	73587257	Hypothetical protein LOC521254
498	3	3	42.49	13	7.86E+03	23610.8	6.44	Bos taurus	NCBInr	84579874	hypothetical protein LOC616503
499	3	3	42.41	4	1.81E+04	78733.3	6.05	Bos taurus	NCBInr	76658374	PREDICTED: similar to cysteinyl-tRNA synthetase isoform b
500	3	3	41.98	5	2.22E+04	51529.6	5.31	Bos taurus	NCBInr	74354621	Hypothetical protein LOC508535
501	3	3	41.87	8	1.29E+04	46285.2	5.67	Bos taurus	NCBInr	62946669	muscle endopin 1a
502	4	3	41.72	9	1.64E+04	49368.3	8.72	Bos taurus	NCBInr	27806759	adipose differentiation-related protein
503	10	2	41.09	10	2.98E+04	24529.1	4.98	Bos taurus	NCBInr	30794348	casein alpha-S1
504	2	2	41.08	9	1.56E+04	32453.7	9.14	Bos taurus	NCBInr	76651922	PREDICTED: similar to vesicle-associated membrane protein-associated prot
505	3	3	41.06	9	2.32E+04	35723	5.5	Bos taurus	NCBInr	76631732	PREDICTED: similar to Potassium channel tetramerisation domain containing
506	3	3	40.89	7	1.39E+04	47991.2	8.98	Bos taurus	NCBInr	74354968	CNP protein
507	3	3	40.85	6	1.61E+04	42791.7	8.06	Canis familia	NCBInr	73949258	Purine-rich element binding protein A
508	3	3	40.74	7	1.64E+04	38964.7	5.13	Bos taurus	NCBInr	76611318	PREDICTED: similar to nuclear distribution gene C homolog (A. nidulans) isof
509	2	2	40.52	12	1.80E+04	34503.3	5.11	Bos taurus	NCBInr	28603812	epsilon subunit of coatomer protein complex
510	4	3	40.52	12	2.29E+04	25542.2	4.9	Bos taurus	NCBInr	75948245	Proteasome (prosome, macropain) subunit, beta type, 6
511	2	2	40.3	4	7.37E+03	59659.5	5.6	Canis familia	NCBInr	74003011	PREDICTED: chaperonin containing TCP1, subunit 5 (epsilon)
512	4	3	40.23	8	1.05E+04	69164.6	5.92	Bos taurus	NCBInr	76648175	PREDICTED: similar to programmed cell death 6 interacting protein isoform 1
513	3	3	40.11	2	1.52E+04	129064.2	9.23	Bos taurus	NCBInr	27806257	collagen, type I, alpha 2
514	3	3	40.09	14	1.25E+04	28929.8	4.82	Bos taurus	NCBInr	76620202	PREDICTED: similar to E-1 enzyme isoform 1
515	5	3	39.84	10	2.12E+04	52804.6	6.26	Bos taurus	NCBInr	76610565	PREDICTED: similar to aspartyl aminopeptidase isoform 7
516	3	3	39.43	6	1.93E+04	59190.2	5.32	Bos taurus	NCBInr	76678376	STK25 protein
517	4	3	39.2	7	3.27E+04	38400.2	5.34	Bos taurus	NCBInr	81674303	Unknown (protein for MGC:134348)
518	4	3	39.08	6	3.31E+04	45385.6	7.58	Bos taurus	NCBInr	76658398	cathepsin D
519	2	2	39.05	7	1.46E+04	42880.8	5.64	Bos taurus	NCBInr	76632304	PREDICTED: similar to selenophosphate synthetase isoform 2
520	2	2	39.03	5	6.80E+03	69136.6	5.5	Bos taurus	NCBInr	76622026	PREDICTED: similar to thyroid hormone receptor interactor 10 isoform 4

groupNun	numSpecI	unique peptide	scoreUnique	% coverage	totalIntensity	mw	pI	species	database	accession	Protein name
521	2	2	38.98	5	7.18E+03	56428.8	6.42	Bos taurus	NCBInr	76634486	PREDICTED: similar to Serine/threonine-protein kinase Sgk3 (Serum/glucocc
522	2	2	38.89	12	2.39E+04	30606.6	4.75	Bos taurus	NCBInr	74354078	Hypothetical protein LOC518321
523	2	2	38.71	8	9.67E+03	25944.8	6.91	Bos taurus	NCBInr	61810775	PREDICTED: similar to Proteasome subunit alpha type 2 (Proteasome compc
524	2	2	38.7	6	1.07E+04	44962.9	4.8	BOVIN	NCBInr	125197	cAMP-dependent protein kinase type II-alpha regulatory subunit
525	3	3	38.63	9	6.41E+03	26723.4	4.42	Bos taurus	NCBInr	27806687	clathrin, light polypeptide (Lca)
526	3	3	38.55	15	1.21E+04	25976.7	6.07	Bos taurus	NCBInr	74267640	Mesoderm development candidate 2
527	9	3	38.43	44	8.93E+04	103253.3	7.23	Bos taurus	NCBInr	76638698	RPS27A protein
528	3	3	38.39	11	9.45E+03	32477.3	6.27	Bos taurus	NCBInr	76632643	PREDICTED: similar to isopentenyl-diphosphate delta isomerase isoform 2
529	2	2	38.38	5	1.16E+04	56493.4	5.84	Bos taurus	NCBInr	76648361	PREDICTED: similar to Dynein light intermediate chain 1, cytosolic (Dynein lig
530	4	2	38.05	2	3.90E+04	87052.1	4.92	Homo sapiei	NCBInr	51470849	PREDICTED: heat shock 90kDa protein 1, alpha-like 3
531	2	2	37.85	6	1.27E+04	39232.3	5.29	Bos taurus	NCBInr	76621211	PREDICTED: similar to N-acylglucosamine 2-epimerase (GlcNAc 2-epimeras
532	2	2	37.81	7	8.39E+03	70825.1	8.75	Bos taurus	NCBInr	76645718	PREDICTED: similar to signal recognition particle 68kDa isoform 1
533	2	2	37.8	1	3.14E+04	311133.9	8.68	Pan troglody	NCBInr	55666933	WD repeat domain 1
534	6	2	37.52	14	1.36E+05	15973.6	8.55	Canis familia	NCBInr	73952614	PREDICTED: similar to Glyceraldehyde-3-phosphate dehydrogenase (GAPDI
535	3	3	37.32	13	1.60E+04	21673.6	5.13	Bos taurus	NCBInr	74354937	Hypothetical protein LOC539524
536	5	2	37.3	4	1.89E+04	44542.9	5.85	Bos taurus	NCBInr	74353978	Lysosomal-associated membrane protein 2
537	3	3	37.19	2	1.60E+04	208347.6	5.97	Bos taurus	NCBInr	76617277	PREDICTED: similar to Plexin B2 precursor (MM1) isoform 4
538	2	2	37.14	14	6.50E+03	19825.2	4.7	Bos taurus	NCBInr	76610984	PREDICTED: similar to MARCKS-like protein
539	3	3	37.08	11	6.43E+03	27997.3	6.02	Bos taurus	NCBInr	74267695	Phosphomannomutase 2
540	3	3	37.07	8	3.51E+03	36687.9	4.76	Bos taurus	NCBInr	27805823	dermatan sulfate proteoglycan 3
541	2	2	37.04	10	1.08E+04	24167.5	6.6	Bos taurus	NCBInr	76627105	PREDICTED: similar to RAB2B protein isoform 1
542	3	3	37.03	2	8.67E+03	83035.5	6.11	Bos taurus	NCBInr	76629583	PREDICTED: similar to inner membrane protein, mitochondrial, partial
543	2	2	36.86	10	2.12E+04	21856.2	8.86	Bos taurus	NCBInr	76679364	PREDICTED: similar to 3-oxoacid CoA transferase 1, partial
544	6	2	36.71	4	4.78E+04	83596.7	6.47	Homo sapiei	NCBInr	16741721	Lysyl hydroxylase, precursor
545	8	2	36.71	5	2.52E+04	49882.3	8.62	Bos taurus	NCBInr	73587285	Solute carrier family 29 (nucleoside transporters), member 1
546	3	3	36.69	12	1.02E+04	54824.9	4.81	Bos taurus	NCBInr	83405836	Hypothetical protein LOC511198
547	3	3	36.66	4	1.67E+04	57927.5	5.93	Bos taurus	NCBInr	76648284	Ste-20 related kinase SPAK
548	2	2	36.54	3	5.99E+03	64520.5	6.77	Bos taurus	NCBInr	76685863	PREDICTED: similar to Beta-glucuronidase precursor (Beta-G1), partial
549	2	2	36.26	15	2.60E+04	22262.6	5.96	Bos taurus	NCBInr	76644487	PREDICTED: similar to Coatomer zeta-2 subunit (Zeta-2 coat protein) (Zeta-2
550	4	3	36.21	5	1.79E+04	65453.1	8.23	Bos taurus	NCBInr	76639264	PREDICTED: similar to Y37D8A.2 isoform 3
551	3	3	36.19	3	5.74E+04	61049.6	5.7	HUMAN	SwissProt	P13674	Prolyl 4-hydroxylase alpha-1 subunit precursor (EC 1.14.11.2) (4-PH alpha-1)
552	3	3	36.02	5	2.13E+04	64847	5.59	Bos taurus	NCBInr	62460512	hypothetical protein LOC512642
553	2	2	35.96	13	1.79E+04	24907.9	5.62	Bos taurus	NCBInr	41386729	high-mobility group box 1
554	2	2	35.9	9	1.93E+04	37164.7	6.34	Bos taurus	NCBInr	27806265	chondromodulin I precursor [leukocyte cell-derived chemotaxin 1]
555	4	2	35.83	4	5.09E+04	63827.5	7.66	Canis familia	NCBInr	73955102	Pafah1b2 protein
556	2	2	35.82	42	8.38E+03	9249.8	5.69	Bos taurus	NCBInr	76647179	PREDICTED: similar to Electron transfer flavoprotein alpha-subunit, mitochon
557	4	2	35.75	17	1.22E+04	17512.3	5.75	Bos taurus	NCBInr	76611597	PREDICTED: similar to cell division cycle 42, partial
558	2	2	35.73	4	4.65E+03	80098.4	6.68	Bos taurus	NCBInr	76607875	PREDICTED: similar to Importin alpha-4 subunit (Karyopherin alpha-4 subuni
559	2	2	35.64	5	2.04E+04	37493.2	4.74	Homo sapiei	NCBInr	37181971	MWRP239
560	3	3	35.63	8	1.22E+04	32538.7	6.85	Bos taurus	NCBInr	74354146	Hypothetical protein LOC512891
561	3	2	35.63	5	1.67E+04	44891.7	7.65	Bos taurus	NCBInr	76639484	PREDICTED: similar to dolichyl-di-phosphooligosaccharide-protein glycotrans
562	4	3	35.56	12	5.70E+03	27901.6	9.2	Bos taurus	NCBInr	74354925	Hypothetical protein LOC533949
563	2	2	35.55	6	9.29E+03	45274.9	9.35	Bos taurus	NCBInr	76623702	PREDICTED: similar to ubiquitin-like domain containing CTD phosphatase 1
564	5	2	35.51	9	3.13E+04	37476.3	6.57	Rattus norve	NCBInr	12002054	transaldolase
565	2	2	35.26	15	7.03E+03	19860.3	6.44	Bos taurus	NCBInr	76619843	PREDICTED: similar to sec1 family domain containing 2
566	6	3	35.25	40	2.37E+04	7348.3	9.82	Bos taurus	NCBInr	45645223	cell division cycle 10
567	2	2	35.08	3	7.83E+03	73498.3	5.77	Homo sapiei	NCBInr	28317368	TPA: aminopeptidase B
568	2	2	34.93	11	3.33E+04	17337.1	4.83	Bos taurus	NCBInr	76677759	PREDICTED: similar to NADP-dependent malic enzyme (NADP-ME) (Malic e
569	3	2	34.88	7	1.37E+04	42761.7	5.28	BOVIN	NCBInr	125192	cAMP-dependent protein kinase type I-alpha regulatory subunit
570	2	2	34.87	4	2.16E+04	68576.8	5.99	Canis familia	NCBInr	73984484	Ribophorin I
571	2	2	34.76	4	1.32E+04	77182.6	8.16	Canis familia	NCBInr	73988830	SWA-70 protein
572	2	2	34.68	8	1.44E+04	28749	4.57	Bos taurus	NCBInr	73587053	Hypothetical protein LOC515499

groupNun	numSpect	unique peptide	scoreUnique	% coverage	totalIntensity	mw	pI	species	database	accession	Protein name
573	2	2	34.66	11	1.12E+04	25377.4	5.38	Bos taurus	NCBInr	76654970	PREDICTED: similar to glutathione-S-transferase omega 1
574	3	2	34.61	6	1.79E+04	47412.1	10.96	Bos taurus	NCBInr	62460480	hypothetical protein LOC510547
575	3	2	34.49	3	9.31E+03	74236.8	6.47	Bos taurus	NCBInr	76639900	Craniofacial development protein 2 (p97 bucentaur protein)
576	2	2	34.48	11	1.15E+04	34525	5.02	Bos taurus	NCBInr	76664539	PREDICTED: similar to vesicle transport-related protein isoform a
577	2	2	34.3	4	1.01E+04	73260	8.91	Bos taurus	NCBInr	76616889	PREDICTED: similar to DEAD box polypeptide 17 isoform 1 isoform 9
578	2	2	34.24	12	3.39E+04	26892.9	8.4	Bos taurus	NCBInr	76701956	PREDICTED: similar to RAN, member RAS oncogene family
579	4	3	34.17	6	1.17E+04	40654	5.08	Bos taurus	NCBInr	74268122	Hypothetical protein LOC526612
580	2	2	34.06	12	1.32E+04	22487.2	8.07	Bos taurus	NCBInr	76655610	caspase-3
581	2	2	33.86	4	1.13E+04	66269.4	5.94	Canis familia	NCBInr	74006523	CTP synthase II
582	2	2	33.8	6	1.28E+04	50287.4	8.72	Pan troglody	NCBInr	55620724	Coproporphyrinogen oxidase
583	3	3	33.7	5	9.77E+03	73144.5	6.32	Bos taurus	NCBInr	76659559	PREDICTED: similar to DEAD-box protein 3, X-chromosomal (Helicase-like p
584	2	2	33.69	16	1.75E+04	23421.5	5.12	Bos taurus	NCBInr	28603774	Rho GDP dissociation inhibitor (GDI) alpha
585	3	2	33.66	3	1.13E+04	86469.6	5.82	Bos taurus	NCBInr	76653827	PREDICTED: similar to procollagen-lysine, 2-oxoglutarate 5-dioxygenase 3 pı
586	2	2	33.65	4	4.89E+03	96894.1	6.12	Canis familia	NCBInr	73998369	NF-kB2 splice variant 4
587	3	3	33.58	8	1.28E+04	47629.2	9.21	Bos taurus	NCBInr	76656245	PREDICTED: similar to coiled-coil domain containing 6
588	3	2	33.56	9	2.21E+04	25258	6.31	Bos taurus	NCBInr	27806911	CD9 antigen (p24)
589	2	2	33.47	6	9.03E+03	54118.8	5.41	Bos taurus	NCBInr	81673074	Unknown (protein for MGC:127205)
590	2	2	33.45	5	1.04E+04	49063.7	5.16	Pan troglody	NCBInr	55648517	tropomyosin 4-anaplastic lymphoma kinase fusion protein
591	2	2	33.43	9	8.22E+03	22896.4	6.52	Bos taurus	NCBInr	74354591	Proteasome (prosome, macropain) subunit, beta type, 2
592	4	2	33.19	6	4.27E+04	35836.2	8.57	Sus scrofa	NCBInr	2407184	glyceraldehyde 3-phosphate dehydrogenase
593	2	2	33.18	10	1.81E+04	35155.5	6.01	Bos taurus	NCBInr	76656965	PREDICTED: similar to CG9119-PA
594	2	2	33.12	8	1.18E+04	33340.2	8.38	Bos taurus	NCBInr	28603744	mitochondrial carrier homolog 2
595	2	2	33.05	3	1.63E+04	81297.4	5.84	Canis familia	NCBInr	74001097	glycogen branching enzyme
596	2	2	33.05	4	1.43E+04	63931	5.78	Bos taurus	NCBInr	74354907	Eukaryotic translation initiation factor 3, subunit 7 zeta, 66/67kDa
597	2	2	32.89	10	5.54E+03	28024.8	11.04	Bos taurus	NCBInr	74267654	Hypothetical protein LOC535056
598	2	2	32.85	2	1.38E+04	88772.6	7.93	Bos taurus	NCBInr	76626705	PREDICTED: similar to ADP-dependent glucokinase
599	4	2	32.83	9	3.37E+04	21920.1	8.25	Bos taurus	NCBInr	76689040	PREDICTED: similar to Tissue alpha-L-fucosidase precursor (Alpha-L-fucosic
600	2	2	32.79	4	1.71E+04	69306.6	5.95	Bos taurus	NCBInr	74355010	Leukotriene A4 hydrolase
601	2	2	32.78	6	1.92E+04	49407.5	6.75	bovine	NCBInr	2119917	translation elongation factor EF-Tu precursor
602	3	2	32.76	5	1.52E+04	40921.5	9.06	Canis familia	NCBInr	73990431	muscleblind-like 1
603	2	2	32.71	5	1.70E+04	54187.5	7.59	Bos taurus	NCBInr	76615127	PREDICTED: similar to Dihydrolipoyl dehydrogenase, mitochondrial precurso
604	2	2	32.71	7	1.11E+04	55465.2	6.34	Bos taurus	NCBInr	76616970	PREDICTED: similar to adenylosuccinate lyase isoform 2
605	2	2	32.67	6	1.28E+04	31521.4	6.74	Bos taurus	NCBInr	74354619	ATPase, Na+/K+ transporting, beta 3 polypeptide
606	3	2	32.53	4	1.92E+04	43803.2	6.13	Bos taurus	NCBInr	73587133	Hypothetical protein LOC540272
607	4	2	32.52	4	5.48E+03	64888	9.6	Bos taurus	NCBInr	76625300	PREDICTED: similar to Plasminogen activator inhibitor 1 RNA-binding protein
608	2	2	32.48	6	7.88E+03	59125.7	6.4	Bos taurus	NCBInr	66792842	dihydroxyacetone kinase 2 homolog
609	2	2	32.06	11	8.39E+03	31905.9	9.93	Bos taurus	NCBInr	76615572	PREDICTED: similar to transmembrane emp24 protein transport domain cont
610	2	2	31.82	5	1.30E+04	40638.9	6.29	Bos taurus	NCBInr	72536789	MHC class I antigen
611	2	2	31.67	9	4.87E+03	23626.9	5.98	Bos taurus	NCBInr	83638639	Unknown (protein for MGC:133754)
612	2	2	31.61	5	5.46E+03	58428.9	6	Bos taurus	NCBInr	27805931	intercellular adhesion molecule 1 (CD54), human rhinovirus receptor
613	2	2	31.44	1	3.01E+04	71187	7.54	Rattus norve	NCBInr	12018252	transketolase
614	2	2	31.44	6	9.11E+03	38032.8	7.13	Bos taurus	NCBInr	81673705	Hypothetical protein LOC515837
615	2	2	31.36	8	1.43E+04	28594	6.18	Bos taurus	NCBInr	73587251	Hypothetical protein LOC505403
616	2	2	31.34	4	1.71E+04	53807.4	5.04	Bos taurus	NCBInr	76617221	PREDICTED: similar to Arylsulfatase A precursor (ASA) (Cerebroside-sulfata
617	2	2	31.3	5	7.21E+03	53650.8	5.6	Homo sapie	NCBInr	12654479	UBX domain containing 8
618	2	2	31.26	7	1.38E+04	55199.6	6.77	Bos taurus	NCBInr	75775064	Hypothetical protein LOC525106
619	2	2	31.22	4	4.79E+03	75541.5	5.6	Bos taurus	NCBInr	2920652	GTP-binding protein
620	2	2	31.2	5	1.51E+04	40619.9	8.71	Bos taurus	NCBInr	633	protein kinase
621	2	2	31.13	10	9.81E+03	19934.4	5.69	Bos taurus	NCBInr	74354962	Hypothetical protein LOC534704
622	2	2	31.07	30	4.83E+03	12547.9	9.07	Bos taurus	NCBInr	76646969	PREDICTED: similar to Ras GTPase-activating-like protein IQGAP1 (p195)
623	2	2	31.04	9	1.09E+04	31414.4	5.92	Bos taurus	NCBInr	76633047	PREDICTED: similar to Vesicle-associated membrane protein-associated pro
624	2	2	30.98	11	7.51E+03	27735	5.37	Bos taurus	NCBInr	76646451	PREDICTED: similar to 3-oxoacid CoA transferase 1

groupNun	numSpect	unique peptide	scoreUnique	% coverage	totalIntensity	mw	pI	species	database	accession	Protein name
625	3	3	30.87	3	2.19E+04	67569.3	7.06	Bos taurus	NCBInr	76608746	PREDICTED: similar to Mitochondrial precursor proteins import receptor (Trai
626	3	2	30.81	5	6.24E+03	69214.4	5.48	Bos taurus	NCBInr	74267729	Hypothetical protein LOC534231
627	2	2	30.81	6	1.84E+04	38631.6	6.2	Homo sapiei	NCBInr	56790945	protein phosphatase 1, catalytic subunit, alpha isoform 3
628	2	2	30.68	7	8.55E+03	35178.6	5.98	Bos taurus	NCBInr	76654275	PREDICTED: similar to JTV1 isoform 2
629	3	2	30.68	8	4.37E+04	32117.1	4.12	Bos taurus	NCBInr	83638675	MGC134241 protein
630	4	2	30.63	3	5.14E+03	94235.5	8.27	Pan troglody	NCBInr	55588614	PREDICTED: a disintegrin and metalloproteinase with thrombospondin motifs
631	2	2	30.62	12	9.46E+03	21535.5	11.69	Bos taurus	NCBInr	75775560	Ribosomal protein L18
632	2	2	30.57	9	1.12E+04	31537.4	8.56	Bos taurus	NCBInr	73586945	Unknown (protein for MGC:126965)
633	2	2	30.52	3	1.22E+04	56776.2	5.94	Bos taurus	NCBInr	76629869	PREDICTED: similar to prenylcysteine oxidase 1
634	2	2	30.47	4	1.51E+04	43877.4	9.56	Bos taurus	NCBInr	27807207	plasminogen activator inhibitor type 1, member 2
635	3	3	30.34	4	2.36E+03	103926.2	8.07	Bos taurus	NCBInr	76607473	PREDICTED: similar to Eukaryotic translation initiation factor 4 gamma 1 (eIF
636	2	2	30.25	2	1.24E+04	87539.8	9	Pan troglody	NCBInr	55633929	CCDC6 protein
637	2	2	30.05	3	9.53E+03	117520.9	7.18	Bos taurus	NCBInr	76607227	PREDICTED: similar to optic atrophy 1 isoform 8 isoform 16
638	11	2	30.05	8	3.66E+04	25692.1	4.88	Bos taurus	NCBInr	76651328	PREDICTED: similar to Translocon-associated protein alpha subunit precursc
639	2	2	30.03	11	9.85E+03	25073.9	4.81	Bos taurus	NCBInr	74354266	Hypothetical protein LOC515326
640	2	2	30	5	2.84E+03	33216.7	8.74	Bos taurus	NCBInr	76652799	PREDICTED: similar to 3,2-trans-enoyl-CoA isomerase, mitochondrial precur:
641	2	2	29.98	3	6.59E+03	82249.9	5.42	Bos taurus	NCBInr	18652676	micromolar calcium activated neutral protease 1
642	2	2	29.89	9	5.04E+03	55762.9	9.03	Bos taurus	NCBInr	76657043	PREDICTED: similar to phosphatidylinositol-binding clathrin assembly protein
643	3	3	29.77	7	5.46E+03	36914.3	4.88	Bos taurus	NCBInr	83638659	MGC133704 protein
644	2	2	29.7	10	6.93E+03	33049.7	6.1	Bos taurus	NCBInr	76656104	PREDICTED: similar to translin-associated factor X
645	2	2	29.69	4	9.77E+03	51979.2	7.19	Bos taurus	NCBInr	61817521	cathepsin C
646	3	2	29.6	5	7.71E+03	29728.1	9.47	Bos taurus	NCBInr	27807365	ubiquinol-cytochrome c reductase, Rieske iron-sulfur polypeptide 1
647	3	2	29.45	5	3.71E+03	60619.4	5.49	Bos taurus	NCBInr	76665976	PREDICTED: similar to Tenascin precursor (TN) (Hexabrachion) (Cytotactin)
648	3	2	29.18	6	1.48E+04	48114.1	9.36	Bos taurus	NCBInr	76626004	PREDICTED: similar to SH3-domain GRB2-like B1 (endophilin) (predicted), p
649	3	3	29.18	8	4.69E+03	33154.1	6.26	Bos taurus	NCBInr	76652711	PREDICTED: hypothetical protein XP_880973 isoform 5
650	2	2	29.13	8	3.47E+03	28761.3	4.75	Canis familia	NCBInr	74000397	Tropomyosin 1, alpha, isoform h
651	4	2	29.04	7	2.34E+04	35655.3	5.87	Bos taurus	NCBInr	73586725	Unknown (protein for MGC:128341)
652	2	2	29.04	6	3.15E+03	47302.5	4.85	Bos taurus	NCBInr	78174362	Hypothetical protein LOC508273
653	2	2	29.01	7	1.39E+04	37298	5.55	Bos taurus	NCBInr	78042550	thioredoxin-like
654	2	2	28.94	5	9.57E+03	39221.2	4.83	Bos taurus	NCBInr	74268242	ADP-ribosylhydrolase like 2
655	8	2	28.93	6	1.28E+04	25111.5	10.06	Bos taurus	NCBInr	16418492	cyanogen bromide
656	3	2	28.79	0	1.65E+04	387090.7	8.9	Pan troglody	NCBInr	55620347	Galphai2 protein
657	2	2	28.75	6	9.48E+03	41384.6	4.68	Bos taurus	NCBInr	61554723	proteasome 26S non-ATPase subunit 4 isoform 1
658	2	2	28.52	5	3.84E+03	33886.4	6.55	Bos taurus	NCBInr	76632995	PREDICTED: similar to cathepsin Y isoform 1
659	2	2	28.48	2	3.21E+03	148222	6.09	Pan troglody	NCBInr	55633999	PREDICTED: vinculin
660	2	2	28.37	3	9.57E+03	74705	5.81	Bos taurus	NCBInr	77404189	thimet oligopeptidase
661	2	2	28.3	8	8.55E+03	29943.5	6.72	Bos taurus	NCBInr	74267697	Hypothetical protein LOC509643
662	3	3	28.23	1	1.98E+03	229100.4	5.44	BOVIN	SwissProt	Q27991	Myosin heavy chain, nonmuscle type B (Cellular myosin heavy chain, type B)
663	2	2	28.15	6	5.61E+03	31201.7	5.44	Bos taurus	NCBInr	28461185	mannose-6-phosphate receptor (cation dependent)
664	2	2	28.08	4	1.89E+04	45444.5	4.91	Bos taurus	NCBInr	76671220	MGC129137 protein
665	2	2	28.07	2	1.45E+04	87335.2	5.74	HUMAN	SwissProt	P42224	Signal transducer and activator of transcription 1-alpha/beta (Transcription fac
666	2	2	28.02	9	1.08E+04	36988.4	5.36	Bos taurus	NCBInr	74353904	MGC127154 protein
667	2	2	28.01	5	1.03E+04	46091.3	6.57	Bos taurus	NCBInr	74268319	Hypothetical protein LOC535740
668	2	2	27.74	8	1.03E+04	41388.3	4.86	Bos taurus	NCBInr	74267606	Protein phosphatase 1, regulatory subunit 7
669	3	2	27.66	8	1.86E+04	28311.9	4.16	Bos taurus	NCBInr	76647200	PREDICTED: similar to Reticulocalbin-2 precursor (Calcium-binding protein E
670	2	2	27.62	2	6.44E+03	63683.6	6.23	Bos taurus	NCBInr	76625619	PREDICTED: fibroblast growth factor receptor 3, partial
671	3	2	27.4	6	1.29E+04	35471.7	5.21	Bos taurus	NCBInr	73586980	Unknown (protein for MGC:127895)
672	2	2	27.35	13	1.13E+04	24489.6	5.65	MOUSE	SwissProt	P46638	Ras-related protein Rab-11B
673	2	2	27.33	1	3.18E+03	196523	6.09	Rattus norve	NCBInr	62640787	IQ motif containing GTPase activating protein 1
674	2	2	27.2	7	1.44E+04	38217.5	8.75	Bos taurus	NCBInr	75773792	DnaJ (Hsp40) homolog, subfamily B, member 1
675	2	2	27.17	2	9.48E+02	127328.6	5.87	Bos taurus	NCBInr	76629029	PREDICTED: similar to latent transforming growth factor beta binding protein
676	2	2	27.15	2	8.74E+03	90828.4	6.28	Bos taurus	NCBInr	76613142	PREDICTED: similar to upstream of NRAS isoform 2

groupNun	numSpect	unique peptide	scoreUnique	% coverage	totalIntensity	mw	pI	species	database	accession	Protein name
677	2	2	27.15	6	9.62E+03	52378	6.36	Bos taurus	NCBInr	76647377	PREDICTED: similar to vesicle transport-related protein isoform a
678	3	2	27.07	2	8.18E+03	131855.5	7.63	Pan troglody	NCBInr	55621128	PREDICTED: transferrin
679	3	2	27.04	1	1.58E+04	132117.9	4.8	Bos taurus	NCBInr	76629332	PREDICTED: similar to Reticulon 4 (Neurite outgrowth inhibitor) (Nogo protei
680	2	2	26.96	10	8.74E+03	28857.5	4.74	Pan troglody	NCBInr	83674988	rcTPM3
681	3	2	26.76	3	9.01E+03	57142	7.23	Bos taurus	NCBInr	76647423	PREDICTED: similar to sorting nexin 6
682	2	2	26.55	1	3.12E+03	226339.3	5.49	RAT	SwissProt	Q62812	Myosin heavy chain, nonmuscle type A (Cellular myosin heavy chain, type A)
683	2	2	26.48	3	5.64E+03	88268.8	5.25	Bos taurus	NCBInr	27805959	integrin, beta 1 subunit (fibronectin receptor, beta polypeptide, antigen CD29
684	2	2	26.48	2	1.08E+03	140787.5	8.15	Bos taurus	NCBInr	76611807	PREDICTED: similar to Coatomer alpha subunit (Alpha-coat protein) (Alpha-C
685	2	2	26.41	3	1.31E+04	52243.2	4.99	Canis familia	NCBInr	74006545	Chromatin assembly factor 1 subunit C (CAF-1 subunit C) (Chromatin assemI
686	2	2	26.41	2	1.40E+04	65294.2	9.06	Bos taurus	NCBInr	76671059	Glutamine synthetase (Glutamate--ammonia ligase) (GS)
687	5	2	26.35	2	1.81E+04	75818.7	9.24	Pan troglody	NCBInr	55640967	SPARC-related modular calcium-binding protein 1 precursor (Secreted modul
688	2	2	26.34	8	4.45E+03	31738	5.54	Bos taurus	NCBInr	76615500	PREDICTED: similar to 3-hydroxyisobutyrate dehydrogenase, mitochondrial p
689	2	2	26.27	4	6.83E+03	50875.8	5.43	Bos taurus	NCBInr	76642670	PREDICTED: similar to serine carboxypeptidase 1 precursor protein isoform 3
690	2	2	26.25	4	4.89E+03	37231.8	9.15	Bos taurus	NCBInr	21450879	beta-1,4-galactosyltransferase
691	2	2	26.23	4	5.60E+03	52191.1	5.71	Bos taurus	NCBInr	74267627	Eukaryotic translation initiation factor 3, subunit 6 48kDa
692	2	2	26.09	6	1.35E+04	31667.9	8.4	Bos taurus	NCBInr	76634058	PREDICTED: similar to tissue specific transplantation antigen P35B
693	2	2	26.07	3	4.48E+03	63206.9	9.43	Bos taurus	NCBInr	76670135	PREDICTED: similar to Melanoma-associated antigen D2 (MAGE-D2 antigen
694	2	2	26.03	12	6.54E+03	22018.6	8.89	Bos taurus	NCBInr	74354772	Hypothetical protein LOC509056
695	3	2	25.74	4	8.97E+03	44010	6.44	Bos taurus	NCBInr	76639752	PREDICTED: similar to v-crk sarcoma virus CT10 oncogene homolog (avian)
696	2	2	25.67	1	4.87E+03	104841.9	7.91	Bos taurus	NCBInr	12034659	ribeye
697	3	2	25.61	3	2.49E+04	53942.3	5.46	RABIT	SwissProt	P28863	Stromelysin-1 precursor (EC 3.4.24.17) (Matrix metalloproteinase-3) (MMP-3)
698	2	2	25.57	2	2.01E+03	137001.2	4.96	Bos taurus	NCBInr	76654996	PREDICTED: similar to serine/threonine kinase 2, partial
699	2	2	25.21	2	1.26E+04	73338.4	5.21	Canis familia	NCBInr	74004542	dynein, cytoplasmic, intermediate polypeptide 2
700	2	2	25.11	12	2.50E+03	26722.2	5.38	Bos taurus	NCBInr	83588810	vinculin
701	2	2	25.04	6	6.78E+03	35742.5	5.86	Bos taurus	NCBInr	76671392	PREDICTED: similar to 26S proteasome non-ATPase regulatory subunit 14 (2
702	3	2	24.99	3	4.61E+03	65238.8	5.16	Bos taurus	NCBInr	73587017	Hypothetical protein LOC534150
703	4	2	24.98	7	6.80E+03	25623.7	8.92	Bos taurus	NCBInr	76657975	PREDICTED: similar to Protein FAM3C precursor (Protein GS3786) isoform 3
704	2	2	24.77	6	1.01E+04	51447.6	8.3	Bos taurus	NCBInr	74356509	Integrin linked kinase
705	2	2	24.76	2	3.95E+03	106671.1	6.22	Bos taurus	NCBInr	62084374	ATP-dependent Lon protease
706	2	2	24.74	2	4.59E+03	106655.5	5.3	Bos taurus	NCBInr	76639846	PREDICTED: similar to Alanyl-tRNA synthetase (Alanine--tRNA ligase) (AlaR
707	2	2	24.73	2	6.70E+03	81315.3	5.81	Bos taurus	NCBInr	73587129	minichromosome maintenance protein 7
708	2	2	24.56	16	1.46E+03	18988.1	6.86	Bos taurus	NCBInr	81294235	Hypothetical protein LOC615197
709	3	2	24.51	2	6.68E+03	94316.8	5.89	Bos taurus	NCBInr	76618599	signal transducer and activator of transcription 6
710	2	2	24.46	7	3.54E+03	32657.1	5.88	Bos taurus	NCBInr	76629502	PREDICTED: similar to Trans-Golgi network integral membrane protein 2 pre
711	2	2	24.44	5	5.28E+03	76213.2	4.59	HUMAN	SwissProt	P19338	Nucleolin (Protein C23)
712	2	2	24.34	6	6.85E+03	32050.6	7	Bos taurus	NCBInr	81673606	Unknown (protein for MGC:133821)
713	2	2	24.25	10	2.54E+04	36978.1	5.68	Bos taurus	NCBInr	76655751	protein phosphatase 2, catalytic subunit, alpha isoform
714	2	2	24.17	7	1.01E+04	33876.6	9.91	Bos taurus	NCBInr	27807191	solute carrier family 25 (mitochondrial carrier
715	2	2	24.09	12	1.12E+04	21258.8	6.73	Mus musculi	NCBInr	74207606	cell division cycle 42 (GTP binding protein, 25kDa)
716	2	2	24.07	2	2.95E+03	107968.2	7.73	Homo sapie	NCBInr	15559717	AP2A1 protein
717	2	2	24.02	9	4.84E+03	24708.9	6.05	RAT	SwissProt	P70470	Acyl-protein thioesterase 1 (EC 3.1.2.-) (Lysophospholipase I)
718	2	2	23.98	20	2.50E+03	21139.4	6.6	Bos taurus	NCBInr	76608281	PREDICTED: similar to Nucleoside diphosphate-linked moiety X motif 16 (Nu
719	2	2	23.92	0	1.22E+03	265650.8	6.61	Bos taurus	NCBInr	76640531	PREDICTED: similar to CCR4-NOT transcription complex, subunit 1 isoform a
720	2	2	23.86	2	4.95E+03	104607.2	4.94	HUMAN	SwissProt	Q10567	Adapter-related protein complex 1 beta 1 subunit (Beta-adaptin 1) (Adaptor pr
721	2	2	23.83	5	1.06E+04	50974.1	8.9	Bos taurus	NCBInr	76616245	PREDICTED: similar to Nedd8 ultimate buster-1, partial
722	2	2	23.8	5	2.46E+04	43079.1	5.86	Bos taurus	NCBInr	76645595	PREDICTED: similar to Galactokinase (Galactose kinase) isoform 3
723	2	2	23.75	5	1.46E+04	65236.8	5.13	Bos taurus	NCBInr	76609484	PREDICTED: similar to Dynein intermediate chain 2, cytosolic (DH IC-2) (Cyt
724	2	2	23.44	0	1.17E+04	410108.1	10.45	Macaca mul	NCBInr	44893813	abnormal spindle-like
725	2	2	23.27	2	6.82E+03	93890.7	5.85	Bos taurus	NCBInr	76651457	LOC533188 protein
726	2	2	23.2	7	1.03E+04	29031.3	5.52	Bos taurus	NCBInr	74267624	Proteasome (prosome, macropain) subunit, beta type, 4
727	2	2	23.07	3	2.15E+03	123630.7	4.83	HUMAN	SwissProt	O00410	Importin beta-3 (Karyopherin beta-3) (Ran-binding protein 5) (RanBP5)
728	1	1	22.92	5	8.39E+03	45712	6.06	Canis familia	NCBInr	73969820	actin-related protein 2 isoform a

groupNun	numSpect	unique peptide	scoreUnique	% coverage	totalIntensity	mw	pI	species	database	accession	Protein name
729	2	2	22.76	1	1.83E+03	164586.7	9.18	Canis familia	NCBInr	50978924	ribosome receptor
730	2	2	22.72	3	5.45E+03	60387.5	5.46	Bos taurus	NCBInr	76689594	PREDICTED: similar to Transcription factor p65 (Nuclear factor NF-kappa-B p
731	2	2	22.66	7	1.36E+04	36899.9	5.73	HUMAN	SwissProt	Q9NQG5	Protein C20orf77
732	2	2	22.52	4	1.95E+04	44401.4	7.61	Bos taurus	NCBInr	76665742	PREDICTED: similar to stromal cell derived factor receptor 1 isoform b isoforr
733	1	1	22.5	3	1.21E+04	49269	9.11	Pan troglody	NCBInr	55642977	PREDICTED: electron transfer flavoprotein, alpha polypeptide
734	2	2	22.45	3	8.69E+03	59673.8	7.85	Bos taurus	NCBInr	86438303	Unknown (protein for MGC:137200)
735	2	2	22.44	3	2.76E+03	96885.8	5.46	Bos taurus	NCBInr	76633288	PREDICTED: similar to Band 4.1-like protein 1 (Neuronal protein 4.1) (4.1N) i
736	2	2	22.28	1	2.44E+03	287831.3	5.2	Bos taurus	NCBInr	76630702	PREDICTED: similar to Spectrin alpha chain, brain (Spectrin, non-erythroid al
737	2	2	21.7	5	1.90E+03	46690.1	10.32	Bos taurus	NCBInr	76609486	PREDICTED: similar to cytochrome b reductase 1
738	1	1	21.63	3	4.20E+03	40463.4	8.78	Bos taurus	NCBInr	83405025	Hypothetical protein LOC514902
739	1	1	21.57	7	3.31E+03	28134.7	4.82	Mus musculi	NCBInr	74219534	14-3-3 protein beta
740	2	2	21.48	2	9.95E+03	69276	5.83	MOUSE	SwissProt	P26040	Ezrin (p81) (Cytovillin) (Villin 2)
741	2	2	21.36	1	1.03E+03	166628.5	5.65	Bos taurus	NCBInr	76627657	PREDICTED: similar to Nidogen-2 precursor (NID-2) (Osteonidogen)
742	2	2	21.29	14	7.36E+03	14465.6	7.98	Bos taurus	NCBInr	76676769	PREDICTED: similar to LIN-7 homolog A (LIN-7A) (Mammalian LIN-seven pro
743	1	1	21.2	4	2.34E+03	60055	4.32	Bos taurus	NCBInr	83405382	Hypothetical protein LOC512427
744	2	2	21.01	3	1.91E+03	136658	6.54	Pan troglody	NCBInr	55652893	CSE1 chromosome segregation 1-like protein, isoform a
745	1	1	20.92	2	4.63E+03	70872.9	8.97	Bos taurus	NCBInr	17941422	vitrin
746	1	1	20.89	7	5.86E+03	32120.3	4.84	HUMAN	SwissProt	O43396	Thioredoxin-like protein 1 (32 kDa thioredoxin-related protein)
747	1	1	20.87	5	5.52E+03	38305.9	5.15	Bos taurus	NCBInr	76641888	PREDICTED: similar to Ubiquitin-like 1 activating enzyme E1A (SUMO-1 activ
748	1	1	20.75	2	5.46E+03	59915.6	6.79	Bos taurus	NCBInr	78369302	hypothetical protein LOC531682
749	1	1	20.65	2	2.89E+03	82978.1	6.26	Bos taurus	NCBInr	76624028	PREDICTED: similar to palladin
750	1	1	20.65	8	7.22E+03	21376.3	8.74	Bos taurus	NCBInr	76614877	PREDICTED: similar to Cell division protein kinase 6 (Serine/threonine-protei
751	1	1	20.5	3	2.83E+03	80998.7	9.79	Bos taurus	NCBInr	76631025	PREDICTED: similar to DEAD (Asp-Glu-Ala-Asp) box polypeptide 31 isoform
752	1	1	20.44	1	6.43E+03	78675.7	6.68	HUMAN	SwissProt	Q06210	Glucosamine--fructose-6-phosphate aminotransferase [isomerizing] 1 (EC 2.6
753	7	1	20.4	9	7.11E+04	13401.5	8.52	Canis familia	NCBInr	74006684	PREDICTED: similar to eukaryotic translation elongation factor 1 alpha 2 isof
754	1	1	20.16	1	5.06E+03	90121.5	8.33	Bos taurus	NCBInr	76616225	PREDICTED: similar to Cullin-1 (CUL-1) isoform 2
755	2	2	20.15	4	5.04E+03	36163.7	5.47	HUMAN	SwissProt	Q7L5N1	COP9 signalosome complex subunit 6 (Signalosome subunit 6) (SGN6) (JAB
756	2	2	20.15	5	5.38E+03	55003.7	9.11	HUMAN	SwissProt	O95822	Malonyl-CoA decarboxylase, mitochondrial precursor (EC 4.1.1.9) (MCD)
757	1	1	20.09	9	4.23E+03	17439.7	5.06	Bos taurus	NCBInr	76676232	PREDICTED: similar to golgi phosphoprotein 3, partial
758	1	1	12.58	4	7.87E+02	329984.3	5.33	Bos taurus	NCBInr	76648072	PREDICTED: similar to AHNAK nucleoprotein isoform 1